

Development of Hydrogen Isotope Exchange Methodologies for the Deuteration of Aromatic Substrates

Dissertation

in kumulativer Form
zur Erlangung des akademischen Grades
Doktor rerum naturalium (Dr. rer. nat.)
der Mathematisch-Naturwissenschaftlichen Fakultät
der Universität Rostock

vorgelegt von Sara Kopf,
geboren am 29.10.1995 in Magdeburg

Rostock, 15.06.2022

Leibniz

Die vorliegende Arbeit entstand am Leibniz-Institut für Katalyse e.V. an der Universität Rostock, am Lehrstuhl für Angewandte Homogenkatalyse in der Gruppe von Prof. Matthias Beller in der Zeit von April 2020 bis Juni 2022.

The present work was accomplished at the Leibniz Institute for Catalysis e. V. at the University of Rostock, at the chair for Applied Catalysis in the group of Prof Matthias Beller during the period from April 2020 to June 2022.

Gutachter:

Prof. Dr. Dr. h.c. mult. Matthias Beller, Leibniz-Institut für Katalyse e.V., Rostock, Deutschland

Dr. Grégory Pieters, CEA Paris-Saclay, Frankreich

Prof. Dr. Matthias Tamm, Technische Universität Braunschweig, Deutschland

Jahr der Einreichung: 2022

Jahr der Verteidigung: 2022

Statement of Authorship

I hereby affirm that I have written the present work by myself without outside assistance. No other resources were utilized than stated. All references as well as verbatim extracts were quoted, and all sources of information were specifically acknowledged.

Ich versichere hiermit an Eides statt, dass ich die vorliegende Arbeit selbstständig angefertigt und ohne fremde Hilfe verfasst habe. Dazu habe ich keine außer der von mir angegebenen Hilfsmittel und Quellen verwendet. Die den benutzten Werken inhaltlich und wörtlich entnommenen Stellen habe ich als solche kenntlich gemacht.

Place, date, signature

Acknowledgments

The first section of this thesis is dedicated to thanking all those who made this work possible. First of all, I would like to thank my supervisor, Prof Matthias Beller. Thank you for allowing me to work in your research group and this way giving me a chance after I decided to change PhD programs. Thank you for welcoming me warmly with lots of nice project ideas and the prospects to finish my PhD in less than three years. Thank you for all the knowledge and experience that you have shared with me. It was always a great pleasure to learn from you and to discuss science with you. You have been the best supervisor I could have dreamed of, and I could not be more grateful to you for your constant support.

I would like to thank my supervisor Dr Helfried Neumann for his everyday support and for his invaluable advice on all types of laboratory techniques. Thank you for giving me great freedom and for creating a friendly and relaxed atmosphere in our group. Thank you for always reading my texts with the utmost attention and finding mistakes that no one else saw. I am glad for having had the opportunity to work with you for the past 2 years.

I would like to acknowledge funding for my PhD provided by the European Union within the FLIX project. I would also like to thank all collaboration partners within the FLIX project, especially Dr Grégory Pieters and Dr Sophie Feuillastre, not only for organizing the partnership, but also for the stimulating exchange in our (online) meetings and at other conferences.

I owe gratitude to my collaboration partners: Thank you, Dr Fei Ye, for giving me a suggestion that led to my first project at LIKAT! Thank you, Dr Kangkang Sun, for our nice collaboration on my first industrial project. I would like to thank Dr Wu Li and Florian Bourriquen for writing a massive review together with me. Thank you, Florian, for collaboration far beyond our review! Thank you for all our discussions on deuteration, for sharing experiences with this wonderful research field and – of course – for co-edition of the Deuteration Newsletter. Thank you, Jiali Liu, for your computational work on our pyridine deuteration project and for our insightful scientific conversations. Additionally, I would like to thank the collaboration partners of ongoing projects that are not part of this thesis: Many thanks go to Dr Volker Derdau for allowing me to get to know his isotope lab at Sanofi and for giving me the opportunity of exploring an interesting project. I would also like to thank Prof Anat Milo and Dr Danilo Machado Lustosa for our wonderful collaboration and invaluable input on our ongoing project. I have learned a lot from you.

Further thanks go to the analytical departments of LIKAT and especially to Susanne Buchholz, Dr Christine Fischer, Dr Wolfgang Baumann and Astrid Lehmann for measuring numerous NMR samples and a good amount of mass spectra. In this context, I would also like to thank the PhD representatives of the year 2021, Paul Hünemörder, Hilario Huerta and Dr David Leonard for establishing student participation in the NMR service.

I owe gratitude to the readers of my thesis, Prof Matthias Beller, Dr Helfried Neumann, Dr Danilo Machado Lustosa, and Florian Bourriquen.

I would like to thank all group members of the Catalysis for Life Sciences group for the friendly working atmosphere. Thank you, Sandra Leiminiger, Dr Fei Ye, Dr Patrick Piehl, Dr Maximilian Marx, Dr Kangkang Sun, Dr Peng Wang, Dr Yaxin Wang, Raquel Pérez, and Zhusong Cao. Many thanks go to my long-time labmate Vishwas Chandrashekhar for being a wonderful colleague. Thank you also for letting me borrow all your compounds and for standing all the smelly chemistry I have worked with. My PhD would have been much harder without our daily conversations.

I would also like to thank Bei, Fairoosa, Hilario, Fábio, Everaldo, Patrick, Ricarda, Gordon, and Conni for nice conversations and enjoyable lunch breaks. Moreover, I would like to thank my PhD/Postdoc representation colleagues Priyanka and Weiheng for their motivation and our friendly meetings.

Thank you, Zé Tiago, Banny, Klaudia, Davide, and Adriana for all the good time we spent together in Tarragona. Thank you, Basudev, for sharing your experience at LIKAT with me and thus for motivating me to apply here.

I would like to thank my friends for making my life happier. Special thanks go to Sonja, Clara and Karolin. Thank you, Sonja, for our friendship from the early days of our undergraduation and all the wonderful time we have spent together since then. It was much easier mastering all the challenges on the way together with you. Thank you, Clara and Karolin, for being faithful friends since our childhood and for always staying in touch and visiting me, no matter if I live in Heidelberg, Cambridge, Tarragona, or Rostock.

I would like to thank my family for all they have given to me. Above all, I would like to thank my mom. Thank you for your constant support, love and understanding! Thank you for always worrying about me, for driving all the way to Rostock to help me moving, and for sending me Dampfnudeln by mail when I could only walk on crutches. And for all the other things that I cannot list here if I still want to make space for my thesis.

Lastly and most importantly, I would like to thank my boyfriend. I do not know how I can express my gratitude for all you have done for me in the past five years, for all your support, love and encouragement. Thank you for standing by my side in the most difficult moments of my life, for comforting me in a way no one else is capable of, for building my confidence, and for making me happy. And, yes, thank you for teaching me so much about chemistry and research. Thank you for being the balance I needed during my PhD and for always being there for me despite 4000 km distance and more than a year of covid-caused travel bans. Without you, I could not have conducted a single experiment or written a single word for this thesis.

Abstract

This thesis entails the development of practical and cost-efficient hydrogen isotope exchange methodologies for the deuteration of aromatic and heteroaromatic substrates. At the outset, the first C–H activation and deuteration of aromatic substrates using a catalyst based on earth-abundant manganese was reported. Transient directing groups allowed for the unprecedented use of weakly coordinating aldehyde directing groups in manganese-catalyzed C–H activation and enabled high *ortho* selectivity. Secondly, the transient directing group strategy was transferred to an application-oriented ruthenium-catalyzed hydrogen isotope exchange reaction on aromatic aldehydes and ketones. For the latter substrates, three different labeling patterns, namely combined *ortho* and α -deuteration, *ortho*-deuteration, and α -deuteration, were accessible by judicious choice of reaction conditions. Both methodologies employ abundant and cost-efficient heavy water as isotope source. Lastly, the electronic characteristics of pyridine derivatives were harnessed for a transition metal-free, base-mediated deuteration protocol. Selectivity for the aromatic sites remote from the nitrogen atom was obtained and complements pre-existing strategies for the hydrogen isotope exchange on heteroarenes. All projects are accompanied by mechanistic investigations and are expected to inspire future developments in the realms of sustainable hydrogen isotope exchange.

Kurzzusammenfassung

Diese Dissertation befasst sich mit der Entwicklung praktischer und kostengünstiger Wasserstoffisotopenaustauschmethoden zur Deuterierung aromatischer und heteroaromatischer Substrate. Zunächst wurde über die erste C–H-Aktivierung und Deuterierung aromatischer Verbindungen mittels eines mangankatalysierten Katalysators berichtet. Transiente dirigierende Gruppen ermöglichten hierbei erstmals die Verwendung schwach koordinierender aldehydbasierter dirigierender Gruppen für die mangankatalysierte C–H-Aktivierung und erbrachten hohe *ortho*-Selektivität. Weiterhin wurde die Strategie der transienten dirigierenden Gruppen auf eine anwendungsbezogene rutheniumkatalysierte Wasserstoffisotopenaustauschreaktion an aromatischen Aldehyden und Ketonen übertragen. Durch gezielte Auswahl der Reaktionsbedingungen und -abfolge wurden für letztere Substrate drei verschiedene Markierungsmuster zugänglich: kombinierte *ortho*- und α -Deuterierung, *ortho*-Deuterierung und α -Deuterierung. Sowohl die mangankatalysierte als auch die rutheniumkatalysierte Methodik verwendeten vielfach vorkommendes und günstiges schweres Wasser als Isotopenquelle. Zuletzt wurde ein übergangsmetallfreies, basenvermitteltes Deuterierungsprotokoll entwickelt, das sich die elektronischen Eigenschaften von Pyridinderivaten zunutze macht. Die Reaktion zeigte sich selektiv für die aromatischen Positionen, die entfernt vom Stickstoffatom stehen, und eröffnete somit eine komplementäre Selektivität zu literaturbekannten Strategien für den Wasserstoffisotopenaustausch von Heteroaromaten. Alle Projekte wurden von mechanistischen Studien begleitet und sind Inspiration für zukünftige Entwicklungen auf dem Gebiet des nachhaltigen Wasserstoffisotopenaustauschs.

List of Abbreviations

°	Degree
Δ	Difference
σ -CAM	σ -Complex-Assisted Metathesis
Ac	Acyl
Ad	Adamantyl
ADME	Absorption, Distribution, Metabolism, Excretion
Ar	Aryl
BArF ⁻	Tetrakis-(3,5-bis(trifluoromethyl)phenyl)-borate
BIES	Base-assisted Internal Electrophilic-type Substitution
Bn	Benzyl
Boc	<i>tert</i> -Butyloxycarbonyl
Bu	Butyl
Bz	Benzoyl
C	Celsius
cat.	catalytic
<i>cf.</i>	confer
CMD	Concerted Metalation Deprotonation
cod	cyclooctadiene
Cp [*]	Pentamethylcyclopentadienyl
Cy	Cyclohexyl
cym	cymene
D	Deuterium
DCE	1,2-Dichloroethane
DCM	Dichloromethane
DFT	Density Functional Theory
DG	Directing Group
DiPP	2,6-Diisopropylphenyl
DME	1,2-Dimethoxyethane
DMSO	Dimethylsulfoxide
eq.	equivalent
Et	Ethyl
FDA	Federal Drug Agency
FG	Functional Group
G	Gibbs free energy
GC	Gas Chromatography

Gly	Glycine
h	hour
HIE	Hydrogen Isotope Exchange
<i>i</i>	<i>iso</i>
J	Joule
JohnPhos	(2-Biphenyl)-di- <i>tert</i> -butylphosphine
k	kilo
KIE	Kinetic Isotope Effect
LC	Liquid Chromatography
m	milli
<i>m</i>	<i>meta</i>
Me	Methyl
Mes	Mesityl
MS	Mass Spectrometry
<i>n</i>	<i>normal</i>
NHC	<i>N</i> -Heterocyclic Carbene
NMR	Nuclear Magnetic Resonance
Np	Nanoparticle
NWAs	Nanowire Arrays
<i>o</i>	<i>ortho</i>
Oct	Octyl
OLED	Organic Light-Emitting Diode
<i>p</i>	<i>para</i>
Ph	Phenyl
Pr	Propyl
PVP	Polyvinylpyrrolidone
R	organic rest
RDS	Rate-Determining Step
rt	room temperature
SET	Single Electron Transfer
SILS	Stable Isotope Labeled internal Standard
SMD	Solvation Model based on Density
Solv	Solvent
SPhos	Dicyclohexyl(2',6'-dimethoxy[1,1'-biphenyl]-2-yl)phosphine
<i>T</i>	<i>tert</i>
Tf	Triflate
TFA	Trifluoroacetic Acid

THF

Tetrahydrofuran

TM

Transition Metal

U

atomic mass unit

Table of Contents

1 Significance of Deuterated Compounds.....	1
2 Methodologies for the Preparation of Deuterated Organic Compounds	2
3 HIE of Aromatic Substrates	4
3.1 Directed Aromatic HIE.....	4
3.1.1 Iridium-Catalyzed Directed Aromatic HIE.....	4
3.1.2 Alternative Transition Metals and Deuterium Sources	8
3.1.3 A Focus on Carbonyl Directing Groups.....	10
3.2 Selectivity in Non-directed Approaches for HIE of Aromatic Substrates	12
4 Deuteration of Heteroaromatic Substrates.....	14
5 Transition Metal-Catalyzed C(sp ²)–H Activation	16
5.1 Ruthenium-Catalyzed C(sp ²)–H Activation	16
5.2 Manganese-Catalyzed C(sp ²)–H Activation.....	18
5.3 Transient Directing Groups in Transition Metal-Catalyzed C(sp ²)–H Activation	20
6 Objectives of this Work.....	21
7 Summary of Published Results.....	21
7.1 Manganese-Catalyzed Selective C–H Activation and Deuteration by Means of a Catalytic Transient Directing Group Strategy.....	21
7.2 Ruthenium-Catalyzed Deuteration of Aromatic Carbonyl Compounds with a Catalytic Transient Directing Group.....	28
7.3 Base-Mediated Remote Deuteration of <i>N</i> -Heteroarenes – Scope and Mechanism	34
8 Outlook.....	40
9 Publications.....	43
9.1 Manganese-Catalyzed Selective C–H Activation and Deuteration by Means of a Catalytic Transient Directing Group Strategy.....	43
9.2 Ruthenium-Catalyzed Deuteration of Aromatic Carbonyl Compounds with a Catalytic Transient Directing Group.....	49
9.3 Base-Mediated Remote Deuteration of <i>N</i> -Heteroarenes – Broad Scope and Mechanism	57
10 Appendix	69
10.1 Additional publication	69

10.2 Curriculum Vitae	156
11 References	159

1 Significance of Deuterated Compounds

The smallest and simplest element, hydrogen, possesses the most remarkable isotope chemistry: While the most abundant and familiar hydrogen isotope is protium and contains one proton and one electron, the heavier isotopes deuterium and tritium additionally comprise one or two neutrons. The fact that protium has a small atomic mass of only 1.008 u dictates that this change in nuclear composition leads to a doubled or tripled atomic mass, respectively, and consequently goes along with significantly altered quantum chemical properties. In this sense, C–D bonds exhibit lower vibrational frequencies compared to C–H bonds, giving rise to lower zero-point energies and consequently higher activation barriers for the respective bond breaking step. This important phenomenon is known as the primary kinetic isotope effect (KIE).¹

Besides the implied changed reactivity, a hydrogen isotope in an organic molecule can – like isotopes of other elements – simply function as a label: Protium, deuterium and tritium are all NMR-active nuclei that are brought in resonance under distinct conditions, leading to specific coupling patterns in interaction with other nuclei such as ^{13}C .² Moreover, the changed molecular mass can be detected in mass spectrometric analyses.³ Tritium further opens up the possibilities of radioactive imaging.⁴

At the same time, bearing isotopes of the same element, protium and deuterium-containing molecules have identical physical properties, structure, and biological function.^{3a} Unlike tritium, deuterium is not radioactive, allowing chemists and scientists of other disciplines to safely probe the differences brought upon by the replacement of protium by deuterium without the need for laborious precautions.

One such application that most organic chemists are familiar with is the use of deuterated compounds for the elucidation of reaction mechanisms. On the one hand, deuterium can function as a label in scrambling experiments with detection by NMR and MS to understand which parts of a molecule participate in a specific reaction.⁵ On the other hand, the KIE is the basis for analyses of the C–H cleavage step as the turnover-limiting or rate-determining step (RDS) of specific reactions. In these frequently performed experiments, initial rates of the unmodified substrate of a reaction and its deuterated counterpart are compared.⁶ For both types of mechanistic experiments, deuterium-labeled organic molecules are needed in which the deuterium atom is precisely installed in a specific position imposed by the studied reaction. Conversely, solvents for NMR spectroscopy, the other popular organic chemistry laboratory application of deuterated compounds, require complete deuteration.⁷

Hydrogen isotopes are further used as labels at various stages of the drug discovery process. The radioactive tritium plays a bigger role here, for instance in the context of binding site characterization or metabolism studies.⁸ However, deuterium gains increasing importance for the preparation of stable isotope labeled internal standards (SILS) for LC-MS/MS applications.^{3a} If a sufficient number of deuterium atoms is incorporated into the reference molecule,

quantitative analysis for various applications such as pharmacokinetic studies of drug molecules in early development or environmental contamination tests becomes possible.^{3a,9} For this application, the deuteration site matters less than the efficiency of the deuteration reaction. Typically, an incorporation of at least four deuterium atoms and the absence of residual non-labeled material are required to preclude overlap of internal standard and sample.^{3a}

With the US Federal Drug Agency's (FDA) approval of the first deuterated drug, deutetrabenazine, in 2017,¹⁰ the replacement of protium by deuterium in metabolically labile sites of existing drugs has gained increasing attention. Medicinal chemists make use of this strategy to improve absorption, distribution, metabolism, and excretion (ADME) properties thanks to the increased drug stability induced by the KIE. This way, lower and less frequent doses compared to the non-deuterated congeners provide undoubted benefits for patients. A second deuterated drug was recently approved for the Chinese market¹¹ and further candidates are currently in clinic trials, indicating further continuation of this trend.¹² In a similar fashion, KIE-driven increased stability and improved properties of deuterated organic light-emitting diodes (OLEDs) and polymers have lately been explored in the field of material science.¹³ Accordingly, a demand for techniques for the preparation of various compounds that are deuterated in specific positions is growing alongside these developments.

As can be seen from the paragraphs above, the variety of applications of deuterated compounds is mirrored by the requirement for manifold deuteration procedures that match the distinct needs of each type of use. For this reason, several chemists around the globe are working towards expanding the toolbox of deuteration methodologies. This thesis takes part in this endeavor. On the following pages, the state of the art of deuteration techniques will be summarized to situate the work of this thesis within its broader context.

2 Methodologies for the Preparation of Deuterated Organic Compounds

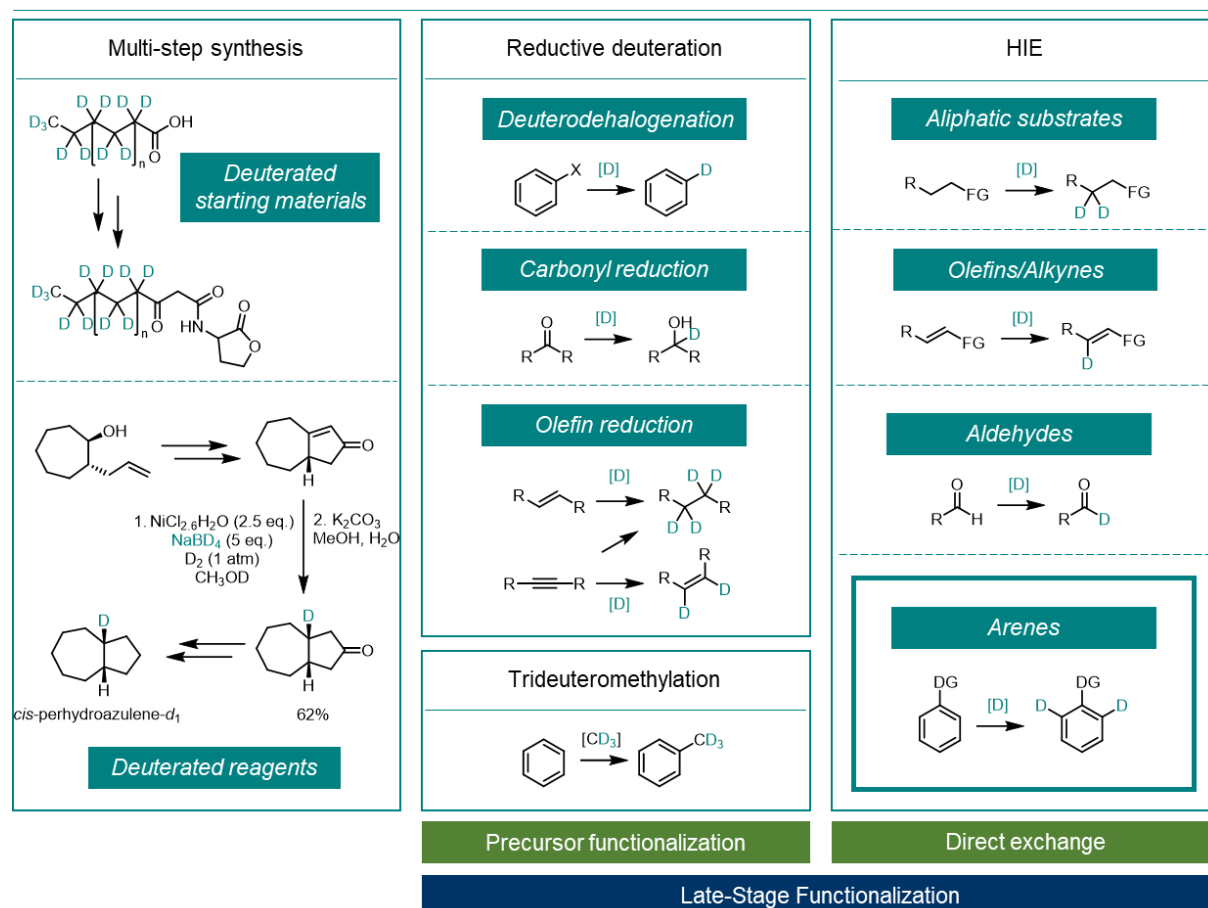
When reading reports from industry on the synthesis of deuterated compounds for some of the applications cited in Chapter 1, it appears striking that the *de novo* preparation of these targets in multi-step synthetic sequences often represents the method of choice.¹⁴ For this purpose, commercially available deuterated building blocks^{14a,d} such as deuterated fatty acids¹⁵ or deuterated reagents,^{14b,c} like sodium borodeuteride,¹⁶ are employed as isotope sources (Scheme 1, left). This way, the regiospecific installation of the label with high isotopic purity (>99% deuterium incorporation in the desired position) can be ensured. Depending on the application, these requirements are crucial, justifying the higher cost associated with the often lengthy syntheses.^{17,18}

However, this approach is neither in line with green chemistry principles nor with the rushed timelines inherent to the pharmaceutical industry. Moreover, for some applications such as the use as SILS, regioselectivity is secondary (*cf.* Chapter 1) and a rapid and cost-efficient

technology appears more attractive. Consequently, the development of late-stage labeling methodologies that employ abundant deuterium sources can be considered the main goal of the field of hydrogen isotope chemistry of our time.

Approaches such as reductive deuteration,¹⁹ deuterodehalogenation²⁰ or trideuteromethylation²¹ present an important advance compared to multi-step procedures (Scheme 1, center). Here, the label is installed on a precursor to the target molecule in the final step of the synthetic sequence. However, true late-stage deuteration is achieved with hydrogen isotope exchange (HIE) where protium atoms on the target molecule itself are directly replaced by deuterium atoms (Scheme 1, right).²² Therefore, HIE is often a C–H activation reaction and can serve as a basic study for this broader field in parallel to delivering labeled molecules.^{Error! Bookmark not defined.c} High deuterium incorporations usually rely on an excess of the deuterium source which can drive the equilibrium to the deuterated compound. In some cases, the KIE and slowed-down reverse protonation reactions contribute to an efficient build-up of high deuteration degrees.

Methodologies for the Preparation of Deuterated Compounds



Scheme 1 Overview of methodologies for the preparation of deuterated compounds. DG = Directing Group.

Given the variety of potential HIE substrates and the number of protons in each of them, two fundamental challenges of HIE are (i) finding methodologies for the activation of a plethora of

organic molecules and (ii) achieving selective deuterium incorporation in one or more specific positions thereof. Only if global labeling of the entire molecule is desired, selectivity becomes less relevant.²³ Moreover, almost quantitative deuterium incorporation is desirable to meet the demands of many applications and to render HIE competitive with alternative methods.

Early deuteration methods were considered model experiments for tritiation and this remains one of the functions of HIE experiments with deuterium. Due to tritium gas being the safest source of this radioactive isotope, deuteration reactions were often conducted under an atmosphere of deuterium gas to guarantee transferable reaction conditions. However, as the understanding of the importance of deuterated compounds for their own specific applications grew, this development went along with a surge for using safer and easier-to-handle liquid isotope sources. Among them, especially heavy water is of significance as it is the cheapest and most abundant deuterium source from which all other deuterated reagents are made.

To address the issues mentioned above, several approaches have been presented in recent years. Different types of aliphatic substrates have undergone isotopic exchange with various deuteration patterns depending on the applied methodology.²⁴ Acid/base catalysis,²⁵ biocatalysis,²⁶ hydrogen autotransfer,²⁷ catalysis with transition metal nanoparticles,²⁸ and homogeneous transition metal-catalyzed directed C(sp³)–H²⁹ activation have all advanced this field while recently photoredox catalysis seems to open up new avenues.³⁰ Further HIE reactions have been presented for olefinic substrates,³¹ alkynes³² and aldehydes.³³ However, a focus of HIE research remains on aromatic substrates which are desirable substrates for deuteration reactions due to their ubiquity in pharmaceuticals and organic materials. As this substrate class builds the essence of this thesis, underlying strategies for C–H activation and selectivity control in the realm of aromatic HIE will be discussed in the following two chapters.

3 HIE of Aromatic Substrates

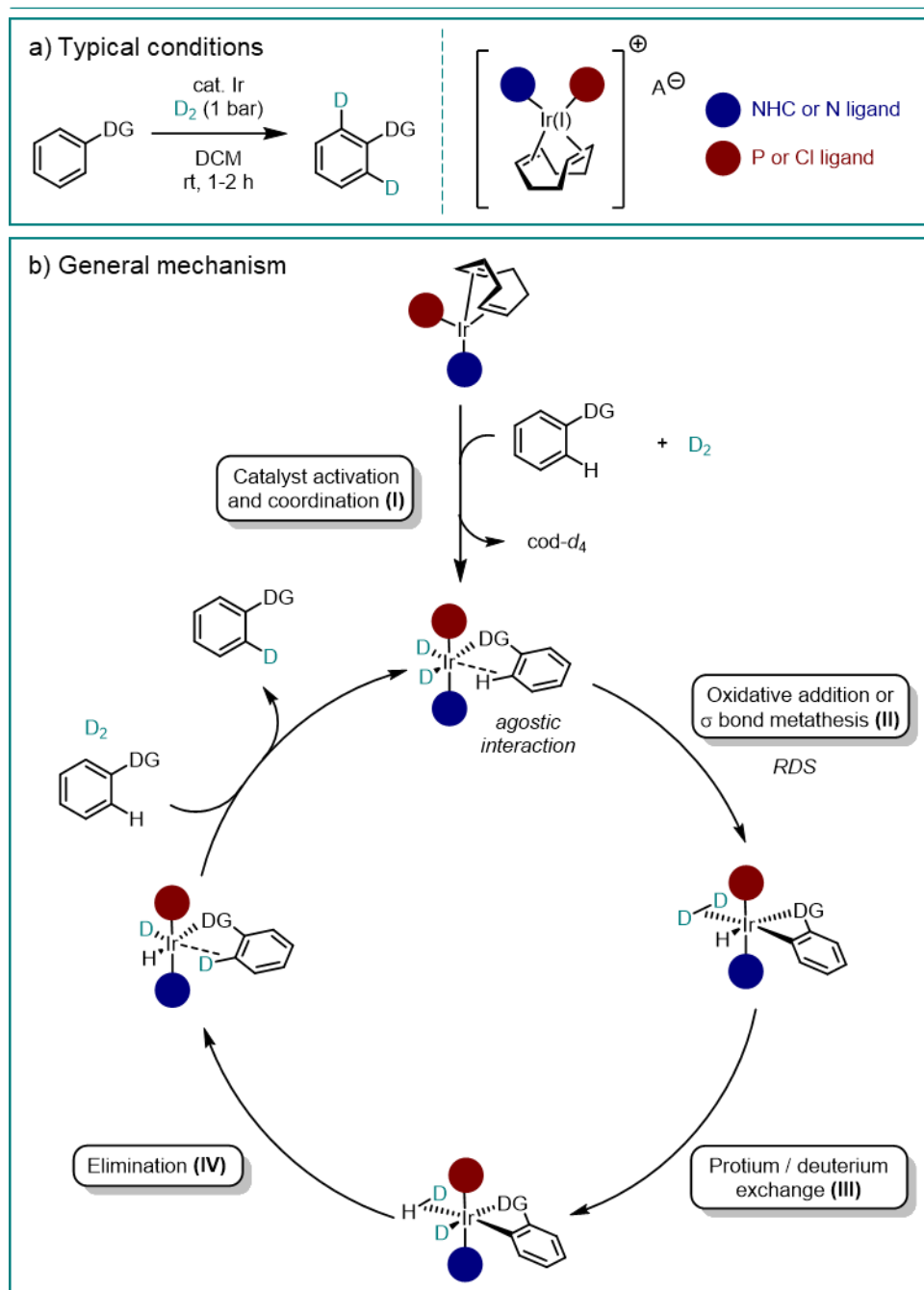
3.1 Directed Aromatic HIE

3.1.1 Iridium-Catalyzed Directed Aromatic HIE

Decades of intense research have rendered iridium-catalyzed C–H activation the standard method for HIE of aromatic substrates.³⁴ Currently, iridium-catalyzed HIE reactions are typically carried out under ambient conditions (room temperature, 1 bar deuterium gas atmosphere) without any additives and are finished after short reaction times (often 1–2 h; Scheme 2a). For this mild protocol, it is necessary that the starting materials exhibit Lewis basic groups (so-called directing groups) which can coordinate to the metal center of the catalyst and bring it in proximity to the *ortho* C–H bonds for establishment of an agostic interaction (Scheme 2b; I). Following this step, cationic iridium complexes will undergo oxidative addition or σ bond metathesis with the activated C–H bond (RDS of the reaction), furnishing a 5-membered

cyclometalated dideuterium hydride complex in the presence of deuterium gas (II). Thanks to hydride fluxionality, protium and deuterium atoms can exchange (III) prior to the elimination/bond-forming step (IV) which will deliver the selectively *ortho*-deuterated product.³⁵ As products and starting materials are virtually indistinguishable, these elementary steps will be repeated on *ortho*-unsubstituted substrates, affording dideuterated compounds with deuterium incorporation in both *ortho* positions.

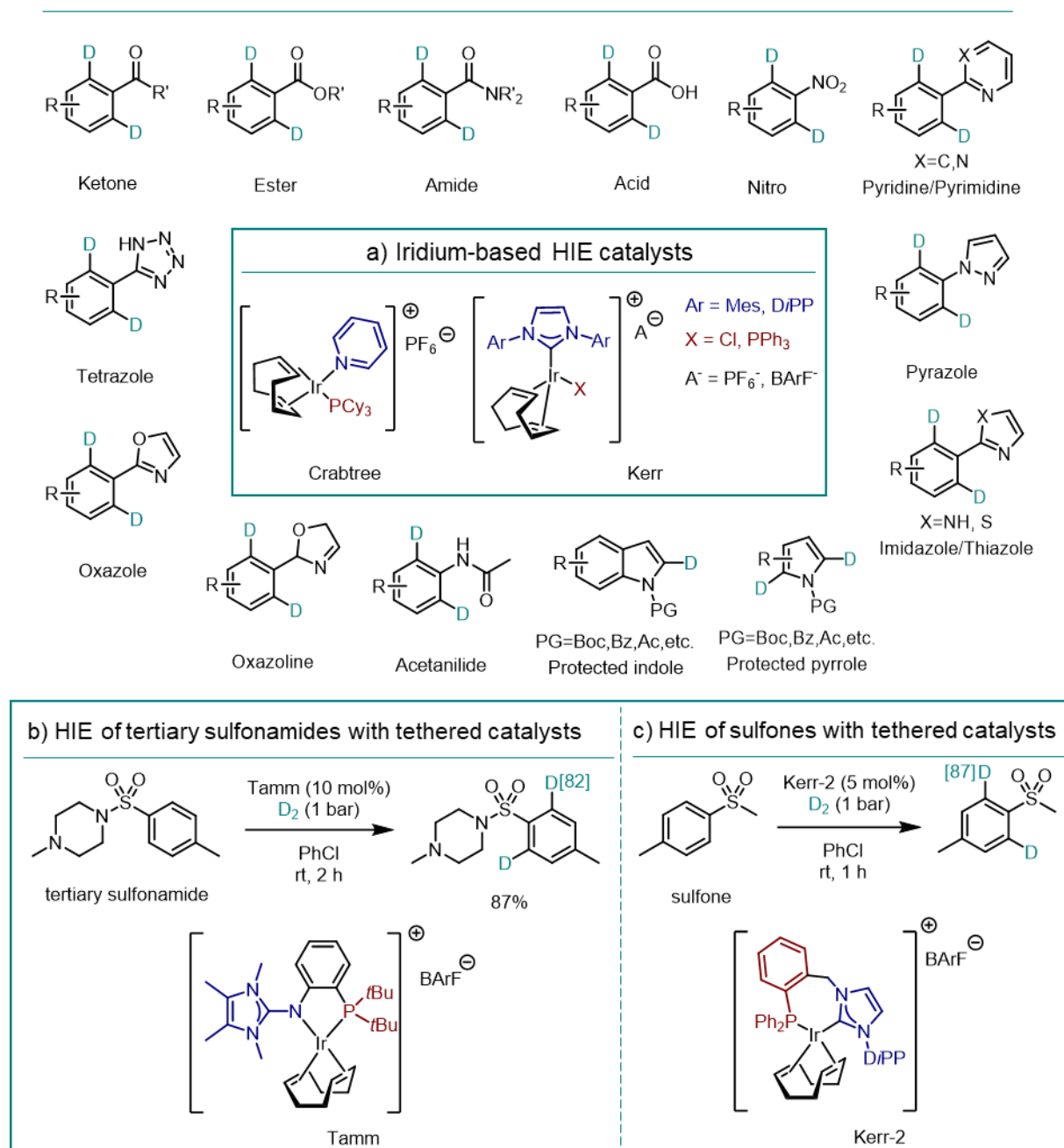
Iridium-Catalyzed Directed Aromatic HIE



Scheme 2 Features of iridium-catalyzed *ortho*-directed aromatic HIE. a) Typical reaction conditions and catalyst structure. b) General mechanism. DCM = dichloromethane; cod = cyclooctadiene.

To stay in line with its late-stage nature, a vital aspect of the field is the use of native directing groups rather than complex scaffolds. The obtained deuterated compounds can then directly be employed as starting materials for mechanistic experiments, especially in the context of KIE measurements. Furthermore, if at least two directing groups are present in a more complex molecule, four or more deuterium atoms can be incorporated, allowing the application as SILS (see Chapter 1). Of course, these are only two of many possible examples for the application of *ortho*-deuterated arenes.

Directing Groups in Iridium-Catalyzed Aromatic HIE

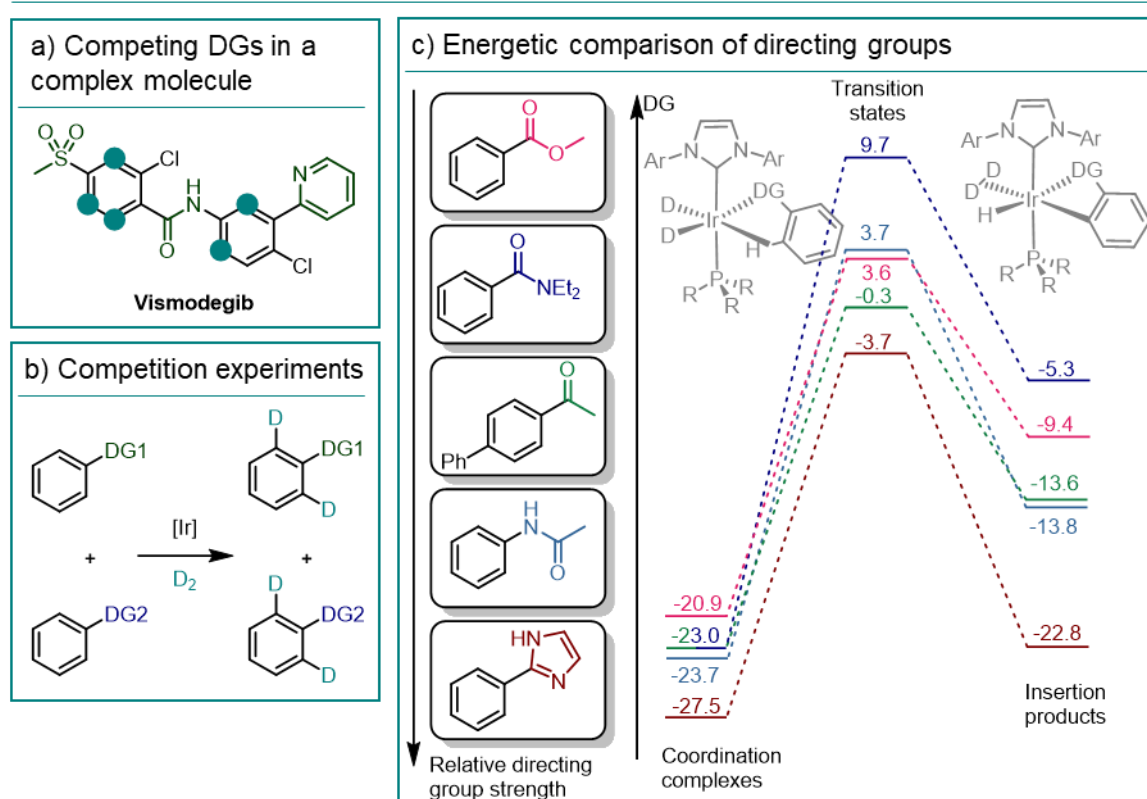


Scheme 3 Scope of iridium-catalyzed HIE: catalysts and directing groups. a) The originally used Crabtree catalyst and the more versatile Kerr catalyst for HIE. b) Tethered ligand enabled HIE of sterically demanding tertiary sulfonamides. c) Tethered ligand enabled HIE of sterically demanding sulfones. Mes = Mesityl; DiPP = 2,6-Diisopropylphenyl; BArF⁻ = tetrakis-(3,5-bis(trifluoromethyl)phenyl)-borate; Boc = *tert*-butoxycarbonyl; Bz = Benzoyl; Ac = Acyl.

Building on the first breakthrough in the field achieved with the Crabtree hydrogenation catalyst,³⁶ the Kerr group has successively improved related cationic iridium complexes until arriving at the current *N*-heterocyclic carbene (NHC)- and phosphine-ligated workhorses of HIE (Scheme 3a).^{35a,37} Compared to their historic congeners, these efficient catalysts enable higher deuterium incorporations (typically >90%) for a broader scope of substrates.

Besides the more traditional *N*-heteroarene^{35a,37,38} and ketone^{35a,37,38b,c,f,h,i-l,39} directing groups, a plethora of coordinating groups such as esters,^{35b,38h,k,l,39,40} amides,^{35a,b,37,38c,d,f,i,j,l,39,40} carboxylic acids^{38a,i,41} and nitro groups^{35a,37,38c,h,k,39} can render deuterated compounds under unchanged conditions (Scheme 3). For especially challenging, sterically hindered substrates, further catalyst tuning is possible. For instance, it has been shown that tethered phosphine-NHC ligands provide more room at the iridium center and can consequently more easily accommodate sterically hindered tertiary sulfonamide or sulfone directing groups (Scheme 3b and c).^{38h,42}

Competing Directing Groups and Selectivity in Iridium-Catalyzed Aromatic HIE



Scheme 4 Competing directing groups in iridium-catalyzed aromatic HIE. a) Example of how various directing groups can lead to unselective deuteration in complex pharmaceuticals. b) Design of competition experiments. c) DFT calculations on the C–H insertion step comparing five different directing groups.

While the broad applicability of this methodology is of course highly useful, it can pose problems if selective deuteration at a single site in a complex substrate with various coordinating groups is desired (Scheme 4a). However, as iridium-catalyzed HIE is an established and well-understood field, tools are available to predict the main deuteration site for competing directing

groups. In this sense, intermolecular competition experiments along with density functional theory (DFT) studies have established that directing group strengths correlate well with the relative free energy of the iridium-substrate coordination complex (Scheme 4b and c).⁴³ It was demonstrated that the activation barrier for the C–H insertion step governs selectivity only if the two directing groups form similarly stable complexes with the catalyst. DFT analysis of the binding energies of directing groups competing intramolecularly within one molecule can provide accurate predictions of selectivity and go beyond the more rudimentary guidelines discussed previously.⁴⁴ Nevertheless, complete selectivity will probably not be achieved and more specific methodologies, potentially relying on alternative catalysts and mechanisms, would be valuable.

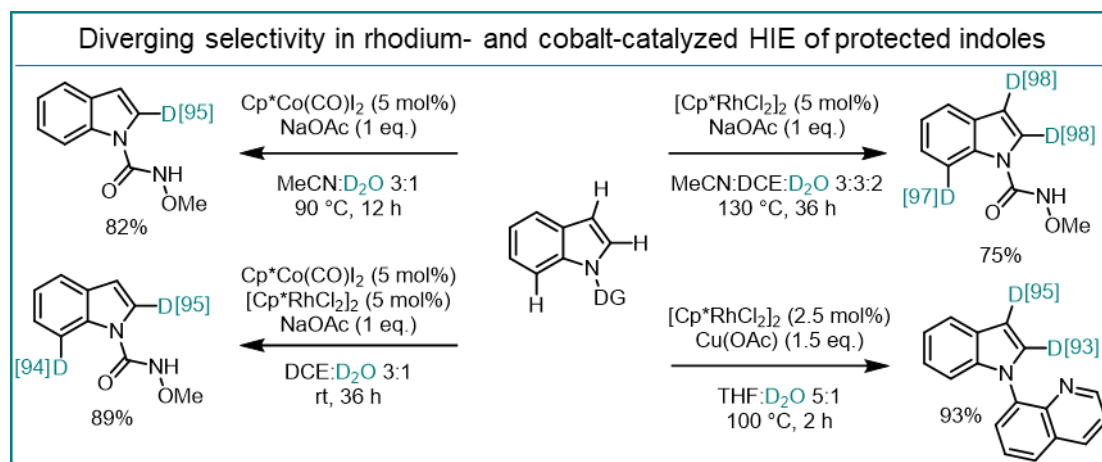
3.1.2 Alternative Transition Metals and Deuterium Sources

Aside from the above-mentioned goal of finding complementary deuteration selectivity, more benefits can be drawn from the use of alternative transition metals. Being the scarcest noble metal, iridium is a very expensive catalyst component whose replacement by more cost-efficient transition metals is highly desirable.⁴⁵ Consequently, recent HIE methodologies build upon the rich precedence of C–H functionalization chemistry with other metals such as rhodium,⁴⁶ palladium,⁴⁷ and ruthenium.⁴⁸ The fact that the C–H bond cleavage step with these catalysts usually differs mechanistically from iridium-catalyzed C–H activation (*vide infra*) has implications for the corresponding HIE reaction conditions.⁴⁹ On the one hand, base additives are frequently needed, potentially limiting the substrate scope to more robust examples. On the other hand, the metallacyclic intermediates resulting from C–H activation with rhodium, palladium, and ruthenium are easily hydrolyzed by protic deuterium sources, allowing for a replacement of deuterium gas by easier-to-handle liquid deuterium sources such as deuterated methanol, water, or acetic acid. Especially the use of heavy water is particularly desirable in the context of deuteration as it represents the most available and cost-effective isotope source (*cf.* Chapter 2).

Although rhodium catalysts have been used from the early days of HIE,⁵⁰ they were outcompeted for the use as general HIE catalysts by the above-described iridium complexes in the last two decades. However, more recent research using pentamethylcyclopentadienyl (Cp*) rhodium complexes has not only shown that they can enable the *ortho*-deuteration of benzoic acids with D₂O instead of D₂ (Scheme 8d),⁵¹ but has also revealed how combinations of rhodium and cobalt catalysts or their individual use can afford diverging selectivities in the deuteration of indoles equipped with directing groups (Scheme 5).⁵²

New selectivity aspects are also brought upon by a palladium-catalyzed methodology that preferentially undergoes deuteration *via* less stable and therefore more reactive 6-membered metallacycles,⁵³ thus affording among others *ortho*-deuterated phenylacetic acids. Conversely,

iridium-catalyzed HIE usually proceeds *via* 5-membered intermediates given that substrate coordination or C–H activation determine selectivity rather than C–D bond formation (Figure 1; Scheme 8c).^{35a}



Scheme 5 Reaction condition-dependent diverging selectivity in the deuteration of protected indoles by Cp* complexes of rhodium and cobalt. DCE = 1,2-dichloroethane; THF = tetrahydrofuran.

Recent ruthenium-catalyzed HIE methodologies have shown to be broadly applicable to a range of directing groups in the presence of heavy water.⁵⁴ After a dihydridosilyl ruthenium complex^{54b} or $[\text{RuCl}_2(\text{PPh}_3)_3]$ ^{54c} were reported to afford good deuterium incorporation in the *ortho* positions of native *N*-heterocyclic and carbonyl directing groups, the *ortho*-deuteration of carboxylic acids, sulfonamides and *N*-heterocycles with a *p*-cymene ruthenium carboxylate catalyst was achieved more recently (Scheme 6 and Scheme 8e).^{54d} Concluding from these versatile results, ruthenium catalysts can be considered cost-efficient substitutes to iridium.

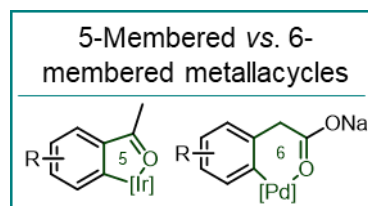
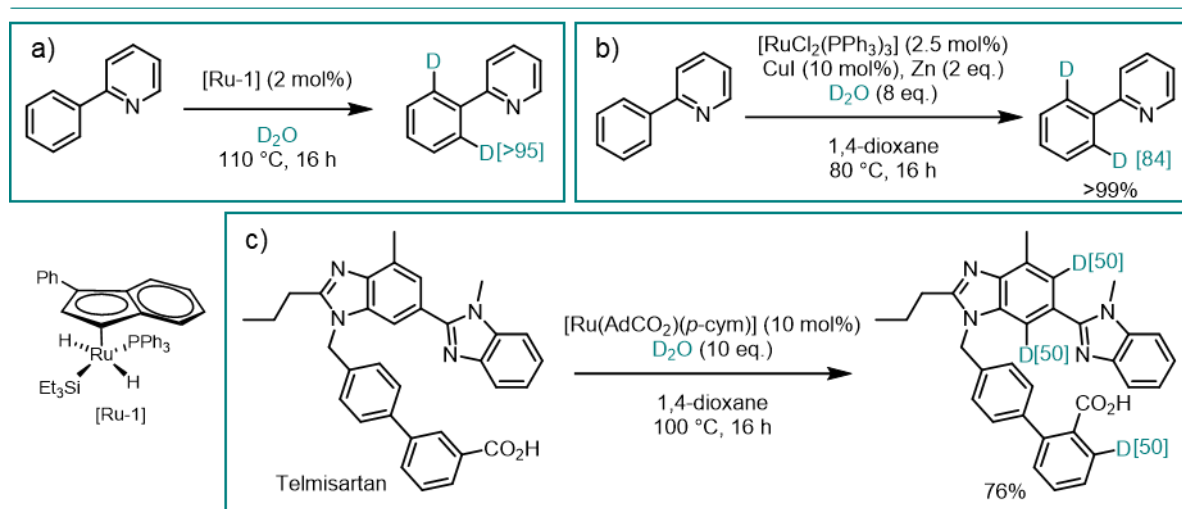


Figure 1 Different preferred ring sizes in metallacyclic intermediates in Ir- and Pd-catalyzed HIE.

Ruthenium-Catalyzed Directed Aromatic HIE

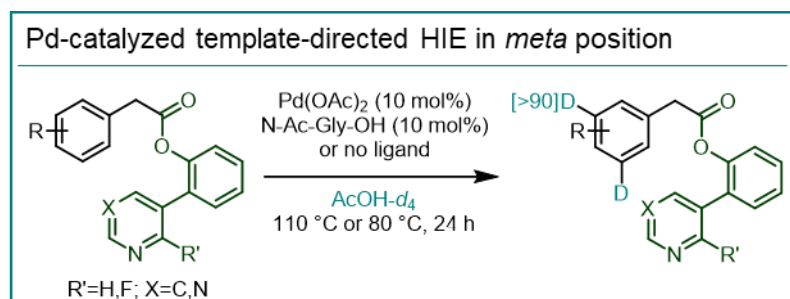


Scheme 6 Ruthenium-catalyzed *ortho*-directed HIE. a) Dihydridosilyl ruthenium-catalyzed *ortho*-directed HIE of heteroarenes. b) *In situ* ruthenium hydride-catalyzed *ortho*-directed HIE of heteroarenes

with superstoichiometric zinc and small excess of heavy water. c) Ruthenium carboxylate-catalyzed *ortho*-directed HIE of pharmaceuticals. Ad = Adamantyl; cym = cymene.

Drawing further inspiration from the field of C–H functionalization, template directing groups for palladium catalysts as well as ruthenium-initiated electrophilic aromatic substitution have recently enabled *meta*-deuteration, going beyond what has been known for iridium-catalyzed HIE (Scheme 7).⁵⁵

In this context, it should be noted that tremendous progress has been made with nanocatalysts.^{28,56} Compared to conventional heterogeneous catalysts such as Pd/C or Pt/C, supported metal nanoparticles



Scheme 7 Template-directed remote HIE with palladium catalysts. Gly = glycine.

are more selective and facilitate labeling under milder conditions (Figure 2).^{Error! Bookmark not defined.} Usually, exchange takes place in all positions in the proximity of coordinating heteroatoms. This type of selectivity differs from and complements homogeneous *ortho*-directed HIE. Despite the narrated valuable advances in terms of complementing iridium-catalyzed HIE, some shortcomings persist. To date, all alternative homogeneous methodologies require relatively high temperatures (usually around 100 °C) and long reaction times. Moreover, progress to abundant and non-toxic 3d metal catalysts remains to be seen and access to more directing groups would be desirable.

Comparison of Heterogeneous, Homogeneous and Nanocatalysts for HIE

Heterogeneous Catalysts	Nanoparticles	Homogeneous Catalysts
<i>Global Deuteration</i>	<i>α-Heteroatom Deuteration</i>	<i>ortho Deuteration</i>

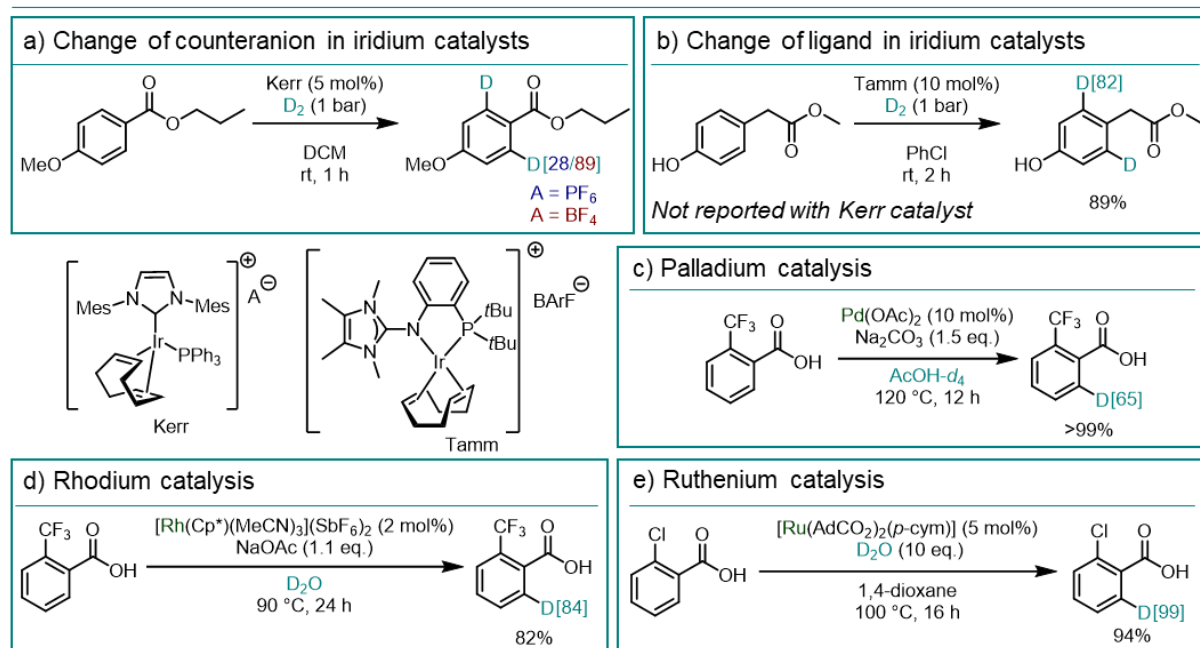
Figure 2 Schematic and simplified comparison of the selectivity of heterogeneous, homogeneous and nanocatalytic HIE methodologies.

3.1.3 A Focus on Carbonyl Directing Groups

Carbonyl groups are useful handles for the installation of chelating⁵⁷ or template directing groups.^{55b-d} While the latter find application for the emerging field of *meta*-directed HIE (*cf.* Chapter 3.1.2), the use of the former has been largely abandoned in favor of native directing groups. However, due to their prevalence in bioactive compounds and pharmaceuticals,

unmodified carbonyl groups such as amides, esters, carboxylic acids and ketones remain important in the field and are routinely tested directing groups for general *ortho*-directed HIE methodologies, albeit with mixed success.^{35a,37,38a-d,f,h,i-l,39,41} As a result of their weaker coordinating abilities compared to *N*-heterocycles, the activation of carbonyl groups can be challenging.⁵⁸ This can be noted in the absence of carboxylic acids and esters in the scope of seminal iridium-catalyzed HIE methodologies despite their importance.^{35a,37,38c,h} Moreover, a broadly applicable ruthenium-catalyzed HIE reaction failed to deuterate acetophenone derivatives.^{54b} To close this gap, these challenges have recently been taken up by studies dedicated to specific carbonyl groups. In this context, it was found that iridium catalysts with a BARF[−] counteranion instead of PF₆[−] are more active for the deuteration of aromatic esters (Scheme 8a).⁴⁰ Further, the Tamm catalyst appeared to be advantageous compared to the Kerr catalyst for the deuteration of benzylic esters and amides *via* 6-membered metallacycles (Scheme 8b).^{35b} The challenging deuteration of carboxylic acids has been solved by the use of alternative transition metal catalysts (see chapter 3.1.2), but high temperatures were still required (Scheme 8c-e).^{51,53a,54d} Knowledge from previously reported carboxylate-directed C–H functionalization reactions with palladium,^{58,59} rhodium,⁶⁰ and ruthenium⁶¹ was instrumental for these achievements.

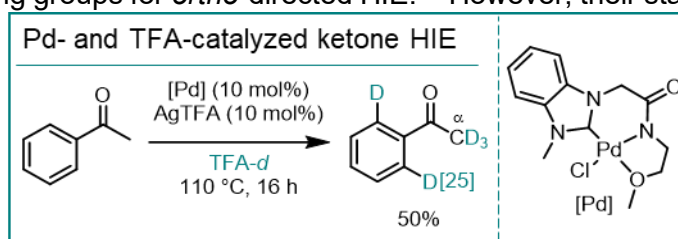
Strategies towards Access to Carbonyl Directing Groups



Scheme 8 HIE with weakly coordinating carbonyl directing groups. a) Change of the counterion of an iridium catalyst can enable ester-directed HIE. b) A tethered ligand shows good reactivity for benzylic ester-directed HIE *via* 6-membered metallacyclic intermediates. c)-e) Experience from carboxylic acid-directed C–H functionalization with palladium, rhodium, and ruthenium catalysts can be transferred to corresponding HIE reactions.

Conversely, attempts to use palladium catalysis for the *ortho*-deuteration of aromatic ketones were met with limited success.⁶² In spite of high temperatures and highly acidic reaction media (trifluoroacetic acid (TFA)-*d* as deuterium source and solvent), only low deuteration levels were

obtained. Interestingly, high deuteration efficiency was observed in the aliphatic α -carbonyl position instead, stemming from acid-catalyzed enolization (Scheme 9). Isotopic exchange at these metabolically labile sites in drug molecules can be valuable for their stabilization through the KIE¹² which is why corresponding deuteration reactions are studied in their own right.^{25b,63} As aldehydes are rarely present in pharmaceuticals because they are prone to oxidation, they have hardly been investigated as directing groups for *ortho*-directed HIE.³⁸ⁱ However, their status as versatile synthetic intermediates has recently sparked interest in formyl isotopic exchange³³ and it can be expected that this surge in aldehyde deuteration methodologies spills over to other areas of HIE.



Scheme 9 Palladium- and AgTFA-catalyzed HIE on acetophenone derivatives with concomitant α -carbonyl deuteration.

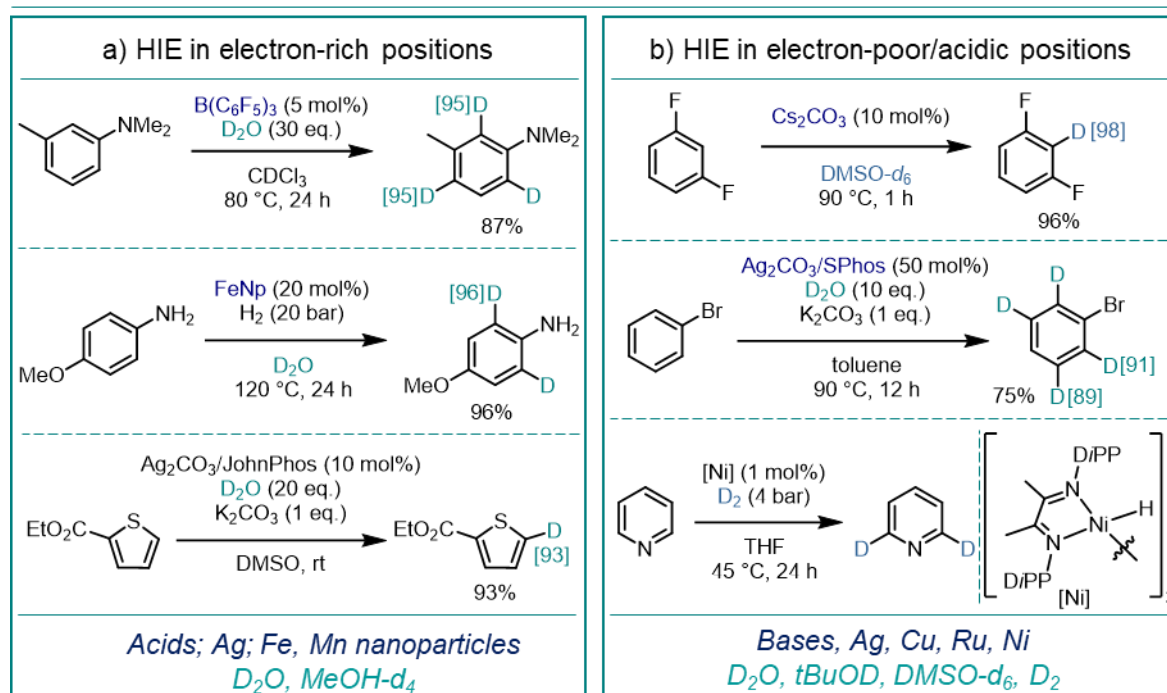
3.2 Selectivity in Non-directed Approaches for HIE of Aromatic Substrates

While directed labeling approaches afford precise selectivity and have provided many viable deuteration methodologies for applications, they are inherently limited. The existence of a directing group, albeit native functionality can be exploited, remains a necessary requirement, implying that substrates without coordinating moieties are not amenable to these procedures. Moreover, at the current state of art, directed HIE at remote sites cannot be considered a late-stage methodology as it requires expensive acidic deuterium sources and complex template directing groups (*cf.* Chapter 3.1.2).⁵⁵ Consequently, to supplement directed HIE, alternative, non-directed methodologies have been devised from the early days of the field and often give rise to complementary labeling patterns. Traditional approaches rely on acid and base catalysis and often use deuterium oxide as isotope source. To enable these reactions, harsh conditions as well as some activating functionality in the substrate are usually required. In this sense, anilines and similar electron-rich arenes can be deuterated in the most electron-rich positions (*ortho* and *para*) in the presence of Brønsted or Lewis acids and at elevated temperature *via* electrophilic aromatic substitution (Scheme 10a, top).⁶⁴ Due to the facile protonation of the amine functionality, primary amines require especially harsh conditions.^{64a,b} Conversely, slightly acidic protons, for example in the *ortho* positions of fluoro substituents, can be exchanged in a base-mediated fashion and at elevated temperature (Scheme 10b, top).⁶⁵

To enable non-directed HIE under milder conditions and with a broader selection of deuterium sources, transition metal-catalyzed methodologies have been developed in the past years. Seminal contributions have been made especially using earth-abundant 3d metal catalysts that often discriminate between different C–H bonds in the substrate based on electronic differences. A preferential exchange in *ortho* and *para* positions of electron-donating substituents reminiscent of acid-mediated HIE has been described with nanoparticles based on iron and

manganese for the labeling of anilines, phenols and electron-rich *N*-heteroarenes (Scheme 10a, center).⁶⁶ Interestingly, though, the mechanism of this exchange seems to be rather different from acid-catalyzed methodologies: Here, a radical pathway *via* D₂O splitting at the metal surface is proposed.

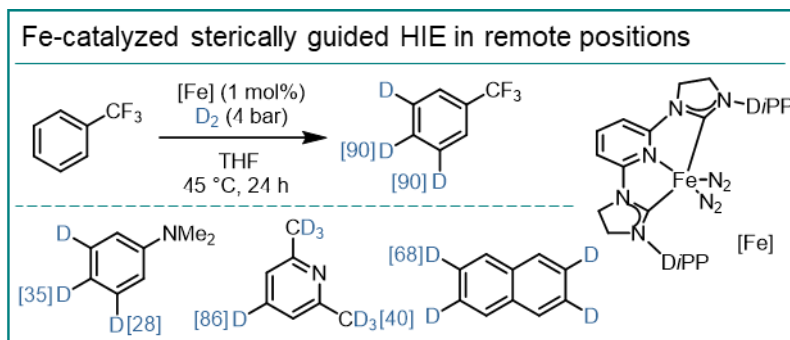
Electronically Controlled Selectivity in Non-Directed HIE



Scheme 10 Examples for electronically controlled non-directed HIE. a) Examples for Lewis-acid- and iron nanoparticle-catalyzed HIE in electron-rich positions of aniline derivatives. b) Examples of base-catalyzed HIE in acidic positions of polyfluoroarenes, silver-catalyzed HIE in acidic positions in haloarenes and nickel-catalyzed HIE in electron-deficient positions of azines. DMSO = dimethylsulfoxide; Np = nanoparticle; SPHos = dicyclohexyl(2',6'-dimethoxy[1,1'-biphenyl]-2-yl)phosphine; JohnPhos = (2-biphenyl)-di-*tert*-butylphosphine.

Further advances for the labeling of electron-rich heteroarenes have been made with homogeneous silver catalysis. A complex formed *in situ* from silver carbonate and bulky monodentate phosphine ligands was shown to undergo non-directed concerted metalation-deprotonation (CMD)-type C–H activation (*vide infra*) in the most acidic positions of thiophenes and other 5-membered heteroarenes, thus enabling selective labeling based on electronic control (Scheme 10a, bottom).⁶⁷ This system can additionally be applied to the labeling of haloarenes where the more acidic *ortho* (and *meta*) hydrogen atoms are preferentially exchanged (Scheme 10b, center).⁶⁸ On the contrary, the most electron-deficient positions in azines can be labeled with ruthenium carbonyl and a protic deuterium source⁶⁹ as well as more mildly with a diimine-ligated nickel complex under a deuterium gas atmosphere (Scheme 10b, bottom).⁷⁰ Although electronically controlled non-directed HIE broadens the toolbox of labeling strategies, specifically activated substrates are nonetheless required.

This is not the case for sterically guided HIE where any substituent can induce selective labeling. In this context, molecularly defined iron pincer complexes were reported to catalyze HIE in the most sterically accessible positions of non-activated aromatic substrates in the presence of deuterium gas or deuterated benzene (Scheme 11).⁷¹ Usually, several deuterium atoms are incorporated into each molecule, rendering this methodology useful for the preparation of LC/MS internal standards. However, this also means that precise selectivity cannot be achieved this way. Although a considerable number of substrates and types of selectivity has been covered in recent years through non-directed labeling approaches, further methodologies leading to diverging labeling patterns or precise installation of deuterium atoms stay in high demand.

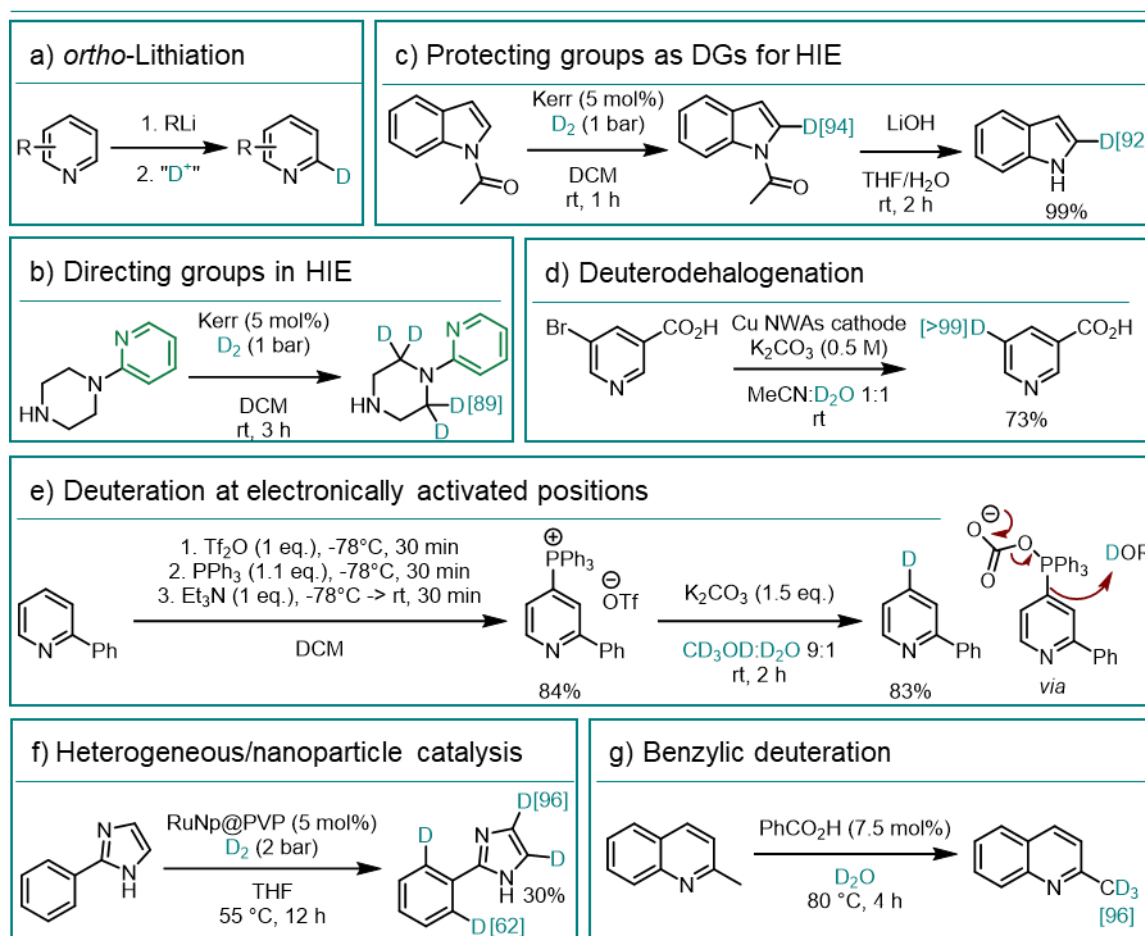


Scheme 11 Iron-catalyzed HIE in sterically accessible positions of unactivated arenes.

4 Deuteration of Heteroaromatic Substrates

Heteroaromatic compounds are a substrate class that receives special attention in the field of deuteration not only due to their importance as ubiquitous moieties in bioactive compounds or pharmaceuticals but also because of their distinct chemical characteristics that open up additional opportunities for functionalization reactions.⁷² Originally seen as prime substrates for *ortho*-lithiation followed by deuterolysis (Scheme 12a),⁷³ heteroarenes are now labeled under milder reaction conditions and with higher functional group tolerance. Firstly, heteroarenes are of prime importance for directed HIE: Nitrogen-containing heterocycles do not only serve as directing groups in aromatic^{35a,37,38} and aliphatic^{29a} isotope exchange, affording deuteration in the adjacent aromatic ring or aliphatic chain (*cf.* Chapter 3.1; Scheme 12b), but they can also be equipped with orthogonal directing groups themselves for deuteration on the heterocyclic core (Scheme 12c). In this context, common nitrogen protecting groups such as benzoyl or acetyl groups can direct HIE in position 2 of indole derivatives under iridium catalysis.⁷⁴ The fact that these groups can be removed easily and without affecting the deuterium incorporation in the aromatic ring is an additional advantageous aspect of this methodology. In a different study, further positions in the indole moiety could be accessed depending on the specific reaction conditions and catalysts used, leading to divergent labeling patterns (Chapter 3.1.2; Scheme 5).⁵² The intrinsic reactivity of the electronically activated, nucleophilic position 3 plays an important role here.

Deuteration of Heteroarenes



Scheme 12 Methodologies for the deuteration of heteroarenes. a) *via ortho*-Lithiation and subsequent deuterolysis. b) In adjacent moieties *via* directed HIE. c) By directed HIE with *N*-protecting groups as coordinating functionalities. d) By deuterodehalogenation of prefunctionalized substrates. e) Utilization of electronic bias in heterocyclic structures. f) Deuteration proximal to heteroatoms by heterogeneous or nanoparticle catalysis. g) Deuteration in acidified benzylic positions by acid catalysis. NWAs = nanowire arrays; Tf = triflate; PVP = polyvinylpyrrolidone.

Moreover, just like other aryl halides, adequately substituted heteroarenes can be subjected to deuterodehalogenation reactions and similar transformations if the need for high deuterium incorporations in specific positions with high reliability justifies the use of prefunctionalized substrates (Scheme 12d).^{20b-e,75} However, in some cases, heteroarenes can act as catalyst poisons owing to their strong coordination to some transition metal catalysts and are then not amenable to directed HIE and reductive deuteration systems.^{51,53d}

This limitation can be easily compensated though as different and sometimes transition metal-free activation methods are possible for heteroarenes thanks to the electronic bias exerted on the aromatic ring by the heteroatom. Based on this effect, selective deuteration of position 4 of pyridines by a two-step protocol involving the formation of pyridine phosphonium ions was recently reported (Scheme 12e).⁷⁶ These intermediates can react with carbonate salts and, after extrusion of triphenylphosphine oxide and CO₂, act as pyridine C4 anion equivalents that are quenched in the presence of a mixture of heavy water and deuterated methanol. The

various possibilities for non-directed HIE on especially electron-rich or electron-poor positions in heteroarenes have been discussed in the previous chapter (Chapter 3.2).^{64d,e,66,67,69,70} Sometimes the role of the heteroatom in non-directed HIE can go beyond electronic activation of the substrate: For the nickel-catalyzed HIE of electron-deficient arenes, the diimine-ligated nickel dimer needs to dissociate to produce the catalytically active monomeric species (Chapter 3.2; Scheme 10b, bottom).^{70a} This dissociation is facilitated by coordinating azines, rendering this methodology specific for such substrates. Similarly, substrate specificity can be observed in metal nanoparticle catalysis where coordinating elements in the substrate are needed to bring it in proximity to the catalyst (Scheme 12f).^{28,56,77}

Lastly, it should be mentioned that the stabilizing effect that heteroarenes have on benzylic anions can be exploited in the facile base-mediated deuteration of alkylated pyridines and related substrates (Scheme 12g).^{25a,64e,78}

5 Transition Metal-Catalyzed C(sp²)–H Activation

It should have become evident from the previous chapters that research on HIE reactions stands in symbiosis with the field of C–H activation, where the former borrows expertise from the latter but also fuels new development. In the following, a brief introduction into the aspects of C–H activation that are relevant to this thesis will be given while a broader discussion of the general field of C–H activation cannot be provided within the space limitations of this work. As the thesis is exclusively concerned with the directed activation of aromatic C–H bonds *via* organometallic intermediates, the introduction will also be restricted to this subfield.

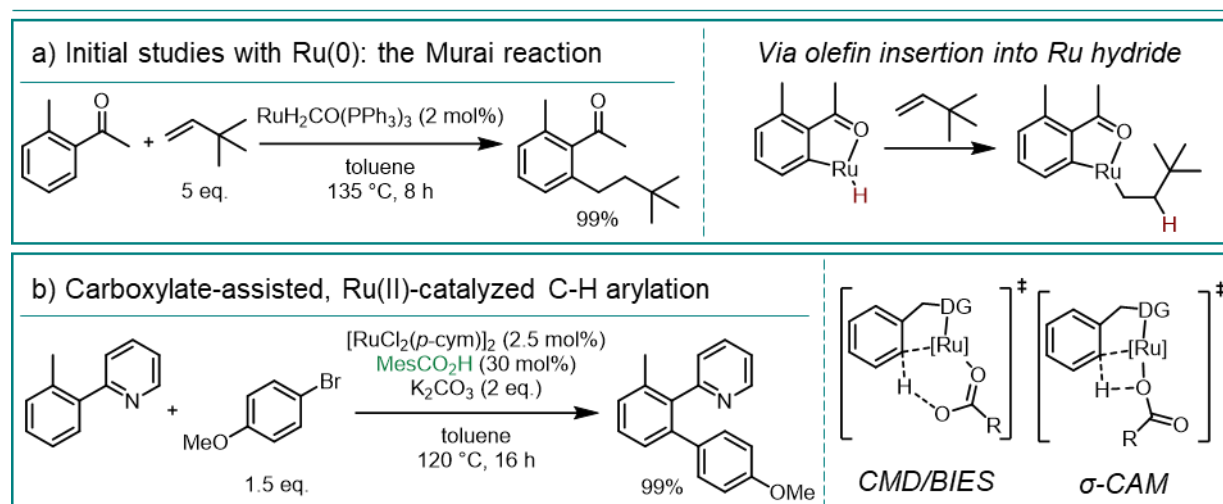
5.1 Ruthenium-Catalyzed C(sp²)–H Activation

Building on the pioneering studies on C–H activation reactions using palladium⁴⁷ and rhodium⁴⁶ catalysts, the search for less expensive transition metal catalysts led to the development of ruthenium-catalyzed C–H activations.⁴⁸ In this context, early work was based on the discovery that ruthenium(0) complexes can undergo oxidative addition into C–H bonds in the *ortho* positions of directing groups such as ketones or heteroarenes. Olefinic reaction partners were shown to insert into the ruthenium–hydrogen bond of the resulting aryl ruthenium(II) hydrides, affording hydroarylation products after reductive elimination (Murai reaction; Scheme 13a).⁷⁹ When it was found that the more air- and water-stable ruthenium(II) complexes can be catalytically active for C–H arylation reactions in the presence of phosphine or phosphine oxide ligands,⁸⁰ the field gained momentum and developments were accelerated with the discovery of carbonate or carboxylate additives as promoters for ruthenium-catalyzed C–H activation reactions (Scheme 13b, left).^{54a,81} Under ruthenium(II) catalysis, arylations^{80,81} and alkylations⁸² with the corresponding halides were possible *via* oxidative addition and intermediary formation

of ruthenium(IV) species. Acylation reactions could proceed by electrophilic substitution of the ruthenacycles with acyl chlorides without the need for Lewis acidic activators.⁸³ Further, in the presence of oxidants, dehydrogenative cross coupling reactions, for instance olefinations with Michael acceptors, became possible.^{61b,c,84}

The role of the carboxylate additives is ascribed to a C–H activation mechanism that is fundamentally different from the ruthenium(0)-catalyzed reactions.⁸⁵ Following coordination to the ruthenium(II) center, the carboxylate ligands facilitate the activation step through formation of a six-membered transition state in which deprotonation of the aryl C–H bond by the carboxylate and C–Ru bond formation take place simultaneously (Scheme 13b, right). In contrast to the oxidative addition mechanism, the oxidation state of the ruthenium center does not change in this so-called CMD mechanism.^{81b} For reactions in which electron-rich arenes react faster than electron-poor substrates, a slightly different mechanism is discussed: Here, the C–H bond is mainly activated by interaction of the arene with the ruthenium center in an electrophilic substitution type regime, generating a partial positive charge on the hydrogen atom which will again be deprotonated by the carboxylate ligand (base-assisted internal electrophilic-type substitution, BIES, Scheme 13b, right).⁸⁶ In some cases, σ -complex-assisted metathesis (σ -CAM) is considered as an alternative pathway in which simultaneous C–H bond cleavage and C–Ru bond formation take place in a four-membered transition state involving the O–Ru σ bond between base and metal center (Scheme 13b).^{81a} In all cases, the directing group plays a pivotal role by lowering the entropy cost of the metalation step through pre-association of the ruthenium complex.^{85b}

Ruthenium-Catalyzed C(sp²)-H Activation



Scheme 13 Examples and mechanistic details of ruthenium-catalyzed C–H activation. a) Murai reaction: Ru(0)-catalyzed hydroarylation of olefins by olefin insertion into the intermediary ruthenium(II) hydride. b) Carboxylate-assisted, ruthenium(II)-catalyzed C–H arylation and transition states of CMD, BIES and σ -CAM-type C–H cleavage mechanisms.

In the past years, new developments have expanded the scope of ruthenium-catalyzed C–H functionalization reactions. In this context, *meta*-selective transformations have been achieved

via radical electrophilic substitution reactions on *ortho*-cyclometalated ruthenium complexes^{87,88} and the selective activation of various specific positions in indole substrates remains a complex field of research.⁸⁹ Moreover, photocatalytic⁹⁰ and electrochemical⁹¹ methodologies have enabled ruthenium-catalyzed C–H functionalization under milder conditions while further efforts have been devoted to protocols that proceed in water⁹² or that rely on weakly coordinating directing groups.^{61d,86,91b,92b,93} Lastly, the established technique of ruthenium-catalyzed C–H functionalization is increasingly used in an application-driven manner to build complex molecular architectures *via* annulation and cascade reactions^{61d,91c,94} or to functionalize biologically relevant substrates.⁹⁵

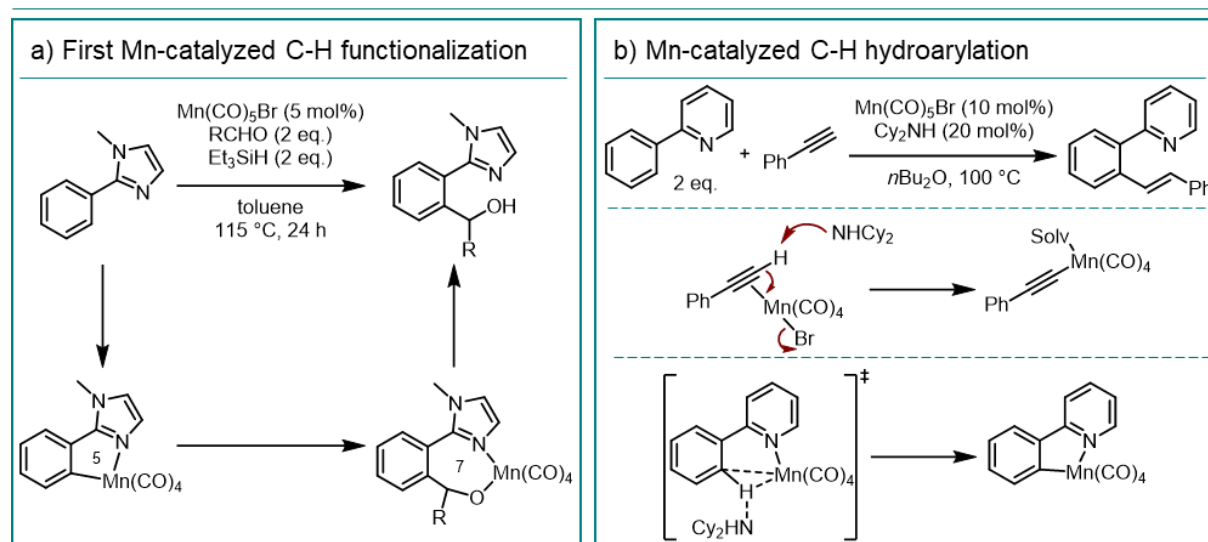
5.2 Manganese-Catalyzed C(sp²)–H Activation

Striving to reduce the economic barriers and sustainability concerns in the way of broad applicability of C–H functionalization, a fortified interest in abundant 3d metal catalysts has manifested itself within the field.^{45,96} Besides iron,⁹⁷ cobalt,⁹⁸ nickel,⁹⁶ and copper,⁹⁹ manganese is an important exponent in this class,¹⁰⁰ given its abundance as the third most commonly found transition metal in the earth crust, its low toxicity, as well as its relevance in biological systems.^{96,100a} While stoichiometric reactions¹⁰¹ and aliphatic C–H oxidation with homolytic bond cleavage¹⁰² have been reported before, it was not until 2007 that the first manganese-catalyzed C–H functionalization of arenes with organometallic intermediates was reported.¹⁰³ In this study, arenes equipped with imidazole directing groups formed 5-membered manganacycles which could perform a nucleophilic attack on aldehydes, thus enabling a transformation similar to the Grignard reaction (Scheme 14a). In the presence of superstoichiometric silane additives, the product could be released from the 7-membered manganacyclic intermediate and catalyst turnover was obtained.¹⁰³ This initial report inspired consecutive studies that lead to significant expansion and improvements of this type of reactions so that now, depending on the reaction partner, stoichiometric additives are often not needed anymore as protodemetalation steps release the products.¹⁰⁴ Aside from the trapping of aldehydes,¹⁰⁵ the reaction with isocyanates could afford amide products^{104c} and nucleophilic addition to nitriles furnished ketones.^{105,106} Moreover, transformations such as the hydroarylation of alkynes (Scheme 14b),^{104f,107} Michael acceptors,¹⁰⁸ and allenes^{104e} or various annulation reactions with unsaturated^{104e,109} or strained¹¹⁰ reaction partners are possible nowadays. Lastly, substitutive transformations on allylic,¹¹¹ allenic,¹¹² and other reagents with leaving groups¹¹³ or alkylations with Grignard reagents¹¹⁴ form an important part of manganese-catalyzed C–H functionalization reactions. On the application side, transformations of biologically relevant structures gained momentum.¹¹⁵ When compared to noble metal-catalyzed C–H activation reactions, manganese catalysis notably offers a partially complementary scope, focusing more on redox-neutral insertion¹¹⁶

reactions with electrophiles terminated by protodemetalation in an isohypsic fashion rather than oxidative transformations or arylations involving reductive elimination steps.^{100a,c}

Another noteworthy difference between manganese- and ruthenium-catalyzed C–H activation lies in the mechanism for the C–H cleavage step. Manganese-catalyzed reactions are often carried out in the presence of mild organic bases such as dicyclohexylamine^{107a,115b} or without basic additives,^{104c,109a,b,f} implying that knowledge from carboxylate-assisted cyclometalation cannot be simply applied to manganese catalysis. Instead, in the presence of sufficiently reactive reaction partners such as terminal alkynes, initial catalyst activation is likely to take place by π -coordination of the alkyne followed by deprotonation of the acidified acetylenic proton (Scheme 14b, center).^{104b} Coordination of the directing group of the C–H activation substrates only follows after formation of the manganese acetylide. However, in the absence of suitable reaction partners, initial C(sp²)–H activation by base-assisted deprotonation and manganese cycle formation is possible (Scheme 14b, bottom).^{104b} Considering how manganese-catalyzed C–H cleavage depends on the specific reaction under study, a broad understanding of this step remains to be attained.

Manganese-Catalyzed C(sp²)-H Activation



Scheme 14 Examples of manganese-catalyzed C–H functionalization. a) First catalytic manganese-mediated C–H activation. b) Example of manganese-catalyzed C–H hydroarylation and possible catalyst activation steps. Cy = Cyclohexyl; Solv = solvent.

Compared to ruthenium catalysis, manganese-catalyzed C–H functionalization continues to be underdeveloped and significant limitations persist. Most protocols developed to date use the rather expensive manganese(I) precursor $\text{Mn}(\text{CO})_5\text{Br}$ or carbonyl complex $\text{Mn}_2(\text{CO})_{10}$ while the naturally occurring Mn(II) salts are rarely employed and often involve radical intermediates.^{100c} Manganese carbonyl complexes suffer from significant catalyst deactivation forming manganese carbonyl clusters which is why high catalyst loadings between 10 and 20 mol% are often spent.^{104b} While initial success with bipyridine-type ligands has been seen for reactions catalyzed by Mn(II) precursors,^{114c,d,117} the right ligand type for Mn(I) catalysts still needs

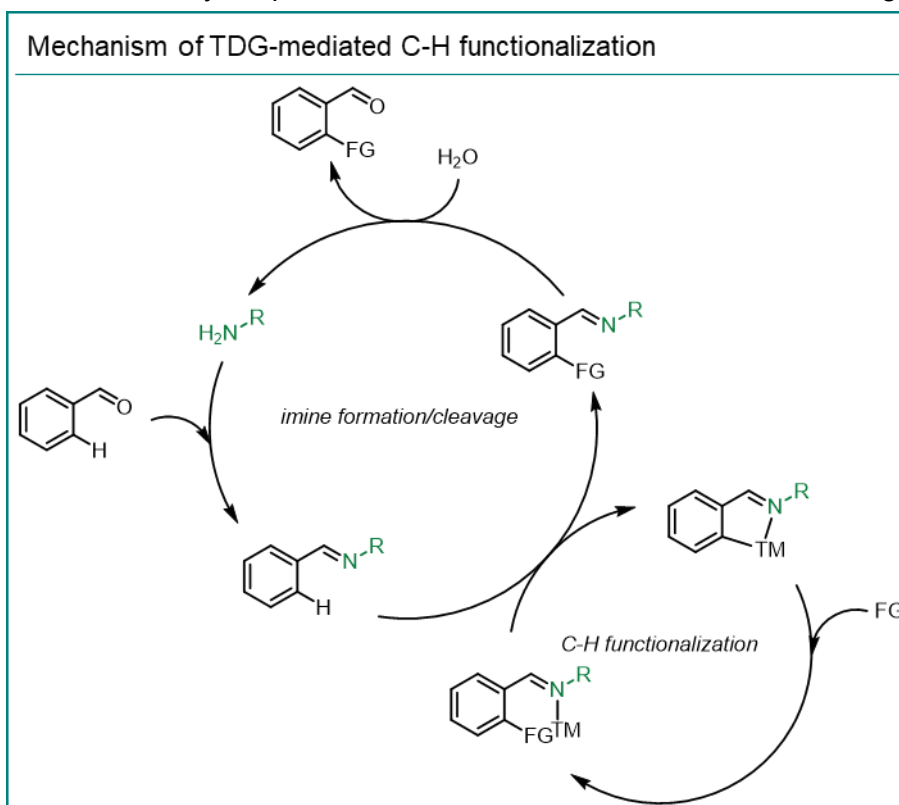
to be found. Currently, the addition of ligands to the latter complexes frequently results in a loss of activity. Although other 3d metals and especially cobalt have been explored for reactions using weakly coordinating directing groups,¹¹⁸ manganese-catalyzed C–H activation is largely limited to nitrogen-containing strongly coordinating moieties. This limitation translates to the need for additional directing group installation and deinstallation steps depending on the substrate of interest.^{111a} Initial examples with native amide^{114b,c} and ketone^{109d,119} directing groups should encourage further studies although π -bonding reaction partners are often required to provide additional stabilization of the metallacycle.¹¹⁸

5.3 Transient Directing Groups in Transition Metal-Catalyzed C(sp²)–H Activation

A strategy to circumvent the above-mentioned problem of the inefficient and waste-generating preformation of strongly coordinating directing groups for more weakly coordinating carbonyl compounds is the use of so-called transient directing groups.¹²⁰ Here, amine additives are present in solution which can react with the weakly coordinating aromatic ketone or aldehyde C–H activation substrates under acid catalysis, affording intermediary imines with enhanced coordinating properties. Being excellent directing groups, the imines can then enable metalation. Subsequently, functionalization and demetalation followed by acid-catalyzed hydrolysis of the imine moiety takes place, ensuring the release of the aldehyde or ketone products as well as catalytic turnover of the transient amine (Scheme 15). The reversibility of the imine formation is key in this context as not only the preformation but also the removal of the directing

groups in additional steps can be avoided. The latter often requires forcing conditions, thus being unsuitable for the transformation of sensitive substrates and for the use within late-stage functionalization projects in general.^{120b} Such transient directing groups have enabled massive advances in both C(sp²)–H¹²¹ and C(sp³)–H¹²²

functionalization and



Scheme 15 General mechanism of transient directing group-mediated C–H functionalization reactions. FG = functional group; TM = transition metal.

judicious choice and tuning of the respective catalytic amines can even give rise to divergent regioselectivities¹²³ as well as enantioselective transformations.¹²⁴ Especially for palladium catalysis, bidentate ligands have been generated through the use of catalytic amino acid additives^{121a,d,122a,c,123d,e, 124e} whereas monodentate imines derived from aniline derivatives are more commonly employed in rhodium-,¹²⁵ iridium-,^{121a,126} and ruthenium¹²⁷-catalyzed C–H functionalization of aldehydes. Importantly, it should be highlighted that transient directing groups have been applied to various transformations and to C–H functionalization with different metals. However, at the outset of the studies leading to this thesis, transient directing groups had never been used to enable the deuteration of weakly coordinating substrates or to facilitate manganese-catalyzed transformations.¹²⁸

6 Objectives of this Work

While the development of new methodologies for the preparation of deuterated molecules is undoubtedly important due to the crucial role these compounds play in life sciences and beyond, several aspects of deuteration chemistry require special attention. First and foremost, late-stage technologies and especially HIE should be in the focus of future research. Within this field, current shortcomings concern particularly the requirement for expensive iridium catalysts and strongly coordinating directing groups.

This thesis aims to address both mentioned issues. First, deuteration methodologies relying on catalysts based on more abundant transition metals were to be explored along with an investigation of metal-free options. Second, these endeavors were intended to be combined with strategies to avoid strongly coordinating directing groups, either by enhancing the coordinating abilities of substrates *in situ* or through activation of C–H bonds based on inherent electronic activation.

7 Summary of Published Results

7.1 Manganese-Catalyzed Selective C–H Activation and Deuteration by Means of a Catalytic Transient Directing Group Strategy

The selectivity and precision of noble metal-catalyzed *ortho*-directed HIE of aromatic substrates is unparalleled by alternative labeling methodologies (*cf.* Chapter 3.1). However, the sustainability of this late-stage catalytic approach is diminished by the necessity to employ rare and expensive transition metals.¹⁷ Indeed, most reports rely on iridium complexes with catalyst loadings of 5 to 10 mol%.^{35,36,37,38b-c,e-i,k,39,40,42} On the other hand, homogeneous and nanocatalysts based on abundant and less toxic 3d metals have gained popularity in the context of non-directed labeling in recent years but have only scarcely been employed for selective HIE (*cf.*

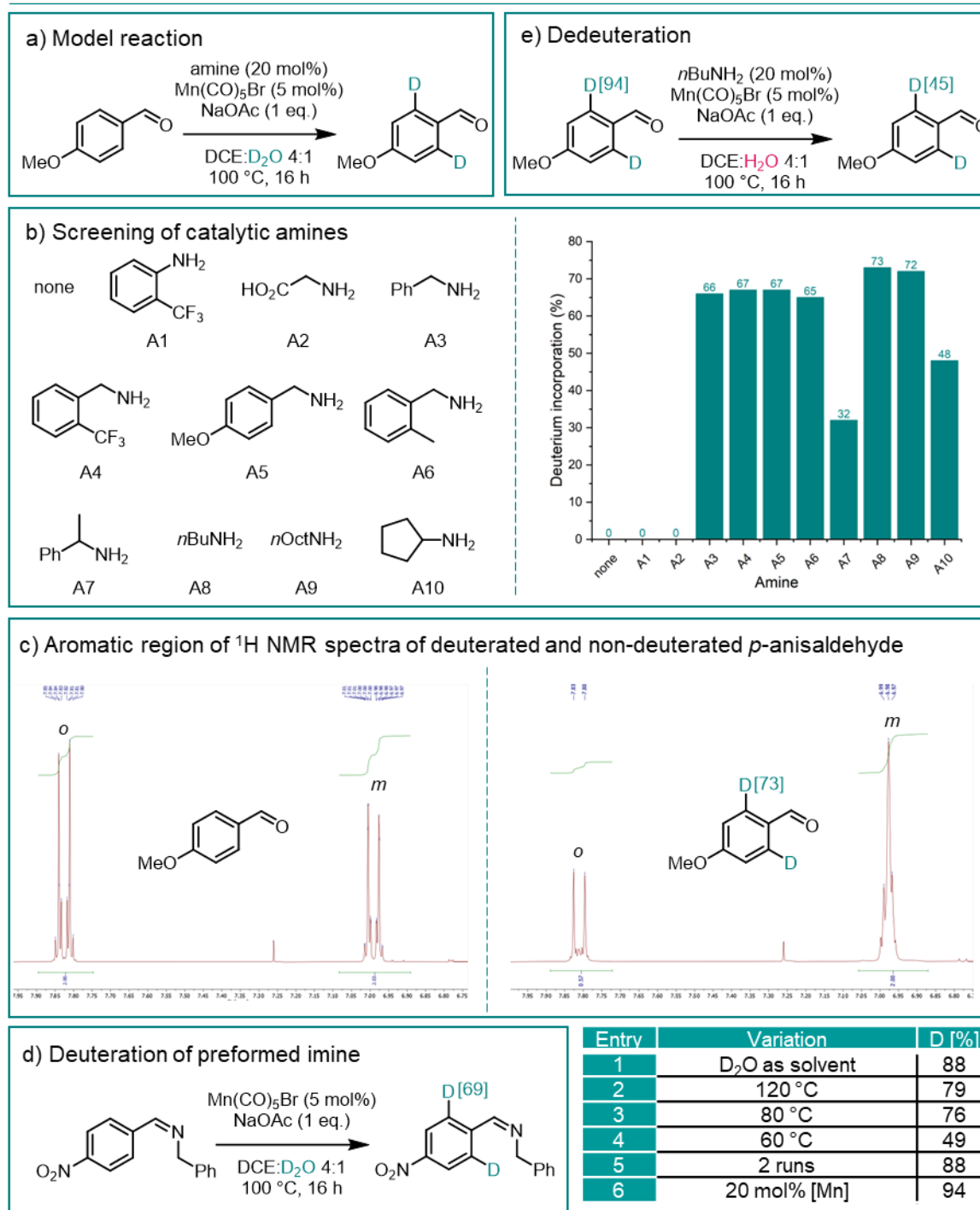
Chapter 3.2).^{56c,66,70,71} Aside from our own work, only one cobalt-catalyzed directed HIE on indole derivatives has been reported.⁵² We therefore reasoned that the precedence on C–H functionalization with the even more abundant manganese could be harnessed to develop a sustainable HIE procedure (*cf.* Chapter 5.2).¹⁰⁰ At the same time, we were interested in solving challenges associated with manganese-catalyzed C–H activation and therefore decided to combine 3d metal catalysis with the transient directing group strategy in order to provide access to weakly coordinating benzaldehyde substrates (*cf.* Chapter 5.3).¹²⁰

At the outset of our studies, we chose commercially available *para*-anisaldehyde as starting material for the benchmark reaction (Scheme 16a). We further employed Mn(CO)₅Br as catalyst due to its precedence in manganese-catalyzed C–H activation (*cf.* Chapter 5.2).^{103,104d-f,105,107,108,109a,c-g,110b,111,112,113,115b-e} However, with our aim of developing a sustainable procedure in mind, we decided to restrict the catalyst loading to 5 mol%, a comparably small amount in the field of manganese-catalyzed C–H activation (*cf.* Chapter 5.2). In the same line of thought, deuterium oxide was chosen as practical and cost-efficient deuterium source and the excess was restricted to 10 eq. to additionally provide tritiation-friendly conditions (*cf.* Chapter 2).¹⁷ Lastly, sodium acetate was added to allow for base-assisted C–H bond cleavage^{104b} and the reactions were set up in 1,2-dichloroethane (DCE) at 100 °C and run overnight (16 h), reflecting typical reaction conditions in the field.^{105,109b,d,110a,112}

Before diving into the screening of transient directing groups, we confirmed that the model substrate can indeed not be activated by manganese in the absence of amine additives. We then tested frequently used amines for the formation of transient directing groups such as aniline derivatives^{121a,b,125,126,127} and glycine as an amino acid^{121a,d} (Scheme 16b). However, no deuterium incorporation in the substrate was observed. Gratifyingly, in the presence of 20 mol% benzylamine, previously used for rhodium-catalyzed C–H functionalization with transient directing groups,¹²⁹ 66% deuterium was incorporated selectively in the *ortho* positions of *para*-anisaldehyde as determined by ¹H NMR spectroscopy through the decrease of the corresponding peaks (Scheme 16c). No exchange was observed in any of the other positions in the molecule. To confirm that deuteration takes place through an imine intermediate, we submitted a pre-synthesized imine to the reaction conditions and obtained a similar result in which deuteration took place in the *ortho* positions of the aldehyde-derived aromatic ring only (no deuteration in the benzylamine moiety; Scheme 16d).¹³⁰ As the stability of imines derived from electron-rich aldehydes is low, *para*-nitrobenzaldehyde was used as starting material for this experiment.¹³¹ Electronic variation of the aromatic core of benzylamine did not affect the deuteration efficiency but sterically hindered amines such as 1-phenylethylamine reduced the level of deuteration, indicating a sterically sensitive C–H cleavage transition state (Scheme 16b). Replacing benzylamine by simple aliphatic amines such as *n*-butylamine or *n*-octylamine slightly improved the deuterium incorporation. Motivated by aspects of cost-effectiveness, we

decided to use *n*-butylamine for further experiments despite considering benzylamine as a viable alternative.

Reaction Optimization



Scheme 16 Optimization of the manganese-catalyzed *ortho*-directed HIE of benzaldehyde derivatives with transient directing groups. a) Model reaction. b) Investigated catalytic amines for *in situ* imine formation and graphic representation of the deuterium incorporation obtained in the *ortho* positions of *para*-anisaldehyde for each of them. c) Comparison of the aromatic regions of the ¹H NMR spectra of non-deuterated and deuterated model substrate. d) Deuteration of preformed imine. e) Reverse reaction. Table: further optimization data.

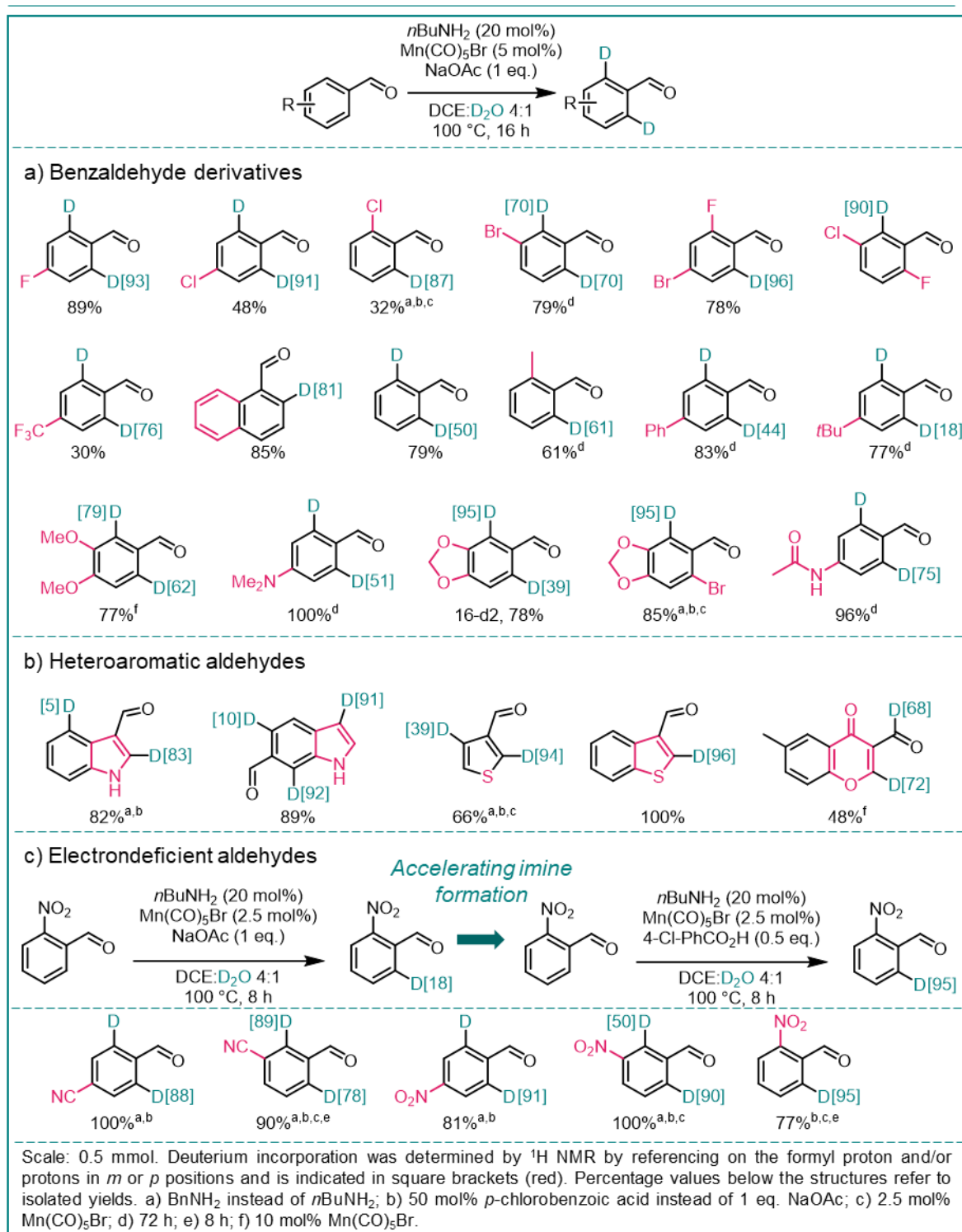
Investigation of further parameters showed comparable reactivity in 1,2-dimethoxyethane (DME) as solvent and increased deuteration in the absence of cosolvents (Scheme 16, Table

entry 1). However, as the latter went along with an increased excess of deuterium oxide (55 eq.), the use of co-solvents was considered more applicable. Sodium acetate was superior to all other inorganic and organic bases or acids investigated and the optimal base loading was found to be 1.0 eq. Importantly, deuteration efficiency was not impacted when lowering the temperature to 80 °C and no beneficial effects went along with increased temperatures (Scheme 16, Table entries 2-4). Finally, no reaction took place in the absence of a manganese catalyst or with Mn(II) salts as confirmed by control experiments. At the end of our optimization studies, *ortho*-deuterated *para*-anisaldehyde could be afforded with 73% deuterium incorporation. Although this is a good value, for some applications higher deuteration levels are needed. Accordingly, means to increase the deuterium incorporation further were explored. It was thus found that a resubmission of the isolated deuterated product to the reaction conditions could increase the deuteration level to 88% (Scheme 16, Table entry 5). Further, with a catalyst loading of 20 mol%, 94% deuteration could be achieved in the first run (Scheme 16, Table entry 6). Lastly, it could be shown that the deuteration is reversible: Submitting deuterated *para*-anisaldehyde to the general reaction conditions but exchanging D₂O for H₂O, the deuterium content was reduced from 94% to 45%, indicative of a back-exchange of deuterium for protium (Scheme 16e). In line with this observation, kinetic experiments revealed a KIE of 1.0 for this reaction.¹³⁰

In the interest of balancing cost-effectiveness and a broad applicability to a range of benzaldehyde derivatives, the originally found conditions with 5 mol% catalyst loading were utilized for the ensuing exploration for the substrate scope. Although good or even superior results had been achieved with Mn₂(CO)₁₀ and at 80 °C for the model substrate, both parameters failed to afford deuteration for other compounds which is why Mn(CO)₅Br and 100 °C were favored as general conditions (Scheme 17, top).

A variety of benzaldehyde derivatives proved to be reactive under these conditions and selective deuterium incorporation in the *ortho* positions was observed in all cases (Scheme 17a). Notably, the reaction exhibited high chemoselectivity so that even halogen substituents were tolerated and did not afford deuterodehalogenated side products.²⁰ Consequently, the recovery of the deuterated compounds was only affected by residues of non-hydrolyzed imine intermediate or by losses during purification due to the volatility and oxidation-sensitivity of some aldehydes. The reaction proved to be insensitive to sterically hindered substituents such as *tert*-butyl and tolerated substitution in *ortho*, *meta* and *para* positions well. Lewis-basic substituents such as methoxy or nitrile presumably coordinate to manganese during the reaction, affording higher deuterium incorporation in their proximity and overriding potentially competing steric effects.^{111a,113b} Interestingly, the coordinating effect of a proximal ketone moiety furnished deuteration of the formyl hydrogen in a chromone-derived substrate (Scheme 17b).

Substrate Scope



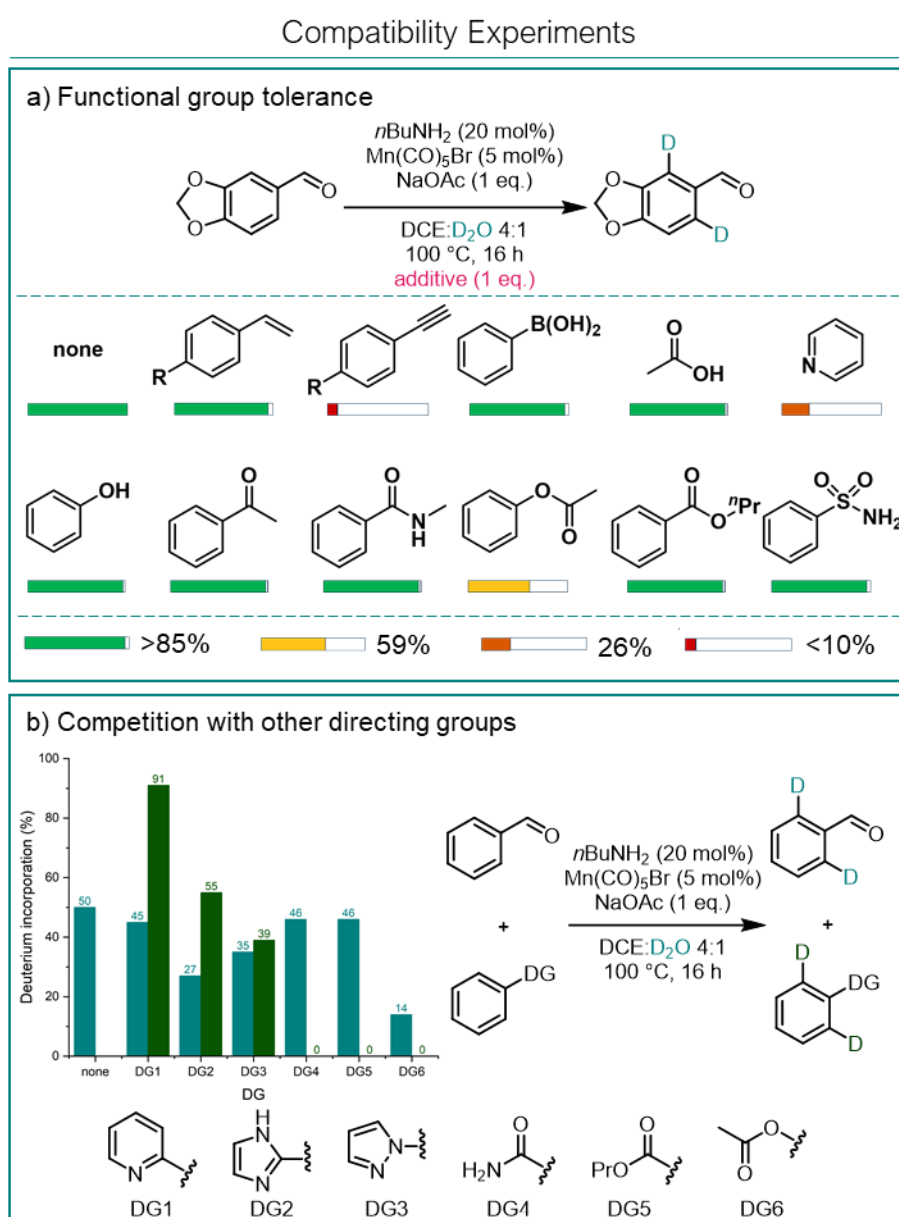
Scheme 17 Substrate scope of the manganese-catalyzed *ortho*-selective HIE of aldehydes with transient directing groups. a) Scope of benzaldehyde derivatives. b) Scope of heteroaromatic aldehydes. c) Adapted reaction conditions for electron-deficient benzaldehyde derivatives. Bn = Benzyl.

Electron-rich heterocyclic aldehydes derived from indole or thiophene were suitable substrates for the reaction (Scheme 17b). For the 3-unsubstituted indole derivative, presumably base-mediated concomitant deuteration in this position was observed additionally (*cf.* Chapter 4). Only the chelating effects of substrates with heteroatoms *ortho* to the formyl moiety as well as

the strong coordination of pyridines resulted in catalyst poisoning. Accordingly, substrates containing these structural elements were not deuterated under our conditions. Further limitations of this methodology include terminal alkynes and free hydroxy groups. Moreover, homologous benzaldehyde underwent significant side reactions and decomposition, probably based on aldol reactivity.

Initially, only poor results were observed for strongly electron-deficient substrates such as *ortho*-nitrobenzaldehyde or *meta*-cyanobenzaldehyde (Scheme 17c). We reasoned that the lack of reactivity in these cases can be attributed to the increased stability of the corresponding intermediary imines and insufficient amine turnover as a consequence.¹³¹ As imine formation and hydrolysis can be accelerated in the presence of acid catalysts, the replacement of sodium acetate by *para*-chlorobenzoic acid afforded excellent deuterium incorporations for this class of substrates even at catalyst loadings as low as 2.5 mol%.

Further assessments of functional group compatibility were carried out by conducting the deuteration of piperonal in the presence of equimolar additives of compounds exhibiting various functional groups (Scheme 18a).¹³² In these experiments, the deuteration of piperonal was unaffected by a terminal olefin, phenylboronic acid, phenol, acetophenone, *N*-methyl



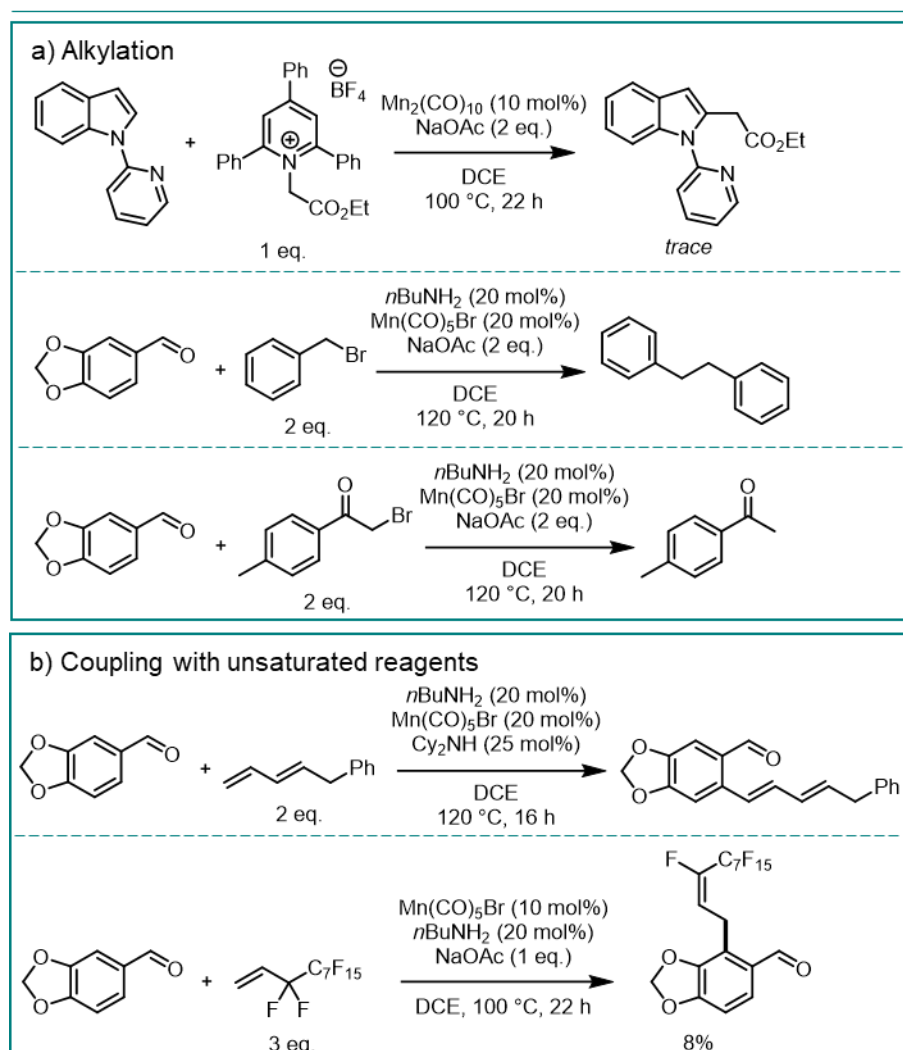
Scheme 18 Compatibility experiments. a) Functional group tolerance tests with equimolar additives. b) Competition experiments with various native directing groups.

benzamide, propyl benzoate, phenylsulfonamide and acetic acid. In contrast, the presence of phenylacetate, pyridine and especially a terminal alkyne diminished the reactivity of the manganese catalyst.

To evaluate the preference of the newly developed catalytic system for specific directing groups, intermolecular one-pot competition experiments were conducted with benzaldehyde and other monosubstituted arenes exhibiting native directing groups (*cf.* Chapter 3.1.1; Scheme 18b).⁴³ Unsurprisingly, the strongly coordinating pyridine directing group outcompeted the transient system. Similarly, imidazole afforded more deuterium incorporation compared to imines formed *in situ*. Pyrazole appeared to be equally reactive whereas a clear preference of the manganese-catalytic system for transient imine over other weakly coordinating carbonyl directing groups was observed: Amides, esters and ketones were not deuterated under the conditions investigated. Especially the latter fact is interesting given the possible formation of ketimines from ketones and amines.

To demonstrate generality for the reported protocol, we attempted the deuteration of benzylamines in the presence of catalytic amounts of aldehydes.¹³⁰ However, no deuterium incorporation was observed under a range of tested conditions. Further, C–H functionalizations beyond deuteration were investigated, too.¹³⁰ Experiments for alkylations *via* single electron transfer (SET) mechanism with Katritzky salts as radical precursors

Other Transformations



Scheme 19 Other attempted manganese-catalyzed C–H functionalization reactions. a) Alkylation with Katritzky salts and alkyl halides. b) Coupling with 1,3-dienes and an allylic fluorinated compound.

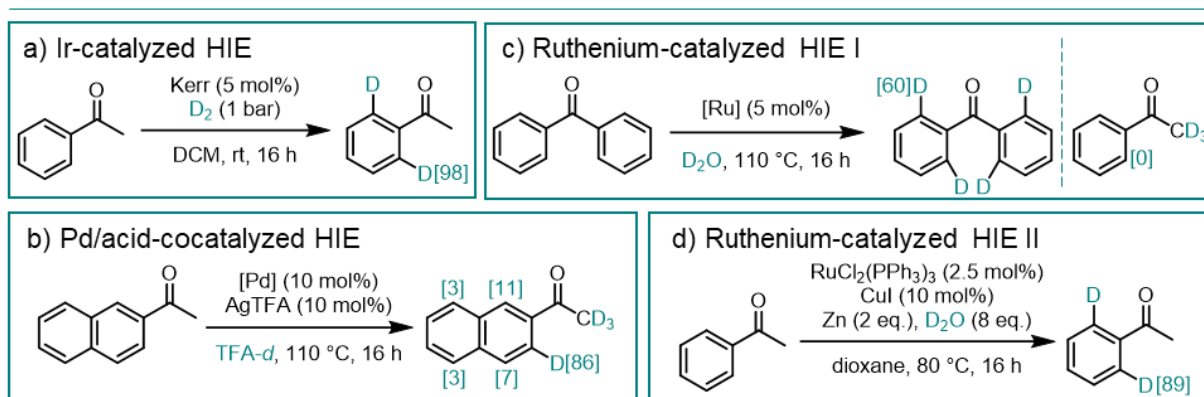
only led to trace products as observed by GC-MS with a preformed directing group and not under the transient directing group regime, whereas alkyl halide reagents afforded dimerization or protodehalogenation instead of the desired alkylation (Scheme 19a).¹¹⁷ In the presence of 2 eq. 5-phenyl-1,3-pentadiene, dehydrogenative coupling was observed by GC-MS instead of the attempted hydroarylation or annulation (Scheme 19b).^{104e,f,107,109,133} Defluorinative allylation afforded 8% isolated yield of the desired product, indicating that the transient directing group and/or the manganese catalyst are not catalytic in this reaction.^{113b} However, further optimization of the reaction conditions might lead to a catalytic protocol.

In conclusion, transient directing groups were reported to enable manganese-catalyzed *ortho*-selective C–H activation of weakly coordinating aldehydes for the first time. It is expected that this report will inspire the development of further transformations using this catalytic system. Further, we introduced the transient directing group strategy to the field of HIE and thus achieved a cost-efficient alternative to iridium-catalyzed *ortho*-directed HIE using an abundant 3d metal catalyst as well as a convenient and cost-effective deuterium source. Our concept has already inspired a similar palladium-catalyzed HIE reaction *via* transient imines and it can be assumed that more reports along these lines will follow. The reported protocol allows for the selective preparation of *ortho*-deuterated compounds with useful deuterium incorporation and recovery of deuterated compounds as well as good functional group tolerance. The thus prepared compounds can be applied as starting materials for KIE studies or as intermediates for the preparation of deuterated drugs or metabolism probes. Given the low amount of heavy water used, the development of a tritiation technology based on our protocol is also possible.

7.2 Ruthenium-Catalyzed Deuteration of Aromatic Carbonyl Compounds with a Catalytic Transient Directing Group

Transition metal-catalyzed HIE guided by native carbonyl directing groups is a particularly fruitful technology given the significance and broad applicability of these types of compounds in the life sciences. Accordingly, a versatile toolkit for labeling methodologies that includes various catalysts and deuterium sources to choose from is desirable. As detailed in Chapter 3.1.3 of the introduction, efforts towards this goal have not been scarce and resulted in a number of carboxylic acid-directed HIE reactions catalyzed by several different transition metal catalysts.^{51,53a,54d} In contrast, enabling the deuteration of aromatic ketones with more cost-efficient catalysts and deuterium sources compared to the iridium-catalyzed standard methodology has been more difficult.^{35a,37,38b,c,f,h,i-k,39} Although much better deuterium incorporation compared to previous palladium-⁶² and ruthenium-catalyzed^{54b} reactions has been achieved with a recent ruthenium-catalyzed methodology, the superstoichiometric amounts of zinc metal used renders this approach less economic (Scheme 20).^{54c}

HIE of Aromatic Ketones: Precedence



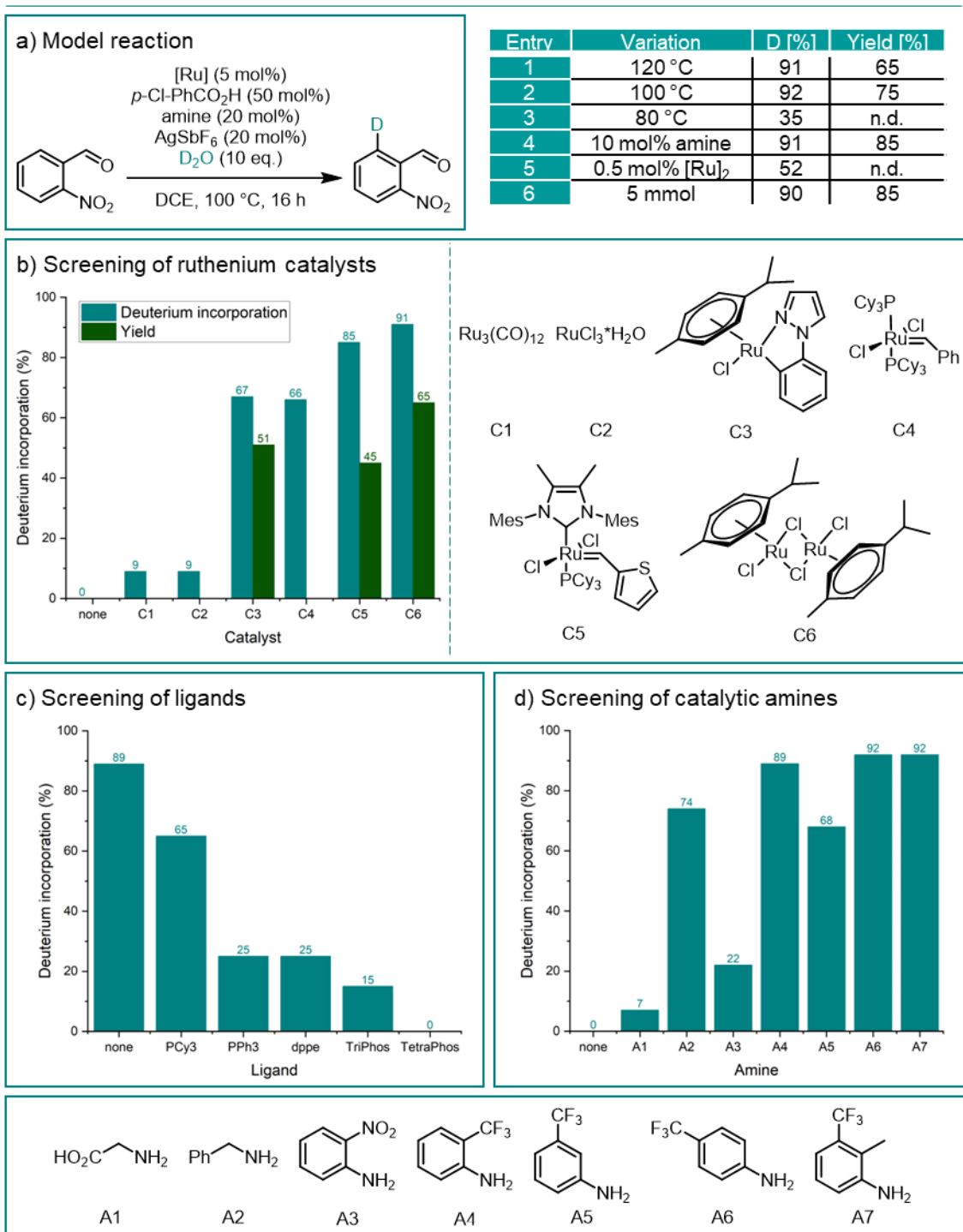
Scheme 20 Precedence of transition metal-catalyzed, ketone-directed HIE of aromatic substrates. a) Iridium-catalyzed HIE on acetophenone. b) Pd/acid-cocatalyzed HIE on acetophenone derivatives. c) Ruthenium-catalyzed HIE on aromatic ketones. d) Ruthenium-catalyzed HIE on acetophenone.

Aiming to improve existing protocols and aware of the difficulties associated with the activation of the weakly coordinating carbonyl groups, we decided to apply knowledge from previously reported ruthenium-catalyzed transformations with transient directing groups^{124c,d,127,134} as well as our own experience with the manganese-catalyzed HIE of benzaldehyde derivatives described above (Chapter 7.1)¹³⁵ to the development of a general ruthenium-catalyzed carbonyl HIE strategy *via* the formation of transient directing groups.

Looking for further applications of NHC-ruthenium catalysts¹³⁶ as well as cyclometalated ruthenium complexes¹³⁷ previously developed by our group, we investigated the *ortho*-directed deuteration of *ortho*-nitrobenzaldehyde as model substrate mediated by transient directing group-forming catalytic amines (Scheme 21a).

To increase the success chances of this project, reaction conditions were taken from a previously published ruthenium-catalyzed C–H alkylation with electron-deficient anilines as transient directing groups.¹²⁷ Accordingly, catalytic amounts of *para*-chlorobenzoic acid were employed to ensure efficient imine formation and cleavage by acid catalysis and to assist with the C–H bond cleavage step (*cf.* Chapter 5.1).⁸⁵ Silver hexafluoroantimonate was used to enable catalyst activation by chloride abstraction and precipitation of insoluble silver chloride and the reaction was run at 120 °C in DCE overnight (16 h). For a practical deuteration protocol with potential application to tritiation, a small excess (10 eq.) of heavy water was chosen as deuterium source and an initial screening of ruthenium catalysts was conducted in the presence of 20 mol% of *ortho*-aminobenzotrifluoride as catalytic amine additive. While the metathesis catalyst and the cyclometalated ruthenium complex afforded moderate to very good deuterium incorporation, the recovery of deuterated compound was too low for application purposes, indicating detrimental side reactions (Scheme 21b). The yield of the deuterated compound could be improved when moving to the commercially available *para*-cymene ruthenium(II) chloride dimer and an excellent deuterium incorporation of 91% could be measured by ¹H NMR spectroscopy.

Optimization of the HIE of aldehydes

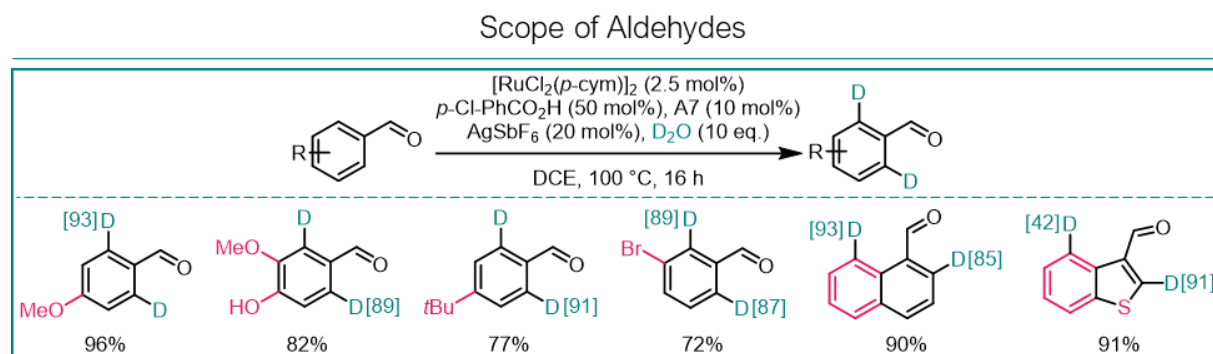


Scheme 21 Optimization of the ruthenium-catalyzed *ortho*-HIE of aromatic aldehydes with transient directing groups. a) Model reaction. b) Screening of ruthenium catalyst precursors. c) Screening of phosphine ligands. d) Screening of catalytic amines. Table: additional optimization data.

The necessity for a ruthenium(II) precursor was confirmed by the low reactivity of Ru(0) and Ru(III) catalysts (<10%) and no reaction took place in the absence of a ruthenium source. Interestingly, the addition of various phosphine ligands only resulted in decreased deuteration efficiencies (Scheme 21c). The high reactivity of the encountered system encouraged us to lower the temperature to 100 °C (Scheme 21, Table entries 1 and 2). Gratifyingly, the

deuterium incorporation remained high under these conditions and the stability of the substrate improved, reflected by an improved isolated yield. Lowering the temperature further slowed down the reaction more drastically (Scheme 21, Table entry 3). Investigation of a series of aniline cocatalysts revealed that specific substitution patterns are important to allow for a suitable balance between transient directing group turnover and imine stability (Scheme 21d). Besides *ortho*-aminobenzotrifluoride, *para*-aminobenzotrifluoride and 2-methyl-3-trifluoroaniline afforded high deuterium incorporation. On the other hand, *meta*-aminobenzotrifluoride, *ortho*-nitroaniline, and benzylamine yielded lower deuterium incorporations while glycine did not form catalytically active transient directing groups. In the absence of amine additives, no deuteration takes place, confirming the requirement for transient imine formation.

A decreased amount of amine improved the recovery of deuterated compound by reducing the percentage of aldehyde that remains as residual imine after the reaction (Scheme 21, Table entry 4). Changing the other parameters such as acid cocatalyst, silver salt and solvent only resulted in deteriorated deuteration levels, indicating that the conditions thus found were optimal. It appears worth noting that 52% deuterium incorporation can still be obtained with a catalyst loading as low as 0.5 mol% for the dimeric structure (that is, 1 mol% per ruthenium atom) and that the reaction can be scaled up 10-fold without affecting deuterium incorporation or yield (Scheme 21, Table entries 5 and 6). Lastly, differences in the C–H activation mechanism compared to the manganese-catalyzed methodology (*cf.* Chapters 5.1 and 5.2) could be seen in a positive KIE of 2.2 for the ruthenium-catalyzed reaction, indicating that the C–H bond cleavage represents the turnover-limiting step of this reaction.¹³⁵ When exploring the substrate scope of the optimized conditions for aldehyde deuteration, a special focus was given to understanding further differences between the two methodologies (Scheme 22). In this context, it was found that free hydroxy groups such as in vanillin were tolerated by the ruthenium catalyst and that reaction conditions did not have to be modified when moving from electron-rich to electron-deficient substrates.



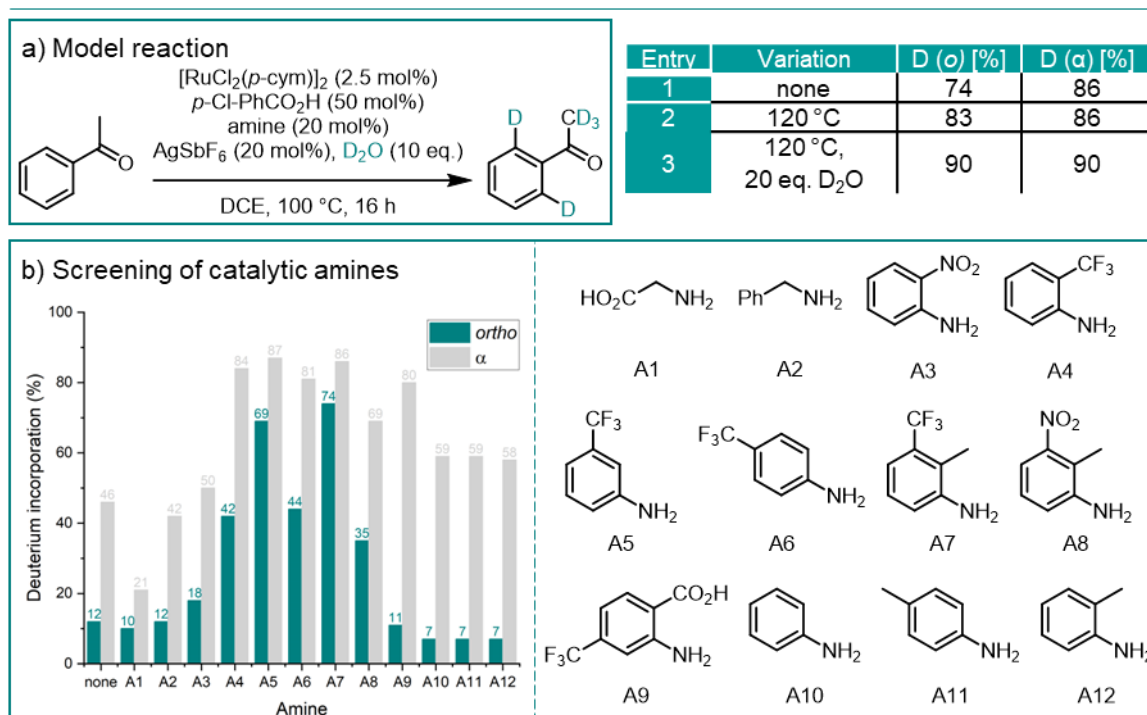
Scheme 22 Scope of the ruthenium-catalyzed *ortho*-directed HIE of benzaldehyde derivatives with transient directing groups.

Further, the complementarity of the two methodologies was demonstrated by diverging reactivity on bicyclic substrates: Whereas the manganese catalyst was selective for the *ortho*

positions of 1-naphthaldehyde and 3-formylbenzothiophene, deuteration of both *ortho* and *peri* positions was possible using the ruthenium catalyst.

In an initial experiment, it was found that – in contrast to the manganese-catalyzed methodology¹³⁵ – acetophenone could be labeled with 74% deuterium incorporation in the *ortho* positions (Scheme 23a, Table entry 1). To gain insight into the mode of action for this reaction, a control reaction in the absence of aniline additive was performed and resulted in only 12% deuterium incorporation in the aromatic core, indicating that transient imine directing groups are again required for efficient C–H activation. Given the diminished electrophilicity of ketones compared to aldehydes, less electron-deficient and consequently more nucleophilic anilines such as *meta*-aminobenzotrifluoride showed the best results here, while A7 proved to be the most general amine catalyst with good activity on both aldehyde and ketone substrates (Scheme 23b). Further compensation of lower substrate reactivity was obtained by raising the temperature to 120 °C and increasing the amount of deuterium oxide to 20 eq., culminating in a deuterium incorporation in the *ortho* positions acetophenone of 90% (Scheme 23, Table entries 2 and 3).

Optimization of the HIE of Ketones

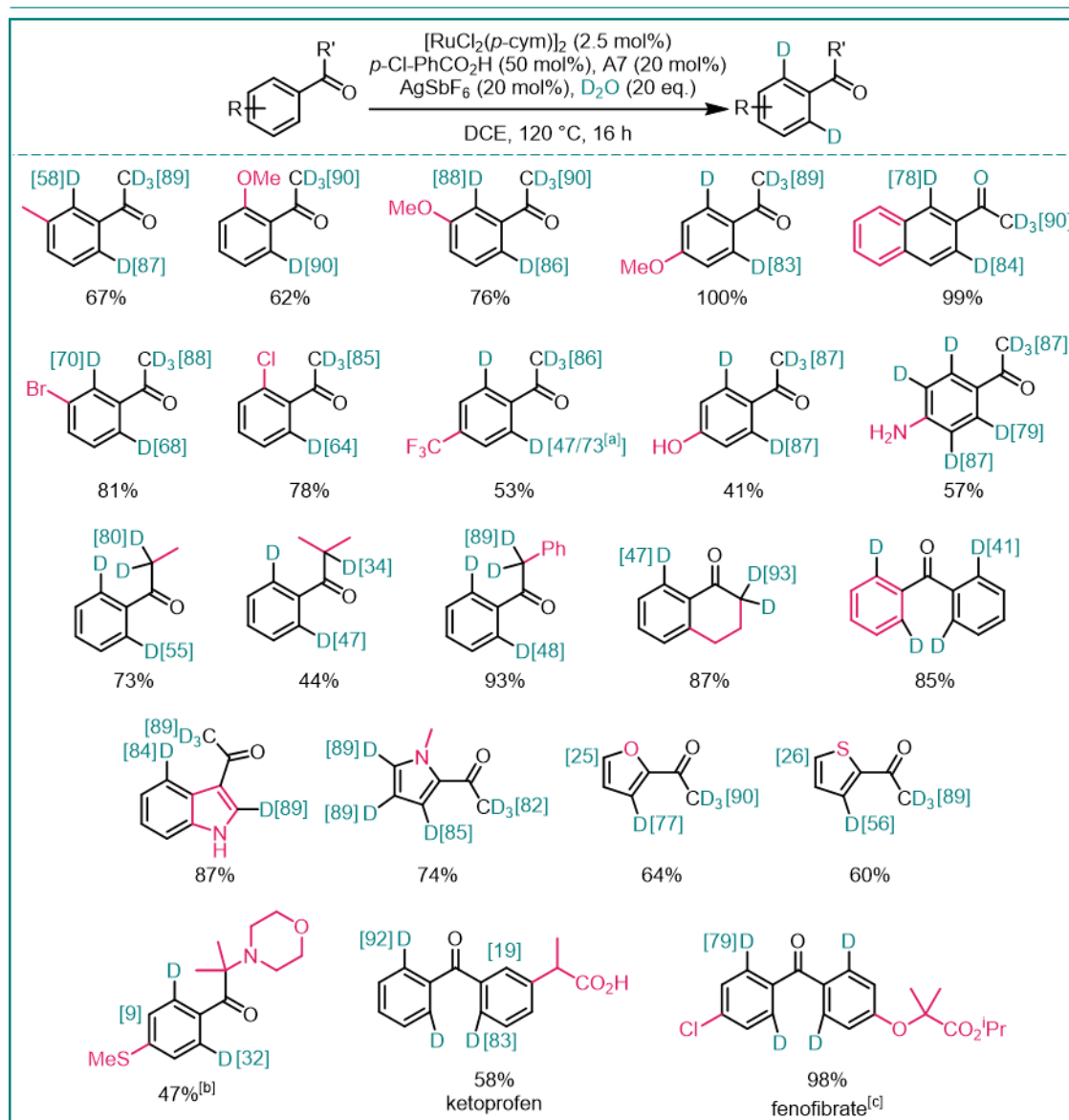


Scheme 23 Optimization of the ruthenium-catalyzed HIE of aromatic ketones. a) Model reaction. b) Screening of catalytic amines. Table: additional optimization data.

Interestingly, concomitant deuteration in the α -carbonyl methyl group was observed, stemming from Lewis- or Brønsted acid-catalyzed enamine formation and deuteration as confirmed by control experiments in the absence of the ruthenium catalyst. Similarly, additional acid mediated HIE was observed in the aromatic core of highly electron-rich substrates and presumably proceeds by electrophilic aromatic substitution (Scheme 24). This additional deuteration is not

only beneficial due to the potential for stabilization of metabolically labile α -carbonyl positions in drug molecules, but it also facilitates the introduction of a higher number of deuterium atoms into the substrate, paving the way for applications as SILS in various analytical studies (cf. Chapters 1 and 3.1.3). In this context, it is worth noting that in almost all cases mass-spectrometric analysis of the products confirmed the absence of non-deuterated compounds in the mixture of isotopomers, a vital requirement for such applications.

Scope of Aromatic Ketones



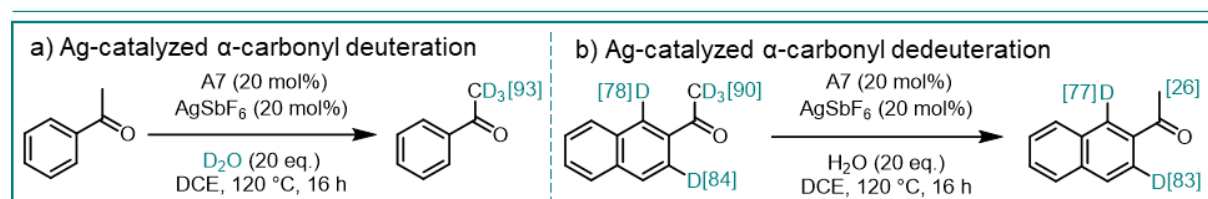
Scheme 24 Scope of the ruthenium-catalyzed HIE of aromatic ketones with a transient directing group.

During the investigation of the substrate scope, electron-rich acetophenones were found to be more reactive than electron-deficient derivatives (Scheme 24). As the latter effect could be compensated by increasing the amine loading to 20 mol%, it can be assumed that the decreased reactivity stems from the fleeting nature of the imine intermediates derived from these substrates. The functional group tolerance of this methodology can be considered good despite the observation of side reactions for substrates exhibiting terminal alkynes, boronic acids

or carbamates (not shown). Longer or branched aliphatic chains appeared to hamper either imine formation or ruthenium coordination, resulting in decreased deuteration efficiencies (Scheme 24).

Overall, the presented methodology enables the preparation of compounds with three different deuteration patterns: a) The optimized conditions afford deuteration in *ortho* and α position, b) the metal-free variant selectively delivers α -deuterated compounds and c) conditions a) followed by metal-free dedeuteration with H₂O furnish *ortho*-deuterated acetophenone derivatives (Scheme 25). Lastly, applicability to the preparation of deuterated pharmaceuticals was demonstrated in the successful HIE of marketed drugs ketoprofen and fenofibrate (Scheme 24).

α -Carbonyl Deuteration



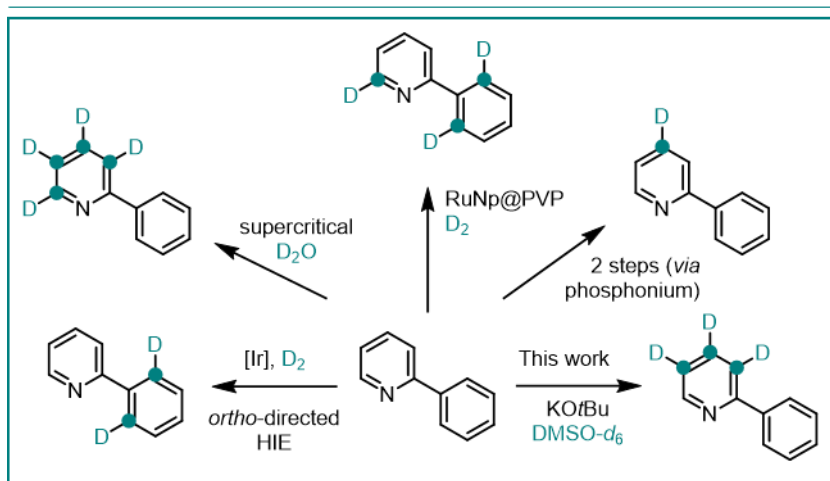
Scheme 25 Access to various deuteration pattern with the ruthenium/amine/silver catalytic system. a) Selective deuteration of the α -carbonyl position in the absence of the ruthenium catalyst. b) Dedeuteration of the *ortho*- and α -deuterated ketone to provide the *ortho*-deuterated derivative.

In conclusion, HIE in the *ortho*- and α -carbonyl positions of aromatic aldehydes and ketones under ruthenium catalysis with *in situ* formation of transient imines in the presence of catalytic aniline additives was reported. This novel methodology shows a broad substrate scope and provides access to compounds with varying deuteration patterns. The reaction is thus deemed suitable for the preparation of deuterated compounds for applications in drug discovery and analytic LC-MS quantification problems while serving as a sustainable alternative to standard HIE methodologies relying on iridium catalysts and deuterium gas.

7.3 Base-Mediated Remote Deuteration of *N*-Heteroarenes – Scope and Mechanism

Thanks to their unique electronic characteristics, heteroarenes are prime substrates for directing group-free HIE reactions (*cf.* Chapters 3.2 and 4). In this context, many reports concerning the deuteration of the ubiquitous pyridine moiety have been published since the early days of HIE (Scheme 26).^{72b,75a,b,138,139} Aside from a plethora of heterogeneous¹⁴⁰ and nanoparticle-catalyzed HIE^{56c,77a,141} reactions targeting positions in the proximity of the nitrogen atom, the global deuteration of pyridines by transition metal catalysis¹⁴² or base-mediated HIE in a supercritical medium¹⁴³ is worth mentioning. However, as depicted in the introduction, the diverse applications for deuterated compounds demand a toolkit of synthetic methodologies that provides access to a broad range of deuteration patterns (*cf.* Chapters 1 and 2). Especially HIE in positions remote from functional groups or activating atoms are still needed to complement

Labeling Patterns in Pyridine HIE



Scheme 26 Divergent HIE of 2-phenylpyridine with various methods.

developed a novel base-mediated methodology which will be introduced on the following pages.¹⁴⁴

During exploratory studies on manganese-catalyzed HIE of quinolines, we discovered that such hetarenes can be labeled in the remote positions under metal-free conditions using a combination of the super base system potassium *tert*-butoxide and deuterated dimethylsulfoxide (DMSO).^{145,146} Consequently, we decided to investigate this reactivity further and chose 2-phenylpyridine as model substrate due to the several possibilities this compound offers for diverging deuteration patterns (Scheme 26). In sharp contrast to previously reported pyridine HIE reactions,^{56c,76,77a,139,140,141,142,143} high deuterium incorporation (>80%) was observed in positions 3, 4 and 5 with only 23% deuterium incorporation in position 6 and no deuteration in the phenyl ring in the presence of 1 eq. potassium *tert*-butoxide and 3 eq. DMSO-*d*₆ at 120 °C under argon atmosphere (Table 1, entry 1). When using the deuterium source as solvent (16 eq.), the deuterium incorporation could be increased above 90% (Table 1, entry 2). Moreover, by decreasing the basicity of the reaction system, the addition of a stoichiometric amount of water resulted in decreased deuteration in position 6 and thus in an improved selectivity (Table 1, entry 3). Reactivity was maintained at a milder temperature (90 °C) while the recovery of the substrate improved under these conditions (Table 1, entry 4). Generally, the reaction only afforded small amounts of one byproduct which was presumably formed through a Minisci-type radical trideuteromethylation pathway. Notably, highly specific reagents were required as no other deuterium source or *tert*-butoxide bases with other alkali metal counter cations furnished any deuterium incorporation at all (Table 1, entries 7-11). The importance of potassium ions for the reaction was further proven by a slowed down reaction in the presence of potassium-sequestering crown ether and by the fact that potassium hydroxide was the only other investigated base besides potassium *tert*-butoxide that lead to measurable deuteration levels (Table 1, entries 12 and 13). Lastly, the deuterium incorporation could be raised to 98% in a

sequential deuteration of the isolated deuterated product although this went along with a decreased selectivity due to concomitant deuteration in the *ortho* positions of the phenyl ring (Table 1, entry 6).

Table 1 Optimization of the base-mediated remote deuteration of 2-phenylpyridine.

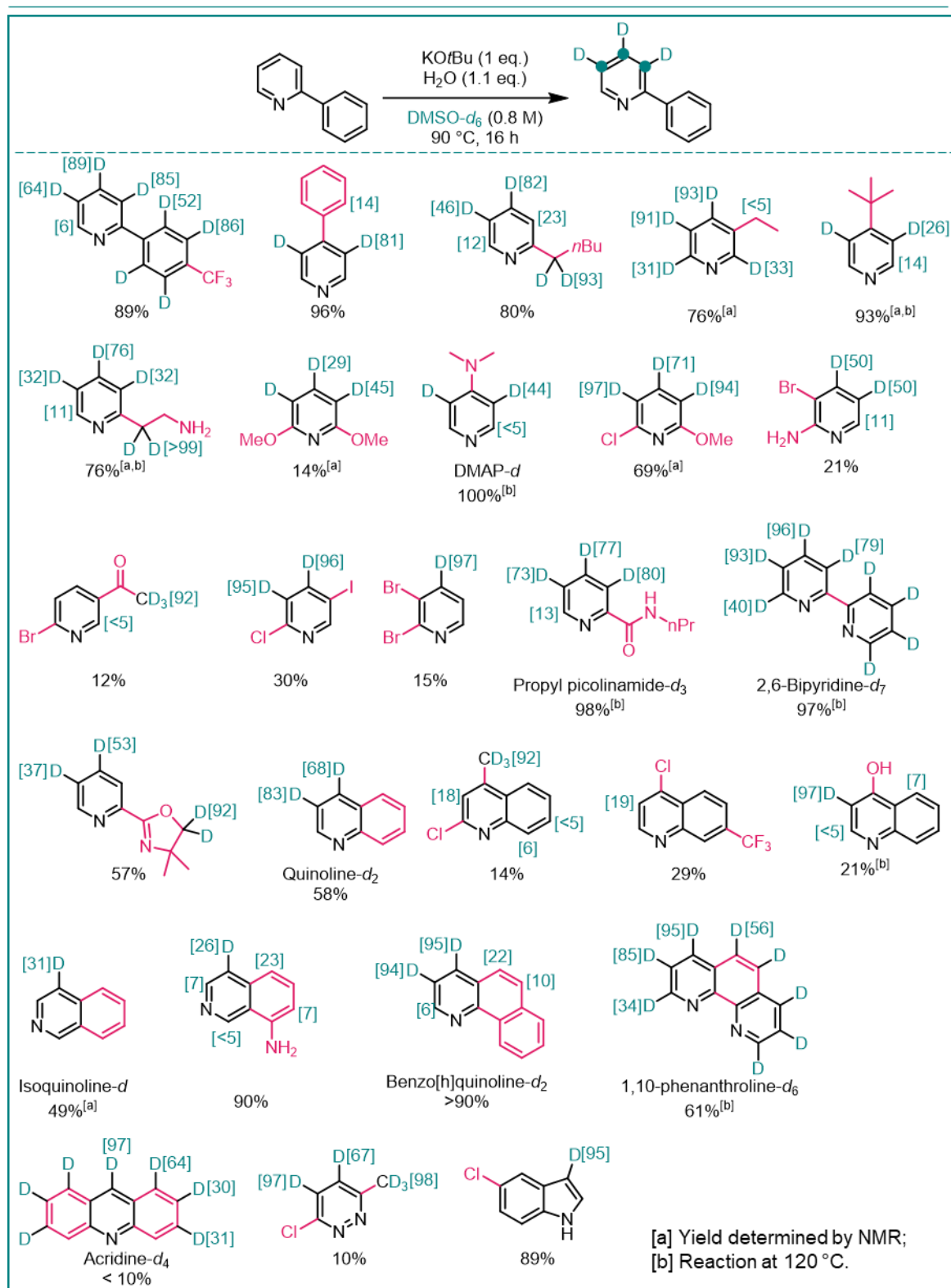
Optimization

Entry ^[a]	Variation	D (3/4/5) [%] ^[b]	D (6) [%]	D (o/m/p) [%]	Yield [%] ^[c]
1 ^[d]	none	86	23	<10	83
2 ^[e]	DMSO- <i>d</i> ₆ as solvent (17 eq.)	96	20	13 (o)	82
3 ^[d]	DMSO- <i>d</i> ₆ as solvent, 1.1 eq. H ₂ O	95	14	<10	84
4 ^[e]	DMSO- <i>d</i> ₆ as solvent, 1.1 eq. H ₂ O, 90 °C	94	18	<10	89
5	DMSO- <i>d</i> ₆ as solvent, 1.1 eq. H ₂ O, 90 °C, 2 nd cycle	98	12	15	n.d.
6	D ₂ O	<10	<10	<10	n.d.
7	Acetone- <i>d</i> ₆	<10	<10	<10	n.d.
8	THF- <i>d</i> ₈	<10	15	<10	n.d.
9	NaOtBu, DMSO- <i>d</i> ₆ as solvent, 90 °C	<10	<10	<10	n.d.
10	LiOtBu	<10	<10	<10	n.d.
11	KOH, DMSO- <i>d</i> ₆ as solvent, 90 °C	43 ^[f] , 70 ^[g]	16	<10	n.d.
12	18-C-6 (1 eq.)	48	<10	<10	n.d.

[a] Scale: 0.5 mmol, work-up: extraction, then NMR in CDCl₃, deuterium incorporation was determined by ¹H NMR using the resonances of the non-deuterated *meta* and *para* positions in the phenyl substituent as a reference; [b] average; [c] isolated yield; [d] average of 2 runs; [e] average of 5 runs; [f] average of positions 3 and 5; [g] position 45.

The selectivity for HIE on remote positions was maintained for a broad scope of pyridine derivatives including important ligands as well as pharmaceuticals (Scheme 27 and Scheme 28). Additional exchange was observed for slightly acidic protons in benzylic and α -carbonyl positions as well as in arenes exhibiting electron-withdrawing trifluoromethyl or chloro substituents. Moreover, electron-rich substituents afforded increased deuterium incorporation in their proximity although the overall deuteration efficiency on these types of substrates was lower which could be due to a shift towards an electrophilic substitution-type mechanism in these cases. Lower deuteration levels were found for sterically hindered substrates such as those containing larger aliphatic residues (Scheme 27). For halogenated compounds, a decreased chemoselectivity was manifested in lower yields due to the formation of several side products (Scheme 27). It can be assumed that competing halogen transfer plays a role under the reaction conditions.¹⁴⁷ Further, cyano, formyl, vinyl and alkynyl substituents present in the substrates afforded decomposition.

Scope of Pyridine Derivatives

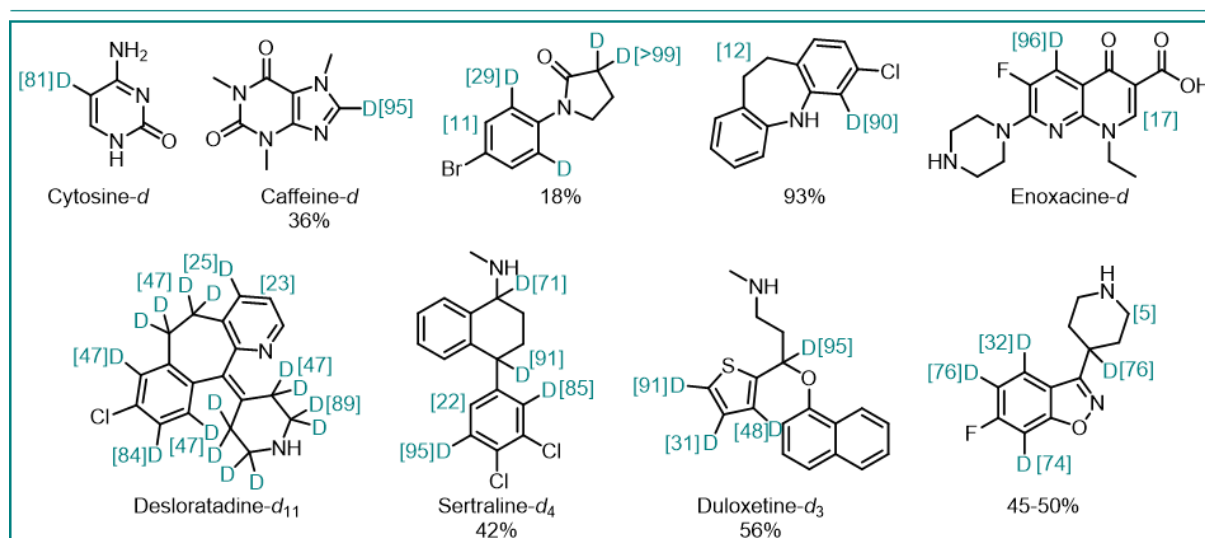


Scheme 27 Scope of pyridine derivatives and fused *N*-heteroarenes.

Intrigued by the persistent and unusual selectivity pattern of this reaction, we commenced more detailed mechanistic studies. Provided that hints towards a radical mechanism were seen in the impaired deuteration efficiency in the presence of radical scavengers, we suspected a formation of dimeric organic super electron donors through deprotonation of the azine substrates

by potassium *tert*-butoxide under the reaction conditions (Scheme 29a).^{148,149} According to our hypothesis, a subsequent single electron transfer step could initiate a radical chain reaction. The fact that an intense red color was observed when adding the substrate to a previously colorless solution of potassium *tert*-butoxide in DMSO-*d*₆ seemed to support a fast formation of conjugated dianionic species. At the same time, other methodologies that rely on organic super electron donors exhibited a remarkable dependence on the presence of potassium ion, just like our system.

Scope of Bioactive Compounds

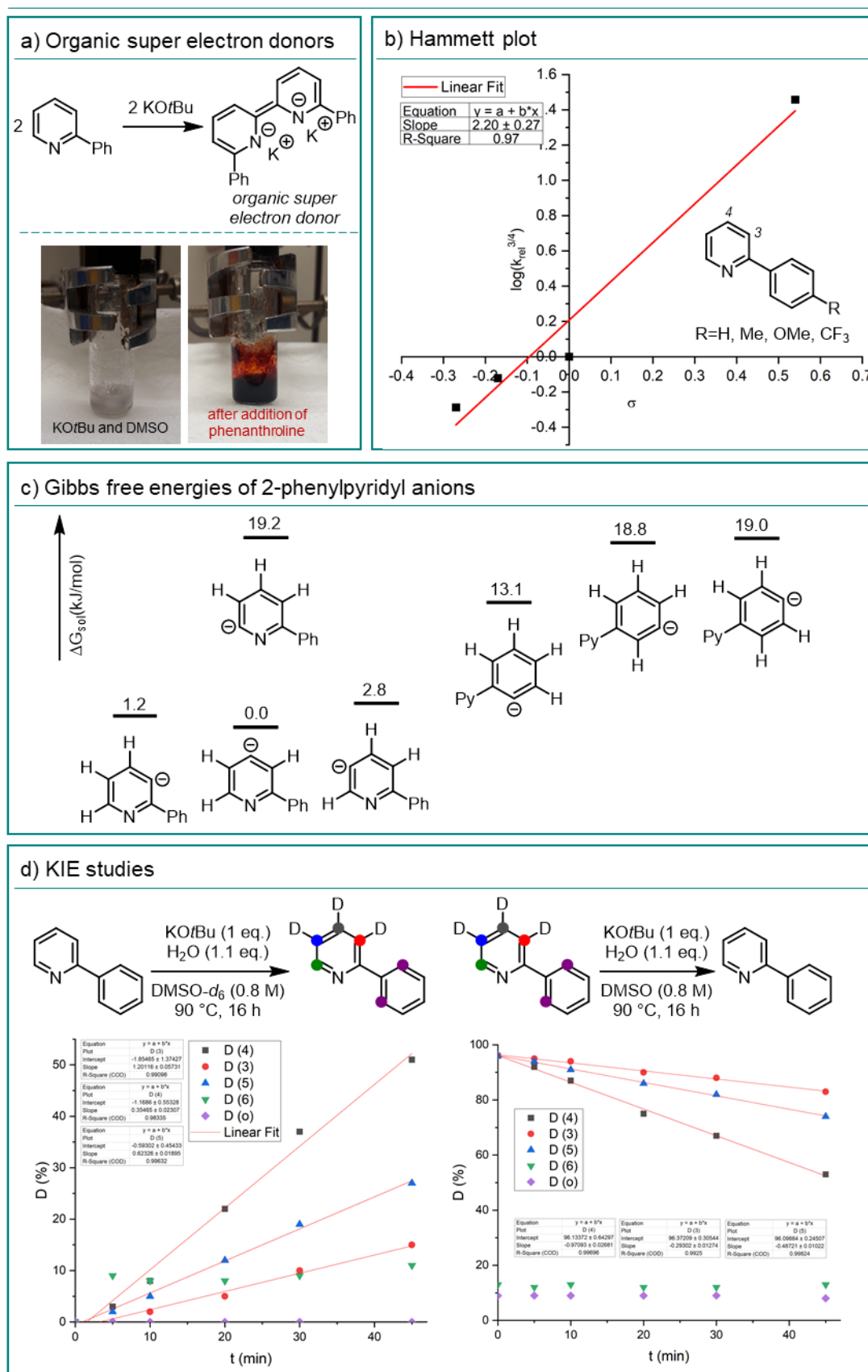


Scheme 28 Scope of bioactive compounds.

However, in contrast to the assumptions listed above, a study of linear free energy relationships with Hammett parameters offered an excellent correlation and a positive slope for polar Hammett σ and σ^- values whereas no fit was found with radical σ^\cdot parameters (Scheme 29b). These experiments suggested a polar pathway with a build-up of negative charge in the transition state rather than a radical reaction.

To shed more light on the deuteration mechanism, DFT calculations (M062X/6-311+G(d,p)/SMD(DMSO))¹⁵⁰ were carried out, comparing the thermodynamic stabilities of pyridyl anions and pyridyl radicals in seven different positions (Scheme 29c). In agreement with the Hammett experiments, the three most thermodynamically stable anions result from deprotonation in positions 3, 4 and 5 whereas the most stable radical would form after hydrogen atom abstraction in position 6. Accordingly, the main deuteration sites of further heteroaromatic compounds could be successfully predicted by determining the most stable anion by DFT calculations. Moreover, comparison of the DFT data with a kinetic profile of the reaction showed that the rate of deuteration is fastest at the site of the most stable pyridyl anion. Consequently, the experimental results agree with a deprotonation-deuteration pathway.

Mechanistic Studies



Scheme 29 Mechanistic studies on the base-mediated deuteration of pyridine derivatives. a) Initial hypothesis: formation of organic super electron donors based on experimental observations such as a color change upon addition of substrate. b) Hammett plot. c) DFT-calculated Gibbs free energies of 2-phenylpyridyl anions. d) KIE studies.

Given that only a small KIE of 1.2 was measured for positions 3 and 4 and of 1.3 for position 5, it is likely that the deprotonation is not the RDS of the reaction (Scheme 29d). Instead, the generation of the dimsyl anion or the final deuteration step might correspond to the highest barriers.

In conclusion, a base-mediated methodology for the remote HIE of pyridine derivatives has been reported and gives access to deuterated ligands as well as bioactive compounds. Experimental and computational mechanistic studies have elucidated that the reaction likely proceeds *via* regioselective deprotonation of the pyridine substrate, affording the most thermodynamically stable pyridyl anion. These insight may inspire future transformations based on anionic pyridyl intermediates besides providing labeled compounds for drug discovery programs.

8 Outlook

This thesis comprises the development of three novel HIE methodologies which enable deuteration of arenes in the absence of iridium catalysts, strongly coordinating directing groups or deuterium gas. The presented works therefore embody a small contribution towards the goal of more applicable, sustainable, and efficient deuteration reactions.

Further contributions to the development of new labeling methods have been made in terms of selectivity. While precise installation of deuterium atoms in *ortho* positions of weakly coordinating carbonyl groups was achieved under manganese- and ruthenium catalysis, a new selectivity concept was discovered in the base-mediated protocol for the remote and non-directed labeling of heteroarenes. Although this achievement constitutes a new addition to the catalogue of labeling reactions with divergent selectivity, more directing group-free HIE methodologies will continue to be in high demand. In this context, reports like ours are expected to inspire new methodologies that allow for a more precise incorporation of deuterium at only one of the described sites.

Building on our proof-of-concept studies, the introduction of transient directing groups to HIE bears the potential of replacing the tedious installment of template directing groups by atom- and step-economic *in situ* formation. This way, precise installation of deuterium atoms at remote *meta* and *para* sites could finally enter the realm of truly applicable HIE reactions. Besides, utilizing dynamic covalent bonds beyond the imine linkage, a broader scope of substrates could become amenable to HIE with 3d metal catalysts. It can be expected that further manganese-catalyzed C–H activation catalysts will be adopted for deuteration, ideally culminating in the direct use of the most abundant manganese(II) salts as HIE catalysts.

While the works within this thesis are focused on the labeling of arenes, transition metal-catalyzed C(sp³)–H activation with transient directing groups could provide access to less explored aliphatic labeling reactions in a similar fashion.

However, more fundamental challenges also remain to be tackled. Iridium-free homogeneous HIE reactions often require temperatures above 50 °C and the methodologies reported herein are no exception. It can be hoped that future studies focus on the development of more active catalysts, for instance through ligand design, that would enable aromatic HIE at lower temperatures and with shorter reaction times. Further, as both heavy water and deuterium gas are desirable isotope sources in their own right, methodologies that allow to switch between these reagents without major changes to the reaction conditions would represent valuable additions to the HIE toolbox.

9 Publications

9.1 Manganese-Catalyzed Selective C–H Activation and Deuteration by Means of a Catalytic Transient Directing Group Strategy

Sara Kopf, Helfried Neumann, and Matthias Beller.

Chem. Commun. **2021**, 57, 1137–1140.

DOI: 10.1039/D0CC07675A

© The Royal Society of Chemistry 2021

Electronic supporting information is available online.

Contribution: For this manuscript, I discovered the reaction and planned and performed the experimental work, including optimization, evaluation of the substrate scope as well as additional tests regarding reaction robustness, mechanism, and further reactivity. In addition, I evaluated all analytical data, wrote the first draft of the manuscript and the supporting information. My contribution approximately amounts to 80%.

Signature of the student
(Sara Kopf)

Signature of the supervisor
(Prof. Matthias Beller)



Manganese-catalyzed selective C–H activation and deuteration by means of a catalytic transient directing group strategy†

Sara Kopf,  Helfried Neumann * and Matthias Beller Cite this: *Chem. Commun.*, 2021, 57, 1137Received 23rd November 2020,
Accepted 18th December 2020

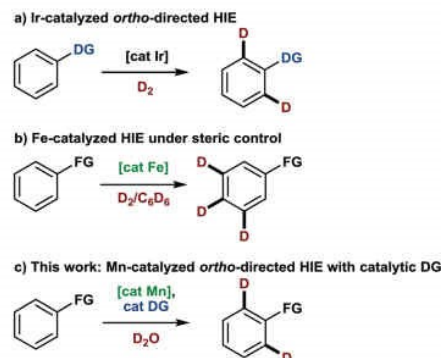
DOI: 10.1039/d0cc07675a

rsc.li/chemcomm

A novel manganese-catalyzed C–H activation methodology for selective hydrogen isotope exchange of benzaldehydes is presented. Using D₂O as a cheap and convenient source of deuterium, the reaction proceeds with excellent functional group tolerance. High *ortho*-selectivity is achieved in the presence of catalytic amounts of specific amines, which *in situ* form a transient directing group.

Not only since the first deuterated drug was accepted by the U.S. Food and Drug Administration (FDA) in 2017, an increasing interest in the development of methodologies for the selective late-stage incorporation of deuterium into organic molecules has manifested itself within the field of organic synthesis.¹ As a result, the current toolbox for labeling reactions comprises a number of established techniques for diverse substrates. As an example, deuteration of arenes predominantly relies on iridium-catalyzed hydrogen isotope exchange (HIE) (Scheme 1a). Here, the most important representative, the NHC-ligated Kerr catalyst, affects deuteration under deuterium gas atmosphere *ortho* to a number of pre-installed directing groups, including N-heterocycles, carbonyl groups and sulfur-containing functional groups.² Most recently, base metal-catalyzed methodologies have expanded the field by presenting new selectivity concepts based on steric and/or electronic control. In this context, the deuteration of the least sterically hindered positions in arenes and heteroarenes has been achieved under catalysis with iron pincer complexes (Scheme 1b),³ whereas a diamine nickel complex preferentially enabled HIE on electron-deficient positions of pyridine derivatives.⁴ However, the precision of a directed approach has so far been unmet by alternative strategies. In this respect, the development of metal catalyzed directed HIE methodologies,⁵ combining inexpensive and available metals with predictable selectivity, is desirable.

Among the different earth-abundant 3d metals, manganese is a most promising candidate, having proven its efficacy for catalytic directed C(sp²)-H functionalization reactions by enabling a plethora of transformations.⁶ Moreover, although manganese-catalyzed deuteration of arenes has only been scarcely investigated yet,⁷ some mechanistic investigations already hint at the potential success of such an endeavor.⁸ However, despite these advances, manganese-catalyzed C–H activation is still limited to substrates comprising nitrogen-containing directing groups⁹ and thus often demands additional synthetic steps. For instance, a recently disclosed allylation reaction of arenes required the pre-formation of an imine as a directing group, which subsequently needed to be hydrolyzed in a separate step.¹⁰ A methodology that allows this imine formation to occur *in situ* with a catalytic amount of amine and thus reduces time and waste would certainly be more appealing. Interestingly, such a transient directing group strategy has been utilized in noble metal catalysis,¹¹ but has thus far not been applied to either manganese-catalyzed C–H activation or directed HIE. We believed that both fields could be merged thus report herein on the first

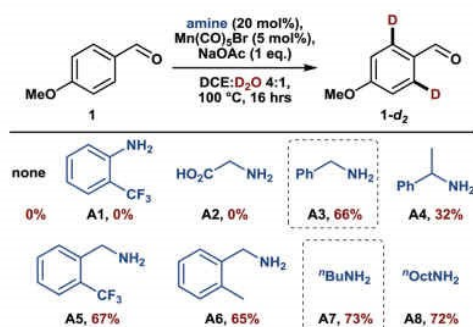


Scheme 1 Selectivity control of deuteration methodologies.

Leibniz-Institut für Katalyse, Albert-Einstein-Str. 29a, Rostock 18059, Germany.

E-mail: matthias.beller@katalyse.de

† Electronic supplementary information (ESI) available. See DOI: 10.1039/d0cc07675a



Scheme 2 Mn-catalyzed *ortho*-deuteration of *p*-anisaldehyde in the presence of catalytic amine additives for the *in situ* formation of transient directing groups. Scale: 0.5 mmol 1. Deuterium incorporation was determined by ¹H NMR through the decrease of the doublet at 7.81 ppm while referencing on the protons in *meta* position.

manganese-catalyzed *ortho*-selective C–H deuteration of aromatic aldehydes through transient formation of a catalytic directing group (Scheme 1c). We started our investigations by studying the deuteration of *para*-anisaldehyde under typical conditions for base-assisted manganese-catalyzed C–H activation. More specifically, we used 5 mol%¹² manganese pentacarbonyl bromide along with D₂O as the cheapest source of deuterium in the presence of catalytic amounts of different amines (Scheme 2).

Firstly, in the absence of amine additives, no deuteration was observed, confirming that the aldehyde moiety is not a feasible directing group for such C–H activation. Furthermore, established transient directing groups such as anilines and glycine¹¹ could not afford any deuteration either. Surprisingly, the addition of 20 mol% of benzylamine to the reaction mixture enabled selective deuteration in the *ortho* positions of the aldehyde with a deuterium incorporation of 66% (A3). The use of sterically more hindered 1-phenylethylamine led to a drop in deuterium incorporation whereas substituents on the aromatic ring did not have a major influence on the reactivity (A5 and A6). A slightly increased deuteration was observed with aliphatic amines such as *n*-butylamine (A7) so that both benzylic and aliphatic amines can be considered efficient catalytic additives for transient directing group formation.

Notably, the deuterium incorporation can be simply increased by re-submitting the isolated, partially deuterated compound to the reaction conditions (Table 1, entry 1). Interestingly, the reaction does not benefit from elevated temperature (120 °C) but works equally well at 80 °C (Table 1, entries 2–4). Finally, in the absence of a manganese catalyst, no deuteration took place (Table 1, entry 5).

Having gained insights into the influence of various parameters on the deuteration efficiency, we moved on to explore the substrate scope of this novel deuteration methodology. For this purpose, we conducted reactions at a temperature of 100 °C to ensure that less reactive substrates are also deuterated efficiently. To our delight, a variety of benzaldehyde derivatives

Table 1 Mn-catalyzed *ortho*-deuteration of *p*-anisaldehyde under various conditions

Entry	Variation	D [%]
1	1- <i>d</i> ₂ (73% D) instead of 1	88
2	120 °C	79
3	80 °C	76
4	60 °C	49
5	No [Mn]	0

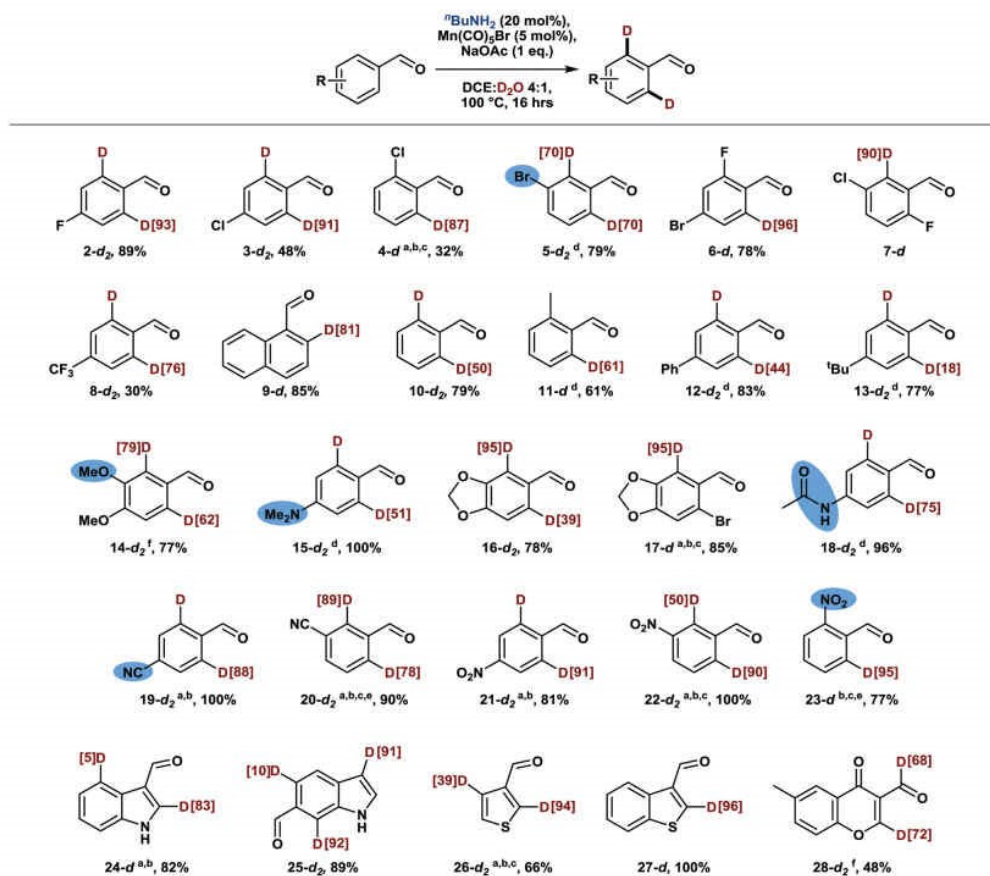
Scale: 0.5 mmol 1. Deuterium incorporation was determined by ¹H NMR through the decrease of the doublet at 7.81 ppm while referencing on the protons in *meta* position.

proved to be amenable substrates, being selectively deuterated in *ortho* position without any side product formation (Scheme 3). In this context, halogenated benzaldehydes proved to be particularly viable substrates and did not undergo competing deutero-dehalogenation (2–7 and 17).¹³ Only remaining amounts of the intermediary imine or the volatility of the substrates sometimes slightly impacted the recovery of the aldehyde. Further, substituents in *ortho*, *meta* and *para* positions as well as multi-substituted benzaldehydes are all well tolerated while guidance by Lewis-basic substituents is observed in the presence of two non-identical *ortho* positions, overriding potential steric effects (14, 16, 20).¹⁴

Strongly electron-deficient benzaldehydes comprising nitro or cyano substituents (19–23) required slightly modified reaction conditions: due to the increased stability of the intermediary imine,¹⁵ a switch from base to acid catalysis facilitated turnover of the catalytic amine, thus yielding the corresponding aldehydes with high deuterium incorporation even at a low catalyst loading of 2.5 mol%. Similarly, good results were achieved with heterocyclic aldehydes (24–28), demonstrating the broad applicability of this methodology. Only substrates containing heteroatoms in α -position to the aldehyde moiety as well as pyridine derivatives appeared to form unreactive manganese complexes instead. Notably, chromone derivative 28 undergoes formyl deuteration additionally, presumably aided by coordination of the proximal keto group.

To test the functional group compatibility of this reaction beyond the groups already mentioned in the text and highlighted in Scheme 3, further deuteration experiments were conducted in the presence of equimolar amounts of a terminal olefin, a boronic acid, a sulfonamide, and phenol. All these additives were well-tolerated and did not affect the deuterium incorporation in the aldehyde substrate. On the other hand, hydroxy-substituted aldehydes as well as substrates comprising terminal alkynes were not deuterated.

From a synthetic point of view it is interesting that the reaction is selective for aldehydes, leaving aromatic ketones untouched despite their ability to form ketimines. Moreover, other carbonyl groups which had previously been employed as

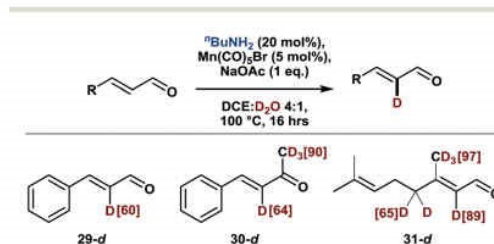


Scheme 3 Mn-catalyzed *o*-deuteration of various benzaldehyde derivatives. Scale: 0.5 mmol. Deuterium incorporation was determined by ¹H NMR by referencing on the formyl proton and/or protons in *m* or *p* positions and is indicated in square brackets (red). Percentage values below the structures refer to isolated yields. ^a BnNH₂ instead of ^tBuNH₂. ^b 50 mol% *p*-chlorobenzoic acid instead of 1 eq. NaOAc. ^c 2.5 mol% Mn(CO)₅Br. ^d 72 h. ^e 8 h. ^f 10 mol% Mn(CO)₅Br.

directing groups for manganese catalyzed C-H functionalization¹⁶ did not induce *ortho*-deuteration under our conditions, whereas heterocyclic directing groups could potentially enable additional deuteration patterns in more complex substrates.

While a variety of methods exists for the labeling of arenes (*vide supra*), the deuteration of olefinic substrates is much less developed.¹⁷ Notably, current methodologies for the labeling of α,β -unsaturated carbonyl compounds either exchange all olefinic protons alike or are slightly selective for the β position.^{17c,e,f} Likewise, a previously reported manganese-catalyzed olefinic C-H activation also led to exclusive functionalization in β position.¹⁸ In this context, we explored the deuteration of α,β -unsaturated aldehydes and ketones. Indeed, as shown in Scheme 4, labelling proceeded smoothly with high selectivity for the α -position. While this work was in progress, an amine-mediated

α -selective deuteration of α,β -unsaturated aldehydes and ketones was published.¹⁹ Accordingly, substrates 29–31 can



Scheme 4 α -Deuteration of α,β -unsaturated aldehydes and ketones. Scale: 0.5 mmol. Deuterium incorporation was determined by ¹H NMR.

be also deuterated in the absence of the manganese catalyst, whereby the amine acts as a nucleophilic catalyst rather than a transient directing group.

In conclusion, we describe a new base metal-catalyzed *ortho*-selective deuteration methodology using the most practical labelling reagent (D_2O). This convenient alternative to current iridium-catalyzed directed hydrogen isotope exchange reactions shows broad scope of (hetero)aromatic aldehydes and versatile functional group compatibility. Moreover, we have introduced the transient directing group concept to the field of manganese-catalyzed $C(sp^2)$ -H activation which will undoubtedly improve the step economy of future transformations by alleviating the need for pre-installed directing groups.

We acknowledge the financial support from the European Union (Flow Chemistry for Isotope Exchange, FLIX, 862179), the BMBF and the State of Mecklenburg-Western Pomerania. We thank the analytical team of LIKAT for their kind support.

Conflicts of interest

There are no conflicts to declare.

Notes and references

- [a] J. Atzrodt, V. Derdau, W. J. Kerr and M. Reid, *Angew. Chem., Int. Ed.*, 2018, 57, 1758; [b] J. Atzrodt, V. Derdau, W. J. Kerr and M. Reid, *Angew. Chem., Int. Ed.*, 2018, 57, 3022.
- [a] J. A. Brown, A. R. Cochrane, R. Irvine, W. J. Kerr, B. Mondal, J. A. Parkinson, L. C. Paterson, M. Reid, T. Tuttle, S. Andersson and G. N. Nilsson, *Adv. Synth. Catal.*, 2014, 356, 3551; [b] W. J. Kerr, M. Reid and T. Tuttle, *ACS Catal.*, 2015, 5, 402; [c] M. Valero, T. Kruissink, J. Blass, R. Weck, S. Güssregen, A. T. Plowright and V. Derdau, *Angew. Chem., Int. Ed.*, 2020, 59, 5626; [d] W. J. Kerr, G. J. Knox, M. Reid, T. Tuttle, J. Bergare and R. A. Bragg, *ACS Catal.*, 2020, 10, 11120.
- [a] R. P. Yu, D. Hesk, N. Rivera, I. Pelczar and P. J. Chirik, *Nature*, 2016, 529, 195; [b] J. Corpas, P. Viereck and P. J. Chirik, *ACS Catal.*, 2020, 10, 8640; [c] S. Garhwal, A. Kaushansky, N. Fridman, L. J. W. Shimon and G. de Ruiter, *J. Am. Chem. Soc.*, 2020, 142, 17131.
- [a] H. Yang, C. Zarate, W. N. Palmer, N. Rivera, D. Hesk and P. J. Chirik, *ACS Catal.*, 2018, 8, 10210; [b] C. Zarate, H. Yang, M. J. Bezdek, D. Hesk and P. J. Chirik, *J. Am. Chem. Soc.*, 2019, 141, 5034.
- J. Zhang, S. Zhang, T. Gogula and H. Zou, *ACS Catal.*, 2020, 10, 7486.
- [a] W. Liu and L. Ackermann, *ACS Catal.*, 2016, 6, 3743; [b] P. Gandeepan, T. Müller, D. Zell, G. Cera, S. Warratz and L. Ackermann, *Chem. Rev.*, 2019, 119, 2192; [c] R. Cano, K. Mackey and G. P. McGlacken, *Catal. Sci. Technol.*, 2018, 8, 1251.
- There is a report on manganese catalyzed aliphatic HIE, though: S. Kar, A. Goepfert, R. Sen, J. Kothandaraman and G. K. S. Prakash, *Green Chem.*, 2018, 20, 2706.
- [a] B. Zhou, P. Ma, H. Chen and C. Wang, *Chem. Commun.*, 2014, 50, 14558; [b] S. Wu, Q. Yang, Q. Hu, Y. Wang, L. Chen, H. Zhang, L. Wu and J. Li, *Org. Chem. Front.*, 2018, 5, 2852; [c] C. Zhu, R. Kuniyil and L. Ackermann, *Angew. Chem., Int. Ed.*, 2019, 58, 5338.
- A few exceptions exist but need bimetallic C-H activation systems: [a] S. Sueki, Z. Wang and Y. Kuninobu, *Org. Lett.*, 2016, 18, 304; [b] B. Zhou, Y. Hu, T. Liu and C. Wang, *Nat. Commun.*, 2017, 8, 1169; [c] Y. Hu, B. Zhou, H. Chen and C. Wang, *Angew. Chem., Int. Ed.*, 2018, 57, 12071; [d] X. Kong and B. Xu, *Org. Lett.*, 2018, 20, 4495; [e] S. Ali, J. Huo and C. Wang, *Org. Lett.*, 2019, 21, 6961.
- W. Liu, S. C. Richter, Y. Zhang and L. Ackermann, *Angew. Chem., Int. Ed.*, 2016, 55, 7747.
- [a] P. Gandeepan and L. Ackermann, *Chemistry*, 2018, 4, 199; [b] S. John-Campbell and J. A. Bull, *Org. Biomol. Chem.*, 2018, 16, 4582; [c] B. Niu, K. Yang, B. Lawrence and H. Ge, *ChemSusChem*, 2019, 12, 2955; [d] J. I. Higham and J. A. Bull, *Org. Biomol. Chem.*, 2020, 18, 7291.
- Catalyst loadings of 10 mol% are most common for manganese-catalyzed C-H activation procedures. Cf. ref. 7, 8b, e.
- Recent examples of deuterodehalogenation: [a] Z.-Z. Zhou, J.-H. Zhao, X.-Y. Guo, X.-M. Chen and Y.-M. Liang, *Org. Chem. Front.*, 2019, 6, 1649; [b] J. J. Gair, R. L. Grey, S. Giroux and M. A. Brodney, *Org. Lett.*, 2019, 21, 2482; [c] M. Kuriyama, G. Yano, H. Kiba, T. Morimoto, K. Yamamoto, Y. Demizu and O. Onomura, *Org. Process Res. Dev.*, 2019, 23, 1552.
- This effect has previously been observed in manganese catalyzed C-H activation: cf. ref. 9 and D. Zell, U. Dhawa, V. Müller, M. Bursch, S. Grimme and L. Ackermann, *ACS Catal.*, 2017, 7, 4209.
- R. W. Layer, *Chem. Rev.*, 1963, 63, 489.
- T. S. Amide, T. Yoshida, H. H. A. Mamari, L. Ilies and E. Nakamura, *Org. Lett.*, 2017, 19, 5458; ester: ref. 8a.
- Examples for olefinic deuteration: [a] S. K. S. Tse, P. Xue, Z. Lin and G. Jia, *Adv. Synth. Catal.*, 2010, 352, 1512; [b] A. Di Giuseppe, R. Castarlenas, J. J. Pérez-Torrente, R. L. Lahoz, V. Polo and L. A. Oro, *Angew. Chem., Int. Ed.*, 2011, 50, 3938; [c] W. J. Kerr, R. J. Mudd, L. C. Paterson and J. A. Brown, *Chem. – Eur. J.*, 2014, 20, 14604; [d] M. Hatano, T. Nishimura and H. Yorimitsu, *Org. Lett.*, 2016, 18, 3674; [e] A. L. Garreau, H. Zhou and M. C. Young, *Org. Lett.*, 2019, 21, 7044; [f] A. Bechtold and L. Ackermann, *ChemCatChem*, 2019, 11, 435.
- B. Zhou, Y. Hu and C. Wang, *Angew. Chem., Int. Ed.*, 2015, 54, 13659.
- V. G. Landge, K. K. Shrestha, A. J. Grant and M. C. Young, *Org. Lett.*, 2020, 22, 9745.



9.2 Ruthenium-Catalyzed Deuteration of Aromatic Carbonyl Compounds with a Catalytic Transient Directing Group

Sara Kopf, Fei Ye, Helfried Neumann, and Matthias Beller.

Chem. Eur. J. **2021**, 27, 9768–9773.

DOI: 10.1002/chem.202100468

© 2021 The Authors. Chemistry – A European Journal published by Wiley-VCH GmbH.

Electronic supporting information is available online.

Highlighted as Front Cover: <https://doi.org/10.1002/chem.202101156>

Contribution: For this manuscript, I planned and performed the experimental work, including optimization, evaluation of the substrate scope as well as mechanistic experiments. In addition, I evaluated all analytical data, wrote the first draft of the manuscript and the supporting information. Lastly, I was involved in the design of the cover picture. My contribution approximately amounts to 75%.

Signature of the student
(Sara Kopf)

Signature of the supervisor
(Prof. Matthias Beller)



Ruthenium-Catalyzed Deuteration of Aromatic Carbonyl Compounds with a Catalytic Transient Directing Group

Sara Kopf,^[a] Fei Ye,^[a, b] Helfried Neumann,^{*,[a]} and Matthias Beller^{*,[a]}

Abstract: A novel ruthenium-catalyzed C–H activation methodology for hydrogen isotope exchange of aromatic carbonyl compounds is presented. In the presence of catalytic amounts of specific amine additives, a transient directing group is formed *in situ*, which directs selective deuteration. A high degree of deuteration is achieved for α -carbonyl and aromatic *ortho*-positions. In addition, appropriate choice of conditions allows for exclusive labeling of the α -carbonyl position while a procedure for the preparation of merely *ortho*-deuterated

compounds is also reported. This methodology proceeds with good functional group tolerance and can be also applied for deuteration of pharmaceutical drugs. Mechanistic studies reveal a kinetic isotope effect of 2.2, showing that the C–H activation is likely the rate-determining step of the catalytic cycle. Using deuterium oxide as a cheap and convenient source of deuterium, the methodology presents a cost-efficient alternative to state-of-the-art iridium-catalyzed procedures.

Introduction

Being an elegant approach to label a compound without altering its physical properties, structure, or biological function, the selective exchange of hydrogen for its heavier isotope deuterium continues to be of interest for many scientists.^[1] Especially in the context of medicinal chemistry, the introduction of deuterium as a bioisosteric replacement of protium in specific, metabolically labile or racemization prone positions of drug candidates such as α carbonyl positions can mitigate deleterious pathways thanks to the kinetic isotope effect (KIE).^[2] The formation of potentially toxic metabolites is thereby prevented while a more general improvement of the absorption, distribution, metabolism and excretion (ADME) properties of the drug candidate is possible at the same time.^[2] The development of selective hydrogen isotope exchange (HIE) methodologies can further be important for the preparation of starting materials for KIE studies relevant for the investigation of reaction mechanisms.^[3] Here, substrates with deuteration

ortho to a functional group can be interesting.^[4] In contrast, the preparation of MS standards for metabolism studies requires the incorporation of several deuterium atoms at once rather than selective deuteration to avoid overlap of unlabeled and labeled compounds in the mass spectrum.^[5a] For this purpose, acetophenone derivatives are particularly attractive substrates, given their prevalence in biologically relevant compounds on the one hand, as well as the presence of two potential labeling sites in their structure on the other hand: While the slightly acidic α -carbonyl hydrogen atoms are subject to acid- or base-catalyzed hydrogen isotope exchange (HIE),^[5] the ketone moiety has also been explored as a directing group in iridium-catalyzed *ortho*-selective deuteration.^[6] Having focused largely on unsubstituted acetophenone and benzophenone as substrates, excellent deuterium incorporation has been observed among others with the so-called Kerr catalyst under deuterium gas atmosphere and mild conditions (Scheme 1a).^[6a]

Although it would be worth investigating scope and functional group tolerance of these methodologies further, the use of alternative transition metal catalysts as well as cheaper deuterium sources is also appealing. However, attempts to replace iridium by ruthenium^[7] or palladium^[8] for ketone-directed HIE have been met with only limited success so far.^[9] In spite of delivering moderate deuterium incorporations for benzophenones (Scheme 1b), these methodologies showed reduced or no reactivity for acetophenone derivatives.^[7a,8] Moreover, using deuterated trifluoroacetic acid as deuterium source, concomitant electrophilic aromatic substitution hampers the *ortho*-selectivity of the directed palladium-catalyzed approach (Scheme 1c).^[8]

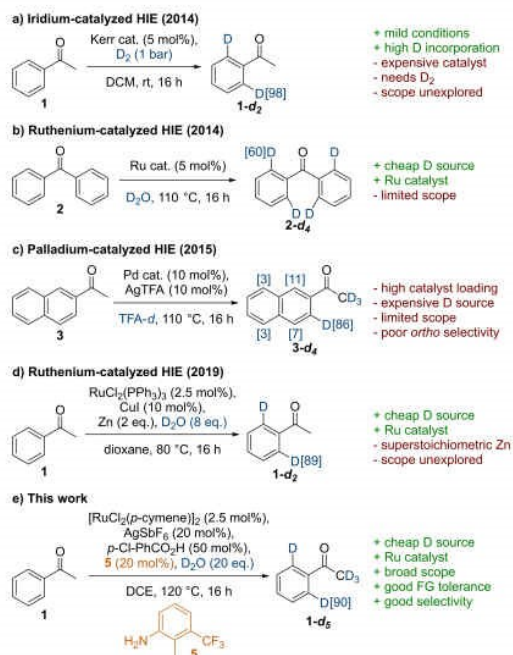
Interestingly, Plietker and co-workers achieved moderate to good deuteration levels in acetophenone derivatives under ruthenium catalysis in the presence of (over)stoichiometric amounts of zinc additives (Scheme 1d).^[7b] An alternative concept for homogeneous ruthenium-catalyzed aromatic HIE makes use of nitrogen containing directing groups.^[7,10] Circum-

[a] S. Kopf, Dr. F. Ye, Dr. H. Neumann, Prof. Dr. M. Beller
Leibniz-Institut für Katalyse e. V., Rostock
Albert-Einstein-Straße 29a, 18059 Rostock (Germany)
E-mail: Helfried.Neumann@catalysis.de
Matthias.Beller@catalysis.de

[b] Dr. F. Ye
Key Laboratory of Organosilicon Chemistry and
Material Technology of Ministry of Education
Key Laboratory of Organosilicon Material Technology of Zhejiang Province
Hangzhou Normal University
No. 2318, Yuhangtang Road, 311121, Hangzhou (P. R. China)

Supporting information for this article is available on the WWW under
<https://doi.org/10.1002/chem.202100468>

© 2021 The Authors. Chemistry – A European Journal published by Wiley-VCH GmbH. This is an open access article under the terms of the Creative Commons Attribution Non-Commercial License, which permits use, distribution and reproduction in any medium, provided the original work is properly cited and is not used for commercial purposes.



Scheme 1. Homogeneous transition metal-catalyzed HIE of aromatic ketones.

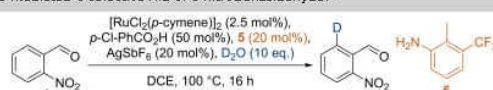
venting the need to pre-synthesize such directing groups, we recently reported a manganese-catalyzed deuteration of benzaldehydes in the presence of catalytic amine additives that form a transient directing group (TDG) in situ.^[11] This concept had previously been shown to be effective under ruthenium catalysis among others^[12] for the alkylation,^[13] amination,^[14] and radical difluoroalkylation^[15] of aromatic aldehydes, but can also

be used for the C–H functionalization of ketones when using palladium^[6a] and rhodium^[17] catalysts. Building on this knowledge and aiming towards a cost-efficient procedure for the deuteration of ketones, we wish to report herein a novel useful ruthenium-catalyzed deuteration of aromatic aldehydes and ketones (Scheme 1e).

Results and Discussion

Inspired by the work on ruthenium-catalyzed functionalization of aromatic aldehydes in the presence of anilines,^[13a] we investigated the deuteration of *o*-nitrobenzaldehyde as model substrate with 10 eq. of deuterium oxide as deuterium source in the presence of common ruthenium catalysts. While cyclo-metallated ruthenium complexes as developed in our group^[8a] as well as NHC ligated metathesis catalysts performed well, the best results were achieved with the simple and commercially available ruthenium chloride *p*-cymene dimer (Table 1, entry 1). Notably, the addition of *p*-chlorobenzoic acid and silver hexafluoroantimonate are necessary to activate the ruthenium complex. Alternative ruthenium precursors such as ruthenium chloride or dodecacarbonyl ruthenium(0) were not effective and the addition of various phosphine ligands slowed down the reaction. In the absence of the ruthenium catalyst no reaction took place although high deuteration was still obtained with a catalyst loading as low as 1.25 mol% (Table 1, entries 2–4). Notably, the exact substitution pattern of the transient directing group plays a minor role. A good balance between a sufficiently stable imine intermediate and good catalytic turnover is achieved with electron-deficient anilines such as *o*- and *p*-aminobenzotrifluoride as well as 2-methyl-3-trifluoromethyl aniline **5**. Further, the isolation of deuterated aldehyde could be improved without impacting the deuterium incorporation by decreasing the aniline loading to 10 mol% which lowered the amount of remaining imine after the reaction (Table 1, entry 5). No deuteration takes place in the absence of the aniline, confirming that the TDG is needed for this transformation (Table 1, entry 6). In this context, it is worth mentioning that

Table 1. Ruthenium-catalyzed and TDG-mediated *o*-selective HIE of *o*-nitrobenzaldehyde.^[a]



Entry	Variation	D [%] ^[b]	Yield [%] ^[c]
1	none	92	75
2	no [Ru] ^[d]	0	n.d.
3	1.25 mol% [Ru] ₂	84	n.d.
4	0.5 mol% [Ru] ₂	52	n.d.
5	10 mol% 5	91	85
6	no 5	0	n.d.
7	80 °C	35	n.d.
8	120 °C	91	65
9	10 mol% 5 , 5 mmol scale	90	84

[a] 0.5 mmol scale. Further optimization details can be found in the Supporting Information. [b] Determined by ¹H NMR using the aldehyde or *m/p*-resonances as reference. [c] Isolated yields. [d] 120 °C, 24 h.

previous attempts to deuterate aldehydes under ruthenium catalysis but without a transient directing group strategy had failed.^[9a] Lowering the temperature to 80 °C diminished the deuterium incorporation significantly whereas the recovery of deuterated aldehyde was reduced at elevated temperature (Table 1, entries 7 and 8). Lastly, the scale of the reaction can be increased 10-fold without affecting deuterium incorporation and yield (Table 1, entry 9).

Having established optimal reaction conditions for the ruthenium- and aniline-catalyzed deuteration of aldehydes, we explored the scope of this transformation, particularly seeking to address some of the limitations of our previously published manganese-catalyzed HIE reaction which showed diminished reactivity for sterically hindered substrates and did not tolerate free hydroxy groups.^[11] Besides, slightly modified reaction conditions were needed for electron-deficient substrates. This new methodology on the other hand appears to be remarkably robust, delivering excellent deuterium incorporations and yields for both electron-deficient and electron-rich (hetero)arenes under unchanged conditions (Scheme 2). Moreover, free hydroxy groups as in vanillin are tolerated and even the sterically hindered *tert*-butylbenzaldehyde is deuterated smoothly.

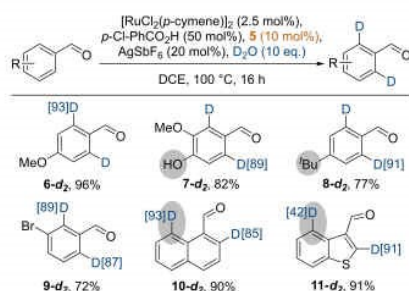
Interestingly, in the case of naphthaldehyde and benzothio-phenone-3-carboxaldehyde, both *ortho*- and *peri*-positions are

deuterated, whereas our previously reported methodology furnished exclusive labeling in the *ortho*-position.

Encouraged by these results, we attempted the TDG-enabled deuteration of aromatic ketones. Under the optimized conditions see above but in the absence of catalytic amines, only 12% deuterium incorporation in the *ortho*-positions of acetophenone was observed, confirming the challenging nature of HIE on this type of substrates (Table 2, entry 1). However, adding 20 mol% of aniline **5** as TDG, the deuteration efficiency was raised significantly (Table 2, entry 2). In contrast to the reaction on aldehydes, other anilines including *o*- and *p*-aminobenzotrifluoride afforded moderate to low deuterium incorporation whereas *m*-aminobenzotrifluoride delivered very good results comparable to **5**. We explain this different behavior by the lower reactivity of ketones compared to aldehydes towards imine formation, requiring more nucleophilic amines. Finally, a deuteration degree of 90% could be obtained after raising the temperature and increasing the amount of deuterium oxide (Table 2, entry 3). Under these conditions, high deuteration levels are additionally achieved in the α -carbonyl position, furnishing an overall incorporation of five deuterium atoms per molecule.

As shown by control experiments (Table 3), this latter reaction likely proceeds via an amine-mediated enamine formation and requires the Lewis acidic silver salt or the benzoic acid derivative as a catalyst. Indeed, in the absence of the ruthenium catalyst, ketones are solely deuterated in α -position. Finally, a broad range of acetophenone derivatives could be successfully converted to the *ortho*- and α -deuterated analogues using this newly developed methodology (Scheme 3). Substituents in *ortho*-, *meta*-, and *para*-positions were all tolerated and deuteration levels appeared to be only slightly affected by steric effects. Especially electron-rich and neutral arenes afforded very good deuterium incorporation, whereas electron-deficient acetophenone derivatives were somewhat less feasible substrates.

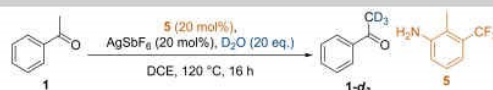
However, using 50 mol% rather than 20 mol% of the TDG, the deuterium incorporation of trifluoromethyl-substituted ketone **20** increased markedly. It can thus be deduced that the lower deuterium incorporation observed under standard conditions can be explained by the short-lived nature of the corresponding imine intermediate rather than factors involving the C–H activation step.



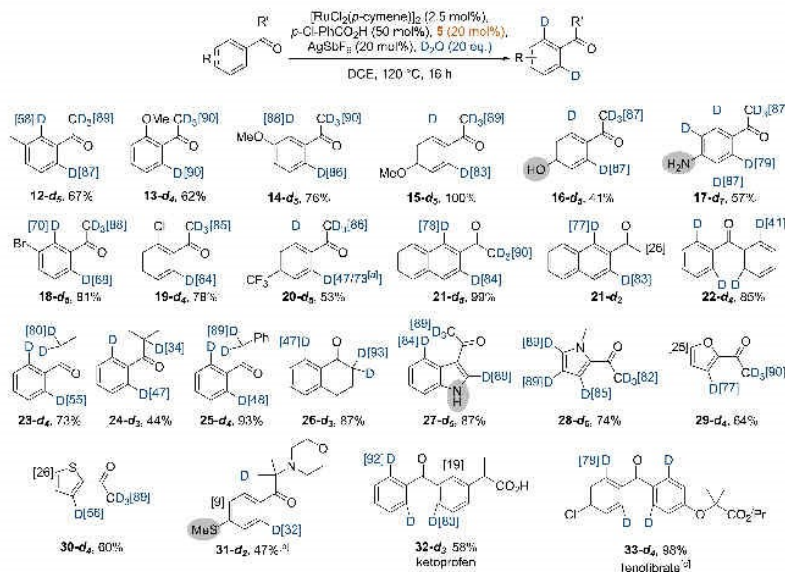
Scheme 2. Scope of aldehydes (0.5 mmol scale). Deuterium incorporations were determined by ¹H NMR using the aldehyde or *m/p*-resonances as reference and are indicated in square brackets. Yields are given under the structures.

Entry	Variation	D (α) [%] ^[b]	D (α) [%] ^[b]
1	no TDG	12	46
2	none	74	86
3	120 °C, 20 equiv. D ₂ O	90	90

[a] 0.5 mmol scale. Further optimization details can be found in the Supporting Information. [b] Determined by ¹H NMR using the resonance for the *p*-position as reference.

		
Entry	Variation	D (α) [%] ^[b]
1	none	93
2	no AgSbF ₆	62
3	no 5	46

[a] 0.5 mmol scale. [b] Determined by ¹H NMR using the resonance for the *p*-position as reference.



Scheme 3. Ruthenium-catalyzed HIE in the presence of a TDG: Scope of ketones. Deuterium incorporations were determined by ¹H NMR using the resonances for the *p*-position as reference and is indicated in square brackets. Yields are given under the structures. [a] 50 mol % TDG used. [b] 4 days reaction time. [c] 4 consecutive deuteration cycles.

Furthermore, the reaction is compatible with reactive functional groups such as free alcohols (16), tertiary as well as free amino groups (31 and 17), unprotected heterocycles (27), and thioethers (31).^[19] Highly electron-rich substrates such as compounds 17 and 28 engage in concomitant deuteration by electrophilic aromatic substitution, affording perdeuterated products. Increasing the chain length of acetophenone (23) and including branched structures (24) led to decreased deuterium incorporation. It thus appears that increased steric hindrance on this side of the ketone substrate interferes with either imine formation or coordination to the ruthenium catalyst.

If exclusive labeling in the *ortho*-position is desired, the deuterated compounds can simply be reacted with water under silver and amine catalysis, thus reversing the deuteration of the methyl group (21-d₃).

Mass spectrometric analysis of the isolated deuterated products showed that in almost all cases no non-deuterated compounds were present, rendering the herein presented procedure relevant for the preparation of isotopically labeled LC–MS standards. Besides, the preparation of deuterated pharmaceuticals is also feasible as demonstrated in the successful deuteration of marketed drugs ketoprofen (32) and fenofibrate (33).

In agreement with previous reports,^[13a] it can be proposed that the ruthenium catalyst is activated by silver-mediated halide abstraction and coordination of the *p*-chlorobenzoic acid additive. At the same time, acid-catalyzed condensation of aniline and aldehyde or ketone to the imine intermediate takes place, preparing for subsequent coordination to ruthenium followed by C–H activation. For *o*-nitrobenzaldehyde, we measured a kinetic isotope effect (KIE) of 2.2, indicating that the

C–H activation is likely the rate-determining step of the reaction. Its reverse finally leads to the deuterated product while the excess of deuterium oxide along with the KIE enable high conversions.

Conclusion

In conclusion, we have reported a novel ruthenium-catalyzed hydrogen isotope exchange reaction of aromatic aldehydes and ketones using the cheapest deuterium source as a viable alternative to the more expensive state-of-the-art iridium-catalyzed methodologies. Using a catalytic transient directing group strategy, the difficulties in the C–H activation of such substrates could be mitigated. Furthermore, appropriate choice of reaction conditions allows for selective deuteration in either *ortho*- or α -positions or at both sites at the same time. The importance of this methodology in the context of drug design and metabolism studies is showcased by the successful preparation of deuterated analogues of marketed drugs.

Experimental Section

Representative procedure for the deuteration of aldehydes: The aldehyde (0.5 mmol), *p*-chlorobenzoic acid (39 mg, 0.25 mmol, 0.5 equiv.), 2-methyl-3-trifluoromethyl-aniline (8.8 mg, 50 μ mol, 10 mol%), dichloro(*p*-cymene)ruthenium(II) dimer (7.7 mg, 12.5 μ mol, 2.5 mol%), and silver hexafluoroantimonate (34 mg, 0.1 mmol, 20 mol%) were weighed into a 25 mL pressure-resistant Schlenk tube equipped with a magnetic stirring bar. The Schlenk tube was evacuated and backfilled with argon three times. DCE (900 μ L) and D₂O (100 μ L) were added. Liquid aldehydes were also added at this stage. The reaction mixture was subsequently heated to 100°C and stirred at this temperature for 16 hours. The resulting suspension was diluted with DCM, washed with an aqueous saturated solution of sodium bicarbonate (20 mL), and extracted with DCM (2 \times 20 mL). The combined organic layers were washed with distilled water (20 mL), dried over sodium sulfate and concentrated. The deuterated products were then purified by silica column chromatography with eluent systems of pentane and ethyl acetate.

Representative procedure for the deuteration of ketones: The ketone (0.5 mmol), *p*-chlorobenzoic acid (39 mg, 0.25 mmol, 0.5 equiv.), 2-methyl-3-trifluoromethyl-aniline (18 mg, 0.1 mmol, 20 mol%), dichloro(*p*-cymene)ruthenium(II) dimer (7.7 mg, 12.5 μ mol, 2.5 mol%), and silver hexafluoroantimonate (34 mg, 0.1 mmol, 20 mol%) were weighed into a 25 mL pressure-resistant Schlenk tube equipped with a magnetic stirring bar. The Schlenk tube was evacuated and backfilled with argon three times. DCE (300 μ L) and D₂O (200 μ L) were added. Liquid ketones were also added at this stage. The reaction mixture was subsequently heated to 120°C and stirred at this temperature for 16 hours. The resulting suspension was diluted with DCM, washed with an aqueous saturated solution of sodium bicarbonate (20 mL), and extracted with DCM (2 \times 20 mL). The combined organic layers were washed with water (20 mL), dried over sodium sulfate and concentrated. The deuterated products were then purified by silica column chromatography with eluent systems of pentane and ethyl acetate.

Acknowledgements

We acknowledge the support from the European Union (Flow Chemistry for Isotope Exchange, FLIX, 862179), the BMBF and the State of Mecklenburg-Western Pomerania. F.Y. thanks the National Natural Science Foundation of China (No. 21801056) for financial support. We thank Dr. Wolfgang Baumann for the measurement of ²H NMR spectra and the whole analytical team of UKAT for their kind support. Open access funding enabled and organized by Projekt DEAL.

Conflict of Interest

The authors declare no conflict of interest.

Keywords: C–H activation · hydrogen isotope exchange · ketones · ruthenium · transient directing group

- [1] a) J. Atzrodt, V. Derau, W. J. Kerr, M. Reid, *Angew. Chem. Int. Ed.* **2018**, *57*, 3022–3047; *Angew. Chem.* **2018**, *130*, 3074–3101; b) J. Atzrodt, V. Derau, W. J. Kerr, M. Reid, *Angew. Chem. Int. Ed.* **2018**, *57*, 1758–1784; *Angew. Chem.* **2018**, *130*, 1774–1802.
- [2] T. Pirali, M. Serafini, S. Carnini, A. A. Genazzani, *J. Med. Chem.* **2019**, *62*, 5276–5297.
- [3] E. M. Simmons, J. F. Hartwig, *Angew. Chem. Int. Ed.* **2012**, *51*, 3066–3072; *Angew. Chem.* **2012**, *124*, 3120–3126.
- [4] Recent examples: a) Q. Dherbassy, J.-P. Djukic, J. Wencel-Delord, F. Colobert, *Angew. Chem. Int. Ed.* **2018**, *57*, 4668–4672; *Angew. Chem.* **2018**, *130*, 4758–4762; b) R. A. Jagtap, C. P. Vinod, B. Punji, *ACS Catal.* **2019**, *9*, 431–441.
- [5] a) C. Rappe, W. H. Sachs, *Tetrahedron* **1968**, *24*, 6287–6290; b) J. Yao, R. F. Ervilia, *J. Am. Chem. Soc.* **1994**, *116*, 11229–11233; c) C. Berthelette, J. Scheigetz, *J. Labelled Compd. Radiopharm.* **2004**, *47*, 891–894; d) M. Zhan, T. Zhang, H. Huang, Y. Xie, Y. Chen, *J. Labelled Compd. Radiopharm.* **2014**, *57*, 533–539; e) Y. Chang, T. Myers, M. Wasa, *Adv. Synth. Catal.* **2020**, *362*, 360–364; f) K. I. Galkin, E. G. Gordeev, V. P. Ananikov, *Adv. Synth. Catal.* **2021**, *363*, 1368–1378.
- [6] a) J. R. Heys, A. Y. L. Shu, S. G. Senderoff, N. M. Phillips, *J. Labelled Compd. Radiopharm.* **1993**, *33*, 431–438; b) D. Heslop, P. R. Das, B. Evans, *J. Labelled Compd. Radiopharm.* **1995**, *36*, 497–502; c) G. J. Ellames, J. S. Gibson, J. M. Herbert, A. H. McNeill, *Tetrahedron* **2001**, *57*, 9487–6597; d) J. A. Brown, S. Irvine, A. R. Kennedy, W. J. Kerr, S. Andersson, G. N. Nilsson, *Chem. Commun.* **2008**, 1115–1117; e) A. R. Cochrane, S. Irvine, W. J. Kerr, M. Reid, S. Andersson, G. N. Nilsson, *J. Labelled Compd. Radiopharm.* **2013**, *56*, 451–454; f) J. A. Brown, A. R. Cochrane, S. Irvine, W. J. Kerr, B. Mondal, J. A. Parkinson, L. C. Paterson, M. Reid, T. Tuttle, S. Andersson, G. N. Nilsson, *Adv. Synth. Catal.* **2014**, *356*, 3551–3562; g) M. Parmentier, T. Hartung, A. Pfaltz, D. Muri, *Chem. Eur. J.* **2014**, *20*, 11496–11504; h) K. Jess, V. Derau, R. Weck, J. Atzrodt, M. Freytag, P. G. Jones, M. Tamm, *Adv. Synth. Catal.* **2017**, *359*, 629–638.
- [7] a) L. Piola, J. A. Fernández-Salas, S. Manzini, S. P. Nolan, *Org. Biomol. Chem.* **2014**, *12*, 8683–8688; b) P. Eisele, F. Ullwer, S. Scholz, B. Plietker, *Chem. Eur. J.* **2019**, *25*, 16550–16554.
- [8] R. Giles, G. Ahn, K. W. Jung, *Tetrahedron Lett.* **2015**, *56*, 6231–6235.
- [9] Concerning directing groups other than ketones, both ruthenium and palladium-catalyzed methodologies have been demonstrated as viable alternatives to iridium-catalyzed HIE. See ref. [7a] and: a) V. Müller, R. Weck, V. Derau, L. Ackermann, *ChemCatChem* **2020**, *12*, 100–104; b) S. Ma, G. Villa, P. S. Thuy-Boun, A. Homs, J.-Q. Yu, *Angew. Chem. Int. Ed.* **2014**, *53*, 734–737; *Angew. Chem.* **2014**, *126*, 753–756.
- [10] L.-L. Zhao, W. Liu, Z. Zhang, H. Zhao, Q. Wang, X. Yan, *Org. Lett.* **2019**, *21*, 10023–10027.
- [11] S. Kopf, H. Neumann, M. Beller, *Chem. Commun.* **2021**, *57*, 1137–1140.
- [12] a) P. Gandeepan, L. Ackermann, *Chem* **2018**, *4*, 199–222; b) S. St John-Campbell, J. A. Bull, *Org. Biomol. Chem.* **2018**, *16*, 4582–4595; c) B. Niu, K. Yang, B. Lawrence, H. Ge, *ChemSusChem* **2019**, *12*, 2955–2969; d) J. I. Higham, J. A. Bull, *Org. Biomol. Chem.* **2020**, *18*, 7291–7315.

- [13] a) F. Li, Y. Zhou, H. Yang, D. Liu, B. Sun, F.-L. Zhang, *Org. Lett.* **2018**, *20*, 146–149; b) Z.-Y. Li, H. H. C. Lakmal, X. Qian, Z. Zhu, B. Donnadieu, S. J. McClain, X. Xu, X. Cui, *J. Am. Chem. Soc.* **2019**, *141*, 15730–15736; c) G. Li, Q. Liu, L. Vasamsetty, W. Guo, J. Wang, *Angew. Chem. Int. Ed.* **2020**, *59*, 3475–3479; *Angew. Chem.* **2020**, *132*, 3503–3507.
- [14] O. K. Rasheed, *Synlett* **2018**, *29*, 1033–1036.
- [15] Y. Cheng, Y. He, J. Zheng, H. Yang, J. Liu, G. An, G. Li, *Chin. Chem. Lett.*, doi:10.1016/j.cclet.2020.09.044.
- [16] a) J. Xu, Y. Liu, Y. Wang, Y. Li, X. Xu, Z. Jin, *Org. Lett.* **2017**, *19*, 1562–1565; b) J. Wang, C. Dong, L. Wu, M. Xu, J. Lin, K. Wei, *Adv. Synth. Catal.* **2018**, *360*, 3709–3715.
- [17] A. E. Hande, V. B. Ramesh, K. R. Prabhu, *Chem. Commun.* **2018**, *54*, 12113–12116.
- [18] P. Piehl, R. Amuso, E. Alberico, H. Junge, B. Gabriele, H. Neumann, M. Beller, *Chem. Eur. J.* **2020**, *26*, 6050–6055.
- [19] Substrates 16 and 17 engage in some side reactions and thus give somewhat diminished, but nevertheless synthetically useful yields of deuterated products.

Manuscript received: February 5, 2021
Accepted manuscript online: April 12, 2021
Version of record online: June 14, 2021

9.3 Base-Mediated Remote Deuteration of *N*-Heteroarenes – Broad Scope and Mechanism

Sara Kopf, Jiali Liu, Robert Franke, Haijun Jiao, Helfried Neumann, and Matthias Beller.

Eur. J. Org. Chem. **2022**, e202200204.

DOI: 10.1002/ejoc.202200204

© 2021 The Authors. European Journal of Organic Chemistry published by Wiley-VCH GmbH.

Electronic supporting information is available online.

Highlighted as Front Cover: <https://doi.org/10.1002/ejoc.202200524>

Contribution: The work on this manuscript was carried out in collaboration with Jiali Liu. I discovered the reaction and planned and performed the experimental work, including optimization, evaluation of the substrate scope as well as mechanistic experiments. I was involved in discussions regarding planning and analysis of the DFT calculations. In addition, I evaluated all analytical data and wrote the experimental part of the supporting information. I wrote the first draft of introduction, experimental results, and conclusions of the manuscript. Lastly, I was involved in the design of the cover picture. My contribution approximately amounts to 65%.

Signature of the student
(Sara Kopf)

Signature of the supervisor
(Prof. Matthias Beller)

Very Important Paper



Base-Mediated Remote Deuteration of *N*-Heteroarenes – Broad Scope and Mechanism

Sara Kopf,^[a] Jiali Liu,^[a, b, c] Robert Franke,^[b, c] Haijun Jiao,^{*,[a]} Helfried Neumann,^{*,[a]} and Matthias Beller^{*,[a]}

Deuterated organic molecules provide the basis for many applications in life sciences and material research. Thus, methodologies to access labeled compounds with defined selectivity continue to be important. Using KOtBu as base and DMSO-*d*₆ as deuterium source, we present a general and applicable method for the selective deuteration of a set of

nitrogen-containing heterocycles (pyridines, azines and bioactive molecules). Experimental and DFT mechanistic studies indicate that this reaction proceeds *via* deprotonation of the substrates by the dimsyl anion. The relative thermodynamic stability of the heterocycle anions determines the distribution and degree of deuteration.

Introduction

Kinetic isotope effects stemming from the replacement of the lightest isotope of hydrogen, protium, by its heavier congeners, deuterium and tritium, is a common concept in physical organic chemistry for mechanistic studies of many organic transformations.^[1] The profound mass difference of the isotopes of hydrogen results in a measurably lower zero-point energy for C–D bonds compared to C–H bonds, leading to higher activation barriers,^[2] and the comparative measurement of reaction rates for substrates containing C–H and C–D bonds is an important tool to probe the participation of the C–H bond cleavage step in mechanisms of organic reactions.^[3] The significant difference in stability and activity between C–H and C–D bonds provides the basis for applications in life sciences where the selective replacement of protium by deuterium at specific, metabolically labile, sites in a drug molecule can enhance the pharmacokinetic properties such as metabolic stability.^[2] Successfully employing this approach, the first deuterated drug, Austedo (deutetrabenazine), was launched in 2017 and currently more deuterated drug candidates are in clinic trials.^[2] While this application requires chemical reactions

that enable selective installation of deuterium atoms in drug scaffolds, methodologies that drive the incorporation of several deuterium atoms at once are highly sought after for the preparation of stable isotopically labeled internal standards for mass spectrometric bioanalytics.^[4,5]

In this context, reactions targeting structural moieties common in bioactive compounds are especially useful. Being the second most common nitrogen heterocycle and the most common nitrogen-containing aromatic heterocycle in drugs approved by the federal drug administration in the US (FDA) as of 2014, pyridines appear to be particularly attractive substrates for deuteration reactions.^[6] Their further use as ligands in material science^[7] and homogeneous catalysis^[8] may open up more possible applications for deuterated compounds.^[9,8] It is therefore not surprising that methodologies for the deuteration of pyridines have been developed as early as in the 1960s.^[9]

For the selective deuterium installation in specific positions of pyridines, prefunctionalized substrates, such as pyridine carboxylic acids or halogenated pyridines, have been used in deuterodehalogenation^[9a,10] and other reductive deuteration reactions.^[9a] Similarly, directed lithiation with subsequent hydrolysis can afford good selectivity.^[11] However, the former reaction may suffer from less accessible substrates and selectivity problems in the prefunctionalization step, while the latter requires harsh reaction conditions, impeding the use for late stage deuteration of sensitive substrates. Therefore, methodologies allowing for the direct exchange of a hydrogen atom for a deuterium atom in one step (hydrogen isotope exchange, HIE) at a late stage are more desirable.^[4,3] While the moiety of pyridine has been famously used as a directing group for the iridium-catalyzed HIE in the *ortho* positions of adjacent aromatic rings (Scheme 1)^[12] and the increased reactivity of benzylic positions at pyridine rings can be exploited for acid-catalyzed HIE,^[13] more drastic conditions such as heating the substrate in a solution of NaOD in supercritical D₂O can enable complete deuteration of all positions in a pyridine ring (Scheme 1).^[14] Heterogeneous^[9,5] and homogeneous^[16] noble metal catalysts facilitate this transformation under milder conditions. However, the selective deuteration of positions

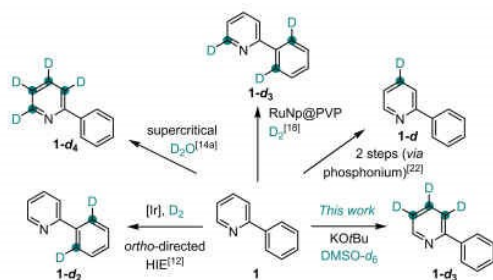
[a] S. Kopf, J. Liu, Dr. H. Jiao, Dr. H. Neumann, Prof. Dr. M. Beller
Leibniz-Institut für Katalyse e. V., Rostock
Albert-Einstein-Straße 29a, 18059 Rostock, Germany
E-mail: Helfried.Neumann@catalysis.de
Haijun.Jiao@catalysis.de
Matthias.Beller@catalysis.de
www.catalysis.de

[b] J. Liu, Prof. Dr. R. Franke
Evanik Operations GmbH
Paul-Baumann-Straße 1, 45772 Marl, Germany

[c] J. Liu, Prof. Dr. R. Franke
Lehrstuhl für Theoretische Chemie
Ruhr-Universität Bochum, 44780 Bochum, Germany

Supporting information for this article is available on the WWW under
<https://doi.org/10.1002/ejoc.202200204>

© 2022 The Authors. European Journal of Organic Chemistry published by Wiley-VCH GmbH. This is an open access article under the terms of the Creative Commons Attribution Non-Commercial License, which permits use, distribution and reproduction in any medium, provided the original work is properly cited and is not used for commercial purposes.



Scheme 1. Selectivity patterns accessed with various HIE methodologies for the labeling of 2-phenylpyridine.

proximal to the heteroatom has been observed more often when using heterogeneous catalysts^[17] and especially good results under milder conditions have been achieved with ruthenium nanoparticles (Scheme 1).^[8] In this case, the observed selectivity results from the directing effect of the nitrogen atom when coordinated to the metal surface.^[18] On the other hand, when homogeneous catalysts are sufficiently tuned to preferentially undergo C–H activation in electron-rich positions, similar results have been achieved.^[19]

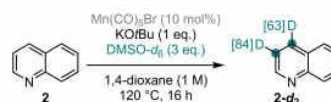
To allow for a broad range of labeling possibilities, it is desirable to have a toolkit that can access various selectivity patterns in the deuteration of pyridines. To this end, interesting approaches have been the combination of homogeneous and heterogeneous catalysts to combine their respective selectivities,^[20] the use of catalysts that exhibit a purely sterically driven selectivity^[21] as well as the implementation of a two-step protocol that enables selective deuteration in position 4 of pyridines (Scheme 1).^[22] On the other hand, a preference for the distal positions of pyridine derivatives was observed in kinetic experiments with osmium complexes^[23] as well as with NaOD.^[24] These reports arose our interest in remote labeling strategies, leading to the development of a methodology for the HIE of distal positions in pyridine derivatives with the aim to complement the existing labeling strategies for this substrate class. It should be noted that during the preparation of this manuscript, a related study on the deuteration of pyridines was published.^[25] Herein, we report our work including a complementary scope and additional mechanistic insights based on experiments and DFT analysis.

Results and Discussion

Inspired by a manganese-catalyzed methodology for the reduction of quinolines reported by our group^[26] and aiming to extend our recent efforts in using manganese catalysts for HIE,^[27] we tested the reaction of various deuterium sources with quinoline with and without base in the presence of 10 mol% manganese pentacarbonyl bromide. Using DMSO-*d*₆ and KOtBu, we were pleased to see that a significant amount of deuterium

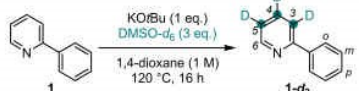
had been introduced into the substrate. Surprisingly, assignment of the NMR resonances using 2D NMR spectroscopy revealed that deuterium had been incorporated in positions 3 and 4, remote from the potentially coordinating nitrogen atom (Scheme 2). Intrigued by this selectivity, we performed control reactions in the absence of the manganese complex and found that the same result can be achieved with only base and deuterium source. A quick survey of the literature showed that the combination of KOtBu and DMSO-*d*₆ had previously been used for the base-mediated deuteration of benzylic positions, although the pyridine and quinoline aromatic positions themselves remained largely unreactive towards isotopic exchange in the corresponding reports.^[28] Other base-mediated HIE methodologies have targeted α -carbonyl positions or alkynes among others but have not been used on pyridines.^[29] Encouraged by the complementarity of this reaction to other reports using the same deuteration system and to the existing strategies for the deuteration of azines, we decided to develop a general methodology for the remote deuteration of pyridine derivatives as well as bioactive molecules based on our findings.

To ensure a more general reaction and to allow for better comparison with a variety of previously reported methodologies, we used 2-phenylpyridine as model substrate for optimization. Under our initial reaction conditions and under an inert atmosphere, high deuterium incorporation was observed in distal positions 3, 4 and 5 (> 80%), whereas only 23% of the hydrogen atom in α -nitrogen position 6 was exchanged and the phenyl ring remained untouched (Table 1, entry 1). This observed selectivity is remarkably different from previous HIE methodologies on pyridine substrates (*vide supra*). Deuterium incorporation for the targeted positions could be raised above 90% by using DMSO-*d*₆ as solvent (Table 1, entry 2) and selectivity was further improved by adding small amounts of water to the reaction mixture (Table 1, entry 3). This is probably due to the diminished overall basicity of the reaction mixture and the resulting slightly decreased reactivity. Lastly, it was found that reactivity was not impaired by increasing the scale of the reaction or by lowering the temperature to 90 °C (Table 1, entries 4 and 5). At the same time, the recovery of the deuterated product was slightly improved to 89% (Table 1, entry 4), hinting at a better chemoselectivity at lower temperature. Sequential deuteration of the isolated product could increase the deuterium content to 98% in the remote positions (entry 6), but a third run failed to raise the deuterium incorporation further (entry 7). Interestingly, the second and third deuteration cycle additionally resulted in an increased deuterium incorporation in the *ortho* positions of the phenyl



Scheme 2. Initial experiment: Remote deuteration of quinoline with KOtBu and DMSO-*d*₆.

Table 1. Optimization of the deuteration of 2-phenylpyridine.



Entry ^[a]	Variation	D (3/4/5) [%] ^[b]	D (6) [%]	D (o/m/p) [%]	yield [%] ^[c]
1 ^[d]	none	86	23	<10	83
2 ^[e]	DMSO- <i>d</i> ₆ as solvent (17 eq.)	96	20	13 (o)	82
3 ^[f]	DMSO- <i>d</i> ₆ as solvent, 1.1 eq. H ₂ O	95	14	<10	84
4 ^[g]	DMSO- <i>d</i> ₆ as solvent, 1.1 eq. H ₂ O, 90 °C	94	18	<10	89
5	DMSO- <i>d</i> ₆ as solvent, 1.1 eq. H ₂ O, 90 °C, 5 mmol	95	11	<10	83
6	DMSO- <i>d</i> ₆ as solvent, 1.1 eq. H ₂ O, 90 °C, 2 nd cycle	98	12	15	n.d.
7	DMSO- <i>d</i> ₆ as solvent, 1.1 eq. H ₂ O, 90 °C, 3 rd cycle	98	13	20	n.d.
8	DMSO- <i>d</i> ₆ as solvent, 1.1 eq. H ₂ O, 0.5 eq. KOtBu	83	11	<10	n.d.
9	D ₂ O	<10	<10	<10	n.d.
10	Acetone- <i>d</i> ₆	<10	<10	<10	n.d.
11	THF- <i>d</i> ₈	<10	15	<10	n.d.
12	NaOtBu, DMSO- <i>d</i> ₆ as solvent, 90 °C	<10	<10	<10	n.d.
13	LiOtBu	<10	<10	<10	n.d.
14	KOH, DMSO- <i>d</i> ₆ as solvent, 90 °C	43 ^[h] , 70 ^[i]	16	<10	n.d.
15	18-C-6 (1 eq.)	48	<10	<10	n.d.
16	<i>n</i> BuLi (1 eq.) and KOtBu (1 eq.), dry DMSO- <i>d</i> ₆ as solvent, rt	92 ^[j] , 66 ^[k]	39	10	n.d.

[a] Scale: 0.5 mmol, work-up: extraction, then NMR in CDCl₃; deuterium incorporation was determined by ¹H NMR using the resonances of the non-deuterated *meta* and *para* positions in the phenyl substituent as a reference; [b] average; [c] isolated yield; [d] average of 2 runs; [e] average of 5 runs; [f] average of positions 3 and 5; [g] position 4; [h] average of positions 3 and 4; [i] position 5.

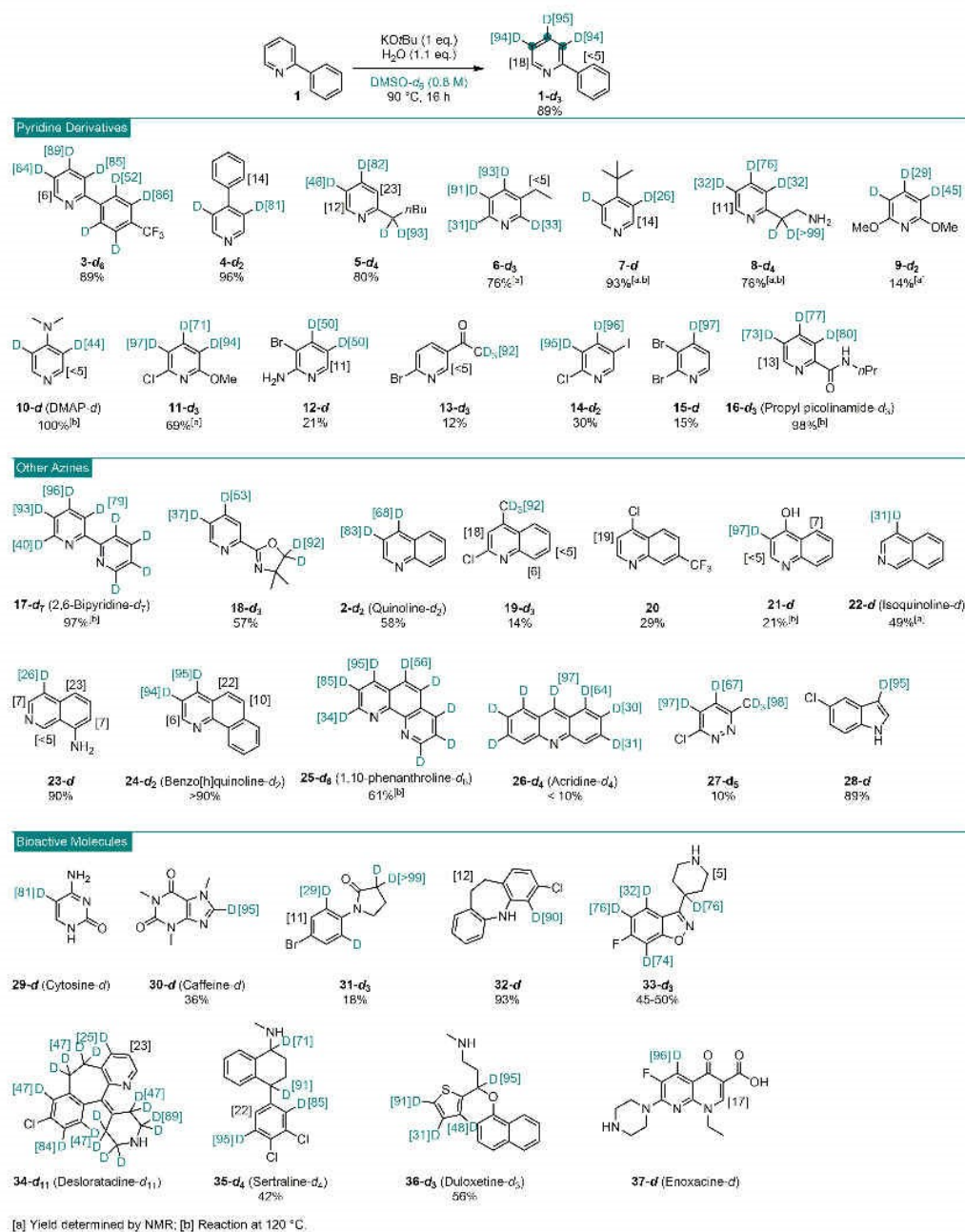
substituent. Overall, the reaction was very clean with small amounts (4% yield) of 2-phenyl-6-trideuteromethylpyridine being the only observed byproduct. Its formation likely stems from a competing Minisci-type radical trideuteromethylation as reported previously with DMSO-*d*₆.^[10] Appreciable results could still be achieved with base loadings as low as 0.5 eq. (Table 1, entry 8). Interestingly, the reaction proved to be remarkably specific to both the deuterium source and the base: Other deuterium sources did not afford any isotopic exchange at all (Table 1, entries 9–11) and even simple replacement of KOtBu by NaOtBu or LiOtBu completely shut down reactivity (Table 1, entries 12 and 13), whereas some reactivity was retained with KOH (Table 1, entry 14). Moreover, sequestration of potassium by addition of 18-C-6 significantly lowered the efficiency of the reaction (Table 1, entry 15), indicating that the cation plays a significant role in this transformation. When moving to Schlosser's base, the reaction could be carried out at room temperature, albeit with a different selectivity (Table 1, en-

try 16). Presumably, the reaction partially proceeds *via* dianions resulting from deprotonation of the *ortho*-metalated intermediate under these strongly basic conditions. This hypothesis would explain the higher amount of deuterium incorporation observed in position 6 compared to the reaction with KOtBu as well as the reduced deuteration in position 5. The latter can be tentatively explained by the low stability of the vicinal dianion.

The reaction conditions explored above were applicable to a range of substituted pyridines and the selectivity pattern was maintained irrespective of the substitution sites (Scheme 3). High deuterium incorporation is usually obtained for the distal positions while deuteration in pyridine α -positions remained low. Concomitant deuteration was observed at more acidic sites such as in benzylic^[21] (Scheme 3, compounds 5-*d*₂ and 8-*d*₂) and α carbonyl (Scheme 3, compound 13-*d*₂) positions as well as in a trifluoromethyl-substituted phenyl ring (Scheme 3, compound 3-*d*₂). The reaction appeared to be somewhat sensitive to sterics and lower deuterium contents were measured in the proximity of larger aliphatic residues (Scheme 3, position 3 in compound 5-*d*₂; positions 3 and 5 in compound 7-*d*). While the reactivity appears to be higher for electron-deficient substrates, for more electron-rich substrates a bias of the deuteration towards the *ortho* positions of electron-donating substituents could be observed, hinting at a change in mechanism in these cases (Scheme 3, compounds 9-*d*₂ and 10-*d*). High recoveries of the deuterated products were observed for pyridines exhibiting aromatic, aliphatic, trifluoromethyl, amide, as well as tertiary and free amine substituents, indicative of a good tolerance for these functional groups. However, halogenated substrates afforded a range of side products and therefore lower yields, presumably resulting from competing halogen transfer reactions under the basic reaction conditions.^[21] Pyridines exhibiting cyano substituents, aldehyde moieties or terminal deins and alkynes decomposed under the reaction conditions.

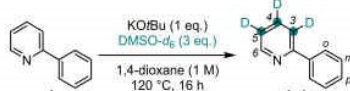
When moving beyond simple substituted pyridine derivatives, we were especially delighted to see that widely used ligands such as 2,6-bipyridine (Scheme 3, compound 17-*d*₂), 1,10-phenanthroline (Scheme 3, compound 25-*d*₂) and oxazolidinone 18-*d*₂ afforded high deuterium contents along with useful yields. Further, some bioactive molecules could be successfully labeled applying our methodology (Scheme 3, compounds 29–37). For these molecules, deuterium was not only incorporated in heterocycles (Scheme 3, compounds 29-*d*, 30-*d*, 33-*d*₂, 34-*d*₂, 36-*d*₂, 37-*d*) but also in chloro-substituted arenes (Scheme 3, 32-*d*, 34-*d*₁₁, 35-*d*₂) as previously reported for HIE reactions using KOtBu and DMSO-*d*₆.^[22]

Having confirmed that the unusual remote deuteration pattern is consistently observed in the labeling reactions of several substrates, we became interested in understanding its origins. Initially, the fact that the reaction was significantly impaired when carried out at air (Table 2, entry 2) or in the presence of known radical scavengers such as (2,2,6,6-tetramethylpiperidin-1-yl)oxyl (TEMPO; Table 2, entry 3 and 4), *p*-benzoquinone (Table 2, entry 5) or butylated hydroxytoluene (BHT; Table 2, entry 6) led us to assume that free radicals could be involved in the reaction mechanism.^[22] Besides, as no drastic differences were observed for the control reaction in the dark



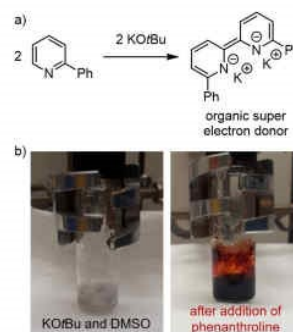
Scheme 3. Scope of the remote deuteration of pyridine derivatives.

Table 2. Effects of air and radical scavengers on the deuteration of pyridines.



Entry ^[a]	Variation	D (3) [%]	D (4) [%]	D (5) [%]
1 ^[b]	none	94	95	94
2	at air	2	11	6
3	TEMPO (1 eq.)	24	66	38
4	TEMPO (3 eq.)	15 ^[c]	15 ^[c]	16
5	<i>p</i> -benzoquinone (1 eq.)	1	1	1
6	BHT (1 eq.)	0	0	0
7	in the dark	66	94	84

[a] Scale: 0.5 mmol, crude NMRs were taken directly taken in the reaction solvent (DMSO-*d*₆), deuterium incorporation was determined by ¹H NMR using the resonances of the non-deuterated *meta* and *para* positions in the phenyl substituent as a reference. [b] Average of 5 runs. [c] Positions 3 and 4 are average values.



Scheme 4. a) Initially assumed formation of organic super electron donors from pyridine derivatives with KOtBu. b) Color change observed after the addition of heteroarenes (in this case: 1,10-phenanthroline) to a solution of KOtBu in DMSO-*d*₆.

(Table 2, entry 7), we reasoned that the reaction most likely proceeds by a ground-state pathway.

Given the rich literature precedence for this type of chemistry and its concordance with our results, we hypothesized that dimeric organic super electron donors might form from deprotonation of the substrate by KOtBu (Scheme 4a).^[33] They could then participate in single electron transfer (SET) pathways, thus kick-starting a radical chain reaction. In line with this hypothesis, we had observed intense color change when adding substrate to a solution of KOtBu in DMSO-*d*₆ (Scheme 4b), indicative of the formation of conjugated dianionic species. Further, a similarly remarkable specificity for certain potassium-containing bases has been observed for previously reported reactions that proceed *via* the formation of organic super electron donors.

To further evaluate the possibility of a radical mechanism, we performed density functional theory (DFT) calculations and

started by comparing the relative thermal stabilities of hypothesized intermediates to the observed selectivity. Based on previous theoretical studies,^[34] we chose the M062X functional^[35] with the 6-311+G(d,p) basis set for optimization in DMSO-*d*₆ solvent based on solute electron density (SMD).^[36] Corrected Gibbs free energies at 298 K and 1 atm with solvation effect are used for our following discussions.

We computed the relative stability of all possible positional isomers of the radical species for 2-phenylpyridine (Figure 1). It was shown that the most stable radical isomer is at the D6 position (−21.0 kJ/mol), followed by the *ortho* position (−5.7 kJ/mol) of the phenyl ring and the D3 position (−1.6 kJ/mol) of the pyridine ring. The radical at the D4 position (0.0 kJ/mol) as well as those at the *meta* and *para* positions (0.9 and 1.8 kJ/mol) are close in energy. The least stable radical is at the D5 position (9.2 kJ/mol). Considering that the deuteration degree will follow the stability order of the radical species, the

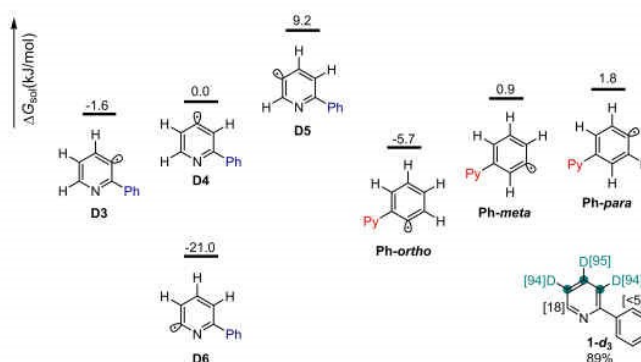


Figure 1. Relative Gibbs free energies of radical species of 2-phenylpyridine.

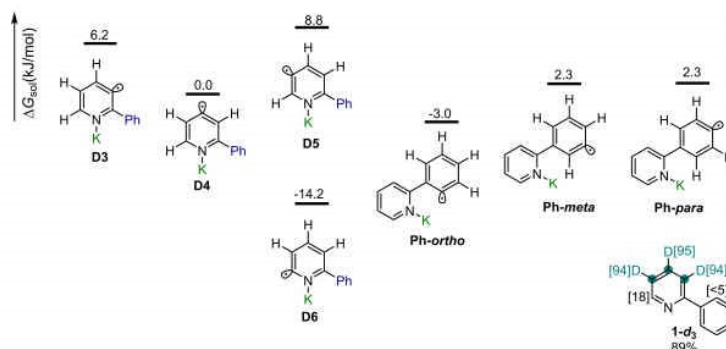


Figure 2. Relative Gibbs free energy of K^+ coordinated radical species of 2-phenylpyridine.

corresponding relative stability of these radical species does not agree with the deuteration distributions found experimentally.

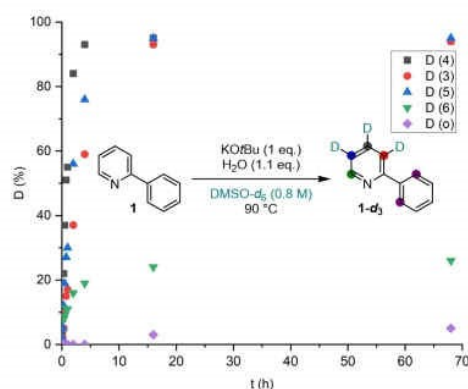
In searching an alternative explanation for our experimentally observed selectivity, we explored the effect of potassium coordination on the stability of hypothesized radical intermediates. It was found that K^+ prefers coordinating with the nitrogen center instead of the radical center and the aromatic face site. As shown in Figure 2, the presence of K^+ changes the relative stability to some extent, however, it does not change the relative order; and the **D6** radical is still the most abundant intermediate.

Next, we briefly investigated steric effects from $KOtBu$ coordination to the pyridine nitrogen atom that could override thermodynamic preferences. However, we quickly discarded this hypothesis after observing a clear indication for a polar mechanism from additional experimental work for the analysis of linear free energy relationships with Hammett parameters. As shown in Figure 3, we found a very good correlation and a positive slope for Hammett σ and σ^- values with the relative initial reaction rates of substrates with various substituents at the *p*-position in the phenyl ring of 2-phenylpyridine, indicative of a transition state with a build-up of negative charge (Figure 3a and b), while only poor correlation was observed for radical σ parameters (Figure 3c).

In general, the combination of DMSO and $KOtBu$ is considered as a super-base system²⁷¹ and the corresponding anionic mechanism has been proposed.^{28b1} Thus, we calculated the relative Gibbs free energies of the anionic species of 2-phenylpyridine (Figure 4). Apparently, the stability of these anions can be divided into two groups, the more stable one including the **D3** (1.2 kJ/mol), **D4** (0.0 kJ/mol) and **D5** (2.8 kJ/mol) anions in very close energy; and the much less stable one including the **D6** anion (19.2 kJ/mol) as well as the *ortho*-, *meta*- and *para*-anions of the phenyl ring (13.1, 18.8 and 19.0 kJ/mol, respectively). This shows that deuteration at the 3, 4 and 5-positions of the pyridine ring should be most favored thermodynamically and deuteration at other positions is less likely. This agrees perfectly with our experimental observation,

i.e., 3-, 4 and 5-positions of the pyridine ring are nearly equally populated (94, 95 and 94%, respectively). In addition, long time and sequential experimental results also show the possible deuteration at the **D6** position as well as at the *ortho* position of the phenyl ring (Scheme 5). Remarkably, kinetic analysis revealed that the most stable anion is deuterated first (Scheme 5, position 4). Therefore, the anionic mechanism can explain the generation of the main product thermodynamically.

Considering the existence of potassium in the reaction system, we contemplated the effect of this cation on the stability of anions and the corresponding data is shown in Figure 5. The optimized structures show that the pyridine nitrogen atom interacts with K^+ for **D6** and **Ph-ortho** anions which increases the thermal stability. However, those more stable **D6** (−5.3 kJ/mol) and **Ph-ortho** (−6.8 kJ/mol) anions pose lower yield than less stable **D4** (0.0 kJ/mol) and **D5** (0.8 kJ/mol), so this mechanism is not consistent with “thermal selectivity”. In summary, the coordination of K^+ can affect the relative stability



Scheme 5. Kinetic profile for the deuteration of 2-phenylpyridine.

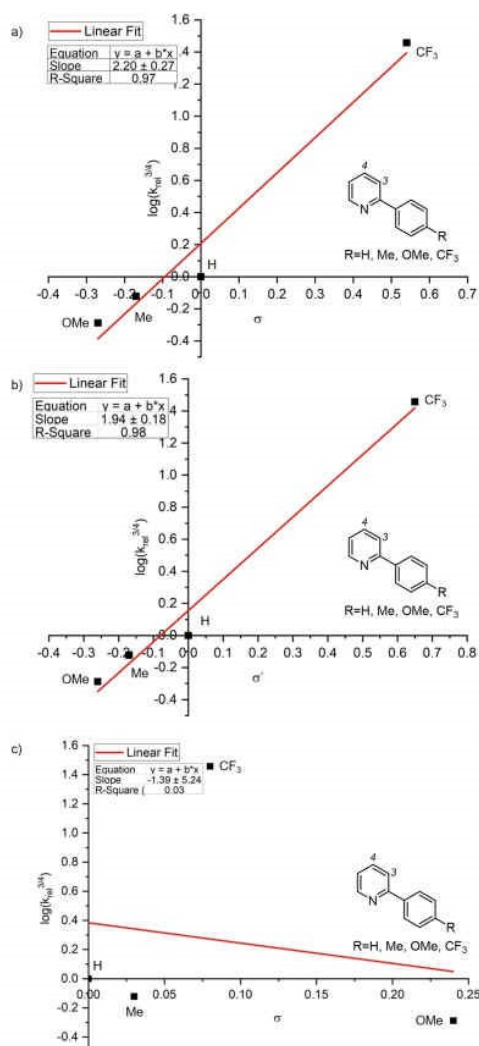


Figure 3. Hammett plots for the relative rates of deuteration in positions 3 and 4 for variously substituted 2-phenylpyridines a) with standard σ parameters, $R^2 = 0.97$; b) with σ^+ parameters, $R^2 = 0.98$; c) with σ parameters, $R^2 = 0.93$.

of anions and there is no correlation between relative Gibbs free energy and deuteration yield. Therefore, this reaction mechanism is not possible thermodynamically.

From the above experimental and computational results, we know that the free anionic mechanism can account well for the deuteration preference in experiment for 2-phenylpyridine. The more thermally stable the pyridine ring anion, the higher

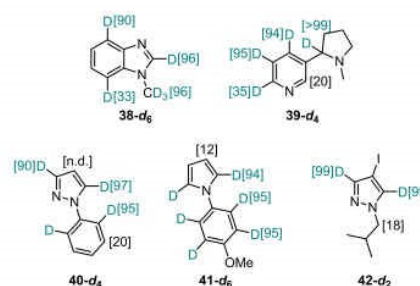
the experimental deuterated yield. In addition, we computed the effect of pre-deuteration on the phenyl substituent (Table S13) and found that starting with 1- d_1 , 1- d_2 and 1- d_3 , the stability of the corresponding anions at the phenyl substituent does not change and the observed increase in the deuteration degree at the *ortho* position of the phenyl ring should be due to the excess of the deuterium source.

Furthermore, we found the relative deuterated yield for other pyridine derivatives, *N,N*-dimethylpyridin-4-amine, 4-(*tert*-butyl)pyridine, 2-(4-(trifluoromethyl)phenyl)pyridine, 2,2'-bipyridine, 4-chloro-7-(trifluoromethyl)quinoline, quinoline and phenanthroline, can also be consistent with an anionic mechanism (Figure S11.1–S11.7). Besides, excellent correlation between relative thermal stability of anionic species and deuteration yield are also found for other experimental results^{25,28b} of the remote deuteration of pyridine derivatives, such as pyridine, 3,4-dimethylpyridine, 2,3-dimethylpyridine, 2-bromopyridine, 2-bromo-5-methylpyridine, 6-bromonicotinonitrile and 1-(difluoromethyl)-4-fluorobenzene (Figure S11.8–S11.14), as well as the deuteration of bioactive molecules in our own scope (caffeine, Figure S11.15). Using the anion stabilities, we have been able to successfully predict the order of deuterium incorporation in the different positions of new substrates (Scheme 6, Figure S11.16–S11.19). Although we have tried to explain and predict the deuteration yield on the basis of the ability of neutral substrates to generate anionic species, this has failed due to the different kinetic properties of different substrates.

Lastly, a measured ΔE of 1.2 for positions 3 and 4 and 1.3 for position 5 hint at a reversible reaction. Since the ΔE is small, the rate-determining step might not involve C–H cleavage at the substrate (Scheme 7). Rather, deuteration of the pyridyl anions or the generation of the dimethyl anion in the first place may represent the steps with the highest barriers.

Conclusion

In conclusion, we report a general and applicable base-mediated methodology for the remote deuteration of pyridine derivatives and other aromatic heterocycles with DMSO- d_6 as



Scheme 6. Results of the deuteration reaction on substrates previously studied computationally.

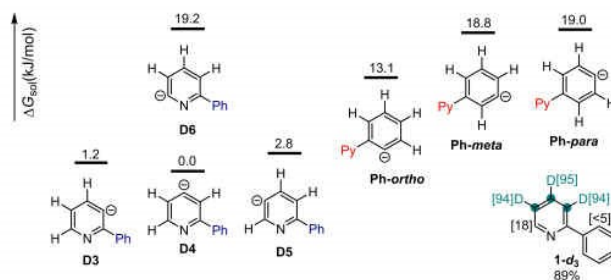


Figure 4. Relative Gibbs free energy of anionic species of 2-phenylpyridine.

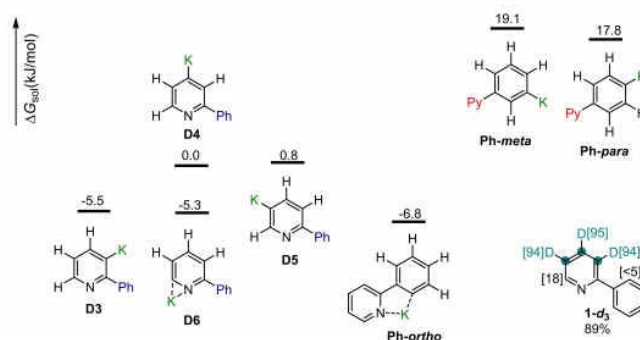


Figure 5. Relative Gibbs free energy of coordinated K⁺ and anion species of 2-phenylpyridine.

deuterium source. Experimental and mechanistic studies including DFT calculations indicate that the reaction takes place via an anionic pathway and that thermodynamic stability of the respective anions corresponds well with the regioselectivity of deuteration. We have shown how these insights can be applied to predict the main deuteration sites of new substrates and we believe that these results will prove useful for the preparation of labeled MS standards and deuterated drugs. In a broader context, new transformations based on the generation of pyridyl anions by deprotonation with the dimsyl anion might be inspired by this report.

Experimental Section

General Deuteration Procedure: Potassium *tert*-butoxide (56 mg, 0.5 mmol, 1.0 eq.) and the substrate (if solid; 0.5 mmol) were weighed into a 25 mL pressure-resistant Schlenk tube equipped with a magnetic stirring bar. The Schlenk tube was capped with a rubber septum and evacuated and backfilled with argon three times. DMSO-*d*₆ (600 µL, 8.5 mmol, 17.0 eq.) was added followed by the substrate (if liquid; 0.5 mmol) and distilled water (10 µL, 5.6 mmol, 1.1 eq.). The Schlenk tube was closed, and the reaction mixture was subsequently heated to 90 °C and stirred at this temperature for 16 h. The resulting mixture was diluted with DCM, washed with brine (20 mL), and extracted with DCM (2 × 20 mL).

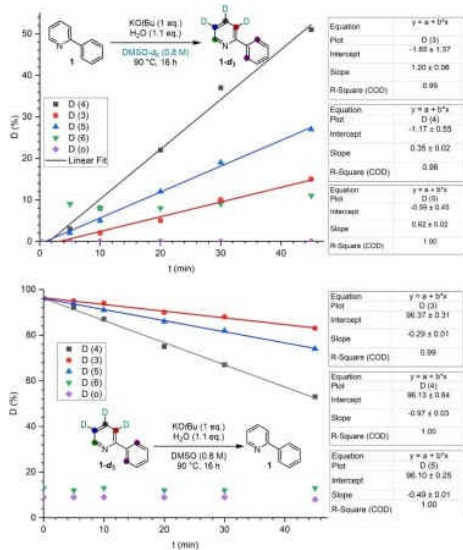
The combined organic layers were dried over sodium sulfate and concentrated. Some compounds were sufficiently pure after extraction. The other deuterated products were purified by silica column chromatography.

Acknowledgements

We acknowledge the support from the European Union (Flow Chemistry for Isotope Exchange, FLIX, 862175), the BMBF and the State of Mecklenburg-Western Pomerania. We thank the analytical team of LIKAT for their kind support. J.L. thanks the European Union's Horizon 2020 research and innovation programme under the Marie Skłodowska-Curie grant agreement No. 859910. We thank Florian Bourriquen for insightful discussions. Open Access funding enabled and organized by Projekt DEAL.

Conflict of Interest

The authors declare no conflict of interest.



Scheme 7. Plots of initial velocities of the deuteration and the reverse reaction for the determination of kinetic isotope effects.

Data Availability Statement

The data that support the findings of this study are available in the supplementary material of this article.

Keywords: Density functional calculations • Deuterium • Heterocycles • Hydrogen isotope exchange • Isotopic labeling

- [1] a) S. A. Blum, K. L. Tan, R. G. Bergman, *J. Org. Chem.* 2003, 68, 4127–4137; b) G. Lloyd-Jones, M. P. Muñoz, *J. Labelled Compd. Radiopharm.* 2007, 50, 1072–1087; c) M. Gómez-Gallego, M. A. Sierra, *Chem. Rev.* 2011, 111, 4857–4963; d) E. M. Simmons, J. F. Hartwig, *Angew. Chem. Int. Ed.* 2012, 51, 3066–3072; *Angew. Chem.* 2012, 124, 3120–3126; e) S. Kopf, F. Bourriquet, W. Li, H. Neumann, K. Junge, M. Beller, *Chem. Rev.* 2022, 122, 6634–6718.
- [2] a) J. Atzrodt, V. Derdau, W. J. Kerr, M. Reid, *Angew. Chem. Int. Ed.* 2018, 57, 1758–1784; *Angew. Chem.* 2018, 130, 1774–1802; b) T. Pirali, M. Serafini, S. Cargini, A. A. Genazzani, *J. Med. Chem.* 2019, 62, 5276–5297.
- [3] J. Atzrodt, V. Derdau, W. J. Kerr, M. Reid, *Angew. Chem. Int. Ed.* 2018, 57, 3022–3047; *Angew. Chem.* 2018, 130, 3074–3101.
- [4] E. Vitaku, D. T. Smith, J. T. Njardarson, *J. Med. Chem.* 2014, 57, 10257–10274.
- [5] a) V. Marin, E. Holder, R. Hoogenboom, U. S. Schubert, *Chem. Soc. Rev.* 2007, 36, 618–635; b) B. Happ, A. Winter, M. D. Hager, U. S. Schubert, *Chem. Soc. Rev.* 2012, 41, 2222–2255; c) A. Gorczyński, J. M. Harrowfield, V. Patroniak, A. R. Stefankiewicz, *Chem. Rev.* 2016, 116, 14620–14674.
- [6] a) G. Desimoni, G. Faita, P. Quadrelli, *Chem. Rev.* 2003, 103, 3119–3154; b) V. C. Gibson, C. Redshaw, C. A. Solan, *Chem. Rev.* 2007, 107, 1745–1776; c) J. I. van der Vlugt, J. N. H. Reek, *Angew. Chem. Int. Ed.* 2009, 48, 8832–8846; *Angew. Chem.* 2009, 121, 8990–9004; d) G. Yang, W. Zhang, *Chem. Soc. Rev.* 2018, 47, 1783–1810.
- [7] a) J. B. Grimm, L. Xie, J. C. Casler, R. Patel, A. N. Tkachuk, N. Falco, H. Choi, J. Lippincott-Schwartz, T. A. Brown, B. S. Glick, Z. Liu, L. D. Davis, *JACS Au* 2021, 1, 690–696; b) H. J. Bae, J. S. Kim, A. Yakubovich, J. Jeong, S. Park, J. Chwae, S. Ishibe, Y. Jung, V. K. Rai, W.-J. Son, S. Kim, H. Choi, M. H. Baik, *Adv. Opt. Mater.* 2021, 9, 2170059.
- [8] J. Chen, R. J. M. Klein Gebbink, *ACS Catal.* 2019, 9, 3564–3575.
- [9] a) C. G. Macdonald, J. S. Shannon, *Tetrahedron Lett.* 1964, 45, 3351–3354; b) J. A. Zoltewicz, C. L. Smith, *J. Am. Chem. Soc.* 1966, 88, 4766–4767; c) J. A. Zoltewicz, C. L. Smith, *J. Am. Chem. Soc.* 1967, 89, 3358–3359; d) G. E. Calf, J. L. Garnett, V. A. Pickles, *Aust. J. Chem.* 1968, 21, 961–972; e) J. A. Zoltewicz, C. L. Smith, J. D. Meyer, *Tetrahedron* 1968, 24, 2269–2274.
- [10] a) X. Wang, M.-H. Zhu, D. P. Schuman, D. Zhong, W.-Y. Wang, L.-Y. Wu, W. Liu, B. M. Stoltz, W.-B. Liu, *J. Am. Chem. Soc.* 2018, 140, 10970–10974; b) C. Liu, S. Han, M. Li, X. Chong, B. Zhang, *Angew. Chem. Int. Ed.* 2020, 59, 18527–18531; *Angew. Chem.* 2020, 132, 18685–18689; c) W. Li, R. Qu, W. Liu, F. Bourriquet, S. Bartling, N. Rockstroh, K. Junge, M. Beller, *Chem. Sci.* 2021, 12, 14033–14038; d) Y. Li, Z. Ye, Y.-M. Lin, Y. Liu, Y. Zhang, L. Gong, *Nat. Commun.* 2021, 12, 2894–2906.
- [11] a) N. Plé, A. Turck, K. Couture, G. Quéguiner, *J. Org. Chem.* 1995, 60, 3781–3786; b) P. Pierrat, P. Gros, Y. Fort, *Synlett* 2004, 13, 2319–2322; c) J. Hawad, O. Bayh, C. Hoarau, F. Trécourt, G. Quéguiner, F. Marsais, *Tetrahedron* 2008, 64, 3236–3245.
- [12] a) J. A. Brown, S. Irvine, A. R. Kennedy, W. J. Kerr, S. Andersson, G. N. Nilsson, *Chem. Commun.* 2008, 1115–1117; b) J. A. Brown, A. R. Cochrane, S. Irvine, W. J. Kerr, B. Mondal, J. A. Parkinson, L. C. Paterson, M. Reid, T. Tuttle, S. Andersson, G. N. Nilsson, *Adv. Synth. Catal.* 2014, 356, 3551–3562; c) M. Parmentier, T. Hartung, A. Pfaltz, D. Muri, *Chem. Eur. J.* 2014, 20, 11496–11504; d) K. Jess, V. Derdau, R. Weck, J. Atzrodt, M. Freytag, P. G. Jones, M. Tamm, *Adv. Synth. Catal.* 2017, 359, 629–638.
- [13] M. Liu, X. Chen, T. Chen, S.-F. Yin, *Org. Biomol. Chem.* 2017, 15, 2507–2511.
- [14] a) N. H. Werstik, C. Ju, *Can. J. Chem.* 1989, 67, 5–10; b) J. Yao, R. F. Evila, *J. Am. Chem. Soc.* 1994, 116, 11229–11233.
- [15] a) H. Esaki, N. Ito, S. Sakai, T. Maegawa, Y. Monguchi, H. Sajiki, *Tetrahedron* 2006, 62, 10954–10961; b) V. Derdau, J. Atzrodt, J. Zimmermann, C. Kroll, F. Brückner, *Chem. Eur. J.* 2009, 15, 10397–10404.
- [16] V. H. Mai, O. B. Gadzhiev, S. K. Ignatov, G. I. Nikonov, *Catal. Sci. Technol.* 2019, 9, 3398–3407.
- [17] a) C. G. Macdonald, J. S. Shannon, *Tetrahedron Lett.* 1964, 45, 3351–3354; b) G. E. Calf, J. L. Garnett, V. A. Pickles, *Aust. J. Chem.* 1968, 21, 961–972; c) R. B. Moyes, P. B. Welles, *J. Catal.* 1971, 21, 86–92; d) G. M. Rubottom, E. J. Evain, *Tetrahedron* 1990, 46, 5055–5064; e) E. Alexis, J. R. Jones, W. J. S. Lockley, *Tetrahedron Lett.* 2006, 47, 5022–5028; f) J. A. Sullivan, K. A. Flanagan, H. Hain, *Catal. Today* 2008, 139, 154–160; g) S. C. Schou, *J. Labelled Compd. Radiopharm.* 2009, 52, 376–381; h) K. R. Guy, J. R. Shapley, *Organometallics* 2009, 28, 4020–4027; i) D. Bouzoutta, J. M. Asensio, V. Pfeiffer, A. Palazzolo, P. Lecante, G. Pieters, S. Feuillestre, S. Tricard, B. Chaudret, *Nanoscale* 2020, 12, 15736–15742.
- [18] G. Pieters, C. Taglang, E. Bonnefille, T. Gutmann, C. Puente, J.-C. Berthet, C. Dugave, B. Chaudret, S. Rousseau, *Angew. Chem. Int. Ed.* 2014, 53, 230–234; *Angew. Chem.* 2014, 126, 234–238.
- [19] a) B. Gröll, M. Schnürch, M. D. Mihovilovic, *J. Org. Chem.* 2012, 77, 4432–4437; b) H. Yang, C. Zarate, W. N. Palmer, N. Rivera, D. Hesk, P. J. Chirik, *ACS Catal.* 2018, 8, 10210–10218; c) C. Zarate, H. Yang, M. J. Bezdek, D. Hesk, P. J. Chirik, *J. Am. Chem. Soc.* 2019, 141, 5034–5044.
- [20] M. Daniel-Bertrand, S. Garcia-Argote, A. Palazzolo, I. M. Marin, P.-F. Fazzini, S. Tricard, B. Chaudret, V. Derdau, S. Feuillestre, G. Pieters, *Angew. Chem. Int. Ed.* 2020, 59, 21114–21120; *Angew. Chem.* 2020, 132, 21300–21306.
- [21] R. P. Yu, D. Hesk, N. Rivera, I. Pelczar, P. J. Chirik, *Nature* 2016, 529, 195–199.
- [22] J. L. Koniarczyk, D. Hesk, A. Overgard, I. W. Davies, A. McNally, *J. Am. Chem. Soc.* 2018, 140, 1990–1993.
- [23] B. Eguillor, M. A. Esteruelas, J. García-Raboso, M. Oliván, E. Oñate, *Organometallics* 2009, 28, 3700–3709.
- [24] J. A. Zoltewicz, C. L. Smith, *J. Am. Chem. Soc.* 1967, 89, 3358–3359.
- [25] Y. Li, C. Zheng, Z.-J. Jiang, J. Tang, B. Tang, Z. Gao, *Chem. Commun.* 2022, 58, 3497–3500.
- [26] V. Papa, Y. Cao, A. Spannenberg, K. Junge, M. Beller, *Nat. Catal.* 2020, 3, 135–142.
- [27] S. Kopf, H. Neumann, M. Beller, *Chem. Commun.* 2021, 57, 1137–1140.
- [28] a) Y. Hu, L. Liang, W.-T. Wei, X. Sun, X.-J. Zhang, M. Yan, *Tetrahedron* 2015, 71, 1425–1430; b) L. Huang, W. Liu, L.-L. Zhao, Z. Zhang, X. Yan, *J. Org. Chem.* 2021, 86, 3981–3988.
- [29] a) S. P. Bew, G. D. Hiatt-Gipson, J. A. Lovell, C. Poullain, *Org. Lett.* 2012, 14, 456–459; b) M. Zanatta, F. P. dos Santos, C. Biehl, G. Marin, G. Ebeling, P. A. Netz, J. Dupont, *J. Org. Chem.* 2017, 82, 2622–2629; c) T. R.

- Puleo, A. J. Strong, J. S. Bandar, *J. Am. Chem. Soc.* **2019**, *141*, 1467–1472; d) V. Salamanca, A. C. Albéniz, *Eur. J. Org. Chem.* **2020**, 3206–3212; e) K. I. Galkin, E. G. Gordeev, V. P. Ananikov, *Adv. Synth. Catal.* **2021**, *363*, 1368–1378.
- [30] a) R. Caporaso, S. Manna, S. Zinken, A. R. Kochnev, E. R. Lukyanenko, A. V. Kurkin, A. P. Antonchick, *Chem. Commun.* **2016**, *52*, 12486–12489; b) R. Zhang, X. Shi, Q. Yan, Z. Li, Z. Wang, H. Yu, X. Wang, J. Qi, M. Jiang, *RSC Adv.* **2017**, *7*, 38830–38833; c) R. A. Garza-Sanchez, T. Patra, A. Tlahuext-Aca, F. Strieth-Kalkhoff, F. Glorius, *Chem. Eur. J.* **2018**, *24*, 10064–10068.
- [31] a) A. Vaitiekunas, F. F. Nord, *Nature* **1951**, *168*, 875–876; b) M. Schnürch, M. Spina, A. F. Khan, M. D. Mihovilovic, P. Stanetty, *Chem. Soc. Rev.* **2007**, *36*, 1046–1057; c) T. R. Puleo, D. R. Klaus, J. S. Bandar, *J. Am. Chem. Soc.* **2021**, *143*, 12480–12486.
- [32] C. L. Øpstad, T.-B. Melo, H.-R. Sliwka, V. Partali, *Tetrahedron* **2009**, *65*, 7616–7619.
- [33] a) S. Yanagisawa, K. Ueda, T. Taniguchi, K. Itami, *Org. Lett.* **2008**, *10*, 4673–4676; b) W. Liu, H. Cao, H. Zhang, H. Zhang, K. H. Chung, C. He, H. Wang, F. Y. Kwong, A. Lei, *J. Am. Chem. Soc.* **2010**, *132*, 16737–16740; c) E. Shirakawa, K.-I. Itoh, T. Higashino, T. Hayashi, *J. Am. Chem. Soc.* **2010**, *132*, 15537–15539; d) A. Studer, D. P. Curran, *Angew. Chem. Int. Ed.* **2011**, *50*, 5018–5022; *Angew. Chem.* **2011**, *123*, 5122–5127; e) E. Shirakawa, T. Hayashi, *Chem. Lett.* **2012**, *41*, 130–134; f) S. Zhou, G. M. Anderson, B. Mondal, E. Doni, V. Ironmonger, M. Kranz, T. Tuttle, J. A. Murphy, *Chem. Sci.* **2014**, *5*, 476–482; g) J. P. Barham, G. Coulthard, R. G. Kane, N. Delgado, M. P. John, J. A. Murphy, *Angew. Chem. Int. Ed.* **2016**, *55*, 4492–4496; *Angew. Chem.* **2016**, *128*, 14568–14572; h) J. P. Barham, G. Coulthard, K. J. Emery, E. Doni, F. Cumine, G. Nocera, M. P. John, L. E. A. Berlouis, T. McGuire, T. Tuttle, J. A. Murphy, *J. Am. Chem. Soc.* **2016**, *138*, 7402–7410; i) L. Zhang, H. Yang, L. Jiao, *J. Am. Chem. Soc.* **2016**, *138*, 7151–7160; j) M. Patil, *J. Org. Chem.* **2016**, *81*, 632–639; k) J. Madasu, S. Shinde, R. Das, S. Patel, A. Shard, *Org. Biomol. Chem.* **2020**, *18*, 8346–8365.
- [34] a) L. Zhang, H. Yang, L. Jiao, *J. Am. Chem. Soc.* **2016**, *138*, 7151–7160; b) W.-B. Liu, D. P. Schuman, Y.-F. Yang, A. A. Toutov, Y. Liang, H. F. T. Klare, N. Nesnas, M. Oestreich, D. G. Blackmond, S. C. Virgil, S. Banerjee, R. N. Zare, R. H. Grubbs, K. N. Houk, B. M. Stoltz, *J. Am. Chem. Soc.* **2017**, *139*, 6867–6879; c) S. Banerjee, Y.-F. Yang, I. D. Jenkins, Y. Liang, A. A. Toutov, W.-B. Liu, D. P. Schuman, R. H. Grubbs, B. M. Stoltz, E. H. Krenske, K. N. Houk, R. N. Zare, *J. Am. Chem. Soc.* **2017**, *139*, 6880–6887.
- [35] Y. Zhao, D. G. Truhlar, *Theor. Chem. Acc.* **2008**, *120*, 215–241.
- [36] A. V. Marenich, C. J. Cramer, D. G. Truhlar, *J. Phys. Chem. B* **2009**, *113*, 6378–6396.
- [37] B. A. Trofimov, E. Y. Schmidt, *Acc. Chem. Res.* **2018**, *51*, 1117–1130.

Manuscript received: February 22, 2022

Revised manuscript received: March 14, 2022

Accepted manuscript online: March 15, 2022

10 Appendix

10.1 Additional publication

The following review was written as part of my PhD work in collaboration with Florian Bourriquen and Dr. Wu Li and contributed to the writing of the introduction of this thesis.

Sara Kopf,⁺ Florian Bourriquen,⁺ Wu Li, Helfried Neumann, Kathrin Junge, and Matthias Beller.

⁺ contributed equally.

Chem. Rev. **2022**, 122, 6634–6718.

DOI: 10.1021/acs.chemrev.1c00795

© 2022 The Authors. Published by American Chemical Society.

Recent Developments for the Deuterium and Tritium Labeling of Organic Molecules

Sara Kopf,[†] Florian Bourriquet,[†] Wu Li, Helfried Neumann, Kathrin Junge, and Matthias Beller*



Cite This: *Chem. Rev.* 2022, 122, 6634–6718



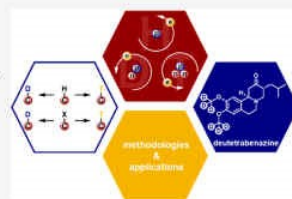
Read Online

ACCESS |

Metrics & More

Article Recommendations

ABSTRACT: Organic compounds labeled with hydrogen isotopes play a crucial role in numerous areas, from materials science to medicinal chemistry. Indeed, while the replacement of hydrogen by deuterium gives rise to improved absorption, distribution, metabolism, and excretion (ADME) properties in drugs and enables the preparation of internal standards for analytical mass spectrometry, the use of tritium-labeled compounds is a key technique all along drug discovery and development in the pharmaceutical industry. For these reasons, the interest in new methodologies for the isotopic enrichment of organic molecules and the extent of their applications are equally rising. In this regard, this Review intends to comprehensively discuss the new developments in this area over the last years (2017–2021). Notably, besides the fundamental hydrogen isotope exchange (HIE) reactions and the use of isotopically labeled analogues of common organic reagents, a plethora of reductive and dehalogenative deuteration techniques and other transformations with isotope incorporation are emerging and are now part of the labeling toolkit.



CONTENTS

1. Introduction	6635	4. Miscellaneous Transformations with Deuterium Incorporation	6679
2. Hydrogen Isotope Exchange	6636	4.1. Trideuteromethylation	6679
2.1. HIE on Aromatic Compounds	6636	4.2. Insertion of the Trideuteromethoxy Group. Deuteration of Thiols, Selenides, and Carboxylic Acids	6682
2.1.1. <i>ortho</i> -Directed HIE	6636	4.3. Deuterodifluoromethylation	6683
2.1.2. <i>meta</i> -Directed HIE	6646	4.4. Deuterated Aldehydes	6685
2.1.3. HIE under Steric Control	6647	4.5. Deuterated Chloroform	6686
2.1.4. HIE under Electronic Control	6648	4.6. Further Approaches	6687
2.1.5. Perdeuteration of Arenes by HIE	6650	4.7. Multistep Syntheses with Deuterium Incorporation	6691
2.1.6. Conclusions	6654	4.7.1. Deuterated Reagents	6691
2.2. HIE on Olefins	6654	4.7.2. Deuterated Starting Materials	6692
2.3. HIE on Alkynes	6656	5. Applications for Deuterated and Tritiated Compounds	6692
2.4. HIE on Aliphatic Substrates	6656	5.1. Mechanistic Investigation	6693
2.4.1. Deuteration of Aliphatic Alcohols and Amines by HIE	6656	5.1.1. Primary Kinetic Isotopic Effect	6694
2.4.2. Deuteration of Aliphatic Carbonyl Compounds by HIE	6659	5.1.2. Secondary Kinetic Isotopic Effect	6694
2.4.3. HIE in Benzylic Positions	6661	5.2. Drug Development	6695
2.4.4. Conclusions	6661	6. Conclusions and Outlook	6706
2.5. Deuteration of Aldehydes by HIE	6662	Author Information	6707
3. Reductive Deuteration	6664	Corresponding Author	6707
3.1. Deuterodehalogenation	6664		
3.1.1. Deuteration of Prefunctionalized Arenes	6665		
3.1.2. Deuterodehalogenation of Vinyl and Allyl Halides	6668		
3.1.3. Deuterodehalogenation of Alkyl Halides	6669		
3.2. Reductive Deuteration of Carbonyl Groups	6670		
3.3. Reductive Deuteration of Olefins	6673		
3.4. Reductive Deuteration of Alkynes	6676		
3.5. Reductive Deuteration of Arenes	6678		

Received: September 14, 2021

Published: February 18, 2022



Authors	6707
Author Contributions	6707
Funding	6707
Notes	6707
Biographies	6707
References	6708

1. INTRODUCTION

Discovered in 1931 by Harold Clayton Urey,¹ and soon after already awarded by the Nobel Prize in Chemistry in 1934, deuterium is a stable and nonradioactive isotope of hydrogen differing only by an additional neutron. Deuterium mainly occurs in the form of HDO or D₂O with a natural abundance of 0.0115% of the hydrogen atoms present in the oceans^{2–4} and is consequently a relatively rare isotope. Compared with the isotopes of other elements, deuterium exhibits a unique isotope weight ratio. When a hydrogen atom possesses an atomic mass of 1.008 u, the mass exhibited by a deuterium atom is 2.014 u. This 2-fold increase induces a lower vibrational frequency in C–D bonds compared with C–H bonds. Therefore, there is a lower zero-point energy of the bonds involving a deuterium atom (of 1.2–1.5 kcal/mol) and thus a higher activation energy for C–D bond cleavage compared with the corresponding C–H bond.⁵ This effect is called the primary kinetic isotope effect (KIE). In general, exchange of hydrogen by deuterium modifies the physicochemical properties of (organic) molecules. For example, decreased lipophilicity and acidity of carboxylic acids and phenols are reported for the deuterated species compared with the nondeuterated counterparts, as well as an increased basicity of amines.^{6–8}

The distinctive properties of deuterium compared with protium generate a vast demand in numerous fields. In medicinal chemistry, introduction of a deuterium atom is utilized to modify drug's absorption, distribution, metabolism, and excretion (ADME) properties. Taking advantage of the KIE, the pharmacokinetic and pharmacodynamic properties are modified, enhancing the metabolic stability and therefore allowing for lower doses.^{9–11} Notably, deuterium-labeled compounds are used for the elucidation of the metabolism of most small molecule drugs.¹² Moreover, precisely labeled compounds find wide applications in quantitative mass spectrometry as well as internal standards.^{13–15} The use of deuterium also allows the determination of protein conformations. In the presence of D₂O, the hydrogen of an amide linkage undergoes H/D exchange. Depending on protein folding and involvement of this labile hydrogen in hydrogen bonding, this exchange will take place with different rates. Careful labeling experiments followed by mass spectrometry analyses permit investigation of these noncovalent interactions and thereof provide information on 3D structures.^{16,17} Furthermore, the investigation of chemical reaction pathways highly relies on deuterated compounds.^{5,18} In addition, the number of applications of hydrogen-labeled molecules in materials science is rising. For instance, taking advantage of kinetic isotope effects, the properties of organic light-emitting diodes (OLEDs)^{19–23} and fluorophores²⁴ could be improved. Last but not least, deuterated solvents are routinely used for NMR spectroscopy, a prime methodology for structural characterization of organic compounds.

By comparison, containing two neutrons, with a half-life of 12.32 (±0.02) years²⁵ and an abundance of 1.10^{–18}, tritium is a rare and radioactive isotope of hydrogen.²⁶ This radioisotope,

detected for the first time in 1934,²⁷ undergoes β decay leading to helium-3 and features a specific activity of 9700 Ci/g.²⁸ Another interesting characteristic of tritium is the low mean energy of its β particles (5.69 keV),²⁹ which can only travel 6 mm in the air and are unable to penetrate human skin, resulting in minimal safety risks to health if appropriately handled.³⁰ Particularly, because of its high specific activity, tritium distribution can be efficiently monitored with high sensitivity by scintillation measurements. Therefore, tritium-labeled organic molecules are valuable radiotracers in biological studies to investigate interactions with the corresponding receptors, ligands, or enzymes.^{31,32} Except for tritiated organic compounds, other uses of tritium, mainly in the form of T₂ gas, include for example its use as a fuel for radioluminescent objects in the presence of a phosphor, as well as a source for nuclear fusion.³⁰

Overall, hydrogen isotope labeled organic molecules are needed on the grounds that (i) they provide new compounds with improved properties in comparison with their protio-containing counterparts, (ii) they allow chemical and metabolic investigations which are not achievable by other techniques, and (iii) their use permits quantitative and reliable studies using either mass spectrometry or radioactivity measurement. Notably, in 2017, deutetrabenazine—the first deuterated drug—was approved by the American Food and Drug Administration (FDA) for the treatment of chorea associated with Huntington's disease, paving the way for deuterium-containing medicines.^{33,34}

Because of all these applications, development of methodologies for the synthesis of deuterated and tritiated compounds continued to receive an impressive attention over the years. General reviews,^{32,35–38} as well as more specific ones dedicated to subareas in the field of deuteration such as hydrogen isotope exchange (HIE),³⁹ visible-light photocatalytic deuteration reactions,⁴⁰ nanocatalyzed HIE,⁴¹ trideuteromethyl incorporation,^{42,43} reductive deuteration,⁴⁴ base metal-catalyzed HIE,⁴⁵ HIE catalysis in alkanes,⁴⁶ iridium-catalyzed HIE,⁴⁷ specific labeling of the α position of heteroatoms,⁴⁸ of the C(sp²)-H,⁴⁹ as well as of the C(sp³)-H positions have been published in recent years.⁵⁰ Similarly, the number of scientific publications dealing with hydrogen isotopes is constantly increasing. Over the last 5 years only, more than 18,000 scientific publications including the word "deuterium" were issued according to the SciFinder database (Figure 1). In comparison, the number of publications with "tritium" peaked around 1971–1975, which is possibly due to its use in military applications,⁵¹ and is now stable with around 5,000 publications for 5-year periods.

Following the early works in metal-catalyzed HIE reactions using platinum,⁵² iridium,⁵³ and rhodium salts by Garnett with deuterated solvents as isotope sources,⁵⁴ a breakthrough was the use of molecularly defined iridium complexes. Here, the commercially available Crabtree catalyst was reported in 1995 for the deuteration of acetanilides and derivatives using deuterium gas (Figure 2).⁵⁵ After a short period of disuse, the research in H/D exchange reactions regained interest at the end of the 2000s decade. As an example, in 2008, the Kerr group described a new family of iridium complexes bearing *N*-heterocyclic carbene (NHC) ligands, once again highlighting the importance of this metal for HIE reactions.⁵⁶ Four years later, our group showed the efficiency of the ruthenium-based Shvo catalyst for H/D exchange at the α and β positions of amines.⁵⁷ In 2014, Chaudret, Rousseau, and co-workers presented ruthenium nanoparticles for the efficient deuteration of nitrogen-containing compounds.⁵⁸ Iron-mediated deutera-

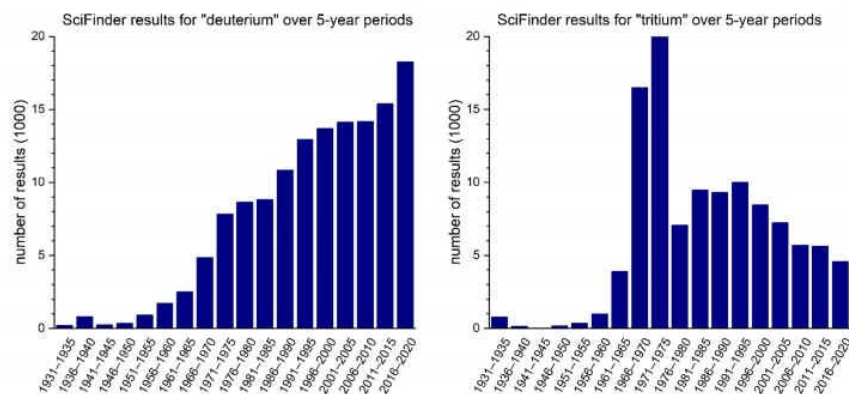


Figure 1. SciFinder search results for "deuterium" and "tritium" over 5-year periods.

tion and tritiation of arenes and heteroarenes were reported by the group of Chirik, revealing that H/D exchange is not limited to noble metals.⁵⁹ In 2017, MacMillan and co-workers described the use of photocatalysts for the selective insertion of deuterium at the α position of *N*-alkyl amines in drug molecules.⁶⁰ Later, the Chirik group developed nickel dihydride systems, first limited to azine substrates but ultimately improved to a broader scope of electron-rich heteroarenes.⁶¹ More recently, Pieters, Chaudret, Derdau, and co-workers demonstrated the utility of NHC-stabilized iridium nanoparticles for the more challenging HIE in anilines.⁶²

Here, we aim to summarize all the recent developments regarding deuterium and tritium incorporation chemistry and present a comprehensive Review on this topic. Supplementary to previous works, several types of deuteration reactions, namely, HIE reactions, deuterodehalogenation, and reductive deuterations, will be covered and critically compared.

2. HYDROGEN ISOTOPE EXCHANGE

For several applications, such as the synthesis of deuterated drugs or the preparation of stable-isotope-labeled internal standards (SILS) for LC-MS quantification studies, the introduction of isotopic labels into organic molecules is best conducted at a late stage, rendering direct exchange of hydrogen for its isotopes via a C–H activation mechanism the most useful and most investigated method. However, the elimination of additional synthetic steps comes at the cost of a difficult-to-control regioselectivity and chemoselectivity. Furthermore, the remaining unlabeled compounds can be problematic because in a HIE domain, starting materials and products are virtually inseparable. Despite these problems, the past decades have seen tremendous success in driving HIE reactions to completion so that nowadays many protocols have been established which afford specific compounds with a deuterium incorporation of more than 90%. Interestingly, an important inspiration for these developments have been new achievements in the topical field of C–H activation processes, giving rise to highly selective HIE protocols. In the following paragraphs, the recent developments in this area will be summarized.

2.1. HIE on Aromatic Compounds

2.1.1. *ortho*-Directed HIE. 2.1.1.1. The Importance of Iridium Catalysis for *ortho*-Directed HIE. In principle any

organic compound is amenable to HIE; however, most of the published methodologies concern HIE on arenes, often enabled by late transition-metal catalysts and directing groups with deuterium or tritium gas as the isotope source. Specifically, numerous new phosphine-coordinated iridium(I) catalysts have been developed since the early efforts using the Crabtree catalyst,^{63–70} leading to the highly efficient contemporary HIE reactions which exhibit exceptionally mild conditions (ambient temperature, short reaction times, no additives). Especially, *ortho*-directed aromatic HIE continues to be dominated by iridium catalysis. In recent years, most examples employed an iridium catalyst family developed by the Kerr group (Figure 3).⁶³ Whereas bulky NHC ligands are mandatory for these catalysts, neutral chloride-containing iridium complexes have been used as well as cationic phosphine-ligated catalysts with the particular choice of catalyst often depending on the type of substrate.

Another effective iridium-based HIE catalyst system developed by the Tamm group became popular more recently.⁶⁸ The authors of this study presented a new family of iridium(I) complexes with *P,N* ligands exhibiting strongly donating nitrogen atoms (Figure 3). One representative of this series not only served as an effective HIE catalyst in the presence of a broad range of previously established directing groups such as heterocycles, the nitro functionality, and a range of carbonyl groups but also realized for the first time Boc protecting group-directed HIE *ortho* to correspondingly protected anilines and indoles which is unattainable using the Kerr catalyst (Scheme 1a). The Tamm catalyst was later also applied to the *ortho*-deuteration of phenylacetic acid esters and amides via 6-membered iridacycles (Scheme 1b)⁷¹ as well as to the deuteration of arenes with sulfonamide (*vide infra*), *N*-oxide, and phosphonamide directing groups (Scheme 1c).⁷²

The general mechanism of iridium-catalyzed aromatic HIE under deuterium gas atmosphere has been elucidated in detail both experimentally and computationally in recent years.^{63,71,73} It has been found that the precatalysts are activated by reduction and dissociation of the cyclooctadiene (COD) ligand in the presence of the gaseous isotope source, furnishing a coordinatively unsaturated iridium species, which is subsequently stabilized by binding of the substrate's directing group along with an agostic interaction of the *ortho* C–H bond

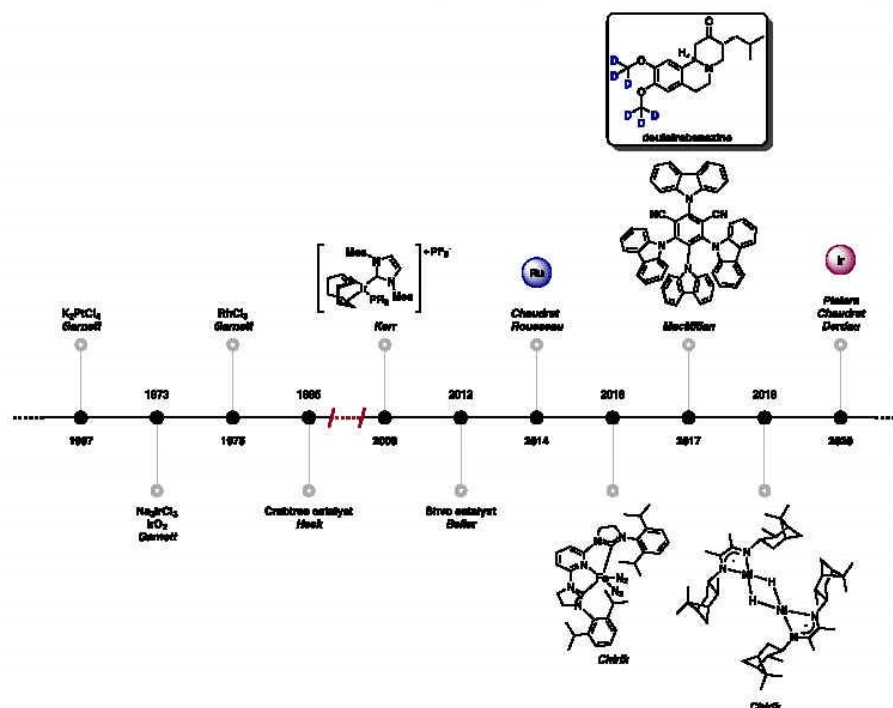


Figure 2. Developments in deuterium labeling chemistry—structure of deutetrabenazine.

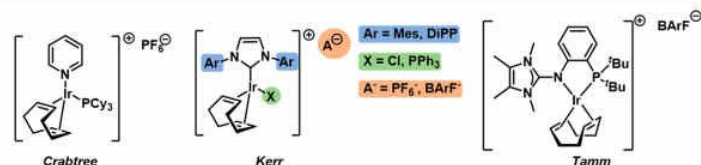


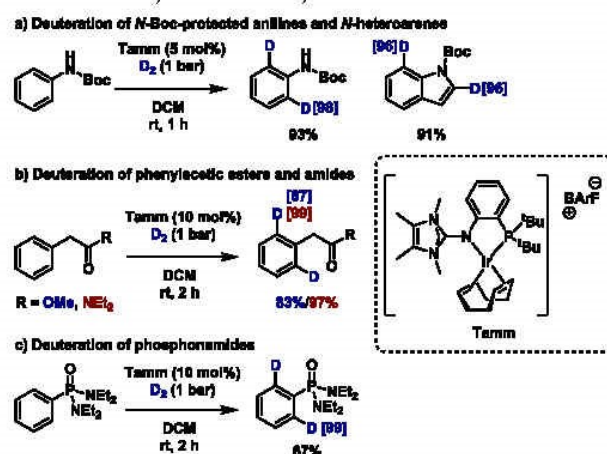
Figure 3. Selected iridium(I) catalysts for *ortho*-directed aromatic HIE.

(Scheme 2). Depending on the nature of the catalyst, either the NHC ligand (in the Kerr catalyst family) or the agostic C–H bond (in the case of the Tamm catalysts) can be found *trans* to the phosphine (or chloride) ligand in this intermediate. C–H activation via oxidative addition (Kerr) or σ -bond metathesis (Tamm) follows as the rate-determining step (RDS), leading to a dihydrogen hydride complex. Hydride fluxionality preceding the elimination step finally allows the formation of the isotopically labeled product.

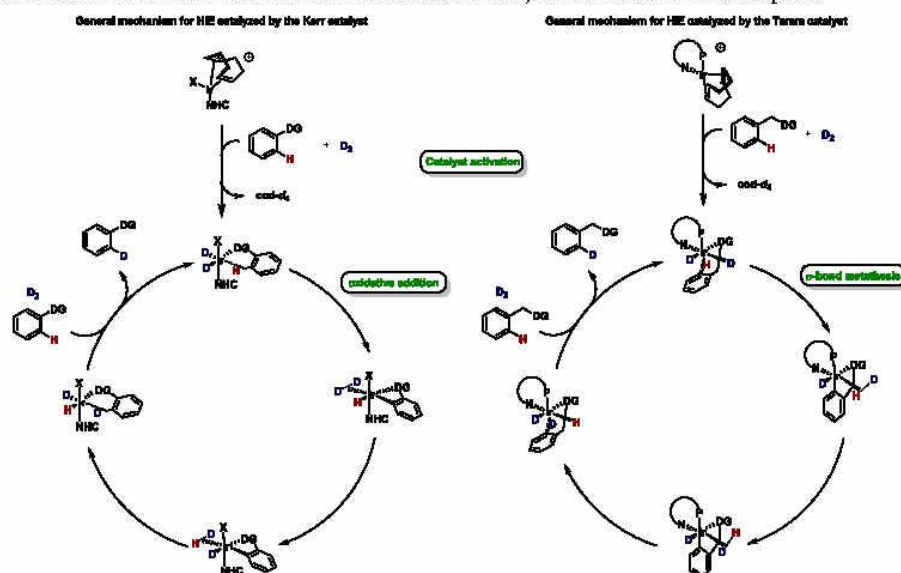
Although the exceptionally mild conditions achieved with iridium catalysts are mostly still out of reach, more and more directed HIE reactions catalyzed by alternative transition metals are being developed, sometimes allowing access to new substrates or selectivities. Often this goes along with the use of deuterium sources other than deuterium gas such as heavy water or, if a more acidic reaction medium is beneficial, deuterated acetic acid or trifluoroacetic acid (TFA) (Table 1, Figure 4). Deuterated benzene, on the other hand, is a common deuterium

source for nondirected aromatic HIE. Further deuterium sources such as the deuterated versions of isopropanol, potassium formate, diphenylmethanol, sodium borohydride, and tetramethyldisiloxane or deuterated amines and boranes as even more specialized examples hardly play a role in the context of HIE but are rather relevant for deuterodehalogenation or reductive deuteration processes. Whereas the use of deuterium oxide for deuteration is desirable because of its low price (Figure 5), high availability, and convenient use, tritiation usually requires the use of gaseous tritium because of the high risk of radioactive contamination that even small amounts of tritium oxide bear. Besides easier handling at small scales, tritium gas is—other than tritiated water—available at near theoretical specific activity. Consequently, the elaboration of deuteration processes under a deuterium atmosphere can serve as a model for a tritiation platform and should be continued to be investigated despite their higher cost and less convenient handling. For deuteration purposes where the use of deuterium

Scheme 1. HIE Transformations Enabled by the Tamm Catalyst



Scheme 2. General Mechanisms for Aromatic HIE under Iridium Catalysis and Deuterium Gas Atmosphere



gas is unavoidable because of the reaction mechanism, the *ex situ* preparation of deuterium gas from heavy water and a diboron compound in a two-chamber reactor can be considered as a convenient alternative.⁷⁴

As HIE reactions are equilibrium processes, high isotopic enrichments can hardly be achieved with just stoichiometric quantities of the isotope source. Consequently, they are usually carried out with an excess of the labeling reagent, while a commendable trend for lowering the necessary equivalents over the past years can be identified. In this context, it should be stated that in some cases, the maximum possible isotope incorporation is limited by the presence of labile protons in the

substrate or through residual amounts of nonlabeled substance in the isotope source. In this instance, authors tend to compare the achieved isotopic yield with the maximum theoretical yield.

Apart from iridium, the reaction conditions for other HIE reactions are far less broad, and a generalized mechanism can therefore not be provided. Instead, interesting mechanistic aspects will be discussed *vide infra* where applicable.

In the following sections, recent developments in transition-metal-catalyzed HIE on arenes are discussed categorized by substrate class, directing groups and selectivity, comparing achievements using various catalysts.

Table 1. Price and Use of Common Deuterium Sources. The Columns “Stoichiometry” and “Application” Refer to Published Examples Since 2017

deuterium source	price/mol (approx.)	stoichiometry	application
D ₂ O	15 € (Deutero, 100 mL)	excess (10 equiv to solvent quantities)	broadly applied in all areas
CDCl ₃	23 € (Deutero, 100 mL)	excess (solvent)	imidazolium-catalyzed HIE on aliphatic substrates and terminal alkynes
MeOD	53 € (Deutero, 25 mL)	excess (solvent)	Mn-catalyzed α -methylation-deuteration of ketones
AcOD	75 € (Sigma-Aldrich, 250 g)	excess (solvent)	metal-free HIE on Michael acceptors
EtOD	92 € (Sigma-Aldrich, 100 mL)	4.5 equiv	reductive deuteration with Na
DMSO- <i>d</i> ₆	100 € (Deutero, 100 mL)	excess (solvent)	base-catalyzed HIE, trideuteromethylation
MeOH- <i>d</i> ₄	115 € (Deutero, 100 mL)	excess (solvent)	HIE on arenes, NHC-catalyzed aldehyde HIE, trideuteromethylation
Acetone- <i>d</i> ₆	120 € (Deutero, 100 mL)	excess (around 10 equiv)	metal-free HIE on aliphatic substrates
CD ₃ CN	160 € (Deutero, 100 mL)	excess (solvent)	deuterodehalogenation of arenes
C ₆ D ₆	200 € (Deutero, 100 mL)	excess (solvent)	nondirected HIE on arenes
DCI 35% in D ₂ O	200 € (Deutero, 10 mL)	-	preparation of deuterium source for reductive deuteration of olefins
D ₂	230 € (Eurisotop, 25 L)	excess (D ₂ atmosphere, usually 1 bar)	broadly applied in metal-catalyzed HIE and reductive deuteration
TFA- <i>d</i>	290 € (Eurisotop, 10 mL)	excess (solvent)	homogeneous TM-catalyzed directed HIE on arenes, acid-catalyzed HIE of benzylic positions
CD ₃ OH	305 € (Deutero, 5 mL)	excess (solvent)	trideuteromethylation
AcOH- <i>d</i> ₄	310 € (Deutero, 10 mL)	excess (solvent)	homogeneous TM-catalyzed directed and S _E Ar HIE on arenes
^t PrOD	615 € (Sigma-Aldrich, 25 g)	5 equiv	Cu-catalyzed reductive deuteration of alkynes
DCO ₂ D	650 € (Deutero, 5 mL)	8 equiv	Ir-catalyzed reductive deuteration of carbonyl compounds
^t PrOH- <i>d</i> ₈	735 € (Deutero, 5 mL)	excess (solvent)	deuterodefunctionalization of arenes, reductive deuteration of carbonyl compounds
KOD 40 mol % in D ₂ O	770 € (Sigma-Aldrich, 50 g)	0.25 equiv	base in Ru-catalyzed HIE on arenes
THF- <i>d</i> ₈	940 € (Deutero, 25 mL)	excess (solvent)	palladium-catalyzed-/light-mediated deuterodehalogenation of aliphatic substrates
CD ₃ I	1020 € (Sigma-Aldrich, 50 g)	-	preparation of deuterium source for light-mediated deuterodebromination of arenes
NaBD ₄	1240 € (Deutero, 5 g)	5.5 equiv	reductive deuteration, preparation of DBpin, preparation of deuterium source for light-mediated deuterodebromination of arenes
EtOH- <i>d</i> ₅	1390 € (Deutero, 5 mL)	-	-
TFE- <i>d</i>	1400 € (Sigma-Aldrich, 25 mL)	excess (solvent)	homogeneous Pt-catalyzed nondirected deuteration of arenes (together with D ₂ O)
DMF- <i>d</i> ₂	1970 € (5 mL, Deutero)	excess (solvent)	trideuteromethylation
DCOOH	1970 € (Sigma-Aldrich, 5 g)	-	preparation of DCOOK and DCOONa
Ac ₂ O- <i>d</i> ₆	3000 € (Sigma-Aldrich, 5 g)	3 equiv	trideuteromethylation
aniline- <i>d</i> ₅	5240 € (Sigma-Aldrich, 5 g)	-	preparation of deuterium source for the light-mediated deuterodebromination of arenes
LiAlD ₄	6720 € (Deutero, 1 g)	-	preparation of Ph ₂ CDOH

2.1.1.2. Palladium, Rhodium, Ruthenium, and Manganese: Alternatives to Iridium-Catalyzed *ortho*-Directed HIE of Carbonyl Compounds. Compared with other carbonyl compounds, carboxylic acids are less explored as directing groups for HIE. However, building on the first selective deuteration of weakly coordinated palladacycles with benzoic and phenylacetic acids as substrates (Scheme 3a),⁷⁵ recent reports showed the potential of other transition-metal catalysts for this methodology, enabling transformations at milder conditions. In this context, *ortho*-deuteration of benzoic acids catalyzed by a Cp* rhodium complex⁷⁶ was achieved using cheaper deuterium oxide as a solvent, whereas the previously

published method only works in deuterated acetic acid (Scheme 3b). Meanwhile, the temperature could also be lowered from 120 to 90 °C, and the scope was extended to cinnamic acids. The economy of the deuterium source was further improved in a recently published ruthenium biscalboxylate-catalyzed *ortho*-directed benzoic acid deuteration, which only requires 10 equiv of deuterium oxide, while achieving high levels of deuteration (Scheme 3c).⁷⁷ Harnessing this deuterium source under palladium-catalyzed conditions is more challenging as seen in a recent report in which a more strongly coordinating bidentate pyridone directing group is needed to access *ortho*-deuterated phenylacetic amides.⁷⁸

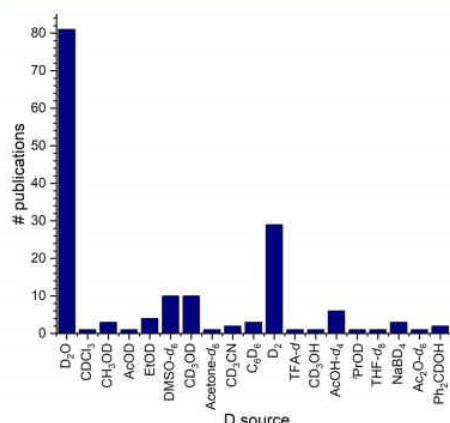


Figure 4. Selected deuterium sources and the number of publications in which they have been used (2017–2021).

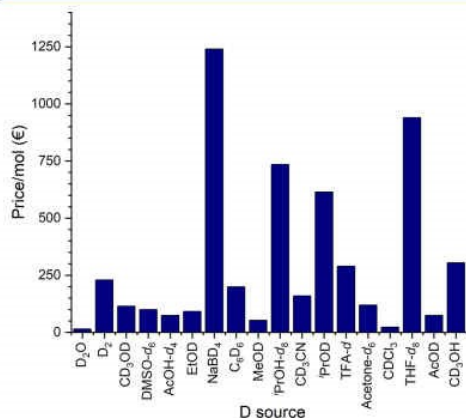
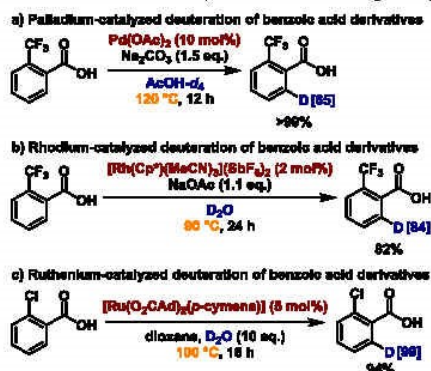


Figure 5. Selected deuterium sources and price/mol.

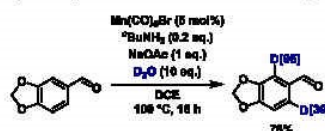
Scheme 3. HIE with Carboxylic Acids as Directing Groups



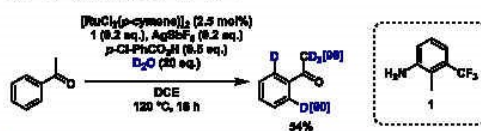
When moving to more abundant transition metals such as manganese, it can be difficult to activate substrates with less-coordinating oxygen-containing functional groups as directing groups. However, a transient directing group approach in which catalytic amounts of specific amines condense with aldehyde substrates *in situ* and form transient imine directing groups has recently been utilized for the *ortho*-selective deuteration of benzaldehyde derivatives catalyzed by simple manganese pentacarbonyl bromide (Scheme 4).⁷⁹ Similarly, aromatic

Scheme 4. HIE with Transient Directing Groups

a) Mn-catalyzed *ortho*-directed HIE of aromatic aldehydes



b) Ru-catalyzed HIE of aromatic ketones

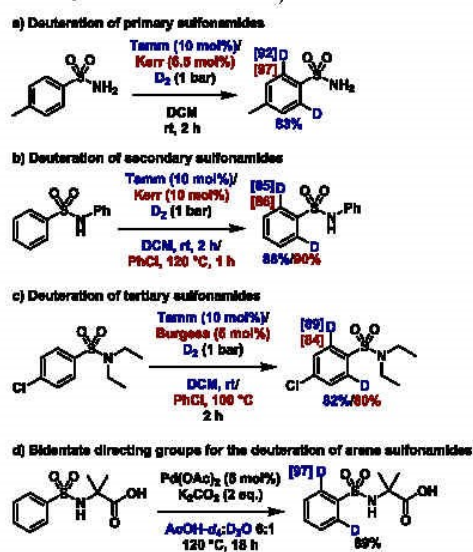


ketones can be deuterated under ruthenium catalysis using catalytic amounts of anilines as transient directing groups. Notably, both aromatic *ortho* and α -carbonyl positions are deuterated under the reaction conditions with the latter being a result of acid- and amine-catalyzed deuteration.⁸⁰

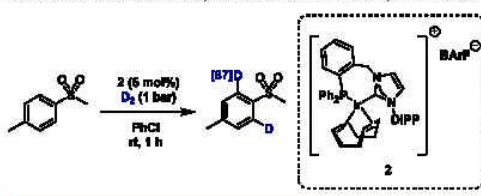
2.1.1.3. Sulfur-Containing Directing Groups. Previously considered as highly challenging substrates, arenes with sulfur-containing directing groups could be successfully *ortho*-deuterated in the presence of iridium catalysts in the last years. Following a seminal study by the Kerr group on the *ortho*-deuteration of primary sulfonamides under mild conditions (Scheme 5a),⁷³ HIE of secondary sulfonamides and sulfonylureas was made accessible later by employing harsher reaction conditions (Scheme 5b).⁸¹ Furthermore, tertiary sulfonamides which delivered only poor results under these conditions could be labeled efficiently using the Burgess catalyst (Scheme 5c).⁸¹ In addition, the Tamm catalyst proved to be effective for the *ortho*-deuteration under mild conditions of primary, secondary, and tertiary sulfonamides alike (Scheme 5a–c).⁷² Secondary sulfonamides derived from α -amino acids have furthermore been used as bidentate directing groups for a palladium-catalyzed HIE of arenes (Scheme 5d).⁸²

Because of the sterically crowded nature of the substrate-bound iridium complex, aryl sulfones are even more challenging substrates. Nevertheless, a general protocol for their iridium-catalyzed *ortho*-deuteration was recently reported by Kerr and co-workers (Scheme 6).⁸³ For this purpose, an *in silico* catalyst screening aimed at increasing the binding energy of the sulfone to the iridium complex was performed and resulted in the finding of tethered NHC-phosphine iridium complexes as workable catalysts for this transformation. Subsequent optimization of the solvent of the reaction led to good deuterium incorporation on a range of aryl sulfones under mild conditions.

2.1.1.4. Deuteration of Anilines. An unusual directing group for HIE in arenes are amine functionalities in anilines. Whereas

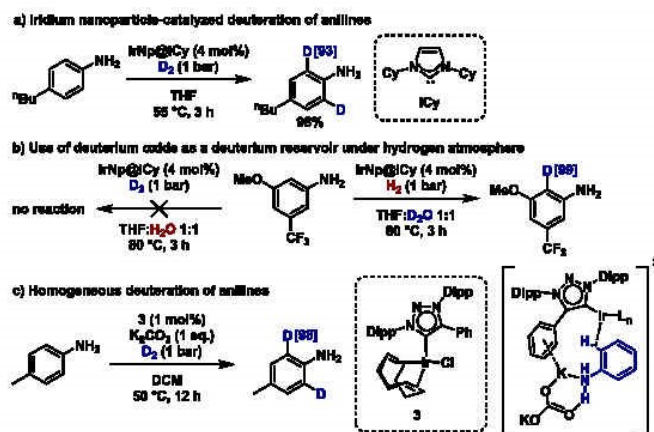
Scheme 5. *ortho*-Deuteration of Aryl Sulfonamides

Scheme 6. Iridium-Catalyzed Deuteration of Aryl Sulfones



in the past this type of substrates had rather been used for transition-metal-free electrophilic substitution chemistry,^{84,85}

Scheme 7. Deuteration of Anilines Catalyzed by Iridium Nanoparticles and Homogeneous Mesionic Iridium NHC Complexes



6641

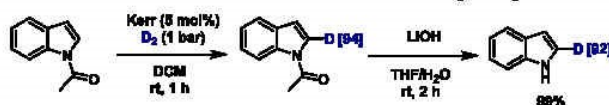
<https://doi.org/10.1021/acs.chemrev.1c00795>
Chem. Rev. 2022, 122, 6634–6718

recently also two transition-metal-catalyzed HIE methodologies for the *ortho*-directed deuteration of anilines have been published. The first one uses air-stable NHC-stabilized iridium nanoparticles.⁶² Having observed sluggish reactivity of ruthenium nanoparticles for this class of substrates along with reduction of the aromatic ring, Pieters, Chaudret, Derdau, and co-workers hypothesized that iridium nanoparticles would perform better given the feasibility of C–H activation with homogeneous iridium complexes as well as the generally poor reduction reactivity of those catalysts. Indeed, using iridium nanoparticles, selective labeling of the *ortho* positions of anilines at 55 or 80 °C in high deuteration levels without reduction side reactions was observed (Scheme 7a). While the method was also developed for the tritiation of pharmaceuticals and hence uses gaseous isotope sources, mechanistic studies discovered that heavy water as a cosolvent can act as a reservoir for deuterium atoms. Accordingly, in the presence of deuterium oxide, hydrogen gas can be used instead of deuterium gas without lowering the deuterium incorporation level (Scheme 7b). Conversely, nondeuterated water with deuterium gas cannot promote deuteration of anilines under iridium nanoparticle catalysis.

Further, mesoionic NHC-ligated iridium complexes have been applied for homogeneous catalysis of the *ortho*-deuteration of anilines in the presence of other directing groups (Scheme 7c).⁸⁶ In this case, addition of potassium carbonate was crucial for the success of the reaction, and the reactivity decreased drastically in the presence of crown ethers. On the basis of these findings, the authors of this study proposed a combination of noncovalent interactions including cation– π interactions between the potassium cation and the phenyl substituent of the NHC ligand to account for the observed selectivity. However, experimental results to support this hypothesis could not be obtained. Perhaps in concordance with this hypothesis, secondary anilines exhibit significantly lower deuterium incorporation, whereas tertiary anilines do not react at all.

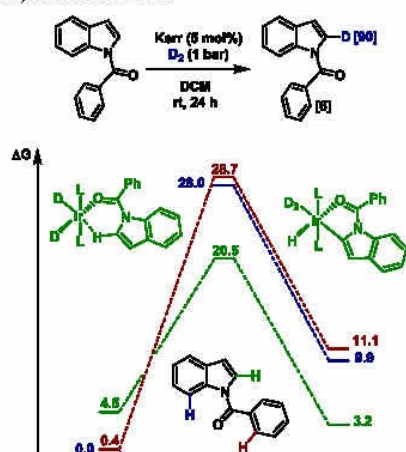
2.1.1.5. Directing-Group-Enabled Deuteration of Heteroaromatic Compounds. Whereas many HIE strategies in the past focused on differently substituted aromatic substrates, recent years have also brought more attention toward the

Scheme 8. Selective HIE in the C2-Position of N-Protected Indoles with Directing Group Removal under Mild Conditions



deuteration of heterocycles. In this context, common nitrogen protecting groups such as benzoyl or acyl have been used by Kerr and co-workers as directing groups for the iridium-catalyzed selective deuteration of 5-membered nitrogen-containing heterocycles such as pyrroles and indoles with subsequent removal of the directing group under mild conditions (Scheme 8).⁸⁷ Notably, the reaction exhibits excellent C2 selectivity, leaving other potentially accessible positions in the indole ring and even the benzoyl protecting group virtually untouched. A density functional theory (DFT)-based comparison of the binding energies of different conformers suggests that the substrate-iridium complex leading to the C2-deuterated product is less thermodynamically stable (by ca. 4 kcal/mol) than the competing complexes. However, its energy barrier for C–H activation is far lower (by ca. 12 kcal/mol), thus rendering it more reactive and explaining the experimentally observed selectivity (Scheme 9).

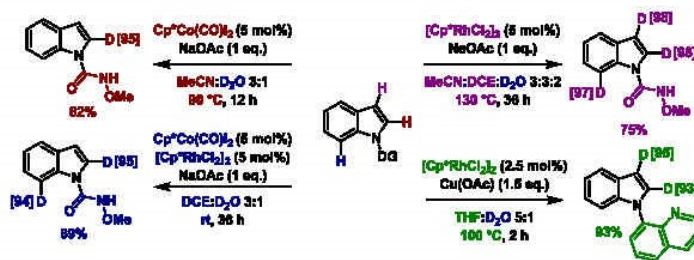
Scheme 9. Energy Profile for the Selective Labeling of Benzoyl-Protected Indole

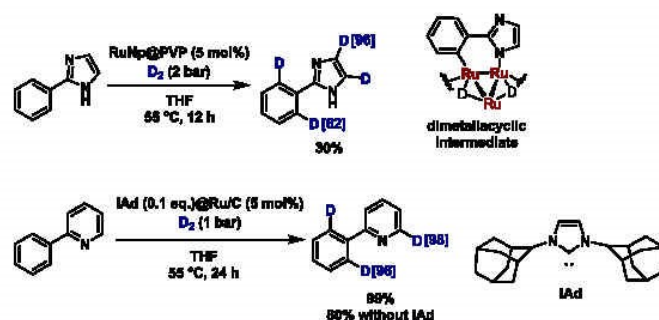


In addition to iridium-based catalysts, a range of recently published methodologies for the directed deuteration of indole derivatives make use of Cp* complexes of rhodium and cobalt. Here, different labeling patterns depending on the catalyst combination and the reaction conditions can be accomplished (Scheme 10).^{88–90} For example, using Cp*Co(CO)₂I₂ as catalyst at 90 °C and with acetonitrile as cosolvent, selective C2-deuteration comparable to the selectivity of Kerr's iridium catalyst (*vide supra*) is achieved.⁸⁸ However, by switching to rhodium catalysis ([Cp*RhCl₂)₂), adding DCE to the solvent mixture and increasing the temperature to 130 °C, trideuterated indoles in C2, C3, and C7 position can be obtained.⁸⁸ Whereas the C2 and C7 positions are activated through metallacycle intermediates, HIE in C3 position probably proceeds via thermal pathways. Consequently, lowering the temperature to 25 °C, only the C2 and C7 positions are deuterated under synergistic Rh/Co catalysis and in DCE as a cosolvent.⁸⁸ Further, blocking the C2 and C3 positions by alkyl substituents enables labeling merely in the C7 position.⁸⁹ Additionally, the C2 and C3 positions can selectively be deuterated under rhodium catalysis and at slightly elevated temperature (100 °C).⁹⁰ Lastly, the rhodium catalyst was used to selectively deuterate all other positions on the indole ring by installing the methoxyamide directing group on varying C-positions.⁸⁸ In this case, HIE of the two adjacent positions and, if applicable, additionally on the C3 position, is affected at 90 °C. Directing group removal was demonstrated for N-methoxyamide-substituted indoles.⁸⁸ However, under the slightly harsh hydrolysis conditions (100 °C, 12 h), deuteration in C3 position is reversed.

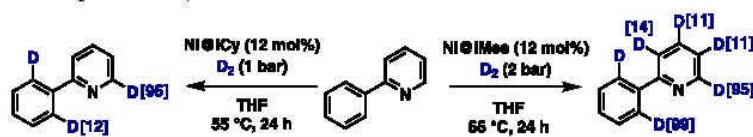
Whereas homogeneous catalysis leads to functionalization in the aromatic rings adjacent to a heterocyclic directing group, catalysis with nanoparticles can enable selective labeling of heterocycles in the positions vicinal to the heteroatom. Making use of this characteristic and aiming toward the incorporation of three deuterium atoms per molecule, Poteau, Pieters, and co-workers recently presented a methodology for the deuteration and tritiation of a range of 5-membered heteroarenes catalyzed by ruthenium nanoparticles on polyvinylpyrrolidone (PVP) support (Scheme 11).⁹¹ According to DFT calculations, HIE in a position within the 5-membered heterocycles proceeds via 4-

Scheme 10. Regioselective Deuteration of Indoles under Rhodium and Cobalt Catalysis



Scheme 11. Ruthenium-Nanoparticle-Catalyzed Deuteration of Heteroarenes in α and β Positions via Dimetallacyclic Intermediates

Scheme 12. Nickel-Nanoparticle-Catalyzed Deuteration of Heteroarenes



membered dimetallacycles, explaining the inability of homogeneous catalysts to afford such transformations. Further labeling of β and γ positions can have 5-membered dimetallacyclic or monometallacyclic intermediates, respectively.

Deuterium labeling of similar heterocyclic substrates is also possible using commercially available heterogeneous Ru/C catalysts. However, as recently demonstrated by Pieters and co-workers, the addition of NHC ligands is essential to avert concomitant reduction of the aromatic rings (Scheme 11).⁹² It is assumed that the presence of ligands on the metal surface impedes flat π -coordination of the substrates which would lead to reduction of the arene rings. In addition, side-on coordination via heteroatoms should be still possible, thus enabling selective C–H activation and subsequent H/D exchange.

NHC-supported nickel nanoparticles have been shown to be similarly active, affording α -heteroatom-labeled heteroaromatic products.⁹³ Depending on the steric requirements of the NHC ligands and the consequently varying substrate coordination modes, additional labeling in the *ortho* positions of the adjacent aromatic ring can be switched on or off (Scheme 12).

2.1.1.6. Regioselectivity and Chemoselectivity in *ortho*-Directed Aromatic HIE. Thanks to catalyst optimization efforts of the past decade, HIE on arenes nowadays works with a broad variety of directing groups, many of which are frequently encountered functional groups rather than complex and difficult-to-synthesize templates (Figure 6).^{94,82} Thereof, carbonyl groups such as ketones, esters and amides as well as *N*-heteroarenes (especially pyridine and pyrazole) are arguably the most established directing groups for this type of C–H activation. Acetophenone is such a reliable substrate for iridium-catalyzed HIE that it often serves as a test substrate for new developments. However, less conventional directing groups such as free and protected amines or sulfur-containing functionalities have also been explored intensively in recent years and can now be viewed as established *ortho* HIE directing groups, too. Apart from this progress, improved methodologies are still needed for carboxylic acids which, by now, can only be

deuterated in the *ortho* position with known catalysts at elevated temperatures. Furthermore, directed HIE on phenol derivatives is a desirable transformation whose applicability to a broader substrate scope is yet to be demonstrated. Finally, it should be mentioned that most directing groups which are regarded as “established” herein, are merely established for iridium-catalyzed HIE under deuterium gas atmosphere. While these conditions are highly suitable in a tritiation setting, the development of alternative methodologies for these substrates using cheaper catalysts (especially base metals) and isotope sources should be encouraged to broaden possibilities for stable isotope labeling.

Given the steadily increasing number of available directing groups for iridium-catalyzed *ortho*-directed HIE, regioselectivity in the presence of more than one potential directing group can be an issue, especially when attempting late-stage deuteration and tritiation on pharmaceuticals. In order to facilitate planning of such transformations, researchers at Sanofi recently developed a predictive model based on both experimental and theoretical studies that allows to estimate the main deuterium incorporation sites in a molecule *before* running the reaction.⁹⁵ For this purpose, the results of extensive intermolecular competition experiments using the Kerr catalyst in the presence of two substrates containing different directing groups were compared to thermodynamic and kinetic data obtained through DFT calculations (Figure 7). Whereas the experimentally found order of directing group strength could not be correlated to the barrier heights for the iridium C–H insertion step, it corresponded well with the relative free energies of the iridium substrate coordination complexes. Consequently, it appears that the population of these complexes is the main factor determining reactivity under standard conditions. In case two directing groups form similarly stable coordination complexes, the activation energy for the C–H insertion step will govern selectivity.

These findings were applied to predict selectivities in intramolecular competition experiments of a set of substrates

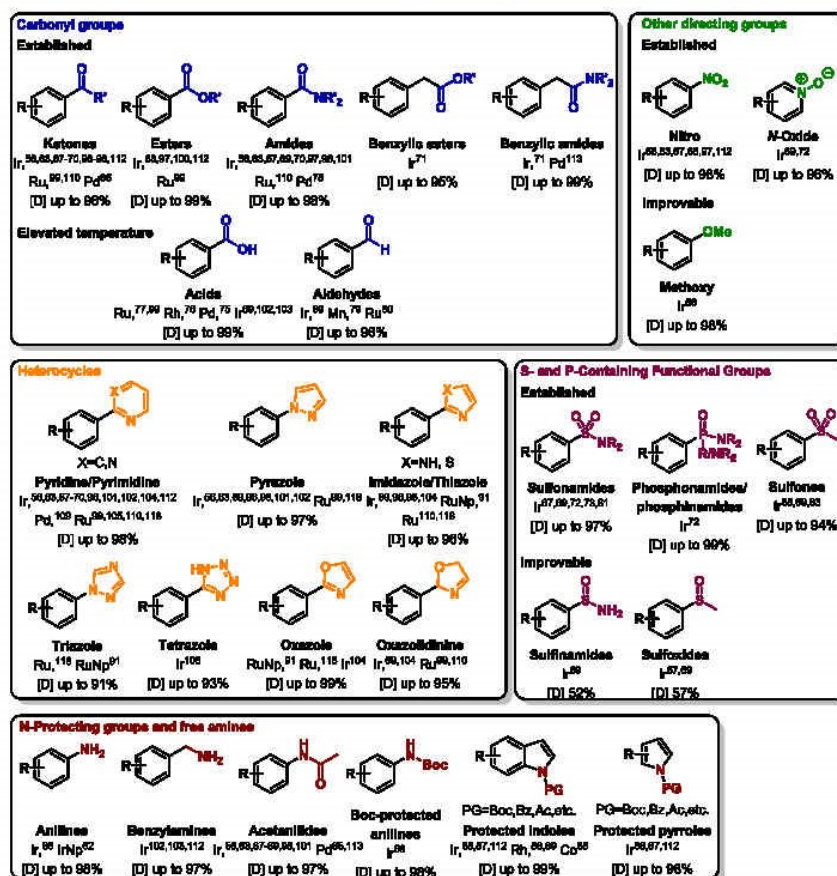


Figure 6. Reported directing groups for transition-metal-catalyzed aromatic HIE.^{56,62,63,67–73,75–77,79–81,83,85–89,91,96–106,109,110,112,113,118}

containing new directing groups which had not been included in the empirical data set as well as on complex molecules. Although a quantitative prediction of deuterium incorporation ratios was not possible, the method serves well to determine the main deuteration site *a priori* for most directing groups except nitro for which the model fails. It has to be noted here that only limited transferability of the results from intermolecular competition experiments to intramolecular competition exists, as two directing groups on the same aromatic ring can mutually affect each other.

A more extensive set of intermolecular competition experiments of directing groups with a neutral and a cationic iridium catalyst was recently contributed by Kerr, Nelson and co-workers.¹⁰⁷ Here, performing reactions using substoichiometric amounts of deuterium gas and thus avoiding full conversion of either substrate allows for a precise distinction of directing group abilities. However, the same order of directing group strength and little difference in reactivity between the two catalysts was observed. Despite having a larger empirical data set compared to the study by Derdaun and co-workers, this method lacks

transferability to nontested directing groups due to the absence of an underlying theoretical model. A fully quantitative prediction of deuteration levels in intramolecular competition experiments is again not given. Interestingly, though, it was observed that qualitative preference for a given substrate in intermolecular competition experiments can be reversed by changing the solvent. This effect was however not thoroughly studied for a larger set of substrates.

In an important case study, Kerr, Reid, and co-workers elaborated on the predictability of intramolecular competition between directing groups.¹⁰⁸ Performing computational and experimental studies on *para*-substituted aromatic compounds containing both a primary sulfonamide and a pyrazole moiety with various substitution patterns, the authors found that, in agreement with the previous studies cited above, the difference in binding energy of the directing groups is again correlated with labeling selectivity. However, the hypothesis stated by Derdaun and co-workers that directing groups on the same molecule mutually affect each other, leading to a lack of transferability from intermolecular binding energies to intramolecular

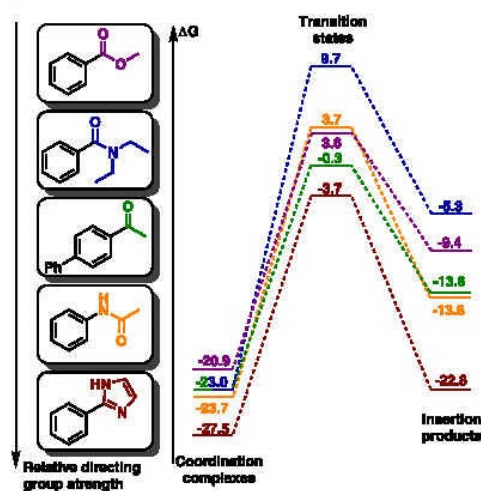


Figure 7. Experimentally found relative directing group strengths compared to thermodynamic data obtained by DFT calculations.

selectivity prediction, was confirmed. Consequently, for accurate predictions, DFT calculations of the binding energy of each directing group need to be carried out on the specific disubstituted molecule of interest rather than on monosubstituted model compounds. Regarding the specific compounds investigated in Kerr's study, unfavorable distorting contributions stemming from secondary interactions of the noncoordinating directing group with the catalyst play an important role and can override favorable attractive interactions, thus changing the overall selectivity. Finally, it should be noted that, depending on the substrate, more expensive calculations which include solvation models as well as thermal corrections to the electronic energies can be needed to accurately reproduce experimental results. Building on these computational results, Kerr, Reid, and co-workers were able to successfully predict catalysts with higher or inverse selectivity by changing the steric properties of the NHC ligand.

Another strategy to achieve selectivity apart from distinguishing two different directing groups can exploit the preferential C–H insertion via 5- or 6-membered metallacycles depending on the specific reaction conditions. In this context, Kerr and co-workers previously demonstrated that such discrimination between positions can be guided by the amount of catalyst used.⁶³ More recently, Yin and Liu found that the choice of the acidic deuterium source in the palladium-catalyzed pyridyl-directed C–H activation of arenes either promotes HIE via a 5-membered palladacycle with a 2-pyridyl directing group

(deuterated acetic acid), or via a 6-membered transition state using an ether-bound pyridyl directing group (deuterated TPA) (Scheme 13).¹⁰⁹ The authors explain this effect by protonation of the pyridyl group by TPA, rendering it incapable of acting as a directing group.

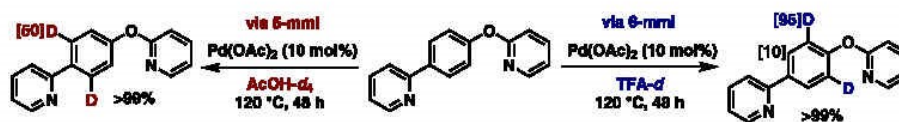
In this context, it is worth mentioning that most directed HIE methodologies rely on 5-membered metallacyclic intermediates whereas more remote directing groups that would require the more challenging formation of larger cyclic intermediates, have only been tackled scarcely.

Another aspect of selectivity in the context of HIE concerns the chemoselective distinction of exchange and reductive labeling pathways. While homogeneous methods usually aim for selective HIE transformations that leave reducible functional groups untouched, a recent study shows that by choosing appropriate cocatalysts, ruthenium-catalyzed *ortho*-directed HIE with or without concomitant reductive labeling of alkynes or ketones can be chosen deliberately.¹¹⁰ Thus, in the presence of catalytic deuterated potassium hydroxide and a slight excess of deuterium oxide, the catalyst $[\text{RuCl}_2(\text{PPh}_3)_3]$ forms a hydroxo species (4) which selectively labels the *ortho* positions of a number of nitrogen-containing directing groups while leaving internal alkynes untouched (Scheme 14a). On the other hand, adding catalytic copper iodide along with an excess of zinc to the precatalyst furnishes a ruthenium hydride species (5). Now, reductive labeling of the alkynes to deuterated (*E*)-alkenes proceeds along with *ortho*-directed HIE, albeit with only moderate deuterium incorporation (Scheme 14b). Under the same conditions, ketones merely act as directing groups. However, a combination of zinc and deuterated potassium hydroxide enables reductive deuteration of ketones to alcohols along with aromatic HIE, catalyzed by the *in situ* formed ruthenium hydride complex 6 (Scheme 14c). Although the possibilities for tuning chemoselectivity as presented in this study are impressive, its synthetic applicability is probably limited by the rather mixed deuterium incorporation levels and the long reaction times required.

2.1.1.7. Increasing Robustness of HIE Methodologies. Besides the quest to find new directing groups and to control selectivity, one goal of recent research on iridium-catalyzed HIE is increasing the robustness of this transformation. In this context, researchers at Sanofi identified temperature windows in which six common iridium-based catalysts show high HIE activity.¹¹¹ While the range of temperatures at which at least 25% deuteration can be achieved is quite large, especially for the Crabtree catalyst which is active between -80 and 130 °C, conducting the reactions at higher temperatures comes at the price of losing selectivity.

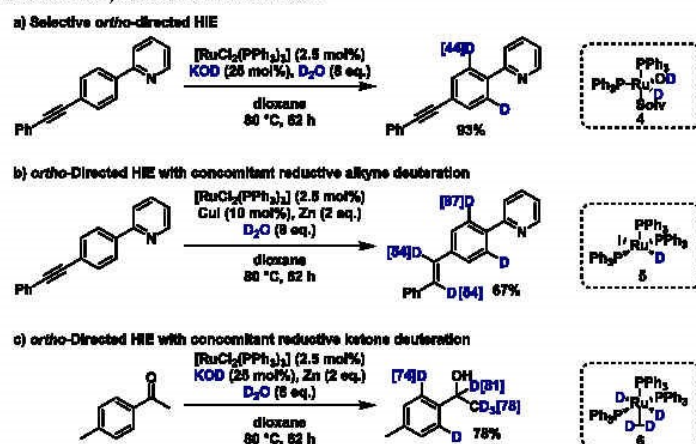
Concerning the solvent scope of iridium-catalyzed HIE, most methodologies have so far been limited to dichloromethane (DCM). In this respect, especially the work of Tamm and co-workers is noteworthy; they recently succeeded in conducting HIE reactions with various directing groups in highly nonpolar

Scheme 13. Palladium-Catalyzed Selective Labeling of Arenes via 5- or 6-Membered Metallacyclic Intermediates Depending on the Deuterium Source



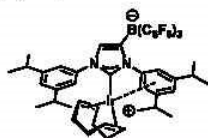
6645

<https://doi.org/10.1021/acs.chemrev.1c00795>
Chem. Rev. 2022, 122, 6634–6718

Scheme 14. Chemoselective *ortho*-Directed HIE vs *ortho*-Directed HIE with Concomitant Reductive Labeling Depending on the Additives in a Ruthenium-Catalyzed Deuteration Protocol

solvents such as cyclohexane by employing a previously reported hydrogenation catalyst and modified versions thereof.¹¹² Instead of consisting of a cationic iridium complex with a counterion, in this case the borate counterion is embedded in the NHC ligand, thus summing up to an overall neutral charge (Scheme 15). However, compared with the *P,N*-chelated Tamm catalyst, these catalysts are slightly less active.

Scheme 15. Neutral Iridium NHC Complex for the Labeling of Arenes in Highly Unpolar Solvents



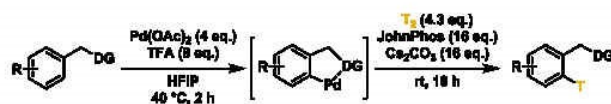
2.1.1.8. *ortho*-Selective Tritiation of Arenes. In medicinal chemistry, tritiation is an important and broadly used tool at various stages of the drug discovery process. Consequently, there is a need for a range of reliable and versatile methodologies for the introduction of radioactive tritium atoms into organic molecules. However, given the high requirements for performing chemical research with radioactive isotopes, preliminary “cold” experiments are often used to gain insight into reactivities before the actual tritiation reactions are carried out. In order to ensure transferability of deuteration results to tritiation, appropriate conditions including the use of gaseous isotope sources need to be used. In this light, deuteration methodologies that employ deuterium gas can often be considered as exemplary studies for tritiation reactions.^{63,73,85,87} Some of the HIE reports

recounted in the previous paragraphs should therefore be kept in mind when reading the following sentences. Moreover, it should be noted that two publications dealing with both deuteration and tritiation^{62,91} have been reviewed in previous subchapters (Section 2.1.1.4 and Section 2.1.1.5).

A palladium-mediated tritiation using coordinating *ortho*-directing groups such as amides, alcohols, amines, carbamates, and *N*-heterocycles was presented by scientists at MSD.¹¹³ In this two-step, one-pot strategy, HIE of the palladacycle intermediate with tritium gas is preceded by an electrophilic C–H activation step which requires excess amounts of palladium (4 equiv) (Scheme 16). This preactivation was necessary as no reaction occurred when tritium gas was present from the beginning, possibly due to the reduction of palladium(II) to palladium(0) species under these conditions. Although such a high amount of transition metal would not be competitive for a deuteration methodology, stoichiometric conditions are unproblematic in a tritiation setting since reactions are usually conducted on a very small scale. Noteworthy, the use of hexafluoroisopropanol (HFIP) as solvent was critical to the success of the reaction. Moderate to good specific activities could be achieved applying this method (17–36 Ci/mmol; Scheme 17). These values could be further increased by extracting the intermediary palladacycles on a bipyridine-containing resin, thus filtering off unreacted starting material before the tritiation step. Furthermore, the C–H activation step of this methodology does not require more than 40 °C to proceed while the tritiation occurs at room temperature. These remarkably mild conditions are unmet by any other recently published palladium-catalyzed HIE.

2.1.2. *meta*-Directed HIE. While *ortho*-directed HIE nowadays is an established method, an upcoming direction in

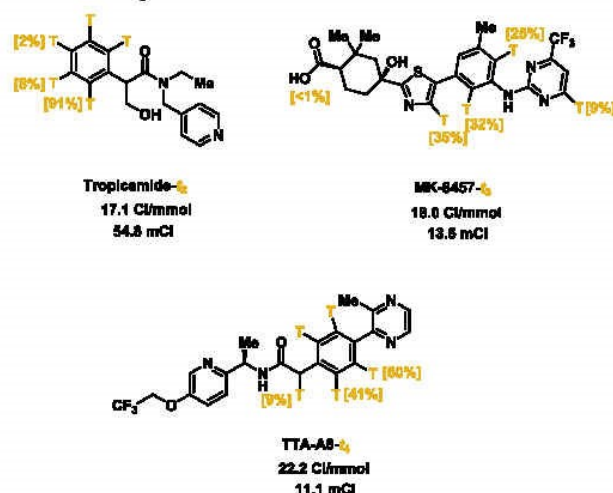
Scheme 16. Tritiation of Pharmaceuticals with Stoichiometric Palladium



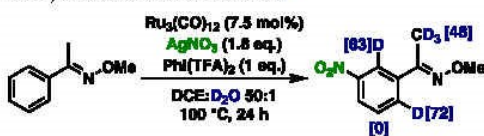
6646

<https://doi.org/10.1021/acs.chemrev.1c00795>
Chem. Rev. 2022, 122, 6634–6718

Scheme 17. Late-Stage Tritiation of Complex Pharmaceuticals



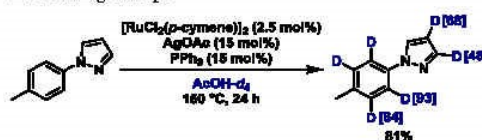
isotopic exchange is *meta*-directed HIE. Clearly, remote deuteration is more challenging than *ortho* deuteration since strategies used for the more general remote C–H functionalization are not necessarily applicable to isotopic exchange. Indeed, accompanying labeling experiments for some ruthenium-catalyzed *meta*-selective C–H functionalizations showed exclusive scrambling in *ortho* position via the corresponding ruthenacycles (Scheme 18).^{114–117} Additionally, such reactions

Scheme 18. Mechanistic Experiment for a Ruthenium-Catalyzed *meta*-Directed Nitration^a

^aDeuterium is only incorporated in the positions *ortho* to the directing group.

often proceed via radical pathways which are difficult to realize for HIE experiments. However, by using deuterated acetic acid as an electrophilic deuterium source and by increasing the electron density on the ruthenium center through addition of a phosphine ligand, Yan and co-workers succeeded in driving *meta* deuteration of aromatics via an electrophilic aromatic substitution pathway (Scheme 19).¹¹⁸ Although concomitant *ortho* deuteration as a result of deuterodemetalation of the intermediary ruthenacycles could not be avoided, the *para* position remained untouched in all cases. *N*-Heteroarenes served as directing groups in this study.

As demonstrated independently by Werz and Maiti¹¹⁹ as well as by Yu and Dai,¹²⁰ palladium catalysis can enable exclusive *meta* labeling without affecting the *ortho* protons and in the presence of competing directing groups (Scheme 20). For this, large template directing groups have to be preinstalled on the substrate which allow for a selective, geometry-directed C–H

Scheme 19. Ruthenium-Catalyzed *ortho*- and *meta*-Deuteration of Arenes in Acidic Media with *N*-Heteroarenes as Directing Groups

insertion of the palladium center at the *meta* position only. In both studies, phenylacetic acids serve as substrates and the directing groups are bound via an ester linkage or, in a more recent study by Kapdi and Maiti,¹²¹ via an amide linkage. Pyridine directing groups appear to be too strongly coordinating and impede reactivity which is why Werz and Maiti employed pyrimidine instead, whereas Yu and Dai modified the pyridyl moiety with fluorine substituents. Both types of directing groups can easily be removed by basic hydrolysis at room temperature. Remarkably, the conditions of Yu and Dai allow to run the reaction at only 80 °C whereas for the other study 110 °C are needed. Additionally, *meta*-directed HIE can be conducted on sulfonic and phosphinic acids as well as on alcohols. In the presence of silver acetate, benzylic protons are exchanged, too. Werz and Maiti further demonstrated that thanks to a KIE of 1, reverse *meta*-selective exchange of deuterium for protium is also possible.

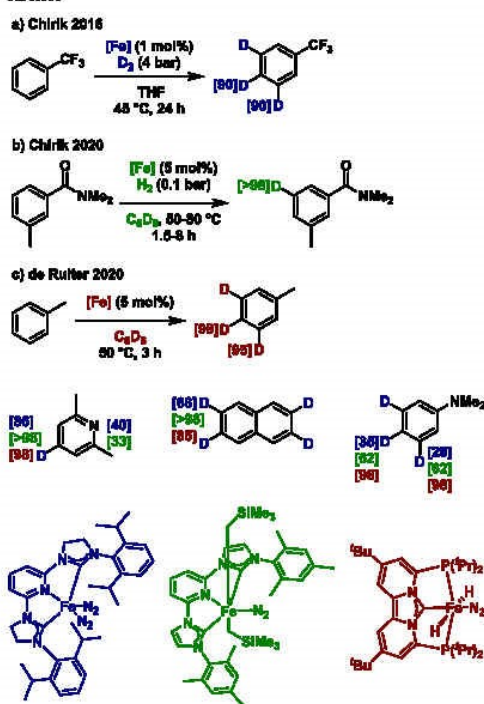
A drawback of currently existing *meta*-selective deuteration methods is that all of them rely on the use of deuterated acetic acid. It is desirable that future research endeavors make these methodologies accessible for labeling with cheaper deuterium sources or with gaseous isotope sources to enable selective tritiation. In addition, as this new direction of remote aromatic HIE is still in its infancy, *para*-selective deuteration has not been achieved so far. Lastly, the development of transient template groups could be a worthwhile approach.

2.1.3. HIE under Steric Control. With directed HIE being a well-explored method, HIE on directing group-free substrates or

Scheme 20. Template-Directed *meta*-Selective Deuteration of Arenes

with orthogonal undirected selectivity is an emerging trend in this field, too. A remarkable example from Chirik and co-workers is the iron-catalyzed deuteration and tritiation of both functionalized and unfunctionalized arenes where selectivity is dominated by steric control and thus complementary to the methodologies recounted so far (Scheme 21a).⁵⁹ In their work,

Scheme 21. Iron-Catalyzed Sterically Controlled HIE on Arenes



Chirik and co-workers elaborated the advantages of using an iron catalyst for tritium labeling such as the possibility to use low pressure of tritium gas under mild reaction conditions. The homogeneous iron catalyst has shown promise in labeling structures that may pose challenges to the existing methodologies and therefore gives medicinal chemists another option to select from in the “toolkit”. However, the highly air and moisture sensitive iron precatalyst requires skilled handling in a glovebox where reactions must be performed with strictly dry equipment and solvents.

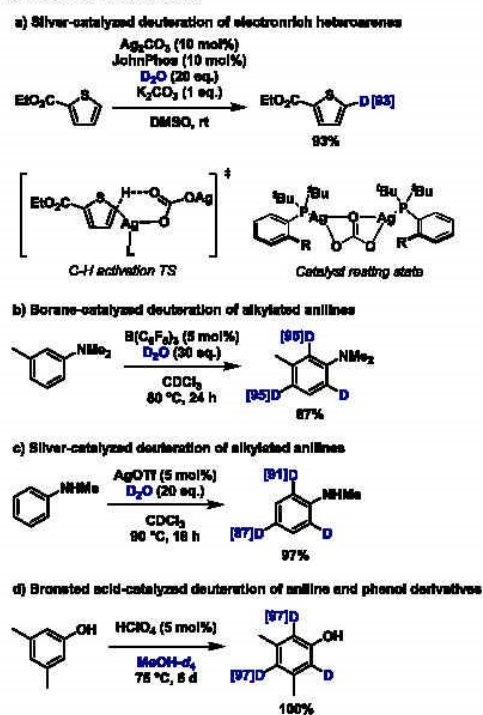
As elucidated in a more recent study by the same group,¹²² iron(II) dihydrides stemming from catalyst activation with hydrogen gas are the catalytically active species involved in the C–H activation step. Besides, using more easily synthesized dialkyl iron complexes as precatalysts and deuterated benzene instead of deuterium gas as the isotope source, this study also presented a more convenient and cheaper method for the preparation of deuterated arenes with excellent deuteration levels (Scheme 21b). Electron-poor arenes were observed to react more readily whereas electron-rich substrates required slightly longer reaction times and higher temperatures. However, the reaction conditions were still sufficiently mild for all substrates and could be even further improved by using a 3,5-dimethyl-substituted pyridine ligand in an optimized version of the iron catalyst.

The same sterically controlled selectivity and even very similar deuterium incorporation levels can alternatively be achieved with an iron PC_{NHC}P instead of PNP pincer complex as recently demonstrated by de Ruiter and co-workers (Scheme 21c).¹²³ Thanks to the good stability of the derived *trans*-dihydride complex, it can be employed directly rather than being formed *in situ* and therefore the reaction does not need to be conducted under an atmosphere of hydrogen. Under otherwise similar conditions, reactions are completed within 3 h. Longer reaction times enable deuteration of less reactive positions, too, thus generating globally labeled arenes. Based on computational and NMR mechanistic studies, the C–H activation step is proposed to proceed via a σ -complex assisted metathesis mechanism with the H–D exchange being facilitated by a subsequent almost barrierless rotation of the iron H–D bond.

2.1.4. HIE under Electronic Control. 2.1.4.1. Labeling of Electron-Rich Positions. Electronically rather than sterically guided regioselectivity plays a bigger role for the directing group-free deuteration of electron-rich heteroarenes including thiophenes under silver catalysis and with only 20 equiv of deuterium oxide as the deuterium source (Scheme 22a).^{124–126} Under mild and open-flask conditions, deuterium is incorporated exclusively in the positions α to the heteroatom. The scope of this reaction was later expanded under base-free conditions and with deuterated methanol as deuterium source.¹²⁷ The presence of carbonate salts was found to be essential under both conditions as carbonate coordination to silver probably assists the deprotonation of the C(sp²)–H bond in a concerted metalation deprotonation regime. Interestingly, the barrier for this step is much lower for carbonate compared to acetate according to DFT calculations and indeed, acetate led to a decreased deuterium incorporation experimentally.¹²⁴ Further mechanistic studies led to the identification of a phosphine-ligated silver complex with bidentate carbonate coordination as catalyst resting state.¹²⁷

Further electron-rich compounds such as aniline and phenol derivatives are traditionally deuterated under acid or base

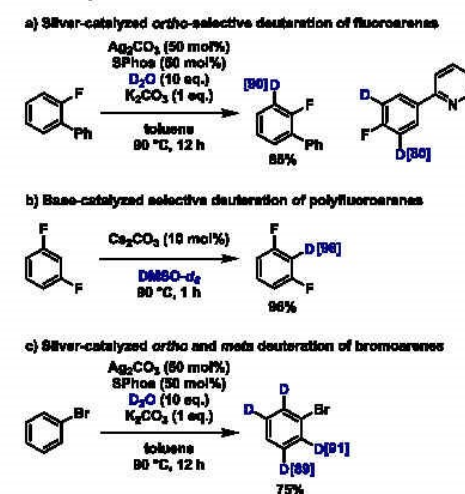
Scheme 22. Electronically Controlled Selective Deuteration of Electron-Rich Arenes



catalysis and harsh conditions.^{84,128} However, also methodologies that enable such reactions under milder conditions appeared in recent years. In this context, very high deuterium incorporation can be achieved for *N*-alkylated aniline derivatives as well as anisoles below 100 °C using Lewis acids such as tris(pentafluorophenyl)-borane (Scheme 22b)¹²⁹ or silver triflate (Scheme 22c)¹³⁰ along with deuterium oxide. Moreover, a combination of perchloric acid and deuterated methanol was additionally applied to the deuteration of free aniline and phenol derivatives at similarly low temperatures but required prolonged reaction times of several days (Scheme 22d).¹⁵¹

2.1.4.2. Labeling of Electron-Poor Positions. While the above-described silver and acid/base-catalyzed deuteration methodologies label electron-rich positions preferentially, a silver/phosphine ligand-catalyzed system similar to the one described above was recently applied to the *ortho*-selective deuteration of monofluoroarenes by the same group (Scheme 23a).^{132,133} Here, the selectivity for the *ortho* position presumably stems from its higher acidity, thus being in line with electronically controlled activation. Remarkably, the presence of pyridine directing groups does not affect the outcome of the silver-catalyzed reaction, rendering this methodology complementary to directed HIE. Polyfluorinated arenes can be deuterated under similar conditions through a base-catalyzed pathway even in the absence of a transition metal (Scheme 23b).¹³⁴ However, solvent quantities of the more expensive deuterated DMSO are required as deuterium source.

Scheme 23. Deuteration of Fluoroarenes and Bromoarenes



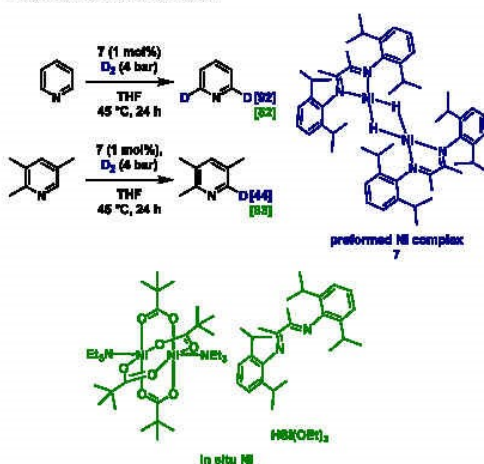
The slightly increased acidity of the positions adjacent to halogen substituents was further harnessed for silver/phosphine-catalyzed HIE of bromoarenes (Scheme 23c).¹³⁵ Interestingly, the positions *ortho* and *meta* to the bromo substituent react preferentially, furnishing polydeuterated arenes with nondeuterated *para* positions. The authors explain this selectivity with the differences in acidity for C–H bonds depending on the distance to the electronegative substituent on the aromatic ring.

A diimine-ligated nickel hydride dimer catalyzes HIE on the least electron-rich positions in electron-deficient nitrogen-containing heteroarenes such as pyridine at 45 °C and under low pressure of deuterium gas (4 bar) while also furnishing *ortho*-directed exchange in adjacent arenes (Scheme 24).¹³⁶

Instead of directly using the nickel hydride dimer, the catalyst can also be generated *in situ* from a nickel precursor, the diamine ligand, and a silane as the source of hydride. Thereby deuteration and tritiation of sterically less accessible positions can be increased. Either way, the catalytically active species is formed by dissociation of the dimeric structure induced by the *N*-heteroarenes thanks to their σ -donating qualities. Compared with previous methods using homogeneous iridium catalysts or also rhodium black and Raney nickel, a different selectivity can be obtained, and deuterium incorporations are generally higher. While homogeneous iridium catalysis shows a directing group-controlled selectivity, deuterium incorporation for this nickel-catalyzed reaction is likely controlled by the acidity of the corresponding C–H bonds as well as proximity to the catalytically active monomeric nickel species that results from substrate-driven catalyst activation.

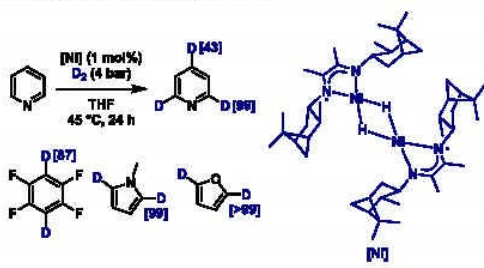
Chirik and co-workers later improved the just-discussed methodology to enable labeling of a much broader selection of aromatic substrates.⁶¹ Using a specially designed bulky, electron-donating diimine ligand, the nickel hydride dimer was now sufficiently destabilized to dissociate even in the absence of nitrogen-containing heteroarenes. Thus, and thanks to their higher activity, electron-rich heteroarenes such as furans and thiophenes as well as polyfluoroarenes became feasible

Scheme 24. Nickel-Catalyzed Deuteration of Electron-Deficient N-Heteroarenes



substrates for deuteration and tritiation even in nonactivated positions, although the highest isotope incorporation levels were still achieved in α positions (Scheme 25). Importantly, the

Scheme 25. Nickel-Catalyzed Deuteration of Electron-Rich and Electron-Poor Heteroarenes

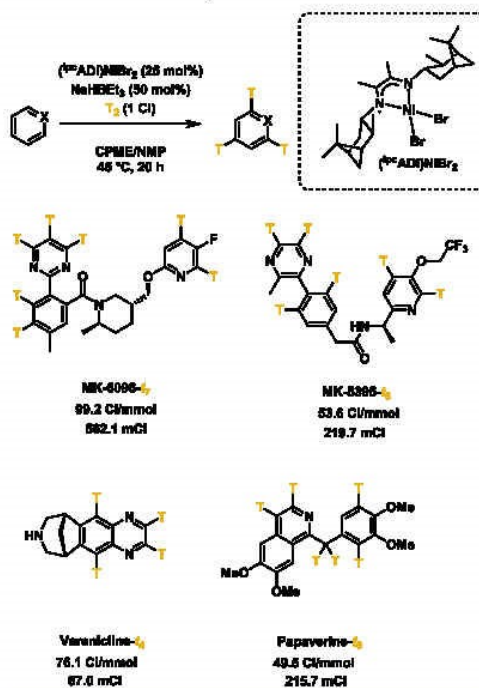


reaction works under mild conditions (45 °C, 4 bar deuterium gas) and tolerates a switch to more polar solvent mixtures which can be necessary for late-stage labeling of pharmaceuticals. The methodology showed good functional group tolerance and a series of complex pharmaceuticals containing diverse functional groups including aryl chlorides, alcohols, amines, sulfones, and unhindered pyridyl groups were tritiated (Scheme 26).

Particularly, the preparation of structurally complex tritiated molecules with a high molar activity (>50 Ci/mmol) is required for some applications. In this respect, the combination of [^{19}C AD]NiBr₂ as a precatalyst with NaHBET₃ allowed achieving high specific activities of >50 Ci/mmol and radiochemical yields ranging from 67 to 562 mCi in the presence of low pressures of tritium gas (~0.15 bar).

A combination of steric and electronic control might play a role in a two-step procedure for the labeling of pyridine derivatives¹³⁷ that exhibits an orthogonal selectivity to both directing group-enabled methodologies and the just mentioned nickel-catalyzed HIE of heterocycles. The method relies on the

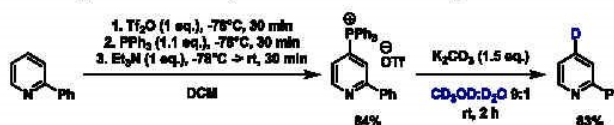
Scheme 26. Nickel-Catalyzed Tritiation



regioselective formation of phosphonium salts in 4-position which, following reaction with a carbonate salt, function as pyridine C4 anion equivalents (Scheme 27). Upon extrusion of carbon dioxide and triphenyl phosphine oxide, the anionic intermediate can abstract a deuterium atom from the mixture of deuterated methanol and deuterium oxide that serves as both solvent and deuterium source. Because of its two-step nature, the methodology does not represent a true HIE reaction and suffers from poor atom economy compared to direct HIE alternatives. However, it is nevertheless applicable to late stage deuteration and even tritiation¹³⁸ of bioactive molecules, thus being a valuable addition to the aromatic HIE toolbox.

2.1.5. Perdeuteration of Arenes by HIE. Depending on the application, comprehensive labeling with a high number of incorporated deuterium atoms can be more desirable than selective labeling of specific positions. For such purposes, most methodologies make use of heterogeneous catalysts. Compared with homogeneous catalysis, one practical benefit of heterogeneous catalysis is the simple isolation of the products by filtration. In addition, the inherent advantages of most of the latter systems are their stability against air and moisture, as well as their convenient recovery and recycling. Furthermore, the reactivity of supported catalysts can be fine-tuned by activation of the catalyst surface. In general, platinum-group metals on carbon (e.g., Pd/C, Pt/C, Ru/C, and Rh/C) are known to catalyze multiple H/D exchange reactions of arenes and heterocyclic amines.¹³⁹ Currently, most established heterogeneous catalysts based on earth abundant metals for HIE are based on nickel and cobalt. In all these examples, either gaseous

Scheme 27. C4-Selective Two-Step Deuteration of Pyridine Derivatives via Phosphonium Salts



deuterium or deuterated protic solvents have been used as labeling reagents. In two review articles, Heys¹⁴⁰ and Hesk¹⁴¹ presented examples of using nickel catalysts for labeling of organic compounds. Surprisingly, to the best of our knowledge, no additional reports on heterogeneous 3d metal catalyzed H/D exchange were published since 2010; thus, this Review will not cover articles in this area.

In contrast to earth-abundant metals, platinum-group metals have proven to be very efficient for H/D exchange,¹⁴² probably because of the oxidative addition of the Ar–H bonds to those metals being more favorable. For example, Sajiki and co-workers reported a series of platinum-group-metal-catalyzed H/D exchanges of various compounds using hydrogen gas in combination with deuterium oxide. There are several reasons for using this unusual combination of hydrogen gas and deuterium oxide in platinum-group metal catalyzed H/D exchange. First, hydrogen acts as a stabilizing ligand or activates the noble metal catalyst for the oxidative insertion step. Second, deuterium gas can conveniently be generated *in situ* in a H₂–D₂O system. Third, the metal catalyst surface is activated using hydrogen gas for the H/D exchange reactions.

As an early example, Sajiki and co-workers reported an *in situ* deuterium gas generation method using a Pd/C-catalyzed H₂–D₂ exchange reaction in a H₂–D₂O system (Scheme 28). In the

corresponding E. The produced D₂ was used for the one-pot reductive deuteration of unsaturated bonds (alkene and alkyne), aromatic halides, epoxides, and nitrile derivatives.¹⁴³ Excellent to quantitative deuterium efficiencies could be achieved in catalytic reduction reactions.

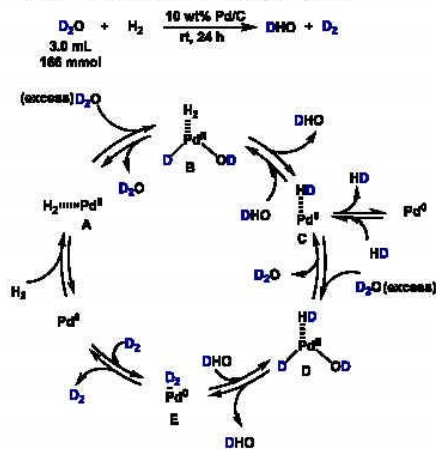
Later on, the same group reported Pd/C as a material for H/D exchange reactions of secondary alcohols and ketones using the H₂–D₂O system.¹⁴⁴ Since then, this principle has been demonstrated successfully on several other occasions, for example H/D exchange on the benzylic positions and alkyl side chains.¹⁴⁵ As another example, electron-rich arenes, such as anilines and phenols but also benzoic acid, were deuterated using deuterium oxide as a deuterium source under hydrogen atmosphere. Consequently, high deuterium incorporation was observed at high temperature (Scheme 29).¹⁴⁶

Later, again Sajiki and co-workers demonstrated that similar H/D exchange reactions of arenes can be catalyzed efficiently in the presence of Pt/C (Scheme 30).¹⁴⁷ These investigations showed that the H/D exchange reaction on an aromatic ring is more efficiently catalyzed by Pt/C, whereas palladium catalysts need higher reaction temperature. This might be due to the formation of the Pt– π -aryl complex being more favorable in the oxidative insertion of Pt(0) into the substrate.

The authors proposed a mechanism based upon oxidative addition of the aromatic C–H bond to Pt centers on the surface (Scheme 31). At the beginning, hydrogen gas most likely acts as a ligand to activate the Pt(0) catalyst. The original step involves the activation of Pt(0) (A) by the coordination of H₂ and D₂O to give complex B. Next, oxidative addition of the Ar–H bond to the Pt– π -aryl complex (C) generates Pt(II) species D. Intramolecular H/D exchange of D and E following reductive elimination gives the deuterium-labeled product Ar–D. The authors proposed that the coordination of the aromatic ring to the platinum generating the Pt– π -aryl complex could be a key step in this reaction. Control experiments showed that no deuterated product is obtained using an aliphatic substrate (octanoic acid) under identical conditions. However, an electrophilic aromatic substitution mechanism could not be excluded in this transformation.

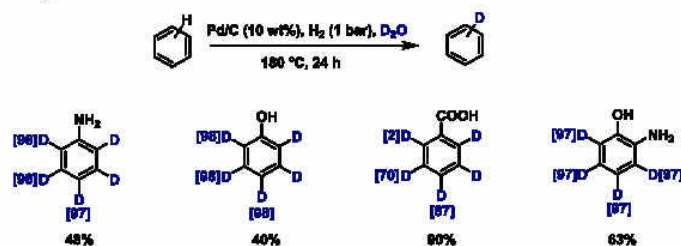
Deuteration of different nitrogen-containing heteroarenes such as pyridines, indoles as well as nucleoside analogues and even diazines could also be directly performed with Pd/C in D₂O in moderate to excellent isolated yields (Scheme 32).¹⁴⁸ Such compounds and related heterocycles are representative structural components of today's pharmaceuticals. Indeed, an analysis showed that 59% of FDA-approved drugs contain such nitrogen heterocyclic motifs.¹⁴⁹

As an interesting example, the deuteration of nucleoside analogues which contain a nucleic acid analogue and a sugar have been investigated for the development of potential antiviral and antitumor agents and as synthetic oligonucleotide probes. In this respect, it is interesting to note that the Pd/C–D₂O–H₂ system can be employed for the deuteration of adenine, guanosine, inosine, hypoxanthine, uracil, cytosine as well as thymine derivatives.¹⁵⁰

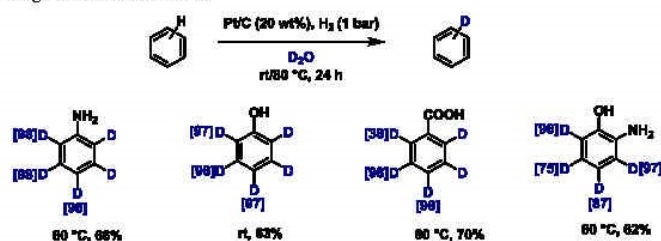
Scheme 28. Proposed Mechanism for the Palladium-Catalyzed Generation of D₂ from D₂O and H₂

H₂–D₂ exchange reaction, they proposed that the key step is the oxidative insertion of Pd⁰ in the H₂–D₂O system. In addition, H₂ or the *in situ* produced HD (or D₂) gas might play a role as a ligand to activate the catalyst. The Pd⁰–HD (C) or D₂ (E) complex is produced *via* ligand exchange reaction of B or D and following reductive elimination. Finally, D₂ gas is generated from

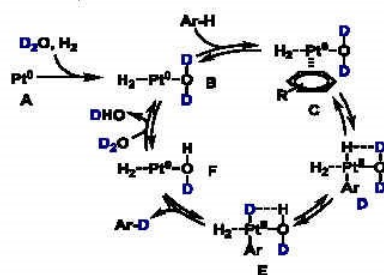
Scheme 29. H/D Exchange of Selected Arenes



Scheme 30. H/D Exchange of Selected Arenes



Scheme 31. Proposed Mechanism for the H/D Exchange of Arenes with Pt/C



More recently, Sajiki and co-workers reported another Pt/C-catalyzed H/D exchange of arenes using a mixed solvent system of 2-propanol and deuterium oxide under argon at room temperature (Scheme 33).¹⁵¹ The formation of dehalogenation products under harsh conditions is often observed utilizing such heterogeneous catalysts. While under these conditions, fluoro substituents are well tolerated, other halogen-containing (e.g., chlorine, bromine, and iodine) derivatives could not be applied, as they mainly produced dehalogenated products.

Interestingly, utilizing mixtures of Pd/C and Ir/C catalysts improved deuteration efficiencies in several cases, for example, salicylic acid, acetanilide derivatives, and 1-naphthol. Unfortunately, no rational explanation is available for this observation so far.

In other early examples, the concurrent use of Pt/C and Pd/C also enhanced deuteration efficiencies, and aliphatic as well as aromatic positions were deuterated with high deuterium incorporation.¹⁵² Notably, in a practical manner, multigram-scale deuteration based on the Pt/C and Pd/C system of bis-aniline derivatives was achieved (Scheme 34). The details of the

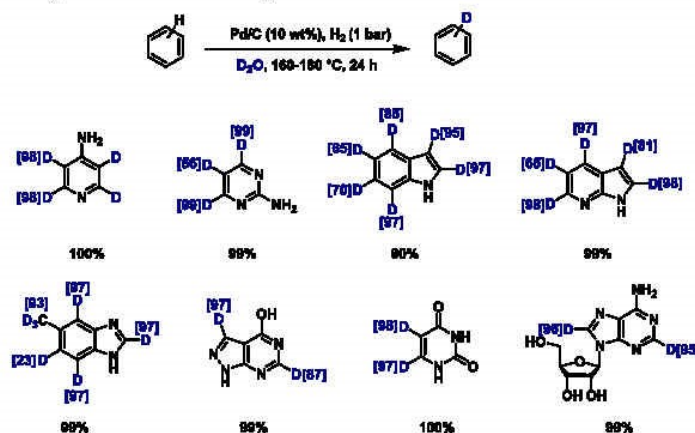
synergic effect using Pt/C and Pt/C are, however, still unexplained.

A new elegant strategy for maximizing the number of incorporated isotopes was recently presented by Pieters and co-workers.¹⁵³ By combining monometallic iridium complexes with iridium nanoparticles formed *in situ* from the same commercially available and air-stable iridium precatalyst, both directed and undirected deuteration and tritiation of diverse aromatic substrates can be achieved, leading to high numbers of incorporated deuterium atoms and high specific activities for tritium labeling (up to 122 Ci/mmol), respectively (Scheme 35 and Scheme 36). More specifically, the presented catalyst system allowed the labeling of azines, indoles, carbazoles, oxa- and thiazoles, thiophenes as well as nucleobases. Moreover, substrates with sensitive functional groups such as nitriles or halogens (Cl, Br, F) could be readily employed. However, compared with the labeling methods discussed above, isotope incorporation is not as comprehensive, leaving some positions completely untouched and affording mixed results for others.

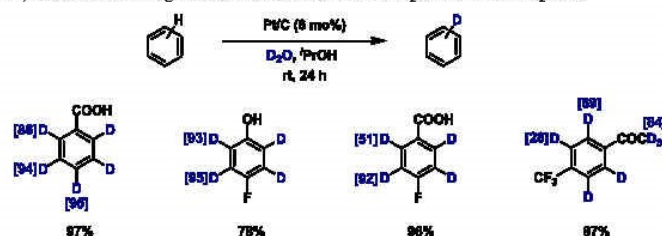
With respect to a more biochemical context, it is interesting to note that all aromatic C–H bonds in purines can be deuterated and tritiated in the presence of ruthenium nanoparticles utilizing gaseous isotope sources (Scheme 37).¹⁵⁴ Remarkably, this method works not only on free purine bases but also on unprotected nucleosides, nucleotides, and even oligonucleotides (up to 12-mer). As required for such diverse substrates, the HIE reaction works under comparably mild conditions (55 °C, 2 bar D₂) over a broad pH range (3–12) and can tolerate different solvents including deuterium oxide. Moreover, depending on the substrate, various NHC- instead of PVP-stabilized nanoparticles led to higher activity by increasing the catalyst solubility. In this sense, oligonucleotides were best labeled with a water-soluble NHC support.

Similarly, ruthenium catalysis afforded complete HIE of nitrogen-containing heteroarenes as well as completely non-activated aromatic substrates such as toluene and naphthalene

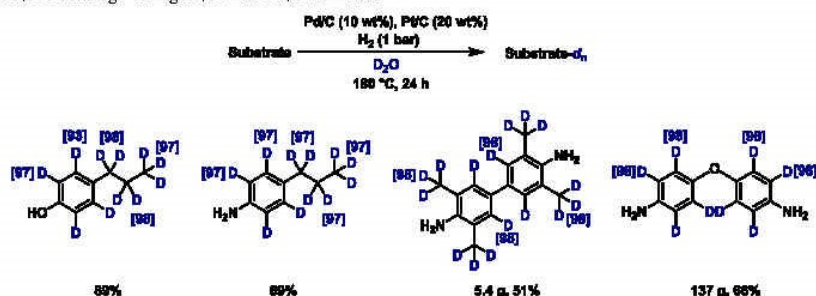
Scheme 32. H/D Exchange of Heteroaromatic Compounds



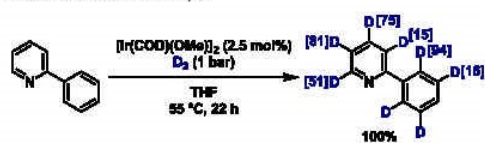
Scheme 33. Pt/C-Catalyzed H/D Exchange Reactions of Aromatic Compounds in 2-Propanol



Scheme 34. H/D Exchange Using Pt/C and Pd/C Mixtures



Scheme 35. HIE on Aromatic Substrates by a Combination of Homogeneous Catalysts and Nanoparticles Derived from the Same Iridium Precatalyst

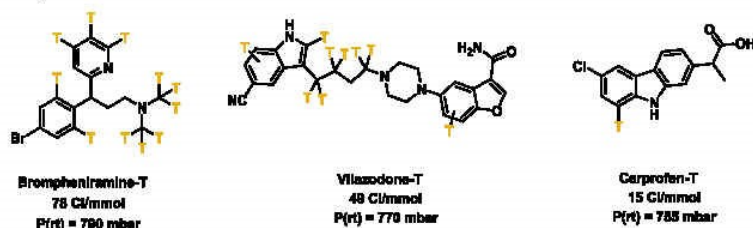


under mild conditions with low catalyst loading (0.1 mol %) (Scheme 38a).¹⁵⁵ Very high deuterium incorporation of

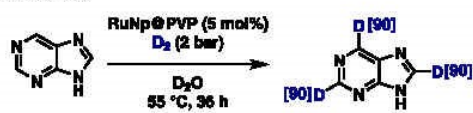
unfunctionalized arenes can simply be achieved by prolonged heating in the presence of catalytic amounts of strong acid in deuterated benzene (Scheme 38b).¹⁵⁶ The deuteration of similar substrates with a platinum CNN pincer complex and a mixture of monodeuterated trifluoroethanol and deuterium oxide resulted in moderate to low deuterium incorporation levels for noncoordinating or weakly coordinating substrates, whereas only catalyst decomposition was observed in the presence of coordinating groups (Scheme 38c).¹⁵⁷

A very general approach for the comprehensive labeling of both plain and complex aromatic substrates was most recently made possible thanks to new achievements in ligand design. In

Scheme 36. Ir-Catalyzed Tritiation of Pharmaceuticals



Scheme 37. Ruthenium Nanoparticle-Catalyzed Deuteration of Purines



this context, a dual ligand system composed of bulky amides derived from amino acids in combination with a pyridine derivative was shown to assist the concerted metalation deprotonation (CMD) step of palladium-catalyzed C–H activation, thus facilitating this reaction.¹⁵⁸ Further modification of the amino-acid-derived ligands by substituting the carboxylic acid functionality by a sulfonamide lead to highly active catalyst systems that prove its value in the HIE of a broad range of aromatic substrates using deuterium oxide as deuterium source.¹⁵⁹ While the exchange proceeds slower at more sterically hindered positions, high deuterium incorporations could generally be achieved (Scheme 38d).

Remarkably, a barium amide complex was recently shown to be capable of catalyzing HIE of aromatic and, preferentially, benzylic C–H bonds in simple arenes under deuterium gas atmosphere (Scheme 38e).¹⁶⁰ It is hypothesized that hydride (deuteride) complexes are the active catalytic species whose aggregation is regulated by the steric requirements of the amide ligands. Bulkier amides inhibited cluster formation and thus led to more active catalysts. Following activation of the aromatic ring by a cation– π interaction with the metal, the reaction probably proceeds *via* a nucleophilic substitution mechanism for aromatic C–H bonds, whereas a sequential deprotonation–protonation mechanism is more likely for benzylic positions. Although the deuterium incorporation levels on the substrates tested so far were rather low, it can be expected that further improvement of alkaline earth metal catalysts for HIE after this inspiring first example can lead to more competitive catalysts.

Deuteration of plain arenes and even alkanes with an iridium PCP pincer complex was very recently demonstrated by Piers and co-workers (Scheme 39).¹⁶¹ Depending on the deuterium source (deuterium oxide or deuterated benzene) and varying amounts of added deuterium gas, the speciation of the iridium complex changes and selectivity can slightly be modulated, albeit at the cost of a lower deuterium incorporation: As an example, in deuterated benzene and with 1.4 mol % deuterium gas, very high deuterium incorporation levels on arenes and reasonable deuteration of alkenes is achieved, whereas with 9 mol % deuterium gas or in deuterium oxide, the overall deuterium incorporation decreases while some selectivity for sterically less hindered positions is observed.

2.1.6. Conclusions. Having been the prevalent technique for deuterium labeling of arenes for decades, nowadays *ortho*-directed HIE under homogeneous catalysis is being increasingly complemented by new methods. On the one hand, nanoparticle catalysis gains more and more attention due to the useful α heteroatom selectivity it offers. On the other hand, selective labeling concepts based on steric or electronic control exerted by the substrates enable access to deuteration patterns that are unattainable under a directed regime. Nevertheless, directed HIE remains an important technique, also thanks to recent efforts that turned ubiquitous and medicinally important functional groups into directing groups.

All in all, the development of selective HIE methodologies continues to attract attention. However, more comprehensively labeled compounds are needed for many applications. Although some progress has been made in this area, future efforts along these lines are especially needed.

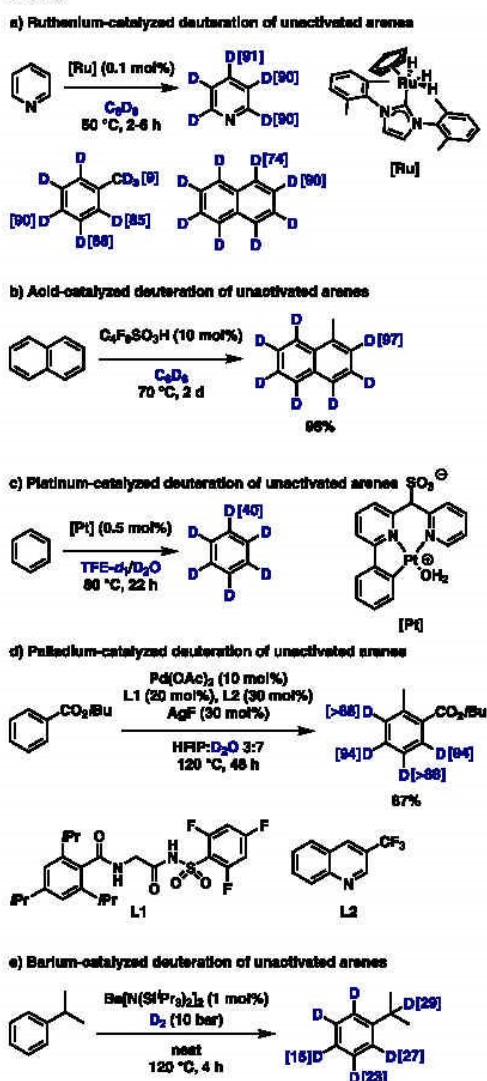
In the broader context of green chemistry, the surge for methodologies catalyzed by abundant available 3d metals has also affected the field of deuteration. Consequently, in the last years, the use of iron, nickel, and even earth alkali metal catalysts became much more popular. It is predicted that these developments will be continued and that robust, easy-to-use methodologies based on Fe, Mn, and other catalysts will be developed in the future.

2.2. HIE on Olefins

Although less common than arenes, olefins are suitable substrates for HIE, too. Their activation in the context of transition-metal catalysis either relies directly on a π -bonding interaction between the olefin and the transition metal^{162–165} or it is assisted by directing groups.^{76,166,167} One example for the latter methodologies has already briefly been mentioned above in the context of carboxylic acid-directed deuteration.⁷⁶ Whereas a rhodium-catalyzed method for arene HIE could be extended for the deuteration of cinnamic acids in β -position, acrylic acid derivatives only exhibited low reactivities to this end and partially gave oligomerization side products (Scheme 40a). In this context, it should be noted that cinnamic *ketones* had previously been reported to undergo selective HIE at the β position under iridium catalysis and deuterium gas atmosphere (Scheme 40b).¹⁶⁶ Given the deuterium source used, a significant challenge was posed by competing reduction side reactions. Eventually, chemoselectivity and good deuterium incorporation were achieved by lowering the catalyst loading and increasing the concentration of the reaction medium.

Aiming for a different selectivity, olefinic *esters* were successfully tackled by a ruthenium-catalyzed HIE methodology that allows the exchange of all olefinic protons with deuterium oxide as solvent and deuterium source (Scheme 40c).¹⁶⁶

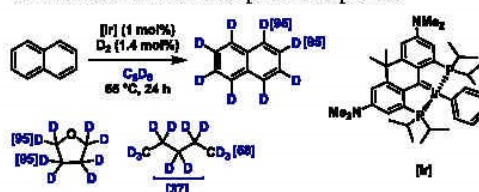
Scheme 38. Recent Examples of Deuteration of Nonactivated Arenes



However, under the described reaction conditions, unactivated terminal olefinic as well as aromatic protons remained untouched, while internal olefins as substrates were not explored.

In 2018, a platinum on carbon catalyzed deuteration of acrylic and methacrylic acid derivatives in deuterium oxide was developed by Sajiki (Scheme 40d).¹⁶⁸ The obtained deuterium-labeled products could be applied as intermediates to prepare the corresponding desired products including a polymer without loss of the deuterium contents.

Scheme 39. Iridium-Catalyzed Comprehensive Labeling of Unactivated Aromatic and Aliphatic Compounds

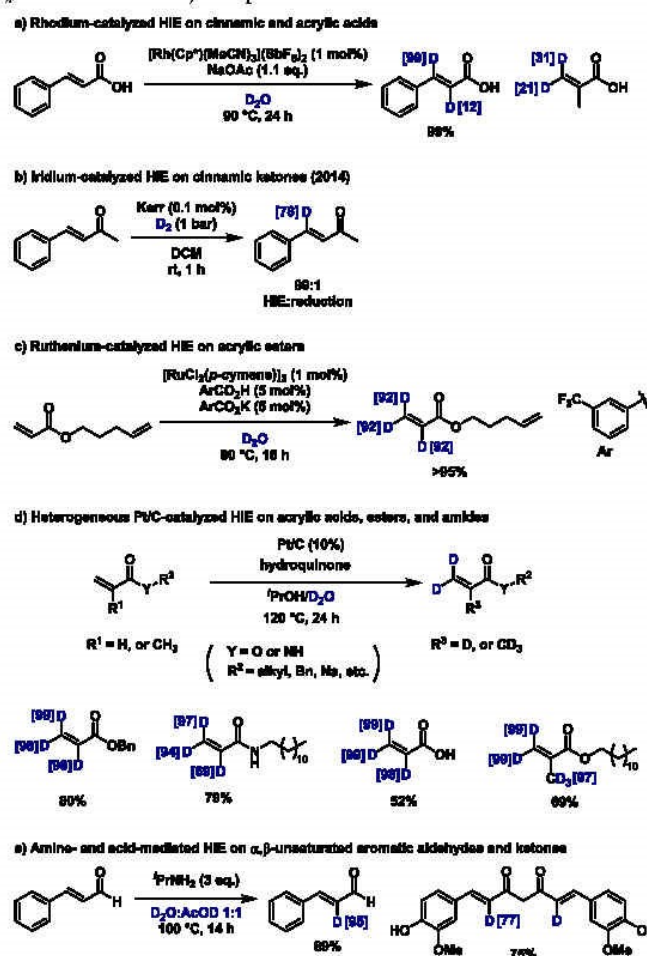


Additionally, α,β -unsaturated aromatic aldehydes and ketones can be selectively deuterated in the α position using a transition-metal-free method (Scheme 40e).¹⁶⁹ Here, an aliphatic amine attacks the Michael acceptor in a conjugate addition fashion, giving rise to a Morita–Baylis–Hillman-type intermediate, which is subsequently deuterated through acid-mediated tautomerization. For this purpose, monodeuterated acetic acid is needed as a deuterium source and cosolvent along with deuterium oxide. While the reaction affords high deuterium incorporations for a range of aromatic and heteroaromatic substrates, it could not be extended to other α,β -unsaturated carbonyl compounds such as cinnamic acids and aliphatic Michael acceptors engaged in isomerization side reactions or decomposed under the reaction conditions.

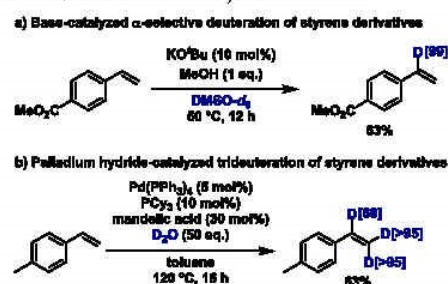
Olefins lacking activation by proximal carbonyl functionalities are arguably more difficult to deuterate selectively. Nevertheless, a base-catalyzed reversible anti-Markovnikov addition–elimination of methanol to styrenes could recently be exploited for α -selective deuteration (Scheme 41a).¹⁷⁰ Deuterated DMSO as solvent and deuterium reservoir enables *in situ* formation of deuterated methanol and allows for equilibration of the reaction to deuterium incorporations of 95% or more. Crucial for the success of this methodology is the amount of alkoxide present in solution. The reactive benzylic anion generated by the anti-Markovnikov addition of methoxide to styrene is rapidly trapped by MeOD. In the presence of too much base, anionic styrene polymerization takes place to a significant extent. Therefore, the reaction conditions were empirically adjusted depending on the substrate. Remarkably, no competing aromatic or β -deuteration was observed. For a S_NAr -reactive substrate use of a bulkier alcohol along with 18-crown-6 sufficiently suppressed the side reaction and afforded nearly complete α -deuteration. However, the fact that reaction conditions had to be optimized for each substrate individually represents a significant limitation of this methodology. Moreover, the reaction could not be extended to electron-rich styrene derivatives.

Complete deuteration of all olefinic protons in styrenes becomes possible in the presence of palladium hydride catalysts, making use of sequential hydropalladation and β -hydride elimination steps, while HIE takes place on the metal center by conducting the reaction in the presence of deuterium oxide (Scheme 41b).¹⁷¹ This reaction appears to be slightly sensitive to steric effects, affording relatively low deuterium incorporation in the α position for a number of more congested substrates.

The allylic positions of polyunsaturated fatty acid derivatives comprising nonconjugated double bonds could selectively be deuterated under ruthenium catalysis (Scheme 42).¹⁶⁵ Interestingly, competing *Z*-to-*E* isomerization as well as the isomerization of skipped to conjugated alkenes under thermodynamic control could be sufficiently suppressed under the reaction conditions.

Scheme 40. HIE on α,β -Unsaturated Carbonyl Compounds

Scheme 41. Deuteration of Styrene Derivatives



2.3. HIE on Alkynes

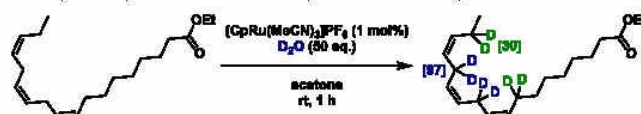
While basic conditions¹⁷² or ruthenium catalysis¹⁷³ had previously been used for the deuteration of terminal alkynes, in a recent report it was found that silver salts can also activate alkyne substrates for labeling processes at the terminal position (Scheme 43).¹⁷⁴ High deuterium incorporations are thus obtained under mild conditions and in the absence of other additives.

Besides, another base-catalyzed methodology using catalytic amounts of potassium hydroxide along with deuterated DMSO as deuterium source was published more recently and can be considered for the fast introduction of deuterium labels in alkynes under mild conditions.¹⁷⁵

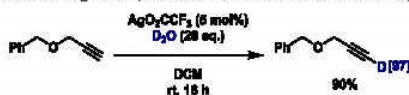
2.4. HIE on Aliphatic Substrates

2.4.1. Deuteration of Aliphatic Alcohols and Amines by HIE. Whereas the past decade has seen a plethora of

Scheme 42. Ruthenium-Catalyzed Allylic Deuteration of Poly-Unsaturated Fatty Acid Derivatives



Scheme 43. Ag-Catalyzed Deuteration of Terminal Alkynes



predominantly ruthenium-catalyzed HIE methodologies for the deuteration of amines^{57,176,177} and alcohols^{178–180} in α - and/or β -position through a hydrogen autotransfer mechanism with imine or carbonyl intermediates; only one new report on this topic appeared in the last 4 years. Consequently, it seems that scope and selectivity of this transformation are sufficiently explored and controllable. A remaining task, however, is to improve the sustainability of such reactions. In this context, the suitability of base metals such as iron and manganese to catalyze HIE of primary and secondary alcohols has recently been demonstrated.¹⁸¹ Interestingly, whereas a manganese pincer complex catalyzes deuteration in α and β positions to an even extent, the iron catalyst selectively affords α -deuterated products (Scheme 44). This is probably due to a higher hydrogenation rate under iron catalysis which renders tautomerization too slow to be competitive.

Harnessing the coordinating ability of the alcohol moiety rather than applying the hydrogen autotransfer concept, Pieters and co-workers recently presented alternative directed labeling of aliphatic alcohols in α position (Scheme 45).⁹² In contrast to established methodologies for this class of substrates, heterogeneous catalysis under deuterium atmosphere in unpolar solvents affords the labeled products here. As discussed in the context of aromatic HIE, the addition of NHC ligands to the Ru/C catalyst efficiently suppresses reductive side reactions while also improving regioselectivity.

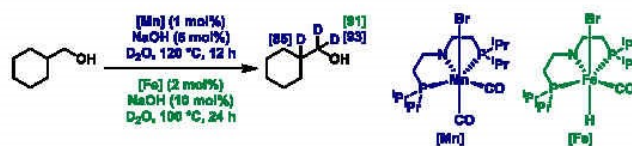
As said above, homogeneous ruthenium catalysts have been widely used in selective HIE reactions. In contrast, supported ruthenium catalysts and nanoparticles have been mainly developed in the past decade. In some specific cases, such supported ruthenium catalysts showed higher activity than Pt/C, Pd/C, and Rh/C. Originally, the regioselective deuteration of carbinol carbon atoms was observed in the presence of Ru/C utilizing hydrogen gas and deuterium oxide.¹⁸²

In 2018, again Pieters and co-workers reported the first ruthenium-catalyzed HIE of C(sp³)-H bonds next to a sulfur atom.¹⁸³ Deuterated and tritiated pharmaceuticals such as methionine, pergolide as well as benzthiazide were obtained (Scheme 46).

In addition, iridium catalysts were used to deuterate tertiary cyclic aliphatic amines in α -position guided by *N*-heteroaromatic directing groups (Scheme 47).¹⁸⁴ For this reaction, the conditions for aromatic iridium-catalyzed HIE with deuterium gas as isotope source could directly be applied to the aliphatic substrates. Whereas secondary amines are less reactive, one example hints at the suitability of ethers as substrates for this transformation.

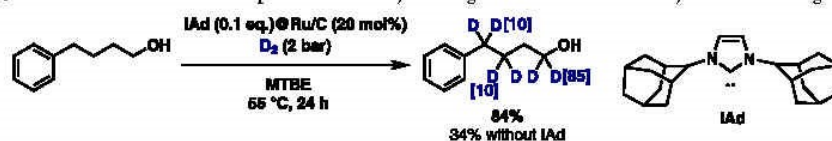
Combining two well-established reactivity modes of photoredox catalysis, namely, the oxidation of alkylamines by a photocatalyst in its excited state, affording α -amino radicals, and hydrogen atom transfer (HAT) catalysis, MacMillan and co-workers successfully demonstrated the α -deuteration and tritiation of complex pharmaceuticals (Scheme 48a).^{60,185} In their studies, bulky thiols exchange with deuterium oxide (or tritium oxide) as the isotope source prior to being subjected to deuterium (tritium) atom abstraction by the intermediary α -amino radical of the substrate.¹⁸⁶ The resulting thiol radical is subsequently reduced, regenerating both HAT and photoredox catalysts. This way, several deuterium (or tritium) atoms can be incorporated in each substrate, affording high specific activities in the case of tritiation. Compared to the iridium-catalyzed methodology described above, the same selectivity is achieved, but a directing group is not required. Further, when adding a slight excess of lithium carbonate, substrates can be directly employed as hydrochloride salts. A slight drawback of this methodology is a lack of general conditions, so that two different photocatalysts, HAT catalysts, and light sources need to be evaluated for each substrate. Switching from mild carbonate salts to a stronger organic base, this methodology could recently be extended to primary amines, rendering the α -deuteration and tritiation of lysine side chains in peptides and peptidic drugs feasible (Scheme 48b).¹⁸⁷ Moreover, unprotected *N*-termini of peptides can be deuterated. However, this labeling reaction is accompanied by racemization, leading to diastereomeric products.

In contrast, a racemization-free α -deuteration of α -amino esters can be achieved in a biocatalytic setting.¹⁸⁸ A pyridoxal phosphate (PLP)-dependent enzyme (SxtA AONS) was used to deprotonate the condensation products of amino acids with pyridoxal, giving rise to a quinonoid intermediate (Scheme 49a). Conducting the reaction in deuterium oxide leads to proton-deuterium exchange at lysine residues, which can subsequently deuterate the quinonoid intermediate, affording α -deuterated amino esters. The reaction showed a broad scope for amino esters but was somewhat less applicable to unprotected amino

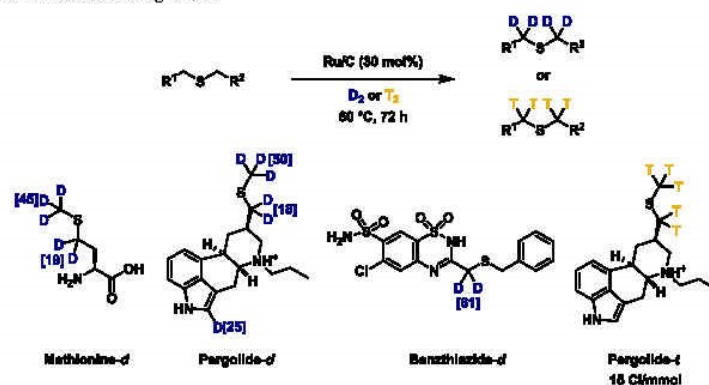
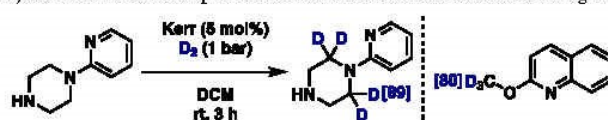
Scheme 44. Manganese- and Iron Pincer Complex-Catalyzed α,β -Deuteration of Aliphatic Alcohols

6657

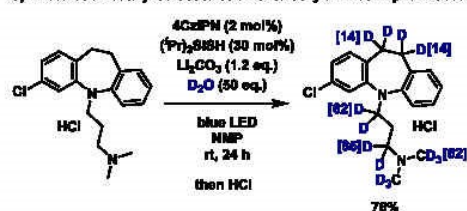
<https://doi.org/10.1021/acs.chemrev.1c00795>
Chem. Rev. 2022, 122, 6634–6718

Scheme 45. Directed α -Deuteration of Aliphatic Alcohols by Heterogeneous Ruthenium Catalysis with NHC Ligands

Scheme 46. HIE on Thioethers Using Ru/C

Scheme 47. Iridium-Catalyzed Deuteration of Aliphatic Amines with *N*-Heteroaromatic Directing GroupsScheme 48. Photoredox-Catalyzed α -Deuteration of Aliphatic Amines

a) Photoredox-catalyzed deuteration of tertiary amines in pharmaceuticals

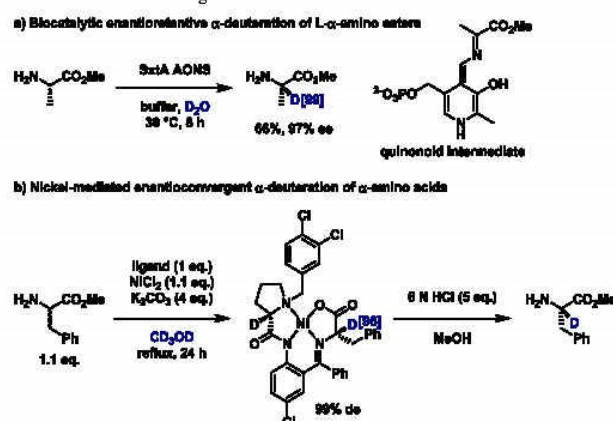


b) Photoredox-catalyzed deuteration of lysine side chains in peptides



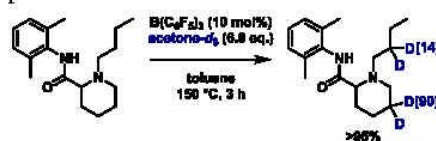
acids. Whereas both ι and ρ enantiomers are amenable substrates for this transformation, only the natural ι -amino esters are deuterated in an enantioselective fashion.

Going one step further, enantioconvergent rather than enantioselective deuteration of amino acids can be achieved by a chiral nickel complex-mediated dynamic kinetic resolution

Scheme 49. Enantioretentive and Enantioconvergent Deuteration of α -Amino Esters and Acids

process (Scheme 49b).¹⁸⁹ Both L and D isomers of α -deuterated amino acids can be prepared by choosing the configuration of the ligand appropriately. However, a significant drawback of this methodology is the need for stoichiometric amounts of the chiral nickel complex from which the deuterated products are released by treatment with hydrochloric acid.

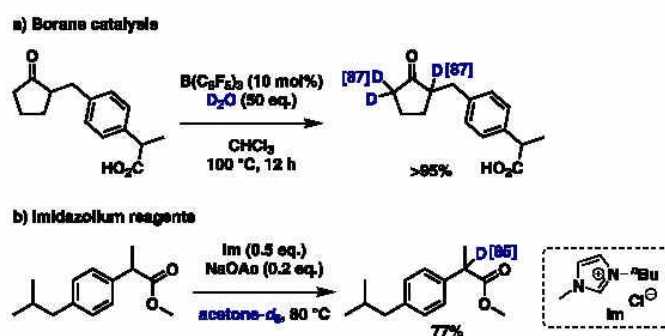
Cooperative Brønsted base and Lewis acid catalysis was exploited for the β -selective deuteration of tertiary aliphatic amines using deuterated acetone as a source of deuterium (Scheme 50).¹⁹⁰ The latter can be activated for nucleophilic

Scheme 50. Borane-Catalyzed β -Selective Deuteration of Aliphatic Amines

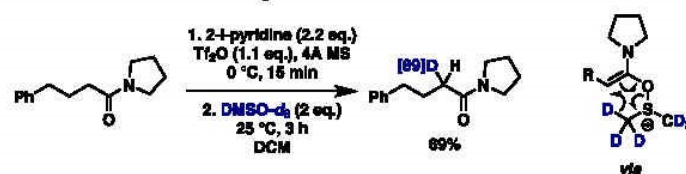
attack by the Lewis-acidic borane prior to deuterium abstraction by the amine substrate, hereby generating a deuterated ammonium salt as the actual deuteration reagent. Thus, the

amine substrate additionally plays the roles of deuteration reagent and base catalyst. Mechanistically, the borane abstracts a hydride from the amine substrate, affording an iminium ion which is deprotonated by another amine functioning as a base. The resulting enamine attacks the deuterated ammonium ion, furnishing a β -deuterated iminium ion which is finally reduced by the borohydride, generating the deuterated product and regenerating the boron catalyst. This concept was successfully applied to a large set of complex tertiary amines with consistently high deuterium incorporation. However, compared with the α -selective amine deuteration methodologies described above, a higher reaction temperature is needed here (150 °C).

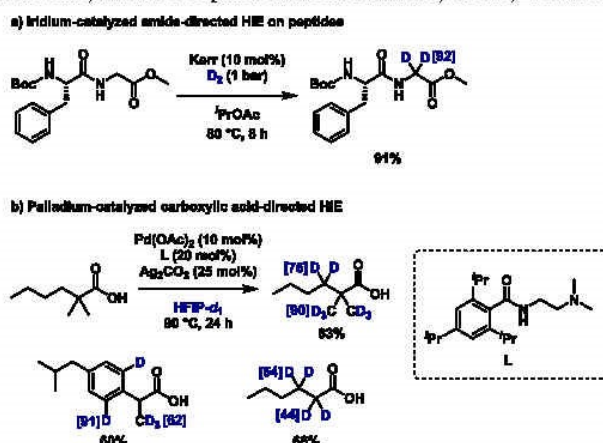
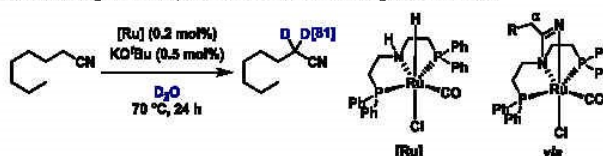
2.4.2. Deuteration of Aliphatic Carbonyl Compounds by HIE. Compared with HIE on aliphatic amines, the α -deuteration of aliphatic ketones is more facile because of increased C–H acidity of α -protons. Thus, activation of the carbonyl group by a Lewis acid catalyst such as tris-(pentafluorophenyl)-borane for exchange of the protons in α position with deuterium oxide at 100 °C affords multideterated compounds with high deuterium incorporation (Scheme 51a).¹⁹¹ Alternatively, α -carbonyl positions can undergo imidazolium salt-mediated H/D exchange where NHC-acetone- d_6 adducts represent the active species (Scheme

Scheme 51. Organocatalyzed α -Deuteration of Aliphatic Ketones

Scheme 52. Monodeuteration of Amides via Electrophilic Amide Activation



Scheme 53. Transition-Metal-Catalyzed HIE of Aliphatic Substrates Directed by Carboxylic Acid Derivatives

Scheme 54. Ruthenium Pincer Complex-Catalyzed α -Deuteration of Aliphatic Nitriles

51b).¹⁹² In a previous related study, deuterated chloroform was used as the deuterium source; however, only low deuterium incorporations were achieved.¹⁹³

Aliphatic amides are somewhat more challenging substrates and have therefore been tackled by different strategies: In this context, selective monodeuteration can be achieved by electrophilic activation of amides with triflic anhydride and a pyridine derivative, followed by nucleophilic attack of deuterated DMSO at the intermediary keteniminium ion (Scheme 52).¹⁹⁴ The resulting enamine subsequently decomposes to an α -deuterated amide in a retro-ene type reaction. The methodology shows good functional group tolerance and high deuterium incorporation on a number of substrates. Moreover, although the second hydrogen atom can be exchanged for deuterium by conducting the procedure twice, deuteration levels for bis-deuterated products are somewhat lower.

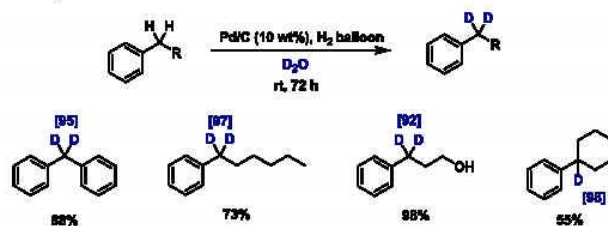
Following the principles of directed C–H activation and demonstrating in another example that iridium-catalyzed directed HIE is not limited to aromatic substrates, Atzrodt, Derdau, and co-workers from Sanofi described an amide-directed HIE on peptides as well as antibody drug conjugate

linkers and payloads (Scheme 53a).¹⁹⁵ With the exception of glycine derivatives, which furnish α -deuterated products, selective labeling in β -position with respect to the amide was achieved under iridium catalysis.

Building on precedence in directed palladium-catalyzed C(sp³)–H functionalization chemistry, a first methodology for the challenging β deuteration of unactivated aliphatic carboxylic acids was achieved most recently using newly developed sterically hindered ethylenediamine ligands (Scheme 53b).¹⁹⁶ Remarkably, under the reaction conditions, both methyl and methylene positions were deuterated to similar extents. However, no reaction took place on tertiary carbon atoms, and the selectivity of this HIE reaction with respect to aliphatic α positions and aromatic C–H bonds is improvable. A further drawback of this methodology lies in the use of expensive deuterated HFIP as deuterium source and solvent. Nevertheless, the labeling of several bioactive compounds using this methodology demonstrates its potential for the field.

Krishnakumar and Gunanathan managed to deuterate aliphatic nitriles in α -position catalyzed by a ruthenium PNP pincer complex (Scheme 54).¹⁹⁷ Mechanistically, it is proposed

Scheme 55. Versatility of Benzylic Deuteration

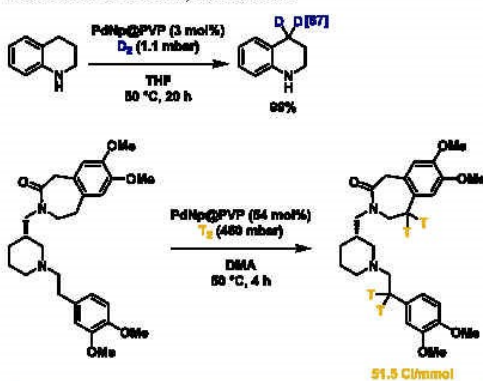


that the nitrile functional group is activated by cycloaddition to the ruthenium center from where an imine/enamine tautomerism along with isotopic exchange on the nitrogen atom leads to the α -deuterated products.

2.4.3. HIE in Benzylic Positions. Using a heterogeneous Pd/C catalyst along with the above-described Pd/C–H₂–D₂O system, benzylic aromatic positions were deuterated very effectively (Scheme 55).¹⁹⁸

A new and alternative methodology for the selective labeling of benzylic positions employs PVP-stabilized palladium nanoparticles as catalyst along with gaseous isotope sources.¹⁹⁹ As high isotopic enrichments could still be observed under subatmospheric pressure, the reaction is ideally suited for tritium labeling which was demonstrated on a number of complex substrates (Scheme 56).

Scheme 56. Palladium Nanoparticle-Catalyzed Deuteration and Tritiation of Benzylic Positions



Being a domain of heterogeneous catalysis, homogeneous transition-metal-catalyzed selective HIE at C(sp³)–H bonds in the absence of directing groups is still very limited until now. Indeed, only one example of a cobalt-catalyzed HIE protocol under deuterium gas atmosphere was published in recent years. Here, an unusual preference for benzylic positions is observed, leaving aromatic C–H bonds almost untouched.²⁰⁰ Although the substrate scope of this methodology shows varying deuterium incorporation levels, the fact that primary, secondary, and tertiary benzylic positions are all deuterated equally well is remarkable. Moreover, complete enantioselective of chiral tertiary centers (Scheme S7a) as well as a diastereoselective deuteration of racemic substrates (Scheme S7b) was observed.

HIE of benzylic C–H bonds is further possible under photocatalysis. Using the tetrabutylammonium decatungstate (TBADT) HAT photocatalyst and, crucially, tetrabutylammonium bromide (TBAB) as an additive, benzylic radicals can be generated and subsequently deuterated with thiol HAT catalysts in the presence of deuterium oxide (cf. the photoredox-catalyzed deuteration of aliphatic amines, *vide supra*).²⁰¹ This way, high deuterium incorporations can be achieved in benzylic positions, while other aliphatic hydrogen atoms such as those in α -position to heteroatoms and at tertiary carbon atoms are exchanged concomitantly (Scheme 58).

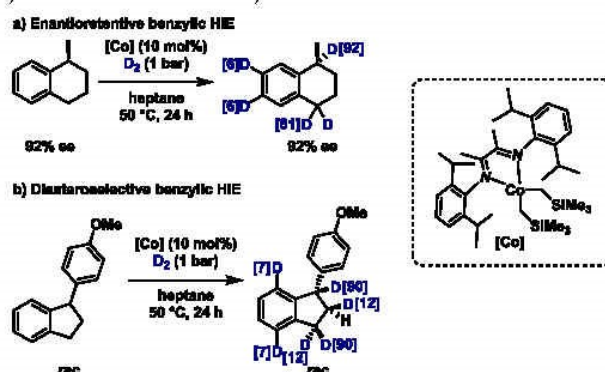
In a number of cases, acid-mediated HIE of polarized C–H bonds is relatively facile. Thus, methyl substituents at pyridine²⁰² and Hantzsch ester²⁰³ derivatives can be transformed into tridenteromethyl groups under Brønsted or Lewis acid¹³⁰ catalysis using deuterium oxide as source of deuterium (Scheme 59).

In contrast, unactivated benzylic methyl groups are efficiently deuterated in the presence of strong base (sodium hydroxide) with deuterated DMSO as the deuterium source (Scheme 60a).²⁰⁴ Using catalytic amounts of potassium *tert*-butoxide instead of sodium hydroxide, the reaction even works at temperatures as low as 30 °C. Similarly, the increased acidity of benzylic and vinylic difluoromethyl as well as monofluoromethyl groups was explored in a base-catalyzed HIE reaction (Scheme 60b).²⁰⁵ Interestingly, depending on the substrate, a small excess of deuterium oxide is needed additionally; however, the reason for this has not been elucidated. Although providing high levels of deuteration in the desired position, the methodology is unfortunately not selective, and concomitant HIE on the aromatic ring and in olefinic positions is observed for many substrates, too.

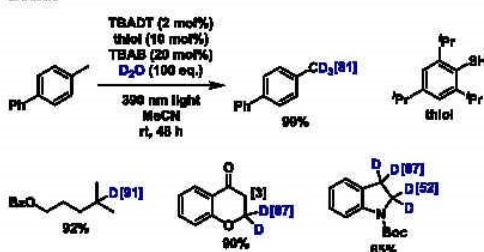
2.4.4. Conclusions. Having been largely limited to the ruthenium-catalyzed α and β deuteration of alcohols and amines in the past, the toolbox for HIE on aliphatic substrates has been significantly expanded in the past few years. Initial examples have shown that iridium-catalyzed HIE is applicable not only to arenes but also to aliphatic substrates provided that suitable directing groups are present. Moreover, significant advances have been made following the introduction of photoredox and HAT catalysis to aliphatic deuteration, while further valuable contributions under Lewis acid catalysis were made.

Although the nondirected cobalt-catalyzed deuteration of benzylic positions holds promise for further nondirected applications, aliphatic labeling is still restricted to deuteration in proximity of activating groups such as amines, alcohols, and carbonyl groups. A general protocol for remote aliphatic HIE remains to be seen.

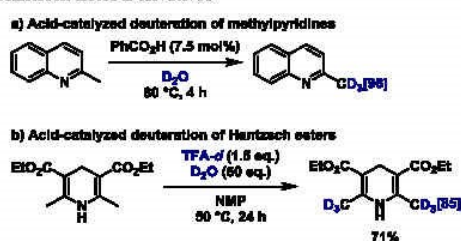
Scheme 57. Cobalt-Catalyzed Nondirected HIE at Benzylic Positions



Scheme 58. Photocatalyzed Deuteration of Hydridic C–H Bonds



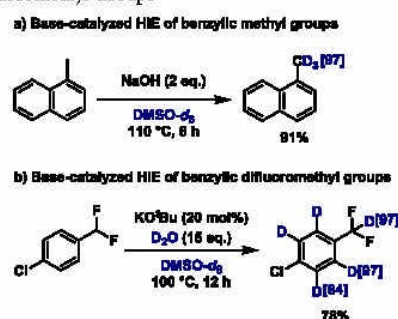
Scheme 59. Acid-Catalyzed Deuteration of Pyridine and Hantzsch Ester Derivatives



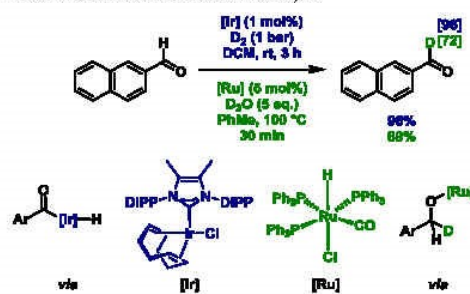
2.5. Deuteration of Aldehydes by HIE

Aromatic aldehydes exhibit several potential deuteration sites: the aromatic protons as well as the formyl hydrogen. Whereas reliable systems for aromatic HIE exist (although less so for benzaldehydes), selective formyl HIE has only been tackled relatively recently in two independent reports (Scheme 61). More specifically, Kerr, Tuttle, and co-workers developed a catalyst for this transformation based on the hypothesis that equatorial coordination of the aldehyde will favor aromatic HIE, while axial coordination may render the formyl hydrogen more accessible.²⁰⁶ Consequently, a small barrier for *cis/trans* isomerization is required in order to permit facile axial coordination. Indeed, formyl selectivity for the NHC-ligated iridium chloride complex was very good and deuterium

Scheme 60. Base-Catalyzed HIE of Benzylic Methyl and Difluoromethyl Groups



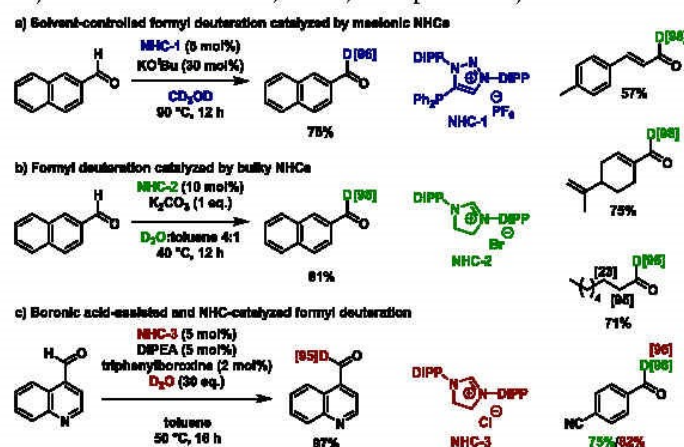
Scheme 61. HIE on the Formyl-H of Aromatic Aldehydes under Iridium and Ruthenium Catalysis



incorporation levels above 95% could be achieved for many substrates.

Interestingly, combining heterogeneous ruthenium catalysts with NHC ligands improved the selectivity of this transformation further (other than under homogeneous iridium catalysis, no trace deuterium incorporation in the aromatic ring was observed). However, this improved selectivity comes at the price of only affording moderate deuterium incorporation levels.⁹²

Scheme 62. NHC-Catalyzed Deuteration of Aromatic, Olefinic, and Aliphatic Aldehydes



An alternative but somewhat less potent method was presented in the same year by the Newman group.²⁰⁷ Instead of inserting into the formyl C–H bond like the iridium catalyst, in this case a ruthenium deuteride adds onto the aldehyde, leading to an alcohol intermediate. Dehydrogenation then affords the labeled aldehyde. Unfortunately, this method was strongly affected by the presence of trace amounts of carboxylic acids, which inhibit the reaction, thus requiring a high purity of the aldehyde starting materials. Unfortunately, neither the iridium nor the ruthenium catalysis could be extended to labeling of aliphatic aldehydes.

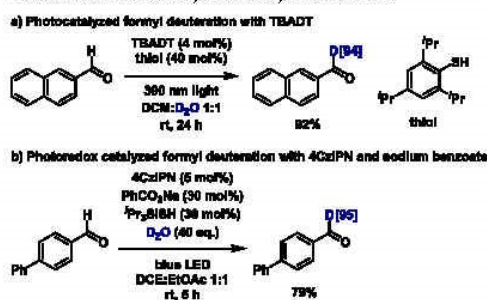
However, such transformations were realized thanks to the independent discovery of two organocatalytic methodologies exploiting the reversible Breslow intermediate formation between aldehydes and NHC catalysts for formyl deuteration (Scheme 62a,b).^{208–210} The main challenge in both cases was sufficient suppression of the competing and kinetically favored benzoin condensation pathway. Whereas one strategy uses a bulky NHC catalyst to impede self-condensation,²¹⁰ the other one relies on solvent-regulated reversible Breslow intermediate formation in deuterated methanol as both solvent and deuterium source.²⁰⁹ Importantly, no concomitant aromatic HIE takes place, and the substrate scope is significantly enlarged compared with the above-mentioned transition-metal catalyzed methodologies, now including olefinic and aliphatic aldehydes. However, α -unsubstituted cinnamaldehydes and aliphatic aldehydes engage in side-reactions under the conditions reported by Bouffard, Bertrand, Yan, and co-workers, and electron-deficient benzaldehydes are not deuterated efficiently.²⁰⁸ Chen, Zhang, Wang, and co-workers managed to deuterate even those more challenging substrates efficiently but needed to choose appropriate NHC catalysts substrate-dependently while reoptimizing reaction conditions.²⁰⁹

Another approach to suppress the benzoin condensation side reaction in NHC-catalyzed formyl deuteration lies in the addition of boronic acids to stabilize the Breslow intermediate, which was shown to be particularly useful for the more problematic electron-deficient benzaldehyde derivatives (Scheme 62c).²¹¹ Moreover, in this report, Milo and co-workers provided a computationally developed guideline to simplify and

accelerate the process of finding ideal reaction conditions for individual substrates.

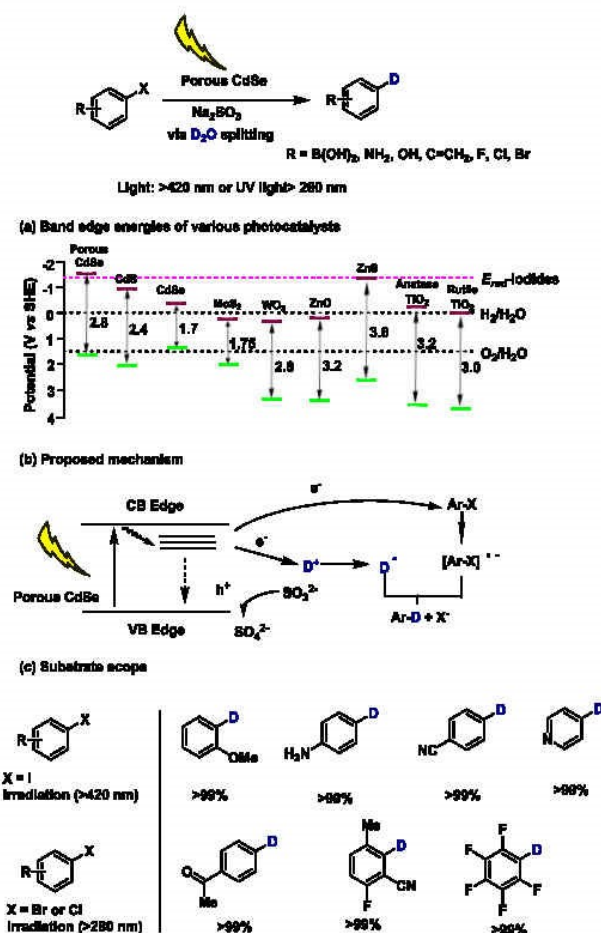
Besides transition-metal and NHC catalysis, photocatalysis has recently been shown to effect efficient HIE at the C1 atom of aldehydes (Scheme 63).^{204,212–214} For this purpose, said

Scheme 63. Photocatalyzed Formyl Deuteration



compounds are activated by hydrogen atom abstraction with either the photocatalyst decatungstate in its excited state or a benzoate radical, generated *in situ* by oxidation of sodium benzoate by the excited organic photoredox catalyst 4CzIPN. The resulting acyl radicals can, in turn, abstract a deuterium atom from *in situ* deuterated thiol HAT catalysts (cf. the photoredox-catalyzed deuteration of aliphatic amines, *vide supra*), thus affording deuterated products. Remarkably, both aromatic and aliphatic aldehydes are susceptible to this transformation and decarbonylation side reactions did not pose a problem under any of the reported conditions. Furthermore, aromatic C–H bonds remained untouched as their bond dissociation energies are too high for decatungstate- or benzoate-mediated HAT.

Scheme 64. Photocatalytic Deuteration



3. REDUCTIVE DEUTERATION

3.1. Deuterodehalogenation

Although HIE is the most common and, considering its high utility for late-stage pharmaceutical applications, arguably also the most desirable method for the preparation of deuterium- and tritium-labeled compounds, alternative transformations such as dehalogenative labeling are important components of the pool of isotopic labeling methods. Especially deuterodehalogenation has some intrinsic advantages: By virtue of its mechanism, complete selectivity for the preselected positions as well as reliable deuterium incorporations of usually more than 99% are guaranteed. Whereas directed HIE usually affords diduterated products unless one of the two accessible *ortho* (or *meta*) positions are blocked, deuterodehalogenation allows the incorporation of a predictable number of deuterium atoms depending on the substrate (that is, if potential HIE side reactions are sufficiently suppressed under the reaction

conditions). Moreover, aryl (and alkyl) halides are widely used and therefore commonly available substrates. Indeed, following the concept of classic halogen chemistry, deuteration can be easily achieved with controlled regioselectivity. In analogy to hydrogenation chemistry, dehalogenative deuteration or tritiation is frequently carried out using a heterogeneous palladium catalyst (Pd/C) along with deuterium or tritium gas.^{215–219} However, protic hydrogen atoms in the substrate or solvent quickly exchange with the isotope source under these conditions, leading to drastically reduced degrees of labeling. Consequently, exchange of all labile protons prior to reduction as well as the use of dry and potentially deuterated solvents are required. Further, chemoselectivity issues can arise in the presence of olefinic moieties in the substrate. Harsh reaction conditions (e.g., *n*-BuLi at -78°C) are often required in further available strategies to cleave C–X bonds first. Alternative and more modern cross-coupling mechanisms generally require nucleophilic deuterides, thus calling for deuterium sources such

as deuterioformates or α -deuterated alcohols. In this context, one of the major improvements in dehalogenative deuteration over the past 5 years has been the application of photocatalytic and electrocatalytic methodologies using D_2O under mild conditions where pretreatment of the substrates for the exchange of labile protons is no longer needed.⁴⁰

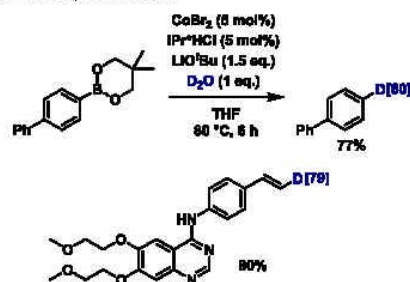
3.1.1.1. Deuteration of Prefunctionalized Arenes. Recently, Loh and co-workers reported the use of porous CdSe as a photocatalyst for the selective deuteration of halides via a radical process. Interestingly, this process proceeds using D_2O as the deuterium source.²²⁰ Among various selected semiconductors, which were tested for this transformation, the designed and synthesized CdSe catalyst outperformed in these C–X bond deuteration studies (Scheme 64a). The proposed mechanism begins with the absorption of substrates on the photocatalysts. Deuterium radicals or the aryl radical anion ($ArX^{\cdot-}$) are generated upon irradiation. Next, the coupling of deuterium radical and $ArX^{\cdot-}$ leads to the formation of deuterium incorporated products. D_2O -splitting is involved for generating active D radicals under photoinduced electron transfer to achieve the deuteration reaction (Scheme 64b). Comparable yields are obtained for C–I to C–D transformation under irradiation (>420 nm). Both electron-rich (e.g., anilines and phenols) and -deficient (aldehydes, ketones, and heterocyclic compounds) iodinated substrates can be deuterated (Scheme 64c). Notably, sensitive groups such as cyano, ester, amino, hydroxyl, aldehyde, and ketone are tolerated. Regarding aryl bromides and chlorides as substrates, stronger light sources were required (>280 nm).

The deutero-debromination of aryl bromides under photoredox catalysis with deuterated isopropanol as solvent and deuterium source was reported recently (Scheme 65a).²²¹ The herein used palladium catalyst exhibited a dual role as both photocatalyst and cross-coupling mediator: It is proposed that the palladium catalyst in the excited state reduces the aryl

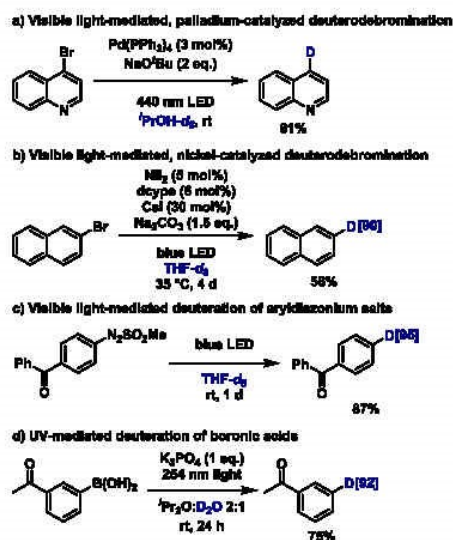
bromide, which upon dissociation of the bromide releases an aryl radical. The aryl radical can subsequently abstract a deuterium atom from deuterated isopropanol, and the so-formed isopropyl radical reduces $Pd(I)$, thus closing the catalytic cycle. A similar concept was used for a light-mediated nickel-catalyzed protodehalogenation reaction in which THF served as the proton source (Scheme 65b).²²² Switching to deuterated THF, the applicability of this methodology for deuteration was demonstrated on three substrates, showing high deuterium incorporation and moderate yields.

Alternatively, aryldiazonium salts²²³ or arylazo sulfone dyes²²⁴ can serve as precursors to aryl radicals under irradiation with blue LEDs (Scheme 65c). Their deuteration with deuterated THF or isopropanol as isotope source proceeds in the absence of a photocatalyst. Similarly, UV-irradiation of arylboronic acids in the presence of a deuterium source afforded deuterated arenes in a catalyst-free regime (Scheme 65d).²²⁵ However, free radicals do not seem to be involved in this reaction and deuterium oxide can be used as isotope source. Using a different NHC/cobalt-catalyzed methodology for the deutero-boronation of aryl and vinyl boronates, only moderate deuterium incorporation was achieved (Scheme 66).²²⁶ In this

Scheme 66. Cobalt/NHC-Catalyzed Protodeboronation of Aryl and Vinyl Boronates



Scheme 65. Light-Mediated Deuteration of Arenes

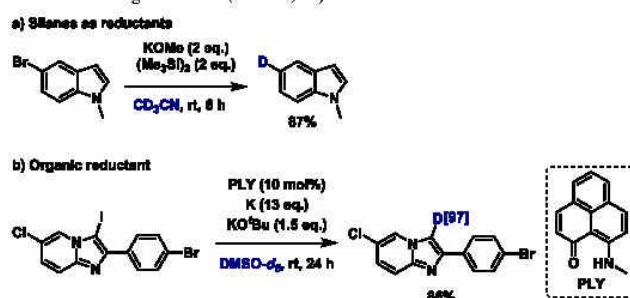


latter case, only 1 equiv of deuterium oxide was used because of the reaction's sensitivity to water. Nevertheless, competing protodeboronation with trace amounts of water was significant. For a deuteration project in which acidic reaction conditions and elevated temperature are tolerable, high deuterium incorporations can be achieved by just heating arylboronates in deuterated acetic acid.²²⁷

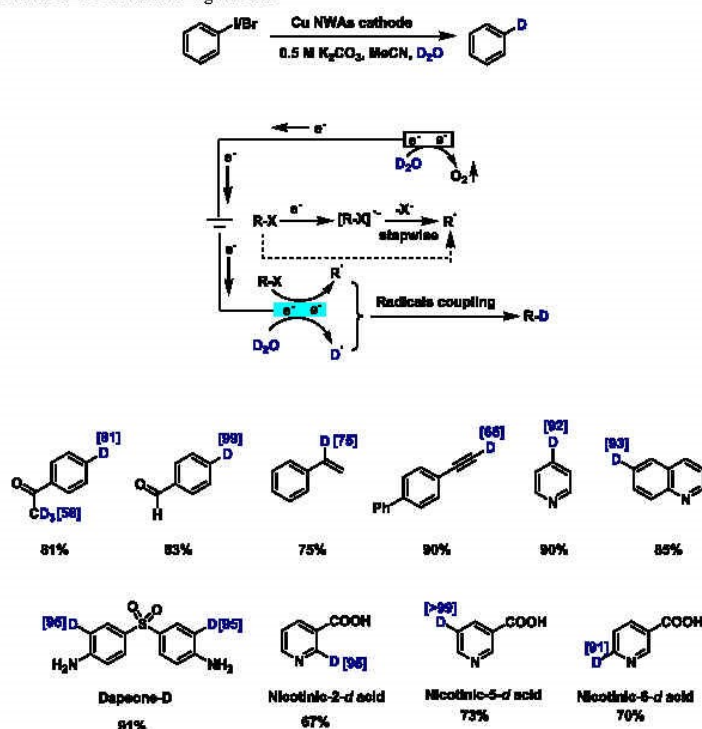
A novel metal-free alternative for the deutero-dehalogenation of aryl bromides makes use of potassium methoxide and a disilane as reagents along with deuterated acetonitrile as deuterium source (Scheme 67a).²²⁸ While the mechanism for this transformation is not fully elucidated yet, its exceptionally mild conditions give rise to a good functional group tolerance, leaving even terminal alkynes and epoxides untouched. Performing well on electron-rich and neutral (hetero)aryl bromides and iodides, the reactivity was not extendable to aryl chlorides and appears to be less suitable for electron-deficient substrates.

Another metal-free methodology for the dehalogenative deuteration of aryl iodides and bromides uses a phenalenyl potassium complex as an organic reductant along with DMSO- d_6 as deuterium source (Scheme 67b).²²⁹ On the basis of experimental radical-trapping experiments and DFT calculations, the authors propose that the phenalenyl compound needs

Scheme 67. Metal-Free Deuterodehalogenation of (Hetero)Aryl Bromides



Scheme 68. Electrochemical Deuterodehalogenation

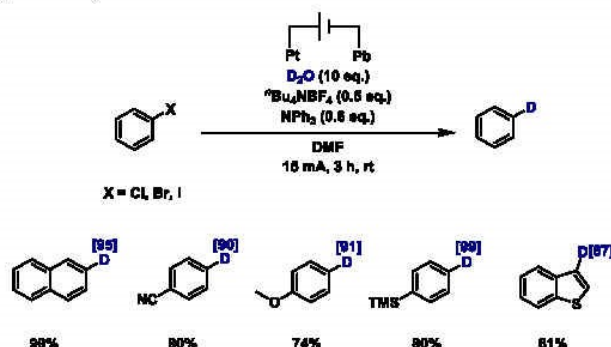


two steps to be activated as a reductant: First, single-electron reduction with potassium *tert*-butoxide affords a radical intermediate which is then further reduced by elementary potassium. Being a sufficiently strong reductant, the phenalenyl anion can now reduce the aryl halogenide substrate, affording an aryl radical that can abstract a deuterium atom from DMSO-*d*₆. The resulting dimethyl radical can react with another molecule of potassium *tert*-butoxide, furnishing a radical anion which can reduce the phenalenyl radical, thus regenerating the organic catalyst. Using this methodology on a number of aromatic substrates, good yields and high deuterium incorporations (above 90%) could be achieved at room temperature, and the

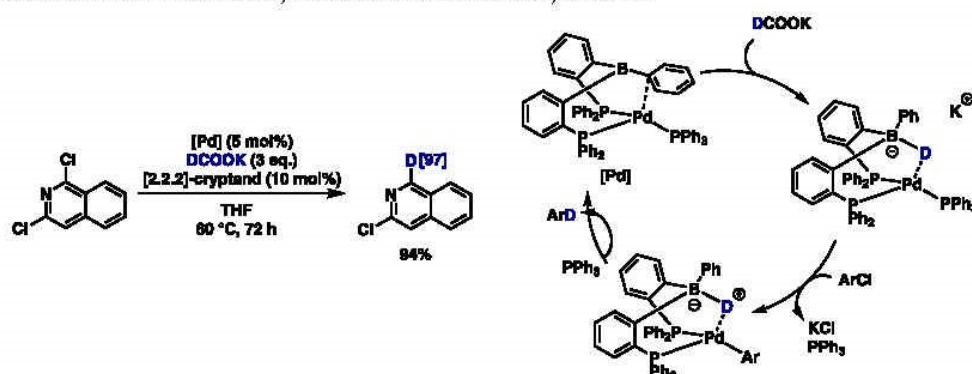
reaction was shown to be selective for the reduction of aryl iodides in the presence of chloride and bromide substituents. However, given that both superstoichiometric amounts of a strong base as well as metallic potassium (albeit in catalytic amounts) need to be present in the reaction mixture, it can be assumed that more sensitive substrates do not survive the reaction conditions.

On the basis of the renewed interest of electrochemical transformations for organic chemistry due to their energy efficiency and avoidance of external redox reagents, recently many reports about reductive dehalogenations at the cathode appeared.²³⁰ In this respect, electrochemical reductive deuter-

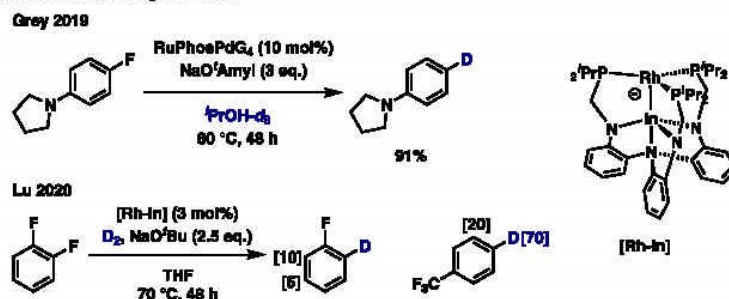
Scheme 69. Electrocatalytic Dehalogenative Deuteration



Scheme 70. Palladium-Borane-Catalyzed Deuterochlorination of Aryl Chlorides



Scheme 71. Defluorinative Labeling of Arenes

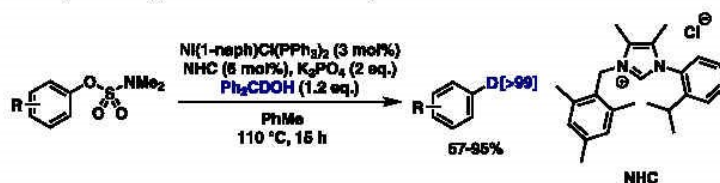


tion of aryl halides also attracted attention.²³¹ As an example, Zhang and co-workers used a Cu nanowire arrays cathode to achieve the deuteration of aryl halides in deuterium oxide.²³² Easily reducible functional groups, such as nitrile, alkyne, alkene, carbonyl, and imine, were well-tolerated, and also less active aryl bromides could be effectively deuterated. Furthermore, deuterated pharmaceuticals such as dapsone and nicotinic acid were prepared using this method (Scheme 68).

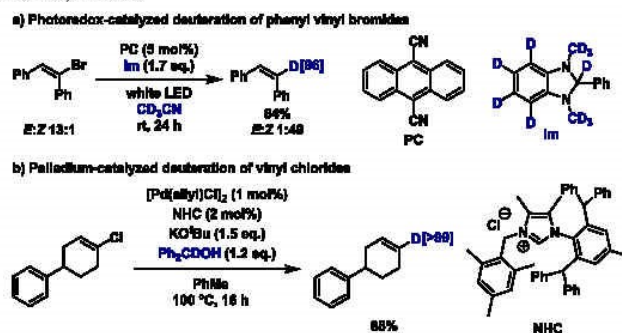
Another electrocatalytic dehalogenative deuteration of (hetero)arylhalides without metal catalysts was reported by Lei and co-workers in 2020.²³³ Aryl iodides and bromides gave the desired deuterated products with relatively high deuterium incorporation. Interestingly, here deuteration was also obtained using aryl chlorides, albeit at moderate levels due to the higher reduction potentials (Scheme 69).

The activation of C–Cl bonds and deuterochlorination of aryl chlorides with deuterated potassium formate as deuterium

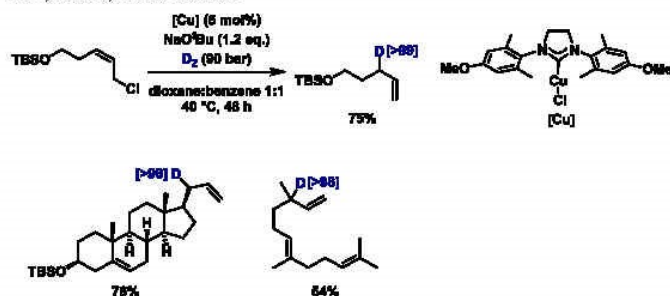
Scheme 72. Nickel-Catalyzed Deoxygenative Deuteration of Aryl Sulfamates



Scheme 73. Deuteration of Vinyl Halides



Scheme 74. Copper-Catalyzed Allylic Deuteration



source was recently realized by palladium-borane complex catalysis.²³⁴ In this transformation, the transition metal–Lewis acid interaction evokes an unusual mechanism in which the nucleophilic deuteride first inserts in the Pd–B bond, giving rise to an anionic Pd(0) species which subsequently undergoes oxidative addition with the aryl chloride (Scheme 70). Because of the electron-rich nature of the Pd–H–B complex, this reaction works best on electron-deficient substrates and can even enable selective monodeuteration of dichlorinated quinolines and isoquinolines.

Among the various aryl halides, aryl fluorides are still most challenging substrates for deuterodehalogenation. Because of significant competing HIE side reactions, only few substrates could be selectively transformed to monodeuterated products so far. However, a pyrrolidine-substituted fluoroarene was successfully deuterated in the presence of a heterogeneous palladium catalyst,²³⁵ and a bimetallic rhodium–indium complex was reported to catalyze the deuterodefluorination of

1,2-difluorobenzene and *p*-fluorobenzotrifluoride with only minor HIE side reactions (Scheme 71).²³⁶

Treating sulfamates as pseudohalides, a nickel-catalyzed deoxygenative deuteration could be realized (Scheme 72).²³⁷ The use of α -deuteriodiphenylmethanol as deuterium source allowed reliably high deuterium incorporation and good yields on a broad scope of aromatic substrates while tolerating other reducible functional groups.

3.1.2. Deuterodehalogenation of Vinyl and Allyl Halides. Making use of imidazolines as strong hydrogen atom donors upon single electron oxidation, deuterated products were prepared for a photoredox-catalyzed deuterodebromination of phenylvinyl bromides (Scheme 73a).²³⁸ The substrates themselves form vinyl radicals upon reduction by an organic photocatalyst in its excited state and subsequently abstract a deuterium atom from the imidazolinium radical cation, forming deuterated styrene derivatives. Because of a background reaction in which the intermediary vinyl radicals abstract hydrogen atoms from the solvent molecules, conducting the reaction in

deuterated solvents ensures higher deuterium incorporation. Electron-deficient phenyl vinyl bromides are deuterated less efficiently, giving rise to significant *E/Z*-isomerization and decomposition side reactions. Furthermore, vinyl chlorides showed low reactivity under the reported conditions. Lastly, it should be noted that the multistep synthesis of the deuterated imidazolines requires the use of several expensive deuterium sources, limiting the practical applicability of this approach.

However, using α -deuteriodiphenylmethanol as the deuterium source in the presence of an NHC-ligated palladium complex, vinyl chlorides could be deuterodechlorinated more efficiently to afford deuterated olefins (Scheme 73b).²³⁹ Moreover, this reaction is not limited to phenyl vinyl chlorides and performed equally well on electron-deficient substrates.

Recently, allylic deuterides were prepared by a copper-catalyzed allylic substitution reaction with deuteride nucleophiles generated through heterolytic cleavage of deuterium gas by a reactive Cu–O species (Scheme 74).²⁴⁰ Remarkably, the judicious choice of the ligand allowed selective allylic substitution without concomitant reduction of the resulting terminal alkene. Furthermore, an excellent selectivity of the branched over the linear product was observed. However, alkynes were not tolerated under the reaction conditions because of semihydrogenation side reactions. The high pressure (90 bar) required for this transformation represents another drawback of this methodology.

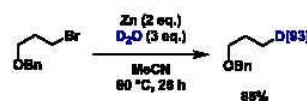
3.1.3. Deuterodehalogenation of Alkyl Halides. Almost all procedures reported for the deuterodehalogenation of alkyl halides since 2017 are based on radical mechanisms. Compared with previous strategies that used organolithium and Grignard reagents,²⁴¹ or stannanes,²⁴² much milder conditions and less toxic reaction profiles have been achieved. In this context, one report for the dehalogenative deuteration of alkyl iodides is based on a radical chain process that is both initiated and activated by triethylborane in conjunction with dry air (Scheme 75a).²⁴³ The resulting ethyl radical abstracts the iodine atom,

hydrogen atom abstraction at the ethyl borane; however, most substrates exhibited deuteration levels above 90%.

An alternative radical deuteration of alkyl (and aryl) iodides makes use of readily prepared deuterated hypophosphites as deuterium source (Scheme 75b).²⁴⁴ On the one hand, these reagents are stable with respect to HIE and consequently render deuterations with water as solvent possible;²⁴⁵ on the other hand, they are amenable to deuterium atom abstraction by alkyl radicals. Following initiation with 2,2'-azobis(2-methylpropionamide) (AIBA) as radical starter, a range of aliphatic and aromatic iodides including unprotected sugars could be deuterated with excellent yields and deuterium incorporations.

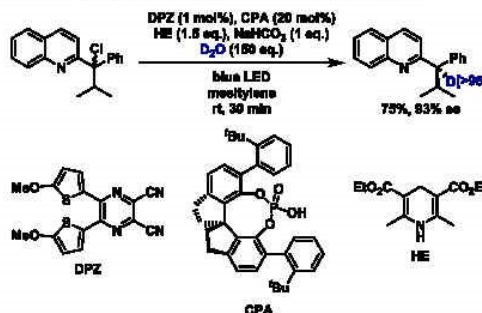
While the above-described methodologies are limited to alkyl iodides as starting materials, superstoichiometric amounts of elementary zinc were shown to activate alkyl bromides for deuteration via *in situ* formation of organozinc intermediates and hydrolysis thereof by deuterium oxide (Scheme 76).²⁴⁶ An especially valuable addition to the toolbox of aliphatic deuterodehalogenations is comprised in the high-yielding transformation of a range of primary alkyl halides.

Scheme 76. Deuteration of Alkyl Bromides via Organozinc Intermediates



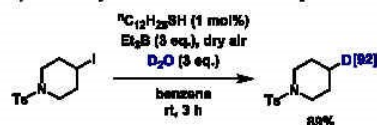
Enantioselective deuterodechlorination of racemic starting materials has so far only been reported for 2-quinoline-substituted benzyl chlorides as a rather specific activated substrate class under photoredox catalysis (Scheme 77).²⁴⁷ The enantioselectivity is achieved by deuteration of the intermediary dechlorinated carbanions with a chiral phosphoric acid using deuterium oxide as isotope source.

Scheme 77. Enantioselective Deuterodechlorination

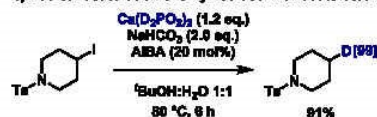


Scheme 75. Radical Deuteration of Alkyl Iodides

a) Thiol-catalyzed radical deuteration of alkyl iodides



b) Radical deuteration of alkyl iodides with deuterated hypophosphites



transforming the substrate into an alkyl radical. Then, deuteration proceeds as seen above for light-mediated methodologies by deuterium atom transfer from a catalytic thiol while deuterium oxide supplies the isotope. The method was applied to tertiary, secondary, and even a primary alkyl iodide, although the latter afforded a moderate yield for the deuterated product only, probably due to the instability of the corresponding radical. Deuterium incorporations can be diminished due to competing

Recently, the concept of frustrated Lewis pairs has been shown to enable the deuteration and tritiation of $C(sp^3)$ –F bonds using deuterium or tritium gas activated by the combination of $B(C_6F_5)_3$ and TMP (Scheme 78).²⁴⁸ Under comparably mild and metal-free reaction conditions, aliphatic C–F bonds led to very high deuterium incorporation (>95%) in the presence of aromatic ones while facilitating tritiation under very low pressures of tritium gas.

Scheme 78. Defluorinative Deuteration and Tritiation Using Frustrated Lewis Pairs



In a more biochemically relevant context, the excited state reactivity of a palladium catalyst was harnessed for the preparation of C2-deuterated 2-deoxy sugars (Scheme 79).²⁴⁹ Interestingly, the reaction uses 1-halo-2-acetoxy-sugars as substrates and, following radical oxidative addition of the C–X bond, a spin-center shift transfers the radical to the C2 position. Finally, the desired deuterated products are obtained after reductive elimination. Although THF-*d*₈ is needed as deuterium source and deuterium incorporations should be improved in subsequent studies, the obtention of those difficult-to-access compounds from readily available starting materials is remarkable.

An alternative to the above-described deuterodehalogenation techniques is the base-mediated deborylative deuteration using deuterated methanol.²⁵⁰ The methodology was demonstrated on aliphatic vicinal diboronates and furnished the corresponding diduterated products with high deuterium incorporations (Scheme 80a). Further, tetradeuterated products could be prepared in two steps by first performing a borylation of internal alkynes in the presence of deuterated methanol followed by the just described deborylative deuteration (Scheme 80b).

3.2. Reductive Deuteration of Carbonyl Groups

Rather than introducing isotopic labels *via* late-stage diversification of complex molecules, isotopes can alternatively also be incorporated during the synthetic sequence. Reduction steps are hereby particularly inviting as labeling can often be achieved by simply replacing hydrogen gas by deuterium gas. Further, the use of deuterated versions of common reducing agents such as sodium borohydride is a frequently encountered approach for the reduction of carbonyl functionalities.

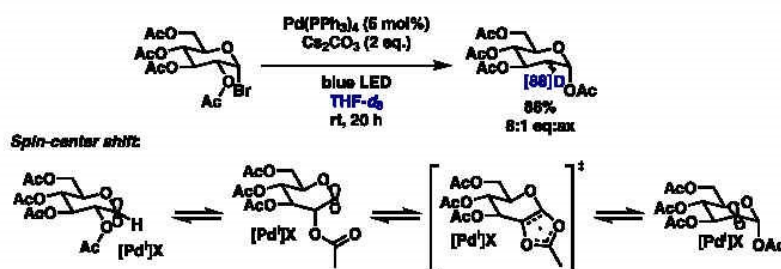
As an example for a more modern approach, using deuterated silanes in combination with deuterated toluene as solvent under nickel/NHC catalysis, Newman and co-workers transformed aromatic esters into trideuteromethyl groups (Scheme 81).²⁵¹ Mechanistically, it is hypothesized that an initial uncatalyzed deuteride addition to the ester is followed by nickel-catalyzed reduction of the intermediary silylated benzyl alcohol. Notably, the reaction is specific for C(sp³)–O bonds and leaves aromatic C(sp²)–O bonds untouched even though anisoles are reduced by nickel catalysis under similar conditions.²⁵²

On the other hand, Bouveault–Blanc-type single electron transfer (SET) reductions of esters stop at the alcohol oxidation state and are thus complementary to the nickel-catalyzed methodology described above. In this context, sodium dispersions along with deuterated ethanol are comparably cost-efficient reagents for the reductive deuteration of aliphatic esters (Scheme 82a),²⁵³ whereas the aromatic congeners were best reduced using a combination of samarium iodide and deuterium oxide (Scheme 82b).^{254,255} For applications demanding extremely high deuterium incorporation, the preparation of activated pentafluorophenyl esters can be worthy (Scheme 82c).²⁵⁴ Being highly active toward reductive deuteration, these compounds afforded deuterated alcohols with deuterium incorporations of 98% and more and can be reduced chemoselectively in the presence of amides, carboxylic acids and even ethyl esters and lactones. Compared with the older but still widely applied reduction with NaBD₄^{256–259} (a recent example for an application of this reagent is shown in Scheme 82d),²⁶⁰ these more recent methodologies offer better cost efficiency due to the much cheaper deuterium sources that are used.

Similar reductions on amides can either afford α -diduterated alcohols or amines, as both C–N and C–O cleavage are possible. Interestingly, in this context, sodium dispersion reductants can selectively produce either product depending on the exact reaction conditions (Scheme 83a).²⁶¹ In this sense, deuterated ethanol led to C–N cleavage and thus diduterated alcohols as products, whereas sodium hydroxide and deuterium oxide furnished deuterated amines. The latter products can alternatively be prepared by a similar reduction process with aliphatic and benzylic nitriles as starting materials (Scheme 83b).²⁶² Extending the substrate scope of nitrile reduction to aromatic nitriles and precluding the concomitant β -deuteration by enolization observed in the sodium dispersion-mediated reductions, samarium iodide represents an attractive alternative as an efficient SET reducing agent, affording high deuterium incorporations and yields on a broad scope of aromatic and aliphatic substrates (Scheme 83c).²⁶³ The samarium iodide-mediated reductive deuteration of oximes afforded the same products (Scheme 83d).²⁶⁴

A continuous-flow reductive deuteration of nitriles to access to α,α -didutero amines was described by Fülöp and co-workers (Scheme 84). They established an individual flow-chemistry-based method for deuteration reactions using deuterated water in an H-Cube system.²⁶⁵ In this method, deuterium gas is generated *in situ* by electrolysis, and Raney nickel is employed as heterogeneous catalyst for reductive deuteration of nitriles. Notably, quantitative conversions and deuterium incorporation

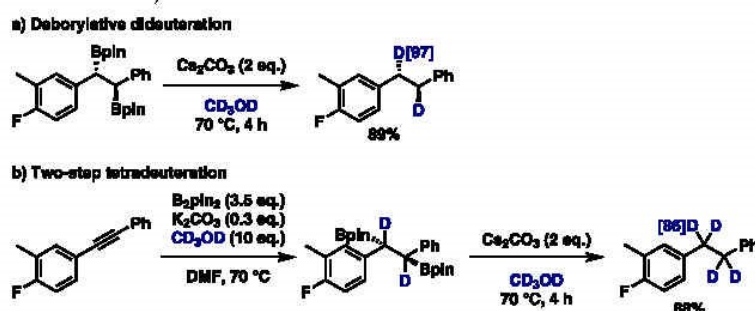
Scheme 79. Visible Light-Mediated and Palladium-Catalyzed C2-Deuteration of 1-Halosugars by a Spin-Center Shift Mechanism



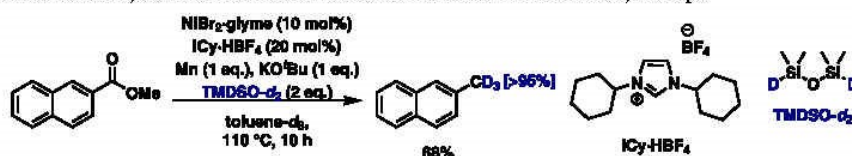
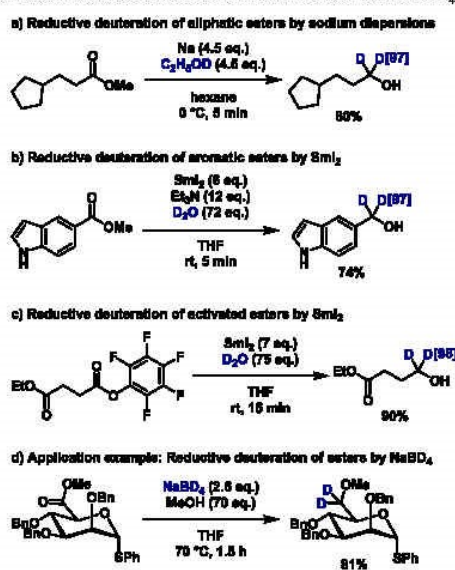
6670

<https://doi.org/10.1021/acs.chemrev.1c00795>
Chem. Rev. 2022, 122, 6634–6718

Scheme 80. Base-Mediated Deborylative Deuteration



Scheme 81. Nickel-Catalyzed Reductive Transformation of Esters into Trideuteromethyl Groups

Scheme 82. (a–c) SET Reductive Deuteration of Esters to α -Deuterated Alcohols; (d) Recent Example for an Application of the Older Reductive Deuteration of Esters with NaBD_4 

values of >99% were obtained for aromatic nitriles, and no dehalogenation is observed in 4-bromobenzonitrile. The continuous-flow method is also feasible to produce deuterated tryptamine on gram scale.

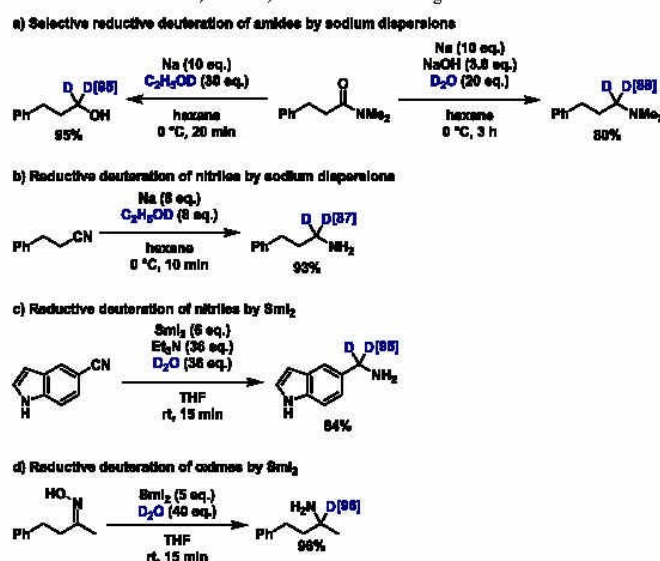
An interesting method for the preparation didetero-methylene groups is the deoxygenative deuteration of ketones. In this respect, biaryl ketones containing a disubstituted amino

group in *para* position were deuterated under iridium hydride catalysis (Scheme 85).²⁶⁶ Both deuterium atoms stem from deuterated formic acid which reacts with the bidentate iridium complex to form iridium hydride species as key catalytic intermediates. The electron-donating *para*-amino substituent further leads to concomitant HIE by electrophilic aromatic substitution. Because of a competing and faster reaction of residual amounts of unlabeled deuteration reagent, deuterium incorporations remained between 72 and 90%.

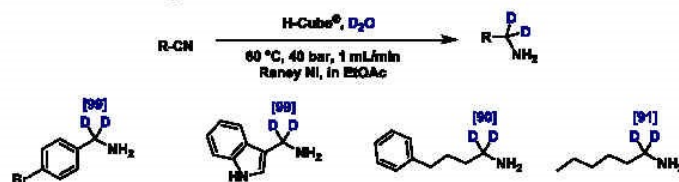
A larger set of aromatic ketones were transformed into the corresponding labeled compounds under mild conditions applying a palladium-catalyzed deoxygenative deuteration methodology (Scheme 86).²⁶⁷ As the reaction required deuterium gas, the authors came up with a special reactor for the *ex situ* generation of deuterium gas from deuterium oxide by electrocatalytic water splitting, enabling a cheaper and safer procedure. Remarkably, the reaction conditions were also applied for the arguably more challenging and far less explored deoxygenative monodeuteration (and, substrate-dependently, occasionally dideuteration) of primary, secondary, and tertiary benzylic alcohols.

At this point, it is worth mentioning that complete reductive deuteration of aromatic ketones is much easier than similar transformations of aliphatic ketones because of the stabilization of the corresponding benzylic intermediates. Hence, the future development of a general selective dideuteration of aliphatic ketones remains an interesting goal in this area.

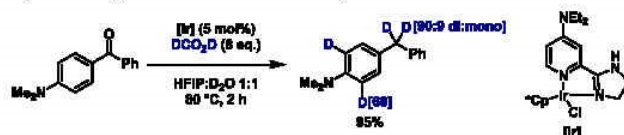
Alternatively, incomplete reductive deuteration transforms ketones into α -deuterated alcohols. In this context, an umpolung reactivity enables the deuteration of biaryl ketones with magnesium as reductant and 1.5 equiv of deuterium oxide, affording very high deuterium incorporations in moderate to good yields (Scheme 87a).²⁶⁸ The addition of 1,2-dibromoethane to the reaction mixture was found to be crucial to suppress competing pinacol coupling reactions. Furthermore, the reducing agent SmI_2 (*vide supra*) can mediate the same transformation²⁶⁹ and the light-mediated enantioselective

Scheme 83. Reductive Deuteration of Amides, Nitriles, and Oximes Leading to α -Deuterated Amines

Scheme 84. Reductive Deuteration of Aliphatic and Aromatic Nitriles



Scheme 85. Iridium-Catalyzed Deoxygenative Deuteration of Biaryl Ketones



reductive deuteration of biaryl ketones containing one *N*-heteroaromatic component was reported to proceed under catalysis by a chiral phosphoric acid (Scheme 87b).²⁷⁰

The preparation of α -deuterated α -hydroxyketones is made possible by means of a cobalt-catalyzed transfer hydrogenation of α -ketoesters (Scheme 88a).²⁷¹ Using deuterium oxide as the deuterium source along with zinc as the reductant, the reaction operates under mild conditions (80 °C) and is also applicable to the racemic reductive deuteration of cyclic sulfonylimides to the α -deuterated reduced form under similar conditions (Scheme 88b).

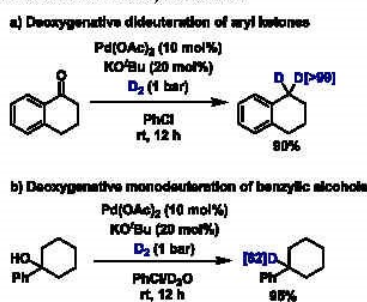
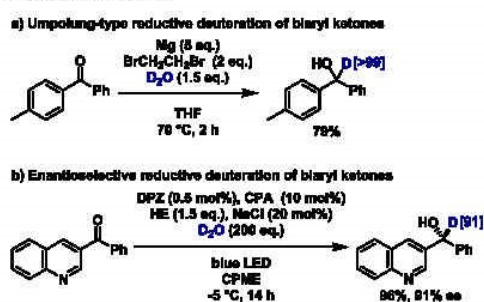
The latter substrate class has been subject of further studies,^{272,273} resulting in the development of a photoredox-catalyzed reduction using phenyl disulfide as HAT catalyst along with deuterium oxide (Scheme 88c)²⁷⁴ as well as a nickel-catalyzed methodology for the enantioselective preparation of α -

deuterated chiral *N*-tosyl-protected amines (Scheme 88d).²⁷⁵

For the latter case, using deuterated isopropanol as deuterium source and a chiral ligand, an intermediary nickel deuteride complex selectively delivers the deuterium atom to the polarized sulfonylimine carbon atom in a stepwise manner, affording excellent yield, deuterium incorporation, and enantioselectivity. An external reductant is not needed as isopropanol additionally acts as a sacrificial reductant, affording acetone as the byproduct of the reduction. The electron-withdrawing nature of the tosyl substituent could efficiently suppress the imine/enamine tautomerism, thus impeding concomitant deuteration of the β position. Consequently, the reaction could not be extended to other classes of imines.

α -Deuterated amines are typically prepared by metal catalyzed hydrogenation or transfer hydrogenation protocols from imines or more conveniently *via* reductive aminations from

Scheme 86. Palladium-Catalyzed Deoxygenative Deuteration of Aryl Ketones and Benzyl Alcohols

Scheme 87. Reductive Deuteration of Biarylketones to α -Deuterated Alcohols

the corresponding amines and aldehydes. As a recent example in this area, Espino, Jalón, and co-workers employed deuterium oxide as the deuterium source along with formic acid and sodium formate in the presence of ruthenium catalysts for hydrogenation of imines.²⁷⁵ However, in heavy water the hydrogenation reaction seemed to outcompete the H-D exchange, consequently affording only low deuterium incorporation levels in the amine products.²⁷⁶ By switching to a biphasic toluene/deuterium oxide system where the starting materials are soluble exclusively in the toluene phase but the catalyst is dissolved in the aqueous phase, the authors managed to sufficiently slow down the transfer hydrogenation, furnishing a significantly increased deuterium incorporation (Scheme 89).

3.3. Reductive Deuteration of Olefins

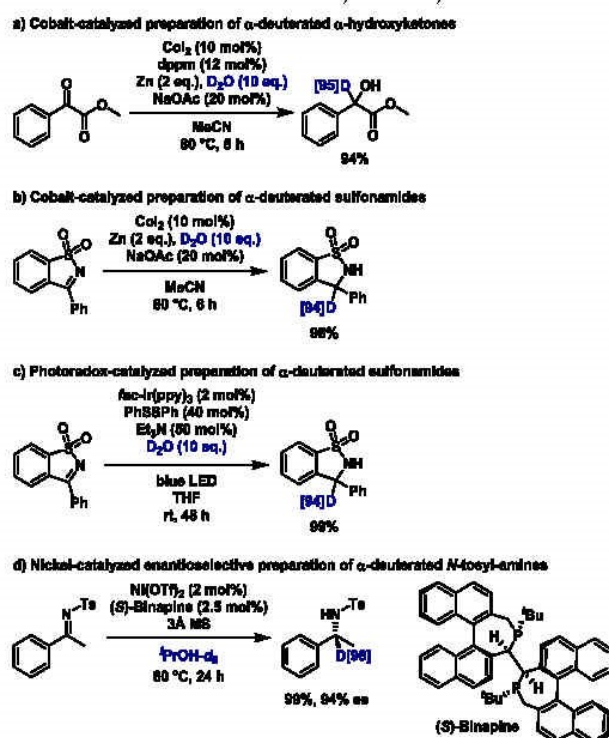
Apart from being reducible moieties themselves, carbonyl groups can activate conjugated olefins for polar transition-metal-catalyzed reductions by bringing them in proximity to the metal center. Avoiding both the use of expensive noble metal catalysts and of pressurized deuterium gas, a nickel-catalyzed asymmetric deuteration of α,β -unsaturated esters represents a recent advance in the field of reductive deuteration of olefins (Scheme 90a).²⁷⁷ Mechanistically, acetic acid protonates the nickel complex, forming a nickel hydride species which can insert into the olefin. The resulting nickel complex is subsequently hydrolyzed, and indium powder serves as the final reductant, regenerating the active Ni(0) species. Conducting the reaction in the presence of deuterium oxide afforded deuterated aliphatic esters with excellent deuterium incorporation levels in β position. Presumably owing to the two-step

mechanism allowing for bond rotation following the addition of the nickel hydride to the double bond, the reaction does not seem to be fully *syn*-selective as only between 60 and 70% deuterium can be found in the *syn*- α -position, whereas the remaining amount of deuterium was incorporated in the *anti*- α -position. In contrast, full *syn* selectivity was achieved in the rhodium-catalyzed asymmetric *syn*-deuteration of β -substituted, α,β -unsaturated esters under deuterium gas atmosphere as both deuterium atoms might be transferred in a concerted fashion (Scheme 90b).²⁷⁸

Whereas the two methods above require either a stoichiometric reductant or the use of the more expensive deuterium gas, electrochemical reduction of α,β -unsaturated carbonyl compounds proceeded in the absence of reductants with deuterium oxide as isotope source thanks to anodic oxygen evolution (Scheme 90c).²⁷⁹ This metal-free methodology was enabled by an almost concerted reduction of the substrate and deuteration of the fleeting carbanion so that dimerizations are precluded. High deuterium incorporations and yields are obtained on olefinic esters, amides, acids, nitriles; and even ester-substituted alkynes are completely reduced to tetraduterated aliphatic esters. Good results were alternatively obtained with sodium dispersions and deuterated ethanol, reminiscent of reductive deuteration reactions described in the previous chapter.²⁸⁰ However, the functional group tolerance of this method is limited compared to the options depicted in Scheme 90.

In analogy to what was mentioned above in the context of dehalogenative deuteration, the older technique using a heterogeneous palladium catalyst such as palladium on charcoal along with deuterium gas remains in use for the reductive deuteration of olefins (and alkynes) as well.^{281–285} A recent example is shown in Scheme 90d.²⁸⁶ However, as the modern techniques can enable enantioselective or stereoselective reduction and are not as sensitive to the presence of labile protons (please note that the conditions in Scheme 90a even allow for the use of nondeuterated acetic acid), they represent a clear advantage.

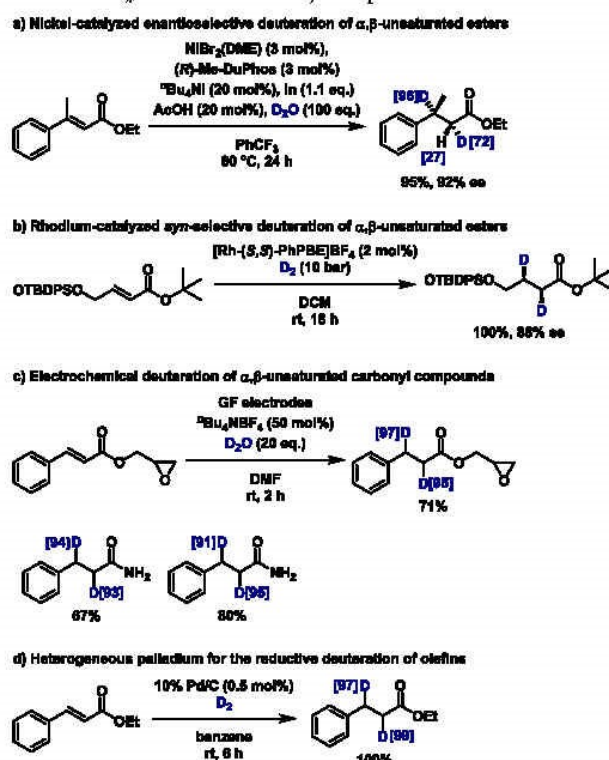
Reductive deuteration of unactivated olefins is significantly more challenging than the deuteration of α,β -unsaturated carbonyl compounds but has recently been achieved under iron catalysis using an ammonia/borane transfer hydrogenation system.²⁸⁷ More specifically, reaction of HBpin as the hydride donor with the iron complex afforded an iron hydride species, which can insert into the olefin. *n*-Butylamine or aniline as the proton source then hydrolyze the iron complex, releasing the reduced product and regenerating the iron catalyst. Thanks to these individual reactivities of boronic ester and amine rather than *in situ* formation of hydrogen or deuterium gas, selective monodeuteration of terminal alkenes can be achieved. Depending on whether (i) DBpin is used along with nondeuterated amine or (ii) HBpin together with deuterated aniline, deuterium is incorporated either at the internal (i, Scheme 91a) or the terminal (ii, Scheme 91b) position. Although the selectivity is not perfect for all substrates, especially for styrenes whose electronics can bias the reaction outcome, this methodology opens new opportunities for deuteration, and most reactions are completed in remarkably short times (often as little as 10 min). Moreover, under the reaction conditions, the ammonia/borane system forms an oligomeric gel, thus keeping the concentration of free amine and borane at a low level and avoiding side reactions such as hydroboration or amine-borane dehydrocoupling.

Scheme 88. Reductive Transfer Deuteration of α -Ketoesters and Cyclic Sulfonylimides under Cobalt Catalysis^a^adpmm: bis(diphenylphosphino)methane.Scheme 89. Ruthenium-Catalyzed Transfer Deuteration of Imines in a Biphasic Solvent System^a^admppy: 4,4-dimethyl-2,2'-bipyridine.

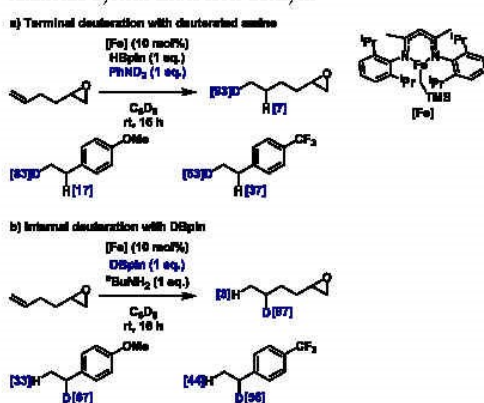
Interestingly, a recently developed similar palladium nanoparticle-catalyzed transfer hydrogenation using HBpin with protic deuterium sources showed an improved selectivity for terminal styrenes, especially in the presence of electron-withdrawing substituents.²⁸⁸ Another reliable deuterohydrogenation and hydrodeuteration of terminal styrene derivatives was offered by a metal-free methodology that exploits 1,4-cyclohexadienes with specific deuterium substitution as HD surrogates (Scheme 92).^{289,290} In the case of hydrodeuteration, the borane Lewis acid catalyst abstracts a deuterium (or hydrogen) atom from the cyclohexadiene, forming a borodeuteride and a so-called Wheland cation which, being a strong acid, can protonate the styrene substrate on the terminal position, forming the stabilized benzylic carbocation. This intermediate can now abstract a deuterium atom from the borodeuteride or directly from the cyclohexadiene, forming a selectively

monodeuterated product. While showing improved results for electron-rich styrenes compared to the iron-catalyzed procedure, this methodology suffers from a somewhat limited scope, performing less well on electron-deficient substrates and failing for unactivated olefins. This reactivity problem was recently successfully tackled by moving to indium(III) bromide as a Lewis acidic catalyst along with increasing the temperature.²⁹¹ While an explanation for the increased reactivity under these conditions was not provided by the authors, electron-deficient as well as trisubstituted olefins are feasible substrates using the improved methodology.

Most recently, the toolbox for transfer hydrodeuteration reactions was expanded by a copper hydride-catalyzed procedure that uses dimethoxymethylsilane and monodeuterated ethanol as more accessible hydrogen/deuterium sources compared with the examples recounted above.²⁹² The method-

Scheme 90. Reductive Deuteration of α,β -Unsaturated Carbonyl Compounds

Scheme 91. Selective Terminal (a) or Internal (b) Monodeuteration of Unactivated Olefins with a Borane/Ammonia System under Iron Catalysis

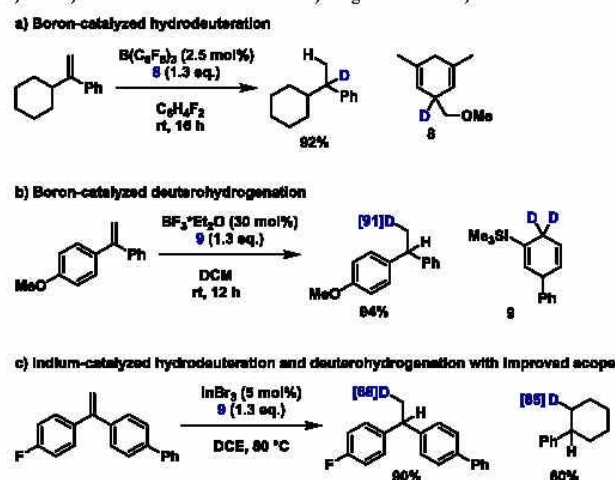


ology relies on the regioselective hydrocupration of styrene derivatives, leading to the thermodynamically favored benzylic organocuprate intermediate while the hydride stemming from nondeuterated silane is delivered to the nonbenzylic position

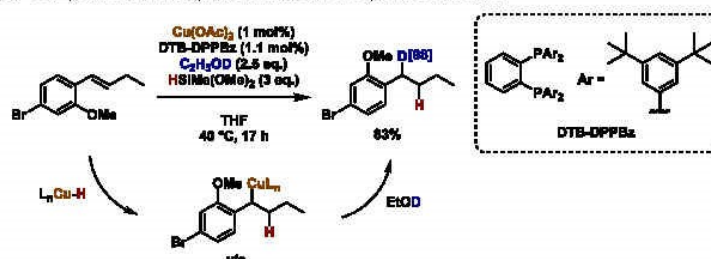
(Scheme 93). This intermediate is subsequently cleaved by deuterated ethanol, affording highly selective deuteration in the benzylic position only. The opposite selectivity could be achieved using a deuterated silane along with nondeuterated ethanol. The reaction shows a broad scope of styrenes with various substitution patterns as well as excellent chemoselectivity of benzylic over nonbenzylic olefins. Moreover, an initial result demonstrates the likely extension of this methodology to unactivated terminal olefins. Only 1,1-disubstituted styrene derivatives suffer decreased regioselectivity, probably imposed by the steric impediments on the benzylic site which hamper cupration. Lastly, it is worth mentioning that the ligand for the copper complex plays a major role for the reactivity as, among the bidentate phosphines investigated by the authors, only the sterically crowded DTB-DPPBz enabled the desired transformation. However, a rationale to explain this observation was not provided.

A biocatalytic enantioselective reductive deuteration of both carbonyl groups and olefins has been reported using reductase enzymes together with a catalytic amount of the NAD cofactor.^{293,294} Under the reaction conditions, the enantioselectively deuterated cofactor is formed and regenerated with deuterium oxide as deuterium source and hydrogen gas as reductant. Interestingly, the deuterium incorporation is not diminished using hydrogen gas since the oxidation of H₂ and the transfer of a deuteron to NAD⁺ take place at different enzymatic

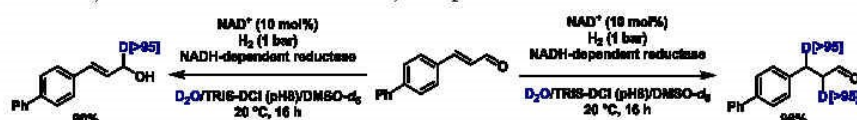
Scheme 92. Borane-Catalyzed Hydrodeuteration and Deuterohydrogenation of Styrenes



Scheme 93. Copper-Catalyzed Transfer Hydrodeuteration of Styrene Derivatives



Scheme 94. Biocatalytic Reduction of Olefins and Carbonyl Compounds



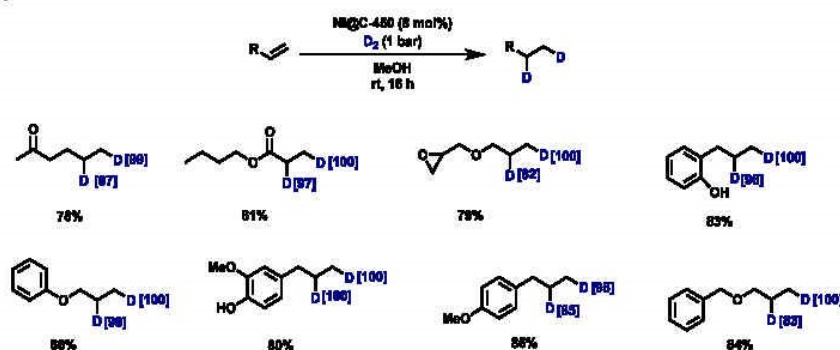
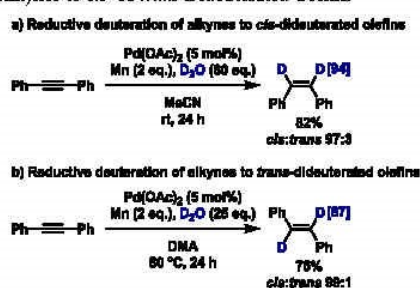
sites while electrons can be transferred from one to the other. Choosing the specific enzyme appropriately depending on the substrate class allows for a highly chemoselective reduction in the presence of other reducible functional groups (Scheme 94).

Very recently, a nanostructured Ni-core-shell catalyzed reductive deuteration of alkenes was achieved at ambient conditions (room temperature, using 1 bar deuterium). Here, a highly active supported nickel catalyst was conveniently prepared by impregnation and subsequent pyrolysis of nickel nitrate on carbon at 450 °C under argon. The resulting materials were tested in the reductive deuteration of a series of alkenes to deuterium-labeled alkanes.²⁹⁵ Notably, functional groups, such as ketone, ester, and epoxide groups, were well tolerated during the deuteration process (Scheme 95).

3.4. Reductive Deuteration of Alkynes

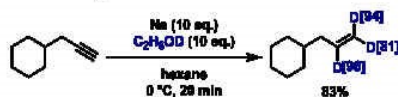
Although the iron-catalyzed ammonia/borane system (*vide supra*) could exhaustively hydrogenate alkynes to alkanes, the deuteration of alkynes was not attempted. However, a palladium-catalyzed method for the reductive semideuteration of alkynes using deuterium oxide was reported previously, which afforded *cis*- and *trans*-diduterated olefins selectively depending on the reaction conditions.^{296,297} Whereas at room temperature and in acetonitrile as solvent *cis*-diduterated alkenes were obtained predominantly (Scheme 96a), elevated temperature (80 °C) and a solvent switch to DMA allowed for complete isomerization to *trans*-diduterated alkenes under the reaction conditions (Scheme 96b). It was corroborated that in the presence of manganese as reductant, palladium nanoparticles were formed and seem to be the catalytically active species.

Scheme 95. Alkenes to Deuterium-Labeled Alkanes

Scheme 96. Palladium-Catalyzed Selective Semideuteration of Alkynes to *cis*- or *trans*-Dideuterated Olefins

Interestingly, if terminal alkynes are reduced to olefins by sodium dispersions in the presence of deuterated ethanol, a third deuterium atom is incorporated through base-catalyzed HIE at the terminal position (Scheme 97).²⁹⁸ Under these reaction

Scheme 97. Semireductive Deuteration of Terminal Alkynes with Sodium Dispersions and Deuterated Ethanol



conditions, terminal alkyl alkynes are selectively deuterated in the presence of unactivated internal alkynes, whereas phenylacetylenes are completely reduced to tetradeterated alkanes due to the intermediary formation of stabilized benzylic radicals.

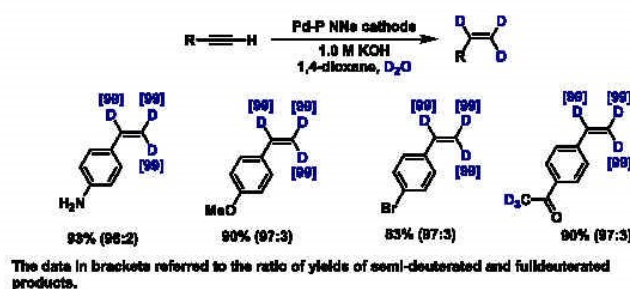
A selective semihydrogenation (deuteration) of terminal and internal alkynes using H_2O (D_2O) as the $H(D)$ source was also accomplished using a Pd-P alloy cathode.²⁹⁹ This electrochemical deuteration of alkynes permitted the selective synthesis of *mono*-, *di*-, and *tri*-deuterated alkenes with high D-incorporation (Scheme 98).

Although many effective methods to form $C(sp^2)-D$ bonds are known, processes for producing $C(sp^3)-D$ bonds often suffer from low site selectivity or require more expensive deuterium reagents. In this respect, the work by Berlinguette and co-workers is noteworthy: Using a tandem electrochemical palladium membrane reactor, reductive deuteration of alkynes, alkenes, aldehydes, and imines proceeded with good site selectivity using D_2O at room temperature.³⁰⁰ They also synthesized a deuteration analogue of cinacalcet, to demonstrate that this methodology can be applied for preparing pharmaceuticals (Scheme 99).

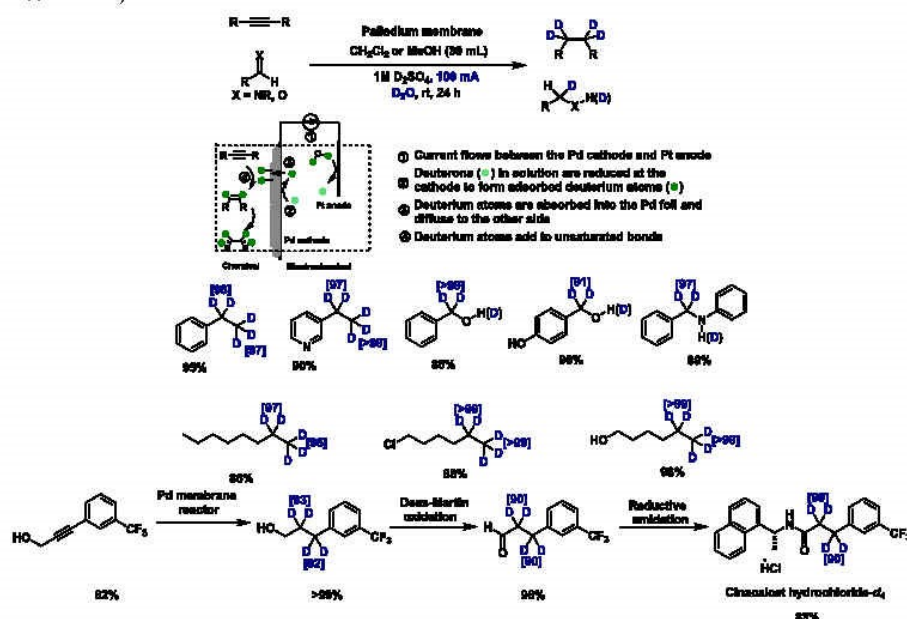
The double reduction of terminal and internal aryl alkynes leading to tetradeterated alkanes was further demonstrated utilizing copper hydride catalysis with a deuterated silane in deuterated isopropanol (Scheme 100).³⁰¹

Heteroatoms adjacent to the alkyne moiety can serve to activate the substrate for metal-free reduction by polar mechanisms.³⁰² In this context, ynamides have recently been explored as starting materials for the preparation of α/β -

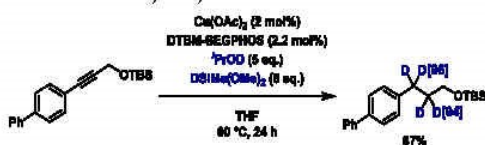
Scheme 98. Electrochemical Semideuteration



Scheme 99. Electrolytic Deuteration of Unsaturated Bonds



Scheme 100. Copper-Hydride-Catalyzed Reductive Deuteration of Aryl Alkynes

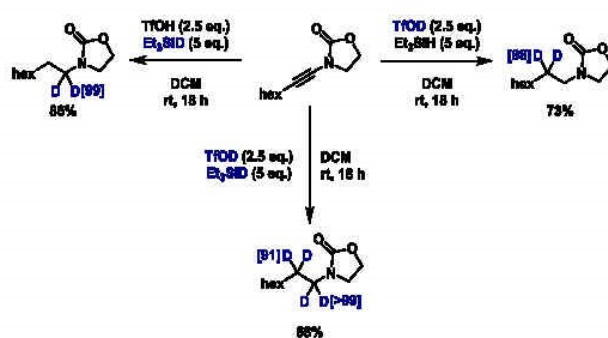


deuterated protected amines *via* an iminium-enamine sequence: In the presence of triflic acid, the substrate is protonated, forming an iminium ion which can subsequently be reduced by addition of a hydride from triethylsilane, yielding an enamine. Under the reaction conditions, this process is repeated to finally

form the fully reduced amine (Scheme 101). Judicious choice of deuterated or nondeuterated acid and hydride source allows for the highly selective deuteration in α position, β position, or both with high deuterium incorporations. To furnish the deuterated free amine, a deprotection step is needed after the reaction. In addition, the authors have demonstrated that this methodology could be extended to the reductive deuteration of ethynyl ethers, yielding deuterated ethers as products. However, due to hydrolysis side reactions, only low yields were obtained for this class of substrates, and thus, further efforts should be devoted to this reaction.

3.5. Reductive Deuteration of Arenes

An extremely precise and controlled way of preparing deuterated cyclohexene isotopomers was recently described by Harman and

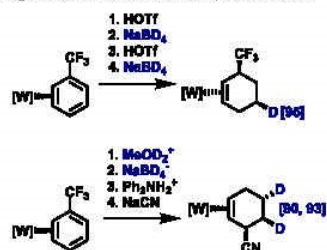
Scheme 101. Reductive Deuteration of Ynamides for the Selective Preparation of α -, β -, and α,β -Deuterated Protected Amines

6678

<https://doi.org/10.1021/acs.chemrev.1c00795>
Chem. Rev. 2022, 122, 6634–6718

co-workers.³⁰³ Starting from a trispyrazolylborate-ligated η^2 benzene tungsten complex, which was prepared in enantio-enriched form, addition of either a proton (e.g., from Ph_2NH_2^+) or a deuterium (e.g., from Ph_2ND_2^+) leads to a cyclohexadienium tungsten complex, and in both cases the proton/deuteron is selectively added *syn* to the tungsten center. Upon treatment with a hydride (BH_4^-) or a deuteride (BD_4^-) source, the hydride/deuteride adds *anti* to the metal center, leading to a defined tungsten-bound cyclohexadiene. This process can be continued until tungsten-bound cyclohexene is obtained, and after oxidation with DDQ and by judiciously choosing the proton/deuteron and hydride/deuteride sources, 52 different stereoisotopomers of cyclohexene could be prepared following this methodology. Furthermore, by employing substituted benzenes as starting materials and nucleophiles or electrophiles other than H^+ , D^+ , H^- , and D^- , the method served to prepare more functionalized deuterated compounds as exemplified for benzotrifluoride as substrate and cyanide as nucleophile in this study (Scheme 102). Currently, this transformation is

Scheme 102. Tungsten-Mediated Preparation of Stereoisotopomers of Substituted Cyclohexenes



stoichiometric in tungsten, but it can be expected that further developments will lead to a catalytic methodology that could ultimately enable the stereoselective synthesis of chiral compounds with highly specific deuteration patterns to be tested in a medicinal chemistry context.

4. MISCELLANEOUS TRANSFORMATIONS WITH DEUTERIUM INCORPORATION

The discussion of the main deuterium incorporation methodologies is presented in the previous chapters, and their respective advantages and limitations are addressed. However, in addition to hydrogen–deuterium exchange reactions, deuterodehalogenations, and reductive deuterations, several other approaches for deuterium labeling are known. These more special procedures will be described in the following lines.

4.1. Trideuteromethylation

Present in 67% of the top-selling drugs from 2011, the methyl group is one of the most common fragments encountered in biologically relevant molecules.^{304,305} The introduction of this small, electronically neutral alkyl fragment can induce tremendous changes in the potency of drug candidates. As an illustration of this “magic methyl effect”, the simple introduction of a methyl group in the structure of a phospholipase D inhibitor induces a 590-fold increase in potency (Figure 8).³⁰⁶ Accordingly, the demand of new methodologies for incorporation of methyl groups is in constant growth.

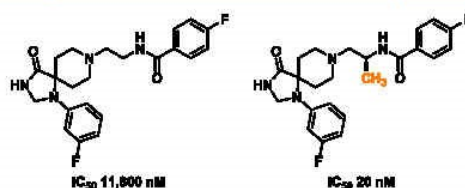


Figure 8. Magic methyl effect.

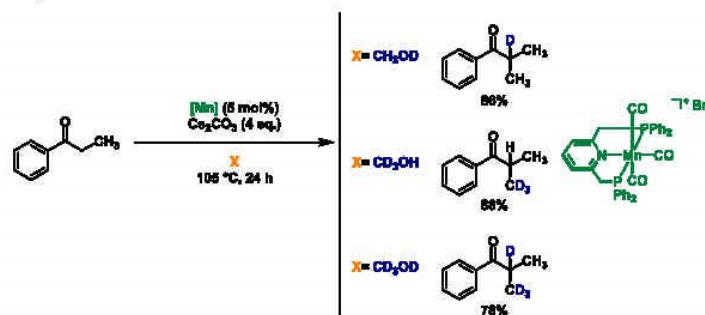
In this respect, the introduction of a trideuteromethyl fragment in small molecules is of significant interest in medicinal chemistry as it combines the benefits of a labeled compound alongside the “magic methyl effect”. While traditionally deuterated alkylating reagents such as deuterated iodomethane have been employed, currently methodologies are of interest which try to avoid the use of such highly toxic and carcinogenic reagents.^{307–310} Besides, achieving high selectivity is a challenging aspect of modern approaches presented in this chapter.

An interesting catalytic trideuteromethylation of ketones was developed by the Rueping group.³¹¹ Using an air- and moisture-stable manganese complex, α -methylation of both aromatic and aliphatic ketones was possible under mild conditions. This method proceeds *via* initial methanol dehydrogenation, subsequent aldol condensation, and final hydrogenation reaction. As expected, the catalytic system operated also in the presence of deuterated methanol, providing the d_4 products in high yields, including substrates containing halogens and heterocycles. Indolinones also underwent trideuteromethylation at the expense of a lower yield despite a higher reaction temperature. H/D exchange was also observed for substrates with benzylic positions, revealing that this catalyst is not limited to C1 deuteromethylation. Double deuteromethylation was achieved when acetophenone and derivatives are used as substrates. This transformation is highly regioselective and allows precise labeling when methanol variants CH_3OD , CD_3OH and $^{13}\text{CH}_3\text{OH}$ are employed (Scheme 103).

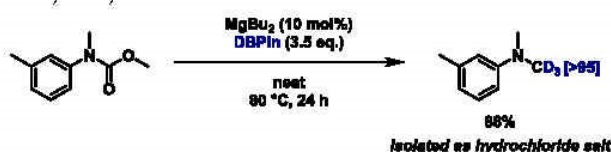
Later, the same group developed a catalytic *N*-methylation and trideuteromethylation of protected amines using a magnesium–pinacolborane system.³¹² Here, BuMgH or BuMgD are *in situ* generated as the active species allowing both the reduction of carbamates to the corresponding formamides followed by the reduction of these latter *via* two hydride or deuteride additions (Scheme 104). Quantitative deuterium incorporations were achieved, yielding N-CD_3 amines in good yields. Even though the labeling part of this methodology was only presented with the *N*-methylating system, these results suggest that amines protected with a Boc moiety can easily be converted to their trideuteromethyl equivalents.

Using a simple iron sulfate salt, Li, Qi, and co-workers developed a new olefin difunctionalization methodology.³¹³ Trideuteromethyl radicals are generated from $\text{DMSO-}d_6$ after H_2O_2 activation, and these methyl radicals were added to olefins (Scheme 105). Moderate to very good yields are obtained, with functionalized olefins including halogen, nitro, or cyano groups. This approach tolerates *N*-alkylacrylamides and styrenes, with the need of $\text{NH}_2\text{OSO}_3\text{H}$ as additive for the latter. To demonstrate the preparative feasibility, gram-scale experiments were performed. Obviously, the resulting products can easily be

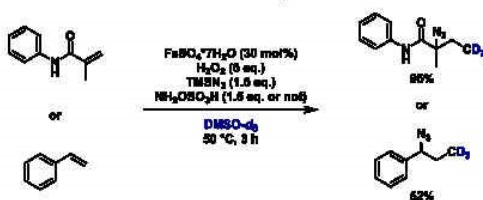
Scheme 103. C1 Methylation of Ketones



Scheme 104. Manganese-Catalyzed Hydroboration of Carbamates



Scheme 105. Azidotrideuteromethylation



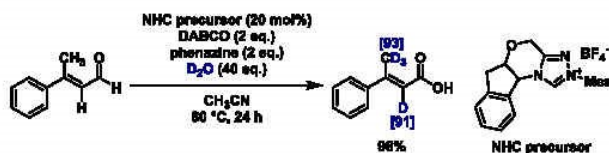
further functionalized, for example, *via* azide–alkyne Huisgen cycloadditions.

The first NHC-catalyzed deuteration at the allylic position of enals was presented by Tian, Chi, and co-workers.³¹⁴ Under oxidative conditions, this aminoindanol-derived precursor allowed high deuterium incorporation not only at the α position but also at the more challenging γ one (Scheme 106). The key intermediate in this metal-free transformation is a vinyl-dienolate that allowed iterative H/D exchanges at both these positions. It is worth noting that the reactivity of (*E*)-enals is more favored than the (*Z*) counterpart and that the β alkyl-substituted enals exhibited a lower yield than the β aryl ones, although the deuterium incorporation is similar.

Employing a palladium photocatalyst activated by visible light, Su and co-workers presented a general method for the synthesis

of *N*-alkyl amines.³¹⁵ The catalyst supported on polymeric carbon nitride allowed the *in situ* generation of hydrogen *via* water splitting, as well as alcohol oxidation to the corresponding aldehyde. After condensation with an amine, the *in situ* generated imine is subsequently reduced. The main advantage of this methodology is its tunability (Scheme 107). By varying the isotope sources between deuterium oxide and the deuterated alcohols, d_0 , d_1 , d_2 , or d_3 *N*-methylation of amines is achieved. Moreover, the use of carbon labeled alcohols permits the insertion of ^{13}C in the alkylating moiety.

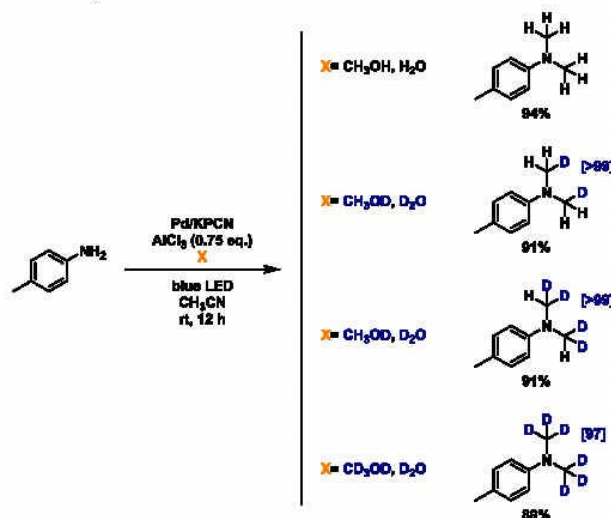
Trideuteromethylation was additionally applied to indoles and to phenols. The key point of this methodology developed by Liu's group was the use of a tosyl protecting group.³¹⁶ This research can be appreciated as the formal replacement of the toluenesulfonyl group by a CD_3 moiety (Scheme 108). Initially, the addition of trideuteromethoxide on the sulfone takes place, followed by desulfonylation of the heteroatom. The latter undergoes a $\text{S}_{\text{N}}2$ reaction with the sulfonic ester affording the labeled compound with quantitative deuterium incorporation. Remarkably, even though the C3 position of indoles is more nucleophilic than the N1 position, no C3-methylated products were detected, underlining the high selectivity of this transformation for the *ipso*-position of the tosyl group. Moreover, the alkylating agent can be generated *in situ* by mixing potassium *tert*-butoxide with the corresponding alcohol providing comparable results.

Scheme 106. α,γ -Deuteration of Enals

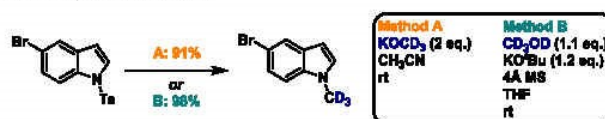
6680

<https://doi.org/10.1021/acs.chemrev.1c00795>
Chem. Rev. 2022, 122, 6634–6718

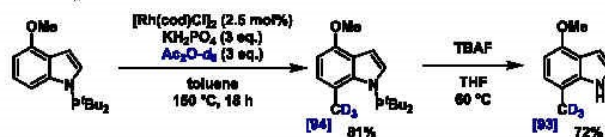
Scheme 107. Supported Photocatalyst for Deuteration of Amines



Scheme 108. N1-Trideuteromethylation of Indoles



Scheme 109. C7 Trideuteromethylation of Indoles



Using a chelation-assisted C–H activation process, Shi and co-workers prepared trideuteromethyl-substituted indoles. Here, an indole containing a *N*-P^tBu₂ group was used in the presence of a rhodium catalyst to insert the desired fragment selectively at the C7 position.³¹⁷ In this case, it is suggested that deuterated acetic anhydride coordinates to a five-membered rhodacycle. Posterior decarboxylation and reductive amination generate the labeled product in medium to good yields with high deuterium incorporation. Easy removal of the directing group is possible using TBAF, delivering the free indole with virtually no isotope loss (Scheme 109).

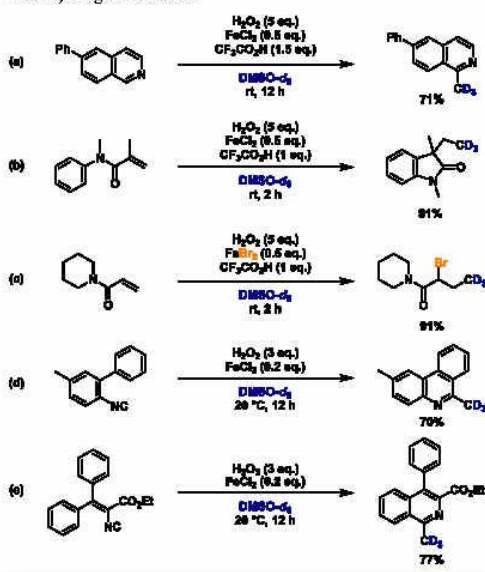
The use of iron salts in combination with hydrogen peroxide for trideuteromethylation was introduced by Antonchick (Scheme 110, a–c),³¹⁸ and further works were realized by Li and Qi (Scheme 110, d–e).³¹⁹ In either case, trideuteromethyl radicals were obtained from deuterated DMSO and added to the most electron-deficient position of the substrate. When possible, cascade cyclization took place providing interesting heterocycles such as oxindoles, phenanthridines, or isoquinolines. Besides,

acrylamides could be converted to labeled α -haloamides by incorporation of the halide anions from the metal salt.

Furthermore, quinolines and isoquinolines were labeled using iridium photocatalysis as elegantly illustrated by Glorius and co-workers.³²⁰ Here, the reaction of DMSO-*d*₆ with the chlorinated electrophile leads to a chloro(ditrideuteromethyl)sulfonium species. Subsequent reduction and homolytic C–S bond cleavage form the trideuteromethyl radicals for the labeling of heteroarenes at the most electron deficient position (Scheme 111). This mild methodology tolerates various functional groups such as esters, amides, methoxy as well as halogen substituents, allowing further functionalization.

Making use of another sophisticated catalytic reaction, deuterated benzofurans and dihydrobenzofurans were generated from phenols and α,β -unsaturated carboxylic acids by Szabo, Maiti, and co-workers via a palladium-catalyzed oxidative annulation.³²¹ The key intermediate in this methodology is a Pd-allyl complex labeled simply by deuterium oxide. In general, two different β -elimination pathways can follow, leading to the

Scheme 110. Radical Trideuteromethylation Using Iron Salts and Hydrogen Peroxide



formation of either 3-(methylene- d_3)-2,3-dihydrobenzofurans or 3-(methyl- d_3)benzofurans (Scheme 112).

Ruthenium catalysis for the methylation at the α position of sulfones was very recently presented by Ling, Zhong, and co-workers.³²² Addition of a sulfone carbanion on formaldehyde generated by *in situ* dehydrogenation of methanol leads to alkene formation. Subsequent reduction of this olefin affords the methylated product. Switching from methanol to deuterated methanol provided a trideuteromethylated product with high deuterium content (Scheme 113).

Precise deuteration of arylacetonitriles is achieved with different amine-borane/ N,N -dimethylformamide systems.³²³ With one hydrogen (or deuterium) atom transferred from the DMF formyl moiety and two hydrides (or deuterides) from the amine-borane, CH_3 , CH_2D , CHD_2 , and CD_3 units can selectively be inserted (Scheme 114). The interest of this methodology relies in its valuable tuneability. As a drawback, only one deuterium atom out of the seven from $\text{DMP-}d_7$ is recovered in the final product, even though this reagent is one of the most expensive deuterium sources discussed in this Review. So far, the reducing agent $\text{Me}_2\text{NH-BD}_3$ is not commercially available and has to be synthesized.

In 2020, the MacMillan group reported a versatile method for late-stage installation of both tritium and carbon-11 into pharmaceutical precursors bearing aryl and alkyl bromides. The key step is a metallaphotoredox-catalyzed methylation (Scheme 115).³²⁴ As mentioned before, methyl groups are common structural elements found in many bioactive molecules, which play a crucial role in a wide range of biological processes, including DNA replication, protein modification, lipid biosynthesis, and various other metabolic pathways. In this study, tritiated and carbon-11-labeled complex pharmaceuticals and positron emission tomography (PET) radioligands were achieved. The authors also used this protocol for preclinical PET imaging and its translation to automated radiosynthesis, which might be applied for regular radiotracer production in human clinical imaging.

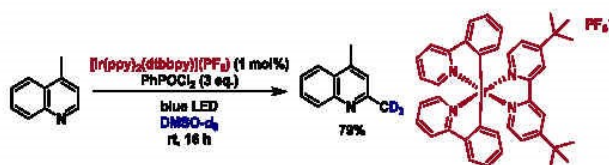
4.2. Insertion of the Trideuteromethoxy Group, Deuteration of Thiols, Selenides, and Carboxylic Acids

An approach for the introduction of deuterated moieties on the C3 position of quinoxalinones was developed by Shen.³²⁵ Via a SET mechanism, alkoxylation using deuterated methanol or ethanol was achieved using *p*-methoxybenzene and peroxyacetic acid. It is postulated that a $\text{ArI}(\text{OAc})_2$ hypervalent iodine(III) species is generated *in situ*, which leads to the active alkoxy radical. Medium to good yields of the corresponding labeled products were obtained with this method (Scheme 116).

A new interesting labeling reagent was introduced by Chen, Wang, and co-workers: they applied trideuteromethyl sulfonium iodide (TDMSOI) for the labeling of phenols, thiols, and nitrogen-containing substrates as well as activated methylene positions.³²⁶ TDMSOI was synthesized *via* sulfoxonium meta-thesis between trimethyl sulfonium iodide (TMSOI) and readily available $\text{DMSO-}d_6$ and was used in a "one pot" manner to insert the CD_3 group (Scheme 117). The generality of this reagent was demonstrated by the labeling of more than 60 substrates, including drugs and natural products such as melatonin derivatives.

Visible-light photochemistry proved to be another efficient approach for thiotrideromethylation, as depicted in the work of Wang and co-workers.³²⁷ Under a nitrogen atmosphere, an eosin Y-mediated cross-coupling reaction between tetrafluoroborate diazonium salts and a *S*-methyl- d_3 sulfonylthioate leads to trideuteromethyl sulfides. Interestingly, by performing this reaction under air, the same conditions lead to the synthesis of trideuteromethylated sulfoxides. The photocatalyst, eosin Y, is supposedly excited under visible-light irradiation and enables the cleavage of the carbon-diazo bond *via* SET, providing an aryl radical. This radical eventually reacts with $\text{PhSO}_2\text{SCD}_3$, yielding the sulfide products. In addition to the sulfur chemistry, this methodology can be applied to generate trideuteromethyl selenide products, with $\text{PhSO}_2\text{SeCD}_3$ as coupling partner (Scheme 118).

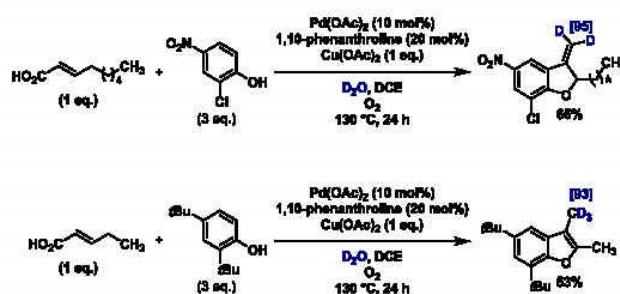
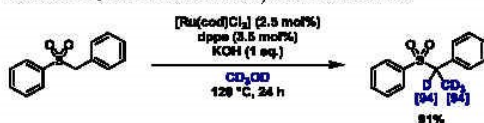
Scheme 111. Iridium Photocatalysis for Trideuteromethylation



6682

<https://doi.org/10.1021/acs.chemrev.1c00795>
Chem. Rev. 2022, 122, 6634–6718

Scheme 112. Deuterated Benzofurans

Scheme 113. α -Trideuteromethylation of Sulfones

Very recently, Shi and co-workers developed DMTT (5-(methyl- d_3)-*SH*-dibenzo[*b,d*]thiophen-5-ium trifluoromethane sulfonate) as an alternative effective methylating agent.³²⁸ Based on a dibenzothiophene motif, the DMTT allows the trideuteromethylation of numerous nucleophilic substrates, such as aliphatic and aromatic carboxylic acids, phenols, sulfonamides, and thiols (Scheme 119). Moreover, in the presence of a catalytic amount of nickel salts, this d_3 -methylating reagent allowed the synthesis of tertiary amines from the corresponding primary amine without the generation of ammonium salts. Also, when a pyridyl group is used as directing group, in the presence of palladium and copper, DMTT allows the *ortho* C–H bond d_3 -methylation in medium yields with high deuterium incorporation.

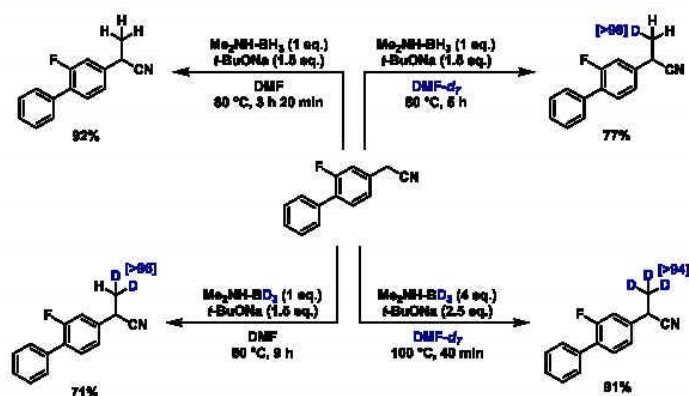
4.3. Deuterodifluoromethylation

Based on previous works of Zafarani, Segall, and co-workers,³²⁹ Zou, Wu, Wu, and co-workers applied the commercially available diethyl bromodifluoromethylphosphonate in the

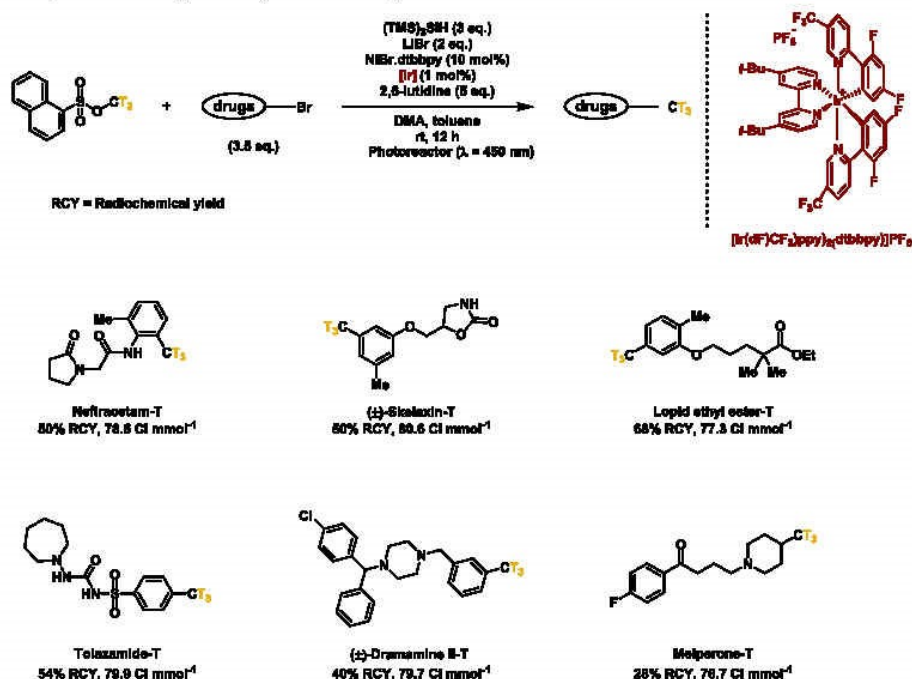
presence of deuterium oxide for the insertion of a CF_2D moiety on phenols, naphthols, benzothiophenol, hydroxyindoline, pyridinol as well as an estrone derivative.³³⁰ P–C bond cleavage via hydrolysis of the phosphonate leads to the unstable bromodifluoromethyl anion that spontaneously eliminates bromide, leading to a difluorocarbene eventually captured by the phenolate ion. D_2O hydrolysis leads to the desired product. This straightforward methodology was easily scaled-up to a 30 g scale without yield or deuterium content erosions (Scheme 120).

In recent years, the topic of flow chemistry attracted significant interest in the pharmaceutical industry as it offers possibilities for easier scale up, improved heat and mass transfers, as well as more facile implementation of multistep processes compared to traditional batch reactions.³³¹ Moreover, this approach suggests advantages when gaseous reagents are used as a precise control of the gas equivalents is possible and high pressure conditions might be avoided. Similarly, safety concerns inherent to toxic gases can be reduced compared with batch processes. These benefits of flow chemistry were used by Jamison and co-worker for the deuteriodifluoromethylation of aldehydes.³³² Specifically, they deprotonated chlorodifluoromethane using a lithiated base, and subsequent α -elimination leads to a singlet difluorocarbene ($:CF_2$), which is trapped in the presence of triphenylphosphine. The difluoromethyl triphenylphosphonium ylide reacts with the aldehyde substrate leading to

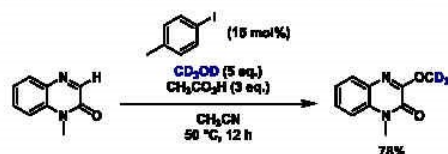
Scheme 114. Labeling of Arylacetonitriles



Scheme 115. Selected Examples of High-Molar-Activity Tritiation

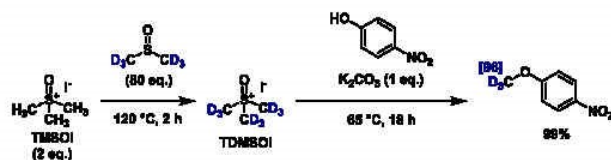


Scheme 116. Trideuteromethylation of Quinoxalines



a key oxaphosphatane intermediate. Alkaline deuterolysis provides the final labeled compounds. Aldehydes including halide, methoxy, thiomethyl, and heteroarene substituents yielded the corresponding deuterated products with high deuterium incorporation, although enolizable aldehydes proved to be not applicable to the standard reaction conditions. The methodology was also scaled-up from 0.832 mmol h⁻¹ to 1.51 mmol h⁻¹, while keeping the same short residence time of 14.9 min (Scheme 121).

Scheme 117. TDMSOI as Trideuteromethylating Reagent



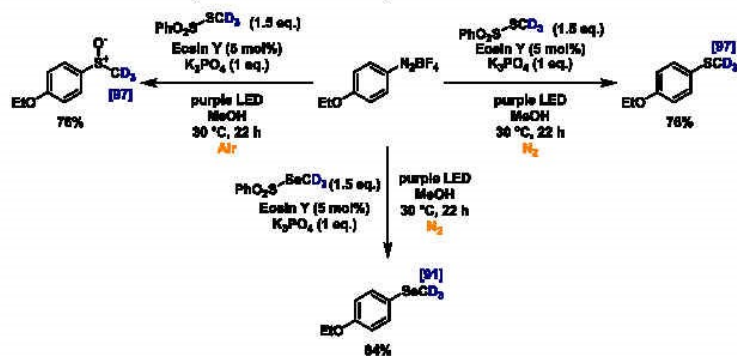
6684

<https://doi.org/10.1021/acs.chemrev.1c00795>
Chem. Rev. 2022, 122, 6634–6718

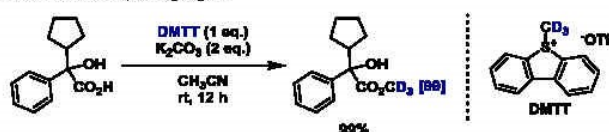
A special method for the preparation of deuteriodifluoromethyl-substituted ketones and related derivatives has been disclosed by Colby and co-workers.³³³ Here, α,α' -perfluorinated *gem*-diols release trifluoroacetate in basic media leading to difluoroenolates. These intermediates easily take part in aldol reactions with various electrophiles. In particular, in the presence of deuterium oxide, α -deutero- α,α' -difluoromethyl ketones are obtained in high yields under very mild conditions. The main disadvantage of this methodology is the availability of the highly fluorinated starting materials: the most general preparation of these latter compounds uses trifluoroacetylation of methyl ketones followed by difluorination. Deuteriodifluoromethyl sulfones were obtained via a similar manner (Scheme 122).

Very recently, $\text{CF}_2\text{DSO}_2\text{Na}$ was introduced by Li and co-workers as a versatile labeling agent, allowing the insertion of the deuteriodifluoromethylthio and deuteriodifluoromethyl moieties on indole backbones, at the C3 and C2 positions, respectively.³³⁴ Notably, this reagent allows the first direct

Scheme 118. Eosin-Mediated Photocatalysis for Trideuteromethylation



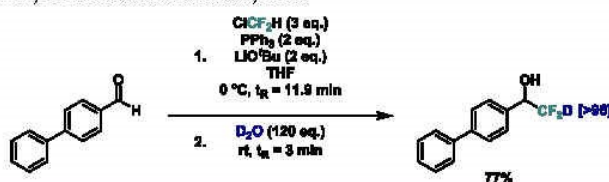
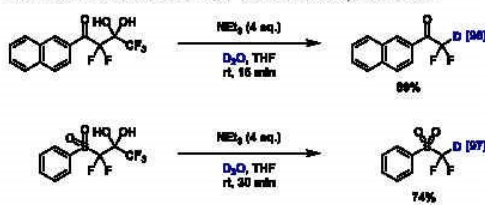
Scheme 119. DMTT as Trideuteromethylating Agent



Scheme 120. Difluorodeuteromethylation of Phenols



Scheme 121. Flow Chemistry for Deuteriodifluoromethylation

Scheme 122. Synthesis of α -Deutero- α,α' -difluoromethyl Ketones and α -Deutero- α,α' -difluoromethyl Sulfones

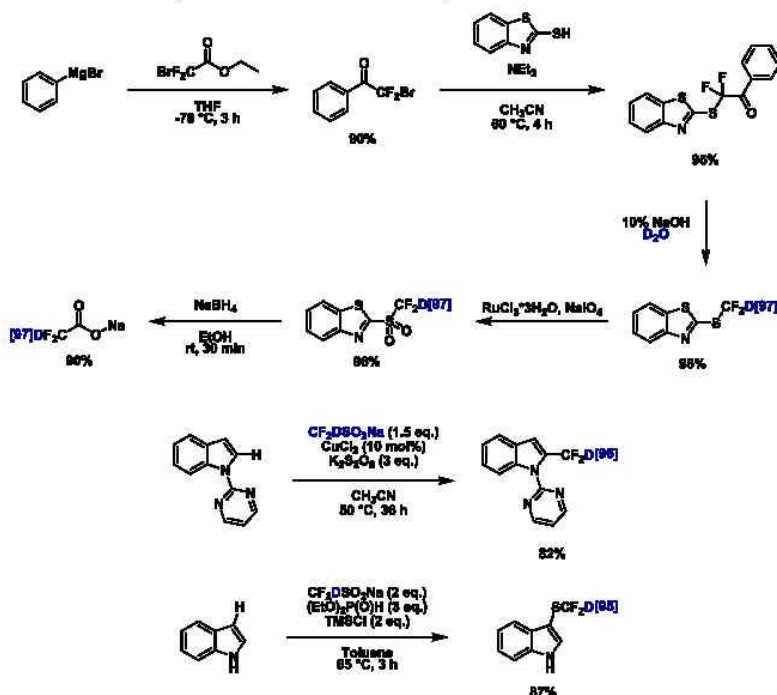
deuteriodifluoromethylation methodology reported. $\text{CF}_2\text{DSO}_2\text{Na}$ is easily synthesized in five reliable steps, with an overall yield of 72% and an overall deuterium incorporation of 97% (Scheme 123). High deuterium incorporations are achieved in both model substrates, as well as in natural and

pharmaceutical compounds notable in the late-stage functionalization of thymol, melatonin, fibronil, and auxin.

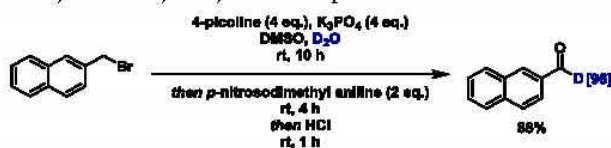
4.4. Deuterated Aldehydes

Luo, Sheng, and co-workers took advantage of the broad availability of arylmethyl halides to synthesize deuterated aldehydes in a one-pot fashion (Scheme 124).³³⁵ In order to avoid the formation of undesired alcohols, pyridinium salts were used as reaction intermediates. In this approach, base-mediated H/D exchange takes place at the benzylic position, subsequent oxidation by *p*-nitrosodimethyl aniline followed by acidification provides the deuterated aldehyde. Arylmethyl bromide as well as chlorides could undergo this transformation, although their aliphatic counterparts failed to generate pyridinium salts. Moreover, this method is also efficient on cinnamyl halides since it allowed a high deuterium incorporation in the labeling of *trans*-cinnamaldehyde.

Scheme 123. Deuteriodifluoromethylation and Deuteriodifluoromethylthiolation

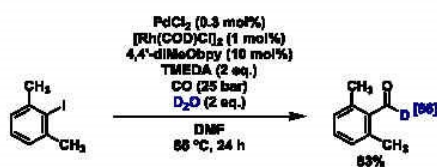


Scheme 124. Deuterated Aldehydes from Arylmethyl Halide Compounds



Deuterated aldehydes were also attained by a cooperative palladium–rhodium catalysis from the corresponding aryl iodides. In this case, the well-known palladium-catalyzed carbonylation of aryl halides is combined with a water–gas shift reaction for the generation of an active rhodium–deuteride species.³³⁶ Highly hindered aldehydes are efficiently labeled by this method, using solely 2 equivalents of deuterium oxide as the isotope source (Scheme 125). However, it should be noted that

Scheme 125. Deuterated Aryl Aldehyde via Water–Gas Shift Reaction



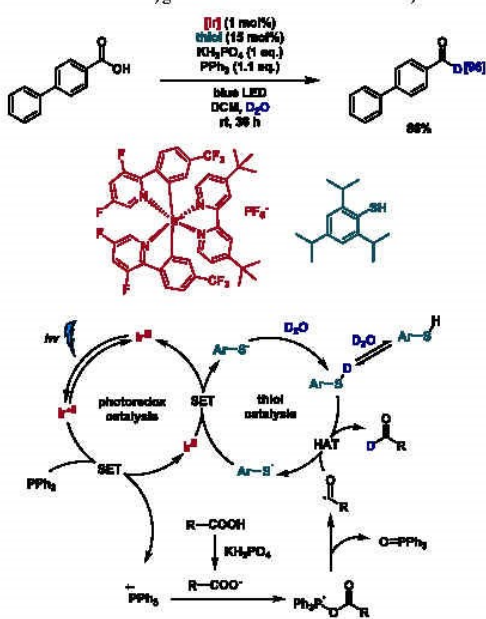
undesired palladium-catalyzed C–H insertion took place when the substrate enabled such reaction (e.g., 2-biphenylcarboxaldehyde, 1-naphthaldehyde). An increased amount of deuterium oxide is thus required to achieve high deuterium incorporation at the formyl position.

A protocol using synergetic photoredox- and organocatalysis was presented by Xie and co-workers for the deoxygenative deuteration of carboxylic acids.³³⁷ Light-induced single-electron oxidation of triphenylphosphine leads to a radical cation which reacts with the deprotonated carboxylic acid. Subsequent β -scission results in a formyl radical which undergoes hydrogen atom transfer (HAT) with a deuterated thiol, leading to the desired labeled aldehyde (Scheme 126). The two catalytic cycles are ultimately closed by reduction of the thiol radical by Ir(II) and successive deuterium abstraction from deuterium oxide.

4.5. Deuterated Chloroform

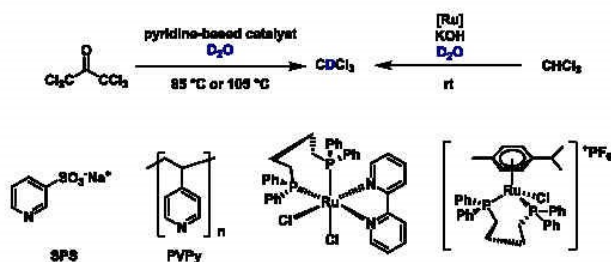
Among the applications of deuterated compounds, their use as solvents for NMR spectroscopy is one of the most important ones as part of chemist's daily routine. Deuterated chloroform,

Scheme 126. Deoxygenative Deuteration of Carboxylic Acids



one of the most used NMR solvents, is mainly produced by either haloform reaction or by treatment of chloral hydrate with sodium deuterioxide.^{338–341} Recently, some catalytic methodologies were presented for the generation of CDCl_3 . For example, pyridine-based catalysts were investigated by Schomaker using hexachloro-2-propanone and deuterium oxide as an isotope source.³⁴² Specifically, sodium 3-pyridine sulfonate (SPS) and poly(4-vinylpyridine) (PVPy) proved to be useful catalysts on a laboratory scale. Both base catalysts are easily recycled as they are non-soluble in CDCl_3 . Especially, the latter being heterogeneous, its reuse permitted clean reactions with a 79% average yield over 11 runs. Other new developments took advantage of two ruthenium complexes bearing a 1,4-bis-(diphenylphosphine)butane (dppb) ligand.³⁴³ Similarly, deuterium oxide was used, although in this case a base is required for the generation of the deuterioxide species that coordinates the ruthenium centers. H/D exchange takes place via a fast-synchronous reaction with the hydrogen atom from chloroform.

Scheme 127. Catalysis for the Synthesis of Deuterated Chloroform



6687

<https://doi.org/10.1021/acs.chemrev.1c00795>
Chem. Rev. 2022, 122, 6634–6718

The active deuterioxide catalyst is finally regenerated by scrambling with deuterium oxide (Scheme 127).

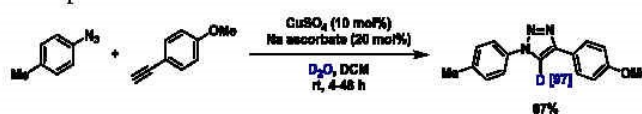
4.6. Further Approaches

In general, triazoles can be efficiently synthesized using azide–alkyne click chemistry. Notably, the copper-catalyzed azide–alkyne cycloaddition (CuAAC) allows the regioselective formation of 1,4-disubstituted 1,2,3-triazoles. Taking advantage of this methodology, Lakshman and co-workers proposed a valuable method for the selective incorporation of a deuterium atom at the C5 position of the triazole ring.³⁴⁴ Using a biphasic reaction medium with D_2O as isotope source, dry copper sulfate, and sodium ascorbate, a variety of deuterated triazoles were generated under mild conditions in good to excellent yields with deuterium incorporation above 92% (Scheme 128). Deuterated versions of bioactive compounds (e.g., resveratrol analogues) and nucleoside-containing substrates were obtained with this method, as well as fully deuterated compounds when phenyl azide- d_5 and ethynylbenzene- d_3 were used.

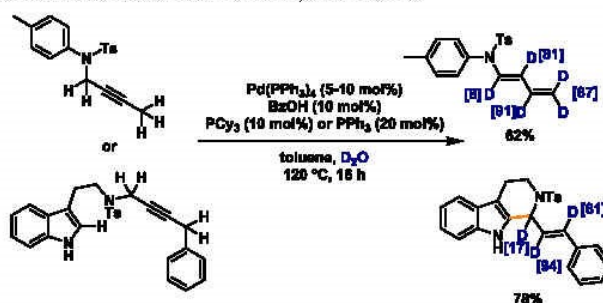
The utility of a low valent palladium complex in the presence of benzoic acid for labeling processes was highlighted by Maestri and co-workers for the generation of polydeuterated 1,3-dienes from propargylamines.³⁴⁵ In this process, deuterium incorporation is however not homogeneous, with high deuteration levels at the β and γ positions, but generally low at the α one (Scheme 129). Mixed outcomes are observed at the δ position. Interestingly, ynamides do not undergo this transformation while it is the case for allenamides, suggesting the latter are intermediates in the catalytic cycle. When tryptamine propargylic derivatives are used, deuterated tetrahydrocarbolines are generated in good yields via C–H activation of the indole ring. Terminal olefins can also undergo this transformation, as a small number of styrene derivatives were deuterated. It is suggested that H/D exchange takes place rapidly between D_2O and a palladium–benzoic acid–hydride complex, followed by up to five sequential insertions and β -hydride eliminations for the generation of dienamides, or three for the carboline derivatives.

Recently, Li and co-workers developed a new transition-metal-free methodology for the direct hydroxylation of heterobenzyl derivatives.³⁴⁶ Using ambient air as oxidant and DMSO as reductant, this simple system allows the rapid and selective hydroxylation without the overoxidation to the ketone, commonly avoided by the *in situ* protection of the hydroxyl groups.^{347,348} When switching the reaction solvent to deuterated DMSO, α -deuterated alcohols were generated in medium to good yields with high deuterium incorporation (Scheme 130). This approach tolerates electron-withdrawing groups as well as

Scheme 128. Deuterium Incorporation in Triazoles



Scheme 129. Synthesis of Deuterated Dienamides and Tetrahydrocarbolines



Scheme 130. Hydroxylation-Deuteration of Heterobenzyl Compounds



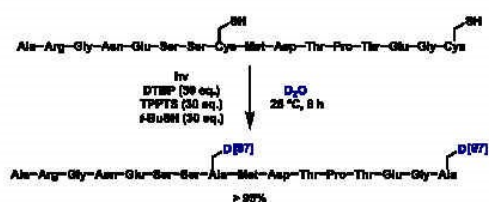
Scheme 131. Desulfurization Deuteration Protocol



electron-donating ones but is substrate limited, since no reactivity is detected when diphenylmethane was tested as substrate. It is suggested that this one-pot hydroxylation deuteration reaction is based on a radical mechanism: The reaction of a DMSO radical with a base-promoted enamine generates a heterobenzylic radical intermediate and subsequent reaction with molecular oxygen leads to the generation of the corresponding hydroperoxide. The latter oxidizes DMSO to dimethyl sulfone forming the desired product.

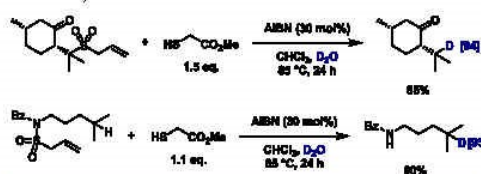
Using a combination of a phosphoric reagent and di-*tert*-butyl peroxide, Sun and co-workers established a specific deuterium labeling methodology based on a desulfurization-deuteration approach.³⁴⁹ Comparably high deuterium incorporations are observed following a radical process mediated by visible light. Applying a combination of deuterium oxide and DCM allowed the deuteration not only of primary, secondary, and tertiary thiols but also of disulfides (Scheme 131). Ethyl acetate/deuterium oxide can also be used as a solvent mixture, providing comparable results in term of yields and deuterium incorporation while being a greener alternative to DCM. Notably, the water-soluble sulfonated phosphine ligand TPPTS allowed to perform this reaction in water and was successfully applied for the deuteration of two cysteine moieties present in a medium size peptide in >95% yield with >97% D incorporation.

While developing a general approach for desulfonylative functionalization of alkyl allyl sulfones, the efficiency of the well-known radical starter AIBN as catalyst for deuterium incorporation was demonstrated by Studer and co-workers.³⁵⁰ The allyl sulfonyl moiety acts as a C radical precursor and reacts with methyl thioglycolate that underwent H/D exchange on the thiol function. This procedure was successfully applied to secondary and tertiary alkyl allyl sulfones and is compatible with



numerous functional groups, albeit the release of a quantitative amount of sulfur dioxide and allyl sulfide are drawbacks (Scheme 132). The same group subsequently implemented this approach

Scheme 132. Synthesis of Labeled Compounds by Desulfonylative Deuteration

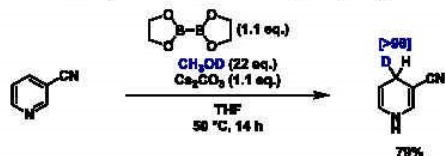


for the labeling of amide containing substrates. When applied to this methodology, *N*-allylsulfonamides were readily deuterated via 1,5- or 1,6-HAT. Notably, this uncommon HIE strategy is effective for primary, secondary, and tertiary C–H bonds.³⁵¹

Another unconventional methodology for the facile synthesis of deuterated 1,4-dihydropyridines was recently presented by Jiao and co-workers via an inverse hydroboration protocol

(Scheme 133).³⁵² In this reaction, a *N*-boryl pyridyl Meisenheimer anion acts as a key intermediate and abstracts a

Scheme 133. Synthesis of 4-Deutero-1,4-dihydropyridines

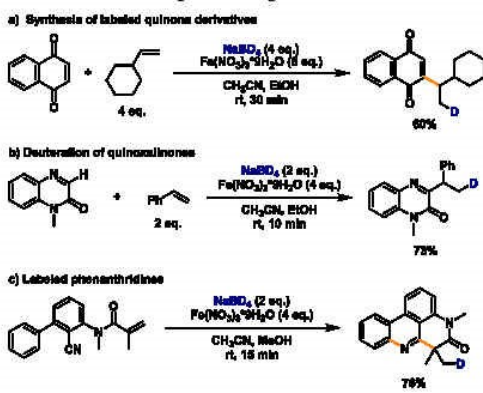


deuterium atom from deuterated methanol. In general, the yields of the desired products were medium to good, and the deuterium incorporation was high. Advantageously, this approach utilizes a cheap deuterium source compared with strong reductants such as LiAlD_4 . However, halogenated pyridines as well as quinolines and acridine are not tolerated by this methodology.

It is well-established to use 1,4-DHP derivatives in hydride transfer reactions. Indeed, deuterated derivatives were also exemplarily shown allowing the deuteride transfer to an α,β -unsaturated aldehyde. The resulting chiral aldehyde was obtained with medium enantiomeric excess and high deuterium incorporation.

Using NaBD_4 as deuterium source, Liu and co-workers prepared deuterium-labeled quinones with a free radical alkylation reaction.³⁵³ From a mechanistic point of view, it was proposed that single-electron oxidation of the deuteride by iron(III) leads to a radical that adds on the less-hindered position of the olefin. The target product is achieved by alkylation of the quinone, second oxidation, and final deprotonation (Scheme 134a). This system tolerates several

Scheme 134. Combination of Sodium Borodeuteride and Iron Nitrate for Isotopic Labeling



functional groups including silanes, halogens, free carboxylic acid, and alcohols. Moreover, the convenient reaction conditions of this labeling technique should be mentioned, as the products are obtained at room temperature in short time (30 min). A related deuteration of quinoxalinones with NaBD_4 and olefins was recently established by Li and co-workers via a three-component reaction following a radical pathway.³⁵⁴

Sodium borodeuteride was used as isotope source, allowing the functionalization of diverse quinoxalinones. However, the substrate scope is limited to this type of backbone as theophyllines and quinazolines did not undergo similar reactions. From a mechanistic point of view, this transformation is permitted by the addition of a deuterium radical generated by the iron(III) salt on the alkene, forming an alkyl radical that reacts with the quinoxalinone. After a 1,2-*H* shift, the more stable tertiary radical is oxidized, and the final product is obtained after deprotonation (Scheme 134b). A very similar approach was later developed by Liu, Sun and co-workers, who labeled phenanthridines from *N*-acrylamides again via a radical pathway.³⁵⁵ Likewise, a deuterium radical is generated by the oxidation of NaBD_4 with an iron(III) salt (Scheme 134c). This radical adds on the terminal olefinic bond of the acrylamide. Subsequent insertion generates an iminyl radical that adds to the adjacent benzene ring. After a second iron(III)-mediated oxidation followed by deprotonation, the newly fused heterocycle is obtained in medium to good yields.

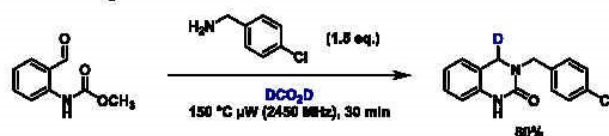
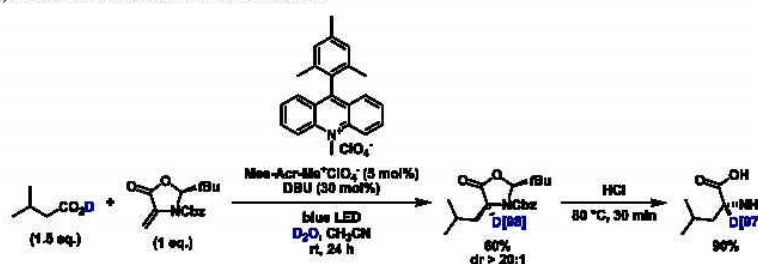
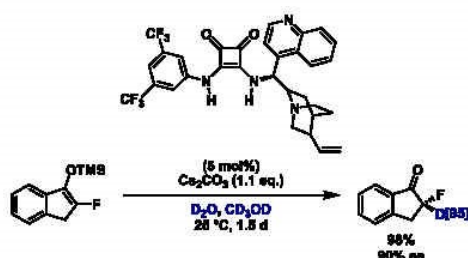
Selective deuterium incorporation at the 4-position of a quinoxalinone scaffold, which is of interest in medicinal chemistry, was achieved by Odell and co-workers via a Leuckart-Wallach type reaction.³⁵⁶ In their metal-free procedure, deuterated formic acid plays the role of solvent, reductant, and isotope source (Scheme 135). Amine condensation on the more reactive aldehyde function forms an imine that subsequently cyclizes on the carbamate moiety leading to an acyl iminium ion. Subsequent reduction generates a deuterium atom at the benzylic position.

An organophotoredox-mediated asymmetric α -deuteration α -amino acid synthesis was presented by Wang and co-workers.³⁵⁷ Here, carboxylic acids were coupled with an oxazolidinone bearing a bulky substituent as amino acid surrogate (Scheme 136). The chiral anion intermediate was trapped with deuterium oxide providing a highly stereoselective deuteration methodology. Noteworthy, bulky carboxylic acids could undergo this transformation, too. Cleavage of the oxazolidinone fragment was easily performed in acidic conditions to generate the desired α -deuterated amino acid. Such products are of interest for example for the determination of the secondary and tertiary structure of peptides and proteins.

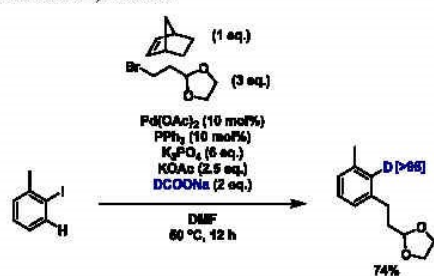
The first highly enantioselective catalytic system for the synthesis of α -deuterated α -fluoro-ketones was reported by Yu, Zhou, and co-workers.³⁵⁸ Here, a bifunctional cinchonidine-derived organocatalyst allowed preferential deuterium addition on the *Si* face of cyclic silyl enol ethers. It is suggested that the silicon interacts with the tertiary amine part, while the fluorine interacts with D_2O bonded to the squaramide part of the catalyst (Scheme 137).

Congested labeled arenes were efficiently synthesized by Zhang, Liu, and co-workers employing a palladium-catalyzed alkylation-deuteration cascade.³⁵⁹ Oxidative addition of the palladium center on the carbon-iodine bond is followed by carbopalladation of norbornene. Subsequent base-mediated palladacycle formation, oxidative addition of the halogenated coupling partner, C–C bond formation via reductive elimination, and β -carbon elimination of the norbornene provided the final palladium(II) species in a Catellani-type approach. Sodium formate-*d* was proven to be the most efficient base for the selective trapping of this final palladium(II) intermediate as its low reactivity toward the other palladium species from the catalytic cycle permits medium to high product yields and high deuterium incorporation (Scheme 138).

Scheme 135. Quinazolinones Labeling

Scheme 136. Synthesis of α -Deuterated α -Amino AcidsScheme 137. Enantioselective Synthesis of α -Deuterated α -Fluoroketones

Scheme 138. Palladium-Catalyzed Alkylation-Deuteration Cascade of Aryl Iodides

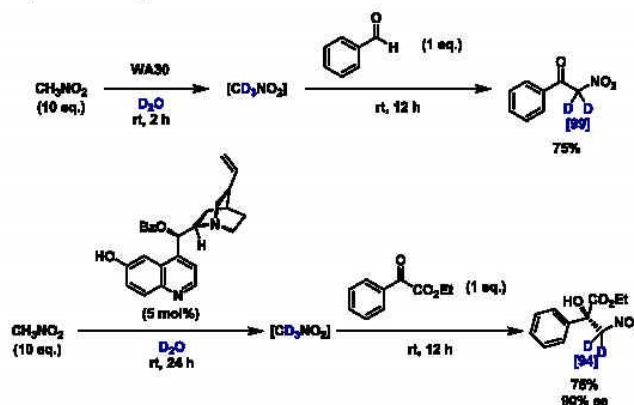


β -Deuterated β -nitroarenes were synthesized in a two-step procedure. First, labeling of nitromethane is achieved with the aid of the basic resin WA30. Successive addition of electrophiles bearing a carbonyl moiety completed the desired nitroaldol reaction.³⁶⁰ Aromatic, heteroaromatic as well as aliphatic aldehydes underwent this transformation. Furthermore, nitroethane and nitropropane were applied to these reaction conditions and provided the corresponding monodeuterated products. Similarly, a quinine-based organocatalyst allowed an asymmetric version of this Henry reaction on α -keto esters

(Scheme 139). Performing the procedure stepwise is not essential for this labeling methodology, as a one-pot version also led to the desired product at the expense of a slightly lower deuterium content.

Vinyl ethers and their sulfur and nitrogen counterparts are often used as building blocks for organic and polymer chemistry. A facile method for the synthesis of such tridentate-labeled substrates starting from the corresponding alcohol, thiol, or amine was disclosed by Ananikov and co-workers.³⁶¹ The key intermediate in these reactions is the dideteroacetylene generated *in situ* with calcium carbide and deuterium oxide (Scheme 140a). Interestingly, when applied to indole derivatives, this methodology also allows H/D exchange on the activated positions of the substrates. Similarly, H/D exchange takes place at the more reactive protons at benzylic positions. This approach was later modified by switching the solvent to 1,4-dioxane and using a smaller amount of DMSO-*d*₆. Doing so, not only the undesired side reaction at the benzylic position was avoided, but the procedure also became more attractive from an economical point of view. Reaction of hydrazonoyl chlorides with these deuterated vinyl ethers leads to interesting 4,5-dideuteropyrazole building blocks (Scheme 140b).³⁶² Besides, taking advantage of a two-chamber reactor, the same group developed a practical methodology for the direct synthesis of similar compounds *via* the *in situ* generation of the two key reagents of a 1,3-dipolar cycloaddition. In one chamber, nitrile amines are obtained *via* deprotonation of hydrazonoyl chlorides. Deuterated acetylene, on the other hand, is generated from CaC₂ and deuterium oxide (Scheme 140c).³⁶³ Notably, this approach is analogous to the one used for the synthesis of labeled isoxazoles.³⁶⁴ Furthermore, aldoximes were converted into the corresponding chloroaldoximes. Subsequent deprotonation in basic media generates a nitrile oxide involved in a 1,3-dipolar cycloaddition with deuterated acetylene (Scheme 140d).

Interestingly, efficient nucleophilic deuteroaddition of indoles, thiols, phenols, and aliphatic alcohols on alkynes is feasible in basic media under metal- and ligand-free conditions.³⁶⁵ Predictably, deuteration takes place at all the acidic and activated positions of the two reagents. Nonetheless,

Scheme 139. Synthesis of β -Deuterated β -Nitroarenes

the interest in this methodology relies in the achieved quantitative deuterium content (Scheme 141).

Very recently, Xie, Li, Zhu, and co-workers modified their previously described photocatalytic system and developed an improved one for the decarboxylative deuteration of carboxylic acids.³⁶⁶ According to the proposed mechanism, an alkyl radical formed by photocatalytic decarboxylation accepts a deuterium atom from the deuterated thiol *via* HAT. Aliphatic as well as benzylic acids were efficiently converted; however, this methodology was not suitable for aromatic carboxylic acids. Noteworthy, activated hydrogen atoms at benzylic positions remained untouched, providing the desired deuterated compounds in high selectivity (Scheme 142). The importance of this methodology relies on the commercial availability of many carboxylic acids, enabling the precise synthesis of numerous deuterated compounds.

Another recently developed metal-free deuteration methodology for the synthesis of β -deuterated methyl-thioether derivatives from unactivated alkenes was reported by Xie and co-workers.³⁶⁷ In their work, the methylsulfenylating agent dimethyl(methylthio)sulfonium trifluoromethanesulfonate (DMTSM) was used to convert olefins to the corresponding episulfonium derivatives. This three-membered ring was eventually opened by deuteride addition (Scheme 143). This approach is efficient for aromatic alkenes and allylic arenes. In the case of aliphatic terminal alkenes, the anti-Markovnikov products are isolated with good regioselectivity. Another interesting feature of this reaction is the simple cleavage of the thioether functionality with Raney nickel.

β -Deuterated tertiary amines can be easily obtained from aldehydes and secondary amines *via* boron catalysis.³⁶⁸ As shown above, nucleophilic attack of an *in situ* generated enamine intermediate followed by deprotonations allowed selective deuterium incorporation. Final iminium reduction by HBPn released the desired products (Scheme 144). Remarkably, this approach is highly regioselective toward the deuteration of aliphatic C–H bonds despite using the same $B(C_6F_5)_3$ derivative utilized by Werner and co-workers¹²⁹ for the labeling of aromatic rings.

Because of the important role of α -hydroxy amides in organic synthesis, as well as their biological activities, new methodologies for their syntheses are of general interest. In this respect,

α,β -deuterated α -hydroxyamide derivatives were produced from the corresponding α -alkyl 1,3-dicarbonyls *via* an interesting cleavage of three C–C bonds.³⁶⁹ In this unusual reaction sequence, cycloalkyl moieties are utilized as leaving groups in a decarboxylative alkylation process (Scheme 145).

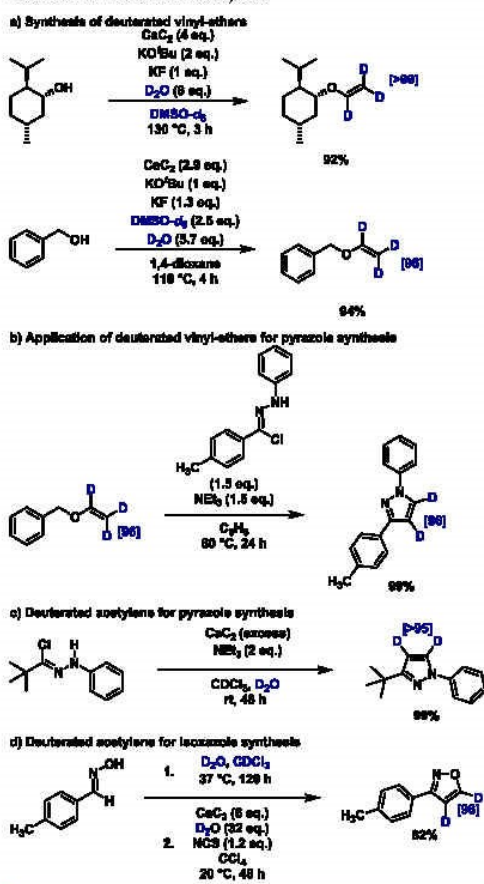
The synthesis of deuterated amides was recently reported by Maulide and co-workers starting from ynamide compounds.³⁷⁰ After activation of the substrate by a strong acid to generate a keteniminium ion and subsequent deuterium oxide addition, the deuterated enol underwent tautomerization to afford the desired product. Besides, the hydrolysis of such bis- α -deuterated carboxylic amides provides an easy entry into the corresponding carboxylic acids. The authors illustrated the potential of their methodology by preparing a deuterated analogue of a synthetic intermediate of the marketed drug guanfacine along with several other drug candidates (Scheme 146).

4.7. Multistep Syntheses with Deuterium Incorporation

In parallel to the methodologies mentioned above, classical synthetic approaches taking advantage of commercially available deuterated reagents or building blocks continue to be valuable for the preparation of specifically labeled compounds. In the following part, we will summarize recent examples of such multistep syntheses.

4.7.1. Deuterated Reagents. Hydrogenation of alkenes is a well-established research field and many methodologies using both heterogeneous as well as homogeneous reagents or catalysts have been proven to be efficient throughout the years. A straightforward way to add deuterium atoms onto olefins relies simply on switching from gaseous hydrogen to gaseous deuterium (Scheme 147). For instance, supported palladium on carbon was utilized in the synthesis of a bicyclic chiral derivatization agent.³⁷¹ Similarly, an α,β -unsaturated ketone was deuterated with nickel boride during the synthesis of *ds*-perhydrazone- d_4 .³⁷² From a homogeneous catalysis point of view, the Wilkinson catalyst has been applied in the synthesis of d_2 amlexanox for the purpose of metabolic studies.³⁷³

Several studies presented above allow the incorporation of a trideuteromethyl moiety into diverse substrates. For this purpose, new and original transformations based on deuterated methanol were developed in recent years. In addition, the use of deuterated analogues of iodomethane was explored for amine alkylations, while synthesizing the first hapten for a heroin

Scheme 140. Deuterium Labeling Reactions Using *In Situ* Generated Deuterated Acetylene

vaccine (Scheme 148a).³⁷⁴ As another example, a simple tunable labeling methodology was recently presented by Sun, Li, and co-workers (Scheme 148b).³⁷⁵ By careful choice of unlabeled or labeled methylation and reductive amination reagents, the synthesis of acylcarnitines bearing a mass shift comprised between 3 and 12 compared with the undeuterated counterparts was feasible.

Nucleophilic CD_3 fragments have also been used in multistep organic syntheses. As an example, the high-order deuterocuprate

$(\text{CD}_3)_5\text{Cu}_3\text{Li}$ obtained from commercially available methyl lithium was applied in the synthesis of 28,28,28-trideutero-25-hydroxydihydrotachysterol.³⁷⁶ In addition, deuterated acetic anhydride was applied in the generation of a library of deuterated lignin model compounds as internal standards for GC–MS quantification.³⁷⁷ Likewise, the multistep synthesis of a geosmin- d_3 was described employing lithium aluminum deuteride for ketone and epoxide reductions.³⁷⁸ The use of deuterated analogues of such common reagents is illustrated in Scheme 149.

SCH 430765 is a potential drug for the treatment of obesity. As another example, the synthesis for the labeled variant of this medication containing both deuterium and carbon-13 atoms was successfully accomplished by Hesk and co-workers, taking advantage of the commercial availability of $[\text{C}^{13}]$ -formaldehyde- d_2 for a Mannich-type reaction (Scheme 150).³⁷⁹

4.7.2. Deuterated Starting Materials. Also, other commercially available deuterated or perdeuterated compounds are prime starting materials in multistep syntheses owing to their high deuterium content. A short selection of syntheses where the authors took advantage of such marketed deuterated substrates is presented in Scheme 151. For example, deuterated acetone, in addition to being an NMR solvent, is an attractive building block for the introduction of a gem-ditrideteromethyl fragment. This moiety is recovered in the labeled aroma fragment β -ionone³⁸⁰ as well as in a leukotriene C4 synthase inhibitor.³⁸¹ MK 3814 was investigated as a potential treatment for Parkinson's disease. Hesk and co-workers modified the ethyl bridge in the structure of this A_{2A} receptor antagonist by starting its synthesis with deuterated ethylene glycol.³⁸² In 2017, two isotope internal standards of serine dipeptide lipids were synthesized in 10 steps by Smith.³⁸³ For these, deuterated butanol was used as labeled starting material. Nasturdexins are an unusual class of natural products found in plants because of their rare dithiocarbamate functionality. Deuterated representatives of this family were synthesized from deuterated benzaldehyde.³⁸⁴ Original deuterated compounds are commercially available, such as (bromomethyl)cyclopropane- d_3 , 2-cyanopyridine- d_4 . The former leads to labeled CHF6001 and a potent phosphodiesterase 4 inhibitor in 10 steps with an overall yield of 9%; the latter initiates the synthesis of a potent lymphocyte function-associated antigen-1 inhibitor. It should be highlighted that this synthesis took advantage of another commercially available labeled building block, BOC-L-alanine- d_4 .

5. APPLICATIONS FOR DEUTERATED AND TRITIATED COMPOUNDS

As mentioned in the introduction, isotope labeling, including deuteration and tritiation, is widely applied in the pharmaceutical industry because of its ability to alter metabolism, to exploit KIEs, and most commonly to perform ADME studies required for registration. While deuteration is an important tool for

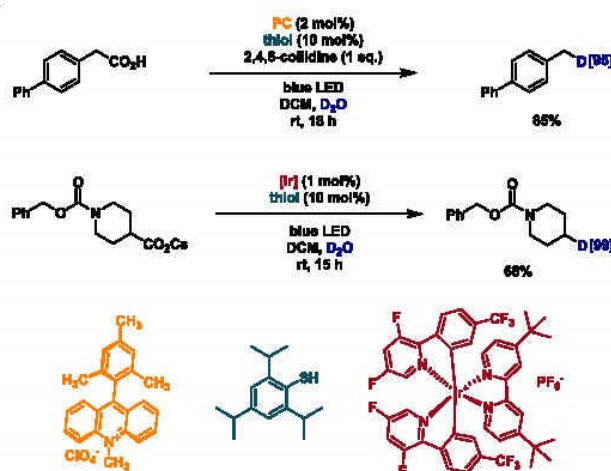
Scheme 141. Nucleophilic Deuterioadditions on Alkynes



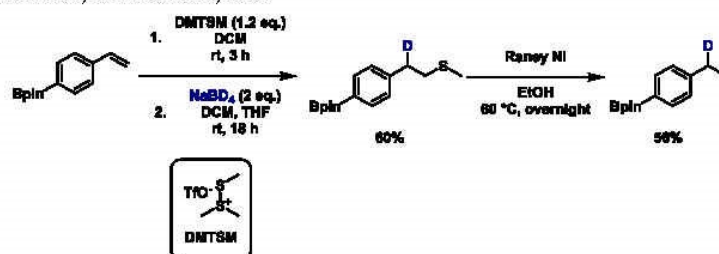
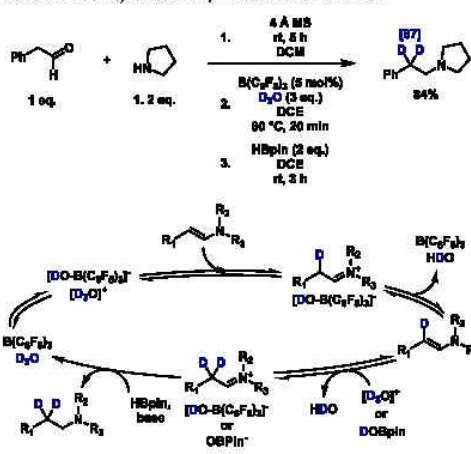
6692

<https://doi.org/10.1021/acs.chemrev.1c00795>
Chem. Rev. 2022, 122, 6634–6718

Scheme 142. Decarboxylative Deuteration

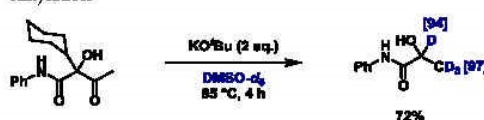


Scheme 143. Deuteromethylthiolation of Styrenes

Scheme 144. Synthesis of β -Deuterated Amines

identification and quantification of drug metabolites, tritiated drug molecules are crucial to support studies containing ligand

Scheme 145. Amide Deuteration via Decarbonylative Alkylation

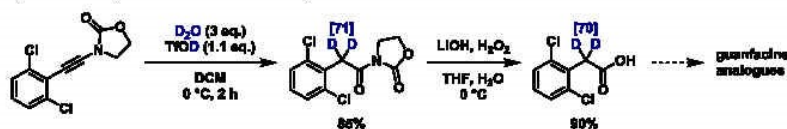


binding interactions, autoradiographic imaging, and drug ADME.

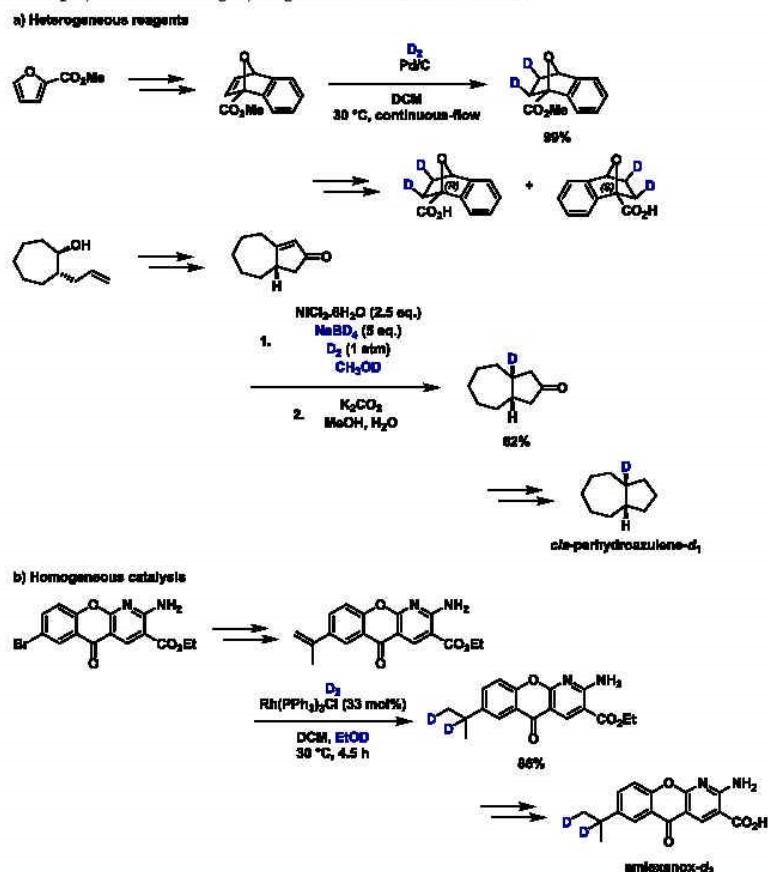
5.1. Mechanistic Investigation

In the last two decades, the development of metal-catalyzed C–H activation reactions continues to be one of the most prominent areas in organic and inorganic chemistry. In those transformations, the cleavage of the respective C–H bond is the crucial step and detailed mechanistic understanding of these processes can be revealed through KIE investigations. Compared with C–H bonds, C–D bonds have intrinsically smaller molar volume, shorter bond length, and a reduced vibrational stretching frequency. Therefore, the activation energy required for C–D bond cleavage is increased compared with C–H bonds. Consequently, the reaction rate (represented by the rate constant k) is slower ($k_H > k_D$).

Scheme 146. Synthesis of α,α -Dideuterated Carboxylic Acid Derivatives via Ynamide Activation



Scheme 147. Multistep Syntheses Utilizing Hydrogenations with Deuterium Gas



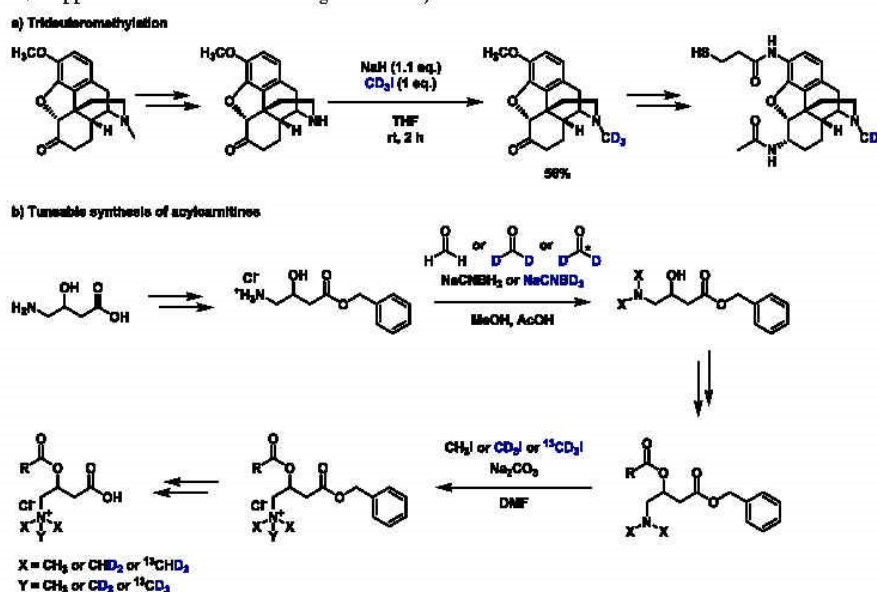
Comprehensive information on the importance of KIEs in mechanistic studies of, for example, C-H activation processes, have been published by Westaway in 2006^{38,9} as well as Simmons and Hartwig in 2012.¹⁸ Thus, in the following section only the main principles will be briefly explained and most recent examples will be shown (Table 2).

5.1.1. Primary Kinetic Isotopic Effect. A primary KIE is observed when the cleavage or formation of an isotopically labeled bond is the slow step of the overall reaction. In general, the KIE values can be calculated by parallel measurements of rates in intermolecular competition vs intramolecular competition. Notably, the observation of a primary KIE is indicative of

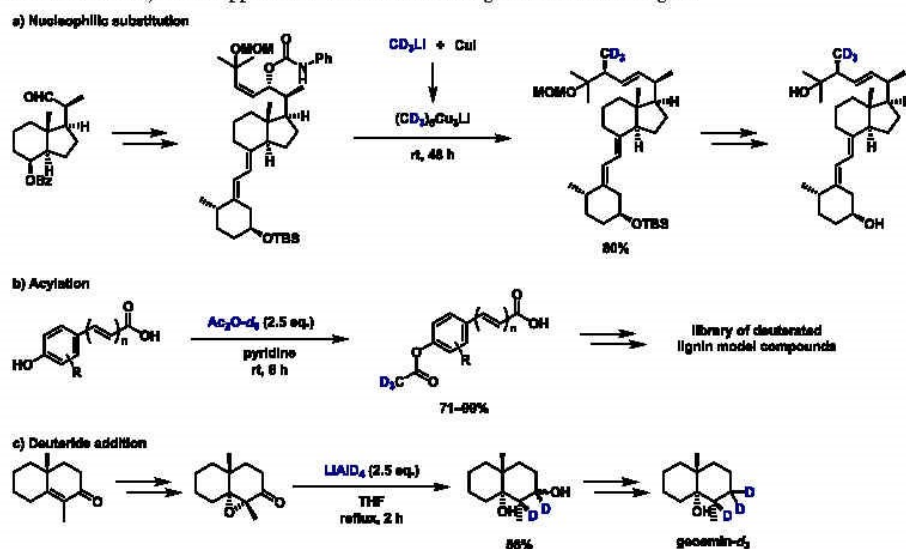
breaking/forming a bond to the isotope at the rate-limiting step, or subsequent product-determining step(s), but no clear proof.

5.1.2. Secondary Kinetic Isotopic Effect. A secondary KIE could result from reactions that bear D or H atoms in positions of the reactant that are not directly involved or formed in the reaction. A secondary KIE is generally much smaller than a primary KIE. Typically, values up to 1.4 or 0.7 (inverse) per deuterium atom are observed (Table 2, entry 13). Noteworthy, secondary kinetic isotope effects offer valuable information to understand the reaction mechanisms.

Scheme 148. Applications of Deuterated Analogues of Methyl Iodide



Scheme 149. Selected Synthetic Applications of Deuterated Analogues of Common Reagents

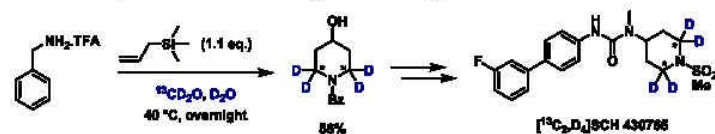


5.2. Drug Development

The introduction of radiolabels to drug molecules enables the direct tracing of these without substantially altering their chemical structure and physical properties compared with the unlabeled counterparts. Thus, both tritium and carbon-14 radioisotopologues are widely deployed diagnostics in clinical

studies. Generally, ^3H labeled drugs can be prepared more easily and quickly than their ^{14}C counterparts. In addition, the extremely high specific activity of 28.8 Ci/mmol of tritium makes it unique for labeling of pharmaceuticals, proteins, oligonucleotides, and antibodies as well as for early labeling strategies to support discovery purposes. Comprehensive literature reviews summarizing tritium incorporation in drug

Scheme 150. Double Labeled Piperidine Backbone Using a Mannich-Type Reaction



Scheme 151. Multistep Syntheses from Deuterated Building Blocks

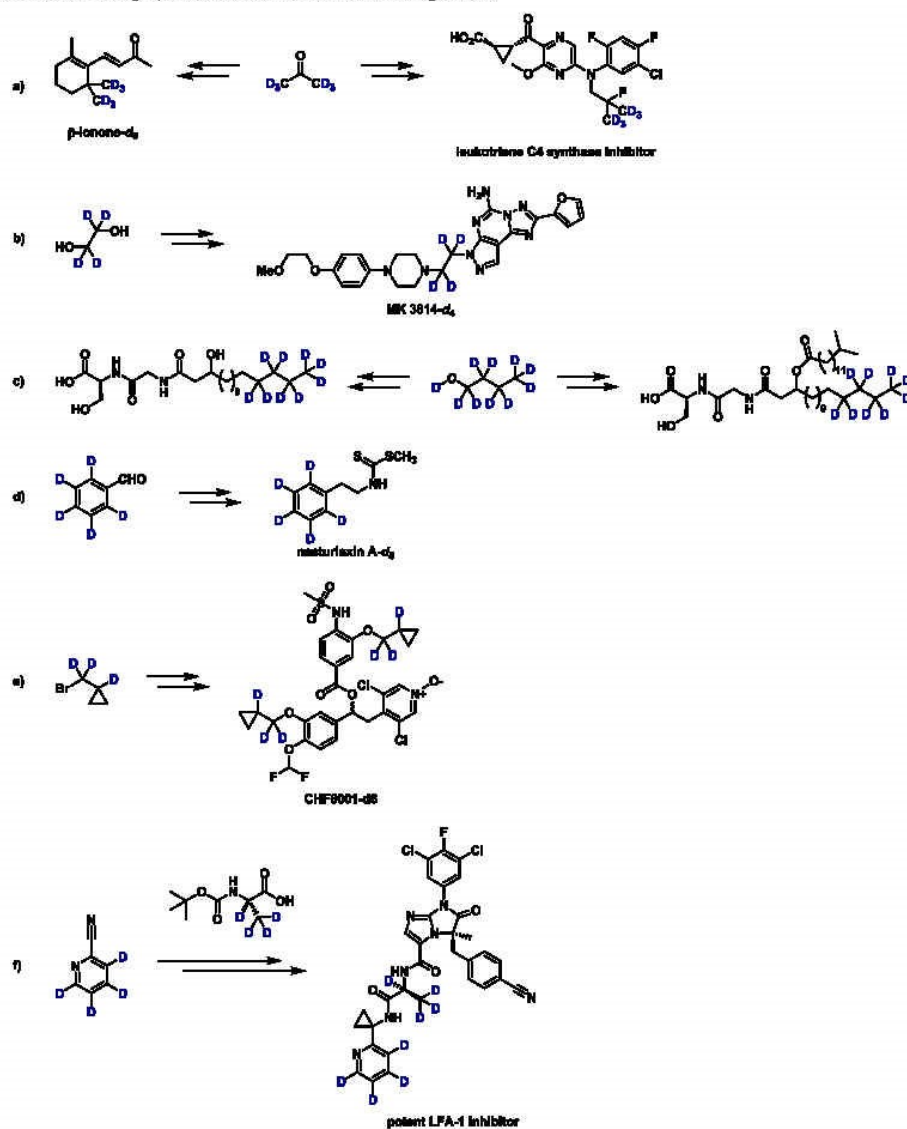


Table 2. Specific Examples of KIEs in Mechanistic Studies (Refs 386–399)

entry	authors	reaction	KIE value
1 ³⁸⁶	He and co-workers		Parallel reactions $k_H/k_D = 1.08$
2 ³⁸⁷	He and co-workers		Parallel reactions $k_H/k_D = 4.8$
			Intermolecular reactions $k_H/k_D = 5.1$
3 ³⁸⁸	Baudoin, Cramer and co-workers		Parallel kinetics $k_H/k_D = 1.8$
4 ³⁸⁹	Mei and co-workers		Parallel kinetics $k_H/k_D = 1.0$

6697

<https://doi.org/10.1021/acs.chemrev.1c00795>
 Chem. Rev. 2022, 122, 6634–6718

Table 2. continued

entry	authors	reaction	KIE value
5 ³⁹⁰	You and co-workers	<p>a-D₇ or a + b $\xrightarrow[\text{AgF, DMF, 60 } ^\circ\text{C}]{[\text{SCpRh}], \text{Ligand}}$ c-D₈ or c</p>	Parallel kinetics $k_{\text{H}}/k_{\text{D}} = 1.0$
		<p>a + b-D₁ or b $\xrightarrow[\text{AgF, DMF, 60 } ^\circ\text{C}]{[\text{SCpRh}], \text{Ligand}}$ c</p>	Parallel kinetics $k_{\text{H}}/k_{\text{D}} = 1.0$
		<p>a-D₇ or a + b-D₁ or b $\xrightarrow[\text{AgF, DMF, 60 } ^\circ\text{C}]{[\text{SCpRh}], \text{Ligand}}$ c</p>	Parallel kinetics $k_{\text{H}}/k_{\text{D}} = 1.1$
6 ³⁹¹	Nakao, Hartwig, and co-workers	<p>D₆-C₆H₅ + C₈H₁₇ $\xrightarrow[\text{Na(acac), Neat, 120 } ^\circ\text{C}]{[\text{Ligand-Ni}(\eta^5\text{-C}_6\text{H}_5)], \text{NaH}}$ C₈H₁₇-D</p>	Parallel kinetics $k_{\text{H}}/k_{\text{D}} = 1.3 \pm 0.1$
7 ³⁹²	Carreira and co-workers	<p>1a-D₃; X = D + 2a $\xrightarrow[\text{MeCN, 70 } ^\circ\text{C}]{\text{Pd(OAc)}_2, \text{PhI(OPiv)}_2, [\text{t-Bu}_4\text{N}]^+\text{I}^-}$ 2a</p> <p>10% yield 21% D-incorporation</p>	Intermolecular reactions $k_{\text{H}}/k_{\text{D}} = 3.3$
		<p>1a-D₁; X = D + 2a $\xrightarrow[\text{MeCN, 70 } ^\circ\text{C}]{\text{Pd(OAc)}_2, \text{PhI(OPiv)}_2, [\text{t-Bu}_4\text{N}]^+\text{I}^-}$ 2a</p>	Parallel reactions $k_{\text{H}}/k_{\text{D}} = 3.4$
8 ³⁹³	van Gemmeren and co-workers	<p>n-Bu-COOH-D₃ + TIPS-alkene $\xrightarrow[\text{Ag}_2\text{O, LiHFIP, HFIP, 60 } ^\circ\text{C}]{\text{Pd(OAc)}_2, \text{Ligand}}$ n-Bu-COOH-D₃</p>	Parallel kinetics $k_{\text{H}}/k_{\text{D}} = 3.5$ Intermolecular reactions $k_{\text{H}}/k_{\text{D}} = 6.0$

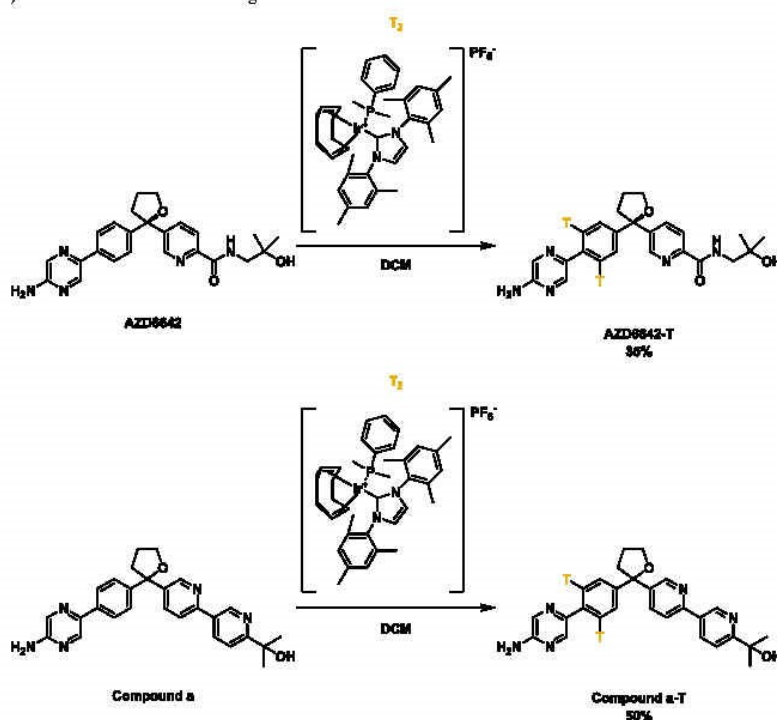
Table 2. continued

entry	authors	reaction	KIE value
9 ¹⁹⁴	Rovis and co-workers		Intermolecular reactions $k_H/k_D = 1.9$
			Intramolecular reactions $k_H/k_D = 2.6$
10 ¹⁹⁵	Duan and co-workers		Parallel kinetics $k_H/k_D = 6.0$
11 ¹⁹⁶	Zhu and co-workers		Intramolecular reactions $k_H/k_D = 3.38$
			Intermolecular reactions $k_H/k_D = 1.33$
12 ¹⁹⁷	Young and co-workers		Intermolecular reactions $k_H/k_D = 3.2$
13 ¹⁹⁸	Cheong, Altman and co-workers		Parallel kinetics $k_H/k_D = 1.0$
			Secondary KIE $k_H/k_D = 1.3$
14 ¹⁹⁹	Zhu and co-workers		$[Fe(A)]$ cat. $k_H/k_D = 4.0$ $[Fe(B)]$ cat. $k_H/k_D = 3.8$

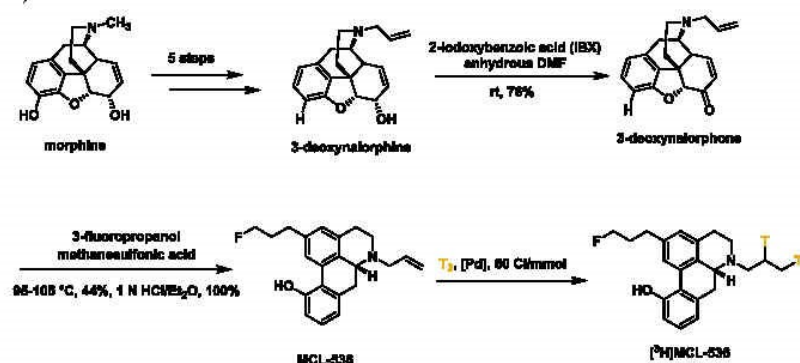
development have been published, and therefore, only the recent results will be briefly explained in the following.⁴⁰⁰

As shown in Scheme 152, a tritiated radioligand was prepared by Artelsmair and co-workers.⁴⁰¹ First, the indole moiety of precursor **a** was iodinated using N-iodosuccinimide (NIS) and

Scheme 152. Synthesis of a Tritiated Radioligand



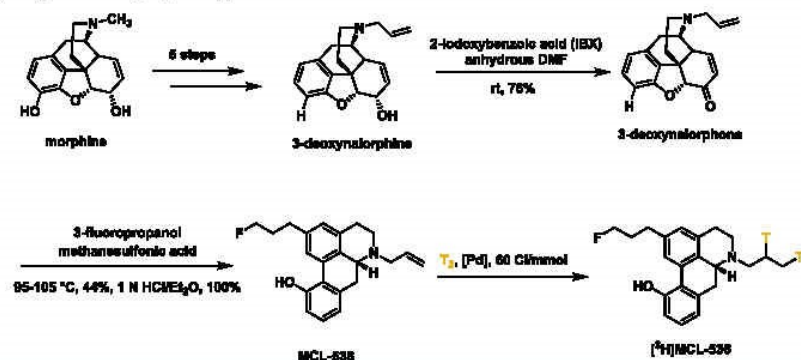
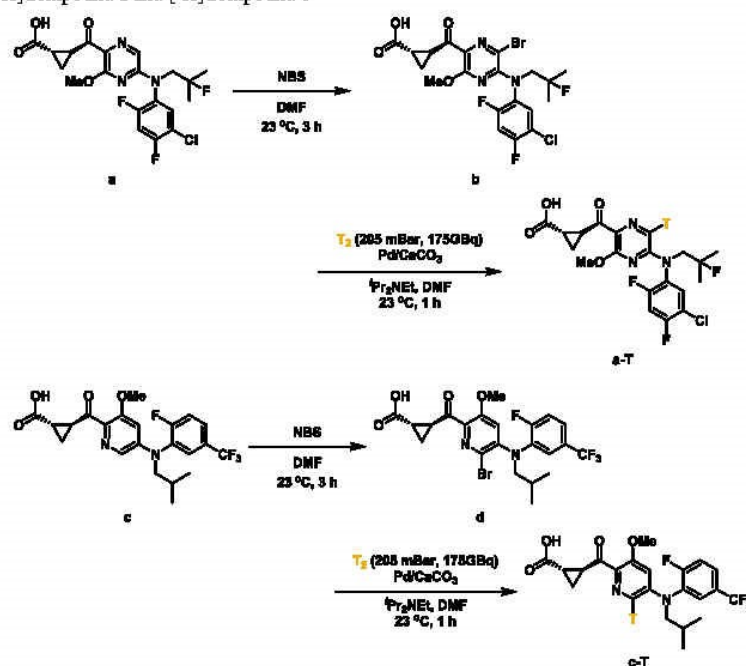
Scheme 153. Synthesis of Tritiated FLAP Inhibitors



TEA in DCM, yielding compound b. Subsequent hydrogenation utilizing tritium gas at low pressure (approximately 50 mbar) provided in short times (15 min and 1 h) the tritium-labeled product c without affecting the olefinic double bond. The product was employed for *in vitro* autoradiography (ARG) studies on fresh frozen human brain slices to establish whether specific binding takes place in Parkinson's disease (PD) tissue.

Leukotrienes are mediators of cellular inflammation, and their overproduction is a major cause of inflammation in asthma and

allergic rhinitis. In this regard, 5-lipoxygenase-activating protein (FLAP) is involved in the conversion of arachidonic acid (AA) to 5-hydroperoxyeicosatetraenoic acid and subsequently to leukotriene. Thus, inhibitors of FLAP should block the production of leukotrienes. As a recent example, AZD6642 and a related derivative show good properties as 5-lipoxygenase-activating protein (FLAP) inhibitors. Consequently, the tritiated analogues were prepared using a specific iridium phosphine carbene catalyst in the presence of tritium to further

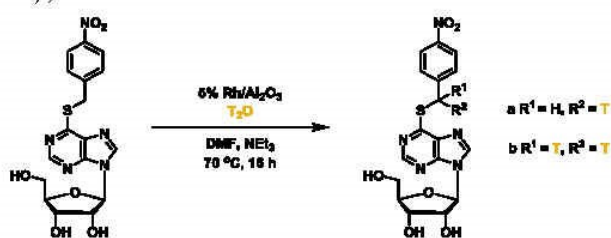
Scheme 154. Preparation of [^3H]MCL-536Scheme 155. [^3H]Compound a and [^3H]Compound c

understand drug metabolism and pharmacokinetic properties (Scheme 153).⁴⁰²

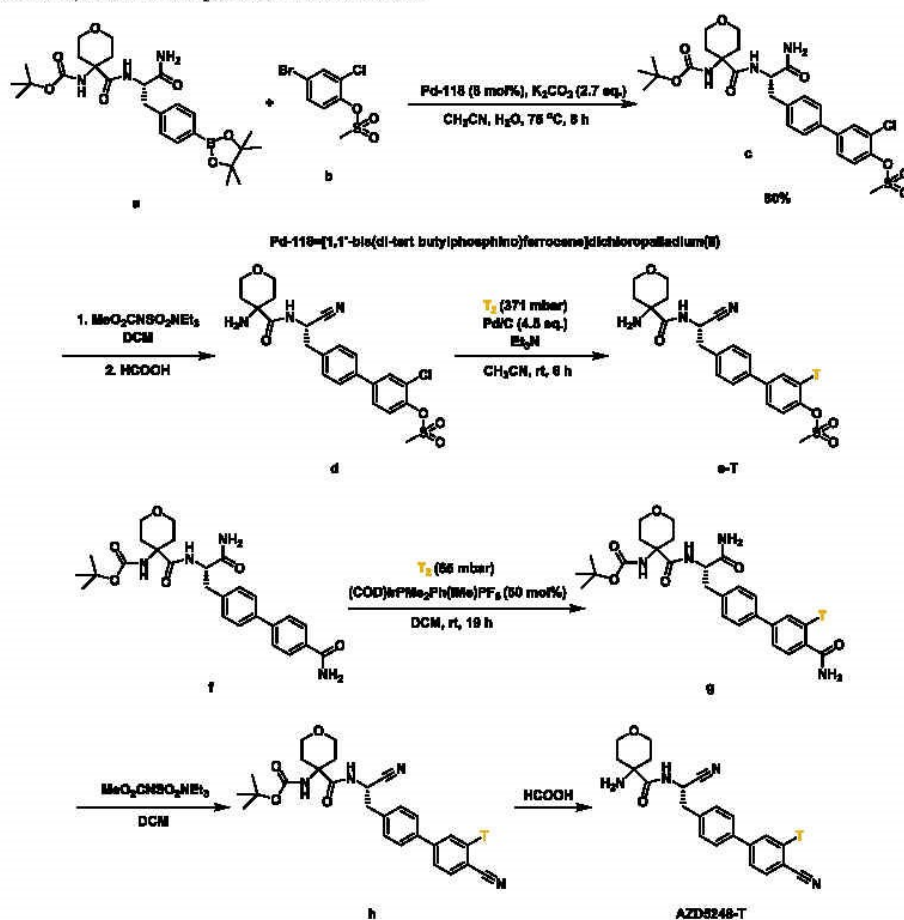
Dopamine receptors, especially those in the D2 family, play a significant role in a variety of disorders involving the central nervous system including Parkinson's disease (PD), restless leg syndrome (RLS), Huntington's chorea, multiple system atrophy (MSA), and so on. As an example, for small molecules which bind with high affinity to these receptors, Subburaju and co-workers developed tritium incorporated MCL-536 which helps to quantify D2 high sites in schizophrenia and PD patients *in vivo* (Scheme 154).⁴⁰³

As a leukotriene, leukotriene C4 (LTC4) has been widely studied in the context of allergy and asthma. It is expected that an enhanced efficacy profile can be gained by hindering the production of LTC4. In this context, a radioactive labeled LTC4S inhibitor is required for developing a leukotriene C4 synthase inhibitor. Later, two tritium labeled ($[^3\text{H}]$ Compound a and [^3H]Compound c) LTC4 inhibitors were prepared from unlabeled analogues a and c by Elmore and co-workers for *in vitro* studies.⁴⁰⁴ First, unlabeled substrates were brominated with *N*-bromosuccinimide (NBS) in DMF to give b and d, respectively (Scheme 155). Subsequent Pd-mediated reduction

Scheme 156. S-(4-Nitrobenzyl)-6-thioinosine-T



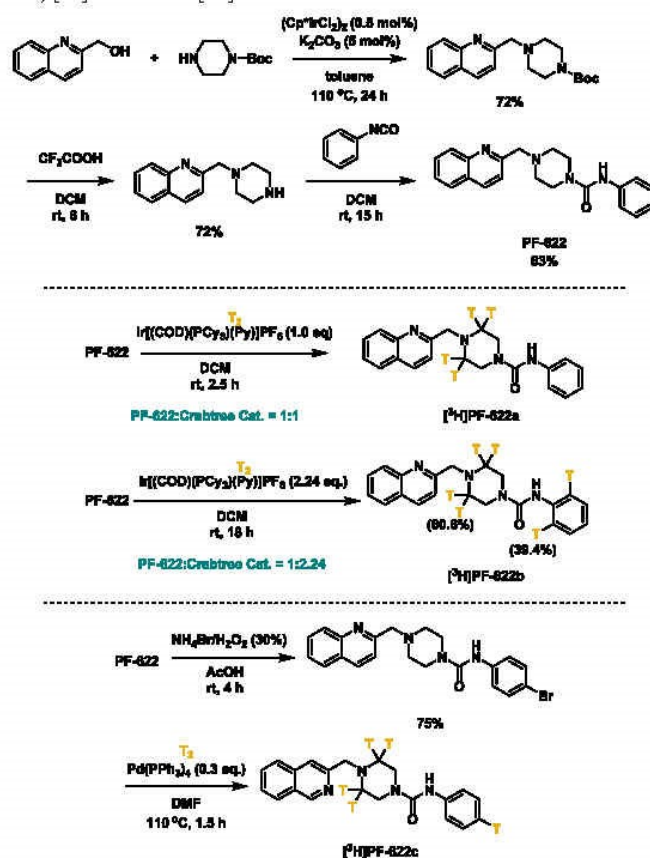
Scheme 157. Synthesis of Compound e-T and AZD5248-T



(stoichiometric in Pd) of the aryl bromides with T₂ afforded the T-labeled compounds [³H]-a and [³H]-c.

Nucleosides continue to be important biological targets. Recent studies discovered that their function could be disrupted by xenobiotics like colchicine and cytochalasin B as well as nucleoside analogues. As an example of the latter compounds,

purine S-(4-nitrobenzyl)-6-thioinosine was identified as a potent transport blocker of nucleosides. More specifically, Filer and Byon reported that [benzyl methylene-³H]S-(4-nitrobenzyl)-6-thioinosine (Scheme 156) has been tritiated to identify the nucleoside transport sites.⁴⁰⁵

Scheme 158. [^3H]PF-622a, [^3H]PF-622b and [^3H]PF-622c

Cathepsin C (CatC), also known as dipeptidyl peptidase I (DPP I), is a lysosomal exocysteine protease that is important for intracellular protein degradation. It functions in the activation of many serine proteases in immune/inflammatory cells. CatC plays a crucial role in the activation of these serine proteases and support the therapeutic strategy of targeting CatC inhibition in inflammatory diseases. In order to develop a highly potent and selective CatC C inhibitor, Bragg and co-workers prepared tritium labeled materials [^3H]compound e and [^3H]AZDS248 (Scheme 157) for preclinical drug metabolism and disposition studies.⁴⁰⁶

Fatty acid amide hydrolase (FAAH) is a member of the serine hydrolase family of enzymes, which degrades the endocannabinoid anandamide. Studies in cells and animals and genetic studies in humans have shown that inhibiting FAAH may be a useful strategy to treat pain, inflammation, and other central nervous system disorders. In this context, *N*-phenyl-4-(quinolin-2-ylmethyl)piperazine-1-carboxamide (PF-622) was developed as an example of FAAH inhibitors. In order to make a comprehensive characterization of the mechanism of inhibition and selectivity of PF-622, three tritium-labeled PF-622 analogues were prepared from PF-622 using the Ir-based

Crabtree catalyst or simply $\text{Pd}(\text{PPh}_3)_4$ under tritium gas atmosphere (Scheme 158).⁴⁰⁷

Bioanalytical tools that allow the identification of drug metabolites hold a great potential to discover new drugs and guide the selection of clinical candidates. In this aspect, isotopes of active drugs are commonly prepared to understand their metabolism and to identify and quantify specific metabolites. Specifically, cytochromes P450 are important enzymes for the metabolism and clearance of many chemical compounds by catalytic oxidations including C–H bond cleavage reactions. In addition, C–X cleavage (e.g., C, N, O, S-dealkylation) processes are also well-known to be catalyzed by this class of proteins. Thus, CYP450-mediated transformations offer many opportunities for the application of KIE strategies. Pioneering work in this area on *N*-demethylation reactions appeared already in 1961.⁴⁰⁸ Since then, in many cases, it has been possible to modulate the *in vivo* metabolism or toxicity of chemicals by using deuterated analogues.

Following the statement of the Nobel Laureate James Black: “The most fruitful basis for the discovery of a new drug is to start with an old drug”,⁴⁰⁹ several pharmaceutical companies are currently interested to improve the properties of approved drugs

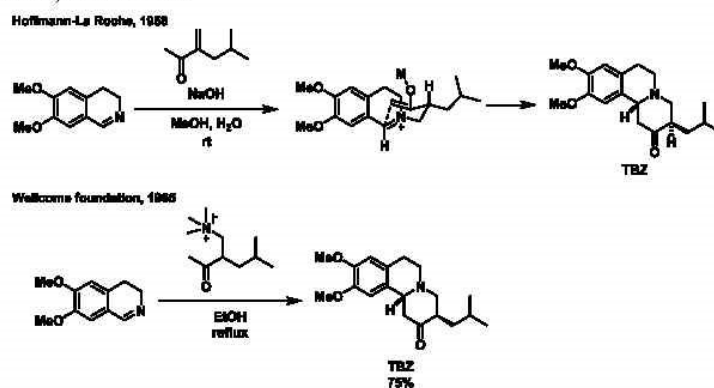
Table 3. Selected Deuterated Drugs and Compounds in Clinical Development

entry	compound name	structure	indication	status
1	Austedo (Deutetrabenazine)		Chorea associated with Huntington disease	Approved
2	AVP-786		Major depressive disorder	Phase 3
3	Donafenib		Differentiated thyroid cancer	Phase 3
4	RT001		Infantile neuroaxonal dystrophy	Phase 3
5	CTP-543		Hair loss (alopecia areata)	Phase 2
6	BMS-986165		Psoriasis	Phase 3
7	CTP-656		Cystic fibrosis	Phase 2
8	ALK-001		Stargardt disease	Phase 2
9	HC-1119		Metastatic castration-resistant prostate cancer	Phase 2
10	VX-984		Solid tumors	Phase 1
11	DRX-065		Non-alcoholic steatohepatitis/adrenoleukodystrophy	Phase 1

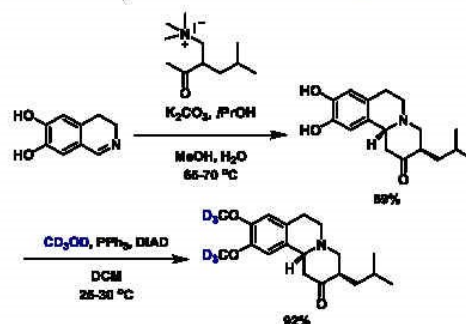
Table 3. continued

entry	compound name	structure	indication	status
12	SD-254		Major depressive disorder	Phase 1
13	CTP-347		Menopause, hot flashes, and vasomotor symptoms	Phase 1
14	CTP-499		Non-dialysis patients associated with moderate chronic kidney disease	Phase 1

Scheme 159. Classical Syntheses of TBZ



by producing “new” labeled drugs with more desirable properties. In fact, specifically deuterated drugs may have the following advantages compared with the original protonated ones: (1) reduced metabolism rates and extended half-life of active compounds; (2) reduced drug dosing; (3) minimization of the formation of potentially toxic metabolites. Notably in 2017, the FDA approved the first deuterated drug, Austedo, for the treatment of Huntington’s disease-related disorders and tardive dyskinesia.³⁴ As a result of the success of Austedo (Table 3, entry 1), several other deuterated drugs are now in clinical phases for various indications (Table 3). Most deuterated derivatives are prepared with D-substitutions on methyl or methylene groups. C–D bonds on those positions are much more resistant toward oxidative degradation processes. For example, tetrabenazine (TBZ) was first approved in 2008, to treat chorea associated with Huntington’s disease (Scheme 159).^{4,10} O-Demethylation is a key step of tetrabenazine metabolism catalyzed by cytochrome 2D6 (CYP2D6). In deutetetrabenazine (Scheme 160), the stronger C–D bond, which attenuates the rate-determining O-demethylation reaction, increases the terminal elimination half-life (Table 3, entry 1).

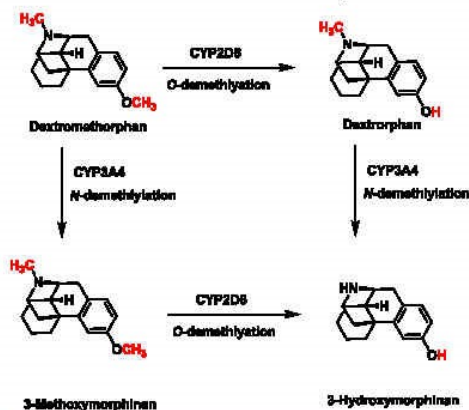
Scheme 160. Synthesis of Deutetetrabenazine^{4f}

^aDIAD: diisopropyl azodicarboxylate.

A similar strategy led to the development AVP-786 (dextromethorphan-*d*₆ + quinidine) for the treatment of agitation in patients with dementia or Alzheimer’s disease.^{4,11} Dextromethorphan was initially developed by E. Hoffman-La Roche

in 1954 as an antitussive agent. Nowadays, it is a common ingredient of more than 125 commercial cough and cold remedies. Both *O*- and *N*-demethylation are key pathways to generate active metabolites. The deuterium analogue AVP-786 showed significant potential for registration trials sufficient for regulatory submission/approval (Scheme 161 and Table 3, entry 2).

Scheme 161. Metabolism of Dextromethorphan



As shown in Table 3, at present four deuterated compounds AVP-786, RT001, Donafenib, and BMS-98616S are considered for regulatory submission/approval. In addition, ALK-001 and HC-1119 have reached phase 3 clinical trials. The increasing number of clinical trials using deuterated drug analogues (Table 3, entries 10–14) clearly indicates the strong interest of the pharmaceutical industry in this area.^{4,12}

Deuterium labeling in vaccine development has been used for other applications, too. In 2020, Janda and co-workers reported a potential vaccine against heroin addiction. To prepare the vaccine, they used a heroin-mimicking molecule in which they replaced several hydrogen atoms with deuterium and found that the new vaccine was significantly improved as shown from titer, affinity, specificity, and behavioral models including antinociception and drug biodistribution (Figure 9).^{4,13}

6. CONCLUSIONS AND OUTLOOK

In the past decade, the strong interest on various aspects regarding the synthesis of isotopically labeled organic molecules has continued. In this respect, both deuteration and tritiation reactions constitute key tools for many basic academic studies as

well as applications, particularly in the life sciences. Thus, in the past 5 years, which is the focus of this Review, many new deuterated and tritiated (complex) molecules have been prepared by well-defined molecular catalysts as well as traditional stoichiometric reactions. While advancements in homogeneous catalysis and organometallic chemistry significantly enriched the repertoire of labeling methodologies in the past, more recently photocatalysis and electrocatalysis are becoming more and more popular for specific applications.

Apart from photocatalysis, electrocatalysis, and organometallic catalysis, so-called nanomaterials are becoming attractive for labeling reactions. In fact, the use of nanostructured materials based on noble and non-noble metals is an exciting area of research for isotope exchange reactions. Compared with their bulk counterparts, supported metal nanoparticles display a large surface-to-volume ratio and can be more active. Interestingly, selective incorporation of deuterium/tritium atoms has been observed for many substrates including pharmaceuticals, although the reasons for these effects are often not fully understood. Nevertheless, the number of publications in this area increases each year, and many recent discoveries have been incorporated into the chemists' toolkit for isotope labeling.

While in the past, the clear focus in this field was on the selective and efficient labeling of pharmaceutically relevant molecules on small scale, recently there is also a growing interest in scalable methods for deuteration. Indeed, a handful of deuterated compounds have already entered the clinic, and in 2017, the FDA approved the first deuterated drug, Austedo, for the treatment of Huntington's disease-related disorders. Due to this launch of deuterated compounds as active drug ingredients, there is an increasing interest in reliable and robust methodologies, which permit large-scale deuterium labeling in industrial settings. In this respect, also the source of deuterium becomes more significant, and the use of D₂O should be preferred.

Although deuteration and tritiation have become well-established methodologies in chemistry, still this field offers interesting potential for innovations (e.g., with respect to catalysts). Most of the homogeneous catalytic systems described above suffer from the high metal price and sophisticated ligands, and in some cases, they are environmentally less acceptable. For example, Ir-based Crabtree and Kerr catalysts along with Ru catalysts are mainly used for C(sp²)-H HIE reactions using D₂ and T₂ gas. Similarly in heterogeneous catalysis, supported Pd, Pt, Ru, and Ir materials are commonly used to catalyze multi H/D exchange of arenes and heterocyclic amines. Unfortunately, the tolerance of these catalysts toward easily reducible functional groups and halogens as well as the selectivity is still challenging. While most academic work concentrates on selectivity aspects, for many applications, the

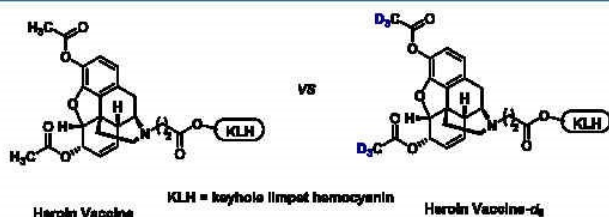


Figure 9. Comparison of heroin and heroin-d₅ vaccines.

efficiency of the process can be more important. To be clear, for a given application often >95% deuteration at the desired position of the compound are mandatory. However, for some drug applications, the synthesis of complex tritiated molecules with a high specific activity (beyond 50 Ci/mmol/1) is required. Thus, there is a growing trend that "design for quality" needs to be considered in the development of new labeling methods.

So far, isotope exchange reactions of C(sp³)-H positions have been primarily developed. In contrast, catalytic systems for the direct and selective HIE of C(sp³)-H sites under mild conditions are still limited. As most of the top-selling commercial drugs contain at least one alkyl moiety, the development of effective HIE reactions targeting C(sp³)-H bonds offers alternative approaches for the isotopic labeling of bioactive molecules. Here, strategies of directed remote functionalization or the use of transient directing groups might help to establish more general protocols.

Last but not least, the importance of labeling methodologies to enable innovations in other areas of chemistry should not be underestimated. For example, HIE reactions of C-H bonds constitute a great source of inspiration for "designing" all kinds of novel C-H functionalization reactions. In addition, the use of labeled ligands and catalysts offers possibilities to better understand catalytic phenomena and study catalysts from cradle to grave. While surface metal hydrides play a crucial role in heterogeneous catalysis including many industrial processes, the behavior of the corresponding isotopes is far less investigated.

AUTHOR INFORMATION

Corresponding Author

Matthias Beller – *Leibniz-Institut für Katalyse e. V., 18059 Rostock, Germany*; orcid.org/0000-0001-5709-0965;
Email: matthias.beller@catalysis.de

Authors

Sara Kopf – *Leibniz-Institut für Katalyse e. V., 18059 Rostock, Germany*; orcid.org/0000-0002-6395-9396

Florian Bourriquet – *Leibniz-Institut für Katalyse e. V., 18059 Rostock, Germany*; orcid.org/0000-0002-3895-7321

Wu Li – *Leibniz-Institut für Katalyse e. V., 18059 Rostock, Germany*; orcid.org/0000-0001-7102-4630

Helfried Neumann – *Leibniz-Institut für Katalyse e. V., 18059 Rostock, Germany*

Kathrin Junge – *Leibniz-Institut für Katalyse e. V., 18059 Rostock, Germany*; orcid.org/0000-0001-7044-8888

Complete contact information is available at:
<https://pubs.acs.org/10.1021/acs.chemrev.1c00795>

Author Contributions

[†]S.K. and F.B. contributed equally to this work.

Funding

We acknowledge the support from the European Union (Flow Chemistry for Isotope Exchange, FLIX, 862179), the BMBF and the State of Mecklenburg-Western Pomerania. Open access funding enabled and organized by Projekt DEAL.

Notes

The authors declare no competing financial interest.

Biographies

Sara Kopf studied chemistry at the University of Heidelberg, Germany and the University of Cambridge, U.K. She carried out her master's

thesis at Boehringer Ingelheim, Biberach, Germany, looking into the applicability of phosphorus-containing functional groups as bioisosteres in medicinal chemistry. Sara moved on to develop a photochemical bioconjugation reaction in the group of Prof. Paolo Melchiorre at ICIQ, Tarragona, Spain, for one year before joining the group of Prof. Matthias Beller at LIKAT, Rostock, Germany as a Ph.D. student in April 2020. Since then, she has been working on the development of new methodologies for hydrogen isotope exchange.

Florian Bourriquet, born in 1995 in Paris, France, studied chemistry at the University of Rennes 1. After a stay at F. Hoffmann-La Roche, Basel, Switzerland in 2018 focused on cross-coupling reactions, he conducted his master's thesis in 2019 at Sanofi, Vitry-sur-Seine, France, developing potential drug candidates. In 2020, he joined the group of Prof. Matthias Beller at the Leibniz-Institute for Catalysis, Germany. His research interests include the development of new methodologies for non-noble metals catalyzed hydrogen/deuterium exchange reactions.

Wu Li was born in 1986 in Anhui, China. He received his Ph.D. degree in 2015 from Wuhan University under the supervision of Prof. Aiwen Lei. In 2016, he joined Prof. Matthias Beller's group at the Leibniz Institute for Catalysis (Germany) as a postdoctoral fellow. His research interests focus on the development of nanometal catalysts for isotopic labeling reaction.

Dr. Helfried Neumann finished his Ph.D. studies in 1995 at the University Erlangen under the supervision of Rainer Herges and Paul Rague von Schleyer. In 1996, he joined the Institute of Organic Catalysis in Rostock (IfOK, which was later renamed to Leibniz-Institut für Katalyse e.V.) and has been project leader since 1998. His current research activities are concerned with carbonylation reactions, "hydrogen-borrowing" concept, perfluoroalkylation of arenes, and the development of new ligands.

Kathrin Junge, born in 1967 in northern Germany, received her Ph.D. degree in Chemistry from the University of Rostock in 1997 working with Prof. E. Popowski. After a postdoctoral appointment position in the Max-Planck group of Uwe Rosenthal, she joined the group led by Matthias Beller in 2000. Since 2008 she has been the group leader for "Sustainable redox reactions" at LIKAT. She has been involved for years in catalysis research, where she has developed efficient catalytic hydrogenations for carboxylic acid derivatives and designed several new ligands, especially for hydrogenation reactions. Her current main interest is the development of environmentally benign and efficient homogeneous and heterogeneous catalytic reactions based on inexpensive, nonprecious metals. Her scientific work has been published in >230 papers in top scientific journals (e.g., *Nature Chemistry*, *Nature Communications*, *Science Advances*), and she has written 6 book chapters. She has 15 562 citations and a 70 h-index. Since 2017, she has been Co-editor of the *Journal of Catalysis*.

Matthias Beller, born in Gudensberg (Germany) in 1962, obtained his Ph.D. in 1989 working with Lutz F. Tietze at the University of Göttingen. After one year of postdoctoral research with Barry Sharpless at MIT (U.S.A.), from 1991 to 1995 he worked at Hoechst AG in Frankfurt. Then, he started his academic career at TU Munich. In 1998, he relocated to Rostock to head the Leibniz-Institute for Catalysis. Matthias Beller is also Vice-president of the Leibniz Association and a member of three German Academies of Sciences including the German National Academia "Leopoldina". The research of his group has been published in more than 1050 original articles and reviews and focused on applying homogeneous and heterogeneous catalysis for the sustainable synthesis of fine/bulk chemicals as well as energy technologies.

REFERENCES

- (1) Urey, H. C.; Brickwedde, F. G.; Murphy, G. M. A Hydrogen Isotope of Mass 2 and Its Concentration. *Phys. Rev.* **1932**, *40*, 1–15.
- (2) Friedman, I. Deuterium Content of Natural Waters and Other Substances. *Geochim. Cosmochim. Acta* **1953**, *4*, 89–103.
- (3) Schiegl, W. E.; Vogel, J. C. Deuterium Content of Organic Matter. *Earth Planet. Sci. Lett.* **1970**, *7*, 307–313.
- (4) Rosman, K. J. R.; Taylor, P. D. P. Isotopic Compositions of the Elements 1997 (Technical Report). *Pure Appl. Chem.* **1998**, *70*, 217–235.
- (5) Wiberg, K. B. The Deuterium Isotope Effect. *Chem. Rev.* **1955**, *55*, 713–743.
- (6) Tayar, N. E.; van de Waterbeemd, H.; Gryllaki, M.; Testa, B.; Trager, W. F. The Lipophilicity of Deuterium Atoms. A Comparison of Shake-Flask and HPLC Methods. *Int. J. Pharm.* **1984**, *19*, 271–281.
- (7) Perrin, C. L.; Dong, Y. Secondary Deuterium Isotope Effects on the Acidity of Carboxylic Acids and Phenols. *J. Am. Chem. Soc.* **2007**, *129*, 4490–4497.
- (8) Perrin, C. L.; Ohta, B. K.; Kuperman, J.; Liberman, J.; Erdelyi, M. Stereochemistry of β -Deuterium Isotope Effects on Amine Basicity. *J. Am. Chem. Soc.* **2005**, *127*, 9641–9647.
- (9) Timmins, G. S. Deuterated Drugs: Updates and Obviousness Analysis. *Expert Opin. Ther. Pat.* **2017**, *27*, 1353–1361.
- (10) Katsnelson, A. Heavy Drugs Draw Heavy Interest from Pharma Backers. *Nat. Med.* **2013**, *19*, 656.
- (11) Pirali, T.; Serafini, M.; Cargnin, S.; Genazzani, A. A. Applications of Deuterium in Medicinal Chemistry. *J. Med. Chem.* **2019**, *62*, S276–S297.
- (12) Gant, T. G. Using Deuterium in Drug Discovery: Leaving the Label in the Drug. *J. Med. Chem.* **2014**, *57*, 3595–3611.
- (13) Atzrodt, J.; Derdau, V. Pd- and Pt-Catalyzed H/D Exchange Methods and Their Application for Internal MS Standard Preparation from a Sanofi-Aventis Perspective. *J. Labelled Compd. Radiopharm.* **2010**, *53*, 674–685.
- (14) Nakanishi, A.; Fukushima, Y.; Miyazawa, N.; Yoshikawa, K.; Maeda, T.; Kurobayashi, Y. Quantitation of Rotundone in Grapefruit (*Citrus Paradisi*) Peel and Juice by Stable Isotope Dilution Assay. *J. Agric. Food Chem.* **2017**, *65*, S026–S033.
- (15) Chace, D. H.; Litt, T.; Hansen, C. R.; Adam, B. W.; Hannon, W. H. Quantification of Malonylcarnitine in Dried Blood Spots by Use of MS/MS Varies by Stable Isotope Internal Standard Composition. *Clin. Chim. Acta* **2009**, *402*, 14–18.
- (16) Konermann, L.; Pan, J.; Liu, Y.-H. Hydrogen Exchange Mass Spectrometry for Studying Protein Structure and Dynamics. *Chem. Soc. Rev.* **2011**, *40*, 1224–1234.
- (17) Lavold, T.; Zubarev, R.; Astorga-Wells, J. Hydrogen-Deuterium Exchange Mass Spectrometry in Drug Discovery - Theory, Practice and Future. In *Applied Biophysics for Drug Discovery*; Huddler, D., Zartler, E. R., Eds.; John Wiley & Sons, Inc.: 2017. DOI: 10.1002/9781119099512.ch4.
- (18) Simmons, E. M.; Hartwig, J. F. On the Interpretation of Deuterium Kinetic Isotope Effects in C-H Bond Functionalizations by Transition-Metal Complexes. *Angew. Chem., Int. Ed.* **2012**, *51*, 3066–3072.
- (19) Bae, H. J.; Kim, J. S.; Yakubovich, A.; Jeong, J.; Park, S.; Chwae, J.; Ishibe, S.; Jung, Y.; Rai, V. K.; Son, W.-J.; et al. Protecting Benzylic C-H Bonds by Deuteration Doubles the Operational Lifetime of Deep-Blue Ir-Phenylimidazole Dopants in Phosphorescent OLEDs. *Adv. Opt. Mater.* **2021**, *9*, 2100630.
- (20) Liu, X.; Chan, C.-Y.; Mathevet, F.; Mamada, M.; Tsuchiya, Y.; Lee, Y.-T.; Nakanotani, H.; Kobayashi, S.; Shiochi, M.; Adachi, C. Isotope Effect of Host Material on Device Stability of Thermally Activated Delayed Fluorescence Organic Light-Emitting Diodes. *Small Sci.* **2021**, *1*, 2000057.
- (21) Abe, T.; Miyazawa, A.; Konno, H.; Kawanishi, Y. Deuteration Isotope Effect on Nonradiative Transition of fac-tris (2-Phenylpyridinato) Iridium (III) Complexes. *Chem. Phys. Lett.* **2010**, *491*, 199–202.
- (22) Wang, P.; Wang, F.-F.; Chen, Y.; Niu, Q.; Lu, L.; Wang, H.-M.; Gao, X.-C.; Wei, B.; Wu, H.-W.; Cai, X.; et al. Synthesis of All-deuterated tris(2-Phenylpyridine)iridium for Highly Stable Electrophosphorescence: the "Deuterium Effect". *J. Mater. Chem. C* **2013**, *1*, 4821–4825.
- (23) Huang, T.; Zhang, D.; Zhan, G.; Wang, Q.; Li, G.; Hong, X.; Liu, Z.; Duan, L. Boosting the Efficiency and Stability of Blue TADF Emitters by Deuteration. *ChemRxiv*, Aug. 19, 2021, version 1.13312484. This content is a preprint and has not been peer-reviewed.
- (24) Grimm, J. B.; Xie, L.; Casler, J. C.; Patel, R.; Tkachuk, A. N.; Falco, N.; Choi, H.; Lippincott-Schwartz, J.; Brown, T. A.; Glick, B. S.; et al. A General Method to Improve Fluorophores Using Deuterated Auxochromes. *JACS Au* **2021**, *1*, 690–696.
- (25) Lucas, L. J.; Unterwieser, M. P. Comprehensive Review and Critical Evaluation of the Half-Life of Tritium. *J. Res. Nat. Inst. Stand. Technol.* **2000**, *105*, S41–S49.
- (26) Grosse, A. V.; Johnston, W. M.; Wolfgang, R. L.; Libby, W. F. Tritium in Nature. *Science* **1951**, *113*, 1–2.
- (27) Oliphant, M. L.; Harteck, P.; Rutherford. Transmutation Effects Observed with Heavy Hydrogen. *Nature* **1934**, *133*, 413–413.
- (28) Okada, S.; Momoshima, N. Overview of Tritium: Characteristics, Sources, and Problems. *Health Phys.* **1993**, *65*, S95–S09.
- (29) U.S. Department of Energy (DOE). DOE-HDBK-1129-2007, Tritium Handling and Safe Storage; DOE, March 4 2007.
- (30) Health Physics Society. Tritium Fact Sheet - January 2020. See the following: https://hps.org/documents/tritium_fact_sheet.pdf.
- (31) Lockley, W.; McEwen, A.; Cooke, R. Tritium: A Coming of Age for Drug Discovery and Development ADME Studies. *J. Labelled Compd. Radiopharm.* **2012**, *55*, 235–257.
- (32) Atzrodt, J.; Derdau, V.; Kerr, W. J.; Reid, M. Deuterium- and Tritium-Labelled Compounds: Applications in the Life Sciences. *Angew. Chem., Int. Ed.* **2018**, *57*, 1758–1784.
- (33) DeWitt, S. H.; Maryanoff, B. E. Deuterated Drug Molecules: Focus on FDA-Approved Deutetrabenazine: Published as Part of the Biochemistry Series "Biochemistry to Bedside". *Biochemistry* **2018**, *57*, 472–473.
- (34) Schmidt, C. First Deuterated Drug Approved. *Nat. Biotechnol.* **2017**, *35*, 493–494.
- (35) Atzrodt, J.; Derdau, V.; Kerr, W. J.; Reid, M. C-H Functionalisation for Hydrogen Isotope Exchange. *Angew. Chem., Int. Ed.* **2018**, *57*, 3022–3047.
- (36) Junk, T.; Catallo, J. W. Hydrogen Isotope Exchange Reactions Involving C-H (D, T) Bonds. *Chem. Soc. Rev.* **1997**, *26*, 401–406.
- (37) Lockley, W. J. S.; Heys, J. R. Metal-Catalysed Hydrogen Isotope Exchange Labelling: A Brief Overview. *J. Labelled Compd. Radiopharm.* **2010**, *53*, 635–644.
- (38) Atzrodt, J.; Derdau, V.; Fey, T.; Zimmermann, J. The Renaissance of H/D Exchange. *Angew. Chem., Int. Ed.* **2007**, *46*, 7744–7765.
- (39) Kang, Q.-K.; Shi, H. Catalytic Hydrogen Isotope Exchange Reactions in Late-Stage Functionalization. *Synlett* **2021**, *32*, A–J.
- (40) Zhou, R.; Ma, L.; Yang, X.; Cao, J. Recent Advances in Visible-light Photocatalytic Deuteration Reactions. *Org. Chem. Front.* **2021**, *8*, 426–244.
- (41) Leprom, M.; Daniel-Bertrand, M.; Mencia, G.; Chaudret, B.; Feuillastre, S.; Pieters, G. Nanocatalyzed Hydrogen Isotope Exchange. *Acc. Chem. Res.* **2021**, *54*, 1465–1480.
- (42) Steverlynck, J.; Sitdikov, R.; Rueping, M. The Deuterated "Magic Methyl" Group - A Guide for Site-Selective Trideuteromethyl Incorporation and Labeling using CD₃-Reagents. *Chem.—Eur. J.* **2021**, *27*, 11751–11772.
- (43) Sun, Q.; Soule, J.-F. Broadening of Horizons in the Synthesis of CD₃-Labeled Molecules. *Chem. Soc. Rev.* **2021**, *50*, 10806–10835.
- (44) Vang, Z. P.; Hintzsche, S. J.; Clark, J. R. Catalytic Transfer Deuteration and Hydrodeuteration: Emerging Techniques to Selectively Transform Alkenes and Alkynes to Deuterated Alkanes. *Chem.—Eur. J.* **2021**, *27*, 9988–10000.
- (45) Yang, H.; Hesk, D. Base Metal-Catalyzed Hydrogen Isotope Exchange. *J. Labelled Compd. Radiopharm.* **2020**, *63*, 296–307.

- (46) Sattler, A. Hydrogen/Deuterium (H/D) Exchange Catalysis in Alkanes. *ACS Catal.* **2018**, *8*, 2296–2312.
- (47) Kerr, W. J.; Knox, G. J.; Paterson, L. C. Recent Advances in Iridium(I) Catalysis towards Directed Hydrogen Isotope Exchange. *J. Labelled Compd. Radiopharm.* **2020**, *63*, 281–295.
- (48) Michelotti, A.; Roche, M. 40 Years of Hydrogen-Deuterium Exchange Adjacent to Heteroatoms: A Survey. *Synthesis* **2019**, *51*, 1319–1328.
- (49) Hesk, D. Highlights of C(sp³)-H Hydrogen Isotope Exchange Reactions. *J. Labelled Compd. Radiopharm.* **2020**, *63*, 247–265.
- (50) Valero, M.; Derdau, V. Highlights of Aliphatic C(sp³)-H Hydrogen Isotope Exchange Reactions. *J. Labelled Compd. Radiopharm.* **2020**, *63*, 266–280.
- (51) Kalinowski, M. B.; Colschen, L. C. International Control of Tritium to Prevent Horizontal Proliferation and to Foster Nuclear Disarmament. *Sci. Glob. Secur.* **1995**, *5*, 131–203.
- (52) Garnett, J. L.; Hodges, R. J. Homogeneous Metal-Catalyzed Exchange of Aromatic Compounds. Isotopic Hydrogen Labeling Procedure. *J. Am. Chem. Soc.* **1967**, *89*, 4546–4547.
- (53) Garnett, J. L.; Long, M. A.; McLaren, A. B.; Peterson, K. B. Iridium(III) Salts as Homogeneous Metal Catalysts for Hydrogen Isotope Exchange in Organic Compounds: A Comparison with Heterogeneous Iridium for the Deuteration of Alkylbenzenes. *J. Chem. Soc., Chem. Commun.* **1973**, *19*, 749–750.
- (54) Blake, M. R.; Garnett, J. L.; Gregor, I. K.; Hannan, W.; Hoa, K.; Long, M. A. Rhodium Trichloride as a Homogeneous Catalyst for Isotopic Hydrogen Exchange. Comparison with Heterogeneous Rhodium in the Deuteration of Aromatic Compounds and Alkanes. *J. Chem. Soc., Chem. Commun.* **1975**, *23*, 930–932.
- (55) Hesk, D.; Das, P. R.; Evans, B. Deuteration of Acetanilides and Other Substituted Aromatics Using [Ir(COD)(Cy3P)(Py)]PF₆ as Catalyst. *J. Labelled Compd. Radiopharm.* **1995**, *36*, 497–502.
- (56) Brown, J. A.; Irvine, S.; Kennedy, A. R.; Kerr, W. J.; Andersson, S.; Nilsson, G. N. Highly Active Iridium(I) Complexes for Catalytic Hydrogen Isotope Exchange. *Chem. Commun.* **2008**, 1115–1117.
- (57) Neubert, L.; Michalik, D.; Bähn, S.; Imm, S.; Neumann, H.; Atzrodt, J.; Derdau, V.; Holla, W.; Beller, M. Ruthenium-Catalyzed Selective α,β -Deuteration of Bioactive Amines. *J. Am. Chem. Soc.* **2012**, *134*, 12239–12244.
- (58) Pieters, G.; Taglang, C.; Bonnefille, E.; Gutmann, T.; Puente, C.; Berthet, J.-C.; Dugave, C.; Chaudret, B.; Rousseau, B. Regioselective and Stereospecific Deuteration of Bioactive Aza Compounds by the Use of Ruthenium Nanoparticles. *Angew. Chem., Int. Ed.* **2014**, *53*, 230–234.
- (59) Yu, R. P.; Hesk, D.; Rivera, N.; Pelczar, I.; Chirik, P. J. Iron-Catalyzed Tritiation of Pharmaceuticals. *Nature* **2016**, *529*, 195–199.
- (60) Loh, Y. Y.; Nagao, K.; Hoover, A. J.; Hesk, D.; Rivera, N. R.; Colletti, S. L.; Davies, I. W.; MacMillan, D. W. C. Photoredox-Catalyzed Deuteration and Tritiation of Pharmaceutical Compounds. *Science* **2017**, *358*, 1182–1187.
- (61) Zarate, C.; Yang, H.; Bezdek, M. J.; Hesk, D.; Chirik, P. J. Ni(I)-X Complexes Bearing a Bulky α -Diimine Ligand: Synthesis, Structure, and Superior Catalytic Performance in the Hydrogen Isotope Exchange in Pharmaceuticals. *J. Am. Chem. Soc.* **2019**, *141*, 5034–5044.
- (62) Valero, M.; Bouzouita, D.; Palazzolo, A.; Atzrodt, J.; Dugave, C.; Tricard, S.; Feullastre, S.; Pieters, G.; Chaudret, B.; Derdau, V. NHC-Stabilized Iridium Nanoparticles as Catalysts in Hydrogen Isotope Exchange Reactions of Anilines. *Angew. Chem., Int. Ed.* **2020**, *59*, 3517–3522.
- (63) Brown, J. A.; Cochrane, A. R.; Irvine, S.; Kerr, W. J.; Mondal, B.; Parkinson, J. A.; Paterson, L. C.; Reid, M.; Tuttle, T.; Andersson, S.; et al. The Synthesis of Highly Active Iridium(I) Complexes and Their Application in Catalytic Hydrogen Isotope Exchange. *Adv. Synth. Catal.* **2014**, *356*, 3551–3562.
- (64) Heys, R. Investigation of [IrH₂(Me₂CO)₂(PPh₃)₂]BF₄ as a Catalyst of Hydrogen Isotope Exchange of Substrates in Solution. *J. Chem. Soc., Chem. Commun.* **1992**, 680–681.
- (65) Hesk, D.; Das, P. R.; Evans, B. J. Deuteration of Acetanilides and Other Substituted Aromatics Using [Ir(COD)(Cy3P)(Py)]PF₆ as Catalyst. *J. Labelled Compd. Radiopharm.* **1995**, *36*, 497–502.
- (66) Powell, M. E.; Elmore, C. S.; Dorff, P. N.; Heys, J. R. Investigation of Isotopic Exchange Reactions Using N-Heterocyclic Iridium (I) Complexes. *J. Labelled Compd. Radiopharm.* **2007**, *50*, S23–S25.
- (67) Parmentier, M.; Hartung, T.; Pfaltz, A.; Muri, D. Iridium-Catalyzed H/D Exchange: Ligand Complexes with Improved Efficiency and Scope. *Chem.—Eur. J.* **2014**, *20*, 11496–11504.
- (68) Jess, K.; Derdau, V.; Weck, R.; Atzrodt, J.; Freytag, M.; Jones, P. G.; Tamm, M. Hydrogen Isotope Exchange with Iridium(I) Complexes Supported by Phosphine-Imidazolin-2-Imine P,N Ligands. *Adv. Synth. Catal.* **2017**, *359*, 629–638.
- (69) Burhop, A.; Prohaska, R.; Weck, R.; Atzrodt, J.; Derdau, V. Burgess Iridium(I)-Catalyst for Selective Hydrogen Isotope Exchange. *J. Labelled Compd. Radiopharm.* **2017**, *60*, 343–348.
- (70) Cochrane, A. R.; Kennedy, A. R.; Kerr, W. J.; Lindsay, D. M.; Reid, M.; Tuttle, T. The Natural Product Lepidiline A as an N-Heterocyclic Carbene Ligand Precursor in Complexes of the Type [Ir(cod)(NHC)PPh₃][X]: Synthesis, Characterisation, and Application in Hydrogen Isotope Exchange Catalysis. *Catalysts* **2020**, *10*, 161.
- (71) Valero, M.; Becker, D.; Jess, K.; Weck, R.; Atzrodt, J.; Bannenberg, T.; Derdau, V.; Tamm, M. Directed Iridium-Catalyzed Hydrogen Isotope Exchange Reactions of Phenylacetic Acid Esters and Amides. *Chem.—Eur. J.* **2019**, *25*, 6517–6522.
- (72) Valero, M.; Burhop, A.; Jess, K.; Weck, R.; Tamm, M.; Atzrodt, J.; Derdau, V. Evaluation of a P,N-Ligated Iridium(I) Catalyst in Hydrogen Isotope Exchange Reactions of Aryl and Heteroaryl Compounds. *J. Labelled Compd. Radiopharm.* **2018**, *61*, 380–385.
- (73) Kerr, W. J.; Reid, M.; Tuttle, T. Iridium-Catalyzed C-H Activation and Deuteration of Primary Sulfonamides: An Experimental and Computational Study. *ACS Catal.* **2015**, *5*, 402–410.
- (74) Flinker, M.; Yin, H.; Juhl, R. W.; Bickel, E. Z.; Overgaard, J.; Nielsen, D. U.; Skrydstrup, T. Efficient Water Reduction with sp³-sp³ Diboron(4) Compounds: Application to Hydrogenations, H-D Exchange Reactions, and Carbonyl Reductions. *Angew. Chem., Int. Ed.* **2017**, *56*, 15910–15915.
- (75) Ma, S.; Villa, G.; Thuy-Boun, P. S.; Horns, A.; Yu, J.-Q. Palladium-Catalyzed ortho-Selective CH Deuteration of Arenes: Evidence for Superior Reactivity of Weakly Coordinated Palladacycles. *Angew. Chem., Int. Ed.* **2014**, *53*, 734–737.
- (76) Garreau, A. L.; Zhou, H.; Young, M. C. A Protocol for the Ortho-Deuteration of Acidic Aromatic Compounds in D₂O Catalyzed by Cationic Rh^{III}. *Org. Lett.* **2019**, *21*, 7044–7048.
- (77) Müller, V.; Weck, R.; Derdau, V.; Ackermann, L. Ruthenium(II)-Catalyzed Hydrogen Isotope Exchange of Pharmaceutical Drugs by C-H Deuteration and C-H Tritiation. *ChemCatChem* **2020**, *12*, 100–104.
- (78) Manna, P.; Kundu, M.; Roy, A.; Adhikari, S. The Palladium-Catalyzed Directed Synthesis of ortho-Deuterated Phenylacetic Acid and Analogues. *Org. Biomol. Chem.* **2021**, *19*, 6244–6249.
- (79) Kopf, S.; Neumann, H.; Beller, M. Manganese-Catalyzed Selective C-H Activation and Deuteration by Means of a Catalytic Transient Directing Group Strategy. *Chem. Commun.* **2021**, *57*, 1137–1140.
- (80) Kopf, S.; Ye, F.; Neumann, H.; Beller, M. Ruthenium-Catalyzed Deuteration of Aromatic Carbonyl Compounds with a Catalytic Transient Directing Group. *Chem.—Eur. J.* **2021**, *27*, 9768–9773.
- (81) Burhop, A.; Weck, R.; Atzrodt, J.; Derdau, V. Hydrogen-Isotope Exchange (HIE) Reactions of Secondary and Tertiary Sulfonamides and Sulfonyleureas with Iridium(I) Catalysts: Hydrogen-Isotope Exchange (HIE) Reactions of Secondary and Tertiary Sulfonamides and Sulfonyleureas with Iridium(I) Catalysts. *Eur. J. Org. Chem.* **2017**, *2017*, 1418–1424.
- (82) Liu, W.; Xu, X.; Zhao, H.; Yan, X. Palladium-Catalyzed Site-Selective Hydrogen Isotope Exchange (HIE) Reaction of Arylsulfonamides Using Amino Acid Auxiliary. *Tetrahedron* **2018**, *74*, 4111–4118.
- (83) Kerr, W. J.; Knox, G. J.; Reid, M.; Tuttle, T.; Bergare, J.; Bragg, R. A. Computationally-Guided Development of a Chelated NHC-P

- Iridium(I) Complex for the Directed Hydrogen Isotope Exchange of Aryl Sulfones. *ACS Catal.* **2020**, *10*, 11120–11126.
- (84) Martins, A.; Lautens, M. A Simple, Cost-Effective Method for the Regioselective Deuteration of Anilines. *Org. Lett.* **2008**, *10*, 4351–4353.
- (85) Giles, R.; Lee, A.; Jung, B.; Kang, A.; Jung, K. W. Hydrogen-Deuterium Exchange of Aromatic Amines and Amides Using Deuterated Trifluoroacetic Acid. *Tetrahedron Lett.* **2015**, *56*, 747–749.
- (86) Liu, W.; Cao, L.; Zhang, Z.; Zhang, G.; Huang, S.; Huang, L.; Zhao, P.; Yan, X. Mesomeric Carbene-Iridium Complex Catalyzed Ortho-Selective Hydrogen Isotope Exchange of Anilines with High Functional Group Tolerance. *Org. Lett.* **2020**, *22*, 2210–2214.
- (87) Kerr, W. J.; Lindsay, D. M.; Owens, P. K.; Reid, M.; Tuttle, T.; Campos, S. Site-Selective Deuteration of *N*-Heterocycles via Iridium-Catalyzed Hydrogen Isotope Exchange. *ACS Catal.* **2017**, *7*, 7182–7186.
- (88) Zhang, J.; Zhang, S.; Gogula, T.; Zou, H. Versatile Regioselective Deuteration of Indoles via Transition-Metal-Catalyzed H/D Exchange. *ACS Catal.* **2020**, *10*, 7486–7494.
- (89) Peng, W.; Liu, W.; Yin, F.; Shi, C.; Ji, L.; Qu, L.; Wang, C.; Luo, H.; Kong, L.; Wang, X. Rhodium(III) Catalyzed Olefination and Deuteration of Tetrahydrocarbazole. *RSC Adv.* **2021**, *11*, 8356–8361.
- (90) Wu, J.; Qian, B.; Lu, L.; Yang, H.; Shang, Y.; Zhang, J. Access to C2 C-H Olefination, Alkylation and Deuteration of Indoles by Rhodium(III) Catalysis: An Entry for Diverse Synthesis. *Org. Chem. Front.* **2021**, *8*, 3032–3040.
- (91) Pfeifer, V.; Certiat, M.; Bouzouita, D.; Palazzolo, A.; Garcia-Argote, S.; Marcon, E.; Buisson, D.-A.; Lesot, P.; Maron, L.; Chaudret, B.; et al. Hydrogen Isotope Exchange Catalyzed by Ru Nanocatalysts: Labelling of Complex Molecules Containing *N*-Heterocycles and Reaction Mechanism Insights. *Chem.—Eur. J.* **2020**, *26*, 4988–4996.
- (92) Palazzolo, A.; Naret, T.; Daniel-Bertrand, M.; Buisson, D.-A.; Tricard, S.; Lesot, P.; Coppel, Y.; Chaudret, B.; Feuillastre, S.; Pieters, G. Tuning the Reactivity of a Heterogeneous Catalyst using *N* Heterocyclic Carbene Ligands for C-H Activation Reactions. *Angew. Chem., Int. Ed.* **2020**, *59*, 20879–20884.
- (93) Bouzouita, D.; Asensio, J. M.; Pfeifer, V.; Palazzolo, A.; Lecante, P.; Pieters, G.; Feuillastre, S.; Tricard, S.; Chaudret, B. Chemoselective H/D Exchange Catalyzed by Nickel Nanoparticles Stabilized by *N*-Heterocyclic Carbene Ligands. *Nanoscale* **2020**, *12*, 15736–15742.
- (94) Directing groups which are not commonly found functional groups are nevertheless used sometimes. Recent examples: Zhao, D.; Luo, H.; Chen, B.; Chen, W.; Zhang, G.; Yu, Y. Palladium-Catalyzed H/D Exchange Reaction with 8-Aminoquinoline as the Directing Group: Access to Ortho-Selective Deuterated Aromatic Acids and β -Selective Deuterated Aliphatic Acids. *J. Org. Chem.* **2018**, *83*, 7860–7866 and reference 82.
- (95) Valero, M.; Kruissink, T.; Blass, J.; Weck, R.; Güssregen, S.; Plowright, A. T.; Derdau, V. C-H Functionalization—Prediction of Selectivity in Iridium(I)-Catalyzed Hydrogen Isotope Exchange Competition Reactions. *Angew. Chem., Int. Ed.* **2020**, *59*, 5626–5631.
- (96) Cochrane, A. R.; Irvine, S.; Kerr, W. J.; Reid, M.; Andersson, S.; Nilsson, G. N. Application of Neutral Iridium(I) *N*-Heterocyclic Carbene Complexes in ortho-Directed Hydrogen Isotope Exchange. *J. Labelled Compd. Radiopharm.* **2013**, *56*, 451–454.
- (97) Kerr, W. J.; Mudd, R. J.; Owens, P. K.; Reid, M.; Brown, J. A.; Campos, S. Hydrogen Isotope Exchange with Highly Active Iridium(I) NHC/Phosphine Complexes: A Comparative Counterion Study. *J. Labelled Compd. Radiopharm.* **2016**, *59*, 601–603.
- (98) Cross, P. W. C.; Herbert, J. M.; Kerr, W. J.; McNeill, A. H.; Paterson, L. C. Isotopic Labelling of Functionalised Arenes Catalysed by Iridium(I) Species of the [(cod)Ir(NHC)(py)]PF₆ Complex Class. *Synlett* **2015**, *27*, 111–115.
- (99) Piola, L.; Fernández-Salas, J. A.; Manzini, S.; Nolan, S. P. Regioselective Ruthenium Catalysed H-D Exchange Using D₂O as the Deuterium Source. *Org. Biomol. Chem.* **2014**, *12*, 8683–8688.
- (100) Devlin, J.; Kerr, W. J.; Lindsay, D. M.; McCabe, T. J. D.; Reid, M.; Tuttle, T. Iridium-Catalysed ortho-Directed Deuterium Labelling of Aromatic Esters—An Experimental and Theoretical Study on Directing Group Chemoselectivity. *Molecules* **2015**, *20*, 11676–11698.
- (101) Cochrane, A. R.; Idziak, C.; Kerr, W. J.; Mondal, B.; Paterson, L. C.; Tuttle, T.; Andersson, S.; Nilsson, G. N. Practically Convenient and Industrially-Aligned Methods for Iridium-Catalysed Hydrogen Isotope Exchange Processes. *Org. Biomol. Chem.* **2014**, *12*, 3598–3603.
- (102) Lockley, W. J. S. Hydrogen Isotope Labelling Using Iridium(I) Donates. *J. Labelled Compd. Radiopharm.* **2010**, *53*, 668–673.
- (103) Krüger, J.; Mammontri, B.; Fels, G. Iridium-Catalyzed H/D Exchange. *Eur. J. Org. Chem.* **2005**, *2005*, 1402–1408.
- (104) Atzrodt, J.; Derdau, V.; Kerr, W. J.; Reid, M.; Rojahn, P.; Weck, R. Expanded applicability of Iridium(I) NHC/Phosphine Catalysts in Hydrogen Isotope Exchange Processes with Pharmaceutically Relevant Heterocycles. *Tetrahedron* **2015**, *71*, 1924–1929.
- (105) Prades, A.; Poyatos, M.; Peris, E. (h⁶-Arene)Ruthenium(*N*-Heterocyclic Carbene) Complexes for the Chelation-Assisted Arylation and Deuteration of Arylpyridines: Catalytic Studies and Mechanistic Insights. *Adv. Synth. Catal.* **2010**, *352*, 1155–1162.
- (106) Kerr, W. J.; Lindsay, D. M.; Reid, M.; Atzrodt, J.; Derdau, V.; Rojahn, P.; Weck, R. Iridium-Catalysed ortho-H/D and -H/T Exchange under Basic Conditions: C-H Activation of Unprotected Tetrazoles. *Chem. Commun.* **2016**, *52*, 6669–6672.
- (107) Timofeeva, D. S.; Lindsay, D. M.; Kerr, W. J.; Nelson, D. J. A Quantitative Empirical Directing Group Scale for Selectivity in Iridium-Catalysed Hydrogen Isotope Exchange Reactions. *Catal. Sci. Technol.* **2020**, *10*, 7249–7255.
- (108) Kerr, W. J.; Knox, G. J.; Reid, M.; Tuttle, T. Catalyst Design in C-H Activation: A Case Study in the Use of Binding Free Energies to Rationalize Intramolecular Directing Group Selectivity in Iridium Catalysis. *Chem. Sci.* **2021**, *12*, 6747–6755.
- (109) Yin, D.-W.; Liu, G. Palladium-Catalyzed Regioselective C-H Functionalization of Arenes Substituted by Two *N*-Heterocycles and Application in Late-Stage Functionalization. *J. Org. Chem.* **2018**, *83*, 3987–4001.
- (110) Eisele, P.; Ullwer, F.; Scholz, S.; Plietker, B. Mild, Selective Ru-Catalyzed Deuteration Using D₂O as a Deuterium Source. *Chem.—Eur. J.* **2019**, *25*, 16550–16554.
- (111) Valero, M.; Mishra, A.; Blass, J.; Weck, R.; Derdau, V. Comparison of Iridium(I) Catalysts in Temperature Mediated Hydrogen Isotope Exchange Reactions. *ChemistryOpen* **2019**, *8*, 1183–1189.
- (112) Koneczny, M.; Phong Ho, L.; Nasr, A.; Freytag, M.; Jones, P. G.; Tamma, M. Iridium(I) Complexes with Anionic *N*-Heterocyclic Carbene Ligands as Catalysts for H/D Exchange in Nonpolar Media. *Adv. Synth. Catal.* **2020**, *362*, 3857–3863.
- (113) Yang, H.; Dormer, P. G.; Rivera, N. R.; Hoover, A. J. Palladium(II)-Mediated C-H Tritiation of Complex Pharmaceuticals. *Angew. Chem., Int. Ed.* **2018**, *57*, 1883–1887.
- (114) Yu, Q.; Hu, L.; Wang, Y.; Zheng, S.; Huang, J. Directed meta-Selective Bromination of Arenes with Ruthenium Catalysts. *Angew. Chem., Int. Ed.* **2015**, *54*, 15284–15288.
- (115) Fan, Z.; Ni, J.; Zhang, A. Meta-Selective CAr-H Nitration of Arenes through a Ru₃(CO)₁₂-Catalyzed Ortho-Metalation Strategy. *J. Am. Chem. Soc.* **2016**, *138*, 8470–8475.
- (116) Fan, Z.; Li, J.; Lu, H.; Wang, D.-Y.; Wang, C.; Uchiyama, M.; Zhang, A. Monomeric Octahedral Ruthenium(II) Complex Enabled meta-C-H Nitration of Arenes with Removable Auxiliaries. *Org. Lett.* **2017**, *19*, 3199–3202.
- (117) Korvorapun, K.; Moselage, M.; Struwe, J.; Rogge, T.; Messinis, A. M.; Ackermann, L. Regiodivergent C-H and Decarboxylative C-C Alkylation by Ruthenium Catalysis: ortho versus meta Position-Selectivity. *Angew. Chem., Int. Ed.* **2020**, *59*, 18795–18803.
- (118) Zhao, L.-L.; Liu, W.; Zhang, Z.; Zhao, H.; Wang, Q.; Yan, X. Ruthenium-Catalyzed Ortho- and Meta-H/D Exchange of Arenes. *Org. Lett.* **2019**, *21*, 10023–10027.
- (119) Bag, S.; Petzold, M.; Sur, A.; Bhowmick, S.; Werz, D. B.; Maiti, D. Palladium-Catalyzed Selective Meta-C-H Deuteration of Arenes: Reaction Design and Applications. *Chem.—Eur. J.* **2019**, *25*, 9433–9437.

- (120) Xu, H.; Liu, M.; Li, L.-J.; Cao, Y.-F.; Yu, J.-Q.; Dai, H.-X. Palladium-Catalyzed Remote Meta-C-H Bond Deuteration of Arenes Using a Pyridine Template. *Org. Lett.* **2019**, *21*, 4887–4891.
- (121) Gholap, A.; Bag, S.; Pradhan, S.; Kapdi, A. R.; Maiti, D. Diverse Meta-C-H Functionalization of Amides. *ACS Catal.* **2020**, *10*, 5347–5352.
- (122) Corpas, J.; Viereck, P.; Chirik, P. J. C(Sp²)-H Activation with Pyridine Dicarbene Iron Dialkyl Complexes: Hydrogen Isotope Exchange of Arenes Using Benzene-d₆ as a Deuterium Source. *ACS Catal.* **2020**, *10*, 8640–8647.
- (123) Garhwal, S.; Kaushansky, A.; Fridman, N.; Shimon, L. J. W.; Ruiter, G. de. Facile H/D Exchange at (Hetero)Aromatic Hydrocarbons Catalyzed by a Stable Trans-Dihydride N-Heterocyclic Carbene (NHC) Iron Complex. *J. Am. Chem. Soc.* **2020**, *142*, 17131–17139.
- (124) Li, E.-C.; Hu, G.-Q.; Zhu, Y.-X.; Zhang, H.-H.; Shen, K.; Hang, X.-C.; Zhang, C.; Huang, W. Ag₂CO₃-Catalyzed H/D Exchange of Five-Membered Heteroarenes at Ambient Temperature. *Org. Lett.* **2019**, *21*, 6745–6749.
- (125) Similar reactivity was previously observed in mechanistic experiments: Whitaker, D.; Burés, J.; Larrosa, I. Ag(I)-Catalyzed C-H Activation: The Role of the Ag(I) Salt in Pd/Ag-Mediated C-H Arylation of Electron-Deficient Arenes. *J. Am. Chem. Soc.* **2016**, *138*, 8384–8387 and reference 124.
- (126) Lotz, M. D.; Camasso, M. N.; Canty, A. J.; Sanford, M. S. Role of Silver Salts in Palladium-Catalyzed Arene and Heteroarene C-H Functionalization Reactions. *Organometallics* **2017**, *36*, 165–171.
- (127) Tlahuext-Aca, A.; Hartwig, J. F. Site-Selective Silver-Catalyzed C-H Bond Deuteration of Five-Membered Aromatic Heterocycles and Pharmaceuticals. *ACS Catal.* **2021**, *11*, 1119–1127.
- (128) Zhan, M.; Xu, R.; Tian, Y.; Jiang, H.; Zhao, L.; Xie, Y.; Chen, Y. A Simple and Cost-Effective Method for the Regioselective Deuteration of Phenols. *Eur. J. Org. Chem.* **2015**, *2015*, 3370–3373.
- (129) Li, W.; Wang, M.-M.; Hu, Y.; Werner, T. B(C₆F₅)₃-Catalyzed Regioselective Deuteration of Electron-Rich Aromatic and Heteroaromatic Compounds. *Org. Lett.* **2017**, *19*, 5768–5771.
- (130) Dong, B.; Cong, X.; Hao, N. Silver-Catalyzed Regioselective Deuteration of (Hetero)Arenes and α -Deuteration of 2-Alkyl Azarenes. *RSC Adv.* **2020**, *10*, 25475–25479.
- (131) Fischer, O.; Hubert, A.; Heimich, M. R. Shifted Selectivity in Protonation Enables the Mild Deuteration of Arenes Through Catalytic Amounts of Brønsted Acids in Deuterated Methanol. *J. Org. Chem.* **2020**, *85*, 11856–11866.
- (132) Hu, G.-Q.; Li, E.-C.; Zhang, H.-H.; Huang, W. Ag(I)-Mediated Hydrogen Isotope Exchange of Mono-Fluorinated (Hetero)Arenes. *Org. Biomol. Chem.* **2020**, *18*, 6627–6633.
- (133) A similar result is additionally shown in a recent mechanistic experiment by Tlahuext-Aca. See the following: Tlahuext-Aca, A.; Lee, S. Y.; Sakamoto, S.; Hartwig, J. F.; et al. Direct Arylation of Simple Arenes with Aryl Bromides by Synergistic Silver and Palladium Catalysis. *ACS Catal.* **2021**, *11*, 1430–1434.
- (134) Salamanca, V.; Albéniz, A. C. Deuterium Exchange between Arenes and Deuterated Solvents in the Absence of a Transition Metal: Synthesis of D-Labeled Fluoroarenes: Deuterium Exchange between Arenes and Deuterated Solvents in the Absence of a Transition Metal: Synthesis of D-Labeled Fluoroarenes. *Eur. J. Org. Chem.* **2020**, *2020*, 3206–3212.
- (135) Hu, G.-Q.; Bai, J.-W.; Li, E.-C.; Liu, K.-H.; Sheng, F.-F.; Zhang, H.-H. Synthesis of Multideuterated (Hetero)Aryl Bromides by Ag(I)-Catalyzed H/D Exchange. *Org. Lett.* **2021**, *23*, 1554–1560.
- (136) Yang, H.; Zarate, C.; Palmer, W. N.; Rivera, N.; Hesk, D.; Chirik, P. J. Site-Selective Nickel-Catalyzed Hydrogen Isotope Exchange in N-Heterocycles and Its Application to the Tritiation of Pharmaceuticals. *ACS Catal.* **2018**, *8*, 10210–10218.
- (137) Koniarczyk, J. L.; Hesk, D.; Overgard, A.; Davies, I. W.; McNally, A. A General Strategy for Site-Selective Incorporation of Deuterium and Tritium into Pyridines, Diazines, and Pharmaceuticals. *J. Am. Chem. Soc.* **2018**, *140*, 1990–1993.
- (138) The tritiation procedure requires previous formation of MeOT by heterogeneously catalyzed HIE between deuterium gas and methanol.
- (139) Maegawa, T.; Fujiwara, Y.; Inagaki, Y.; Esaki, H.; Monguchi, Y.; Sajiki, H. Mild and Efficient H/D Exchange of Alkanes Based on C-H Activation Catalyzed by Rhodium on Charcoal. *Angew. Chem., Int. Ed.* **2008**, *47*, 5394–5397.
- (140) Heys, J. R. Nickel-Catalyzed Hydrogen Isotope Exchange. *J. Labelled Compd. Radiopharm.* **2010**, *53*, 716–721.
- (141) Hesk, D.; Lavey, C. F.; McNamara, P. Tritium Labeling of Pharmaceuticals by Metal-Catalysed Exchange Methods. *J. Labelled Compd. Radiopharm.* **2010**, *53*, 722–730.
- (142) Sajiki, H.; Sawama, Y.; Monguchi, Y. Efficient H-D Exchange Reactions Using Heterogeneous Platinum-Group Metal on Carbon-H₂-D₂O System. *Synlett* **2012**, *23*, 959–972.
- (143) Sajiki, H.; Kurita, T.; Esaki, H.; Aoki, F.; Maegawa, T.; Hirota, K. Complete Replacement of H₂ by D₂ via Pd/C-Catalyzed H/D Exchange Reaction. *Org. Lett.* **2004**, *6*, 3521–3523.
- (144) Esaki, H.; Ohtaki, R.; Maegawa, T.; Monguchi, Y.; Sajiki, H. Novel Pd/C-Catalyzed Redox Reactions between Aliphatic Secondary Alcohols and Ketones under Hydrogenation Conditions: Application to H-D Exchange Reaction and the Mechanistic Study. *J. Org. Chem.* **2007**, *72*, 2143–2150.
- (145) Kurita, T.; Aoki, F.; Mizumoto, T.; Maejima, T.; Esaki, H.; Maegawa, T.; Monguchi, Y.; Sajiki, H. Facile and Convenient Method of Deuterium Gas Generation Using a Pd/C-Catalyzed H₂-D₂ Exchange Reaction and its Application to Synthesis of Deuterium-Labeled Compounds. *Chem.—Eur. J.* **2008**, *14*, 3371–3379.
- (146) Sajiki, H.; Ito, N.; Esaki, H.; Maesawa, T.; Maegawa, T.; Hirota, K. Aromatic Ring Favorable and Efficient H-D Exchange Reaction Catalyzed by Pt/C. *Tetrahedron Lett.* **2005**, *46*, 6995–6998.
- (147) Ito, N.; Esaki, H.; Maesawa, T.; Imamiya, B.; Maegawa, T.; Sajiki, H. Efficient and Selective Pt/C-Catalyzed H-D Exchange Reaction of Aromatic Rings. *Bull. Chem. Soc. Jpn.* **2008**, *81*, 278–286.
- (148) Esaki, H.; Ito, N.; Sakai, S.; Maegawa, T.; Monguchi, Y.; Sajiki, H. General Method of Obtaining Deuterium-Labeled Heterocyclic Compounds Using Neutral D₂O with Heterogeneous Pd/C. *Tetrahedron* **2006**, *62*, 10954–10961.
- (149) Vitaku, E.; Smith, D. T.; Njardarson, J. T. Analysis of the Structural Diversity, Substitution Patterns, and Frequency of Nitrogen Heterocycles among U.S. FDA Approved Pharmaceuticals. *J. Med. Chem.* **2014**, *57*, 10257–10274.
- (150) Sajiki, H.; Esaki, H.; Aoki, F.; Maegawa, T.; Hirota, K. Palladium-Catalyzed Base-Selective H-D Exchange Reaction of Nucleosides in Deuterium Oxide. *Synlett* **2005**, 1385–1388.
- (151) Sawama, Y.; Nakano, A.; Matsuda, T.; Kawajiri, T.; Yamada, T.; Sajiki, H. H-D Exchange Deuteration of Arenes at Room Temperature. *Org. Process Res. Dev.* **2019**, *23*, 648–653.
- (152) Sajiki, H.; Ito, N.; Watahiki, T.; Maesawa, T.; Maegawa, T. H-D Exchange Reaction Taking Advantage of the Synergistic Effect of Heterogeneous Palladium and Platinum Mixed Catalyst. *Synthesis* **2008**, *2008*, 1467–1478.
- (153) Daniel-Bertrand, M.; Garcia-Argote, S.; Palazzolo, A.; Mustieles Marin, I.; Fazzini, P.-F.; Tricard, S.; Chaudret, B.; Derdau, V.; Feuillastre, S.; Pieters, G. Multiple Site Hydrogen Isotope Labelling of Pharmaceuticals. *Angew. Chem., Int. Ed.* **2020**, *59*, 21114–21120.
- (154) Palazzolo, A.; Feuillastre, S.; Pfeifer, V.; Garcia-Argote, S.; Bouzouita, D.; Tricard, S.; Chollet, C.; Marcon, E.; Buisson, D.-A.; Cholet, S.; et al. Efficient Access to Deuterated and Tritiated Nucleobase Pharmaceuticals and Oligonucleotides Using Hydrogen-Isotope Exchange. *Angew. Chem., Int. Ed.* **2019**, *58*, 4891–4895.
- (155) Mai, V. H.; Gadzhiev, O. B.; Ignatov, S. K.; Nikonov, G. I. H/D Exchange in N-Heterocycles Catalysed by an NHC-Supported Ruthenium Complex. *Catal. Sci. Technol.* **2019**, *9*, 3398–3407.
- (156) Liang, X.; Duttwyler, S. Efficient Brønsted-Acid-Catalyzed Deuteration of Arenes and Their Transformation to Functionalized Deuterated Products. *Asian J. Org. Chem.* **2017**, *6*, 1063–1071.
- (157) Kramer, M.; Watts, D.; Vedernikov, A. N. Catalytic Deuteration of C(Sp²)-H Bonds of Substituted (Hetero)Arenes in a Pt(II) CNN-

- Pincer Complex/2,2,2-Trifluoroethanol- d_4 System: Effect of Substituents on the Reaction Rate and Selectivity. *Organometallics* 2020, 39, 4102–4114.
- (158) Wedi, P.; Farizyan, M.; Bergander, K.; Mück-Lichtenfeld, C.; van Gemmeren, M. Mechanism of the Arene-Limited Nondirected C-H Activation of Arenes with Palladium. *Angew. Chem., Int. Ed.* 2021, 60, 15641–15649.
- (159) Farizyan, M.; Mondal, A.; Mal, S.; Deufel, F.; van Gemmeren, M. Palladium-Catalyzed Nondirected Late-Stage C-H Deuteration of Arenes. *J. Am. Chem. Soc.* 2021, 143, 16370–16376.
- (160) Martin, J.; Byslein, J.; Grams, S.; Harder, S. Hydrogen Isotope Exchange with Superbulky Alkaline Earth Metal Amide Catalysts. *ACS Catal.* 2020, 10, 7792–7799.
- (161) Smith, J. D.; Durrant, G.; Ess, D. H.; Gelfand, B. S.; Piers, W. E. H/D Exchange under Mild Conditions in Arenes and Unactivated Alkanes with C_2D_6 and D_2O Using Rigid, Electron-Rich Iridium PCP Pincer Complexes. *Chem. Sci.* 2020, 11, 10705–10717.
- (162) Tse, S. K. S.; Xue, P.; Lin, Z.; Jia, G. Hydrogen/Deuterium Exchange Reactions of Olefins with Deuterium Oxide Mediated by the Carbonylchlorohydrido-tris (Triphenylphosphine) Ruthenium (II) Complex. *Adv. Synth. Catal.* 2010, 352, 1512–1522.
- (163) Di Giuseppe, A.; Castarlenas, R.; Pérez-Torrente, J. J.; Lahoz, F. L.; Polo, V.; Oro, L. A. Mild and Selective H/D Exchange at the β Position of Aromatic α -Olefins by N-Heterocyclic Carbene-Hydride-Rhodium Catalysts. *Angew. Chem., Int. Ed.* 2011, 50, 3938–3942.
- (164) Hatano, M.; Nishimura, T.; Yoritatsu, H. Selective H/D Exchange at Vinyl and Methyldene Groups with D_2O Catalyzed by an Iridium Complex. *Org. Lett.* 2016, 18, 3674–3677.
- (165) Smarun, A. V.; Petković, M.; Shchepinov, M. S.; Vidović, D. Site-Specific Deuteration of Polyunsaturated Alkenes. *J. Org. Chem.* 2017, 82, 13115–13120.
- (166) Kerr, W. J.; Mudd, R. J.; Paterson, L. C.; Brown, J. A. Iridium (I)-Catalyzed Regioselective C-H Activation and Hydrogen-Isotope Exchange of Non-Aromatic Unsaturated Functionality. *Chem.—Eur. J.* 2014, 20, 14604–14607.
- (167) Bechtoldt, A.; Ackermann, L. Ruthenium(II)Bis(carboxylate)-Catalyzed Hydrogen-Isotope Exchange by Alkene C-H Activation. *ChemCatChem* 2019, 11, 435–438.
- (168) Park, K.; Matsuda, T.; Yamada, T.; Monguchi, Y.; Sawama, Y.; Doi, N.; Sasai, Y.; Konodo, S.-i.; Sawama, Y.; Sajiki, H. Direct Deuteration of Acrylic and Methacrylic Acid Derivatives Catalyzed by Platinum on Carbon in Deuterium Oxide. *Adv. Synth. Catal.* 2018, 360, 2303–2307.
- (169) Landge, V. G.; Shrestha, K. K.; Grant, A. J.; Young, M. C. Regioselective α -Deuteration of Michael Acceptors Mediated by Isopropylamine in D_2O /AcOD. *Org. Lett.* 2020, 22, 9745–9750.
- (170) Puleo, T. R.; Strong, A. J.; Bandar, J. S. Catalytic α -Selective Deuteration of Styrene Derivatives. *J. Am. Chem. Soc.* 2019, 141, 1467–1472.
- (171) Camedda, N.; Serafino, A.; Maggi, R.; Bigi, F.; Cera, G.; Maestri, G. Functionalization of Alkenyl C-H Bonds with D_2O via Pd(0)/Carboxylic Acid Catalysis. *Synthesis* 2020, S2, 1762–1772.
- (172) Bew, S. P.; Hiatt-Gipson, G. D.; Lovell, J. A.; Poullain, C. Mild Reaction Conditions for the Terminal Deuteration of Alkynes. *Org. Lett.* 2012, 14, 456–459.
- (173) Chatterjee, B.; Gunanathan, C. The Ruthenium-Catalyzed Selective Synthesis of Mono-Deuterated Terminal Alkynes. *Chem. Commun.* 2016, S2, 4509–4512.
- (174) Wu, D.-C.; Bai, J.-W.; Guo, L.; Hu, G.-Q.; Liu, K.-H.; Sheng, F.-F.; Zhang, H.-H.; Sun, Z.-Y.; Shen, K.; Liu, X. A Practical and Efficient Method for Late-Stage Deuteration of Terminal Alkynes with Silver Salt as Catalyst. *Tetrahedron Lett.* 2021, 66, 152807.
- (175) Kumar, S.; Patel, M.; Verma, A. K. Base-Catalyzed Selective Deuteration of Alkynes. *Asian J. Org. Chem.* 2021, 10, 2365–2369.
- (176) Hale, L. V. A.; Szymczak, N. K. Stereoretentive Deuteration of α -Chiral Amines with D_2O . *J. Am. Chem. Soc.* 2016, 138, 13489–13492.
- (177) Chatterjee, B.; Krishnakumar, V.; Gunanathan, C. Selective α -Deuteration of Amines and Amino Acids Using D_2O . *Org. Lett.* 2016, 18, 5892–5895.
- (178) Tse, S. K. S.; Xue, P.; Lau, C. W. S.; Sung, H. H. Y.; Williams, I. D.; Jia, G. Ruthenium-Catalyzed Regioselective Deuteration of Alcohols at the β -Carbon Position with Deuterium Oxide. *Chem.—Eur. J.* 2011, 17, 13918–13925.
- (179) Khaskin, E.; Milstein, D. Simple and Efficient Catalytic Reaction for the Selective Deuteration of Alcohols. *ACS Catal.* 2013, 3, 448–452.
- (180) Chatterjee, B.; Gunanathan, C. Ruthenium Catalyzed Selective α - and α,β -Deuteration of Alcohols Using D_2O . *Org. Lett.* 2015, 17, 4794–4797.
- (181) Kar, S.; Goepfert, A.; Sen, R.; Kothandaraman, J.; Surya Prakash, G. K. Regioselective Deuteration of Alcohols in D_2O Catalysed by Homogeneous Manganese and Iron Pincer Complexes. *Green Chem.* 2018, 20, 2706–2710.
- (182) Maegawa, T.; Fujiwara, Y.; Inagaki, Y.; Monguchi, Y.; Sajiki, H. A Convenient and Effective Method for the Regioselective Deuteration of Alcohols. *Adv. Synth. Catal.* 2008, 350, 2215–2218.
- (183) Gao, L.; Perato, S.; Garcia-Argote, S.; Taglang, C.; Martinez-Prieto, L. M.; Chollet, C.; Buisson, D. A.; Dauvois, V.; Lesot, P.; Chaudret, B.; et al. Ruthenium-Catalyzed Hydrogen Isotope Exchange of C(sp³)-H Bonds Directed by a Sulfur Atom. *Chem. Commun.* 2018, S4, 2986–2989.
- (184) Kerr, W. J.; Mudd, R. J.; Reid, M.; Atzrodt, J.; Derdau, V. Iridium-Catalyzed Csp³-H Activation for Mild and Selective Hydrogen Isotope Exchange. *ACS Catal.* 2018, 8, 10895–10900.
- (185) Zilate, B.; Fischer, C.; Schneider, L.; Sparr, C. Scalable Synthesis of Acridinium Catalysts for Photoredox Deuterations. *Synthesis* 2019, S1, 4359–4365.
- (186) The use of thiols as HAT agents is necessary due to the high bond dissociation energy of D_2O which impedes deuterium atom abstraction from the solvent.
- (187) Legros, F.; Fernandez-Rodriguez, P.; Mishra, A.; Weck, R.; Bauer, A.; Sandvoss, M.; Ruf, S.; Méndez, M.; Mora-Radó, H.; Rackelmann, N.; et al. Photoredox-Mediated Hydrogen Isotope Exchange Reactions of Amino-Acids, Peptides, and Peptide-Derived Drugs. *Chem.—Eur. J.* 2020, 26, 12738–12742.
- (188) Chun, S. W.; Narayan, A. R. H. Biocatalytic, Stereoselective Deuteration of α -Amino Acids and Methyl Esters. *ACS Catal.* 2020, 10, 7413–7418.
- (189) Takeda, R.; Abe, H.; Shibata, N.; Moriawaki, H.; Izawa, K.; Soloshonok, V. A. Asymmetric Synthesis of α -Deuterated α -Amino Acids. *Org. Biomol. Chem.* 2017, 15, 6978–6983.
- (190) Chang, Y.; Yesilcimen, A.; Cao, M.; Zhang, Y.; Zhang, B.; Chan, J. Z.; Wasa, M. Catalytic Deuterium Incorporation within Metabolically Stable β -Amino C-H Bonds of Drug Molecules. *J. Am. Chem. Soc.* 2019, 141, 14570–14575.
- (191) Chang, Y.; Myers, T.; Wasa, M. B(C₆F₅)₃-Catalyzed α -Deuteration of Bioactive Carbonyl Compounds with D_2O . *Adv. Synth. Catal.* 2020, 362, 360–364.
- (192) Galkin, K. I.; Gordeev, E. G.; Ananikov, V. P. Organocatalytic Deuteration Induced by the Dynamic Covalent Interaction of Imidazolium Cations with Ketones. *Adv. Synth. Catal.* 2021, 363, 1368–1378.
- (193) Zanatta, M.; dos Santos, F. P.; Biehl, C.; Marin, G.; Ebeling, G.; Netz, P. A.; Dupont, J. Organocatalytic Imidazolium Ionic Liquids H/D Exchange Catalysts. *J. Org. Chem.* 2017, 82, 2622–2629.
- (194) Porte, V.; Di Mauro, G.; Schupp, M.; Kaiser, D.; Maulide, N. Chemoselective Alpha-Deuteration of Amides via Retro-Ene Reaction. *Chem.—Eur. J.* 2020, 26, 15509–15512.
- (195) Valero, M.; Weck, R.; Güssregen, S.; Atzrodt, J.; Derdau, V. Highly Selective Directed Iridium-Catalyzed Hydrogen Isotope Exchange Reactions of Aliphatic Amides. *Angew. Chem., Int. Ed.* 2018, 57, 8159–8163.
- (196) Uttry, A.; Mal, S.; van Gemmeren, M. Late-Stage β -C(sp³)-H Deuteration of Carboxylic Acids. *J. Am. Chem. Soc.* 2021, 143, 10895–10901.

- (197) Krishnakumar, V.; Gunanathan, C. Ruthenium-Catalyzed Selective α -Deuteration of Aliphatic Nitriles Using D_2O . *Chem. Commun.* **2018**, *54*, 8705–8708.
- (198) Kurita, T.; Hattori, K.; Seki, S.; Mizumoto, T.; Aoki, F.; Yamada, Y.; Ikawa, K.; Maegawa, T.; Monguchi, Y.; Sajiki, H. Efficient and Convenient Heterogeneous Palladium-Catalyzed Regioselective Deuteration at the Benzylic Position. *Chem.—Eur. J.* **2008**, *14*, 664–673.
- (199) Pfeifer, V.; Zeltner, T.; Fackler, C.; Kraemer, A.; Thoma, J.; Zeller, A.; Kiesling, R. Palladium Nanoparticles for the Deuteration and Tritiation of Benzylic Positions on Complex Molecules. *Angew. Chem., Int. Ed.* **2021**, *60*, 26671.
- (200) Palmer, W. N.; Chirik, P. J. Cobalt-Catalyzed Stereoretentive Hydrogen Isotope Exchange of $C(Sp^3)$ -H Bonds. *ACS Catal.* **2017**, *7*, 5674–5678.
- (201) Kuang, Y.; Cao, H.; Tang, H.; Chew, J.; Chen, W.; Shi, X.; Wu, J. Visible Light Driven Deuteration of Formyl C-H and Hydridic $C(Sp^3)$ -H Bonds in Feedstock Chemicals and Pharmaceutical Molecules. *Chem. Sci.* **2020**, *11*, 8912–8918.
- (202) Liu, M.; Chen, X.; Chen, T.; Yin, S.-F. A Facile and General Acid-Catalyzed Deuteration at Methyl Groups of N-Heteroaryl-methanes. *Org. Biomol. Chem.* **2017**, *15*, 2507–2511.
- (203) Wang, K.; Chen, X.; Peng, X.; Wang, P.; Liang, F. A Highly Selective H/D Exchange Reaction of 1,4-Dihydropyridines. *Org. Biomol. Chem.* **2019**, *17*, 3845–3852.
- (204) Tie, L.; Shan, X.-H.; Qu, J.-P.; Kang, Y.-B. α -Trideuteration of Methylarenes. *Org. Chem. Front.* **2021**, *8*, 2981–2984.
- (205) Huang, L.; Liu, W.; Zhao, L.-L.; Zhang, Z.; Yan, X. Base-Catalyzed H/D Exchange Reaction of Difluoromethylarenes. *J. Org. Chem.* **2021**, *86*, 3981–3988.
- (206) Kerr, W. J.; Reid, M.; Tuttle, T. Iridium-Catalyzed Formyl-Selective Deuteration of Aldehydes. *Angew. Chem., Int. Ed.* **2017**, *56*, 7808–7812.
- (207) Isbrandt, E.; Vandavasi, J.; Zhang, W.; Jamshidi, M.; Newman, S. Catalytic Deuteration of Aldehydes with D_2O . *Synlett* **2017**, *28*, 2851–2854.
- (208) Liu, W.; Zhao, L.-L.; Melaimi, M.; Cao, L.; Xu, X.; Bouffard, J.; Bertrand, G.; Yan, X. Mesomeric Carbene (MIC)-Catalyzed H/D Exchange at Formyl Groups. *Chem.* **2019**, *5*, 2484–2494.
- (209) Geng, H.; Chen, X.; Gui, J.; Zhang, Y.; Shen, Z.; Qian, P.; Chen, J.; Zhang, S.; Wang, W. Practical Synthesis of C1 Deuterated Aldehydes Enabled by NHC Catalysis. *Nat. Catal.* **2019**, *2*, 1071–1077.
- (210) Sawama, Y.; Miki, Y.; Sajiki, H. N-Heterocyclic Carbene Catalyzed Deuteration of Aldehydes in D_2O . *Synlett* **2020**, *31*, 699–702.
- (211) Gadekar, S. C.; Dhayalan, V.; Nandi, A.; Zak, I. L.; Mizrahi, M. S.; Kozuch, S.; Milo, A. Rerouting the Organocatalytic Benzoin Reaction toward Aldehyde Deuteration. *ACS Catal.* **2021**, *11*, 14561–14569.
- (212) Dong, J.; Wang, X.; Wang, Z.; Song, H.; Liu, Y.; Wang, Q. Formyl-Selective Deuteration of Aldehydes with D_2O via Synergistic Organic and Photoredox Catalysis. *Chem. Sci.* **2020**, *11*, 1026–1031.
- (213) Zhang, Y.; Ji, P.; Dong, Y.; Wei, Y.; Wang, W. Deuteration of Formyl Groups via a Catalytic Radical H/D Exchange Approach. *ACS Catal.* **2020**, *10*, 2226–2230.
- (214) Dong, J.-Y.; Xu, W.-T.; Yue, F.-Y.; Song, H.-J.; Liu, Y.-X.; Wang, W.-M. Visible-Light-Mediated Deuteration of Aldehydes with D_2O via Polarity-Matched Reversible Hydrogen Atom Transfer. *Tetrahedron* **2021**, *82*, 131946–131952.
- (215) Waterhouse, A. L.; Rapoport, H. Synthesis and Tritium Labeling of the Food Mutagens IQ and Methyl-IQ. *J. Labelled Compd. Radiopharm.* **1985**, *22*, 201–216.
- (216) Helfenbein, J.; Lartigue, C.; Noirault, E.; Azim, E.; Legaillard, J.; Galmier, M. J.; Madelmont, J. C. Isotopic Effect Study of Propofol Deuteration on the Metabolism, Activity, and Toxicity of the Anesthetic. *J. Med. Chem.* **2002**, *45*, S806–S808.
- (217) Kristensen, J. B.; Johansen, S. K.; Valsborg, J. S.; Martiny, L.; Foged, C. [14C] and [3H]-Labelling of Ragaglitazar: A Dual Acting PPAR α and PPAR γ Agonist with Hypolipidemic and Anti-Diabetic Activity. *J. Labelled Compd. Radiopharm.* **2003**, *46*, 475–488.
- (218) Damont, A.; Garcia-Argote, S.; Buisson, D.-A.; Rousseau, B.; Dollé, F. Efficient Tritiation of the Translocator Protein (18 kDa) Selective Ligand DPA-714. *J. Labelled Compd. Radiopharm.* **2015**, *58*, 1–6.
- (219) Artelsmaier, M.; Miranda-Azpiroz, P.; Kingston, L.; Bergare, J.; Schou, M.; Varrone, A.; Elmore, C. S. Synthesis, 3H-Labeling and in vitro Evaluation of a Substituted Dipiperidine Alcohol as a Potential Ligand for Chemokine Receptor 2. *J. Labelled Compd. Radiopharm.* **2019**, *62*, 265–279.
- (220) Liu, C.; Chen, Z.; Su, C.; Zhao, X.; Gao, Q.; Ning, G. H.; Zhu, H.; Tang, W.; Leng, K.; Fu, W.; et al. Controllable Deuteration of Halogenated Compounds by Photocatalytic D_2O Splitting. *Nat. Commun.* **2018**, *9*, 80.
- (221) Zhou, Z.-Z.; Zhao, J.-H.; Gou, X.-Y.; Chen, X.-M.; Liang, Y.-M. Visible-Light-Mediated Hydrodehalogenation and Br/D Exchange of Inactivated Aryl and Alkyl Halides with a Palladium Complex. *Org. Chem. Front.* **2019**, *6*, 1649–1654.
- (222) Higginson, B.; Sanjosé-Orduna, J.; Gu, Y.; Martin, R. Nickel-Catalyzed Photodehalogenation of Aryl Bromides. *Synlett* **2021**, *32*, 1633–1636.
- (223) Yang, L.; Zhang, C.-P. Additive-Free Visible-Light-Mediated Hydro-/Deuterodiazotization of Arenediazonium Tetrafluoroborates in THF/THF- d_6 . *Asian J. Org. Chem.* **2021**, *10*, 2157–2160.
- (224) Amin, H. I. M.; Raviola, C.; Amin, A. A.; Mannucci, B.; Protti, S.; Fagnoni, M. Hydro/Deutero Deamination of Arylazo Sulfones under Metal- and (Photo)Catalyst-Free Conditions. *Molecules* **2019**, *24*, 2164.
- (225) Lang, Y.; Peng, X.; Li, C.-J.; Zeng, H. Photoinduced Catalyst-Free Deborylation-Deuteration of Arylboronic Acids with D_2O . *Green Chem.* **2020**, *22*, 6323–6327.
- (226) Li, N.; Xiong, F.; Gao, K. Cobalt-Catalyzed Protodeboronation of Aryl and Vinyl Boronates. *J. Org. Chem.* **2021**, *86*, 1972–1979.
- (227) Yang, Y.; Gao, X.; Zeng, X.; Han, J.; Xu, B. Hydrogen-Bond-Donor Solvents Enable Catalyst-Free (Radio)-Halogenation and Deuteration of Organoborons. *Chem.—Eur. J.* **2021**, *27*, 1297–1300.
- (228) Wang, X.; Zhu, M.-H.; Schuman, D. P.; Zhong, D.; Wang, W.-Y.; Wu, L.-Y.; Liu, W.; Stoltz, B. M.; Liu, W.-B. General and Practical Potassium Methoxide/Disilane-Mediated Dehalogenative Deuteration of (Hetero)Arylhalides. *J. Am. Chem. Soc.* **2018**, *140*, 10970–10974.
- (229) Singh, B.; Ahmed, J.; Biswas, A.; Paira, R.; Mandal, S. K. Reduced Phenalenyl in Catalytic Dehalogenative Deuteration and Hydrodehalogenation of Aryl Halides. *J. Org. Chem.* **2021**, *86*, 7242–7255.
- (230) Yan, M.; Kawamata, Y.; Baran, P. S. Synthetic Organic Electrochemical Methods Since 2000: On the Verge of a Renaissance. *Chem. Rev.* **2017**, *117*, 13230–13319.
- (231) Tang, S.; Liu, Y.; Lei, A. Electrochemical Oxidative Cross-Coupling with Hydrogen Evolution: A Green and Sustainable Way for Bond Formation. *Chem.* **2018**, *4*, 27–45.
- (232) Liu, C.; Han, S.; Li, M.; Chong, X.; Zhang, B. Electrocatalytic Deuteration of Halides with D_2O as the Deuterium Source over a Copper Nanowire Arrays Cathode. *Angew. Chem., Int. Ed.* **2020**, *59*, 18527–18531.
- (233) Lu, L.; Li, H.; Zheng, Y.; Bu, F.; Lei, A. Facile and Economical Electrochemical Dehalogenative Deuteration of (Hetero)Aryl Halides. *CCS Chem.* **2021**, *3*, 2669–2675.
- (234) Kameo, H.; Yamamoto, J.; Asada, A.; Nakazawa, H.; Matsuzaka, H.; Bourissou, D. Palladium-Borane Cooperation: Evidence for an Anionic Pathway and Its Application to Catalytic Hydro-/Deutero-Dechlorination. *Angew. Chem., Int. Ed.* **2019**, *58*, 18783–18787.
- (235) Gair, J. J.; Grey, R. L.; Giroux, S.; Brodney, M. A. Palladium Catalyzed Hydrodefluorination of Fluoro-(Hetero)Arenes. *Org. Lett.* **2019**, *21*, 2482–2487.
- (236) Moore, J. T.; Lu, C. C. Catalytic Hydrogenolysis of Aryl C-F Bonds Using a Bimetallic Rhodium-Indium Complex. *J. Am. Chem. Soc.* **2020**, *142*, 11641–11646.
- (237) Kuriyama, M.; Kujirada, S.; Tsukuda, K.; Onomura, O. Nickel-Catalyzed Deoxygenative Deuteration of Aryl Sulfamates. *Adv. Synth. Catal.* **2017**, *359*, 1043–1048.

- (238) Iakovenko, R.; Hlaváč, J. Visible Light-Mediated Metal-Free Double Bond Deuteration of Substituted Phenylalkenes. *Green Chem.* **2021**, *23*, 440–446.
- (239) Kuriyama, M.; Yano, G.; Kiba, H.; Morimoto, T.; Yamamoto, K.; Demizu, Y.; Onomura, O. Palladium-Catalyzed Synthesis of Deuterated Alkenes through Deuterodechlorination of Alkenyl Chlorides. *Org. Process Res. Dev.* **2019**, *23*, 1552–1557.
- (240) Pape, F.; Brechmann, L. T.; Teichert, J. F. Catalytic Generation and Chemoselective Transfer of Nucleophilic Hydrides from Dihydrogen. *Chem.—Eur. J.* **2018**, *25*, 985–988.
- (241) Caldwell, R. A. Quantitative Deuteration of a Grignard Reagent. Preparation of 2-Butene-2-d. *J. Org. Chem.* **1970**, *35*, 1193–1194.
- (242) Curran, D. P.; Ramamoorthy, P. S. I. 2-Asymmetric Induction in Radical Reactions. Deuteration and Allylation Reactions of β -Oxy- α -Bromo Esters. *Tetrahedron* **1993**, *49*, 4841–4858.
- (243) Soulard, V.; Villa, G.; Vollmar, D. P.; Renaud, P. Radical Deuteration with D_2O : Catalysis and Mechanistic Insights. *J. Am. Chem. Soc.* **2018**, *140*, 155–158.
- (244) Song, Z.; Zeng, J.; Li, T.; Zhao, X.; Fang, J.; Meng, L.; Wan, Q. Water Compatible Hypophosphites- d_2 Reagents: Deuteration Reaction via Deutero-Deiodination in Aqueous Solution. *Org. Lett.* **2020**, *22*, 1736–1741.
- (245) They only exchange in highly acidic or basic media.
- (246) Xia, A.; Xie, X.; Hu, X.; Xu, W.; Liu, Y. Dehalogenative Deuteration of Unactivated Alkyl Halides Using D_2O as the Deuterium Source. *J. Org. Chem.* **2019**, *84*, 13841–13857.
- (247) Shao, T.; Li, Y.; Ma, N.; Li, C.; Chai, G.; Zhao, X.; Qiao, B.; Jiang, Z. Photoredox-Catalyzed Enantioselective α -Deuteration of Azaarenes with D_2O . *iScience* **2019**, *16*, 410–419.
- (248) Brož, B.; Marek, A. Tritiodefluorination of Alkyl C-F Groups. *J. Labelled Compd. Radiopharm.* **2019**, *62*, 743–750.
- (249) Zhao, G.; Yao, W.; Mauro, J. N.; Ngai, M.-Y. Excited-State Palladium-Catalyzed 1, 2-Spin-Center Shift Enables Selective C-2 Reduction, Deuteration, and Iodination of Carbohydrates. *J. Am. Chem. Soc.* **2021**, *143*, 1728–1734.
- (250) Kuang, Z.; Mai, S.; Yang, K.; Song, Q. Synthesis of anti-Vicinal Diboronates from Diarylethylenes and $B_{10}pin_2$. *Sci. Bull.* **2019**, *64*, 1685–1690.
- (251) Cook, A.; Prakash, S.; Zheng, Y.-L.; Newman, S. G. Exhaustive Reduction of Esters Enabled by Nickel Catalysis. *J. Am. Chem. Soc.* **2020**, *142*, 8109–8115.
- (252) Alvarez-Bercedo, P.; Martin, R. Ni-Catalyzed Reduction of Inert C–O Bonds: A New Strategy for Using Aryl Ethers as Easily Removable Directing Groups. *J. Am. Chem. Soc.* **2010**, *132*, 17352–17353.
- (253) Han, M.; Ma, X.; Yao, S.; Ding, Y.; Yan, Z.; Adijiang, A.; Wu, Y.; Li, H.; Zhang, Y.; Lei, P.; Ling, Y.; An, J. Development of a Modified Bouveault-Blanc Reduction for the Selective Synthesis of α,α -Dideutero Alcohols. *J. Org. Chem.* **2017**, *82*, 1285–1290.
- (254) Li, H.; Hou, Y.; Liu, C.; Lai, Z.; Ning, L.; Szostak, R.; Szostak, M.; An, J. Pentafluorophenyl Esters: Highly Chemoselective Ketyl Precursors for the Synthesis of α,α -Dideutero Alcohols Using SmI_2 and D_2O as a Deuterium Source. *Org. Lett.* **2020**, *22*, 1249–1253.
- (255) Luo, S.; Weng, C.; Ding, Y.; Ling, C.; Szostak, M.; Ma, X.; An, J. Reductive Deuteration of Aromatic Esters for the Synthesis of α,α -Dideutero Benzyl Alcohols Using D_2O as Deuterium Source. *Synlett* **2021**, *32*, 51–56.
- (256) Ramalingam, K.; Woodard, R. W. Synthesis of Stereospecific Deuterium-Labeled Homoserines and Homoserine Lactones. *J. Org. Chem.* **1988**, *53*, 1900–1903.
- (257) Monnat, F.; Vogel, P.; Meana, R.; Sordo, J. A. Equilibrium and Kinetic Deuterium Isotope Effects on the Hetero-Diels-Alder Addition of Sulfur Dioxide. *Angew. Chem., Int. Ed.* **2003**, *42*, 3924–3927.
- (258) Zhang, Y.-K.; Plattner, J. J.; Easom, B. E.; Liu, L.; Retz, D. M.; Ge, M.; Zhou, H.-H. Benzoxaborole Antimalarial Agents. Part 3: Design and Syntheses of (Carboxy-13C-3,3–2H₂)-labeled and (3–14C)-Labeled 7-(2-Carboxyethyl)-1,3-dihydro-1-hydroxy-2,1-benzoxaboroles. *J. Labelled Compd. Radiopharm.* **2012**, *55*, 201–205.
- (259) Zhu, Y.; Zhou, J.; Jiao, B. Deuterated Clopidogrel Analogues as a New Generation of Antiplatelet Agents. *ACS Med. Chem. Lett.* **2013**, *4*, 349–352.
- (260) Ahmadipour, S.; Pergolizzi, G.; Rejzek, M.; Field, R. A.; Miller, G. J. Chemoenzymatic Synthesis of C6-Modified Sugar Nucleotides to Probe the GDP-d-Mannose Dehydrogenase from *Pseudomonas aeruginosa*. *Org. Lett.* **2019**, *21*, 4415–4419.
- (261) Zhang, B.; Li, H.; Ding, Y.; Yan, Y.; An, J. Reduction and Reductive Deuteration of Tertiary Amides Mediated by Sodium Dispersions with Distinct Proton Donor-Dependent Chemoselectivity. *J. Org. Chem.* **2018**, *83*, 6006–6014.
- (262) Ding, Y.; Luo, S.; Adijiang, A.; Zhao, H.; An, J. Reductive Deuteration of Nitriles: The Synthesis of α,α -Dideutero Amines by Sodium-Mediated Electron Transfer Reactions. *J. Org. Chem.* **2018**, *83*, 12269–12274.
- (263) Ding, Y.; Luo, S.; Weng, C.; An, J. Reductive Deuteration of Nitriles Using D_2O as a Deuterium Source. *J. Org. Chem.* **2019**, *84*, 15098–15105.
- (264) Ning, L.; Li, H.; Lai, Z.; Szostak, M.; Chen, X.; Dong, Y.; Jin, S.; An, J. Synthesis of α -Deuterated Primary Amines via Reductive Deuteration of Oximes Using D_2O as a Deuterium Source. *J. Org. Chem.* **2021**, *86*, 2907–2916.
- (265) Mészáros, R.; Peng, B.-J.; Ötvös, S. B.; Yang, S.-C.; Fülöp, F. Continuous-Flow Hydrogenation and Reductive Deuteration of Nitriles: A Simple Access to α,α -Dideutero Amines. *ChemPlusChem.* **2019**, *84*, 1508–1511.
- (266) Yang, Z.; Zhu, X.; Yang, S.; Cheng, W.; Zhang, X.; Yang, Z. Iridium-Catalyzed Reductive Deoxygenation of Ketones with Formic Acid as Traceless Hydride Donor. *Adv. Synth. Catal.* **2020**, *362*, 5496–5505.
- (267) Ou, W.; Xiang, X.; Zou, R.; Xu, Q.; Loh, K. P.; Su, C. Room-Temperature Palladium-Catalyzed Deuteration of Carbon–Oxygen Bonds towards Deuterated Pharmaceuticals. *Angew. Chem., Int. Ed.* **2021**, *60*, 6357–6361.
- (268) Zhu, N.; Su, M.; Wan, W.-M.; Li, Y.; Bao, H. Practical Method for Reductive Deuteration of Ketones with Magnesium and D_2O . *Org. Lett.* **2020**, *22*, 991–996.
- (269) Li, H.; Hou, Y.; Lai, Z.; Ning, L.; Li, A.; Li, Y.; An, J. Synthesis of α -Deuterioalcohols by Single-Electron Umpolung Reductive Deuteration of Carbonyls Using D_2O as Deuterium Source. *Synlett* **2021**, *32*, 1241–1245.
- (270) Zhang, X.; Chen, J.; Gao, Y.; Li, K.; Zhou, Y.; Sun, W.; Fan, B. Photocatalyzed Transfer Hydrogenation and Deuteration of Cyclic N-Sulfonylimines. *Org. Chem. Front.* **2019**, *6*, 2410–2414.
- (271) Gao, Y.; Zhang, X.; Laishram, R. D.; Chen, J.; Li, K.; Zhang, K.; Zeng, G.; Fan, B. Cobalt-Catalyzed Transfer Hydrogenation of α -Ketoesters and N-Cyclicsulfonylimides Using H_2O as Hydrogen Source. *Adv. Synth. Catal.* **2019**, *361*, 3991–3997.
- (272) Li, B.; Chen, J.; Zhang, Z.; Gridnev, I. D.; Zhang, W. Nickel-Catalyzed Asymmetric Hydrogenation of N-Sulfonyl Imines. *Angew. Chem., Int. Ed.* **2019**, *58*, 7329–7334.
- (273) Yang, P.; Zhang, L.; Fu, K.; Sun, Y.; Wang, X.; Yue, J.; Ma, Y.; Tang, B. Nickel-Catalyzed Asymmetric Transfer Hydrogenation and α -Selective Deuteration of N-Sulfonyl Imines with Alcohols: Access to α -Deuterated Chiral Amines. *Org. Lett.* **2020**, *22*, 8278–8284.
- (274) Zhang, X.; Chen, J.; Gao, Y.; Li, K.; Zhou, Y.; Sun, W.; Fan, B. Photocatalyzed Transfer Hydrogenation and Deuteration of Cyclic N-Sulfonylimines. *Org. Chem. Front.* **2019**, *6*, 2410–2414.
- (275) Ruiz-Castañeda, M.; Carrión, M. C.; Santos, L.; Manzano, B. R.; Espino, G.; Jalon, F. A. A Biphasic Medium Slows Down the Transfer Hydrogenation and Allows a Selective Catalytic Deuterium Labeling of Amines from Imines Mediated by a Ru-H/D + Exchange in D_2O . *ChemCatChem.* **2018**, *10*, 5541–5550.
- (276) Carrión, M. C.; Ruiz-Castañeda, M.; Espino, G.; Aliende, C.; Santos, L.; Rodríguez, A. M.; Manzano, B. R.; Jalon, F. A.; Lledós, A. Selective Catalytic Deuterium Labeling of Alcohols during a Transfer Hydrogenation Process of Ketones Using D_2O as the Only Deuterium Source. Theoretical and Experimental Demonstration of a Ru-H/D + Exchange as the Key Step. *ACS Catal.* **2014**, *4*, 1040–1053.

- (277) Guo, S.; Wang, X.; Zhou, J. S. Asymmetric Umpolung Hydrogenation and Deuteration of Alkenes Catalyzed by Nickel. *Org. Lett.* **2020**, *22*, 1204–1207.
- (278) Lethu, S.; Ano, H.; Murata, M.; Matsuoka, S. Enantioselective Deuteration of β -Substituted α,β -Unsaturated Esters by Rhodium-1,2-Bis(2,5-Diphenylphospholano)Ethane: Enantioselective Deuteration of β -Substituted α,β -Unsaturated Esters by Rhodium-1,2-Bis(2,5-Diphenylphospholano)Ethane. *Eur. J. Org. Chem.* **2018**, *2018*, 235–239.
- (279) Liu, X.; Liu, R.; Qiu, J.; Cheng, X.; Li, G. Chemical-Reductant-Free Electrochemical Deuteration Reaction Using Deuterium Oxide. *Angew. Chem., Int. Ed.* **2020**, *59*, 13962–13967.
- (280) Li, H.; Zhang, B.; Dong, Y.; Liu, T.; Zhang, Y.; Nie, H.; Yang, R.; Ma, X.; Ling, Y.; An, J. A Selective and Cost-Effective Method for the Reductive Deuteration of Activated Alkenes. *Tetrahedron Lett.* **2017**, *58*, 2757–2760.
- (281) Pearlman, W. H.; Pearlman, M. R. J. Preparation of 6,7- d_2 -Estrone Acetate. *J. Am. Chem. Soc.* **1950**, *72*, 5781.
- (282) Saljoughian, M.; Morimoto, H.; Williams, P. G.; Rapoport, H. Specific Labelling of Putrescine Dihydrochloride by Heterogeneous Hydrogenation with Deuterium or Tritium Gas in Dimethyl Sulfoxide. *J. Labelled Compd. Radiopharm.* **1988**, *25*, 313–328.
- (283) Oba, M.; Ishihara, T.; Satake, H.; Nishiyama, K. Stereoselective Synthesis of 1-[2,3,4,5- D_4]Ornithine. *J. Labelled Compd. Radiopharm.* **2002**, *45*, 619–627.
- (284) Zhang, Y.; Tortorella, M. D.; Wang, Y.; Liu, J.; Tu, Z.; Liu, X.; Bai, Y.; Wen, D.; Lu, X.; Lu, Y.; et al. Synthesis of Deuterated Benzopyran Derivatives as Selective COX-2 Inhibitors with Improved Pharmacokinetic Properties. *ACS Med. Chem. Lett.* **2014**, *5*, 1162–1166.
- (285) Haider, A.; Gobbi, L.; Kretz, J.; Ullmer, C.; Brink, A.; Honer, M.; Woltering, T. J.; Muri, D.; Iding, H.; Bürkner, M.; et al. Identification and Preclinical Development of a 2,5,6-Trisubstituted Fluorinated Pyridine Derivative as a Radioligand for the Positron Emission Tomography Imaging of Cannabinoid Type 2 Receptors. *J. Med. Chem.* **2020**, *63*, 10287–10306.
- (286) Enomoto, A.; Kapit, S.; Fujita, K. Convenient Method for the Production of Deuterium Gas Catalyzed by an Iridium Complex and Its Application to the Deuteration of Organic Compounds. *Chem. Lett.* **2019**, *48*, 106–109.
- (287) Espinal-Viguri, M.; Neale, S. E.; Coles, N. T.; Macgregor, S. A.; Webster, R. L. Room Temperature Iron-Catalyzed Transfer Hydrogenation and Regioselective Deuteration of Carbon-Carbon Double Bonds. *J. Am. Chem. Soc.* **2019**, *141*, 572–582.
- (288) Wang, Y.; Cao, X.; Zhao, L.; Pi, C.; Ji, J.; Cui, X.; Wu, Y. Generalized Chemoselective Transfer Hydrogenation/Hydrodeuteration. *Adv. Synth. Catal.* **2020**, *362*, 4119–4129.
- (289) Walker, J. C. L.; Oestreich, M. Regioselective Transfer Hydrodeuteration of Alkenes with a Hydrogen Deuteride Surrogate Using $B(C_6F_5)_3$ Catalysis. *Org. Lett.* **2018**, *20*, 6411–6414.
- (290) Li, L.; Hilt, G. Regiodivergent DH or HD Addition to Alkenes: Deuterohydrogenation versus Hydrodeuteration. *Org. Lett.* **2020**, *22*, 1628–1632.
- (291) Li, L.; Hilt, G. Indium Tribromide-Catalyzed Transfer-Hydrogenation: Expanding the Scope of the Hydrogenation and of the Regiodivergent DH or HD Addition to Alkenes. *Chem.—Eur. J.* **2021**, *27*, 11221–11225.
- (292) Vang, Z. P.; Reyes, A.; Sonstrom, R. E.; Holdren, N. S.; Sloane, S. E.; Alansari, I. Y.; Neill, J. L.; Pate, B. H.; Clark, J. R. Copper-catalyzed Transfer Hydrodeuteration of Aryl Alkenes with Quantitative Isotopomer Purity Analysis by Molecular Rotational Resonance Spectroscopy. *J. Am. Chem. Soc.* **2021**, *143*, 7707–7718.
- (293) Rowbotham, J. S.; Ramirez, M. A.; Lenz, O.; Reeve, H. A.; Vincent, K. A. Bringing Biocatalytic Deuteration into the Toolbox of Asymmetric Isotopic Labelling Techniques. *Nat. Commun.* **2020**, *11*, 1454.
- (294) For a discussion of further NAD regeneration systems, please see the following: Rowbotham, J. S.; Reeve, H. A.; Vincent, K. A. Hybrid Chemo-, Bio-, and Electrocatalysis for Atom-Efficient Deuteration of Cofactors in Heavy Water. *ACS Catal.* **2021**, *11*, 2596–2604.
- (295) Gao, J.; Ma, R.; Feng, L.; Liu, Y.; Jackstell, R.; Jagadeesh, R. V.; Beller, M. Ambient Hydrogenation and Deuteration of Alkenes Using a Nanostructured Ni-Core-Shell Catalyst. *Angew. Chem., Int. Ed.* **2021**, *60*, 18591–18598.
- (296) Zhao, C.-Q.; Chen, Y.-G.; Qiu, H.; Wei, L.; Fang, P.; Mei, T.-S. Water as a Hydrogenating Agent: Stereodivergent Pd-Catalyzed Semihydrogenation of Alkynes. *Org. Lett.* **2019**, *21*, 1412–1416.
- (297) Cf. also a copper-catalyzed transfer semideuteration of alkynes to cis-olefins with EtOD: Bao, H.; Zhou, B.; Jin, H.; Liu, Y. Diboron-Assisted Copper-Catalyzed Z-Selective Semihydrogenation of Alkynes Using Ethanol as a Hydrogen Donor. *J. Org. Chem.* **2019**, *84*, 3579–3589. However, deuteration is only demonstrated in one example.
- (298) Han, M.; Ding, Y.; Yan, Y.; Li, H.; Luo, S.; Adijiang, A.; Ling, Y.; An, J. Transition-Metal-Free, Selective Reductive Deuteration of Terminal Alkynes with Sodium Dispersions and EtOD- d_4 . *Org. Lett.* **2018**, *20*, 3010–3013.
- (299) Wu, Y.; Liu, C.; Wang, C.; Lu, S.; Zhang, B. Selective Transfer Semihydrogenation of Alkynes with H_2O (D_2O) as the H (D) Source over a Pd-P Cathode. *Angew. Chem., Int. Ed.* **2020**, *59*, 21170–21175.
- (300) Kurimoto, A.; Sherbo, R. S.; Cao, Y.; Loo, N. W. X.; Berlinguette, C. P. Electrolytic Deuteration of Unsaturated Bonds without Using D_2 . *Nat. Catal.* **2020**, *3*, 719–726.
- (301) Sloane, S. E.; Reyes, A.; Vang, Z. P.; Li, L.; Behlow, K. T.; Clark, J. R. Copper-Catalyzed Formal Transfer Hydrogenation/Deuteration of Aryl Alkynes. *Org. Lett.* **2020**, *22*, 9139–9144.
- (302) Lecomte, M.; Lahboubi, M.; Thilmany, P.; El Bouzakhi, A.; Evans, G. A General, Versatile and Divergent Synthesis of Selectively Deuterated Amines. *Chem. Sci.* **2021**, *12*, 11157–11165.
- (303) Smith, J. A.; Wilson, K. B.; Sonstrom, R. E.; Kelleher, P. J.; Welch, K. D.; Pert, E. K.; Westendorff, K. S.; Dickie, D. A.; Wang, X.; Pate, B. H.; et al. Preparation of Cyclohexene Isotopologues and Stereoisotopomers from Benzene. *Nature* **2020**, *581*, 288–293.
- (304) Feng, K.; Quevedo, R. E.; Kohrt, J. T.; Oderinde, M. S.; Reilly, U.; White, M. C. Late-Stage Oxidative C(Sp³)-H Methylation. *Nature* **2020**, *580*, 621–627.
- (305) Schönherr, H.; Cernak, T. Profound Methyl Effects in Drug Discovery and a Call for New C-H Methylation Reactions. *Angew. Chem., Int. Ed.* **2013**, *52*, 12256–12267.
- (306) O'Reilly, M. C.; Scott, S. A.; Brown, K. A.; Oguin, T. H.; Thomas, P. G.; Daniels, J. S.; Morrison, R.; Brown, H. A.; Lindsley, C. W. Development of Dual PLD1/2 and PLD2 Selective Inhibitors from a Common 1,3,8-Triazaspiro[4.5]Decane Core: Discovery of ML298 and ML299 That Decrease Invasive Migration in U87-MG Glioblastoma Cells. *J. Med. Chem.* **2013**, *56*, 2695–2699.
- (307) Manley, P. W.; Blasco, F.; Mestan, J.; Aichholz, R. The Kinetic Deuterium Isotope Effect as Applied to Metabolic Deactivation of Imatinib to the Des-Methyl Metabolite, CGP74588. *Bioorg. Med. Chem.* **2013**, *21*, 3231–3239.
- (308) Komarapuri, S.; Krishnan, K.; Covey, D. F. Synthesis of 19-Trideuterated *Ent*-Testosterone and the GABA_A Receptor Potentiators *Ent*-Androsterone and *Ent*-Ethinolanolone. *J. Labelled Compd. Radiopharm.* **2008**, *51*, 430–434.
- (309) Antonchick, A. P.; Schneider, B.; Zhabinskii, V. N.; Khripach, V. A. Synthesis of [26,27– $^{2}H_6$]Brassinosteroids from 23,24-Bisnorcholelic Acid Methyl Ester. *Steroids* **2004**, *69*, 617–628.
- (310) Khripach, V. A.; Zhabinskii, V. N.; Antonchick, A. P.; Konstantinova, O. V.; Schneider, B. Synthesis of Hexadeuterated 23-Dehydroxybrassinosteroids. *Steroids* **2002**, *67*, 1101–1108.
- (311) Sklyaruk, J.; Borghs, J. C.; El-Sepelgy, O.; Rueping, M. Catalytic C1 Alkylation with Methanol and Isotope-Labeled Methanol. *Angew. Chem., Int. Ed.* **2019**, *58*, 775–779.
- (312) Magre, M.; Szewczyk, M.; Rueping, M. N-Methylation and Trideuteromethylation of Amines via Magnesium-Catalyzed Reduction of Cyclic and Linear Carbamates. *Org. Lett.* **2020**, *22*, 3209–3214.
- (313) Zhang, R.; Yu, H.; Li, Z.; Yan, Q.; Li, P.; Wu, J.; Qi, J.; Jiang, M.; Sun, L. Iron-Mediated Azidomethylation or Azidotrideuteromethylation

- tion of Active Alkenes with Azidotrimethylsilane and Dimethyl Sulfoxide. *Adv. Synth. Catal.* **2018**, *360*, 1384–1388.
- (314) Zhang, X.; Chen, Q.; Song, R.; Xu, J.; Tian, W.; Li, S.; Jin, Z.; Chi, Y. R. Carbene-Catalyzed α,γ -Deuteration of Enals under Oxidative Conditions. *ACS Catal.* **2020**, *10*, 5475–5482.
- (315) Zhang, Z.; Qiu, C.; Xu, Y.; Han, Q.; Tang, J.; Loh, K. P.; Su, C. Semiconductor Photocatalysis to Engineering Deuterated N-Alkyl Pharmaceuticals Enabled by Synergistic Activation of Water and Alkanols. *Nat. Commun.* **2020**, *11*, 4722.
- (316) Zhu, M.-H.; Yu, C.-L.; Feng, Y.-L.; Usman, M.; Zhong, D.; Wang, X.; Nesnas, N.; Liu, W.-B. Detosylative (Deutero)Alkylation of Indoles and Phenols with (Deutero)Alkoxides. *Org. Lett.* **2019**, *21*, 7073–7077.
- (317) Han, X.; Yuan, Y.; Shi, Z. Rhodium-Catalyzed Selective C-H Trideuteromethylation of Indole at C7 Position Using Acetic- d_3 Anhydride. *J. Org. Chem.* **2019**, *84*, 12764–12772.
- (318) Caporaso, R.; Manna, S.; Zinken, S.; Kochnev, A. R.; Lukyanenko, E. R.; Kurkin, A. V.; Antonchick, A. P. Radical Trideuteromethylation with Deuterated Dimethyl Sulfoxide in the Synthesis of Heterocycles and Labelled Building Blocks. *Chem. Commun.* **2016**, *52*, 12486–12489.
- (319) Zhang, R.; Shi, X.; Yan, Q.; Li, Z.; Wang, Z.; Yu, H.; Wang, X.; Qi, J.; Jiang, M. Free-Radical Initiated Cascade Methylation or Trideuteromethylation of Isocyanides with Dimethyl Sulfoxides. *RSC Adv.* **2017**, *7*, 38830–38833.
- (320) Garza-Sanchez, R. A.; Patra, T.; Tlahuext-Aca, A.; Strieth-Kalthoff, F.; Glorius, F. DMSO as a Switchable Alkylating Agent in Heteroarene C-H Functionalization. *Chem.—Eur. J.* **2018**, *24*, 10064–10068.
- (321) Agasti, S.; Maity, S.; Szabo, K. J.; Maiti, D. Palladium-Catalyzed Synthesis of 2,3-Disubstituted Benzofurans: An Approach Towards the Synthesis of Deuterium Labeled Compounds. *Adv. Synth. Catal.* **2015**, *357*, 2331–2338.
- (322) Song, D.; Chen, L.; Li, Y.; Liu, T.; Yi, X.; Liu, L.; Ling, F.; Zhong, W. Ruthenium Catalyzed α -Methylation of Sulfones with Methanol as a Sustainable C1 Source. *Org. Chem. Front.* **2021**, *8*, 120–126.
- (323) Xia, H.-M.; Zhang, F.-L.; Ye, T.; Wang, Y.-F. Selective α -Monomethylation by an Amine-Borane/ N,N -Dimethylformamide System as the Methyl Source. *Angew. Chem., Int. Ed.* **2018**, *57*, 11770–11775.
- (324) Pipal, R. W.; Stout, K. T.; Musacchio, P. Z.; Ren, S.; Graham, T. J. A.; Verhoog, S.; Gantert, L.; Lohith, T. G.; Schmitz, A.; Lee, H. S.; et al. Metallaphotoredox Aryl and Alkyl Radiomethylation for PET Ligand Discovery. *Nature* **2021**, *589*, 542–547.
- (325) Jin, J.; Tong, J.; Yu, W.; Qiao, J.; Shen, C. Iodobenzene-Catalyzed Oxidative C-H α -Alkoxylation of Quinoxalinones with Deuterated Alcohols. *Catal. Commun.* **2020**, *141*, 106008.
- (326) Shen, Z.; Zhang, S.; Geng, H.; Wang, J.; Zhang, X.; Zhou, A.; Yao, C.; Chen, X.; Wang, W. Trideuteromethylation Enabled by a Sulfoxonium Metathesis Reaction. *Org. Lett.* **2019**, *21*, 448–452.
- (327) Huang, C.-M.; Li, J.; Ai, J.-J.; Liu, X.-Y.; Rao, W.; Wang, S.-Y. Visible-Light-Promoted Cross-Coupling Reactions of Aryldiazonium Salts with S -Methyl- d_3 Sulfonothioate or Se -Methyl- d_3 Selenium Sulfonate: Synthesis of Trideuteromethylated Sulfides, Sulfoxides, and Selenides. *Org. Lett.* **2020**, *22*, 9128–9132.
- (328) Wang, M.; Zhao, Y.; Zhao, Y.; Shi, Z. Bioinspired Design of a Robust D3-Methylating Agent. *Sci. Adv.* **2020**, *6*, No. eaba0946.
- (329) Zafarani, Y.; Sod-Moriah, G.; Segall, Y. Diethyl Bromodifluoromethylphosphonate: A Highly Efficient and Environmentally Benign Difluorocarbene Precursor. *Tetrahedron* **2009**, *65*, 5278–5283.
- (330) Geng, Y.; Zhu, M.; Liang, A.; Niu, C.; Li, J.; Zou, D.; Wu, Y.; Wu, Y. O-Difluorodeuteromethylation of Phenols Using Difluorocarbene Precursors and Deuterium Oxide. *Org. Biomol. Chem.* **2018**, *16*, 1807–1811.
- (331) Plutschack, M. B.; Pieber, B.; Gilmore, K.; Seeberger, P. H. The Hitchhiker's Guide to Flow Chemistry. *Chem. Rev.* **2017**, *117*, 11796–11893.
- (332) Fu, W. C.; Jamison, T. F. Deuteriodifluoromethylation and gem-Difluoroalkenylation of Aldehydes Using $ClCF_2H$ in Continuous Flow. *Angew. Chem., Int. Ed.* **2020**, *59*, 13885–13890.
- (333) Sowaileh, M. F.; Han, C.; Hazlitt, R. A.; Kim, B. H.; John, J. P.; Colby, D. A. Conversion of Methyl Ketones and Methyl Sulfones into α -Deutero- α,α -difluoromethyl Ketones and α -Deutero- α,α -difluoromethyl Sulfones in Three Synthetic Steps. *Tetrahedron Lett.* **2017**, *58*, 396–400.
- (334) Liang, J.; Wang, G.; Dong, L.; Pang, X.; Qin, J.; Xu, X.; Shao, X.; Li, Z. CF₂DSO₂Na: An Effective Precursor Reagent for Deuteriodifluoromethylthiolation and Deuteriodifluoromethylation. *Org. Lett.* **2021**, *23*, 5545–5548.
- (335) Li, X.; Wu, S.; Chen, S.; Lai, Z.; Luo, H.-B.; Sheng, C. One-Pot Synthesis of Deuterated Aldehydes from Arylmethyl Halides. *Org. Lett.* **2018**, *20*, 1712–1715.
- (336) Ibrahim, M. Y. S.; Denmark, S. E. Palladium/Rhodium Cooperative Catalysis for the Production of Aryl Aldehydes and Their Deuterated Analogues Using the Water-Gas Shift Reaction. *Angew. Chem., Int. Ed.* **2018**, *57*, 10362–10367.
- (337) Zhang, M.; Yuan, X.-A.; Zhu, C.; Xie, J. Deoxygenative Deuteration of Carboxylic Acids with D₂O. *Angew. Chem., Int. Ed.* **2019**, *58*, 312–316.
- (338) Breuer, F. W. Chloroform- d (Deuteriochloroform)1. *J. Am. Chem. Soc.* **1935**, *57*, 2236–2237.
- (339) Earing, M. H.; Cloke, J. B. A New Synthesis of Chloroform- d_1 . *J. Am. Chem. Soc.* **1951**, *73*, 769–770.
- (340) Kluger, R. A Convenient Preparation of Chloroform- d_1 . *J. Org. Chem.* **1964**, *29*, 2045–2046.
- (341) Paulsen, P. J.; Cooke, W. D. Preparation of Deuterated Solvents for Nuclear Magnetic Resonance Spectrometry. *Anal. Chem.* **1963**, *35*, 1560.
- (342) Tansukawat, N. D.; See, A. E.; Jiranuntarat, S.; Corbin, J. R.; Schomaker, J. M. Method for Small-Scale Production of Deuteriochloroform. *J. Org. Chem.* **2018**, *83*, 8739–8742.
- (343) Higuera-Padilla, A. R.; Kock, F. V. C.; Batista, A. A.; Colnago, L. A. A Straightforward Catalytic Approach to Obtain Deuterated Chloroform at Room Temperature. *Magn. Reson. Chem.* **2020**, *58*, 917–920.
- (344) Akula, H. K.; Lakshman, M. K. Synthesis of Deuterated 1,2,3-Triazoles. *J. Org. Chem.* **2012**, *77*, 8896–8904.
- (345) Cera, G.; Della Ca', N.; Maestri, G. Palladium(0)/Benzoic Acid Catalysis Merges Sequences with D₂O-Promoted Labelling of C-H Bonds. *Chem. Sci.* **2019**, *10*, 10297–10304.
- (346) Liu, Y.; Yu, Y.; Sun, C.; Fu, Y.; Mang, Z.; Shi, L.; Li, H. Transition-Metal Free Chemoselective Hydroxylation and Hydroxylation-Deuteration of Heterobenzylic Methylene. *Org. Lett.* **2020**, *22*, 8127–8131.
- (347) Tanwar, L.; Börgel, J.; Ritter, T. Synthesis of Benzylic Alcohols by C-H Oxidation. *J. Am. Chem. Soc.* **2019**, *141*, 17983–17988.
- (348) Guha, S.; Sekar, G. Metal-Free Halogen(I) Catalysts for the Oxidation of Aryl(heteroaryl)methanes to Ketones or Esters: Selectivity Control by Halogen Bonding. *Chem.—Eur. J.* **2018**, *24*, 14171–14182.
- (349) Shi, S.; Li, R.; Rao, L.; Sun, Z. A Mild, General, and Metal-Free Method for Site-Specific Deuteration Induced by Visible Light Using D₂O as the Source of Deuterium Atoms. *Green Chem.* **2020**, *22*, 669–672.
- (350) Xia, Y.; Studer, A. Diversity-Oriented Desulfonylative Functionalization of Alkyl Allyl Sulfones. *Angew. Chem., Int. Ed.* **2019**, *58*, 9836–9840.
- (351) Wang, L.; Xia, Y.; Derdau, V.; Studer, A. Remote Site-Selective Radical C(Sp³)-H Monodeuteration of Amides Using D₂O. *Angew. Chem., Int. Ed.* **2021**, *60*, 18645–18650.
- (352) Yang, H.; Zhang, L.; Zhou, F.-Y.; Jiao, L. An Umpolung Approach to the Hydroboration of Pyridines: A Novel and Efficient Synthesis of N -H 1,4-Dihydropyridines. *Chem. Sci.* **2020**, *11*, 742–747.
- (353) Liu, S.; Shen, T.; Luo, Z.; Liu, Z.-Q. A Free Radical Alkylation of Quinones with Olefins. *Chem. Commun.* **2019**, *55*, 4027–4030.

- (354) Li, W.; Cai, H.; Huang, L.; He, L.; Zhang, Y.; Xu, J.; Zhang, P. Iron(III)-Mediated Rapid Radical-Type Three-Component Deuteration of Quinoxalones with Olefins and NaBD4. *Front. Chem.* **2020**, *8*, 606.
- (355) Ji, L.; Gu, W.; Liu, P.; Sun, P. Iron-Mediated Deuterium Addition Cascade Cyano Insertion/Cyclization of *N*-Arylacrylamides to Access Deuterium-Labelled Phenanthridines. *Org. Biomol. Chem.* **2020**, *18*, 6126–6133.
- (356) Bokale-Shivale, S.; Amin, M. A.; Sawant, R. T.; Stevens, M. Y.; Turanlı, L.; Hallberg, A.; Waghmode, S. B.; Odell, L. R. Synthesis of Substituted 3,4-Dihydroquinazolinones via a Metal Free Leuckart-Wallach Type Reaction. *RSC Adv.* **2021**, *11*, 349–353.
- (357) Ji, P.; Zhang, Y.; Dong, Y.; Huang, H.; Wei, Y.; Wang, W. Synthesis of Enantioenriched α -Deuterated α -Amino Acids Enabled by an Organophotocatalytic Radical Approach. *Org. Lett.* **2020**, *22*, 1557–1562.
- (358) Liao, K.; Hu, X.; Zhu, R.; Rao, R.; Yu, J.; Zhou, F.; Zhou, J. Catalytic Enantioselective Protonation of Monofluorinated Silyl Enol Ethers towards Chiral α -Fluoroketones. *Chin. J. Chem.* **2019**, *37*, 799–806.
- (359) Guo, L.; Xu, C.; Wu, D.-C.; Hu, G.-Q.; Zhang, H.-H.; Hong, K.; Chen, S.; Liu, X. Cascade Alkylation and Deuteration with Aryl Iodides via Pd/Norbornene Catalysis: An Efficient Method for the Synthesis of Congested Deuterium-Labeled Arenes. *Chem. Commun.* **2019**, *55*, 8567–8570.
- (360) Yamada, T.; Kuwata, M.; Takakura, R.; Monguchi, Y.; Sajiki, H.; Sawama, Y. Organocatalytic Nitroaldol Reaction Associated with Deuterium-Labeling. *Adv. Synth. Catal.* **2018**, *360*, 637–641.
- (361) Ledovskaya, M. S.; Voronin, V. V.; Rodygin, K. S.; Posvyatenko, A. V.; Egorova, K. S.; Ananikov, V. P. Direct Synthesis of Deuterium-Labeled O-, S-, N-Vinyl Derivatives from Calcium Carbide. *Synthesis* **2019**, *51*, 3001–3013.
- (362) Ledovskaya, M. S.; Voronin, V. V.; Polynski, M. V.; Lebedev, A. N.; Ananikov, V. P. Primary Vinyl Ethers as Acetylene Surrogate: A Flexible Tool for Deuterium-Labeled Pyrazole Synthesis. *Eur. J. Org. Chem.* **2020**, *2020*, 4571–4580.
- (363) Voronin, V. V.; Ledovskaya, M. S.; Gordeev, E. G.; Rodygin, K. S.; Ananikov, V. P. [3 + 2]-Cycloaddition of in Situ Generated Nitrile Imines and Acetylene for Assembling of 1,3-Disubstituted Pyrazoles with Quantitative Deuterium Labeling. *J. Org. Chem.* **2018**, *83*, 3819–3828.
- (364) Ledovskaya, M. S.; Rodygin, K. S.; Ananikov, V. P. Calcium-Mediated One-Pot Preparation of Isoxazoles with Deuterium Incorporation. *Org. Chem. Front.* **2018**, *5*, 226–231.
- (365) Patel, M.; Saunthwal, R. K.; Verma, A. K. Base-Mediated Deuteration of Organic Molecules: A Mechanistic Insight. *ACS Omega* **2018**, *3*, 10612–10623.
- (366) Xie, J.; Li, N.; Ning, Y.-Y.; Wu, X.; Li, W.; Zhu, C. A Highly Selective Decarboxylative Deuteration of Carboxylic Acids. *Chem. Sci.* **2021**, *12*, 5505–5510.
- (367) Chen, S.; Wang, J.; Xie, L.-G. Transition Metal-Free Formal Hydro/Deuteromethylthiolation of Unactivated Alkenes. *Org. Biomol. Chem.* **2021**, *19*, 4037–4042.
- (368) Wu, R.; Gao, K. B. (C6F5)₃-catalyzed Tandem Protonation/Deuteration and Reduction of in situ-Formed Enamines. *Org. Biomol. Chem.* **2021**, *19*, 4032–4036.
- (369) Sun, C.; Yu, Y.; Zhang, X.; Liu, Y.; Sun, C.; Kai, G.; Shi, L.; Li, H. Transition-Metal-Free Decarbonylative Alkylation towards *N*-Aryl α -Hydroxy Amides via Triple C-C Bond Cleavages and Their Selective Deuteration. *Org. Chem. Front.* **2021**, *8*, 4814–4819.
- (370) Porte, V.; Zhang, H.; Kaiser, D.; Maulide, N. Harnessing Ynamide Activation to Access Deuterated Carbonyls. *Tetrahedron* **2021**, *90*, 132211.
- (371) Soponpong, J.; Dolsophon, K.; Thongpanchang, C.; Linden, A.; Thongpanchang, T. Application of Deuterated THENA for Assigning the Absolute Configuration of Chiral Secondary Alcohols. *Tetrahedron Lett.* **2019**, *60*, 497–500.
- (372) Saito, F.; Gerbig, D.; Becker, J.; Schreiner, P. R. Breaking the Symmetry of a Meso Compound by Isotopic Substitution: Synthesis and Stereochemical Assignment of Monodeuterated Cis-Perhydroazulene. *Org. Lett.* **2021**, *23*, 113–117.
- (373) Gan, X.; Wilson, M. W.; Beyett, T. S.; Wen, B.; Sun, D.; Larsen, S. D.; Tesmer, J. J. G.; Saltiel, A. R.; Showalter, H. D. Synthesis of Deuterium-Labelled Amlexanox and Its Metabolic Stability against Mouse, Rat, and Human Microsomes. *J. Labelled Compd. Radiopharm.* **2019**, *62*, 202–208.
- (374) Makarova, M.; Barrientos, R. C.; Torres, O. B.; Matyas, G. R.; Jacobson, A. E.; Sulima, A.; Rice, K. C. Synthesis of a Deuterated 6-AmHap Internal Standard for the Determination of Hapten Density in a Heroin Vaccine Drug Product. *J. Labelled Compd. Radiopharm.* **2020**, *63*, 564–571.
- (375) Dai, X.; Lv, C.; Sun, J.; Li, S. A Facile Synthesis of Isotope Labeled Acylcarnitines. *J. Labelled Compd. Radiopharm.* **2021**, *64*, 217–224.
- (376) Sigüeiro, R.; Loureiro, J.; González-Berdullas, P.; Mouriño, A.; Maestro, M. A. Synthesis of 28,28,28-Trideutero-25-Hydroxydihydro-tachysterol. *J. Steroid Biochem. Mol. Biol.* **2019**, *185*, 248–250.
- (377) Regner, M.; Bartuce, A.; Padmakshan, D.; Ralph, J.; Karlen, S. D. Reductive Cleavage Method for Quantitation of Monolignols and Low-Abundance Monolignol Conjugates. *ChemSusChem* **2018**, *11*, 1600–1605.
- (378) Porcelli, C.; Kreissl, J.; Steinhaus, M. Enantioselective Synthesis of Tri-Deuterated (–)-Geosmin to Be Used as Internal Standard in Quantitation Assays. *J. Labelled Compd. Radiopharm.* **2020**, *63*, 476–481.
- (379) Hesk, D.; Koharski, D.; McNamara, P.; Royster, P.; Saluja, S.; Truong, V.; Voronin, K. Synthesis of 3H, 13C2, 2H4 14C-SCH 430765 and 35S-SCH 500946, Potent and Selective Inhibitors of the NPY5 Receptor. *J. Labelled Compd. Radiopharm.* **2018**, *61*, 533–539.
- (380) Mosafari, S.; Jelley, R. E.; Fedrizzi, B.; Barker, D. Scalable Synthesis of the Aroma Compounds D6- β -Ionone and D6- β -Cyclo-citral for Use as Internal Standards in Stable Isotope Dilution Assays. *Tetrahedron Lett.* **2020**, *61*, 152642.
- (381) Bergare, J.; Kingston, L.; Guly, D. J.; Dolan, J.; Lewis, R. J.; Elmore, C. S. The Synthesis of One H-2 Labeled and Two H-3 Labeled Leukotriene C4 Synthase Inhibitors. *J. Labelled Compd. Radiopharm.* **2020**, *63*, 434–441.
- (382) Hesk, D.; Borges, S.; Dumpit, R.; Hendershot, S.; Koharski, D.; McNamara, P.; Ren, S.; Saluja, S.; Truong, V.; Voronin, K. Synthesis of ³H, ²H₄ and ³⁸⁴C-MK 3814 (Preladenant). *J. Labelled Compd. Radiopharm.* **2017**, *60*, 194–199.
- (383) Dietz, C.; Clark, R. B.; Nichols, F. C.; Smith, M. B. Convergent Synthesis of a Deuterium-Labeled Serine Dipeptide Lipid for Analysis of Biological Samples. *J. Labelled Compd. Radiopharm.* **2017**, *60*, 274–285.
- (384) Pedras, M. S. C.; To, Q. H. Synthesis of Stable Isotope-Labeled Nasturlexins and Potential Precursors to Probe Biosynthetic Pathways of Cruciferous Phytoalexins. *J. Labelled Compd. Radiopharm.* **2018**, *61*, 94–106.
- (385) Westaway, K. C. Using Kinetic Isotope Effects to Determine the Structure of the Transition States of SN2 Reactions. *Adv. Phys. Org. Chem.* **2006**, *41*, 217–273.
- (386) Mu, D.; Yuan, W.; Chen, S.; Wang, N.; Yang, B.; You, L.; Zu, B.; Yu, P.; He, C. Streamlined Construction of Silicon-Stereogenic Silanes by Tandem Enantioselective C-H Silylation/Alkene Hydrosilylation. *J. Am. Chem. Soc.* **2020**, *142*, 13459–13468.
- (387) Yang, W.; Li, Y.; Zhu, J.; Liu, W.; Ke, J.; He, C. Lewis Acid-Assisted Ir(III) Reductive Elimination Enables Construction of Seven-Membered-Ring Sulfoxides. *Chem. Sci.* **2020**, *11*, 10149–10158.
- (388) Nguyen, Q.-H.; Guo, S.-M.; Royal, T.; Baudoin, O.; Cramer, N. Intermolecular Palladium(0)-Catalyzed Atropo-Enantioselective C-H Arylation of Heteroarenes. *J. Am. Chem. Soc.* **2020**, *142*, 2161–2167.
- (389) Yang, Q.-L.; Wang, X.-Y.; Lu, J.-Y.; Zhang, L.-P.; Fang, P.; Mei, T.-S. Copper-Catalyzed Electrochemical C-H Amination of Arenes with Secondary Amines. *J. Am. Chem. Soc.* **2018**, *140*, 11487–11494.
- (390) Wang, Q.; Zhang, W.-W.; Song, H.; Wang, J.; Zheng, C.; Gu, Q.; You, S.-L. Rhodium-Catalyzed Atroposelective Oxidative C-H/C-H Cross-Coupling Reaction of 1-Aryl Isoquinoline Derivatives with

Electron-Rich Heteroarenes. *J. Am. Chem. Soc.* **2020**, *142*, 15678–15685.

(391) Saper, N. I.; Ohgi, A.; Small, D. W.; Semba, K.; Nakao, Y.; Hartwig, J. F. Nickel-Catalyzed Anti-Markovnikov Hydroarylation of Unactivated Alkenes with Unactivated Arenes Facilitated by Non-Covalent Interactions. *Nat. Chem.* **2020**, *12*, 276–283.

(392) Schreiber, B. S.; Carreira, E. M. Palladium-Catalyzed Regioselective C-H Iodination of Unactivated Alkenes. *J. Am. Chem. Soc.* **2019**, *141*, 8758–8763.

(393) Ghiringhelli, F.; Uttry, A.; Ghosh, K. K.; Gemmeren, M. Direct B- and -C(Sp³)-H Alkynylation of Free Carboxylic Acids**. *Angew. Chem., Int. Ed.* **2020**, *59*, 23127–23131.

(394) Lei, H.; Rovis, T. Ir-Catalyzed Intermolecular Branch-Selective Allylic C-H Amidation of Unactivated Terminal Olefins. *J. Am. Chem. Soc.* **2019**, *141*, 2268–2273.

(395) Wang, C.; Yu, Y.; Liu, W.-L.; Duan, W.-L. Site-Tunable C_{sp}³-H Bonds Functionalization by Visible-Light-Induced Radical Translocation of *N*-Alkoxyphthalimides. *Org. Lett.* **2019**, *21*, 9147–9152.

(396) Li, Z.; Wang, Q.; Zhu, J. Copper-Catalyzed Arylation of Remote C(Sp³)-H Bonds in Carboxamides and Sulfonamides. *Angew. Chem., Int. Ed.* **2018**, *57*, 13288–13292.

(397) Kapoor, M.; Liu, D.; Young, M. C. Carbon Dioxide-Mediated C(Sp³)-H Arylation of Amine Substrates. *J. Am. Chem. Soc.* **2018**, *140*, 6818–6822.

(398) de Azambuja, F.; Yang, M.-H.; Feoktistova, T.; Selvaraju, M.; Brueckner, A. C.; Grove, M. A.; Koley, S.; Cheong, P. H.-Y.; Altman, R. A. Connecting Remote C-H Bond Functionalization and Decarboxylative Coupling Using Simple Amines. *Nat. Chem.* **2020**, *12*, 489–496.

(399) Hu, M.-Y.; He, P.; Qiao, T.-Z.; Sun, W.; Li, W.-T.; Lian, J.; Li, J.-H.; Zhu, S.-F. Iron-Catalyzed Regiodivergent Alkyne Hydrosilylation. *J. Am. Chem. Soc.* **2020**, *142*, 16894–16902.

(400) Saljoughian, M. Synthetic Tritium Labeling: Reagents and Methodologies. *Synthesis* **2002**, *2002*, 1781–1801.

(401) Artelsmair, M.; Miranda-Azpiroz, P.; Kingston, L.; Bergare, J.; Schou, M.; Varone, A.; Elmore, C. S. Synthesis, ³H-Labeling and in vitro Evaluation of a Substituted Dipiperidine Alcohol as a Potential Ligand for Chemokine Receptor 2. *J. Labelled. Compd. Radiopharm.* **2019**, *62*, 265–279.

(402) Lindelof, A.; Ericsson, C.; Simonsson, R.; Nilsson, G.; Gronberg, G.; Elmore, C. S. Synthesis of [³H] and [³H₂]AZD6642, an Inhibitor of S-Lipoxygenase Activating Protein (FLAP). *J. Labelled. Compd. Radiopharm.* **2016**, *59*, 340–345.

(403) Subburaju, S.; Sromek, A. W.; Seeman, P.; Neumeier, J. L. New Dopamine D2 Receptor Agonist, [³H]MCL-536, for Detecting Dopamine D2high Receptors in Vivo. *ACS Chem. Neurosci.* **2018**, *9*, 1283–1289.

(404) Bergare, J.; Kingston, L.; Guly, D. J.; Dolan, J.; Lewis, R. J.; Elmore, C. S. The Synthesis of One H-2 Labeled and Two H-3 Labeled Leukotriene C4 Synthase Inhibitors. *J. Labelled. Compd. Radiopharm.* **2020**, *63*, 434–441.

(405) Filer, C. N.; Byon, C. S-(4-Nitrobenzyl)-6-Thioinosine: Tritium Labeling at High Specific Activity. *J. Labelled. Compd. Radiopharm.* **2020**, *63*, 426–429.

(406) Allen, P.; Bragg, R. A.; Caffrey, M.; Ericsson, C.; Hickey, M. J.; Kingston, L. P.; Elmore, C. S. The Synthesis of a Tritium, Carbon-14, and Stable Isotope-labeled Cathepsin C Inhibitors. *J. Labelled. Compd. Radiopharm.* **2017**, *60*, 124–129.

(407) Zhang, Y. Preparation of Tritium-Labeled PF-622, a Novel Fatty Acid Amide Hydrolase Inhibitor. *J. Labelled. Compd. Radiopharm.* **2017**, *60*, 608–615.

(408) Ellison, C.; Rapoport, H.; Laursen, R.; Elliott, H. W. Effect of Deuteration of N-CH3 Group on Potency and Enzymatic N-Demethylation of Morphine. *Science* **1961**, *134*, 1078–1079.

(409) Raju, T. N. K. The Nobel Chronicles. *Lancet* **2000**, *355*, 1022.

(410) Kaur, N.; Kumar, P.; Jamwal, S.; Deshmukh, R.; Gauttam, V. Tetrabenazine: Spotlight on Drug Review. *Ann. Neurosci.* **2016**, *23*, 176–185.

(411) Garay, R. P.; Grossberg, G. T. AVP-786 for the Treatment of Agitation in Dementia of the Alzheimer's Type. *Expert Opin. Investig. Drugs* **2017**, *26*, 121–132.

(412) Cargnin, S.; Serafini, M.; Pirali, T. A Primer of Deuterium in Drug Design. *Future Med. Chem.* **2019**, *11*, 2039–2042.

(413) Belz, T. F.; Bremer, P. T.; Zhou, B.; Ellis, B.; Eubanks, L. M.; Janda, K. D. Enhancement of a Heroin Vaccine through Hapten Deuteration. *J. Am. Chem. Soc.* **2020**, *142*, 13294–13298.

Recommended by ACS

Catalytic Electrophilic Halogenation of Arenes with Electron-Withdrawing Substituents

Weijun Wang, Ning Jiao, et al.

JULY 15, 2022

JOURNAL OF THE AMERICAN CHEMICAL SOCIETY

READ

Analysis of Metabolic Pathways by ¹³C-Labeled Molecular Probes and HRMAS Nuclear Magnetic Resonance Spectroscopy: Isotopologue Identification and Quantification

Hassiba Ouilafi, Izzie J. Namer, et al.

JUNE 03, 2022

ANALYTICAL CHEMISTRY

READ

Easy-to-Implement Hydrogen Isotope Exchange for the Labeling of *N*-Heterocycles, Alkylamines, Benzylic Scaffolds, and Pharmaceuticals

Etienne Levernier, Grégory Pieters, et al.

APRIL 01, 2022

JACS AU

READ

Photoinduced Dynamic Radical Processes for Isomerizations, Deracemizations, and Dynamic Kinetic Resolutions

Jacob S. DeHovitz and Todd K. Hyster

JULY 11, 2022

ACS CATALYSIS

READ

Get More Suggestions >

SARA KOPF

Leibniz Institute for Catalysis
Albert-Einstein-Str. 29A, Room 1.120, 18059 Rostock
Phone: +493811281178
Email: sara.kopf@catalysis.de
Born 29th October 1995 in Magdeburg, Germany

ORCID: 0000-0002-6395-9396

Languages: German (native), English (fluent), Portuguese (intermediate), Spanish (intermediate), Latinum



EDUCATION

- 2020 – 2022** **PhD in Organic Chemistry** at the Leibniz Institute for Catalysis (LIKAT), Rostock, Germany.
Supervisors: Prof. Matthias Beller, Dr. Helfried Neumann.
Thesis: “*Development of Hydrogen Isotope Exchange Methodologies for the Deuteration of Aromatic Substrates*”
Handed in on 15th June 2022, defended on 25th October 2022
- 2017 – 2019** **MSc in Chemistry** at the University of Heidelberg, Germany and the University of Cambridge, UK.
Master thesis: “*New Dimensions in Bioisosterism: Synthesis of Phosphorus-Containing Acids as Drug Analogues and Evaluation of their Properties for the Use in Medicinal Chemistry.*” (1.0); carried out at Boehringer Ingelheim, Biberach an der Riß, Germany, under the supervision of Prof. Stephen Hashmi and Dr. Jörg Hehn.
Final grade: 1.1 (final oral exam: 1.0)
Supported by a scholarship of the Kaufmann-Peters-Stiftung and an Erasmus+ scholarship.
- 2013 – 2016** **BSc in Chemistry** at the University of Heidelberg, Germany.
Bachelor thesis: “*Fluorescence-based Investigation of Enzyme Kinetics on 5'-NAD-RNA.*” (1.0); carried out under the supervision of Prof. Andres Jäschke.
Final grade: 1.3 (final oral exam: 1.0)
- 2005 – 2013** **Abitur** at Carl-Bosch-Gymnasium in Ludwigshafen am Rhein, Germany.
Final grade: 1.0
GDCh (Gesellschaft Deutscher Chemiker)-Award for the school's best Abitur in chemistry (2013); Award of the mayor of Ludwigshafen for the school's best Abitur (2013)

ADDITIONAL RESEARCH AND WORK EXPERIENCE

- 09 – 10/2021** Guest researcher in isotope chemistry at Sanofi, Frankfurt am Main, Germany. *Deuteration of carbohydrates by borrowing hydrogen techniques.* Supervisor: Dr. Volker Derdau.

2019 – 2020	PhD studies in Organic Chemistry at the Institut Català d'Investigació Química (ICIQ), Tarragona, Spain. <i>Development of a photochemical bioconjugation strategy for the selective modification of tryptophan residues in peptides and DFT studies on catalytic photochemical reactions</i> . Supervisors: Prof. Paolo Melchiorre, Prof. Feliu Maseras.
2015 – 2018	Freelancer at the BASF Teens' Labs, Ludwigshafen am Rhein, Germany (supervised high school students in chemistry projects).
04 – 07/2018	Tutor in organic chemistry for students of molecular biotechnology at the University of Heidelberg, Germany.
02 – 04/2018	Research intern in biophysical chemistry at the Max Planck Institutes for Medical Research (Heidelberg, Germany) and Intelligent Systems (Stuttgart, Germany). <i>Chemically induced growth of giant unilamellar vesicles with encapsulated DNA</i> . Supervisor: Prof. Joachim Spatz.
10 – 12/2017	Research intern in medicinal chemistry at the University of Heidelberg, Germany. <i>Synthesis of peptide β-lactams as flaviviral NS3 protease inhibitors</i> . Supervisor: Prof. Christian Klein.
08 – 09/2017	Industry intern in polymer chemistry at BASF, Ludwigshafen am Rhein, Germany. <i>Tuning the physicochemical properties of polyesteramides</i> . Supervisor: Dr. Martin Rübenacker.
2016 – 2017	Research intern in inorganic chemistry at the University of Cambridge, UK. <i>Coordination chemistry and post-functionalisation of tris-pyridyl aluminates</i> . Supervisor: Prof. Dominic Wright.

PUBLICATIONS

8. [Sara Kopf](#), Jiali Liu, Robert Franke, Haijun Jiao, Helfried Neumann, and Matthias Beller, "Base-Mediated Remote Deuteration of *N*-Heteroarenes – Broad Scope and Mechanism", *Eur. J. Org. Chem.* **2022**, e202200204.
7. [Sara Kopf](#), Florian Bourriquen, Wu Li, Helfried Neumann, Kathrin Junge, and Matthias Beller, "Recent Developments for the Deuterium and Tritium Labeling of Organic Molecules" *Chem. Rev.* **2022**, 122, 6634–6718.
6. [Sara Kopf](#), Fei Ye, Helfried Neumann, and Matthias Beller, "Ruthenium-Catalyzed Deuteration of Aromatic Carbonyl Compounds with a Catalytic Transient Directing Group" *Chem. Eur. J.* **2021**, 27, 9768–9773. Front cover *Chem. Eur. J.* 38/2021.
5. [Sara Kopf](#), Helfried Neumann, and Matthias Beller, "Manganese-Catalyzed Selective C–H Activation and Deuteration by Means of a Catalytic Transient Directing Group Strategy" *Chem. Commun.* **2021**, 57, 1137–1140.
4. Florian Abele, Katharina Höfer, Patrick Bernhard, Julia Grawenhoff, Maximilian Seidel, André Krause, [Sara Kopf](#), Martin Schröter, and Andres Jäschke, "A Novel NAD-RNA Decapping Pathway Discovered by Synthetic Light-up NAD-RNAs" *Biomolecules* **2020**, 10, 513.
3. Tonko Dražić, [Sara Kopf](#), James Corridan, Mila M. Leuthold, Branimir Bertoša, and Christian D. Klein, "Peptide- β -lactam inhibitors of dengue and West Nile virus NS2B-NS3 protease display two distinct binding modes" *J. Med. Chem.* **2020**, 63, 140–156.
2. Alex J. Plajer, [Sara Kopf](#), Annie L. Colebatch, Andrew D. Bond, Dominic S. Wright, and Raúl García-Rodríguez, "Deprotonation, insertion and isomerisation in the post-functionalisation of tris-pyridyl aluminates" *Dalton Trans.* **2019**, 48, 5692–5697.

1. Raúl García-Rodríguez, Sara Kopf, and Dominic S. Wright, "Modifying the donor properties of tris(pyridyl) aluminates in lanthanide(II) sandwich compounds" *Dalton Trans.* **2018**, 47, 2232–2239.

Sara Kopf, Peter Finkbeiner, Stephan Heß, and Jörg Hehn, "New Dimensions in Bioisosterism: Synthesis of Phosphorus-Containing Acids as Drug Analogues and Evaluation of their Properties for the Use in Medicinal Chemistry", *manuscript in preparation*.

PARTICIPATION IN INTERNATIONAL CONFERENCES

4. **Poster** "Base-Mediated Remote Deuteration of *N*-Heteroarenes" at the Belgian Organic Synthesis Symposium (BOSS) XVII in Namur, Belgium.
3. **Oral communication** "Selective Hydrogen Isotope Exchange with Transient Directing Groups" at the International Isotope Society-Central European Division (IIS-CED) Symposium 2021, online.
2. **Poster** "Manganese-catalyzed deuteration with transient directing groups" at the Tetrahedron Symposium 2021, online.
1. **Oral communication** „Selective Hydrogen Isotope Exchange with Transient Directing Groups" at Cutting Edge Homogeneous Catalysis-1 (CEHC-1), online.

VOLUNTEERING

- | | |
|------------------|--|
| 11/2021– 10/2022 | PhD representative at LIKAT, Rostock. |
| 10/2020– 09/2021 | Mentor in CyberMentor program to encourage and motivate female school students for natural sciences. |

11 References

- ¹ K. B. Wiberg. The Deuterium Isotope Effect. *Chem. Rev.* **1955**, *55*, 713–743, doi:10.1021/cr50004a004.
- ² a) K. H. Gardner, L. E. Kay. The Use of ^2H , ^{13}C , ^{15}N Multidimensional NMR to Study the Structure and Dynamics of Proteins. *Annu. Rev. Biophys. Biomol. Struct.* **1998**, *27*, 357–406, doi:10.1146/annurev.biophys.27.1.357; b) C. N. Filer. Progress in Tritium NMR: 1990–2005. *J. Radioanal. Nucl. Chem.* **2006**, *268*, 663–669, doi:10.1007/s10967-006-0187-5; c) B. Reif. Deuteration for High-Resolution Detection of Protons in Protein Magic Angle Spinning (MAS) Solid-State NMR. *Chem. Rev.* **2022**, *122*, 10019–10035, doi:10.1021/acs.chemrev.1c00681.
- ³ a) J. Atzrodt, V. Derdau, W. J. Kerr, M. Reid. Deuterium- and Tritium-Labelled Compounds: Applications in the Life Sciences. *Angew. Chem. Int. Ed.* **2018**, *57*, 1758–1784, doi:10.1002/anie.201704146; b) E. I. James, T. A. Murphree, C. Vorauer, J. R. Engen, M. Guttman. Advances in Hydrogen/Deuterium Exchange Mass Spectrometry and the Pursuit of Challenging Biological Systems. *Chem. Rev.* **2022**, *122*, 7562–7623, doi:10.1021/acs.chemrev.1c00279.
- ⁴ J. A. Krauser. A Perspective on Tritium Versus Carbon-14: Ensuring Optimal Label Selection in Pharmaceutical Research and Development. *J. Labelled Compd. Radiopharm.* **2013**, *56*, 441–446, doi:10.1002/jlcr.3085.
- ⁵ Selected examples: a) D. M. Lustosa, S. Clemens, M. Rudolph, A. S. K. Hashmi. Gold-Catalyzed One-Pot Synthesis of 1,3-Disubstituted Allenes from Benzaldehydes and Terminal Alkynes. *Adv. Synth. Catal.* **2019**, *361*, 5050–5056, doi:10.1002/adsc.201900824; b) Y. Ge, F. Ye, J. Yang, A. Spannenberg, H. Jiao, R. Jackstell, M. Beller. Palladium-Catalyzed Cascade Carbonylation to α,β -Unsaturated Piperidones via Selective Cleavage of Carbon–Carbon Triple Bonds. *Angew. Chem. Int. Ed.* **2021**, *60*, 22393–22400, doi:10.1002/anie.202108120; c) Y. Dong, A. W. Schuppe, B. K. Mai, P. Liu, S. Buchwald. Confronting the Challenging Asymmetric Carbonyl 1,2-Addition Using Vinyl Heteroarene Pronucleophiles: Ligand-Controlled Regiodivergent Processes through a Dearomatized Allyl–Cu Species. *J. Am. Chem. Soc.* **2022**, *144*, 5985–5995, doi:10.1021/jacs.2c00734.
- ⁶ a) M. Gómez-Gallego, M. A. Sierra. Kinetic Isotope Effects in the Study of Organometallic Reaction Mechanisms. *Chem. Rev.* **2011**, *111*, 4857–4963, doi:10.1021/cr100436k; b) E. M. Simmons, J. F. Hartwig. On the Interpretation of Deuterium Kinetic Isotope Effects in C–H Bond Functionalizations by Transition-Metal Complexes. *Angew. Chem. Int. Ed.* **2012**, *51*, 3066–3072, doi:10.1002/anie.201107334.
- ⁷ a) F. W. Breuer. Chloroform-*d* (Deuteriochloroform). *J. Am. Chem. Soc.* **1935**, *57*, 2236–2237, doi:10.1021/ja01314a058; b) T. He, H. F. T. Klare, M. Oestreich. Perdeuteration of Deactivated Aryl Halides by H/D Exchange under Superelectrophile Catalysis. *J. Am. Chem. Soc.* **2022**, *144*, 4734–4738, doi:10.1021/jacs.2c00080.
- ⁸ Selected examples: a) A. Lindelof, C. Ericsson, R. Simonsson, G. Nilsson, G. Gronberg, C. S. Elmore. Synthesis of [^3H] and [$^2\text{H}_6$]AZD6642, an Inhibitor of 5-Lipoxygenase Activating Protein (FLAP). *J. Labelled Compd. Radiopharm.* **2016**, *59*, 340–345, doi:10.1002/jlcr.3409; b) S. Subburaju, A. W. Sromek, P. Seeman, J. L. Neumeyer. New Dopamine D2 Receptor Agonist, [^3H]MCL-536, for Detecting Dopamine D2 High Receptors in Vivo. *ACS Chem. Neurosci.* **2018**, *9*, 1283–

- 1289, doi:10.1021/acscemneuro.8b00096; c) M. Artelsmair, P. Miranda-Azpiazu, L. Kingston, J. Bergare, M. Schou, A. Varrone, C. S. Elmore. Synthesis, ^3H -Labelling and in vitro Evaluation of a Substituted Dipiperidine Alcohol as a Potential Ligand for Chemokine Receptor 2. *J. Labelled Compd. Radiopharm.* **2019**, *62*, 265–279, doi:10.1002/jlcr.3731.
- ⁹ Selected examples: a) J. Atzrodt, J. Blankenstein, D. Brasseur, S. Calvo-Vicente, M. Denoux, V. Derdau, M. Lavis, S. Perard, S. Roy, M. Sandvoss, J. Schofield, J. Zimmermann. Synthesis of Stable Isotope Labelled Internal Standards for Drug–Drug Interaction (DDI) Studies. *Bioorg. Med. Chem.* **2012**, *20*, 5658–5667, doi:10.1016/j.bmc.2012.06.052; b) R. Loos, R. Carvalho, D. C. António, S. Comero, G. Locoro, S. Tavazzi, B. Paracchini, M. Ghiani, T. Lettieri, L. Blaha, B. Jarasova, S. Voorspoels, K. Servaes, P. Haglund, J. Fick, R. H. Lindberg, D. Schwesig, B. M. Gawlik. EU-Wide Monitoring Survey on Emerging Polar Organic Contaminants in Wastewater Treatment Plant Effluents. *Water Res.* **2013**, *47*, 6475–6487, doi:10.1016/j.watres.2013.08.024; c) K. H. Kim, S. Y. Lee, D. G. Kim, S.-Y. Lee, J. Y. Kim, J. S. Yoo. Absolute Quantification of N-Glycosylation of Alpha-Fetoprotein Using Parallel Reaction Monitoring with Stable Isotope-Labeled N-Glycopeptide as an Internal Standard. *Anal. Chem.* **2020**, *92*, 12588–12595, doi:10.1021/acs.analchem.0c02563; d) R. D. Jansen-van Vuuren, R. Vohra. Synthesis of $[2\text{H}_5]$ Baricitinib via $[2\text{H}_5]$ Ethanesulfonyl Chloride. *J. Labelled Compd. Radiopharm.* **2022**, *65*, 156–161, doi:10.1002/jlcr.3969.
- ¹⁰ C. Schmidt. First Deuterated Drug Approved. *Nat. Biotechnol.* **2017**, *35*, 493–494, doi:10.1038/nbt0617-493.
- ¹¹ S. J. Keam, S. Duggan. Donafenib: First Approval. *Drugs* **2021**, *81*, 1915–1920, doi:10.1007/s40265-021-01603-0.
- ¹² T. Pirali, M. Serafini, S. Cargnin, A. A. Genazzani. Applications of Deuterium in Medicinal Chemistry. *J. Med. Chem.* **2019**, *62*, 5276–5297, doi:10.1021/acs.jmedchem.8b01808.
- ¹³ Selected examples: a) M. Shao, J. Keum, J. Chen, Y. He, W. Chen, J. F. Browning, J. Jakowski, B. G. Sumpter, I. N. Ivanov, Y.-Z. Ma, C. M. Rouleau, S. C. Smith, D. B. Geohegan, K. Hong, K. Xiao. The Isotopic Effects of Deuteration on Optoelectronic Properties of Conducting Polymers. *Nat. Commun.* **2014**, *5*, 3180, doi:10.1038/ncomms4180; b) H. J. Bae, J. S. Kim, A. Yakubovich, J. Jeong, S. Park, J. Chwae, S. Ishibe, Y. Jung, V. K. Rai, W.-J. Son, S. Kim, H. Choi, M.-H. Baik. Protecting Benzylic C–H Bonds by Deuteration Doubles the Operational Lifetime of Deep-Blue Ir-Phenylimidazole Dopants in Phosphorescent OLEDs. *Adv. Opt. Mater.* **2021**, *9*, 2100630, doi:10.1002/adom.202100630; c) X. Liu, C.-Y. Chan, F. Mathevet, M. Mamada, Y. Tsuchiya, Y.-T. Lee, H. Nakanotani, S. Kobayashi, M. Shiochi, C. Adachi. Isotope Effect of Host Material on Device Stability of Thermally Activated Delayed Fluorescence Organic Light-Emitting Diodes. *Small Sci.* **2021**, *1*, 2000057, doi:10.1002/smss.202000057.
- ¹⁴ Selected examples: a) D. Hesk, S. Borges, R. Dumpit, S. Hendershot, D. Koharski, P. McNamara, S. Ren, S. Saluja, V. Truong, K. Voronin. Synthesis of ^3H , $^2\text{H}_4$, and ^{3834}C -MK 3814 (Preladenant). *J. Labelled Compd. Radiopharm.* **2017**, *60*, 194–199, doi:10.1002/jlcr.3490; b) D. Hesk, D. Koharski, P. McNamara, P. Royster, S. Saluja, V. Truong, K. Voronin. Potent and Selective Inhibitors of the NPY5 Receptor. *J. Labelled Compd. Radiopharm.* **2018**, *61*, 533–539, doi:10.1002/jlcr.3617; c) M. Makarova, R. C. Barrientos, O. B. Torres, G. R. Matyas, A. E. Jacobsen, A. Sulima, K. C. Rice. Synthesis of a Deuterated 6-AmHap Internal Standard for the

- Determination of Hapten Density in a Heroin Vaccine Drug Product. *J. Labelled Compd. Radiopharm.* **2020**, *63*, 564–571, doi:10.1002/jlcr.3880; d) J. Bergare, L. Kingston, D. J. Guly, R. J. Lewis, C. S. Elmore. The Synthesis of One H-2 Labeled and Two H-3 Labeled Leukotriene C4 Synthase Inhibitors. *J. Labelled Compd. Radiopharm.* **2020**, *63*, 434–441, doi:10.1002/jlcr.3862.
- ¹⁵ Selected examples: a) D. Jakubczyk, C. Barth, A. Kubas, F. Anastassacos, P. Koelsch, K. Fink, U. Schepers, G. Brenner-Weiß, S. Bräse. Deuterium-labelled *N*-acyl-L-homoserine lactones (AHLs)—inter-kingdom signalling molecules—synthesis, structural studies, and interactions with model lipid membranes. *Anal. Bioanal. Chem.* **2012**, *403*, 473–482, doi:10.1007/s00216-012-5839-4; b) N. R. Yepuri, S. A. Jamieson, T. A. Darwish, A. Rawal, J. M. Hook, P. Thordarson, P. J. Holden, M. James. Synthesis of Per-Deuterated Alkyl Amines for the Preparation of Deuterated Organic Pyromellitimide Gelators. *Tetrahedron Lett.* **2013**, *54*, 2538–2541, doi:10.1016/j.tetlet.2013.03.031.
- ¹⁶ Selected examples: a) K. Ramalingam, R. W. Woodard. Synthesis of Stereospecific Deuterium-Labeled Homoserines and Homoserine Lactones. *J. Org. Chem.* **1988**, *53*, 1900–1903, doi:10.1021/jo00244a012; b) F. Monnat, P. Vogel, R. Meana, J. A. Sordo. Equilibrium and Kinetic Deuterium Isotope Effects on the Hetero-Diels-Alder Addition of Sulfur Dioxide. *Angew. Chem. Int. Ed.* **2003**, *42*, 3924–3927, doi:10.1002/anie.200351732; c) Y.-K. Zhang, J. J. Plattner, E. E. Easom, L. Liu, D. M. Retz, M. Ge, H.-H. Zhou. Benzoxaborole Antimalarial Agents. Part 3: Design and Syntheses of (Carboxy-¹³C-3,3-²H₂)-labeled and (3-¹⁴C)-Labeled 7-(2-Carboxyethyl)-1,3-dihydro-1-hydroxy-2,1-benzoxaboroles. *J. Labelled Compd. Radiopharm.* **2012**, *55*, 201–205, doi:10.1002/jlcr.2926; d) Y. Zhu, J. Zhou, B. Jiao. Deuterated Clopidogrel Analogues as a New Generation of Antiplatelet Agents. *ACS Med. Chem. Lett.* **2013**, *4*, 349–352, doi:10.1021/ml300460t; e) F. Saito, D. Gerbig, J. Becker, P. R. Schreiner. Breaking the Symmetry of a *Meso* Compound by Isotopic Substitution: Synthesis and Stereochemical Assignment of Monodeuterated *Cis*-Perhydroazulene. *Org. Lett.* **2021**, *23*, 113–117, doi:10.1021/acs.orglett.0c03795.
- ¹⁷ Please *cf.* throughout the chapter: S. Kopf, F. Bourriquen, W. Li, H. Neumann, K. Junge, M. Beller. Recent Developments for the Deuterium and Tritium Labeling of Organic Molecules. *Chem. Rev.* **2022**, *122*, 6634–6718, doi:10.1021/acs.chemrev.1c00795.
- ¹⁸ *Cf.* further recent reviews on this topic: a) X. Yang, H. Ben, A. J. Ragauskas. Recent Advances in the Synthesis of Deuterium-Labeled Compounds. *Asian J. Org. Chem.* **2021**, *10*, 2473–2485, doi:10.1002/ajoc.202100381; b) G. Prakash, N. Paul, G. A. Oliver, D. B. Werz, D. Maiti. C–H Deuteration of Organic Compounds and Potential Drug Candidates. *Chem. Soc. Rev.* **2022**, *51*, 3123–3163, doi:10.1039/D0CS01496F.
- ¹⁹ Review on reductive deuteration of unsaturated C–C bonds: a) Z. P. Wang, S. J. Hintzsche, J. R. Clark. Catalytic Transfer Deuteration and Hydrodeuteration: Emerging Techniques to Selectively Transform Alkenes and Alkynes to Deuterated Alkanes. *Chem. Eur. J.* **2021**, *27*, 9988–10000, doi:10.1002/chem.202100635; selected examples for the reductive deuteration of carbonyl groups: b) J. S. Rowbotham, M. A. Ramirez, O. Lenz, H. A. Reeve, K. A. Vincent. Bringing Biocatalytic Deuteration into the Toolbox of Asymmetric Isotopic Labelling Techniques. *Nat. Commun.* **2020**, *11*, 1454, doi:10.1038/s41467-020-15310-z; c) A. Cook, S. Prakash, Y.-L. Zheng, S. G. Newman. Exhaustive Reduction of Esters Enabled by Nickel Catalysis. *J. Am. Chem. Soc.* **2020**, *142*, 8109–8115, doi:10.1021/jacs.0c02405; d) W. Ou, X. Xiang, R. Zou, Q. Xu, K. P.

- Loh, C. Su. Room-Temperature Palladium-Catalyzed Deuteroanalysis of Carbon Oxygen Bonds towards Deuterated Pharmaceuticals. *Angew. Chem., Int. Ed.* **2021**, *60*, 6357–6361, doi:10.1002/anie.202014196; Selected example for olefine deuteration: e) J. Gao, R. Ma, L. Feng, Y. Liu, R. Jackstell, R. V. Jagadeesh, M. Beller. Ambient Hydrogenation and Deuteration of Alkenes Using a Nanostructured Ni-Core-Shell Catalyst. *Angew. Chem., Int. Ed.* **2021**, *60*, 18591–18598, doi:10.1002/anie.202105492; Selected examples for the reductive deuteration of olefins with Pd/C and D₂: f) W. H. Pearlman, M. R. J. Pearlman. Preparation of 6,7-*d*₂-Estrone Acetate. *J. Am. Chem. Soc.* **1950**, *72*, 5781, doi:10.1021/ja01168a537; g) M. Saljoughian, H. Morimoto, P. G. Williams, H. Rapaport. Specific Labelling of Putrescine Dihydrochloride by Heterogeneous Hydrogenation with Deuterium or Tritium Gas in Dimethyl Sulfoxide. *J. Labelled Compd. Radiopharm.* **1988**, *25*, 313–328, doi:10.1002/jlcr.2580250311; h) M. Oba, T. Ishihara, H. Satake, K. Nishiyama. Stereoselective Synthesis of L-[2,3,4,5-D₄]Ornithine. *J. Labelled Compd. Radiopharm.* **2002**, *45*, 619–627, doi:10.1002/jlcr.592; i) Y. Zhang, M. D. Tortorella, Y. Wang, J. Liu, Z. Tu, X. Liu, Y. Bai, D. Wen, X. Lu, Y. Lu, J. J. Talley. Synthesis of Deuterated Benzopyran Derivatives as Selective COX-2 Inhibitors with Improved Pharmacokinetic Properties. *ACS Med. Chem. Lett.* **2014**, *5*, 1162–1166, doi:10.1021/ml500299q; j) A. Haider, L. Gobbi, J. Kretz, C. Ullmer, A. Brink, M. Honer, T. J. Woltering, D. Muri, H. Iding, M. Burkler, M. Binder, C. Bartelmus, I. Knuesel, P. Pacher, A. M. Herde, F. Spinelli, H. Ahmed, K. Atz, C. Keller, M. Weber, R. Schibli, L. Mu, U. Grether, S. M. Ametamey. Identification and Preclinical Development of a 2,5,6-Trisubstituted Fluorinated Pyridine Derivative as a Radioligand for the Positron Emission Tomography Imaging of Cannabinoid Type 2 Receptors. *J. Med. Chem.* **2020**, *63*, 10287–10306, doi:10.1021/acs.jmedchem.0c00778.
- ²⁰ Selected examples for deuteroanalysis: a) V. Soulard, G. Villa, D. P. Vollmar, P. Renaud. Radical Deuteration with D₂O: Catalysis and Mechanistic Insights. *J. Am. Chem. Soc.* **2018**, *140*, 155–158, doi:10.1021/jacs.7b12105; b) X. Wang, M.-H. Zhu, D. P. Schuman, D. Zhong, W.-Y. Wang, L.-Y. Wu, W. Liu, B. M. Stoltz, W.-B. Liu. General and Practical Potassium Methoxide/Disilane-Mediated Dehalogenative Deuteration of (Hetero)Arylhalides. *J. Am. Chem. Soc.* **2018**, *140*, 10970–10974, doi:10.1021/jacs.8b07597; c) C. Liu, S. Han, M. Li, X. Chong, B. Zhang. Electrocatalytic Deuteration of Halides with D₂O as the Deuterium Source over a Copper Nanowire Arrays Cathode. *Angew. Chem. Int. Ed.* **2020**, *59*, 18527–18531, doi:10.1002/anie.202009155; d) W. Li, R. Qu, W. Liu, F. Bourriquen, S. Bartling, N. Rockstroh, K. Junge, M. Beller. Copper-Catalysed Low-Temperature Water–Gas Shift Reaction for Selective Deuteration of Aryl Halides. *Chem. Sci.* **2021**, *12*, 14033–14038, doi:10.1039/D1SC04259A; e) Selected example for the reductive deuteration of a pseudohalide: D. Zhao, R. Petzold, J. Yan, D. Muri, T. Ritter. Tritiation of Aryl Thianthrenium Salts with a Molecular Palladium Catalyst. *Nature* **2021**, *600*, 444–449, doi:10.1038/s41586-021-04007-y.
- ²¹ Review: a) J. Steverlynck, R. Sitdikov, M. Rueping. The Deuterated “Magic Methyl” Group: A Guide to Site-Selective Trideuteromethyl Incorporation and Labeling by Using CD₃ Reagents. *Chem. Eur. J.* **2021**, *27*, 11751–11772, doi:10.1002/chem.202101179; example: b) R. W. Pipal, K. T. Stout, P. Z. Musacchio, S. Ren, T. J. A. Graham, S. Verhoog, L. Gantert, T. G. Lohith, A. Schmitz, H. S. Lee, D. Hesk, E. D. Hostetler, I. W. Davies, D. W. C. MacMillan. Metallaphotoredox Aryl and Alkyl

- Radiomethylation for PET Ligand Discovery. *Nature* **2021**, 589, 542–547, doi:10.1038/s41586-020-3015-0.
- ²² a) T. Junk, J. W. Catallo. Hydrogen Isotope Exchange Reactions Involving C-H (D, T) Bonds. *Chem. Soc. Rev.* **1997**, 26, 401–406, doi:10.1039/CS9972600401; b) J. Atzrodt, V. Derdau, T. Fey, J. Zimmermann. The Renaissance of H/D Exchange. *Angew. Chem. Int. Ed.* **2007**, 46, 7744–7765, doi:10.1002/anie.200700039; c) J. Atzrodt, V. Derdau, W. J. Kerr, M. Reid. C-H Functionalisation for Hydrogen Isotope Exchange. *Angew. Chem. Int. Ed.* **2018**, 57, 3022–3047, doi:10.1002/anie.201708903; d) Q.-K. Kang, H. Shi. Catalytic Hydrogen Isotope Exchange Reactions in Late-Stage Functionalization. *Synlett* **2021**, 33, 329–338, doi:10.1055/a-1354-0367.
- ²³ Selected examples of global labeling techniques: a) J. Martin, J. Eyselein, S. Grams, S. Harder. Hydrogen Isotope Exchange with Superbulky Alkaline Earth Metal Amide Catalysts. *ACS Catal.* **2020**, 10, 7792–7799, doi:10.1021/acscatal.0c01359; b) M. Farizyan, A. Mondal, S. Mal, F. Deufel, M. van Gemmeren. Palladium-Catalyzed Nondirected Late-Stage C–H Deuteration of Arenes. *J. Am. Chem. Soc.* **2021**, 143, 16370–16376, doi:10.1021/jacs.1c08233; c) J. D. Smith, G. Durrant, D. H. Ess, B. S. Gelfand, W. E. Piers. H/D Exchange under Mild Conditions in Arenes and Unactivated Alkanes with C₆D₆ and D₂O Using Rigid, Electron-Rich Iridium PCP Pincer Complexes. *Chem. Sci.* **2020**, 11, 10705–10717, doi:10.1039/D0SC02694H.
- ²⁴ Reviews on aliphatic HIE: a) A. Sattler. Hydrogen/Deuterium (H/D) Exchange Catalysis in Alkanes. *ACS Catal.* **2018**, 8, 2296–2312, doi:10.1021/acscatal.7b04201; b) M. Valero, V. Derdau. Highlights of Aliphatic C(sp³)–H Hydrogen Isotope Exchange Reactions. *J. Labelled Compd. Radiopharm.* **2020**, 63, 266–280, doi:10.1002/jlcr.3783; c) A. Michelotti, M. Roche. 40 Years of Hydrogen-Deuterium Exchange Adjacent to Heteroatoms: A Survey. *Synthesis* **2019**, 51, 1319–1328, doi:10.1055/s-0037-1610405.
- ²⁵ Selected examples: a) M. Liu, X. Chen, T. Chen, S.-F. Yin. A Facile and General Acid-Catalyzed Deuteration at Methyl Groups of *N*-Heteroarylmethanes. *Org. Biomol. Chem.* **2017**, 15, 2507–2511, doi:10.1039/C7OB00062F; b) Y. Chang, T. Myers, M. Wasa. B(C₆F₅)₃-Catalyzed α -Deuteration of Bioactive Carbonyl Compounds with D₂O. *Adv. Synth. Catal.* **2020**, 362, 360–364, doi:10.1002/adsc.201901419; c) L. Tie, X.-H. Shan, J.-P. Qu, Y.-B. Kang. α -Trideuteration of Methylarenes. *Org. Chem. Front.* **2021**, 8, 2981–2984, doi:10.1039/D1QO00265A.
- ²⁶ S. W. Chun, A. R. H. Narayan. Biocatalytic, Stereoselective Deuteration of α -Amino Acids and Methyl Esters. *ACS Catal.* **2020**, 10, 7413–7418, doi:10.1021/acscatal.0c01885.
- ²⁷ Selected examples: a) S. K. S. Tse, P. Xue, C. W. S. Lau, H. H. Y. Sung, I. D. Williams, G. Jia. Ruthenium-Catalyzed Regioselective Deuteration of Alcohols at the β -Carbon Position with Deuterium Oxide. *Chem. Eur. J.* **2011**, 17, 13918–13925, doi:10.1002/chem.201101542; b) L. Neubert, D. Michalik, S. Bähn, S. Imm, H. Neumann, J. Atzrodt, V. Derdau, W. Holla, M. Beller. Ruthenium-Catalyzed Selective α,β -Deuteration of Bioactive Amines. *J. Am. Chem. Soc.* **2012**, 134, 12239–12244, doi:10.1021/ja3041338; c) E. Khaskin, D. Milstein. Simple and Efficient Catalytic Reaction for the Selective Deuteration of Alcohols. *ACS Catal.* **2013**, 3, 448–452, doi:10.1021/cs400092p; d) B. Chatterjee, C. Gunanathan. Ruthenium Catalyzed Selective α - and α,β -Deuteration of Alcohols Using D₂O. *Org. Lett.* **2015**, 17, 4794–4797, doi:10.1021/acs.orglett.5b02254; e) L. V. A. Hale, N. K. Szymczak. Stereoretentive Deuteration of α -Chiral Amines with D₂O. *J. Am. Chem.*

- Soc. **2016**, *138*, 13489–13492, doi:10.1021/jacs.6b07879; f) B. Chatterjee, V. Krishnakumar, C. Gunanathan. Selective α -Deuteration of Amines and Amino Acids Using D₂O. *Org. Lett.* **2016**, *18*, 5892–5895, doi:10.1021/acs.orglett.6b02978; g) S. Kar, A. Goeppert, R. Sen, J. Kot-handaraman, G. K. Surya Prakash. Regioselective Deuteration of Alcohols in D₂O Catalysed by Homogeneous Manganese and Iron Pincer Complexes. *Green Chem.* **2018**, *20*, 2706–2710, doi:10.1039/C8GC01052H.
- ²⁸ M. Lepron, M. Daniel-Bertrand, G. Mencia, B. Chaudret, S. Feuillastre, G. Pieters. Nanocatalyzed Hydrogen Isotope Exchange. *Acc. Chem. Res.* **2021**, *54*, 1465–1480, doi:10.1021/acs.accounts.0c00721.
- ²⁹ a) W. J. Kerr, R. J. Mudd, M. Reid, J. Atzrodt, V. Derdau. Iridium-Catalyzed Csp³-H Activation for Mild and Selective Hydrogen Isotope Exchange. *ACS Catal.* **2018**, *8*, 10895–10900, doi:10.1021/acscatal.8b03565; b) M. Valero, R. Weck, S. Güssregen, J. Atzrodt, V. Derdau. Highly Selective Directed Iridium-Catalyzed Hydrogen Isotope Exchange Reactions of Aliphatic Amides. *Angew. Chem. Int. Ed.* **2018**, *57*, 8159–8163, doi:10.1002/anie.201804010; c) A. Uttry, S. Mal, M. van Gemmeren. Late-Stage β -C(sp³)-H Deuteration of Carboxylic Acids. *J. Am. Chem. Soc.* **2021**, *143*, 10895–10901, doi:10.1021/jacs.1c06474.
- ³⁰ Reviews: a) P. Ranjan, S. Pillitteri, E. V. Van der Eycken, U. K. Sharma. Photochemical Methods for Deuterium Labelling of Organic Molecules. *Green Chem.* **2020**, *22*, 7725–7736, doi:10.1039/d0gc02901g; b) R. Zhou, L. Ma, X. Yang, J. Cao. Recent Advances in Visible-light Photocatalytic Deuteration Reactions. *Org. Chem. Front.* **2021**, *8*, 426–244, doi:10.1039/D0QO01299H.
- ³¹ Selected examples: a) A. Di Giuseppe, R. Castarlenas, J. J. Pérez-Torrente, F. L. Lahoz, V. Polo, L. A. Oro. Mild and Selective H/D Exchange at the β Position of Aromatic α -Olefins by N-Heterocyclic Carbene-Hydride-Rhodium Catalysts. *Angew. Chem. Int. Ed.* **2011**, *50*, 3938–3942, doi:10.1002/anie.201007238; b) W. J. Kerr, R. J. Mudd, L. C. Paterson, J. A. Brown. Iridium (I)-Catalyzed Regioselective C-H Activation and Hydrogen-Isotope Exchange of Non-Aromatic Unsaturated Functionality. *Chem. Eur. J.* **2014**, *20*, 14604–14607, doi:10.1002/chem.201405114; c) T. R. Puleo, A. J. Strong, J. S. Bandar. Catalytic α -Selective Deuteration of Styrene Derivatives. *J. Am. Chem. Soc.* **2019**, *141*, 1467–1472, doi:10.1021/jacs.8b12874; d) A. Bechtoldt, L. Ackermann. Ruthenium(II)Biscarboxylate-Catalyzed Hydrogen-Isotope Exchange by Alkene C–H Activation. *ChemCatChem*. **2019**, *11*, 435–438, doi:10.1002/cctc.201801601; e) V. G. Landge, K. K. Shrestha, A. J. Grant, M. C. Young. Regioselective α -Deuteration of Michael Acceptors Mediated by Isopropylamine in D₂O/AcOD. *Org. Lett.* **2020**, *22*, 9745–9750, doi:10.1021/acs.orglett.0c03839.
- ³² Selected examples: a) S. P. Bew, G. D. Hiatt-Gipson, J. A. Lovell, C. Poullain. Mild Reaction Conditions for the Terminal Deuteration of Alkynes. *Org. Lett.* **2012**, *14*, 456–459, doi:10.1021/ol2029178; b) B. Chatterjee, C. Gunanathan. The Ruthenium-Catalysed Selective Synthesis of Mono-Deuterated Terminal Alkynes. *Chem. Commun.* **2016**, *52*, 4509–4512, doi:10.1039/C6CC01401A.
- ³³ Selected examples: a) W. J. Kerr, M. Reid, T. Tuttle. Iridium-Catalyzed Formyl-Selective Deuteration of Aldehydes. *Angew. Chem. Int. Ed.* **2017**, *56*, 7808–7812, doi:10.1002/anie.201702997; b) W. Liu, L.-L. Zhao, M. Melaimi, L. Cao, X. Xu, J. Bouffard, G. Bertrand, X. Yan. Mesoionic Carbene (MIC)-Catalyzed H/D Exchange at Formyl Groups. *Chem.* **2019**, *5*, 2484–2494, doi:10.1016/j.chempr.2019.08.011; c) H. Geng, X. Chen, J. Gui, Y. Zhang, Z. Shen, P. Qian,

- J. Chen, S. Zhang, W. Wang. Practical Synthesis of C1 Deuterated Aldehydes Enabled by NHC Catalysis. *Nat. Catal* **2019**, 2, 1071–1077, doi:10.1038/s41929-019-0370-z; d) J. Dong, X. Wang, Z. Wang, H. Song, Y. Liu, Q. Wang. Formyl-Selective Deuteration of Aldehydes with D₂O via Synergistic Organic and Photoredox Catalysis. *Chem. Sci.* **2020**, 11, 1026–1031, doi:10.1039/C9SC05132E; e) Y. Zhang, P. Ji, Y. Dong, Y. Wei, W. Wang. Deuteration of Formyl Groups via a Catalytic Radical H/D Exchange Approach. *ACS Catal.* **2020**, 10, 2226–2230, doi:10.1021/acscatal.9b05300; f) S. C. Gadekar, V. Dhayalan, A. Nandi, I. L. Zak, M. S. Mizrachi, S. Kozuch, A. Milo. Rerouting the Organocatalytic Benzoin Reaction toward Aldehyde Deuteration. *ACS Catal.* **2021**, 11, 14561–14569, doi:10.1021/acscatal.1c04583.
- ³⁴ W. J. Kerr, G. J. Knox, L. C. Paterson. Recent Advances in Iridium(I) Catalysis towards Directed Hydrogen Isotope Exchange. *J. Labelled Compd. Radiopharm.* **2020**, 63, 281–295, doi:10.1002/jlcr.3812.
- ³⁵ Important mechanistic studies: a) J. A. Brown, A. R. Cochrane, S. Irvine, W. J. Kerr, B. Mondal, J. A. Parkinson, L. C. Paterson, M. Reid, T. Tuttle, S. Andersson. The Synthesis of Highly Active Iridium(I) Complexes and Their Application in Catalytic Hydrogen Isotope Exchange. *Adv. Synth. Catal.* **2014**, 356, 3551–3562, doi:10.1002/adsc.201400730; b) M. Valero, D. Becker, K. Jess, R. Weck, J. Atzrodt, T. Bannenberg, V. Derdau, M. Tamm. Directed Iridium-Catalyzed Hydrogen Isotope Exchange Reactions of Phenylacetic Acid Esters and Amides. *Chem. Eur. J.* **2019**, 25, 6517–6522, doi:10.1002/chem.201901449; c) W. J. Kerr, M. Reid, T. Tuttle. Iridium-Catalyzed C–H Activation and Deuteration of Primary Sulfonamides: An Experimental and Computational Study. *ACS Catal.* **2015**, 5, 402–410, doi:10.1021/cs5015755.
- ³⁶ D. Hesk, P. R. Das, B. Evans. Deuteration of Acetanilides and Other Substituted Aromatics Using [Ir(COD)(Cy₃P)(Py)]PF₆ as Catalyst. *J. Labelled Compd. Radiopharm.* **1995**, 36, 497–502, doi:10.1002/jlcr.2580360514.
- ³⁷ J. A. Brown, S. Irvine, A. R. Kennedy, W. J. Kerr, S. Andersson, G. N. Nilsson. Highly Active Iridium(I) Complexes for Catalytic Hydrogen Isotope Exchange. *Chem. Commun.* **2008**, 1115–1117, doi:10.1039/b715938b.
- ³⁸ a) W. J. S. Lockley. Hydrogen Isotope Labelling Using Iridium(I) Dionates. *J. Labelled Compd. Radiopharm.* **2010**, 53, 668–673, doi:10.1002/jlcr.1806; b) A. R. Cochrane, S. Irvine, W. J. Kerr, M. Reid, S. Andersson, G. N. Nilsson. Application of Neutral Iridium(I) N-Heterocyclic Carbene Complexes in *ortho*-Directed Hydrogen Isotope Exchange. *J. Labelled Compd. Radiopharm.* **2013**, 56, 451–454, doi:10.1002/jlcr.3084; c) M. Parmentier, T. Hartung, A. Pfaltz, D. Muri. Iridium-Catalyzed H/D Exchange: Ligand Complexes with Improved Efficiency and Scope. *Chem. Eur. J.* **2014**, 20, 11496–11504, doi:10.1002/chem.201402078; d) A. R. Cochrane, C. Idziak, W. J. Kerr, B. Mondal, L. C. Paterson, T. Tuttle, S. Andersson, G. N. Nilsson. Practically Convenient and Industrially-Aligned Methods for Iridium-Catalysed Hydrogen Isotope Exchange Processes. *Org. Biomol. Chem.* **2014**, 12, 3598–3603, doi:10.1039/C4OB00465E; e) J. Atzrodt, V. Derdau, W. J. Kerr, M. Reid, P. Rojahn, R. Weck. Expanded applicability of Iridium(I) NHC/Phosphine Catalysts in Hydrogen Isotope Exchange Processes with Pharmaceutically Relevant Heterocycles. *Tetrahedron* **2015**, 71, 1924–1929, doi:10.1016/j.tet.2015.02.029; f) P. W. C. Cross, J. M. Herbert, W. J. Kerr, A. H. McNeill, L. C. Paterson. Isotopic Labelling of Functionalised Arenes Catalysed by

- Iridium(I) Species of the [(cod)Ir(NHC)(py)]PF₆ Complex Class. *Synlett* **2015**, 27, 111–115, doi:10.1055/s-0035-1560518; g) W. J. Kerr, D. M. Lindsay, M. Reid, J. Atzrodt, V. Derdau, P. Rojahn, R. Weck. Iridium-Catalysed *ortho*-H/D and -H/T Exchange under Basic Conditions: C–H Activation of Unprotected Tetrazoles. *Chem. Commun.* **2016**, 52, 6669–6672, doi:10.1039/C6CC02137A; h) K. Jess, V. Derdau, R. Weck, J. Atzrodt, M. Freytag, P. G. Jones, M. Tamm. Hydrogen Isotope Exchange with Iridium(I) Complexes Supported by Phosphine-Imidazolin-2-Imine P,N Ligands. *Adv. Synth. Catal.* **2017**, 359, 629–638, doi:10.1002/adsc.201601291; i) A. Burhop, R. Prohaska, R. Weck, J. Atzrodt, V. Derdau. Burgess Iridium(I)-Catalyst for Selective Hydrogen Isotope Exchange. *J. Labelled Compd. Radiopharm.* **2017**, 60, 343–348, doi:10.1002/jlcr.3512; j) A. R. Cochrane, A. R. Kennedy, W. J. Kerr, D. M. Lindsay, M. Reid, T. Tuttle. The Natural Product Lepidiline A as an N-Heterocyclic Carbene Ligand Precursor in Complexes of the Type [Ir(cod)(NHC)PPh₃]]X: Synthesis, Characterisation, and Application in Hydrogen Isotope Exchange Catalysis. *Catalysts* **2020**, 10, 161, doi:10.3390/catal10020161; k) M. Koneczny, L. Phong Ho, A. Nasr, M. Freytag, P. G. Jones, M. Tamm. Iridium(I) Complexes with Anionic N-Heterocyclic Carbene Ligands as Catalysts for H/D Exchange in Nonpolar Media. *Adv. Synth. Catal.* **2020**, 362, 3857–3863, doi:10.1002/adsc.202000438; l) M. Peters, D. Bockfeld, M. Tamm. Cationic Iridium(I) NHC-Phosphinidene Complexes and their Application in Hydrogen Isotope Exchange Reactions. *Eur. J. Inorg. Chem.* **2022**, e202200148, doi:10.1002/ejic.202200148.
- ³⁹ W. J. Kerr, R. J. Mudd, P. K. Owens, M. Reid, J. A. Brown, S. Campos. Hydrogen Isotope Exchange with Highly Active Iridium(I) NHC/Phosphine Complexes: A Comparative Counterion Study. *J. Labelled Compd. Radiopharm.* **2016**, 59, 601–603, doi:10.1002/jlcr.3427.
- ⁴⁰ J. Devlin, W. J. Kerr, D. M. Lindsay, T. J. D. McCabe, M. Reid, T. Tuttle. Iridium-Catalysed *ortho*-Directed Deuterium Labelling of Aromatic Esters – An Experimental and Theoretical Study on Directing Group Chemoselectivity. *Molecules* **2015**, 20, 11676–11698, doi:10.3390/molecules200711676.
- ⁴¹ J. Krüger, B. Manmontri, G. Fels. Iridium-Catalyzed H/D Exchange. *Eur. J. Org. Chem.* **2005**, 1402–1408, doi:10.1002/ejoc.200400669.
- ⁴² a) M. Valero, A. Burhop, K. Jess, R. Weck, M. Tamm, J. Atzrodt, V. Derdau. Evaluation of a P,N-Ligated Iridium(I) Catalyst in Hydrogen Isotope Exchange Reactions of Aryl and Heteroaryl Compounds. *J. Labelled Compd. Radiopharm.* **2018**, 61, 380–385; b) W. J. Kerr, G. J. Knox, M. Reid, T. Tuttle, J. Bergare, R. A. Bragg. Computationally-Guided Development of a Chelated NHC-P Iridium(I) Complex for the Directed Hydrogen Isotope Exchange of Aryl Sulfones. *ACS Catal.* **2020**, 10, 11120–11126, doi:10.1021/acscatal.0c03031.
- ⁴³ M. Valero, T. Kruissink, J. Blass, R. Weck, S. Güssregen, A. T. Plowright, V. Derdau. C–H Functionalization – Prediction of Selectivity in Iridium(I)-Catalyzed Hydrogen Isotope Exchange Competition Reactions. *Angew. Chem. Int. Ed.* **2020**, 59, 5626–5631, doi:10.1002/anie.201914220.
- ⁴⁴ W. J. Kerr, G. J. Knox, M. Reid, T. Tuttle. Catalyst Design in C–H Activation: A Case Study in the Use of Binding Free Energies to Rationalize Intramolecular Directing Group Selectivity in Iridium Catalysis. *Chem. Sci.* **2021**, 12, 6747–6755, doi:10.1039/D1SC01509E.
- ⁴⁵ T. Dalton, T. Faber, F. Glorius. C–H Activation: Toward Sustainability and Applications. *ACS Cent. Sci.* **2021**, 7, 245–261, doi:10.1021/acscentsci.0c01413.

- ⁴⁶ a) K. Fagnou, M. Lautens. Rhodium-Catalyzed Carbon-Carbon Bond Forming Reactions of Organometallic Compounds. *Chem. Rev.* **2003**, *103*, 169–196, doi:10.1021/cr020007u; b) D. A. Colby, R. G. Bergman, J. A. Ellman. Rhodium-Catalyzed C–C Bond Formation via Heteroatom-Directed C–H Bond Activation. *Chem. Rev.* **2010**, *110*, 624–655, doi:10.1021/cr900005n; c) G. Song, F. Wang, X. Li. C–C, C–O and C–N Bond Formation via Rhodium(III)-Catalyzed Oxidative C–H Activation. *Chem. Soc. Rev.* **2012**, *41*, 3651–3678, doi:10.1039/c2cs15281a.
- ⁴⁷ a) X. Chen, K. M. Engle, D.-H. Wang, J.-Q. Yu. Palladium(II)-Catalyzed C–H Activation/C–C Cross-Coupling Reactions: Versatility and Practicality. *Angew. Chem. Int. Ed.* **2009**, *48*, 5094–5115, doi:10.1002/anie.200806273; b) T. W. Lyon, M. S. Sanford, Palladium-Catalyzed Ligand-Directed C–H Functionalization Reactions. *Chem. Rev.* **2010**, *110*, 1147–1169, doi:10.1021/cr900184e.
- ⁴⁸ P. B. Arockiam, C. Bruneau, P. H. Dixneuf. Ruthenium(II)-Catalyzed C–H Bond Activation and Functionalization. *Chem. Rev.* **2012**, *112*, 5879–5918, doi:10.1021/cr300153j.
- ⁴⁹ a) D. Balcells, E. Clot, O. Eisenstein. C–H Bond Activation in Transition Metal Species from a Computational Perspective. *Chem. Rev.* **2010**, *110*, 749–823, doi:10.1021/cr900315k.
- ⁵⁰ a) M. R. Blake, J. L. Garnett, I. K. Gregor, W. Hannan, K. Hoa, M. A. Long. Rhodium Trichloride as a Homogeneous Catalyst for Isotopic Hydrogen Exchange. Comparison with Heterogeneous Rhodium in the Deuteration of Aromatic Compounds and Alkanes. *J. Chem. Soc., Chem. Commun.* **1975**, 930–932, doi:10.1039/C39750000930; b) W. J. S. Lockley. Regioselective Deuteration of Aromatic and α,β -Unsaturated Carboxylic Acids via Rhodium(III) Chloride Catalysed Exchange with Deuterium Oxide. *Tetrahedron Lett.* **1982**, *23*, 3819–3822, doi:10.1016/S0040-4039(00)87716-3; c) W. J. S. Lockley. Regioselective Deuterium Labelling of Aromatic Acids, Amides and Amines Using Group VIII Metal Catalysts. *J. Labelled Compd. Radiopharm.* **1984**, *21*, 45–57, doi:10.1002/jlcr.2580210105; d) W. J. S. Lockley. Regioselective Labelling of Anilides with Deuterium. *J. Labelled Compd. Radiopharm.* **1985**, *22*, 623–630, doi:10.1002/jlcr.2580220612; e) D. Hesk, J. R. Jones, W. J. S. Lockley. Regiospecific Tritium Labeling of Aromatic Acids, Amides, Amines and Heterocyclics Using Homogeneous Rhodium Trichloride and Ruthenium Acetylacetonate Catalysts. *J. Labelled Compd. Radiopharm.* **1990**, *28*, 1427–1436, doi:10.1002/jlcr.2580281211.
- ⁵¹ A. Garreau, H. Zhou, M. C. Young. A Protocol for the *Ortho*-Deuteration of Acidic Aromatic Compounds in D₂O Catalyzed by Cationic Rh^{III}. *Org. Lett.* **2019**, *21*, 7044–7048, doi:10.1021/acs.orglett.9b02618.
- ⁵² J. Zhang, S. Zhang, T. Gogula, H. Zou. Versatile Regioselective Deuteration of Indoles via Transition-Metal-Catalyzed H/D Exchange. *ACS Catal.* **2020**, *10*, 7486–7494, doi:10.1021/acscatal.0c01674.
- ⁵³ a) S. Ma, G. Villa, P. S. Thuy-Boun, A. Homs, J.-Q. Yu. Palladium-Catalyzed *ortho*-Selective C–H Deuteration of Arenes: Evidence for Superior Reactivity of Weakly Coordinated Palladacycles. *Angew. Chem. Int. Ed.* **2014**, *53*, 734–737, doi:10.1002/anie.201305388; cf. further Pd-catalyzed HIE methodologies; b) H. Yang, P. G. Dormer, N. R. Rivera, A. J. Hoover. Palladium(II)-Mediated C–H Tritiation of Complex Pharmaceuticals. *Angew. Chem. Int. Ed.* **2018**, *57*, 1883–1887, doi:10.1002/anie.201711364; c) D.-W. Yin, G. Liu. Palladium-Catalyzed Regioselective C–H Functionalization of Arenes Substituted by Two *N*-Heterocycles and Application in Late-Stage Functionalization. *J. Org. Chem.* **2018**, *83*, 3987–4001, doi:10.1021/acs.joc.8b00322; d) J. Kong, Z.-J. Jiang,

- J. Xu, Y. Li, H. Cao, Y. Ding, B. Tang, J. Chen, Z. Gao. *Ortho*-Deuteration of Aromatic Aldehydes via a Transient Directing Group-Enabled Pd-Catalyzed Hydrogen Isotope Exchange. *J. Org. Chem.* **2021**, *86*, 13350–13359, doi:10.1021/acs.joc.1c01411.
- ⁵⁴ a) A. Prades, M. Poyatos, E. Peris. (η^6 -Arene)ruthenium(*N*-heterocyclic carbene) Complexes for the Chelation-Assisted Arylation and Deuteration of Arylpyridines: Catalytic Studies and Mechanistic Insights. *Adv. Synth. Catal.* **2010**, *352*, 1155–1162, doi:10.1002/adsc.201000049; b) L. Piola, J. A. Fernández-Salas, S. Manzini, S. P. Nolan. Regioselective Ruthenium Catalysed H–D Exchange Using D₂O as the Deuterium Source. *Org. Biomol. Chem.* **2014**, *12*, 8683–8688, doi:10.1039/c4ob01798f; c) P. Eisele, F. Ullwer, S. Scholz, B. Plietker. Mild, Selective Ru-Catalyzed Deuteration Using D₂O as a Deuterium Source. *Chem. Eur. J.* **2019**, *25*, 16550–16554, doi:10.1002/chem.201904927; d) V. Müller, R. Weck, V. Derdau, L. Ackermann. Ruthenium(II)-Catalyzed Hydrogen Isotope Exchange of Pharmaceutical Drugs by C–H Deuteration and C–H Tritiation. *ChemCatChem*. **2020**, *12*, 100–104, doi:10.1002/cctc.201902051.
- ⁵⁵ a) L.-L. Zhao, W. Liu, Z. Zhang, H. Zhao, Q. Wang, X. Yan. Ruthenium-Catalyzed *Ortho*- and *Meta*-H/D Exchange of Arenes. *Org. Lett.* **2019**, *21*, 10023–10027, doi:10.1021/acs.orglett.9b03955; b) S. Bag, M. Petzold, A. Sur, S. Bhowmick, D. B. Werz, D. Maiti. Palladium-Catalyzed Selective *Meta*-C–H Deuteration of Arenes: Reaction Design and Applications. *Chem. Eur. J.* **2019**, *25*, 9433–9437, doi:10.1002/chem.201901317; c) H. Xu, M. Liu, L.-J. Li, Y.-F. Cao, J.-Q. Yu, H.-X. Dai. Palladium-Catalyzed Remote *Meta*-C–H Bond Deuteration of Arenes Using a Pyridine Template. *Org. Lett.* **2019**, *21*, 4887–4891, doi:10.1021/acs.orglett.9b01784; d) A. Gholap, S. Bag, S. Pradhan, A. R. Kapdi, D. Maiti. Diverse *Meta*-C–H Functionalization of Amides. *ACS Catal.* **2020**, *10*, 5347–5352, doi:10.1021/acscatal.0c01306.
- ⁵⁶ Selected examples: a) M. Valero, D. Bouzouita, A. Palazzolo, J. Atzrodt, C. Dugave, S. Tricard, S. Feuillastre, G. Pieters, B. Chaudret, V. Derdau. NHC-Stabilized Iridium Nanoparticles as Catalysts in Hydrogen Isotope Exchange Reactions of Anilines. *Angew. Chem. Int. Ed.* **2020**, *59*, 3517–3522, doi:10.1002/anie.201914369; b) V. Pfeifer, M. Certiat, D. Bouzouita, A. Palazzolo, S. Garcia-Argote, E. Marcon, D.-A. Buisson, P. Lesot, L. Maron, B. Chaudret. Hydrogen Isotope Exchange Catalyzed by Ru Nanocatalysts: Labelling of Complex Molecules Containing *N*-Heterocycles and Reaction Mechanism Insights. *Chem. Eur. J.* **2020**, *26*, 4988–4996, doi:10.1002/chem.201905651; c) D. Bouzouita, J. M. Asensio, V. Pfeifer, A. Palazzolo, P. Lecante, G. Pieters, S. Feuillastre, S. Tricard, B. Chaudret. Chemoselective H/D Exchange Catalyzed by Nickel Nanoparticles Stabilized by *N*-Heterocyclic Carbene Ligands. *Nanoscale* **2020**, *12*, 15736–15742, doi:10.1039/D0NR04384B.
- ⁵⁷ a) D. Zhao, H. Luo, B. Chen, W. Chen, G. Zhang, Y. Yu. Palladium-Catalyzed H/D Exchange Reaction with 8-Aminoquinoline as the Directing Group: Access to *ortho*-Selective Deuterated Aromatic Acids and β -Selective Deuterated Aliphatic Acids. *J. Org. Chem.* **2018**, *83*, 7860–7866, doi:10.1021/acs.joc.8b00734; b) P. Manna, M. Kundu, A. Roy, S. Adhikari. The Palladium-Catalyzed Directed Synthesis of *ortho*-Deuterated Phenylacetic Acid and Analogues. *Org. Biomol. Chem.* **2021**, *19*, 6244–6249, doi:10.1039/d1ob00663k.
- ⁵⁸ K. M. Engle, T.-S. Mei, M. Wasa, J.-Q. Yu. Weak Coordination as a Powerful Means for Developing Broadly Useful C–H Functionalization Reactions. *Acc. Chem. Res.* **2012**, *45*, 788–802, doi:10.1021/ar200185g.

- ⁵⁹ Selected examples: a) M. Miura, T. Tsuda, T. Satoh, S. Pivsa-Art, M. Nomura. Oxidative Cross-Coupling of *N*-(2'-Phenylphenyl)benzene-sulfonamides or Benzoic and Naphthoic Acids with Alkenes Using a Palladium–Copper Catalyst System under Air. *J. Org. Chem.* **1998**, *63*, 5211–5215, doi:10.1021/jo980584b; b) R. Giri, N. Mangel, J.-J. Li, D.-H. Wang, S. P. Breazzano, L. B. Saunders, J.-Q. Yu. Palladium-Catalyzed Methylation and Arylation of sp² and sp³ C–H Bonds in Simple Carboxylic Acids. *J. Am. Chem. Soc.* **2007**, *129*, 3510–3511, doi:10.1021/ja0701614; c) H. A. Chiong, Q.-N. Pham, O. Daugulis. Two Methods for Direct *ortho*-Arylation of Benzoic Acids. *J. Am. Chem. Soc.* **2007**, *129*, 9879–9894, doi:10.1021/ja071845e; d) R. Giri, J.-Q. Yu. Synthesis of 1,2- and 1,3-Dicarboxylic Acids via Pd(II)-Catalyzed Carboxylation of Aryl and Vinyl C–H Bonds. *J. Am. Chem. Soc.* **2008**, *130*, 14082–14083, doi:10.1021/ja8063827; e) D.-H. Wang, K. Engle, B.-F. Shi, J.-Q. Yu. Ligand-Enabled Reactivity and Selectivity in a Synthetically Versatile Aryl C–H Olefination. *Science* **2009**, *327*, 315–319, doi:10.1126/science.1182512.
- ⁶⁰ Selected examples: a) K. Ueura, T. Satoh, M. Miura. An Efficient Waste-Free Oxidative Coupling via Regioselective C–H Bond Cleavage: Rh/Cu-Catalyzed Reaction of Benzoic Acids with Alkynes and Acrylates under Air. *Org. Lett.* **2007**, *9*, 1407–1409, doi:10.1021/ol070406h; b) P. Mamone, G. Dagnoun, L. J. Gooßen. Rhodium-Catalyzed *ortho* Acylation of Aromatic Carboxylic Acids. *Angew. Chem. Int. Ed.* **2013**, *52*, 6704–6708, doi:10.1002/anie.201301328; c) H. Gong, H. Zeng, F. Zhou, C.-J. Li. Rhodium(I)-Catalyzed Regiospecific Dimerization of Aromatic Acids: Two Direct C–H Bond Activations in Water. *Angew. Chem. Int. Ed.* **2015**, *54*, 5718–5721, doi:10.1002/anie.201500220.
- ⁶¹ General review: a) S. De Sarkar, W. Liu, S. I. Kozhushkov, L. Ackermann. Weakly Coordinating Directing Groups for Ruthenium(II)-Catalyzed C–H Activation. *Adv. Synth. Catal.* **2014**, *356*, 1461–1479, doi:10.1002/adsc.201400110; Selected examples: b) T. Ueyama, S. Mochida, T. Fukutani, K. Hirano, T. Satoh, M. Miura. Ruthenium-Catalyzed Oxidative Vinylation of Heteroarene Carboxylic Acids with Alkenes via Regioselective C–H Bond Cleavage. *Org. Lett.* **2011**, *13*, 706–708, doi:10.1021/ol102942w; c) L. Ackermann, J. Pospech. Ruthenium-Catalyzed Oxidative C–H Bond Alkenylations in Water: Expedient Synthesis of Annulated Lactones. *Org. Lett.* **2011**, *13*, 4153–4155, doi:10.1021/ol201563r; d) S. Warratz, C. Kornhaas, A. Cajaraville, B. Niepötter, D. Stalke, L. Ackermann. Ruthenium(II)-Catalyzed C–H Activation/Alkyne Annulation by Weak Coordination with O₂ as the Sole Oxidant. *Angew. Chem. Int. Ed.* **2015**, *54*, 5513–5517, doi:10.1002/anie.201500600.
- ⁶² R. Giles, G. Ahn, K. W. Jung. H–D Exchange in Deuterated Trifluoroacetic Acid via Ligand-Directed NHC–Palladium Catalysis: a Powerful Method for Deuteration of Aromatic Ketones, Amides, and Amino Acids. *Tetrahedron Lett.* **2015**, *56*, 6231–6235, doi:10.1016/j.tetlet.2015.09.100.
- ⁶³ a) C. Rape, W. H. Sachs. Enolization of Ketones—VI : The Base-Catalyzed Deuteration of Some Cyclic Ketones. *Tetrahedron* **1968**, *24*, 6287–6290, doi:10.1016/S0040-4020(01)96361-6; b) C. Berthelette, J. Scheigetz. Base-Catalyzed Deuterium and Tritium Labelling of 1-Biphenyl-4-ylpropane-1,2-dione and Deuteration of Aryl Methyl Ketones. *J. Labelled Compd. Radiopharm.* **2004**, *47*, 891–894, doi:10.1002/jlcr.879; c) C. Sabot, K. K. Kumar, C. Antheaume, C. Mioskowski. Triazabicyclodecene: An Effective Isotope Exchange Catalyst in CDCl₃. *J. Org. Chem.* **2007**, *13*, 5001–5004, doi:10.1021/jo070307h; d) M. Zhan, T. Zhang, H. Huang, Y. Xie, Y. Chen. A Simple Method for α -Position Deuterated Carbonyl Compounds with Pyrrolidine as Catalyst. *J. Labelled Compd. Radiopharm.* **2014**, *57*, 533–539, doi:10.1002/jlcr.3210; e) M. Zanatta, F. P. dos Santos, C. Biehl, G.

- Marin, G. Ebeling, P. A. Netz, J. Dupont. Organocatalytic Imidazolium Ionic Liquids H/D Exchange Catalysts. *J. Org. Chem.* **2017**, *82*, 2622–2629, doi:10.1021/acs.joc.6b03029; f) K. I. Galkin, E. G. Gordeev, V. P. Ananikov. Organocatalytic Deuteration Induced by the Dynamic Covalent Interaction of Imidazolium Cations with Ketones. *Adv. Synth. Catal.* **2020**, *363*, 1368–1378, doi:10.1002/adsc.202001507; g) M. Peng, H. Li, Z. Qin, J. Li, Z. Sun, X. Zhang, L. Jiang, H. Do, J. An. Pentafluorophenyl Group as Activating Group: Synthesis of α -Deuterio Carboxylic Acid Derivatives via Et₃N Catalyzed H/D Exchange. *Adv. Synth. Catal.* **2022**, doi:10.1002/adsc.202200258.
- ⁶⁴ a) J. M. Barthez, A. V. Filikov, L. B. Frederiksen, M.-L. Huguet, J. R. Jones, S.-Y. Lu. Microwave-Enhanced Metal- and Acid-Catalysed Hydrogen Isotope Exchange Reactions. *Can. J. Chem.* **1998**, *76*, 726–728, doi:10.1139/v98-045; b) A. Martin, M. Lautens. A Simple, Cost-Effective Method for the Regioselective Deuteration of Anilines. *Org. Lett.* **2008**, *10*, 4351–4353, doi:10.1021/ol801763j; c) R. Giles, A. Lee, E. Jung, A. Kang, K. W. Jung. Hydrogen–Deuterium Exchange of Aromatic Amines and Amides Using Deuterated Trifluoroacetic Acid. *Tetrahedron Lett.* **2015**, *56*, 747–749, doi:10.1016/j.tetlet.2014.12.102; d) W. Li, M.-M. Wang, Y. Hu, T. Werner. B(C₆F₅)₃-Catalyzed Regioselective Deuteration of Electron-Rich Aromatic and Heteroaromatic Compounds. *Org. Lett.* **2017**, *19*, 5768–5771, doi:10.1021/acs.orglett.7b02701; e) B. Dong, X. Cong, N. Hao. Silver-Catalyzed Regioselective Deuteration of (Hetero)arenes and α -Deuteration of 2-Alkyl Azaarenes. *RSC Adv.* **2020**, *10*, 25475–25479, doi:10.1039/D0RA02358B; f) O. Fischer, A. Hubert, M. R. Heinrich. Shifted Selectivity in Protonation Enables the Mild Deuteration of Arenes Through Catalytic Amounts of Bronsted Acids in Deuterated Methanol. *J. Org. Chem.* **2020**, *85*, 11856–11866, doi:10.1021/acs.joc.0c01604; g) B. Liu, G. Wang, Z. Xu. M. Wang, Y. Nie, Z. Luo. Ionic Liquid/Boronic Acid System Enabled Deuteration with D₂O. *Chin. Chem. Lett.* **2022**, doi:10.2139/ssrn.4096978.
- ⁶⁵ a) M. Zhan, R. Xu, Y. Tian, H. Jiang, L. Zhao, Y. Xie, Y. Chen. A Simple and Cost-Effective Method for the Regioselective Deuteration of Phenols. *Eur. J. Org. Chem.* **2015**, 3370–3373, doi:10.1002/ejoc.201500192; b) V. Salamanca, A. C. Albéniz. Deuterium Exchange between Arenes and Deuterated Solvents in the Absence of a Transition Metal: Synthesis of D-Labeled Fluoroarenes. *Eur. J. Org. Chem.* **2020**, 3206–3212, doi:10.1002/ejoc.202000284.
- ⁶⁶ a) W. Li, J. Rabeah, F. Bourriquen, D. Yang, C. Kreyenschulte, N. Rockstroh, H. Lund, S. Bartling, A.-E. Surkus, K. Junge, A. Brückner, A. Lei, M. Beller. Scalable and Selective Deuteration of (Hetero)arenes. *Nat. Chem.* **2022**, *14*, 334–341, doi:10.1038/s41557-021-00846-4; b) F. Bourriquen, N. Rockstroh, S. Bartling, K. Junge, M. Beller. Manganese Catalysed Deuterium Labelling of Anilines and Electron-Rich (Hetero)Arenes. *Angew. Chem. Int. Ed.* **2022**, e202202423, doi:10.1002/anie.202202423.
- ⁶⁷ a) E.-C. Li, G.-Q. Hu, Y.-X. Zhu, H.-H. Zhang, K. Shen, X.-C. Hang, C. Zhang, W. Huang. Ag₂CO₃-Catalyzed H/D Exchange of Five-Membered Heteroarenes at Ambient Temperature. *Org. Lett.* **2019**, *21*, 6745–6749, doi:10.1021/acs.orglett.9b02369; b) A. Tlahuext-Aca, J. F. Hartwig. Site-Selective Silver-Catalyzed C–H Bond Deuteration of Five-Membered Aromatic Heterocycles and Pharmaceuticals. *ACS Catal.* **2021**, *11*, 1119–1127, doi:10.1021/acscatal.0c04917.
- ⁶⁸ a) G.-Q. Hu, E.-C. Li, H.-H. Zhang, W. Huang. Ag(i)-Mediated Hydrogen Isotope Exchange of Mono-Fluorinated (Hetero)arenes. *Org. Biomol. Chem.* **2020**, *18*, 6627–6633, doi:10.1039/D0OB01273D;

- b) G.-Q. Hu, J.-W. Bai, E.-C. Li, K.-H. Liu, F.-F. Sheng, H.-H. Zhang. Synthesis of Multideuterated (Hetero)aryl Bromides by Ag(I)-Catalyzed H/D Exchange. *Org. Lett.* **2021**, *23*, 1554–1560, doi:10.1021/acs.orglett.0c04139.
- ⁶⁹ B. Gröll, M. Schnürch, M. D. Mihovilovic. Selective Ru(0)-Catalyzed Deuteration of Electron-Rich and Electron-Poor Nitrogen-Containing Heterocycles. *J. Org. Chem.* **2012**, *77*, 4432–4437, doi:10.1021/jo300219v.
- ⁷⁰ a) H. Yang, C. Zarate, N. Palmer, N. Rivera, D. Hesk, P. J. Chirik. Site-Selective Nickel-Catalyzed Hydrogen Isotope Exchange in *N*-Heterocycles and Its Application to the Tritiation of Pharmaceuticals. *ACS Catal.* **2018**, *8*, 10210–10218, doi:10.1021/acscatal.8b03717; b) C. Zarate, H. Yang, M. J. Bezdek, D. Hesk, P. J. Chirik. Ni(I)–X Complexes Bearing a Bulky α -Diimine Ligand: Synthesis, Structure, and Superior Catalytic Performance in the Hydrogen Isotope Exchange in Pharmaceuticals. *J. Am. Chem. Soc.* **2019**, *141*, 5034–5044, doi:10.1021/jacs.9b00939.
- ⁷¹ a) R. P. Yu, D. Hesk, N. Rivera, I. Pelczar, P. J. Chirik. Iron-Catalysed Tritiation of Pharmaceuticals. *Nature* **2016**, *529*, 195–199, doi:10.1038/nature16464; b) J. Corpas, P. Viereck, P. J. Chirik. C(Sp²)-H Activation with Pyridine Dicarbene Iron Dialkyl Complexes: Hydrogen Isotope Exchange of Arenes Using Benzene-*d*₆ as a Deuterium Source. *ACS Catal.* **2020**, *10*, 8640–8647, doi:10.1021/acscatal.0c01714; c) S. Garhwal, A. Kaushansky, N. Fridman, L. J. W. Shimon, G. de Ruiter. Facile H/D Exchange at (Hetero)Aromatic Hydrocarbons Catalyzed by a Stable Trans-Dihydride *N*-Heterocyclic Carbene (NHC) Iron Complex. *J. Am. Chem. Soc.* **2020**, *142*, 17131–17139, doi:10.1021/jacs.0c07689.
- ⁷² a) A. Gomtsyan. Heterocycles in Drugs and Drug Discovery. *Chem. Heterocycl. Comp.* **2012**, *48*, 7–10, doi:10.1007/s10593-012-0960-z; b) E. Vitaku, D. T. Smith, J. T. Njardarson. Analysis of the Structural Diversity, Substitution Patterns, and Frequency of Nitrogen Heterocycles among U.S. FDA Approved Pharmaceuticals. *J. Med. Chem.* **2014**, *57*, 10257–10274, doi:10.1021/jm501100b; c) M. D. Delost, D. T. Smith, B. J. Anderson, N. J. Njardarson. From Oxiranes to Oligomers: Architectures of U.S. FDA Approved Pharmaceuticals Containing Oxygen Heterocycles. *J. Med. Chem.* **2018**, *61*, 10996–11020, doi:10.1021/acs.jmedchem.8b00876.
- ⁷³ a) N. Plé, A. Turck, K. Couture, G. Quéguiner. Diazines 13: Metalation without *Ortho*-Directing Group – Functionalization of Diazines via Direct Metalation. *J. Org. Chem.* **1995**, *60*, 3781–3786, doi:10.1021/jo00117a033; b) P. Pierrat, P. Gros, Y. Fort. Unusual *t*-BuLi Induced Ortholithiation versus Halogen-Lithium Exchange in Bromopyridines: Two Alternative Strategies for Functionalization. *Synlett* **2004**, *13*, 2319–2322, doi:10.1055/s-2004-831337; c) J. Hawad, O. Bayh, C. Hoarau, F. Trécourt, G. Quéguiner, F. Marsais. Deprotonation of Pyridine Carboxamides Using Lithium Magnesiates Bases. *Tetrahedron* **2008**, *64*, 3236–3245, doi:10.1016/j.tet.2008.01.064.
- ⁷⁴ W. J. Kerr, D. M. Lindsay, P. K. Owens, M. Reid, T. Tuttle, S. Campos. Site-Selective Deuteration of *N*-Heterocycles via Iridium-Catalyzed Hydrogen Isotope Exchange. *ACS Catal.* **2017**, *7*, 7182–7186, doi:10.1021/acscatal.7b02682.
- ⁷⁵ a) J. A. Zoltewicz, C. L. Smith. Hydrogen-Deuterium Exchange in Some Halopyridines and the Mechanism of Pyridyne Formation. *J. Am. Chem. Soc.* **1966**, *88*, 4766–4767, doi:10.1021/ja00972a068; b) J. A. Zoltewicz, C. L. Smith, J. D. Meyer. Deuterodecarboxylation: A Convenient Method for the Preparation of Labeled Pyridines. *Tetrahedron* **1968**, *24*, 2269–2274, doi:10.1016/0040-

4020(68)88128-1; c) M. Rudzki, A. Alcalde-Aragonés, W. I. Dzik, N. Rodríguez, L. J. Gooßen. Selective Copper- or Silver-Catalyzed Decarboxylative Deuteration of Aromatic Carboxylic Acids, *Synthesis* **2012**, *44*, 184–193, doi:10.1055/s-0031-128963; d) R. Grainger, A. Nikmal, J. Cornella, I. Larrosa. Selective Deuteration of (Hetero)aromatic Compounds via Deutero-Decarboxylation of Carboxylic Acids. *Org. Biomol. Chem.* **2012**, *10*, 3172–3174, doi:10.1039/c2ob25157d; e) C. S. Donald, T. A. Moss, G. M. Noonan, B. Roberts, E. C. Durham. Deuterodehalogenation – a Mild Method for Synthesising Deuterated Heterocycles. *Tetrahedron Lett.* **2014**, *55*, 3305–3307, doi:10.1016/j.tetlet.2014.04.025; f) H.-H. Zhang, P. V. Bonnesen, K. Hong. Palladium-Catalyzed Br/D Exchange of Arenes: Selective Deuterium Incorporation with Versatile Functional Group Tolerance and High Efficiency. *Org. Chem. Front.* **2015**, *2*, 1071–1075, doi:10.1039/c5qo00181a; g) M. Kuriyama, N. Hamaguchi, G. Yano, K. Tsukuda, K. Sato, O. Onomura. Deuterodechlorination of Aryl/Heteroaryl Chlorides Catalyzed by a Palladium/Unsymmetrical NHC System. *J. Org. Chem.* **2016**, *81*, 8934–8946, doi:10.1021/acs.joc.6b01609; h) M. Janni, S. Perunchelatan. Catalytic Selective Deuteration of Halo(hetero)arenes. *Org. Biomol. Chem.* **2016**, *14*, 3091–3097, doi:10.1039/c6ob00193a; i) M. Kuriyama, S. Kujirada, K. Tsukuda, O. Onomura. Nickel-Catalyzed Deoxygenative Deuteration of Aryl Sulfamates. *Adv. Synth. Catal.* **2017**, *359*, 1043–1048, doi:10.1002/adsc.201601105; j) C. Liu, Z. Chen, C. Su, X. Zhao, Q. Gao, G. H. Ning, H. Zhu, W. Tang, K. Leng, W. Fu, B. Tian, X. Peng, J. Li, Q.-H. Xu, W. Zhou, K. P. Loh. Controllable Deuteration of Halogenated Compounds by Photocatalytic D₂O Splitting. *Nat. Commun.* **2018**, *9*, 80, doi:10.1038/s41467-017-02551-8; k) Z.-Z. Zhou, J.-H. Zhao, X.-Y. Gou, X.-M. Chen, Y.-M. Liang. Visible-Light-Mediated Hydrodehalogenation and Br/D Exchange of Inactivated Aryl and Alkyl Halides with a Palladium Complex. *Org. Chem. Front.* **2019**, *6*, 1649–1654, doi:10.1039/c9qo00240e; l) H. Kameo, J. Yamamoto, A. Asada, H. Nakazawa, H. Matsuzaka, D. Bourissou. Palladium-Borane Cooperation: Evidence for an Anionic Pathway and Its Application to Catalytic Hydro-/Deutero-Dechlorination. *Angew. Chem. Int. Ed.* **2019**, *58*, 18783–18787, doi:10.1002/anie.201909675; m) Y. Li, Z. Ye, Y.-M. Lin, Y. Liu, Y. Zhang, L. Gong. Organophotocatalytic Selective Deuterodehalogenation of Aryl or Alkyl Chlorides. *Nat. Commun.* **2021**, *12*, 2894–2906, doi:10.1038/s41467-021-23255-0; n) B. Singh, J. Ahmed, A. Biswas, R. Paira, S. K. Mandal. Reduced Phenalenyl in Catalytic Dehalogenative Deuteration and Hydrodehalogenation of Aryl Halides. *J. Org. Chem.* **2021**, *86*, 7242–7255, doi:10.1021/acs.joc.1c00573; o) B. Yan, Y. Zhou, J. Wu, M. Ran, H. Li, Q. Yao. Catalyst-Free Reductive Hydrogenation or Deuteration of Aryl–Heteroatom Bonds Induced by Light. *Org. Chem. Front.* **2021**, *8*, 5244–5249, doi:10.1039/D1QO00978H.

⁷⁶ J. L. Koniarczyk, D. Hesk, A. Overgard, I. W. Davies, A. McNally. A General Strategy for Site-Selective Incorporation of Deuterium and Tritium into Pyridines, Diazines, and Pharmaceuticals. *J. Am. Chem. Soc.* **2018**, *140*, 1990–1993, doi:10.1021/jacs.7b11710.

⁷⁷ a) G. Pieters, C. Taglang, E. Bonnefille, T. Gutmann, C. Puente, J.-C. Berthet, C. Dugave, B. Chaudret, B. Rousseau. Regioselective and Stereospecific Deuteration of Bioactive Aza Compounds by the Use of Ruthenium Nanoparticles. *Angew. Chem. Int. Ed.* **2014**, *53*, 230–234, doi:10.1002/anie.201307930; b) A. Palazzolo, S. Feuillastre, V. Pfeifer, S. Garcia-Argote, D. Bouzouita, S. Tricard, C. Chollet, E. Marcon, D.-A. Buisson, S. Cholet, F. Fenaille, G. Lippens, B.

- Chaudret, G. Pieters. Efficient Access to Deuterated and Tritiated Nucleobase Pharmaceuticals and Oligonucleotides Using Hydrogen-Isotope Exchange. *Angew. Chem. Int. Ed.* **2019**, *58*, 4891–4895, doi:10.1002/anie.201813946; c) M. Daniel-Bertrand, S. Garcia-Argote, A. Palazzolo, I. Mustieles Marin, P.-F. Fazzini, S. Tricard, B. Chaudret, V. Derdau, S. Feuillastre, G. Pieters. Multiple Site Hydrogen Isotope Labelling of Pharmaceuticals. *Angew. Chem. Int. Ed.* **2020**, *59*, 21114–21120, doi:10.1002/anie.202008519; d) E. Levernier, K. Tatoueix, S. Garcia-Argote, V. Pfeifer, R. Kiesling, E. Gravel, S. Feuillastre, G. Pieters. Easy-to-Implement Hydrogen Isotope Exchange for the Labeling of *N*-Heterocycles, Alkylamines, Benzylic Scaffolds, and Pharmaceuticals. *JACS Au* **2022**, *2*, 801–808, doi:10.1021/jacsau.1c00503.
- ⁷⁸ K. Wang, X. Chen, X. Peng, P. Wang, F. Liang. A Highly Selective H/D Exchange Reaction of 1,4-Dihydropyridines. *Org. Biomol. Chem.* **2019**, *17*, 3845–3852, doi:10.1039/C9OB00575G.
- ⁷⁹ a) S. Murai, F. Kakiuchi, S. Sekine, Y. Tanaka, A. Kamatani, M. Sonoda, N. Chatani. Efficient Catalytic Addition of Aromatic Carbon–Hydrogen Bonds to Olefins. *Nature* **1993**, *366*, 529–531, doi:10.1038/366529a0; b) F. Kakiuchi, S. Murai. Catalytic C–H/Olefin Coupling. *Acc. Chem. Res.* **2002**, *35*, 826–834, doi:10.1021/ar960318p.
- ⁸⁰ Pioneering examples: a) S. Oi, S. Fukita, N. Hirata, N. Watanuki, S. Miyano, Y. Inoue. Ruthenium Complex-Catalyzed Direct *Ortho* Arylation and Alkenylation of 2-Arylpyridines with Organic Halides. *Org. Lett.* **2001**, *3*, 2579–2581, doi:10.1021/ol016257z; b) S. Oi, Y. Ogino, S. Fukita, Y. Inoue. Ruthenium Complex Catalyzed Direct *Ortho* Arylation and Alkenylation of Aromatic Imines with Organic Halides. *Org. Lett.* **2002**, *4*, 1783–1875, doi:10.1021/ol025851l; c) L. Ackermann, A. Althammer, R. Born. Catalytic Arylation Reactions by C–H Bond Activation with Aryl Tosylates. *Angew. Chem. Int. Ed.* **2006**, *45*, 2619–2622, doi:10.1002/anie.200504450; d) L. Ackermann. Phosphine Oxides as Pre-ligands in Ruthenium-Catalyzed Arylations via C–H Bond Functionalizations Using Aryl Chlorides. *Org. Lett.* **2005**, *7*, 3123–3125, doi:10.1021/ol051216e.
- ⁸¹ a) I. Özdemir, S. Demir, B. Çetinkaya, C. Gourlaouen, F. Maseras, C. Bruneau, P. H. Dixneuf. Direct Arylation of Arene C–H Bonds by Cooperative Action of NHCarbene-Ruthenium(II) Catalyst and Carbonate via Proton Abstraction Mechanism. *J. Am. Chem. Soc.* **2008**, *130*, 1156–1157, doi:10.1021/ja710276x; b) L. Ackermann, R. Vicente, A. Althammer. Assisted Ruthenium-Catalyzed C–H Bond Activation: Carboxylic Acids as Cocatalysts for Generally Applicable Direct Arylations in Apolar Solvents. *Org. Lett.* **2008**, *10*, 2299–2302, doi:10.1021/ol800773x; c) F. Požgan, P. H. Dixneuf. Ruthenium(II) Acetate Catalyst for Direct Functionalisation of *sp*²-C–H Bonds with Aryl Chlorides and Access to Tris-Heterocyclic Molecules. *Adv. Synth. Catal.* **2009**, *351*, 1737–1743, doi:10.1002/adsc.200900350; d) P. B. Arockiam, C. Fischmeister, C. Bruneau, P. H. Dixneuf. C–H Bond Functionalization in Water Catalyzed by Carboxylate Ruthenium(II) Systems. *Angew. Chem. Int. Ed.* **2010**, *49*, 6629–6632, doi:10.1002/anie.201002870; e) L. Ackermann, R. Vicente, H. K. Potukuchi, V. Pirovano. Mechanistic Insight into Direct Arylations with Ruthenium(II) Carboxylate Catalysts. *Org. Lett.* **2010**, *12*, 5032–5035, doi:10.1021/ol102187e; f) L. Ackermann, A. V. Lygin. Ruthenium-Catalyzed Direct C–H Bond Arylations of Heteroarenes. *Org. Lett.* **2011**, *13*, 3332–3335, doi:10.1021/ol2010648; g) B. Li, C. B. Bheeter, C. Darcel, P. H. Dixneuf. Sequential Catalysis for the Production of Sterically Hindered Amines: Ru(II)-Catalyzed C–H Bond Activation and Hydrosilylation of Imines. *ACS Catal.* **2011**, *1*, 1221–1224, doi:10.1021/cs200331m; h) W. Li, P. B. Arockiam, C.

- Fischmeister, C. Bruneau, P. H. Dixneuf. C–H Bond Functionalisation with [RuH(codyl)₂BF₄] Catalyst Precursor. *Green Chem.* **2011**, *13*, 2315–2319, doi:10.1039/C1GC15642J; i) L. Ackermann, E. Diers, A. Manvar. Ruthenium-Catalyzed C–H Bond Arylations of Arenes Bearing Removable Directing Groups via Six-Membered Ruthenacycles. *Org. Lett.* **2012**, *14*, 1154–1157, doi:10.1021/ol3000876.
- ⁸² Selected examples: L. Ackermann, P. Novák, R. Vicente, N. Hofmann. Ruthenium-Catalyzed Regioselective Direct Alkylation of Arenes with Unactivated Alkyl Halides through C–H Bond Cleavage. *Angew. Chem. Int. Ed.* **2009**, *48*, 6045–6048, doi:10.1002/anie.200902458; b) L. Ackermann, P. Novák. Regioselective Ruthenium-Catalyzed Direct Benzylations of Arenes through C–H Bond Cleavages. *Org. Lett.* **2009**, *11*, 4966–4969, doi:10.1021/ol902115f; c) L. Ackermann, N. Hofmann, R. Vicente. Carboxylate-Assisted Ruthenium-Catalyzed Direct Alkylations of Ketimines. *Org. Lett.* **2011**, *13*, 1875–1877, doi:10.1021/ol200366n.
- ⁸³ a) T. Kochi, S. Urano, H. Seki, E. Mizushima, M. Sato, F. Kakiuchi. Ruthenium-Catalyzed Amino- and Alkoxy-carbonylations with Carbamoyl Chlorides and Alkyl Chloroformates via Aromatic C–H Bond Cleavage. *J. Am. Chem. Soc.* **2009**, *131*, 2792–2793, doi:10.1021/ja8097492; b) O. Sadi, J. Marafie, A. E. W. Ledger, P. M. Liu, M. F. Mahon, G. Kociok-Köhn, M. K. Whittlesey, C. G. Frost. Ruthenium-Catalyzed *Meta* Sulfonation of 2-Phenylpyridines. *J. Am. Chem. Soc.* **2011**, *133*, 19298–19301, doi:10.1021/ja208286b; c) T. Kochi, A. Tazawa, K. Honda, F. Kakiuchi. Ruthenium-Catalyzed Acylation of Arylpyridines with Acyl Chlorides via *ortho*-Selective C–H Bond Cleavage. *Chem. Lett.* **2011**, *40*, 1018–1020, doi:10.1246/cl.2011.1018.
- ⁸⁴ Perspective: a) S. I. Kozhushkov, K. Ackermann. Ruthenium-Catalyzed Direct Oxidative Alkenylation of Arenes through Twofold C–H Bond Functionalization. *Chem. Sci.* **2013**, *4*, 886–896, doi:10.1039/c2sc21524a; selected examples: b) H. Weissman, X. Song, D. Milstein. Ru-Catalyzed Oxidative Coupling of Arenes with Olefins Using O₂. *J. Am. Chem. Soc.* **2001**, *123*, 337–338, doi:10.1021/ja003361n; c) K. Cheng, B. Yao, J. Zhao, Y. Zhang. RuCl₃-Catalyzed Alkenylation of Aromatic C–H Bonds with Terminal Alkynes. *Org. Lett.* **2008**, *10*, 5309–5312, doi:10.1021/ol802262r; d) P. B. Arockiam, C. Fischmeister, C. Bruneau, P. H. Dixneuf. Ruthenium Diacetate-Catalysed Oxidative Alkenylation of C–H Bonds in Air: Synthesis of Alkenyl *N*-Arylpyrazoles. *Green Chem.* **2011**, *13*, 3075–3078, doi:10.1039/C1GC15875A; e) K. Padala, M. Jeganmohan. Ruthenium-Catalyzed *Ortho*-Alkenylation of Aromatic Ketones with Alkenes by C–H Bond Activation. *Org. Lett.* **2011**, *13*, 6144–6147, doi:10.1021/ol202580e; f) B. Li, J. Ma, N. Wang, H. Feng, S. Xu, B. Wang. Ruthenium-Catalyzed Oxidative C–H Bond Olefination of *N*-Methoxybenzamides Using an Oxidizing Directing Group. *Org. Lett.* **2012**, *14*, 736–739, doi:10.1021/ol2032575; g) Y. Hashimoto, K. Hirano, T. Satoh, F. Kakiuchi, M. Miura. Ruthenium(II)-Catalyzed Regio- and Stereoselective Hydroarylation of Alkynes via Directed C–H Functionalization. *Org. Lett.* **2012**, *14*, 2058–2061, doi:10.1021/ol300579m; h) M. Schinkel, I. Marek, L. Ackermann. Carboxylate-Assisted Ruthenium(II)-Catalyzed Hydroarylations of Unactivated Alkenes through C–H Cleavage. *Angew. Chem. Int. Ed.* **2013**, *52*, 3977–3980, doi:10.1002/anie.201208446.
- ⁸⁵ a) L. Ackermann. Carboxylate-Assisted Transition-Metal-Catalyzed C–H Bond Functionalizations: Mechanism and Scope. *Chem. Rev.* **2011**, *111*, 1315–1345, doi:10.1021/cr100412j; b) C. Shan, L. Zhu, L.-B. Qu, R. Bai, Y. Lan. Mechanistic View of Ru-Catalyzed C–H Bond Activation and Functionalization: Computational Advances. *Chem. Soc. Rev.* **2018**, *47*, 7552–7576,

- doi:10.1039/c8cs00036k; c) T. Rogge, J. C. A. Oliveira, R. Kuniyil, L. Hu, L. Ackermann. Reactivity-Controlling Factors in Carboxylate-Assisted C–H Activation under 4d and 3d Transition Metal Catalysis. *ACS Catal.* **2020**, *10*, 10551–10558, doi:10.1021/acscatal.0c02808.
- ⁸⁶ Q. Bu, T. Rogge, V. Kotek, L. Ackermann. Distal Weak Coordination of Acetamides in Ruthenium(II)-Catalyzed C–H Activation Processes. *Angew. Chem. Int. Ed.* **2018**, *57*, 765–768, doi:10.1002/anie.201711108.
- ⁸⁷ Reviews: a) J. A. Leitch, C. G. Frost. Ruthenium-Catalysed σ -Activation for Remote *Meta*-Selective C–H Functionalisation. *Chem. Soc. Rev.* **2017**, *46*, 7145–7153, doi:10.1039/c7cs00496f; b) F. F. Khan, S. K. Sinha, G. K. Lahiri, D. Maiti. Ruthenium-Mediated Distal C–H Activation. *Chem. Asian J.* **2018**, *13*, 2243–2256, doi:10.1002/asia.201800545; c) K. Korvorapun, R. C. Samanta, T. Rogge, L. Ackermann. Remote C–H Functionalizations by Ruthenium Catalysis. *Synthesis* **2021**, *53*, 2911–2946, doi:10.1055/a-1485-5156.
- ⁸⁸ Selected examples: a) N. Hofmann, L. Ackermann. *meta*-Selective C–H Bond Alkylation with Secondary Alkyl Halides. *J. Am. Chem. Soc.* **2013**, *135*, 5877–5884, doi:10.1021/ja401466y; b) J. Li, K. Korvorapun, S. De Sarkar, T. Rogge, D. J. Burns, S. Warratz, L. Ackermann. *Nat. Commun.* **2017**, *8*, 15430, doi:10.1038/ncomms15430; c) K. Korvorapun, N. Kaplaneris, T. Rogge, S. Warratz, A. C. Stückl, L. Ackermann. Sequential *meta*/*ortho*-C–H Functionalizations by One-Pot Ruthenium(II/III) Catalysis. *ACS Catal.* **2018**, *8*, 886–892, doi:10.1021/acscatal.7b03648; d) K. Korvorapun, M. Moselage, J. Struwe, T. Rogge, A. M. Messinis, L. Ackermann. Regiodivergent C–H and Decarboxylative C–C Alkylation by Ruthenium Catalysis: *ortho* versus *meta* Position-Selectivity. *Angew. Chem. Int. Ed.* **2020**, *59*, 18795–18803, doi:10.1002/anie.202007144; e) K. Korvorapun, R. Kuniyil, L. Ackermann. Late-Stage Diversification by Selectivity Switch in *meta*-C–H Activation: Evidence for Singlet Stabilization. *ACS Catal.* **2020**, *10*, 435–440, doi:10.1021/acscatal.9b04592; f) W. Wei, H. Yu, A. Zangarelli, L. Ackermann. Deaminative *meta*-C–H Alkylation by Ruthenium(II) Catalysis. *Chem. Sci.* **2021**, *12*, 8073–8078, doi:10.1039/D1SC00986A; g) H.-C. Liu, X.-P. Gong, Y.-Z. Wang, Z.-J. Niu, H. Yue, X.-Y. Liu, Y.-M. Liang. Three-Component Ru-Catalyzed Regioselective Alkylarylation of Vinylarenes via *Meta*-Selective C(sp²)-H Bond Functionalization. *Org. Lett.* **2022**, *24*, 3043–3047, doi:10.1021/acs.orglett.2c00999.
- ⁸⁹ Selected examples: a) J. A. Leitch, C. L. McMullin, M. F. Mahon, Y. Bhonoah, C. G. Frost. Remote C6-Selective Ruthenium-Catalyzed C–H Alkylation of Indole Derivatives via σ -Activation. *ACS Catal.* **2017**, *7*, 2616–2623, doi:10.1021/acscatal.7b00038; b) I. Choi, A. M. Messinis, L. Ackermann. C7-Indole Amidations and Alkenylations by Ruthenium(II) Catalysis. *Angew. Chem. Int. Ed.* **2020**, *59*, 12534–12540, doi:10.1002/anie.202006164.
- ⁹⁰ Selected examples: a) D. C. Fabry, M. A. Ronge, J. Zoller, M. Rueping. C–H Functionalization of Phenols Using Combined Ruthenium and Photoredox Catalysis: *In Situ* Generation of the Oxidant. *Angew. Chem. Int. Ed.* **2015**, *54*, 2801–2805, doi:10.1002/anie.201408891; b) A. Sagadevan, M. F. Greaney. *meta*-Selective C–H Activation of Arenes at Room Temperature Using Visible Light: Dual-Function Ruthenium Catalysis. *Angew. Chem. Int. Ed.* **2019**, *58*, 9826–9830, doi:10.1002/anie.201904288; c) P. Gandeepan, J. Knoeller, K. Korvorapun, J. Mohr, L. Ackermann. Visible-Light-Enabled Ruthenium-Catalyzed *meta*-C–H Alkylation at Room Temperature. *Angew. Chem. Int. Ed.* **2019**, *58*, 9820–9825, doi:10.1002/anie.201902258; d) K. Korvorapun, J. Struwe, R. Kuniyil, A.

- Zangarelli, A. Casnati, M. Waeterschoot, L. Ackermann. Photo-Induced Ruthenium-Catalyzed C–H Arylations at Ambient Temperature. *Angew. Chem. Int. Ed.* **2020**, *59*, 18103–18109, doi:10.1002/anie.202003035; e) A. Sagadevan, A. Charitou, F. Wang, M. Ivanova, M. Vuagnat, M. F. Greaney. *Ortho* C–H Arylation of Arenes at Room Temperature Using Visible Light Ruthenium C–H Activation. *Chem. Sci.* **2020**, *11*, 4439–4443, doi:10.1039/d0sc01289.
- ⁹¹ For a general review, see: a) N. Sauermann, T. H. Meyer, Y. Qiu, L. Ackermann. Electrocatalytic C–H Activation. *ACS Catal.* **2018**, *8*, 7086–7103, doi:10.1021/acscatal.8b01682; selected examples: b) L. Massignan, X. Tan, T. H. Meyer, R. Kuniyil, A. M. Messinis, L. Ackermann. C–H Oxygenation Reactions Enabled by Dual Catalysis with Electrogenated Hypervalent Iodine Species and Ruthenium Complexes. *Angew. Chem. Int. Ed.* **2020**, *59*, 3184–3189, doi:10.1002/anie.201914226; c) L. Yang, R. Steinbock, A. Scheremetjew, R. Kuniyil, L. H. Finger, A. M. Messinis, L. Ackermann. Azaruthena(II)-bicyclo[3.2.0]heptadiene: Key Intermediate for Ruthenaelectro(II/III/I)-Catalyzed Alkyne Annulations. *Angew. Chem. Int. Ed.* **2020**, *59*, 11130–11135, doi:10.1002/anie.202000762.
- ⁹² Selected examples: a) A. Tlili, J. Schranck, J. Pospech, H. Neumann, M. Beller. Ruthenium-Catalyzed Carbonylative C–C Coupling in Water by Directed C–H Bond Activation. *Angew. Chem. Int. Ed.* **2013**, *52*, 6293–6297, doi:10.1002/anie.201301663; b) S. R. Yetra, T. Rogge, S. Warratz, J. Struwe, W. Peng, P. Vana, L. Ackermann. Micellar Catalysis for Ruthenium(II)-Catalyzed C–H Arylation: Weak-Coordination-Enabled C–H Activation in H₂O. *Angew. Chem. Int. Ed.* **2019**, *58*, 7490–7494, doi:10.1002/anie.201901856.
- ⁹³ Selected examples: a) J. A. Leitch, P. B. Wilson, C. L. McMullin, M. F. Mahon, Y. Bhonoah, I. H. Williams, C. G. Frost. Ruthenium(II)-Catalyzed C–H Functionalization Using the Oxazolidinone Heterocycle as a Weakly Coordinating Directing Group: Experimental and Computational Insights. *ACS Catal.* **2016**, *6*, 5520–5529, doi:10.1021/acscatal.6b01370; b) P. Nareddy, F. Jordan, S. E. Brenner-Moyer, M. Szostak. Ruthenium(II)-Catalyzed Regioselective C–H Arylation of Cyclic and *N,N*-Dialkyl Benzamides with Boronic Acids by Weak Coordination. *ACS Catal.* **2016**, *6*, 4755–4759, doi:10.1021/acscatal.6b01360; c) X.-Q. Hu, Z.-K. Liu, Y.-X. Hou, J.-H. Xu, Y. Gao. Merging C–H Activation and Strain-Release in Ruthenium-Catalyzed Isoindoline Synthesis. *Org. Lett.* **2021**, *23*, 16, 6332–6336, doi:10.1021/acs.orglett.1c02131; d) S. Dana, C. K. Giri, M. Baidya. Ruthenium(II)-Catalyzed Regioselective C–H Olefination of Aromatic Ketones and Amides with Allyl Sulfones. *Org. Lett.* **2021**, *23*, 17, 6855–6860, doi:10.1021/acs.orglett.1c02424; e) Z. Hu, F. Belitz, G. Zhang, F. Papp, L. J. Gooßen. Ru-Catalyzed (*E*)-Specific *ortho*-C–H Alkenylation of Arenecarboxylic Acids by Coupling with Alkenyl Bromides. *Org. Lett.* **2021**, *23*, 3541–3545, doi:10.1021/acs.orglett.1c00956; f) F. Belitz, A.-K. Seitz, J. F. Goebel, Z. Hu, L. J. Gooßen. Ru-Catalyzed C–H Arylation of Acrylic Acids with Aryl Bromides. *Org. Lett.* **2022**, *24*, 3466–3470, doi:10.1021/acs.orglett.2c01043.
- ⁹⁴ Reviews: a) L. Ackermann. Carboxylate-Assisted Ruthenium-Catalyzed Alkyne Annulations by C–H/Het–H Bond Functionalizations. *Acc. Chem. Res.* **2014**, *47*, 281–295, doi:10.1021/ar3002798; b) M. Gulías, J. L. Mascareñas. Metal-Catalyzed Annulations through Activation and Cleavage of C–H Bonds. *Angew. Chem. Int. Ed.* **2016**, *55*, 11000–11019, doi:10.1002/anie.201511567; c) P. Singh, K. K. Chouhan, A. Mukherjee. Ruthenium Catalyzed Intramolecular C–X (X=C, N, O, S) Bond Formation *via* C–H Functionalization: An Overview. *Chem. Asian J.* **2021**, *16*, 2392–2412, doi:10.1002/asia.202100513; d) L. Song, E. V. Van der Eycken. Transition Metal-Catalyzed

- Intermolecular Cascade C–H Activation/Annulation Processes for the Synthesis of Polycycles. *Chem. Eur. J.* **2021**, *27*, 121–144, doi:10.1002/chem.202002110; selected examples: e) V. P. Mehta, J.-A. García-López, M. F. Greaney. Ruthenium-Catalyzed Cascade C–H Functionalization of Phenylacetophenones. *Angew. Chem. Int. Ed.* **2014**, *53*, 1529–1533, doi:10.1002/anie.201309114; f) R. Prakash, K. Shekarrao, S. Gogoi. Ruthenium(II)-Catalyzed Alkene C–H Bond Functionalization on Cinnamic Acids: A Facile Synthesis of Versatile α -Pyrones. *Org. Lett.* **2015**, *17*, 5264–5267, doi:10.1021/acs.orglett.5b02631; g) Y. Li, Z. Qi, H. Wang, X. Yang, X. Li. Ruthenium(II)-Catalyzed C–H Activation of Imidamides and Divergent Couplings with Diazo Compounds: Substrate-Controlled Synthesis of Indoles and 3*H*-Indoles. *Angew. Chem. Int. Ed.* **2016**, *55*, 11877–11881, doi:10.1002/anie.201606316; h) X. Wu, B. Wang, S. Zhou, Y. Zhou, H. Liu. Ruthenium-Catalyzed Redox-Neutral [4+1] Annulation of Benzamides and Propargyl Alcohols via C–H Bond Activation. *ACS Catal.* **2017**, *7*, 2494–2499, doi:10.1021/acscatal.7b00031; i) L. Song, X. Zhang, X. Tang, L. Van Meervelt, J. Van der Eycken, J. N. Harvey, E. V. Van der Eycken. Ruthenium-Catalyzed Cascade C–H Activation/Annulation of *N*-Alkoxybenzamides: Reaction Development and Mechanistic Insight. *Chem. Sci.* **2020**, *11*, 11562–11569, doi:10.1039/d0sc04434b; j) T. Zhou, P.-F. Qian, J. -Y. Li, Y.-B. Zhou, H.-C. Li, H.-Y. Chen, B.-F. Shi. Efficient Synthesis of Sulfur-Stereogenic Sulfoximines *via* Ru(II)-Catalyzed Enantioselective C–H Functionalization Enabled by Chiral Carboxylic Acid. *J. Am. Chem. Soc.* **2021**, *143*, 6810–6816, doi:10.1021/jacs.1c03111; k) Y. Li, Y. Wang, X. Huang, Y. Shi, Y. Tang, J. Jiao, J. Li, S. Xu. Rapid Construction of Hexacyclic Indolines *via* the Ru(II)-Catalyzed C–H Activation Initiated Cascade Cyclization of Phenidones with Enynones. *Org. Lett.* **2022**, *24*, 435–440, doi:10.1021/acs.orglett.1c04133.
- ⁹⁵ a) A. Schischko, H. Ren, N. Kaplaneris, L. Ackermann. Bioorthogonal Diversification of Peptides through Selective Ruthenium(II)-Catalyzed C–H Activation. *Angew. Chem. Int. Ed.* **2017**, *56*, 1576–1580, doi:10.1002/anie.201609631; b) P. Andrade-Sampedro, J. M. Matxain, A. Correa. Ru-Catalyzed C–H Hydroxylation of Tyrosine-Containing Di- and Tripeptides toward the Assembly of L-DOPA Derivatives. *Adv. Synth. Catal.* **2022**, doi:10.1002/adsc.202200234.
- ⁹⁶ P. Gandeepan, T. Müller, D. Zell, G. Cera, S. Warratz, L. Ackermann. 3d Transition Metals for C–H Activation. *Chem. Rev.* **2019**, *119*, 2192–2452, doi:10.1021/acs.chemrev.8b00507.
- ⁹⁷ R. Shang, L. Ilies, E. Nakamura. Iron-Catalyzed C–H Bond Activation. *Chem. Rev.* **2017**, *117*, 9086–9139, doi:10.1021/acs.chemrev.6b00772.
- ⁹⁸ M. Moselage, J. Li, L. Ackermann. Cobalt-Catalyzed C–H Activation. *ACS Catal.* **2016**, *6*, 498–525, doi:10.1021/acscatal.5b02344.
- ⁹⁹ a) X.-H. Cai, B. Xie. Carbon–Hydrogen Bond Functionalizations Mediated by Copper. *Synthesis* **2015**, *47*, 737–759, doi:10.1055/s-0034-1379720; b) J. Liu, G. Chen, Z. Tan. Copper-Catalyzed or -Mediated C–H Bond Functionalizations Assisted by Bidentate Directing Groups. *Adv. Synth. Catal.* **2016**, *358*, 1174–1194, doi:10.1002/adsc.201600031; c) Z.-K. Li, X.-S. Jia, L. Yin. Recent Advances in Copper(II)-Mediated or -Catalyzed C–H Functionalization. *Synthesis* **2018**, *50*, 4165–4188, doi:10.1055/s-0037-1609932; d) A. A. Almasalma, E. Mejía. Recent Advances on Copper-Catalyzed C–C Bond Formation *via* C–H Functionalization. *Synthesis* **2020**, *52*, 2613–2622, doi:10.1055/s-0040-1707815.

- ¹⁰⁰ a) W. Liu, K. Ackermann. Manganese-Catalyzed C–H Activation. *ACS Catal.* **2016**, *6*, 3743–3752, doi:10.1021/acscatal.6b00993; b) J. R. Carney, B. R. Dillon, S. P. Thomas. Recent Advances of Manganese Catalysis for Organic Synthesis. *Eur. J. Org. Chem.* **2016**, 3912–3929, doi:10.1002/ejoc.201600018; c) R. Cano, K. Mackey, G. P. McGlacken. Recent Advances in Manganese-Catalysed C–H Activation: Scope and Mechanism. *Catal. Sci. Technol.* **2018**, *8*, 1251–1266, doi:10.1039/c7cy02514a; d) T. Aneja, M. Neetha, C. M. A. Afsina, G. Anilkumar. Recent Advances and Perspectives in Manganese-Catalyzed C–H Activation. *Catal. Sci. Technol.* **2021**, *11*, 444–458, doi:10.1039/d0cy02087g.
- ¹⁰¹ Selected examples: a) M. Bruce, M. Iqbal, F. Stone. *o*-Metalation Reactions. I. Reactions of Azobenzene with Some Metal Carbonyl Complexes of Subgroups VI, VII, and VIII. *J. Chem. Soc. A* **1970**, 3204–3209, doi:10.1039/j19700003204; b) M. I. Bruce, B. L. Goodall, M. Z. Iqbal, F. G. A. Stone, R. J. Doedens, R. G. Little. *Ortho*-Metalation of Benzylideneaniline: Structure of Tetracarbonyl[*o*-(phenyliminomethyl)phenyl]manganese. *J. Chem. Soc. D* **1971**, 1595–1596, doi:10.1039/C29710001595; c) A. Suárez, J. Manuel Vila, M. Teresa Pereira, E. Gayoso, M. Gayoso. Cyclometalated Compounds of Manganese(I) with 1-Methylphenylimidazoles. *J. Organomet. Chem.* **1987**, *335*, 359–363, doi:10.1016/S0022-328X(00)99411-7; d) J. M. Cooney, L. H. P. Gommans, L. Main, B. K. Nicholson. *Ortho*-Manganated Arenes in Synthesis. IV. *Ortho*-Manganation of Substituted Acetophenones and of Heteroaromatic Methyl Ketones. Crystal Structures of Two Cyclometalated Acetylthiophene Derivatives. *J. Organomet. Chem.* **1988**, *349*, 197–207, doi:10.1016/0022-328X(88)80449-2; e) C. Morton, D. J. Duncalf, J. P. Rourke. Substituent Effects on the Cyclomanganation Reaction. X-Ray Crystal Structure of $\text{Mn}\{2\text{-(Bu-N:CH)}_5\text{-(NO}_2\text{)C}_6\text{H}_3\}\text{(CO)}_4$. *J. Organomet. Chem.* **1997**, *530*, 19–25, doi:10.1016/S0022-328X(96)06663-6; f) J.-P. Djukic, A. Maisse, M. Pfeffer. Cyclomanganated (η^6 -Arene)tricarbonylchromium Complexes: Synthesis and Reactivity. *Organomet. Chem.* **1998**, *567*, 65–74, doi:10.1016/S0022-328X(98)00669-X; g) M. A. Leeson, B. K. Nicholson, M. R. Olsen. Orthomanganation of the Iminophosphorane $\text{Ph}_3\text{P:NPh}$, and of Triphenylarsine-Oxide and -Sulfide. *J. Organomet. Chem.* **1999**, *579*, 243–251, doi:10.1016/S0022-328X(99)00007-8; h) J. Albert, J. M. Cadena, J. Granell, X. Solans, M. Font-Bardia. Regioselective Cyclomanganation of Schiff Bases. An Unexpected Effect of Chloro Substituents. *J. Organomet. Chem.* **2004**, *689*, 4889–4896, doi:10.1016/j.jorganchem.2004.07.010; i) G. J. Depree, L. Main, B. K. Nicholson, N. P. Robinson, G. B. Jameson. Synthesis and Alkyne-Coupling Chemistry of Cyclomanganated 1- and 3-Acetylindoles, 3-Formylindole and Analogs. *J. Organomet. Chem.* **2006**, *691*, 667–679, doi:10.1016/j.jorganchem.2005.09.049.
- ¹⁰² Reviews: a) A. Gunay, K. H. Theopold. C–H Bond Activations by Metal Oxo Compounds. *Chem. Rev.* **2010**, *110*, 1060–1081, doi:10.1021/cr900269x; b) A. S. Borovik. Role of Metal–Oxo Complexes in the Cleavage of C–H Bonds. *Chem. Soc. Rev.* **2011**, *40*, 1870–1874, doi:10.1039/C0CS00165A; c) W. Liu, J. T. Groves. Manganese-Catalyzed C–H Halogenation. *Acc. Chem. Res.* **2015**, *48*, 1727–1735, doi:10.1021/acs.accounts.5b00062; selected examples: d) R. Breslow, X. Zhang, Y. Huang. Selective Catalytic Hydroxylation of a Steroid by an Artificial Cytochrome P-450 Enzyme. *J. Am. Chem. Soc.* **1997**, *119*, 4535–4536, doi:10.1021/ja9704951; e) S. Das, C. D. Incarvito, R. H. Crabtree, G. W. Brudvig. Molecular Recognition in the Selective Oxygenation of Saturated C–H Bonds by a Dimanganese Catalyst, *Science* **2006**, *312*, 1941–1943, doi:10.1126/science.1127899;

- f) W. Liu, J. T. Groves. Manganese Porphyrins Catalyze Selective C–H Bond Halogenations. *J. Am. Chem. Soc.* **2010**, *132*, 12847–12849, doi:10.1021/ja105548x; g) W. Liu, X. Huang, M.-J. Cheng, R. J. Nielsen, W. A. Goddard III, J. T. Groves. Oxidative Aliphatic C–H Fluorination with Fluoride Ion Catalyzed by a Manganese Porphyrin. *Science* **2012**, *337*, 1322–1325, doi:10.1126/science.1222327; h) S. M. Paradine, J. R. Griffin, J. Zhao, A. L. Petronico, S. M. Miller, M. C. White. A Manganese Catalyst for Highly Reactive Yet Chemoselective Intramolecular C(sp³)–H Amination. *Nat. Chem.* **2015**, *7*, 987–994, doi:10.1038/nchem.2366.
- ¹⁰³ Y. Kuninobu, Y. Nishina, T. Takeuchi, K. Takai. Manganese-Catalyzed Insertion of Aldehydes into a C–H Bond. *Angew. Chem. Int. Ed.* **2007**, *46*, 6518–6520, doi:10.1002/anie.200702256.
- ¹⁰⁴ Mechanistic studies: a) N. P. Yahaya, K. M. Appleby, M. The, C. Wagner, E. Troschke, J. T. W. Bray, S. B. Duckett, L. A. Hammarback, J. S. Ward, J. Milani, N. E. Pridmore, A. C. Whitwood, J. M. Lynam, I. J. S. Fairlamb. Manganese(I)-Catalyzed C–H Activation: The Key Role of a 7-Membered Manganocycle in H-Transfer and Reductive Elimination. *Angew. Chem. Int. Ed.* **2016**, *55*, 12455–12459, doi:10.1002/anie.201606236; b) L. A. Hammarback, A. Robinson, J. M. Lynam, I. J. S. Fairlamb. Mechanistic Insight into Catalytic Redox-Neutral C–H Bond Activation Involving Manganese (I) Carbonyls: Catalyst Activation, Turnover, and Deactivation Pathways Reveal an Intricate Network of Steps. *J. Am. Chem. Soc.* **2019**, *141*, 2316–2328, doi:10.1021/jacs.8b09095; c) L. A. Hammarback, B. J. Aucott, J. T. W. Bray, I. P. Clark, M. Towrie, A. Robinson, I. J. S. Fairlamb, J. M. Lynam. Direct Observation of the Microscopic Reverse of the Ubiquitous Concerted Metalation Deprotonation Step in C–H Bond Activation Catalysis. *J. Am. Chem. Soc.* **2021**, *143*, 1356–1364, doi:10.1021/jacs.0c10409; selected examples: d) W. Liu, J. Bang, Y. Zhang, L. Ackermann. Manganese(I)-Catalyzed C–H Aminocarbonylation of Heteroarenes. *Angew. Chem. Int. Ed.* **2015**, *54*, 14137–14140, doi:10.1002/anie.201507087; e) C. Wang, A. Wang, M. Rueping. Manganese-Catalyzed C–H Functionalizations: Hydroarylations and Alkenylations Involving an Unexpected Heteroaryl Shift. *Angew. Chem. Int. Ed.* **2017**, *56*, 9935–9938, doi:10.1002/anie.201704682; f) S. Cembellín, T. Dalton, T. Pinkert, F. Schäfers, F. Glorius. Highly Selective Synthesis of 1,3-Enynes, Pyrroles and Furans by Manganese(I)-Catalyzed C–H Activation. *ACS Catal.* **2020**, *10*, 197–202, doi:10.1021/acscatal.9b03965.
- ¹⁰⁵ B. Zhou, Y. Hu, C. Wang. Manganese-Catalyzed Direct Nucleophilic C(sp²)–H Addition to Aldehydes and Nitriles. *Angew. Chem. Int. Ed.* **2015**, *54*, 13659–13663, doi:10.1002/anie.201506187.
- ¹⁰⁶ T. Liu, C. Wang. Manganese-Catalyzed C(sp²)–H Addition to Polar Unsaturated Bonds. *Synlett* **2021**, *32*, 1323–1329, doi:10.1055/a-1468-6136.
- ¹⁰⁷ a) B. Zhou, H. Chen, C. Wang. Mn-Catalyzed Aromatic C–H Alkenylation with Terminal Alkynes. *J. Am. Chem. Soc.* **2013**, *135*, 1264–1267, doi:10.1021/ja311689k; b) H. Wang, F. Pesciaioli, J. C. A. Oliveira, S. Warratz, L. Ackermann. Synergistic Manganese(I) C–H Activation Catalysis in Continuous Flow: Chemoselective Hydroarylation. *Angew. Chem. Int. Ed.* **2017**, *56*, 15063–15067, doi:10.1002/anie.201708271.
- ¹⁰⁸ B. Zhou, P. Ma, H. Chen, C. Wang. Amine-Accelerated Manganese-Catalyzed Aromatic C–H Conjugate Addition to α,β -Unsaturated Carbonyls. *Chem. Commun.* **2014**, *50*, 14558–14561, doi:10.1039/C4CC07598F.

- ¹⁰⁹ a) R. He, Z.-T. Huang, Q.-Y. Zheng, C. Wang. Manganese-Catalyzed Dehydrogenative [4+2] Annulation of N–H Imines and Alkynes by C–H/N–H Activation. *Angew. Chem. Int. Ed.* **2014**, *53*, 4950–4953, doi:10.1002/anie.201402575; b) W. Liu, D. Zell, M. John, L. Ackermann. Manganese-Catalyzed Synthesis of *cis*- β -Amino Acid Esters through Organometallic C–H Activation of Ketimines. *Angew. Chem. Int. Ed.* **2015**, *54*, 4092–4096, doi:10.1002/anie.201411808; c) Q. Lu, S. Greßies, S. Cembellín, F. J. R. Klauck, C. G. Daniliuc, F. Glorius. Redox-Neutral Manganese(I)-Catalyzed C–H Activation: Traceless Directing Group Enabled Regioselective Annulation. *Angew. Chem. Int. Ed.* **2017**, *56*, 12778–12782, doi:10.1002/anie.201707396; d) B. Zhou, Y. Hu, T. Liu, C. Wang. Aromatic C–H Addition of Ketones to Imines Enabled by Manganese Catalysis. *Nat. Commun.* **2017**, *8*, 1169, doi:10.1038/s41467-017-01262-4; e) Q. Lu, S. Cembellín, S. Greßies, S. Singha, C. G. Daniliuc, F. Glorius. Manganese(I)-Catalyzed C–H (2-Indolyl)methylation: Expedient Access to Diheteroarylmethanes. *Angew. Chem. Int. Ed.* **2017**, *57*, 1399–1403, doi:10.1002/anie.201710060; f) S.-Y. Chen, X.-L. Han, J.-Q. Wu, Q. Li, Y. Chen, H. Wang. Manganese(I)-Catalyzed Regio- and Stereoselective 1,2-Diheteroarylation of Allenes: Combination of C–H Activation and Smiles Rearrangement. *Angew. Chem. Int. Ed.* **2017**, *56*, 9939–9943, doi:10.1002/anie.201704952; g) C. Zhu, R. Koniyl, L. Ackermann. Manganese(I)-Catalyzed C–H Activation/Diels–Alder/retro-Diels–Alder Domino Alkyne Annulation featuring Transformable Pyridines. *Angew. Chem. Int. Ed.* **2019**, *58*, 5338–5342, doi:10.1002/anie.201900495.
- ¹¹⁰ a) S. Sueki, Z. Wang, Y. Kuninobu. Manganese- and Borane-Mediated Synthesis of Isobenzofuranones from Aromatic Esters and Oxiranes *via* C–H Bond Activation. *Org. Lett.* **2016**, *18*, 304–307, doi:10.1021/acs.orglett.5b0347; b) Y.-F. Liang, V. Müller, W. Liu, A. Münch, D. Stalke, L. Ackermann. Methylenecyclopropane Annulation by Manganese(I)-Catalyzed Stereoselective C–H/C–C Activation. *Angew. Chem. Int. Ed.* **2017**, *56*, 9415–9419, doi:10.1002/anie.201704767.
- ¹¹¹ a) W. Liu, S. C. Richter, Y. Zhang, L. Ackermann. Manganese(I)-Catalyzed Substitutive C–H Allylation. *Angew. Chem. Int. Ed.* **2016**, *55*, 7747–7750, doi:10.1002/anie.201601560; b) Q. Lu, F. J. R. Klauck, F. Glorius. Manganese-Catalyzed Allylation *via* Sequential C–H and C–C/C–Het Bond Activation. *Chem. Sci.* **2017**, *8*, 3379–3383, doi:10.1039/C7SC00230K; c) H. Wang, M. M. Lorion, L. Ackermann. Air-Stable Manganese(I)-Catalyzed C–H Activation for Decarboxylative C–H/C–O Cleavages in Water. *Angew. Chem. Int. Ed.* **2017**, *56*, 6339–6342, doi:10.1002/anie.201702193.
- ¹¹² C. Zhu, J. L. Schwarz, S. Cembellín, S. Greßies, F. Glorius. Highly Selective Manganese(I)/Lewis Acid Cocatalyzed Direct C–H Propargylation Using Bromoallenes. *Angew. Chem. Int. Ed.* **2018**, *57*, 437–441, doi:10.1002/anie.201710835.
- ¹¹³ a) Q. Lu, S. Greßies, F. J. R. Klauck, F. Glorius. Manganese(I)-Catalyzed Regioselective C–H Allenylation: Direct Access to 2-Alkenylindoles. *Angew. Chem. Int. Ed.* **2017**, *56*, 6660–6664, doi:10.1002/anie.201701767; b) D. Zell, U. Dhawa, V. Müller, M. Bursch, S. Grimme, L. Ackermann. C–F/C–H Functionalization by Manganese(I) Catalysis: Expedient (Per)Fluoro-Allylations and Alkenylations. *ACS Catal.* **2017**, *7*, 4209–4213, doi:10.1021/acscatal.7b01208.
- ¹¹⁴ a) W. Liu, G. Cera, J. C. A. Oliveira, Z. Shen, L. Ackermann. MnCl₂-Catalyzed C–H Alkylations with Alkyl Halides. *Chem. Eur. J.* **2017**, *23*, 11524–11528, doi:10.1002/chem.201703191; b) T. Sato, T. Yoshida, H. H. Al Mamari, L. Ilies, E. Nakamura. Manganese-Catalyzed Directed Methylation of C(sp²)–H Bonds at 25 °C with High Catalytic Turnover. *Org. Lett.* **2017**, *19*, 5458–5461,

- doi:10.1021/acs.orglett.7b02778; c) C. Zhu, J. C. A. Oliveira, Z. Shen, H. Huang, L. Ackermann. Manganese(II/III/I)-Catalyzed C–H Arylations in Continuous Flow. *ACS Catal.* **2018**, *8*, 4402–4407, doi:10.1021/acscatal.8b00166; d) L. Massignan, C. Zhu, X. Hou, J. C. A. Oliveira, A. Salamé, L. Ackermann. Manganoelectro-Catalyzed Azine C–H Arylations and C–H Alkylations by Assistance of Weakly Coordinating Amides. *ACS Catal.* **2021**, *11*, 11639–11649, doi:10.1021/acscatal.1c02516.
- ¹¹⁵ Review: a) J. Son. Sustainable Manganese Catalysis for Late-Stage C–H Functionalization of Bioactive Structural Motifs. *Beilstein J. Org. Chem.* **2021**, *17*, 1733–1751, doi:10.3762/bjoc.17.122; examples: b) Z. Ruan, N. Sauermann, E. Manoni, L. Ackermann. Manganese-Catalyzed C–H Alkynylation: Expedient Peptide Synthesis and Modification. *Angew. Chem. Int. Ed.* **2017**, *56*, 3172–3176, doi:10.1002/anie.201611118; c) N. Kaplaneris, T. Rogge, R. Yin, H. Wang, G. Sirvinskaite, L. Ackermann. Late-Stage Diversification through Manganese-Catalyzed C–H Activation: Access to Acyclic, Hybrid, and Stapled Peptides. *Angew. Chem. Int. Ed.* **2019**, *58*, 3476–3480, doi:10.1002/anie.201812705; d) N. Kaplaneris, J. Son, L. Mendive-Tapia, A. Kopp, N. D. Barth, I. Maksso, M. Vendrell, L. Ackermann. Chemodivergent Manganese-Catalyzed C–H Activation: Modular Synthesis of Fluorogenic Probes. *Nat. Commun.* **2021**, *12*, 3389, doi:10.1038/s41467-021-23462-9; e) N. Kaplaneris, F. Kaltenhäuser, G. Sirvinskaite, S. Fan, T. De Oliveira, L.-C. Conradi, L. Ackermann. Late-Stage Stitching Enabled by Manganese-Catalyzed C–H Activation: Peptide Ligation and Access to Cyclopeptides. *Sci. Adv.* **2021**, *7*, eabe6202, doi:10.1126/sciadv.abe6202.
- ¹¹⁶ Mechanistic study on the insertion step in manganese-catalyzed C–H functionalization: L. A. Hammarback, I. P. Clark, I. V. Sazanovich, M. Towrie, A. Robinson, F. Clarke, S. Meyer, I. J. S. Fairlamb, J. M. Lynam. Mapping out the Key Carbon-Carbon Bond-Forming Steps in Mn-Catalysed C–H Functionalization. *Nat. Catal.* **2018**, *1*, 830–840, doi:10.15124/46f25600-736a-408a-b498-8b7f6a5f3f2e.
- ¹¹⁷ R. A. Jagtap, S. K. Verma, B. Punji. MnBr₂-Catalyzed Direct and Site-Selective Alkylation of Indoles and Benzo[*h*]quinoline. *Org. Lett.* **2020**, *22*, 4643–4647, doi:10.1021/acs.orglett.0c01398.
- ¹¹⁸ R. Mandal, B. Garai, B. Sundararaju. Weak-Coordination in C–H Bond Functionalizations Catalyzed by 3d Metals. *ACS Catal.* **2022**, *12*, 3452–3506, doi:10.1021/acscatal.1c05267.
- ¹¹⁹ a) Y. Hu, B. Zhou, H. Chen, C. Wang. Manganese-Catalyzed Redox-Neutral C–H Olefination of Ketones with Unactivated Alkenes. *Angew. Chem. Int. Ed.* **2018**, *57*, 12071–12075, doi:10.1002/anie.201806287; b) X. Kong, B. Xu. Manganese-Catalyzed *ortho*-C–H Amidation of Weakly Coordinating Aromatic Ketones. *Org. Lett.* **2018**, *20*, 4495–4498, doi:10.1021/acs.orglett.8b01770; c) S. Ali, J. Huo, C. Wang. Manganese-Catalyzed Aromatic C–H Allylation of Ketones. *Org. Lett.* **2019**, *21*, 6961–6965, doi:10.1021/acs.orglett.9b02554.
- ¹²⁰ a) P. Gandeepan, L. Ackermann. Transient Directing Groups for Transformative C–H Activation by Synergistic Metal Catalysis. *Chem* **2018**, *4*, 199–222, doi:10.1016/j.chempr.2017.11.002; b) S. St John-Campbell, J. A. Bull. Transient Imines as “Next Generation” Directing Groups for the Catalytic Functionalisation of C–H Bonds in a Single Operation. *Org. Biomol. Chem.* **2018**, *16*, 4582–4595, doi:10.1039/C8OB00926K; c) B. Niu, K. Yang, B. Lawrence, H. Ge. Transient Ligand-Enabled Transition Metal-Catalyzed C–H Functionalization. *ChemSusChem* **2019**, *12*, 2955–2969, doi:10.1002/cssc.201900151; d) J. I. Higham, J. A. Bull. Transient Imine Directing Groups for the C–H Functionalisation of Aldehydes, Ketones and Amines: an Update 2018–2020. *Org. Biomol. Chem.* **2020**, *18*, 7291–7315, doi:10.1039/D0OB01587C; e) N. Goswami, T. Bhattacharya, D. Maiti.

- Transient Directing Ligands for Selective Metal-Catalysed C–H Activation. *Nat. Rev. Chem.* **2021**, *5*, 646–649, doi:10.1038/s41570-021-00311-3; f) C. Jacob, B. U. W. Maes, G. Evano. Transient Directing Groups in Metal–Organic Cooperative Catalysis. *Chem. Eur. J.* **2021**, *27*, 13899–13952, doi:10.1002/chem.202101598.
- ¹²¹ Selected examples: a) X.-H. Liu, H. Park, J.-H. Hu, Y. Hu, Q.-L. Zhang, B.-L. Wang, B. Sun, K.-S. Yeung, F.-L. Zhang, J.-Q. Yu. Diverse *ortho*-C(sp²)–H Functionalization of Benzaldehydes Using Transient Directing Groups. *J. Am. Chem. Soc.* **2017**, *139*, 888–896, doi:10.1021/jacs.6b11188; b) X.-Y. Chen, E. J. Sorensen. Pd-Catalyzed *ortho* C–H Methylation and Fluorination of Benzaldehydes Using Orthoanilic Acids as Transient Directing Groups. *J. Am. Chem. Soc.* **2018**, *140*, 2789–2792, doi:10.1021/jacs.8b00048; c) S. Rej, N. Chatani. Transient Imine as a Directing Group for the Metal-Free *o*-C–H Borylation of Benzaldehydes. *J. Am. Chem. Soc.* **2021**, *143*, 2920–2929, doi:10.1021/jacs.0c13013; d) M. Liu, J. Sun, T. G. Erbay, H.-Q. Ni, R. Martín-Montero, P. Liu, K. M. Engle. Pd(II)-Catalyzed C(alkenyl)–H Activation Facilitated by a Transient Directing Group. *Angew. Chem. Int. Ed.* **2022**, e202203624, doi:10.1002/anie.202203624.
- ¹²² Selected examples: a) F.-L. Zhang, K. Hong, T.-J. Li, H. Park, J.-Q. Yu. Functionalization of C(sp³)–H Bonds Using a Transient Directing Group. *Science* **2016**, *351*, 252–256, doi:10.1126/science.aad7893; b) Y. Xu, M. C. Young, C. Wang, D. M. Magness, G. Dong. Catalytic C(sp³)–H Arylation of Free Primary Amines with an *exo* Directing Group Generated In Situ. *Angew. Chem. Int. Ed.* **2016**, *55*, 9084–9087, doi:10.1002/anie.201604268; c) K. Hong, H. Park, J.-Q. Yu. Methylene C(sp³)–H Arylation of Aliphatic Ketones Using a Transient Directing Group. *ACS Catal.* **2017**, *7*, 6938–6941, doi:10.1021/acscatal.7b02905; d) Y.-Q. Chen, S. Singh, Y. Qu, Z. Wang, W. Hao, P. Verma, J. X. Qiao, R. B. Sunoj, J.-Q. Yu. Pd-Catalyzed γ -C(sp³)–H Fluorination of Free Amines. *J. Am. Chem. Soc.* **2020**, *142*, 9966–9974, doi:10.1021/jacs.9b13537.
- ¹²³ a) Y.-Q. Chen, Z. Wang, Y. Wu, S. R. Wisniewski, J. X. Qiao, W. R. Ewing, M. D. Eastgate, J.-Q. Yu. Overcoming the Limitations of γ - and δ -C–H Arylation of Amines through Ligand Development. *J. Am. Chem. Soc.* **2018**, *140*, 17884–17894, doi:10.1021/jacs.8b07109; b) J. Jiang, D. Yuan, C. Ma, W. Song, Y. Lin, L. Hu, Y. Zhang. Palladium-Catalyzed Regiospecific *peri*- and *ortho*-C–H Oxygenations of Polyaromatic Rings Mediated by Tunable Directing Groups. *Org. Lett.* **2021**, *23*, 279–284, doi:10.1021/acs.orglett.0c03701; c) G. Kuang, D. Liu, Y. Chen, G. Liu, Y. Fu, Y. Peng, H. Li, Y. Zhou. Transient Directing Group Strategy as a Unified Method for Site Selective Direct C4–H Halogenation of Indoles. *Org. Lett.* **2021**, *23*, 8402–8406, doi:10.1021/acs.orglett.1c03131; d) Y.-H. Li, Y. Ouyang, N. Chekshin, J.-Q. Yu. Pd^{II}-Catalyzed Site-Selective β - and γ -C(sp³)–H Arylation of Primary Aldehydes Controlled by Transient Directing Groups. *J. Am. Chem. Soc.* **2022**, *144*, 4727–4733, doi:10.1021/jacs.1c13586; e) Y. Mao, J. Jiang, D. Yuan, X. Chen, Y. Wang, L. Hu, Y. Zhang. Overcoming *peri*- and *ortho*-Selectivity in C–H Methylation of 1-Naphthaldehydes by a Tunable Transient Ligand Strategy. *Chem. Sci.* **2022**, *13*, 2900–2908, doi:10.1039/D1SC05899A.
- ¹²⁴ Reviews: a) M. I. Lapuh, S. Mazeh, T. Besset. Chiral Transient Directing Groups in Transition-Metal-Catalyzed Enantioselective C–H Bond Functionalization. *ACS Catal.* **2020**, *10*, 12898–12919, doi:10.1021/acscatal.0c03317; b) G. Liao, T. Zhang, Z.-K. Lin, B.-F. Shi. Transition Metal-Catalyzed Enantioselective C–H Functionalization via Chiral Transient Directing Group Strategies. *Angew. Chem. Int. Ed.* **2020**, *59*, 19773–19786, doi:10.1002/anie.202008437; selected examples: c) Z.-Y.

- Li, H. H. C. Lakmal, X. Qian, Z. Zhu, B. Donnadieu, S. J. McClain, X. Xu, X. Cui. Ruthenium-Catalyzed Enantioselective C–H Functionalization: A Practical Access to Optically Active Indoline Derivatives. *J. Am. Chem. Soc.* **2019**, *141*, 15730–15736, doi:10.1021/jacs.9b07251; d) G. Li, Q. Liu, L. Vasamsetty, W. Guo, J. Wang. Ruthenium(II)-Catalyzed Asymmetric Inert C–H Bond Activation Assisted by a Chiral Transient Directing Group. *Angew. Chem. Int. Ed.* **2020**, *59*, 3475–3479, doi:10.1002/anie.201913733; e) U. Dhawa, C. Tian, T. Wdowik, J. C. A. Oliveira, J. Hao, L. Ackermann. Enantioselective Pallada-Electrocatalyzed C–H Activation by Transient Directing Groups: Expedient Access to Helicenes. *Angew. Chem. Int. Ed.* **2020**, *59*, 13451–13457, doi:10.1002/anie.202003826.
- ¹²⁵ Selected examples: a) P. W. Tan, N. A. B. Juwaini, J. Seayad. Rhodium(III)-Amine Dual Catalysis for the Oxidative Coupling of Aldehydes by Directed C–H Activation: Synthesis of Phthalides. *Org. Lett.* **2013**, *15*, 5166–5169, doi:10.1021/ol402145m; b) A. E. Hande, V. B. Ramesh, K. R. Prabhu. Rh(III)-Catalyzed *ortho*-C(sp²)-H Amidation of Ketones and Aldehydes under Synergistic Ligand-Accelerated Catalysis. *Chem. Commun.* **2018**, *54*, 12113–12116, doi:10.1039/C8CC07006G.
- ¹²⁶ a) D. Mu, X. Wang, G. Chen, G. He. Iridium-Catalyzed *ortho*-C(sp²)-H Amidation of Benzaldehydes with Organic Azides. *J. Org. Chem.* **2017**, *82*, 4497–4503, doi:10.1021/acs.joc.7b00531; b) X.-Y. Chen, E. J. Sorensen. Ir(III)-Catalyzed *ortho* C–H Alkylations of (Hetero)Aromatic Aldehydes Using Alkyl Boron Reagents. *Chem. Sci.* **2018**, *9*, 8951–8956, doi:10.1039/C8SC03606C.
- ¹²⁷ F. Li, Y. Zhou, H. Yang, D. Liu, B. Sun, F.-L. Zhang. Assembly of Diverse Spirocyclic Pyrrolidines via Transient Directing Group Enabled *Ortho*-C(sp²)-H Alkylation of Benzaldehydes. *Org. Lett.* **2018**, *20*, 146–149, doi:10.1021/acs.orglett.7b03502.
- ¹²⁸ Following our reports, the TDG strategy has been adopted to a palladium-catalyzed *ortho*-deuteration of benzaldehydes (ref. 53d).
- ¹²⁹ W. Hu, Q. Zheng, S. Sun, J. Cheng. Rh(III)-Catalyzed Bilateral Cyclization of Aldehydes with Nitrosos toward Unsymmetrical Acridines Proceeding with C–H Functionalization Enabled by a Transient Directing Group. *Chem. Commun.* **2017**, *53*, 6263–6266, doi:10.1039/C7CC03006A.
- ¹³⁰ Unpublished results.
- ¹³¹ R. W. Layer. The Chemistry of Imines. *Chem. Rev.* **1963**, *63*, 489–510, doi:10.1021/cr60225a003.
- ¹³² K. D. Collins, F. Glorius. A Robustness Screen for the Rapid Assessment of Chemical Reactions. *Nature Chem.* **2013**, *5*, 597–601, doi:10.1038/nchem.1669.
- ¹³³ a) L. Wu, L. Li, H. Zhang, H. Gao, Z. Zhou, W. Yi. Rh(III)-Catalyzed C–H Activation/[3 + 2] Annulation of *N*-Phenoxyacetamides via Carboxygenation of 1,3-Dienes. *Org. Lett.* **2021**, *23*, 3844–3849, doi:10.1021/acs.orglett.1c00945; b) J. L. Knippel, Y. Ye, S. L. Buchwald. Enantioselective C2-Allylation of Benzimidazoles Using 1,3-Diene Pronucleophiles. *Org. Lett.* **2021**, *23*, 2153–2157, doi:10.1021/acs.orglett.1c00306.
- ¹³⁴ a) O. K. Rasheed. Ruthenium-Catalyzed *Ortho* C(sp²)-H Amidation of Benzaldehydes with Organic Azides. *Synlett* **2018**, *29*, 1033–1036, doi:10.1055/s-0036-1591765; b) Y. Cheng, Y. He, J. Zheng, H. Yang, J. Liu, G. An, G. Li. Ruthenium(II)-Catalyzed *para*-Selective C–H Difluoroalkylation of Aromatic Aldehydes and Ketones using Transient Directing Groups. *Chin. Chem. Lett.* **2021**, *32*, 1437–1441, doi:10.1016/j.ccllet.2020.09.044.

- ¹³⁵ S. Kopf, H. Neumann, M. Beller. Manganese-Catalyzed Selective C–H Activation and Deuteration by Means of a Catalytic Transient Directing Group strategy. *Chem. Commun.* **2021**, 57, 1137–1140, doi:10.1039/D0CC07675A.
- ¹³⁶ Y. Li, H. Neumann, M. Beller. Ruthenium-Catalyzed Site-Selective Trifluoromethylations and (Per)Fluoroalkylations of Anilines and Indoles. *Chem. Eur. J.* **2020**, 26, 6784–6788, doi:10.1002/chem.202001439.
- ¹³⁷ a) P. Piehl, R. Amuso, E. Alberico, H. Junge, B. Gabriele, H. Neumann, M. Beller. Cyclometalated Ruthenium Pincer Complexes as Catalysts for the α -Alkylation of Ketones with Alcohols. *Chem. Eur. J.* **2020**, 26, 6050–6055, doi:10.1002/chem.202000396; b) P. Piehl, R. Amuso, A. Spannenberg, B. Gabriele, H. Neumann, M. Beller. Efficient Methylation of Anilines with Methanol Catalysed by Cyclometalated Ruthenium Complexes. *Catal. Sci. Technol.* **2021**, 11, 2512–2517, doi:10.1039/D0CY02210A.
- ¹³⁸ Application in material science: a) V. Marin, E. Holder, R. Hoogenboom, U. S. Schubert. Functional Ruthenium(II)- and Iridium(III)-Containing Polymers for Potential Electro-Optical Applications. *Chem. Soc. Rev.* **2007**, 36, 618–635, doi:10.1039/B610016C; b) B. Happ, A. Winter, M. D. Hager, U. S. Schubert. Photogenerated Avenues in Macromolecules Containing Re(I), Ru(II), Os(II), and Ir(III) Metal Complexes of Pyridine-Based Ligands. *Chem. Soc. Rev.* **2012**, 41, 2222–2255, doi:10.1039/C1CS15154A; c) A. Gorczyński, J. M. Harrowfield, V. Patroniak, A. R. Stefankiewicz. Quaterpyridines as Scaffolds for Functional Metallosupramolecular Materials. *Chem. Rev.* **2016**, 116, 14620–14674, doi:10.1021/acs.chemrev.6b00377; applications as ligands in homogeneous catalysis: d) G. Desimoni, G. Faita, P. Quadrelli. Pyridine-2,6-bis(oxazolines), Helpful Ligands for Asymmetric Catalysts. *Chem. Rev.* **2003**, 103, 3119–3154, doi:10.1021/cr020004h; e) V. C. Gibson, C. Redshaw, C. A. Solan. Bis(imino)pyridines: Surprisingly Reactive Ligands and a Gateway to New Families of Catalysts. *Chem. Rev.* **2007**, 107, 1745–1776, doi:10.1021/cr068437y; f) J. I. van der Vlugt, J. N. H. Reek. Neutral Tridentate PNP Ligands and Their Hybrid Analogues: Versatile Non-Innocent Scaffolds for Homogeneous Catalysis. *Angew. Chem. Int. Ed.* **2009**, 48, 8832–8846, doi:10.1002/anie.200903193; g) G. Yang, W. Zhang. Renaissance of Pyridine-Oxazolines as Chiral Ligands for Asymmetric Catalysis. *Chem. Soc. Rev.* **2018**, 47, 1783–1810, doi:10.1039/C7CS00615B.
- ¹³⁹ Early report on pyridine deuteration: J. A. Zoltewicz, C. L. Smith. Inversion of Positional Reactivity Order and Two Mechanisms of Hydrogen-Deuterium Exchange for Pyridine. *J. Am. Chem. Soc.* **1967**, 89, 3358–3359, doi:10.1021/ja00989a052.
- ¹⁴⁰ a) C. G. Macdonald, J. S. Shannon. Selective Nickel-Catalysed Hydrogen Exchange of Phenol, Aniline and Pyridine Derivatives. *Tetrahedron Lett.* **1964**, 45, 3351–3354, doi:10.1016/0040-4039(64)83098-7; b) G. E. Calf, J. L. Garnett, V. A. Pickles. Catalytic Deuterium Exchange Reactions with Organics. XL. Pyridine, the Quinolines, Azines, and Aniline on Unsupported Group VIII Transition Metals. *Aust. J. Chem.* **1968**, 21, 961–972, doi:10.1071/CH9680961; c) R. B. Moyes, P. B. Welles. Metal-Catalyzed Hydrogen Exchange Between Pyridine and Deuterium. *J. Catalysis* **1971**, 21, 86–92, doi:10.1016/0021-9517(71)90124-2; d) G. M. Rubottom, E. J. Evain. Deuteration of Pyridine Derivatives: A Very Mild Procedure. *Tetrahedron* **1990**, 46, 5055–5064, doi:10.1016/S0040-4020(01)87812-1; e) E. Alexis, J. R. Jones, W. J. S. Lockley. One-Step Exchange-Labeling of

- Pyridines and Other *N*-Heteroaromatics Using Deuterium Gas: Catalysis by Heterogeneous Rhodium and Ruthenium Catalysts. *Tetrahedron Lett.* **2006**, *47*, 5022–5028, doi:10.1016/j.tetlet.2006.05.106; f) J. A. Sullivan, K. A. Flanagan, H. Hain. Selective H–D Exchange Catalysed by Aqueous Phase and Immobilised Pd Nanoparticles. *Catalysis Today* **2008**, *139*, 154–160, doi:10.1016/j.cattod.2008.03.031; g) S. C. Schou. The Effect of Adding Crabtree's Catalyst to Rhodium Black in Direct Hydrogen Isotope Exchange Reactions. *J. Labelled Compd. Radiopharm.* **2009**, *52*, 376–381, doi:10.1002/jlcr.1612.
- ¹⁴¹ K. R. Guy, J. R. Shapley. H–D Exchange between *N*-Heterocyclic Compounds and D₂O with a Pd/PVP Colloid Catalyst. *Organometallics* **2009**, *28*, 4020–4027, doi:10.1021/om900179g
- ¹⁴² Heterogeneous catalysis: a) H. Esaki, N. Ito, S. Sakai, T. Maegawa, Y. Monguchi, H. Sajiki. General Method of Obtaining Deuterium-Labeled Heterocyclic Compounds Using Neutral D₂O with Heterogeneous Pd/C. *Tetrahedron* **2006**, *62*, 10954–10961, doi:10.1016/j.tet.2006.08.088; b) V. Derdau, J. Atzrodt, J. Zimmermann, C. Kroll, F. Brückner. Hydrogen–Deuterium Exchange Reactions of Aromatic Compounds and Heterocycles by NaBD₄-Activated Rhodium, Platinum and Palladium Catalysts. *Chem. Eur. J.* **2009**, *15*, 10397–10404, doi:10.1002/chem.200901107; homogeneous catalysis: c) V. H. Mai, O. B. Gadzhiev, S. K. Ignatov, G. I. Nikonov. H/D Exchange in *N*-Heterocycles Catalysed by an NHC-Supported Ruthenium Complex. *Catal. Sci. Technol.* **2019**, *9*, 3398–3407, doi:10.1039/C9CY00561G.
- ¹⁴³ a) N. H. Werstiuk, C. Ju. Protium–Deuterium Exchange of Substituted Pyridines in Neutral D₂O at Elevated Temperatures. *Can. J. Chem.* **1989**, *67*, 5–10, doi:10.1139/v89-002; b) J. Yao, R. F. Evilia. Deuteration of Extremely Weak Organic Acids by Enhanced Acid-Base Reactivity in Supercritical Deuteroxide Solution. *J. Am. Chem. Soc.* **1994**, *116*, 11229–11233, doi:10.1021/ja00104a003.
- ¹⁴⁴ A similar study was published during the preparation of our manuscript: Y. Li, C. Zheng, Z.-J. Jiang, J. Tang, B. Tang, Z. Gao. Potassium *tert*-Butoxide Promoted Regioselective Deuteration of Pyridines. *Chem. Commun.* **2022**, *58*, 3497–3500, doi:10.1039/D1CC07128A.
- ¹⁴⁵ B. A. Trofimov, E. Y. Schmidt. Acetylenes in the Superbase-Promoted Assembly of Carbocycles and Heterocycles. *Acc. Chem. Res.* **2018**, *51*, 1117–1130, doi:10.1021/acs.accounts.7b00618.
- ¹⁴⁶ Previous use of KO^tBu/DMSO-*d*₆ in HIE: a) Y. Hu, L. Liang, W.-T. Wei, X. Sun, X.-J. Zhang, M. Yan. A Convenient Synthesis of Deuterium Labeled Amines and Nitrogen Heterocycles with KO^tBu/DMSO-*d*₆. *Tetrahedron* **2015**, *71*, 1425–1430, doi:10.1016/j.tet.2015.01.015; b) L. Huang, W. Liu, L.-L. Zhao, Z. Zhang, X. Yan. Base-Catalyzed H/D Exchange Reaction of Difluoromethylarenes. *J. Org. Chem.* **2021**, *86*, 3981–3988, doi:10.1021/acs.joc.0c02827.
- ¹⁴⁷ a) A. Vaitiekunas, F. F. Nord. Tetrabromothiophene from 2-Bromothiophene by Means of Sodium Acetylide in Liquid Ammonia. *Nature* **1951**, *168*, 875–876, doi:10.1038/168875a0; b) M. Schnürch, M. Spina, A. F. Khan, M. D. Mihovilovic, P. Stanetty. Halogen Dance Reactions – A Review. *Chem. Soc. Rev.* **2007**, *36*, 1046–1057, doi:10.1039/B607701N; c) T. R. Puleo, D. R. Klaus, J. S. Bandar. Nucleophilic C–H Etherification of Heteroarenes Enabled by Base-Catalyzed Halogen Transfer. *J. Am. Chem. Soc.* **2021**, *143*, 12480–12486, doi:10.1021/jacs.1c06481.
- ¹⁴⁸ a) S. Yanagisawa, K. Ueda, T. Taniguchi, K. Itami. Potassium *t*-Butoxide Alone Can Promote the Biaryl Coupling of Electron-Deficient Nitrogen Heterocycles and Haloarenes. *Org. Lett.* **2008**, *10*, 4673–4676, doi:10.1021/ol8019764; b) W. Liu, H. Cao, H. Zhang, H. Zhang, K. H. Chung, C. He, H.

- Wang, F. Y. Kwong, A. Lei. Organocatalysis in Cross-Coupling: DMEDA-Catalyzed Direct C–H Arylation of Unactivated Benzene. *J. Am. Chem. Soc.* **2010**, *132*, 16737–16740, doi:10.1021/ja103050x; c) E. Shirakawa, K.-I. Itoh, T. Higashino, T. Hayashi. *tert*-Butoxide-Mediated Arylation of Benzene with Aryl Halides in the Presence of a Catalytic 1,10-Phenanthroline Derivative *J. Am. Chem. Soc.* **2010**, *132*, 15537–15539, doi:10.1021/ja1080822; d) A. Studer, D. P. Curran. Organocatalysis and C–H Activation Meet Radical- and Electron-Transfer Reactions. *Angew. Chem. Int. Ed.* **2011**, *50*, 5018–5022, doi:10.1002/anie.201101597; e) E. Shirakawa, T. Hayashi. Transition-Metal-Free Coupling of Aryl Halides. *Chem. Lett.* **2012**, *41*, 130–134, doi:10.1246/cl.2012.130; d) S. Zhou, G. M. Anderson, B. Mondal, E. Doni, V. Ironmonger, M. Kranz, T. Tettle, J. A. Murphy. Organic Super-Electron-Donors: Initiators in Transition Metal-Free Haloarene-Arene Coupling. *Chem. Sci.* **2014**, *5*, 476–482, doi:10.1039/C3SC52315B; f) J. P. Barham, G. Coulthard, R. G. Kane, N. Delgado, M. P. John, J. A. Murphy. Double Deprotonation of Pyridinols Generates Potent Organic Electron-Donor Initiators for Haloarene–Arene Coupling. *Angew. Chem. Int. Ed.* **2016**, *55*, 4492–4496, doi:10.1002/anie.201511847; g) J. P. Barham, G. Coulthard, K. J. Emery, E. Doni, F. Cumine, G. Nocera, M. P. John, L. E. A. Berlouis, T. McGuire, T. Tuttle, J. A. Murphy. *KOtBu*: A Privileged Reagent for Electron Transfer Reactions? *J. Am. Chem. Soc.* **2016**, *138*, 7402–7410, doi:10.1021/jacs.6b03282; h) L. Zhang, H. Yang, L. Jiao. Revisiting the Radical Initiation Mechanism of the Diamine-Promoted Transition-Metal-Free Cross-Coupling Reaction. *J. Am. Chem. Soc.* **2016**, *138*, 7151–7160, doi:10.1021/jacs.6b03442; i) M. Patil. Mechanistic Insights into the Initiation Step of the Base Promoted Direct C–H Arylation of Benzene in the Presence of Additive. *J. Org. Chem.* **2016**, *81*, 632–639, doi:10.1021/acs.joc.5b02438; j) J. Madasu, S. Shinde, R. Das, S. Patel, A. Shard. Potassium *tert*-Butoxide Mediated C–C, C–N, C–O and C–S Bond Forming Reactions. *Org. Biomol. Chem.* **2020**, *18*, 8346–8365, doi:10.1039/D0OB01382J.
- ¹⁴⁹ The formation of radicals in DMSO in the presence of base has also been reported: C. L. Øpstad, T.-B. Melø, H.-R. Sliwka, V. Partali. Formation of DMSO and DMF Radicals with Minute Amounts of Base. *Tetrahedron* **2009**, *65*, 7616–7619, doi:10.1016/j.tet.2009.06.109.
- ¹⁵⁰ a) Y. Zhao, D. G. Truhlar. The M06 Suite of Density Functionals for Main Group Thermochemistry, Thermochemical Kinetics, Noncovalent Interactions, Excited States, and Transition Elements: Two New Functionals and Systematic Testing of Four M06-Class Functionals and 12 Other Functionals. *Theor. Chem. Acc.* **2008**, *120*, 215–241, doi:10.1007/s00214-007-0310-x; b) A. V. Marenich, C. J. Cramer, D. G. Truhlar. Universal Solvation Model Based on Solute Electron Density and on a Continuum Model of the Solvent Defined by the Bulk Dielectric Constant and Atomic Surface Tensions. *J. Phys. Chem. B* **2009**, *113*, 6378–6396, doi:10.1021/jp810292n.